The Effects of High Temperature on the Strength of Concrete with Reference to Thermal Spalling

A Thesis submitted to the University of London for Degree of Ph.D.

by

John Wilson Dougill

University of London, King's College.

1971

BIBL. LONDIN. UNIV.

Abstract

The work described consists of a broad investigation into the strength of concrete and concrete structures undertaken with the object of understanding the mechanism and causes of thermal spalling under fire conditions.

The main part of the work comprises a study of the temperatures and stresses developed in plain concrete wall panels heated in the manner prescribed in the Standard fire test. A number of fire tests to determine temperatures in wall panels were undertaken, with the co-operation of the Fire Research Station, and this work is supplemented by a numerical analysis for the temperatures with some account being taken of drying. The method of analysis used needs to be improved, to deal more completely with moisture migration, but the results obtained were useful and the method may have further use, in its present form, in studying charring of timber and in some problems in soil mechanics.

Following the thermal investigation, the stresses in heated wall panels were obtained using an iterative step-by-step analysis. This takes into account the occurrence of cracking and crack closure and the behaviour of concrete in compression, including behaviour beyond the peak stress and during unloading. The results of this analysis

illustrate a number of different modes of progressive structural degradation under fire conditions and also suggest the circumstances when sudden failure could occur as a result of instability of the entire panel.

Besides the work on wall panels, the report includes a classification of spalling and a discussion of possible mechanisms of local spalling. In this, new results are reported to support the contention that aggregate splitting may be reduced by using a smaller maximum sized aggregate in the concrete mix. Also, mechanisms for surface spalling, blistering and pitting are proposed and examined.

Preface

This report is concerned with work that arose from the Imperial College research contract 'Temperature Effects on Structural Concrete' undertaken for the Fire Service Research and Training Trust during the period from Septemeber 1961 to August 1964. The contract was undertaken in the Concrete Structures and Technology section of the Department of Civil Engineering, Imperial College, under the direction of Professor A.L.L.Baker.

At the conclusion of the research contract the author took up an appointment in the Department of Civil Engineering, University of London King's College, where the work was continued on a personal basis with the general support of the Head of Department, Professor A.D.Ross.

The author is grateful to Professor A.L.L.Baker for his patient and understanding supervision throughout this work and to the Fire Service Research and Training Trust for their support in the early stages of the work. The author is also grateful to Professor A.D.Ross for his general encouragement and in particular for his interest in the work undertaken at King's.

The author enjoyed the facilities of the University of London and King's College Computer Units, without which the work described in chapters 8 and 10 would not have been possible. In addition, assistance was received in a number of particular aspects of the work and this is acknowledged where the work is described.

Contents

Abstract			II
Preface			IV
Chapter 1	FIRE RESISTANCE AND SPALLING		
	1·1	Background material	2
	1·2	Fire Resistance	3
	1·3	Spalling - Occurrence and Classification	7
	1·4	Spalling Tests	12
	1·5	Mechanisms of Surface Spalling	15
	1·6	Objectives of the Present Work	20
Chapter 2	SOME ASPECTS OF THE STRENGTH OF CONCRETE AT NORMAL TEMPERATURES		
	2·1	Introduction	23
	2·2	Behaviour of concrete in uniaxial compression	23
	2·3	The Compression Test - Instability	30
	2·4	Behaviour under more general stress systems	34
	2·5	Introduction to the theoretical aspects	38
	2·6	The Fracture Mechanics approach	44
	2·7	Applications to Concrete	50
	2·8	A mathematical model for progressive fracture	56
	2·9	Size Effects	66
	2·10	Comments on Criteria for Failure	68

2·11 The Present Problem 71

Chapter 3 PROPERTIES OF CONCRETE AT ELEVATED TEMPERATURES

3·1 Introduction 74

3·2 Thermal Strains 74

3·3 Structural Properties 83

3·4 Effects of heating on conventional strength, or peak stress, in compression 87

3·5 Young's modulus for heated concrete 96

3·6 Time dependent strains induced by loading - creep 99

3·7 Heat Transmission Properties - Introduction 104

3·8 Thermal Conductivity 106

3·9 Specific Heat and thermal diffusivity 114

Chapter 4 STRUCTURAL BEHAVIOUR IN FIRE TESTS AND STRUCTURES

4·1 Introduction 119

4·2 Fire Resistance of Reinforced Concrete Columns 121

4·3 The behaviour of columns when they are part of a structure

The Localised fire 127

4·4 Simply supported flexural members 137

4·5 Longitudinal Restraint 143

	4·6	Conclusions	149
Chapter 5		OBJECT AND METHOD OF INVESTIGATION	
	5·1	Objective	152
	5·2	General Method	153
	5·3	Choice of Variables	155
	5·4	Status of the Analysis	157
Chapter 6		FIRE TEST ON A CONCRETE WALL PANEL	
	6·1	Introduction	161
	6·2	Test and specimen details	161
	6·3	Results and Observations	169
	6·4	Consideration of Drying	170
	6·5	Fire Resistance	171
	6·6	Spalling and Conclusions	171
	6·7	Acknowledgement	172
Chapter 7		THERMAL CONDITIONS: THEORETICAL CONSIDERATIONS	
	7·1	Introduction	184
	7·2	Assessment of the Problem	184
	7·3	Problem specification	186
	7·4	Numerical Analysis of Heat Conduction	190
	7·5	Stability of the Schmidt-Dus/inberre method	193
	7·6	Interface Temperatures	196
	7·7	Boundary Conditions	204
	7·8	Drying within the wall or movement of the interface	207

	7·9	Initial Stages of Drying - drying near the heated surface	210
Chapter 8		CALCULATIONS AND RESULTS FOR TEMPERATURES IN WALLS	
	8·1	Introduction	215
	8·2	Neumann's solution	215
	8·3	Development of TOASTER	221
	8·4	THERMAL	232
	8·5	Results from THERMAL	235
	8·6	Discussion	246
	8·7	Conclusions from the analysis of the Thermal Conditions	253
Chapter 9		STRUCTURAL BEHAVIOUR OF CONCRETE PANELS I	
	9·1	Introduction	255
	9·2	Analytical Preliminaries	255
	9·3	The thick slab	257
	9·4	Pore pressures	261
	9·5	The Thin slab symmetrically heated	262
	9·6	The thin slab heated on one side only	266
	9·7	Creep	267
	9·8	Method of Analysis	269
	9·9	Instability	273

Chapter 10 STRUCTURAL BEHAVIOUR OF CONCRETE PANELS 11

10·1 Introduction 277

10·2 Representation of concrete behaviour at normal temperatures 277

10·3 Behaviour at elevated temperatures 283

10·4 Material State 289

10·5 Arrangements for computation SLOADED 290

10·6 Input and Output 298

10·7 Data for use with SLOADED 303

10·8 Results from SLOADED: Axially Loaded Panels 308

10·9 Flexurally restrained panels with axial load 313

10·10 Panels with less than Full Restraint 325

10·11 Axial Restraint 329

10·12 Discussion 332

Chapter 11 MECHANISMS OF LOCAL SPALLING

11·1 Introduction 338

11·2 Aggregate Splitting 338

11·3 A Thermal Stress Resistance Factor for Aggregate Splitting 342

11·4 Experiments concerned with aggregate splitting 351

11·5 Corner Failures 354

11·6 Surface Spalling: Introduction 361

11·7 Effects of Large Curvature 361

11·8 Effect of local variations in the heating pattern 365

11·9 Local effects due to the presence of reinforcement 369

11·10 Pore Pressure 371

11·11 Mechanism of Surface Spalling 377

11·12 Discussion 384

Chapter 12 DISCUSSION AND CONCLUSIONS

12·1 General Discussion 387

12·2 Conclusions 390

References 396

Subsidiary Material

Chapter 1

FIRE RESISTANCE AND SPALLING

1·1 Background material

The introduction of reinforced concrete into Britain, by L.G.Mouchel in 1897, coincided with a growing interest in the problems of structural fire protection which lead to the incorporation of the British Fire Prevention Committee (B.F.P.C.) in 1899. At first, concrete was often regarded, or described, as being 'fireproof'. This term was an overstatement, even for the generous sections used in the early designs, and the need for factual data on the behaviour of new materials and methods of construction, was soon recognised. This need was later emphasised, as the new materials were soon to include structural steel; the first steel frame building in Britain, the Ritz Hotel, being constructed in 1907.

In this country, the early tests for fire resistance were undertaken by the B.F.P.C. until its responsibilities were taken over by the Department of Scientific and Industrial Research in 1920. The results of the work undertaken by these two organisations lead to the British Standard B.S.476 (1932) which defined the manner in which tests for fire resistance should be undertaken. Following this, in 1935, the Fire Offices' Committee built furnaces at Boreham Wood to test specimens in accordance with the new Standard. Some time later (1946) the D.S.I.R. joined with the Fire Offices' Committee to form the Joint Fire Research Organisation, in order to undertake research in the broad field of fire resistance and prevention, and the facilities at Boreham Wood were subsequently extended to form the present Fire Research Station.

It is of interest to note that formal study of the fire resistance of structures was initiated at the time when the two of the most common modern constructional materials were first introduced. In a sense, our knowledge of the behaviour of structures in fires has always lagged behind the developments and improvements made in the use of these materials. This is almost inevitable, as work, in the field of structural fire resistance, has been mainly empirical and principally aimed at obtaining comparative 'ratings' for different forms of construction. Some work of a more fundamental nature has also been done, but the results of this are not yet sufficient to enable generally acceptable predictions to be made of the behaviour of structures under fire conditions. Thus, any change in design philosophy (such as the adoption of limit state design proposed in the current (1969) draft Code of Practice for the Structural use of Concrete) or the use of a new form of construction, such as that becoming common in high-bay warehouses, produces a gap, in our knowledge, that has to be filled by retrospective testing. This situation is not ideal and will only be improved when a greater body of fundamental knowledge is available, to cover the range of fire induced behaviour.

1·2 Fire Resistance

In general, buildings are designed and constructed to withstand certain specified loadings for an indefinitely long period. However, this philosophy is not adopted when considering the possibility of damage by fire. Here,

it is considered better to insure against the possible financial loss involved rather than to spend additional capital sums in an attempt to construct a building to resist entirely the effects of fire. Clearly though, if a fire occurs in a structure it is a danger to both life and possessions. It is therefore essential that the structure remains intact for a period long enough to enable the occupants to be evacuated and the fire controlled. This is the principal guide line in the method used to deal with the problem of fire. In this approach; the aim of the building regulations is to prevent loss of life, the structure is designed to remain intact for a specified time, and the cost of damage to property is the subject of insurance.

In practice, the damage caused to a structure and the actual period of fire endurance will depend on the severity of the fire. However, in order that the relative performance of different forms of construction can be compared, the concept of a standard exposure condition has been introduced in the form of a specified time/ambient temperature relationship. Great Britain, Sweden, Germany and the United States of America have adopted, as standard, very similar exposure conditions and an international standard (IS . O. 834) is now available which is incorporated in the current draft revision of B.S. 476. This exposure condition is shown in figure 1-1 and on this basis the 'fire resistance' of a structural element is the time during which it continues to perform its function satisfactorily, when

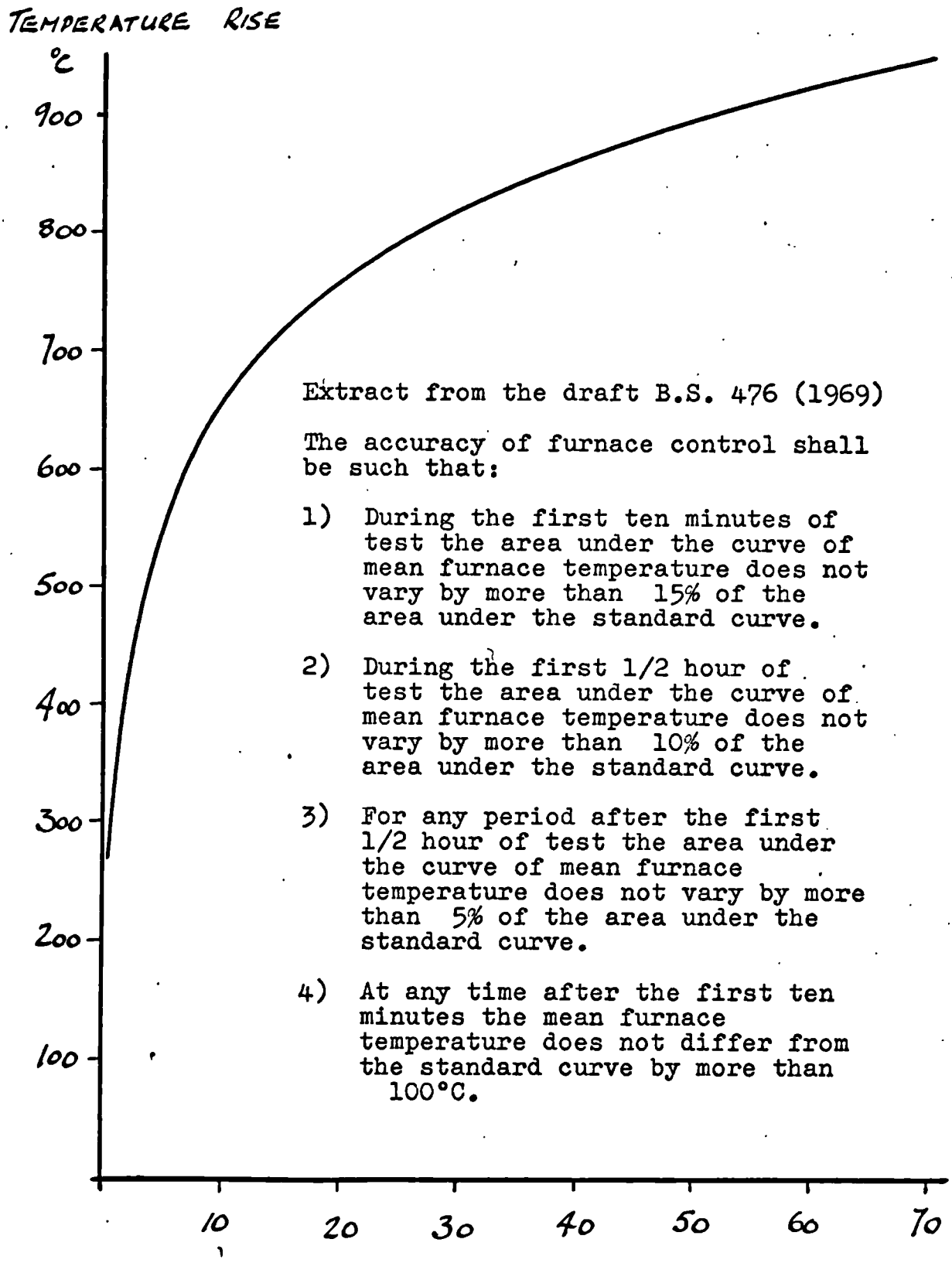


Figure 1-1 STANDARD HEATING CONDITION SPECIFIED IN I.S.O. 834

heated in the specified manner, in a laboratory test.

The standard exposure condition is used in all tests for fire resistance, but the type of test and the criterion of satisfactory performance depend on the function of the member, in the structure, during a fire. This function may be to prevent the spread of fire, by dividing the structure into compartments, or to carry the dead and superimposed loadings. Some members, floor slabs for example, have both these functions whereas others are either primarily barriers to the propagation of fire or purely load bearing.

For members whose only function is to prevent the spread of fire, by forming an adequate barrier for a given time, there appears to be little difficulty in designing experiments to determine their effectiveness in terms of a period of resistance to the standard exposure. Such tests are specified in B.S. 476. The problem is essentially one of heat transmission and, in general, single structural elements can be tested with the knowledge that similar results would be obtained if the tests had been undertaken with the element forming part of a structure.

The problem of testing is not so straightforward for load bearing members, as continuity with the remainder of the structure and the manner in which the loads are applied, can have significant effects on the performance of an individual structural element. In the past, these effects have been generally ignored and only recently has research been undertaken on the effects of restraint and continuity on the fire resistance of structural members. These

questions are taken up in more detail in a later chapter. At this stage, it is sufficient to note that the test for fire resistance is highly idealised and in many cases fails to reproduce the conditions under which a particular element would perform in service.

It must not be supposed that this situation has arisen out of ignorance of the effects of continuity. The decision to ignore the effects of restraint was almost certainly made because of the experimental difficulties, and expense involved, in simulating this effect. However, this policy has the effect that results obtained from fire tests, for modes of failure and local breakdown, may not necessarily be relevant to behaviour in complete structures exposed to fire. This is an important point which will be treated in more detail in a later section.

1·3 Spalling - Occurrence and Classification

In general, reinforced or prestressed concrete members behave reasonably satisfactorily in a fire test and considerable experience has been obtained of the performance of simple elements. However, there are instances (Ashton 1951, Barends 1965 and others) where sudden failure of a concrete member has occurred very soon after it was exposed to rapid heating. This form of behaviour is known as spalling and it may involve complete disintegration of the member or be essentially local in character. The term spalling is also used to refer to the various types of local breakdown that occur at later stages of heating. However, these modes

of failure are more predictable, and so less serious, than the violent mode of failure encountered near the start of heating.

Most information on spalling has been obtained under the particular conditions of the standard test in which spalling invariably leads to a reduction in fire resistance. Clearly, spalling could also have important effects in the more practical situation of a fire in a continuous structure. Thus, although a continuous structure can be expected to accommodate local damage more satisfactorily than a statically determinate one, general spalling could still lead to early collapse or cause the spread of fire by eliminating separating members.

At present, there is no generally accepted theory for the occurrence of spalling. However, the conditions under which spalling has occurred are appreciated. These were discussed by members of the F.I.P. Commission on Fire Resistance of Prestressed Concrete and summarised by Kordina (1965), at the Brunswick symposium, and a similar summary, of Japanese experience, has been given by Saito (1965). These reports, taken together with other workers' experience, give the following picture for the occurrence of spalling.

a) If explosive spalling occurs in the standard test, it does so within 15 - 30 minutes of the start of heating (Kordina 1965). More generally, fast heating rates are required for violent spalling.

b) Explosive spalling is unlikely to occur in members having a large cross-section. (Ashton and Bate 1961, Hill 1965, Kordina 1966

c) Spalling may be promoted by high longitudinal restraint. (Carlson and Abrams 1965, Ashton 1965) or high initial prestress (Saito 1965)

d) A high initial moisture content in the concrete may lead to dangerous spalling (Shorter and Harmathy 1961, Gatenby 1961, Waubke 1966, Akhtaruzzaman and Sullivan 1970.

e) External corners are particularly susceptible to spalling, and

f) the occurrence of spalling may be exacerbated by section geometries giving rise to high thermal stress, the presence of closely spaced reinforcement, or the use of unstable aggregates (Schumann 1965)

Although these statements (a - f) represent a useful summary of current knowledge, some factors that influence spalling are almost certainly missing. For instance the effects of different concrete properties are not dealt with, except by implication. Also, no distinction has been made between the different types of spalling that can occur in practice. This seems important, as it is probable that the various types of spalling may have fundamentally different mechanisms and so would be affected differently by the same variables. Because of this, there is a need to classify the types of spalling

that can occur. Such a classification would be useful when recording impressions of phenomena observed in fire tests and may also be a help in distinguishing between types of behaviour that require separate investigation.

A classification for local spalling has been proposed by Dougill (1964 a) and similar terminology was used by Meyer Ottens (1965) to describe the forms of spalling observed in his own tests. If general spalling is also considered, it seems convenient to describe spalling by means of the classification given in Table 1·3·1. This Table also includes the phenomenon of sloughing off described by Ashton and Bate (1961).

The different forms of spalling will be examined in more detail later in this report. However, it is helpful to note, at this stage, that corner separation and aggregate splitting are, most probably, both forms of cleavage fracture that are primarily due to high thermal stress. Thus, the main difficulty, in considering spalling, is to understand the mechanisms of surface spalling and to explain how destructive spalling can occur. This is the main object of the present work. Before dealing with the mechanisms that have already been proposed to account for spalling it is convenient to review the experimental work undertaken to examine this form of failure.

Table 1·3·1 Types of Spalling

	General or Destructive Spalling
	This is violent and occurs at an early stage of heating. This form of spalling causes extensive damage or complete destruction of a member. The occurrence of general spalling means a fire test is ended.
Local Spalling	Surface Spalling - to include pitting, blistering and local removal of surface material - sometimes violent
	Aggregate Splitting - failure of aggregate near the surface, often accompanied by surface spalling
	Corner Separation - removal of external corners from beams and columns - occasionally violent.
	Sloughing Off
	This is a gradual progressive form of breakdown, noted by Ashton and Bate (1961), involving partial separation of layers of surface material from the member, that may continue slowly through the later stages of heating.

1•4 Spalling Tests

In general our knowledge of spalling is a bonus derived from observations of behaviour in tests for fire resistance and few experiments are undertaken specifically to study spalling under fire conditions. A series of tests undertaken by Meyer Ottens (1965) is a notable exception to this general rule.

Meyer Ottens subjected a series of 27 concrete slabs to rapid heating and observed the temperature rise and forms of spalling that occurred. All the specimens were simply supported reinforced concrete slabs with no super-imposed loading. In most cases only nominal reinforcement was used but in one series of eight tests, a significant amount of steel was included in the cross-section.

A wide range of variables was studied. The whole series included four different concrete mixes, slabs of different dimensions and the use of three different exposure conditions. For most of the tests, the slabs were heated on both sides with the furnace temperature following the German standard exposure condition given in DIN 4102 (1965). However, in some tests, a faster heating rate was used, with the maximum furnace temperature of 1125°C being achieved in only 15 minutes, and in the last two tests, on slabs with nominal reinforcement, the slabs were heated from one side only. The general arrangement for these last two tests is shown in figure 1 - 2.

In all the tests some spalling of the aggregate

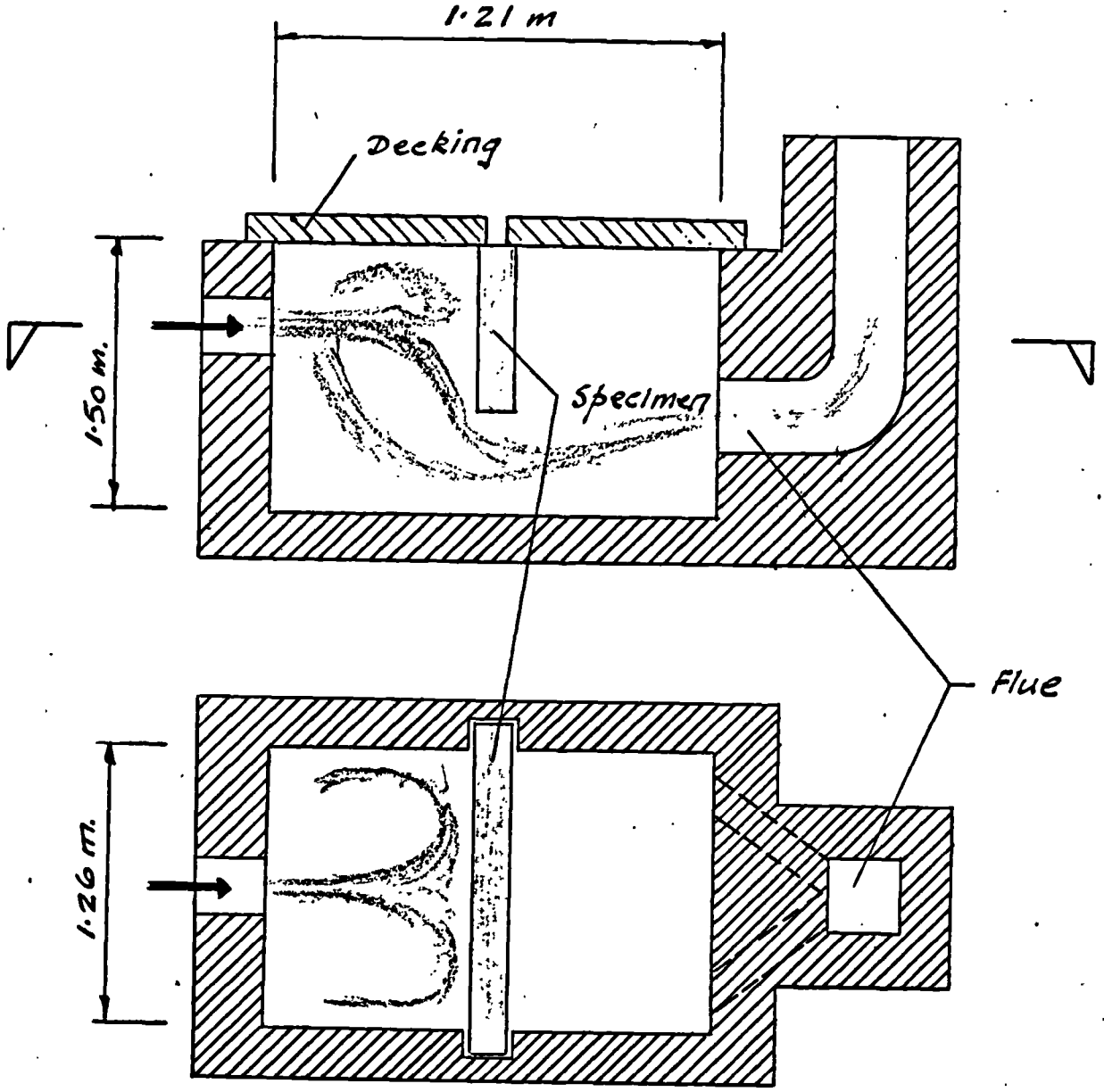


Figure 1-2 GENERAL ARRANGEMENT OF MEYER OTTENS (1965) SPALLING TESTS ON SPECIMENS HEATED FROM ONE SIDE ONLY

(Zuschlagstoff Abplatzungen) occurred. These caused local failure at the heated surface and removal of material in zones up to 80mm in diameter and 5mm deep. The maximum aggregate size in all the four mixes was 15mm. In addition some aggregate pop-out occurred. In some slabs, isolated blocks of Limonite (hydrated iron oxide $2Fe_2O_3 . 3H_2O$ in blocks of size 70x70x20mm) were cast into the slabs. These were included to increase the free water content in the specimen during the test. On heating, Limonite is decomposed to form Hematite (Fe_2O_3) with the liberation of water which thus increases the free water content of the concrete. Unfortunately, there is also a considerable volumetric expansion in the solid phase of this reaction (Schumann 1965) and this may have contributed to the amount of spalling observed.

Spalling was more extensive in the slabs subjected to the faster rate of heating. Here surface spalling (oberflachen Abplatzungen) occurred with removal of material to a depth of 5-10mms from regions 100 - 250mms across. No significant difference in behaviour was observed between the slabs with conventional aggregates and those in which the moisture content had been artificially augmented by the inclusion of Limonite. However, all spalling occurred within the period of visible water vapourisation.

The more heavily reinforced sections were all tested using the standard exposure conditions and extensive surface spalling generally occurred to expose the reinforcement. Destructive spalling (Zerstorende

abplatzungen) occurred in the two thinnest slabs. These were only 50mm thick and heated on both sides. One of these slabs contained reinforcing mesh in the mid plane and the other had reinforcing mesh in each face with the occasional Limonite block between. The sections of these slabs were the thinnest used in the entire series of 27 tests and it is this fact, rather than the reinforcing details, that is probably of most significance in the occurrence of spalling.

Meyer Ottens' tests provide valuable confirmation of the experience derived from fire tests summarised in Section 1·3 (points a - f). The results are slightly disappointing, however, in that they provide little direct guidance to the underlying causes or mechanisms of spalling. These have been the subject of theoretical investigations by other workers which will be discussed in the next section.

1·5 Mechanisms of Surface Spalling

It has generally been supposed that the principal cause of surface spalling is either high thermal stress or the pore pressure induced when steam is generated within the concrete structure. In taking this view, different workers have laid greater emphasis on one or other of these causes. Thus Saito (1965) explains the occurrence of spalling entirely in terms of compression failure caused by thermal stress,whereas Harmathy (1965), in developing the concept of moisture clog spalling, considers that pore pressure generation is the most significant cause of spalling. These two differing views

are now examined in detail.

Compression Failure Mode (after Saito)

Saito (1965) states categorically that explosive spalling is not caused by steam pressure but is due to the compressive stress, induced near the heated surface of a member, reaching a value equal to the compressive strength. Saito takes concrete to be a linear elastic brittle material, in an analysis to determine the stresses caused by heating, and finds that the compressive stress at the surface is increased by longitudinal restraint (or prestress) but is reduced by internal tensile cracking. In this way he explains the influence of restraint and prestress and also demonstrates that prestressed concrete is more likely to spall than reinforced concrete. The effect of moisture is explained by its effect on the temperature distribution and thus on the magnitude of the compressive stresses developed at the surface.

At first sight, Saito's theory is very attractive as it provides an explanation for all but one of the major effects discussed in the previous section. However, in spite of this apparent agreement with reality, there are serious deficiencies in Saito's theory. These arise because concrete is not a linear material and failure does not necessarily occur in concrete when the compressive stress at a point reaches a maximum value. In addition, the theory does not explain why the mode of failure is sudden in occurrence.

These shortcomings rule out Saito's concept of spalling caused by a limiting compressive strength.

Nevertheless, it is clear that very high stresses must occur at the hot face of a heated member and that the concrete near the surface must suffer some damage. It is possible that this damage contributes to spalling but the manner in which this occurs is not clear and is not explained by Saito.

Moisture Clog Spalling

Many workers believe that the pressure of steam generated within the pores of the concrete has a major influence on spalling. This idea has been developed most completely by Shorter and Harmathy (1961) and Harmathy (1965) in their concept of 'moisture clog' spalling. In this they consider that explosive spalling will occur if the pore pressure becomes as great as the tensile strength of the concrete. This is clearly a mechanism that must be considered.

If the surface of a concrete wall panel is heated, desorption of moisture occurs in a thin layer next to the heated surface and some of the vapour produced escapes to the atmosphere through the heated face. The remainder of the vapour moves away from the heated region and may become readsorbed in the pore structure of the cooler material. Continued heating increases the thickness of the dry layer and a completely saturated layer is formed some distance in from the heated surface. After this, desorption only occurs at the interface between the dry and saturated regions. Due to the low permeability of the concrete structure, an appreciable pore pressure

gradient is required to expel the vapour from the hot face and move the body of free water, comprising the saturated layer, towards the cooler regions of the slab.

Harmathy (1965) has attempted to obtain an estimate of the pore pressures developed during heating. He suggests that the pore pressure rises with increase in temperature unless movement of the saturated layer occurs to provide sufficient space to accommodate the liberated vapour without increase in pressure. Looked at in this way, the pressure build up is directly due to the resistance to movement of the saturated region, or 'moisture clog' as it has been called. This is a simplification, as the passage of vapour through the dry region to the atmosphere is equally important, and in this sense the theory is incomplete. However, the analysis does indicate that the rate of heat flow within the dry region and the permeability of the concrete must be considered in addition to the initial saturation.

A more direct estimate of the generated pore pressure can be obtained from the results of fire tests in which temperatures are measured at various depths from the heated surface. Because of the heat required for desorption, the rate of temperature rise is very much reduced at any point during vapourisation. This effect shows itself as a step in a graph of temperature against time and thus the temperature at which vapourisation occurs can be determined.

A number of tests of this type were undertaken simultaneously on a series of eight planks of different

grades of concrete at the Fire Research Station, Boreham Wood, and a description of these tests is given, with the results, in Chapter 6. In these tests the maximum temperature at the interface between the dry and saturated regions was around 150°C and at this temperature the pressure of saturated steam is much less than the tensile strength of concrete. Similar results were obtained by Meyer Ottens (1965) in the tests described in the previous section.

It is suggested that a value of 2·0 MN/m^2. can be taken as a reasonable safe low estimate of the tensile strength of a mature structural concrete. Vapourisation must take place at 215°C in order to produce saturated steam at this pressure and this temperature is considerably higher than the values obtained from the fire test at Boreham Wood or in Meyer Ottens experiments. Consequently, it is considered that it would be exceptional for the pore pressures, generated in a member in a standard fire test, to exceed the tensile strength of a conventional concrete. This suggests that 'moisture clog' spalling is not likely to occur in a standard fire test in the form envisaged by Shorter and Harmathy. However, this conclusion does not rule out the possibility that there is an alternative mechanism by which failure can be induced by pore pressures less than the tensile strength of the material. This possibility will be examined at a later stage.

1·6 Objectives of the Present Work

It is clear that neither Saito's concept of compression spalling nor Harmathy's moisture clog mechanism are entirely satisfactory explanations for the spalling phenomenon. In a way, neither fully describes a mechanism of failure. Harmathy gives a plausible explanation to account for the generation of pore pressure, but does not explain how fracture results at a relatively modest pressure, and Saito pays little attention to the actual behaviour of concrete.

The principal objective of the present work is to arrive at an understanding of the various mechanisms of spalling. This objective may appear to be very limited but it is hoped that greater understanding of the failure process may eventually lead to practical methods of preventing or reducing spalling, where this is important.

Surface spalling is the most difficult of the various related phenomena to explain. Apparently, it is a brittle, cleavage, type of fracture in which material is removed from the concrete surface in a violent manner. Clearly, the mechanism of failure of concrete itself must be appreciated before spalling can be explained. Also, the precise mode of failure must be determined by the state of the concrete at high temperatures, and under stress, near the surface. Thus, before any explanation of spalling can be attempted it is necessary to

a) review existing data and ideas concerned with failure and fracture of concrete, and

b) assess the available information on the structural and thermal properties of concrete at high temperatures.

The next two chapters deal with these topics and the first part of the report is concluded with a further chapter in which the implications of spalling, in fire resistance testing and structures are briefly examined. In the second part of the report the conditions under which spalling occurs are examined in detail whilst the third part is concerned with probable mechanisms of spalling.

Chapter 2

SOME ASPECTS OF THE STRENGTH OF CONCRETE AT NORMAL TEMPERATURES.

2·1 Introduction

In this chapter, the structural properties of concrete at normal temperatures are discussed with the objective of defining the circumstances in which sudden failure can occur. In doing this, no attempt is made to review the entire literature dealing with the strength of concrete. The approach used is to explore what is meant by the term strength and thus to determine how this property should be regarded in considering sudden failure.

At present our knowledge of the behaviour of concrete is mainly empirical in origin and is most complete for concrete in uniaxial compression.

2·2 Behaviour of concrete in uniaxial compression

Under short-term loading, the stress-strain curve for concrete in uniaxial compression is of the form shown in figure 2-1. The duration of loading here is of the order of a few minutes to around half an hour, so that the effect of creep during loading is minimal. Before loading, the concrete already contains some flaws or cracks (Hsu et al. 1963, Hsu 1963) due to internal shrinkage during curing. Some of these miscrocracks may close, during the initial stages of loading, leading to a slight increase in stiffness in the manner described by Brace (1969) for rocks. Most often though, this behaviour is relatively insignificant and the micro-cracks remain stable until the applied stress reaches about half its peak value (see figure 2-1). Around this stage, but not necessarily simultaneously, there is a significant increase in the acoustic energy emitted (Rusch 1959) and a decrease in ultrasonic pulse velocity measured

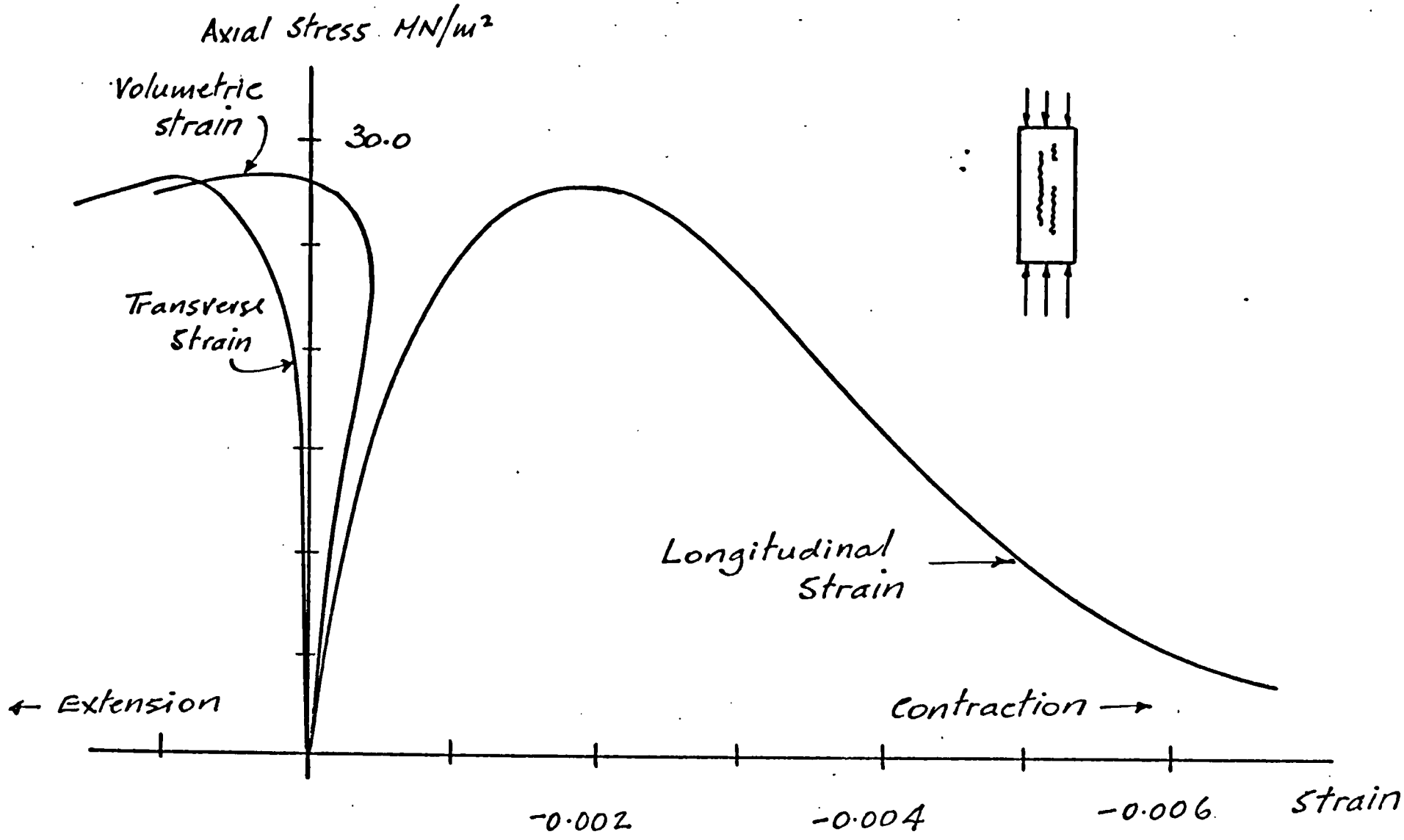


Figure 2-1 TYPICAL STRESS STRAIN CURVES FOR CONCRETE IN COMPRESSION

at right angles to the direction of loading (Jones 1955, Robinson 1965). These changes are considered to be due to the propagation or growth of micro-cracks and these cause the increase in the lateral strains, and in the ratio of lateral to axial strains, referred to in the literature as an increase in Poisson's ratio. With continued loading, the micro-cracks increase in size and join together, causing reduced stiffness and load capacity. Thus, if the axial strain is increased, the induced stress reaches a maximum value before decreasing with further increases in strain and damage.

Although there is general agreement in the literature on the broad aspects of behaviour during progressive failure in compression, there are some differences of opinion concerning the origin of serious cracking or fast crack propagation. For instance, McCreath et al (1969) and the two Newmans (1969) consider that failure originates in the mortar matrix, by cracking in a direction parallel to the applied load, and that these cracks grow until the fracture path is deflected, or divides, to pass around the hard aggregate inclusions. From this stage onwards, they consider that failure is controlled by the aggregate/paste shear bond strength rather than breakdown within the matrix itself. Other workers take the opposite view. Thus, Alexander, Wardlaw and Gilbert (1965) and Vile (1965) all consider that the initial breakdown occurs at the aggregate/cement paste interface. This could then be followed by vertical splitting in the paste, as Shah and Winter (1966) have shown, by tests on isolated interfaces, that the effect of loss of adhesion at these boundaries is to induce tensile stresses

in the matrix and to cause cracking parallel to the direction of the applied compressive load. At present, there is little evidence to suggest that either of these two views is untenable. In fact, if the random structural geometry of a typical concrete is considered, it seems plausible that both sequences of behaviour could occur in different regions of the same specimen. Also, it is probable that even if cracking of the matrix precedes shear bond failure as suggested by the Newmans, further cracking will occur within the matrix during bond breakdown, in the way demonstrated by Shah and Winter.

Discontinuity

It is clearly of interest to know at what stage a material begins to break down under load and the term 'discontinuity' (introduced by Newman in 1964) is now used to describe the stage, in the loading process, at which severe cracking begins. Various techniques have been used to determine the precise stress level at which discontinuity occurs, but the results depend on the method used and the criteria adopted to recognise severe cracking. These difficulties are similar to those encountered in attempting to measure the yield stress of a material such as aluminium, in that the results become subject to an agreed convention which specifies what constitutes the yield stress or, in the case of concrete, discontinuity. Thus, at present, the occurrence of discontinuity in a compression test is taken to coincide with a significant departure from linearity in the relationship between the volumetric strain and the axial compressive strain (Newman and Newman 1969).

The Newmans, and their collaborators, tend to regard the stress level at discontinuity in the same light as the yield stress in the theory of plasticity. Thus, they consider that no significant irreversible strain can be induced in concrete if the discontinuity stress is not exceeded and the loading is of short duration. This is a useful concept, from the design point of view, and may possibly be related to serviceability under repeated short-term loading.

Repeated Loads

Concrete shows some hysteresis with repeated loading at even low stresses but this may usually be disregarded unless the applied stress is above that corresponding to discontinuity. With higher stresses, considerable permanent strain can be induced by repeated cycles of loading and unloading and a typical result is shown in figure 2-2 (after Sinha et al. 1964). Here the strain remaining after each load cycle is related to the amount of cracking that occurs in loading to the higher stress level, although some of these cracks may close during unloading. This suggests that continued deformation, beyond the point corresponding to the peak stress, is accompanied by progressive damage. This is also evident during testing in this range, as the major cracks become easily visible at the surface of a specimen.

Rate of Deformation - Creep

The form of the stress-strain curve in uniaxial compression is affected by the strain rate, as shown in figure 2-3 (after Rusch 1960). With the longer testing periods, there is more opportunity for the stress induced

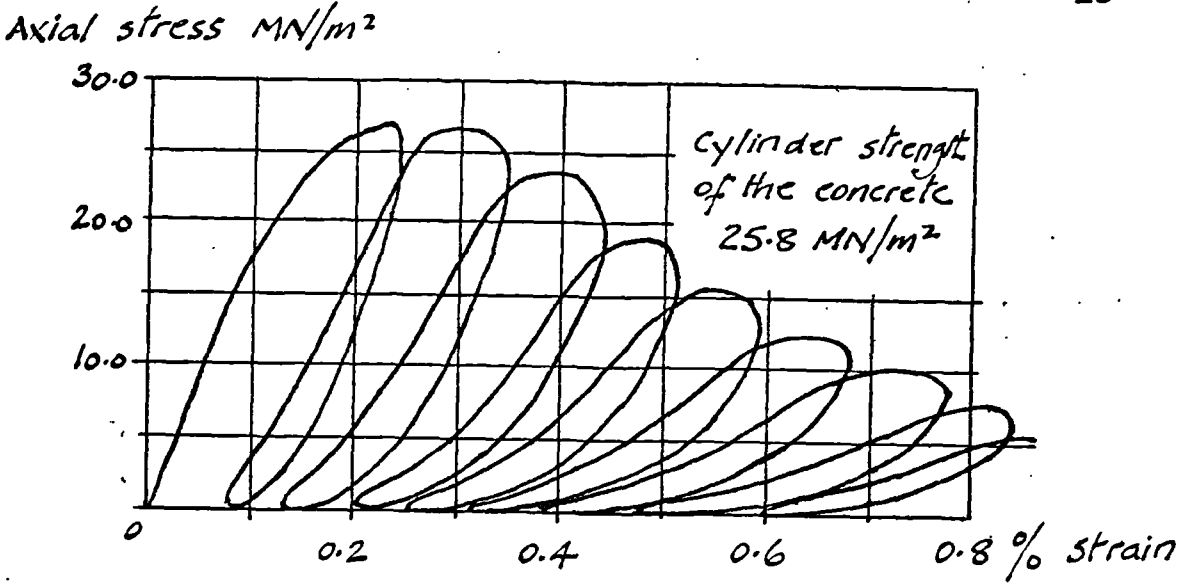


Figure 2-2 AXIAL STRESS - STRAIN CURVES FOR A CONCRETE LOADED REPEATEDLY IN COMPRESSION after SINHA etal. 1964

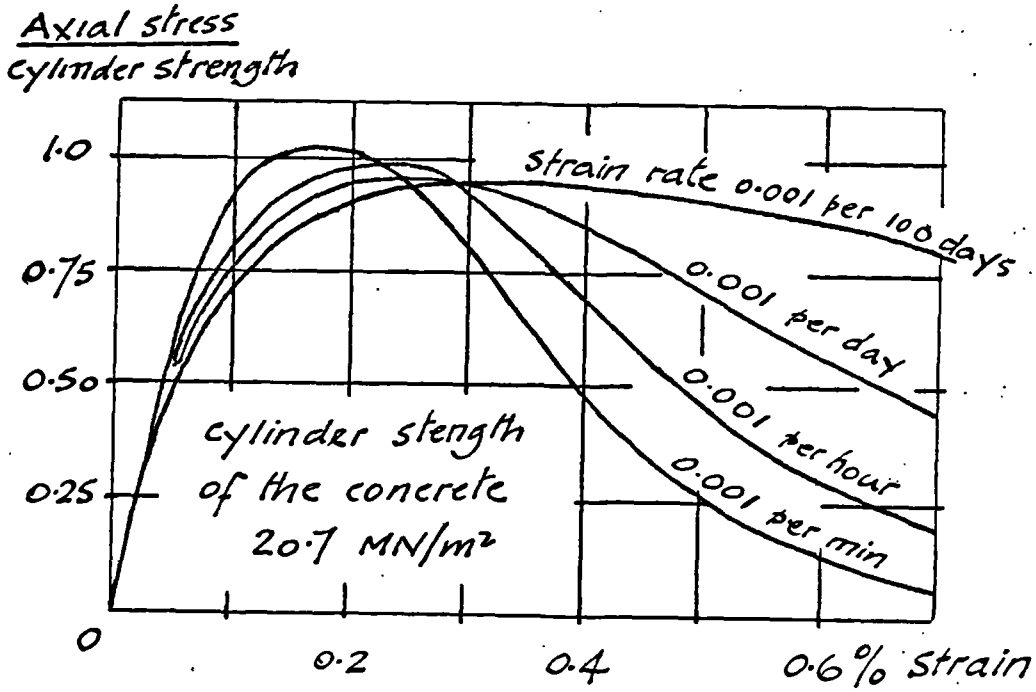


Figure 2-3 STRESS - STRAIN CURVES FOR CONCRETE IN COMPRESSION FOR VARIOUS RATES OF IMPOSED STRAIN after RUSCH (1960)

at a particular strain to relax with time and this causes a considerable change in the form of the stress-strain curve. It is interesting that this change is not necessarily reflected in a changed peak stress, the maximum stress values differing by less than 10% for the four tests reported in the example. The effects of creep are more clearly evident when specimens are maintained under a constant stress for an appreciable period of time. Under moderate stresses, the strain continues to increase with time but at a steadily decreasing rate. However, when the applied stress is an appreciable proportion of the short term peak stress ('ultimate strength') creep is exacerbated by internal disruption of the material and failure eventually occurs (Sell 1959). Results of this type have the form normally associated with creep in metals at elevated temperatures, in that the creep strain/time relationship can be separated into three successive stages. In the first, the creep rate is reduced from an initially high value until it is relatively constant during the second stage. In the final stage (i.e. tertiary creep) the rate of creep increases with time until fracture occurs. With concrete, the second stage is quite short and there is a point of inflexion where the creep rate first starts to increase. Glucklich (1967) considers that this point marks the start of fast crack propagation and that failure of the concrete is inevitable from that time onwards.

Experimental Technique

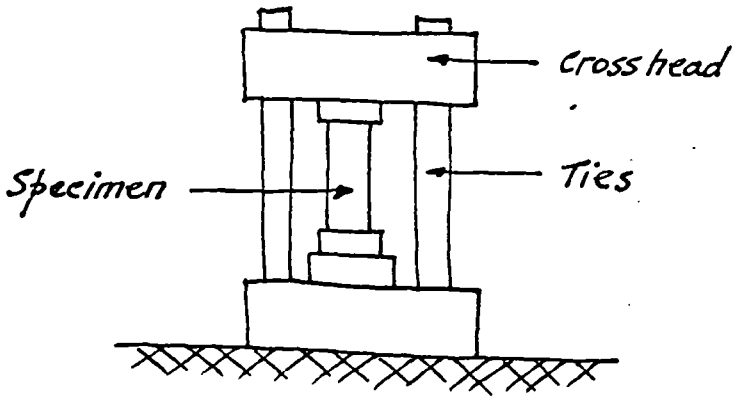
Returning to short term behaviour, it is found that the values of peak stress are very dependent on the

experimental conditions. The size of specimen (Neville 1956), the stiffness of the machine platens (Newman and La-Chance 1964) and the form of ball seating used for alignment (Newman 1965), all have important effects. In addition, it is clear that the full stress-strain curve shown in figure 2-1 can not be obtained under all test conditions. For instance, failure would occur at the peak stress under a gradually applied dead load but the specimen could remain intact if the specimen were subjected to prescribed deformation, even if these exceeded the strain corresponding to the peak stress in the dead load test. In general, the form of loading provided by a conventional testing machine lies between these two extremes and the point of failure of the specimen is dependent on the relative stiffness of the testing machine (Freudenthal 1950, Sigvaldason 1964). This is an important point which has serious implications in defining strength and failure. For this reason, it seems wothwhile to discuss the mechanics of the compression test in more detail.

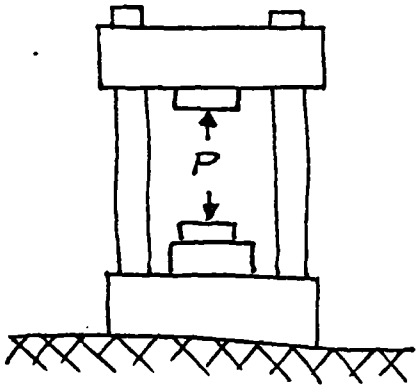
2·3 The Compression Test - Instability

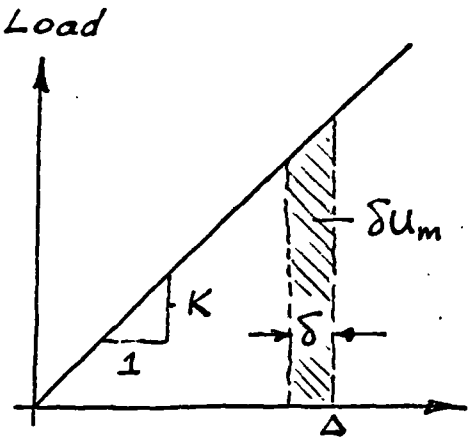
Consider the test machine and specimen shown in figure 2-4. Imagine that the specimen is removed from the machine and replaced by a jack so that the load required to separate the machine platens by an additional prescribed amount can be determined, so providing the load/displacement relationship for the testing machine shown in figure 2-4. We take this relationship to be linear and refer to the slope K as the machine stiffness.

Now consider the specimen in the testing machine under

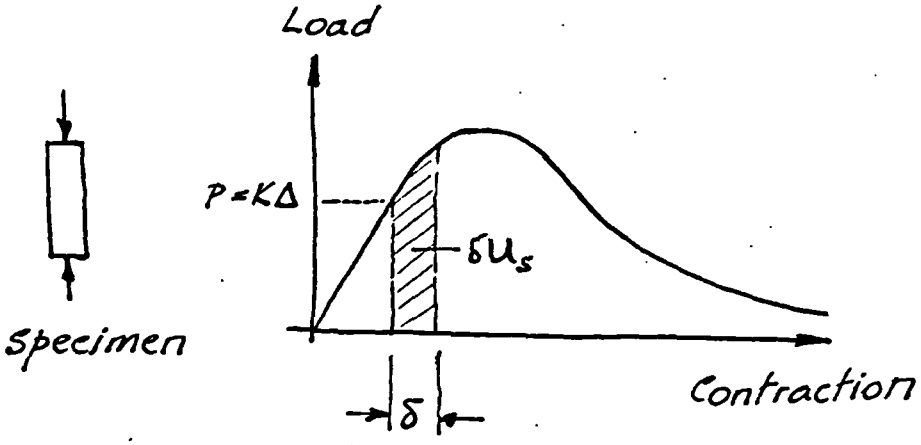


GENERAL ARRANGEMENT FOR THE COMPRESSION TEST





TESTING MACHINE PROPERTIES



SPECIMEN PROPERTIES

Figure 2-4 SYSTEM DETAILS FOR THE COMPRESSION TEST

JWB

a load P. In this state the displacement of the machine (from some datum position) is Δ, the load applied to the specimen is $K\Delta$ and the potential energy of the entire system is π_1. We enquire whether this is a possible equilibrium position, that is one for which the potential energy is a minimum, and examine the effect of a virtual displacement δ of the specimen together with a compatible movement of the test frame. The potential energy in this new configuration is π_2 and the original state is clearly unstable if $\pi_2 \leqslant \pi_1$.

The virtual displacement δ causes an increase in the strain energy of the specimen δu_s and a decrease in the strain energy stored in the machine δu_m represented by the shaded areas in figure 2-4. From this,

$$\delta u_s = K\Delta\delta + \left(\frac{\partial P}{\partial \Delta}\right)_1 \frac{\delta^2}{2} \qquad \text{and } \delta u_m = \frac{K\delta}{2}(2\Delta - \delta) \qquad (2\cdot3\cdot1)$$

where $\left(\frac{\partial P}{\partial \Delta}\right)_1$ is the slope of the load displacement curve for the specimen at the load P carried in the original configuration After the virtual displacement, the potential energy becomes,

$$\pi_2 = \pi_1 + K\Delta\delta + \left(\frac{\partial P}{\partial \Delta}\right)_1 \frac{\delta^2}{2} - \frac{K\delta}{2}(2\Delta - \delta), \qquad (2\cdot3\cdot2)$$

so that for the original configuration to be unstable (i.e. $\pi_2 \leqslant \pi_1$)

$$-\left(\frac{\partial P}{\partial \Delta}\right)_1 \geqslant K \qquad (2\cdot3\cdot3)$$

This condition can only arise when the peak stress has already been achieved. Thus, instability will occur if the

absolute value of the slope of the load displacement curve for the specimen becomes greater than the machine stiffness K. The special cases of dead loading and prescribed displacement correspond to values of $K = 0$ and $K = \infty$ respectively. If instability occurs, the displacements of the specimen and testing machine will change rapidly and the system may 'snap through' to a new equilibrium position. In many cases, however, the strain energy released from the testing machine is available as kinetic energy and the resulting velocity of approach of the platens does not allow the system to settle in a new equilibrium position and catastrophic failure occurs. This form of behaviour becomes more likely with specimens having a steep slope in the decending branch of the stress-strain curve. The results may also be affected by a lack of homogeneity in the concrete specimen.

This analysis of behaviour in a compression test suggests that the occurrence of failure is not determined solely by the peak stress achieved in a compression test and that the explosive mode of failure that is sometimes obtained in the laboratory is the result of instability of the specimen and testing machine considered as a single system. This is a difficult concept to relate to practical situations because it appears that the strength of a concrete structure is not determined by the peak stress achieved at some point but follows from the condition for the structure as a whole to become unstable. However, in spite of the difficulties, this situation has been recognised in formulating rules for the design of reinforced concrete beams, by Whitney (1943) and

Hognestadt et al. (1955) for example, and is an underlying feature of any ultimate load method of analysis (such as Baker's 1956). In both these examples, instability is avoided by setting design limits to the strains or rotation that can be tolerated in a structure. As yet, these ideas have not been extended to more general situations where the state of stress is not so well defined.

2·4 Behaviour under more general stress systems

The occurrence of instability is not confined to behaviour in uniaxial compression as the forms of stress-strain curves obtained from specimens tested with different stress combinations are essentially similar. For example, the stress-strain curve obtained for concrete in uniaxial tension by Hughes and Chapman (1966) has the same form as that of figure 2-1 but with the peak stress reduced and with a much steeper decending branch. Similar results have been obtained by Hughes and Ash (1968), in torsion, and by Davies in flexure (1967) and in combined tension and compression (1968), as obtained in the Brazilian split cylinder test. In all these results, the portion of the stress-strain curve beyond the peak stress is very steep and instability is difficult to avoid, even in a well designed test.

The effect of triaxial compression was studied relatively early in the development of concrete technology by Richart, Brandtzaeg and Brown (1928) who tested jacketed cylindrical specimens in a hydraulic cell so that the specimens could be subjected to an axial stress together with a uniform lateral pressure over the curved surface. Some typical results are shown in figure 2-5 in the form of curves of

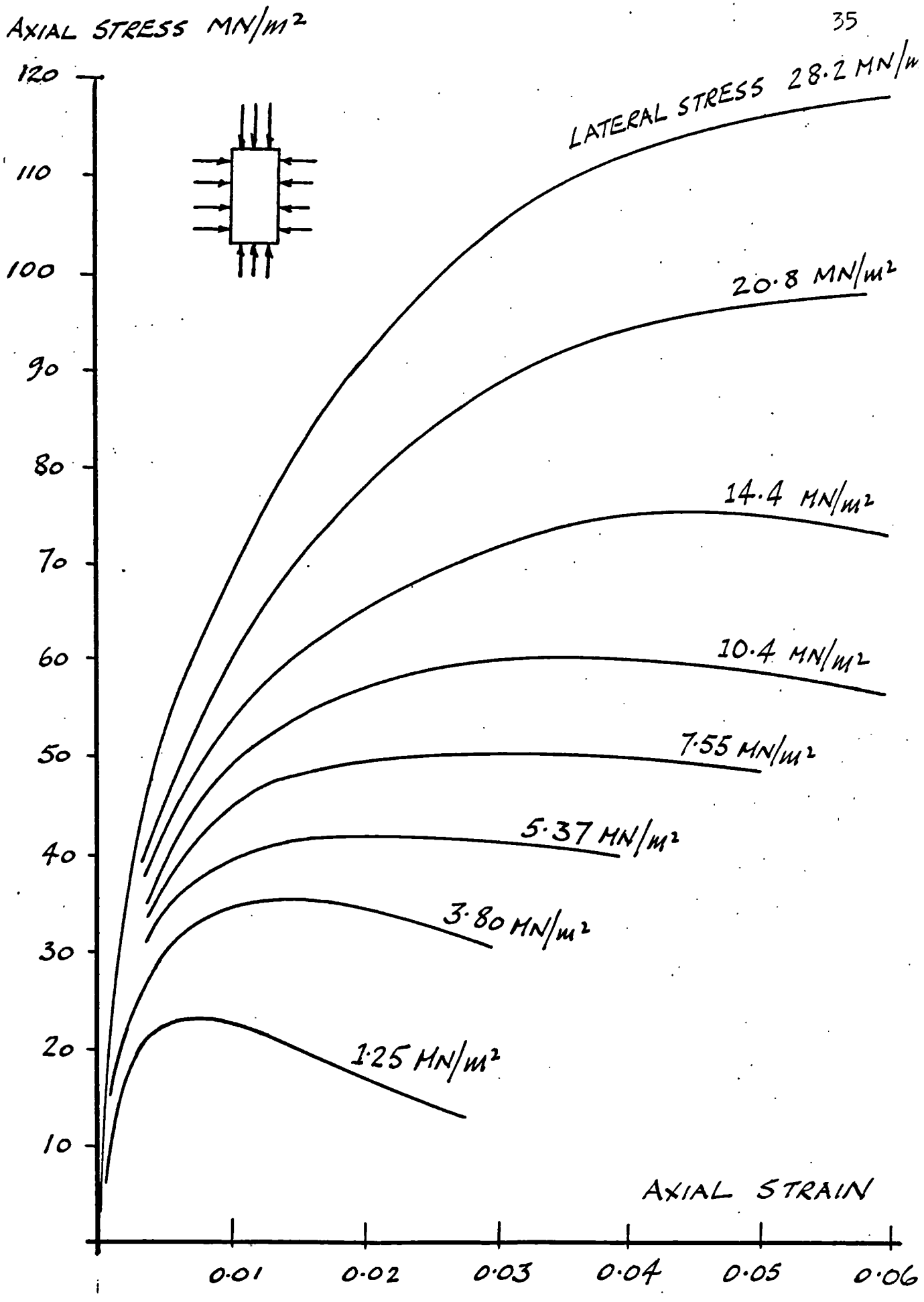


Figure 2-5 STRESS - STRAIN CURVES FOR CONCRETE IN TRIAXIAL COMPRESSIO (after RICHART et al. 1928)

axial stress plotted to a base of axial strain. Similar results have been obtained more recently by Chinn and Zimmerman (1965) and by J.B.Newman (see McCreath et al 1969). At low confining pressures the behaviour is similar to that observed in uniaxial compression, but, an increase in lateral pressure causes a considerable increase in peak stress and a reduction in the slope of the decending branch; so that, at high confining pressures the material appears to be capable of stable plastic deformation. Clearly, the development of internal cracking is inhibited by the lateral stress. This also effectively increases the aggregate/cement paste shear bond strength, which is apparently subject to a Mohr-Coulomb type of law (Taylor and Broms 1964).

Besides triaxial compression, the biaxial state of stress, in which one of the principal stresses is zero, is of considerable interest as the results should indicate the role of the intermediate principal stress in the failure process. Unfortunately, the tests are very difficult to arrange and there are uncertainties regarding the actual states of stress that obtained in much of the published work. (See the discussion by Hilsdorf 1965 for instance). Also, in some tests where care was taken in an attempt to obtain the required state of stress (Robinson 1967, Vile 1965) the full stress-strain curves were not obtained due to instability arising from lack of stiffness in the testing machine. However, reasonably complete data have been obtained by Kupfer et al. at Munich (1969). These results suggest that the decending branch is not so steep as in uniaxial compression and that biaxial stressing may provide

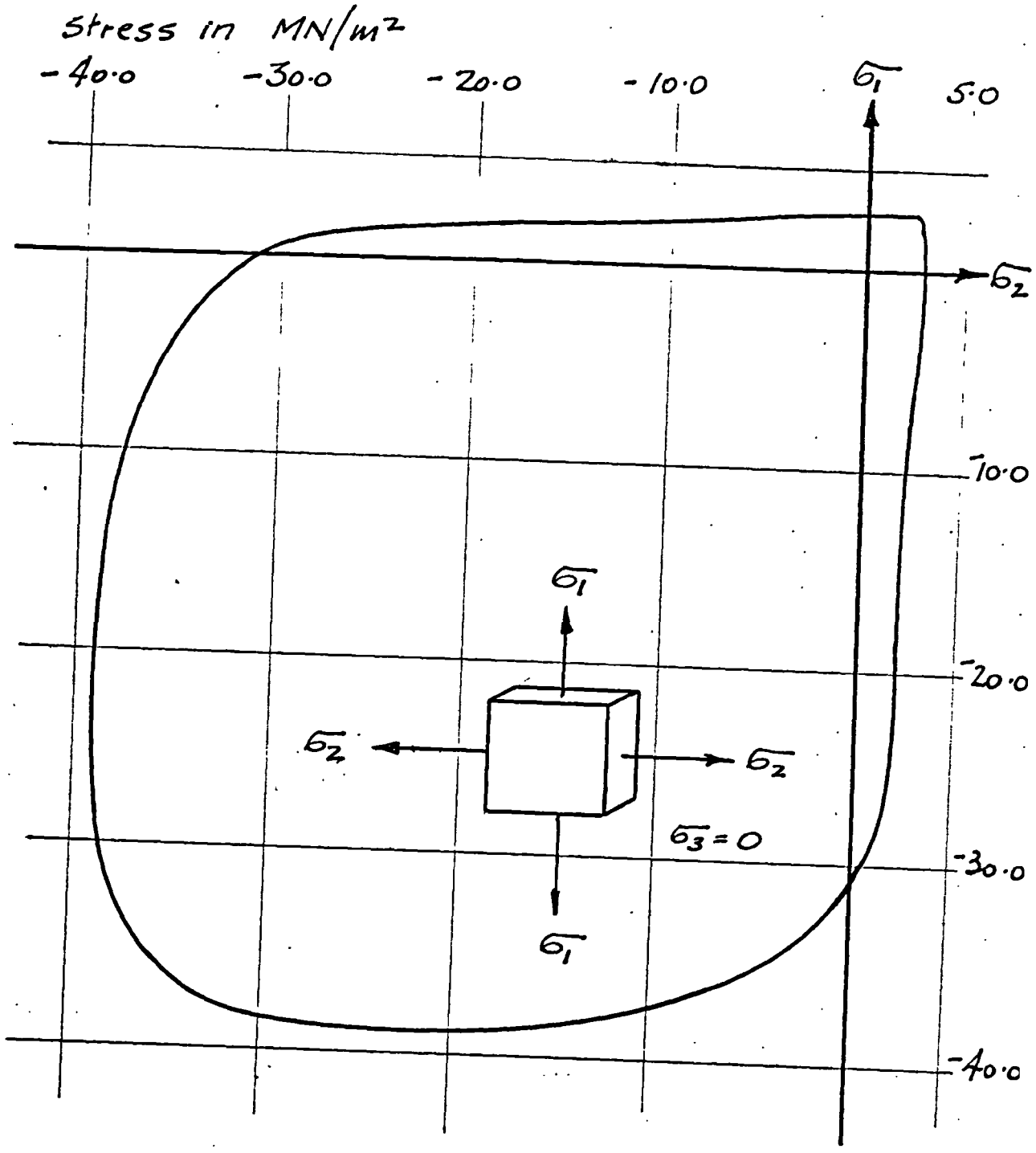


Figure 2-6 VALUES OF PEAK STRESS FOR A CONCRETE TESTED UNDER SHORT-TERM BIAXIAL STRESS (after Kupfer et al. 1969)

a small increase in peak stress over that obtained in simple compression (see figure 2-6).

2·5 Introduction to the theoretical aspects

Although a considerable amount has been accomplished, it is clear that it would need an immense testing programme to furnish data relevant to all possible combinations of stress and load history for even a single concrete. Thus, there have been attempts to develop theories of deformation and failure with the objective of generalising or extending the range of experimental results. In this, most success has been achieved in developing solid models to account for the influence of mix proportions or properties at moderate stress levels when concrete can be considered to be a linear, elastic or visco-elastic, material. The initial application of these ideas to concrete was due to Pickett (1956), Dantu (1958) and Hansen (1958) and useful practical refinements were made later by Hirsch (1962) and Dougill (1962). Following these, many workers have contributed in this field and there are now models available to describe the effects of concrete composition on Young's modulus, Poisson's ratio, shrinkage, thermal expansion, creep and thermal and electrical conductivities. The same degree of success has not followed theoretical work aimed at understanding behaviour at the higher stress levels that obtain as failure is approached. However, there have been a number of notable contributions ranging from the use of structural models to attempts to treat concrete within the framework of fracture mechanics.

Brandtzaeg (1927)

One of the first theoretical studies relating to failure

of concrete was undertaken by Brandtzaeg in 1927. This is still of interest today and a similar approach has been used more recently by Shah and Winter (1966) and Taylor (1970).

Brandtzaeg considered an idealised material made up of separate elements containing planes of weakness along which sliding could occur. He confined his analysis to axisymmetric states of stress and took the material to be linear elastic, homogeneous and isotropic before slip occurred. A representative volume contained a large number of elements with different planes of weakness so that all possible directions of slip were equally represented. During sliding, the shear stress and the normal stress on the slip plane were taken to be related in a linear manner, so suggesting that the behaviour was controlled by a combination of cohesion and friction. It was also assumed that the deformations were the same throughout the specimen.

The results of Brandtzaeg's analysis are both intersting and informative. Under simple compression,the idealised material behaves in a linear elastic manner until slip occurs in one or more elements. With additional loading, more elements yield and there is a loss of stiffness in the axial direction leading to non-linearity in the stress-strain curve together with a redistribution of stress between the elastic regions and those in which slip occurs. As a consequence of this redistribution, tensile stresses are induced in the elastic regions, in directions perpendicular to the applied compression. These stresses increase, as more elements yield, so that tensile failure eventually occurs by splitting in the axial direction. Brandtzaeg used

the term 'critical stress' to refer to the stress applied to the material as a whole when lateral splitting occurred. He recognised that the critical stress did not necessarily correspond to complete collapse of the material, but that it implied that continuity was destroyed so that his homogeneous strain assumption was no longer tenable. Accordingly, Brandtzaeg termed the material 'disorganised' once splitting had occurred.

Below the critical stress, Brandtzaeg's analysis gave results which compared very well with experimental data (Richart et al 1928). In uniaxial compression the critical stress occurred at about 80% of the peak stress which occurred when the volumetric strain was near its minimum value. The analysis also showed that triaxial compression caused an increase in critical stress and that the critical stress in equal biaxial compression was slightly greater than in simple compression. Clearly, there are considerable similarities between Brandtzaeg's 'critical stress' and Newman's (1964) concept of discontinuity, although the latter now refers, in Brandtzaeg's terms, to the first occurrence of slip rather than the onset of disorganisation. The analysis is also relevant to the ideas developed by Taylor and Broms (1964) and Alexander and Wardlaw (1965) on shear bond failure, if the planes of weakness are taken to represent the aggregate/cement paste interface. Thus, it is of interest that Taylor (1970) has attempted to generalise this approach to consider, in numerical terms, the case of three independent principal stresses.

The main disadvantage of Brandtzaeg's approach is that

only the initial stage of the failure process is considered. Also, in assuming that the material is initially homogeneous, the effect of the aggregate inclusions on the stress distribution is omitted. This effect is the principal feature of the structural model proposed by Baker (1959).

Baker's (1959) Lattice.

In this approach, Baker considers that the larger pieces of aggregate in a well compacted concrete form stiff ring structures around regions of relatively soft mortar. Thus, when concrete is loaded in compression, load is attracted to the ring and lateral tensile stresses are induced in the mortar. Baker suggested that this type of behaviour could be simulated by means of a three dimensional pin jointed lattice framework comprising different types of members to represent the separate actions of the thrust rings and the mortar pockets. Although Anson (1964) later extended the work to three dimensions, Baker's first analysis was based on the two dimensional lattice element shown in figure 2-7. In this, the diagonal members represent the short stiff connections between aggregate particles and the horizontal and vertical members represent the bonding action of the mortar enclosed within the thrust ring. Baker recognised that a stiff jointed lattice would be a more appropriate model and that the resultant line of force in the thrust ring is displaced from the diagonal direction obtained from aggregate geometry only. Therefore, he introduced the angle φ, as a lattice property, to define the diagonal direction for use in simple compression. In the analysis it was assumed that failure occurred when the tensile force

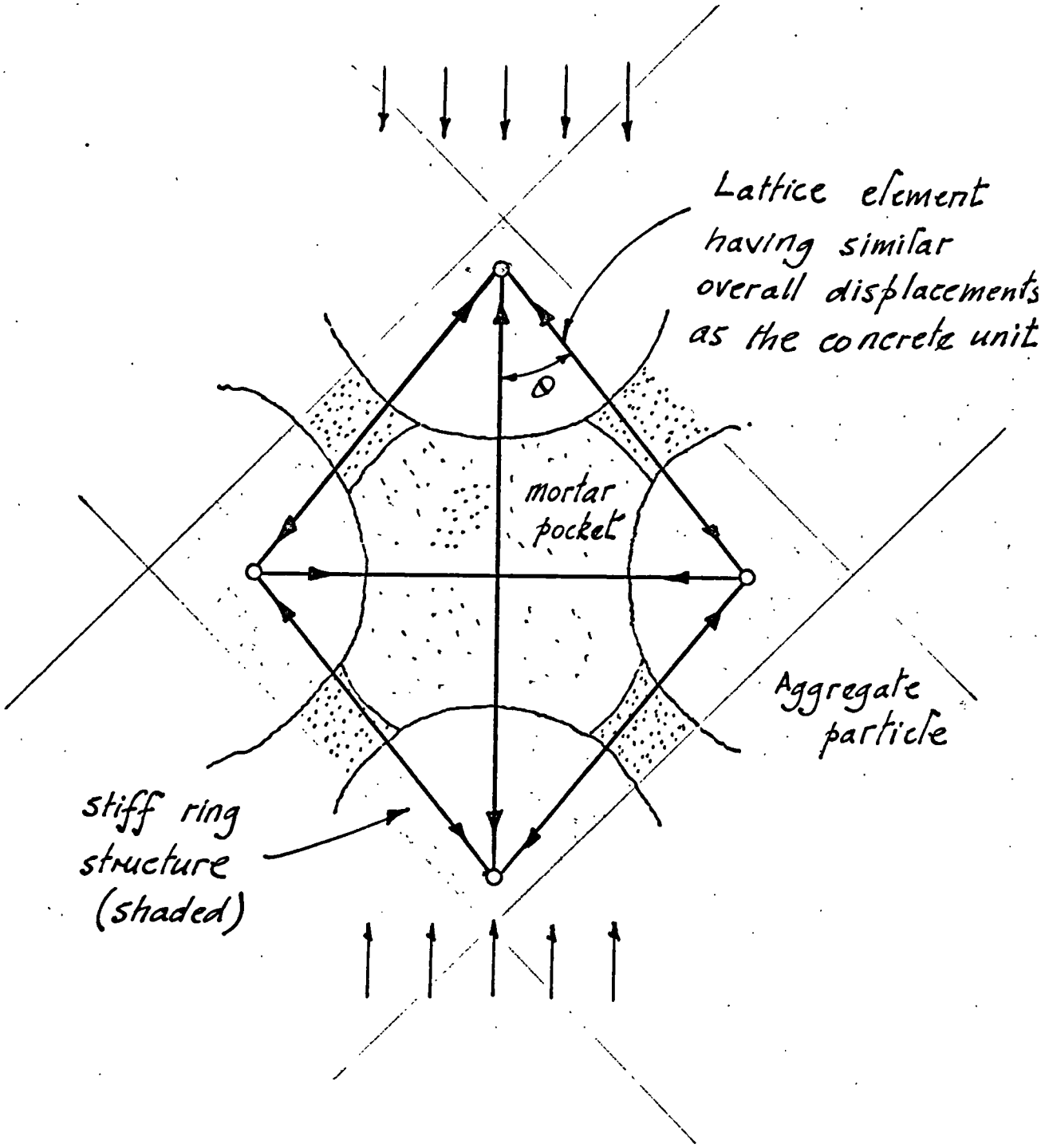


Figure 2-7 BAKER'S (1959) LATTICE ANALOGUE FOR THE STRUCTURAL BEHAVIOUR OF CONCRETE

in a mortar bond reached a critical value and the angle φ and the relative stiffness of the members were chosen to give a suitable value of Poisson's ratio and a ratio of compressive to tensile strength of between 8 and 12. The main results showed how failure in simple compression could be due to axial splitting.

Baker's lattice is noteworthy because it recognises the effects of heterogeneity in the concrete structure as did the earlier model used by Reinius (1955). However, the lattice can not give fundamental information on possible modes of failure in concrete as the results follow from the initial assumption that the principal cause of failure is tensile breakdown within the mortar and no consideration is given to bond failure. Also, it is possible that the angle φ should depend on the stress level and this would complicate the analysis, particularly under combined stresses. It appears, therefore, that the main use for the lattice is as a qualitative tool to help in visualising the interaction between the aggregate and cement paste. This is the manner in which the lattice was used by Dougill (1961), to demonstrate the effects of thermal incompatibility in concrete, and more recently by Baker (1970) in postulating limiting strain criteria for the design strength of concrete.

Neither Brandtzaeg's analysis nor Baker's lattice provides a description of the latter stages of the failure process. In order to do this, attempts have been made by Kaplan (1961 and 1965) and Glucklich (1963) to apply fundamental concepts of brittle fracture to concrete. These followed from the work of Griffith (1920) and Irwin (1948) who can

be regarded as originators of fracture mechanics.

2·6 The Fracture Mechanics approach

Griffith (1920) recognised that the fracture stress for most brittle solids is considerably less than the tensile cleavage strength that could be expected from these materials on the basis of their atomic structure. He postulated that the discrepancy occurs because materials contain defects. These defects, or flaws, cause local stress concentrations which affect the technical strength of a sample of material. This view is now widely accepted and the presence of flaws has been demonstrated using modern methods of non-destructive testing.

Griffith considered the effect of a flaw, having the form of a narrow elliptical cavity, in a sheet of an otherwise homogeneous elastic material. The cavity represented a crack through the thickness of a loaded plate and the ellipse was made narrow in order to represent a slit of negligible thickness in the material.. This would cause difficulties in an elastic analysis, as there is a singularity in the stress field at the tip of the crack which would prevent the direct determination of a stress concentration factor for the assumed flaw (Williams 1969). Griffith avoided this difficulty by investigating the equilibrium of the system, in an indirect manner, using the Theorem of Minimum Potential Energy. This approach is of considerable interest and so will be discussed in detail.

Consider a thin elliptical crack of length 2c in an infinite plate of unit thickness carrying a tensile stress σ in a direction normal to the major axis of the ellipse. In

this configuration the potential energy of the system, π_1, can be written in the form

$$\pi_1 = \pi_o - u(c) \qquad (2\cdot6\cdot1)$$

where the term π_o may be regarded as a convenient datum value of potential energy and the strain energy term u(c) represents the reduction in strain energy in the plate due to the presence of the crack. Now, if the body containing the crack is in stable equilibrium, the potential energy π_1 must have a minimum value and any virtual change of configuration will raise the potential energy. This suggests that if the potential energy π_2 is found, for the system displaced to an alternative neighbouring configuration, and if $\pi_2 \leqslant \pi_1$ the system is unstable in the original configuration. This approach is used frequently in structural mechanics and has already been used (in para. 2·3) in discussing the behaviour of a testing machine and specimen. In the case of the crack, the neighbouring configuration is found by considering a virtual crack extension, the half length becoming c+δc. Griffith realised that the work done in forming new surfaces must be included in the expression for the potential energy, so that

$$\pi_2 = \pi_o - u(c+\delta c) + 4\gamma\delta c \qquad (2\cdot6\cdot2)$$

where γ is the surface energy of the material and has dimensions the same as those of work/unit area. Equation 2·6·2 may be written

$$\pi_2 = \pi_o - \left(u + \frac{du}{dc}\,\delta c\right) + 4\gamma\delta c,$$

so that the condition, $\pi_2 < \pi_1$, for the system to be unstable becomes,

$$\frac{du}{dc} \geqslant 4\gamma \qquad (2\cdot6\cdot3)$$

For the case considered (by Griffith 1920)

$$u = \frac{\pi c^2 \sigma}{E} \qquad (2\cdot6\cdot4)$$

where E is Young's modulus for the material and thus instability occurs for

$$\sigma = \sqrt{\frac{2E\gamma}{\pi c}} \qquad (2\cdot6\cdot5)$$

Equation 2·6·5 shows that the strength of a brittle material is determined by its stiffness, surface energy and the size of the imperfections. In arriving at this conclusion, Griffith had broken new ground in postulating that flaws were present in real materials and in demonstrating that brittle fracture is a form of instability.

Griffith's equation applies to a material that remains linear elastic until fracture occurs. Also, the structure of the material is ignored in the analysis, which is based on an assumed continuum. It is therefore reasonable to restrict the application of the equation to situations where the effective crack length, 2c, controlling brittle fracture is considerably greater than the typical micro-structural dimensions (i.e. grain size) of the material considered. In this way, it is seen that the result is likely to be most applicable to amorphous materials such as glass but may

require modification if it is to be applied to materials with a macroscopic structure such as mortar, brittle rocks or concrete. Objections have also been made at the dimensional level (and discussed by Murrell 1964) to the form of crack adopted by Griffith. In these it is suggested that a description of behaviour at the crack tip must be influenced by the local structure which is of atomic dimensions, and by the inter-atomic forces. Clearly, such a description cannot be provided by the continuum model. However, it appears that Griffith avoids this difficulty, in circumventing the singularity at the crack tip, if the crack extension δc is taken to be large compared with the atomic dimensions but small when compared with c, Some idea of the dimensions of crack that correspond to the known practical limitations on the strength of a brittle material may be obtained by considering glass. For a glass with a technical tensile strength of $150MN/m^2$ and a Young's modulus of $70GN/m^2$ the effective flaw length is found to be only 2 microns, if we take Griffith's value of about 0·5N/m for the surface energy. This value, for the effective crack length, can be compared with an equilibrium atomic spacing of around $2x10^{-4}$microns.

The range of application of Griffith's concept was extended significantly when it was realised by Irwin (1948) and Orowan (1948) that the occurrence of a limited amount of plastic deformation prior to fracture could be accommodated in Griffith's theory. Thus, if the crack extension is accompanied by plastic deformation in a small region near the crack tip, additional work is done which may be represented

by an additional pseudo surface energy p. Equation 2·6·5 now becomes

$$\sigma = \sqrt{\frac{2E(\gamma+p)}{\pi c}} \qquad (2\cdot6\cdot6)$$

This equation can be applied to crystaline materials that show some ductility before fracture. In such an application the effect of plastic deformation completely outweighs effects due to the creation of new surfaces. Thus, for a material such as low carbon steel (Hayden et al. 1965) p can have a value between 100 and 1000 N/m, which is one or two orders of magnitude greater than the solid state surface tension. For this material, the crack, effectively controlling fracture, is a few millimeters long compared with the few microns for an amorphous material.

It seems possible that Griffith's approach can be applied to a wide range of situations if the total work done in propagating the critical flaw is included in the analysis. The results of the analysis typically emerge in the form of equation 2·6·3, in which the term du/dc represents the rate of release of strain energy, G and failure occurs when this quantity reaches a critical value G_c. Irwin (1948) calls this quantity the critical strain energy release rate and, if a limited amount of plastic deformation occurs, it has the value $4(\gamma+p)$ for an isolated crack in an infinite plate. Irwin extended the application of these ideas by noting that the stress field, in the elastic region outside the plastic domain at the tip of a crack, could be expressed in terms of a single stress intensity factor K which is a

function of the stress, the crack length and the mode of crack propagation. As the material is linear, the effects of different stress combinations can be found by adding together the separate stress intensity factors, for each load, to give a total value for K. Irwin shows that

$$G = \frac{du}{dc} = \frac{K^2}{E} \qquad (2\cdot6\cdot7)$$

so that instability occurs for

$$K^2 = EG_c \qquad (2\cdot6\cdot8)$$

As only one mode of crack propagation is considered, the critical strain energy release rate G_c can be regarded as a material property relevant to that form of behaviour. Alternatively, one can consider a critical stress intensity factor K_c for which instability occurs, where

$$K_c = EG_c. \qquad (2\cdot6\cdot9)$$

Further developments in fracture mechanics have followed from this concept. Values of stress intensity factor K has been determined by analysis for many situations that are used in testing, so that test results can be interpreted in terms of a critical value K_c for use in design (Wells 1969). More recently, attention has been drawn to the problem of fracture that occurs after general plastic deformation. Again fracture occurs as a form of instability, but the linear theory is inappropriate and alternative methods have to be used (Wells 1966 and 1967) and alternative modes of failure investigated (McClintock 1968).

2·7 Applications to Concrete

Kaplan (1961) was the first to attempt to measure a value of G_c for concrete. He considered an imperfection in the form of a 30° notch in a plain concrete beam loaded in flexure. Tests of this sort are difficult to perform and interpret and so Kaplan used two methods to find G_c.

In the first method, the strain energy release rate is found experimentally from load deflection measurements on a series of beams with different depth notches. In each test, the relation between the applied load P and the displacement δ, under the load, was found. For moderate loads this is almost linear so that $P = \delta/\lambda$ where λ is the compliance for the particular beam tested. For linear elastic behaviour, the work done in loading the beam is $P\delta/2$ which must equal the strain energy stored in the beam. Thus $u = P^2\lambda/2$ and the strain energy release rate

$$G = \frac{du}{dc} = \frac{P^2}{2}\left(\frac{\partial\lambda}{\partial c}\right) \qquad (2\cdot7\cdot1)$$

where c is the depth of the notch. The values of $\frac{\partial\lambda}{\partial c}$, for notches of different depths, can be found from the combined results of the whole series of tests and G_c follows from the known values of the load at failure. This method was first suggested by Irwin and Kies (1952) and has since been used as the basis for determining stress intensity factors numerically using the finite element method (Dixon and Pook 1969). In his other method, Kaplan used an approximate analytical solution for the strain energy release rate, to find G_c from the known notch depth and the measured

values of the failure load and elastic properties of the concrete.

The two methods gave values of G_c that differed by $\pm$ 20% with the sign of the error depending on whether centre point or third point loading was used. Three different mixes (a mortar, a limestone concrete and a gravel aggregate concrete) were used and the values of G_c were in the range 30·0 - 8·0 N/m for all methods of testing and analysis.

Following Kaplan (1961), a number of other workers+ have also obtained values of G_c, for concretes and mortars, which range from 42·0 - 3·5 N/m. The differences arise partly from the differences in the concretes used but also from the manner in which the results were interpreted in calculating G_c. Different procedures give widely differening results so that it is not possible to quote absolute values of G_c with any confidence. However, for any one method of test and analysis it appears that the critical strain energy release rate increases with an increase in the cement paste content of the concrete or a reduction in the water cement ratio (Welch and Haisman 1969). The difficulties of interpretation arise because of the heterogeneity of the material and the effects of slow crack propagation before instability occurs. Both the analytical approach used by Kaplan and Irwin's

+Footnote

Glucklich (1962 and 1965), Lott and Kesler (1964) and Welch and Haisman (1968, 1969) used notch bend tests similar to Kaplan (1961). Romualdi and Batson (1963) used a slit in a nominally uniform stress field.

compliance calibration method require the original crack to propagate as a single sharp crack without branching. However, it has been suggested (Kaplan 1961, Glucklich 1963) that the region in the vicinity of the crack tip must contain a multitude of micro-cracks. Thus it appears extremely doubtful that the description of crack propagation afforded by an assumed increase in the length of the original crack is sufficiently precise to be generally useful in a quantitative analysis.

In applying the equations of fracture mechanics to concrete it seems advisable to refer to the conditions for which Griffith's analysis is most appropriate (see section 2·6). Thus, for the approach to be successful, the crack considered should be large compared with the dimensions of the structure of the concrete. Also, if the approach is to be extended to include consideration of slow crack propagation, the region in which additional micro-cracking occurs must be small and local to the crack tip. Only in these circumstances is it likely that the effects of slow crack propagation can be included within the strain energy release rate for the crack opening mode, in the manner used in equation 2·6·6 to account for the effects of local plastic deformation.

In these terms, the experiments that have been conducted to date on notched beams are open to critisism. Consider for instance, a concrete having Young's modulus $35GN/m^2$, modulus of rupture, $4MN/m^2$ and a value of the critical strain energy release rate of around 18N/m. These values, which are reasonably typical, can be used to calculate an equivalent notch depth which corresponds to the size of

imperfection that is typically present in a plain beam - i.e. one in which no notch has been introduced for test purposes. Using equation 2·6·5 and putting $2\gamma = G_c$ (for the surface crack) we find the theoretical intrinsic notch depth is approximately 12·5mm. Although this is rather an artificial concept, the result does suggest that tests using notches having depths in the range 12 - 50mm, as is customary, are not likely to highlight effects due to stress concentration. Also, it is clear that the notch depths used in testing are not sufficiently different from the dimensions of the aggregate for an analytical result to be meaningful. This view was taken by Blakey and Beresford (1962) in discussing Kaplan's paper, in which he observed that the reduced load capacity of the beams could be calculated quite satisfactorily by ignoring the stress concentration effect and using simple bending theory for the beam with a reduced depth at the notch. This is evident from the data in Table 2-1, which gives the values of the nominal tensile stress, at the tip of the notch, calculated from Kaplan's results using simple bending theory. Note that the values are approximately constant for any one mix and method of testing and that there is no definite trend with notch depth.

Wright and Byrne (1964) and Evans and Marathe (1967) have studied the effects of stress concentration in concrete by casting holes of different sizes and shapes in tensile specimens. Although the load capacity was reduced by the presence of holes, the tensile strength calculated on the basis of the reduced cross section was relatively unaffected. Evans and Marathe concluded that it is almost impossible to

Table 2·1 Values of the stress at failure, at the tip of the notch of Kaplan's beams, ignoring any effect due to stress concentration

Size of Beam	Type of loading	Notch depth	Stress at Failure MN/m^2 Mix 1	Mix 2	Mix 3
3x4x16	Third point	0·5	4·41	5·19	4·14
		1·0	4·42	5·17	3·67
		1·5	4·68	5·38	4·02
3x4x16	Centre point	0·5	4·78	5·86	3·93
		1·0	4·64	5·82	3·77
		1·5	4·78	5·95	4·30
6x6x20	Third point	1·0	3·75	4·55	3·36
		2·0	3·74	4·95	3·49
		3·0	3·77	5·16	3·49
6x6x20	Centre point	1·0	4·27	5·52	3·43
		2·0	4·16	5·40	3·82
		3·0	4·31	5·23	3·70

Note: All linear dimensions are given in inches.

introduce artificial stress raisers that have a higher stress concentration factor than is already present in concrete by virtue of its heterogeneity. The maximum size of crack or hole used by Evans and Marathe was 25mm. Clearly concrete cannot be regarded as notch sensitive for imperfections of this size and the fracture mechanics approach is not required unless the structural feature, giving rise to a region of high stress concentration, is of a much greater size.

Both Glucklich (1963) and Kaplan (1965) have implied that the existance of micro-cracks in concrete before loading, and the propagation of micro-cracks under load, is sufficient evidence to suggest that the fracture mechanics approach will be useful in studying the strength of concrete itself, in addition to those applications concerned with the effects of abnormally large imperfections on the stability of the material. This seems reasonable when it is recognised that Griffith's approach, using the energy principle, is in fact a procedure for establishing a condition for the material to be in equilibrium in a particular configuration and that this concept must have a universal application. However, the details of the analysis, for a heterogeneous material, are not straightforward as it is difficult to define the stress field in the vicinity of an imperfection. Also, if the heterogeneity is such that there is slow crack propagation before the occurrence of instability, an analysis based on the stability of the material around a single crack is no longer relevant. Both these difficulties exist, but at different dimensional levels, in cement paste, mortars and and concretes. In addition, these materials have a random

structure with individual elements having dimensions that are comparable to those of a theoretical Griffith's crack, calculated for an assumed continuum on the basis of the known technological properties. Further difficulties arise when the structural behaviour can no longer be regarded as brittle. If extensive cracking occurs before failure, the situation is similar to that in some metals that can sustain general plastic deformation before fracture. With concrete, this situation coincides with the appearance of a decending branch of the stress-strain curve. This is in direct contrast to ideal brittle behaviour in which fracture occurs at, or near, the peak stress. These difficulties are such that it is felt that an alternative approach must be developed to deal directly with the effects of heterogeneity in materials such as concrete. This work is still in an early stage of development and will therefore be discussed in outline only. Fuller accounts are available in the published papers.

2·8 A mathematical model for progressive fracture

(Dougill 1967, 1969 and 1971)

In order to avoid the difficulty of specifying the geometry of the micro-structure, Dougill (1967) suggested that heterogeneity could be described in terms of the variation of the stresses in the material considered at the micro-level. In proposing a model for material behaviour under a uniaxial tensile stress σ, it was assumed that the distribution of micro-stress ζ, acting on a plane at right angles to the direction of σ, is as shown in figure 2-8. This is a normal distribution with mean $m\sigma$ and standard deviation $\alpha\sigma$, which is truncated at $\zeta = q_t$ and has a

discontinuity at $\xi = 0$. The cut off follows from the assumption that no micro-element can sustain a stress greater than the intrinsic strength q_t of the material. In this way, the shaded region of figure 2-8 represents the proportion of material fractured under the stress σ and this also corresponds to the discontinuity, at $\xi = 0$, representing the proportion of material carrying a micro-stress having a value of precisely zero. The parameter m can be regarded as a measure of the extent of the stress redistribution that accompanies progressive fracture, whilst the quantity α is a property of the model material that describes heterogeneity through its effect on the micro-stress distribution. In a homogeneous material, α would be zero and the stresses in all the micro-elements would be the same. On the other hand, in a heterogeneous material, the micro-stresses will vary about the mean and this variation is described, in broad terms by using the appropriate value of α.

The analysis for the behaviour of the model material is undertaken in two stages. In the first (Dougill 1967 and 1969) the conditions for equilibrium are used to obtain a relationship between the applied stress and the proportion of material fractured. In the second stage (Dougill 1971), an assessment is made of the energy dissipated in fracturing the material and this leads to conclusions regarding the form of the stress-strain curve.

The results of the equilibrium analysis are shown in figure 2-9. If the heterogeneity parameter α can be considered to be unaffected by stress or damage, these curves represent the behaviour, during progressive fracture, of

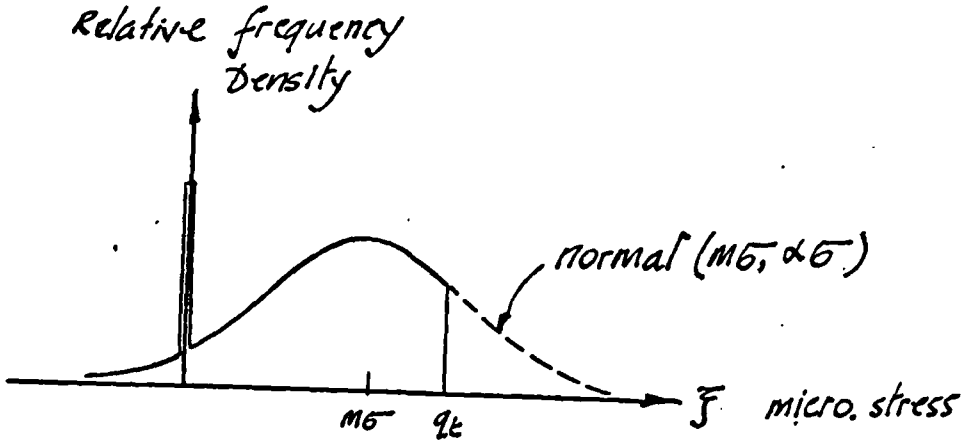


Figure 2-8 ASSUMED DISTRIBUTION OF MICRO-STRES DURING PROPAGATION OF BRITTLE FAILURE

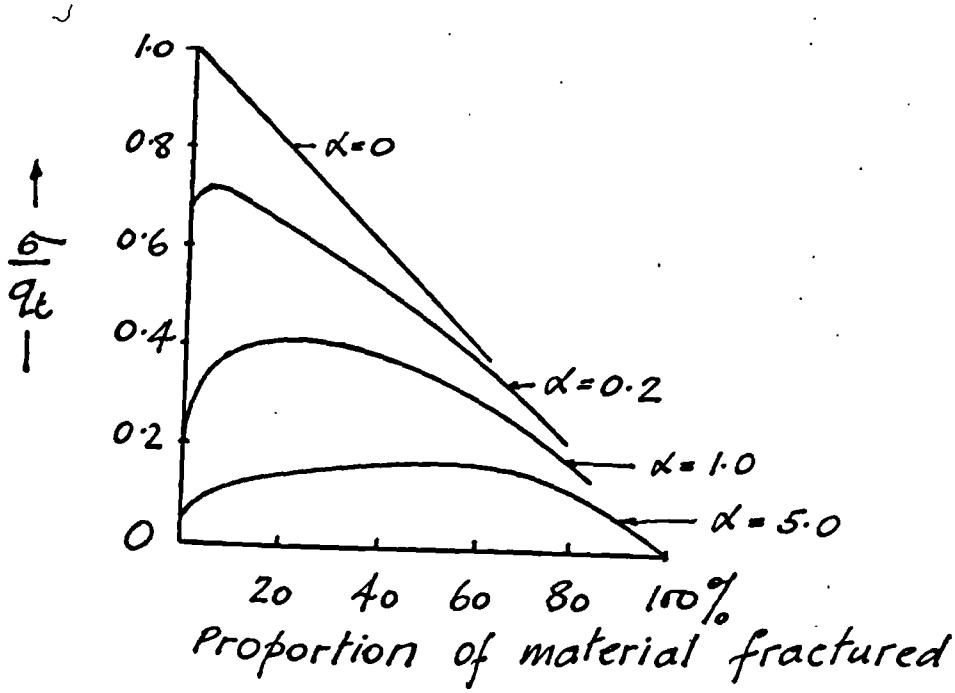


Figure 2-9 PROGRESSIVE FAILURE IN UNIAXIAL TENSION FOR THE MATHEMATICAL MODEL

materials of differing heterogeneity. For a monotonic increase in the proportion of material fractured, the applied stress increases to a maximum value before decreasing to become zero, when the entire section is fractured. A material of this type fails in a load controlled test when the applied stress reaches the peak value and observation of behaviour beyond this point is only possible if the applied load can be relaxed during the continuing process of failure. It is considered that this type of behaviour is similar to that observed with mortars and concretes in tension (see Hughes and Chapman 1966 for example)

The analysis is extended to provide results for the deformations by considering the manner in which the work done on the material is shared between the processes of deformation and fracture. In order to produce an increment of strain $\delta\varepsilon$, energy must be supplied to the material. This energy is equivalent to the work done by the applied loads, which is equal to the sum of the strain energy δu and the energy dissipated δD during the increment of deformation. Thus, the strain can be found by integration of the equation

$$\sigma d\varepsilon = d(u+D), \qquad (2\cdot8\cdot1)$$

which is written for unit volume of material.

In considering the strain energy u, it is assumed that each element of material is linear elastic with Young's modulus E and that only the component of micro-stress contributes to the strain energy. The dissipated energy is taken to be directly proportional to the amount of material fractured F, so that the energy dissipated per unit volume

is given by

$$D = \lambda F, \qquad (2\cdot8\cdot2)$$

The constant λ can be regarded as the product of the surface energy of the material and the number of separate fracture planes that occur in unit length of the model material measured in the direction of loading. In a real material, these separate fracture planes would occur at structural discontinuities or flaws. Thus, λ is dependent on the cohesive strength of the material and the flaw density.

By using the results of the equilibrium analysis, the strain energy u can be expressed as a function of α, E and F, the proportion of material fractured. Thus, equation 2·8·1 can be rewritten, to provide an expression for the strain ε, in the form

$$\varepsilon = \int_0^F \frac{1}{\sigma} \frac{d}{dF} (u + D)\, dF. \qquad (2\cdot8\cdot3)$$

The results are conveniently expressed as relations between the non-dimensional stress σ/q_t and a normalised strain $E\varepsilon/q_t$, for different values of α and a non-dimensional parameter $\lambda E/q_t^2$. Some results of this sort are shown in figure 2-10, for a material with $\alpha = 1\cdot0$. The results for the two highest values of $\lambda E/q_t^2$ follow the expected pattern, for strain controlled tests, in which the stress reaches a maximum value and is then reduced with continued deformation. The difference between these two curves reflects the greater toughness of the material having the higher value of $\lambda E/q_t^2$.

The third curve in figure 2-10, drawn for $\lambda E/q_t^2 = 0{\cdot}15$, is of particular interest. With this material, a stage is reached, under reducing stress, where no additional energy need be supplied in order to propagate failure throughout the material. At this point, the strain energy stored in the material is sufficient to fracture all the material that remains undamaged. If more strain energy is available than is necessary for complete fracture, much of the excess will be dissipated as kinetic energy and the process of failure will be violent. Thus, it appears that instability is possible even under conditions of monotonically increasing strain. It is of interest that failures of this kind have apparently been observed by Wawersik (1968) in compression tests on rock samples.

It is clear from figure 2-10 that instability occurs under conditions of controlled deformation if the gradient of the decending branch of the stress-strain curve becomes infinite. It may be shown (Dougill 1971) that this is equivalent to the condition that the material is unstable for

$$\lambda \leqslant -\frac{du}{dF} \qquad (2{\cdot}8{\cdot}4)$$

In this condition, the term $-\frac{du}{dF}$ represents the rate of release of strain energy per unit volume of material so that the quantity λ is seen to have a similar significance as G_c, the critical strain energy release rate of fracture mechanics. However, there is a fundamental difference between these quantities which occurs because Dougill's analysis is concerned with the variations in microstress

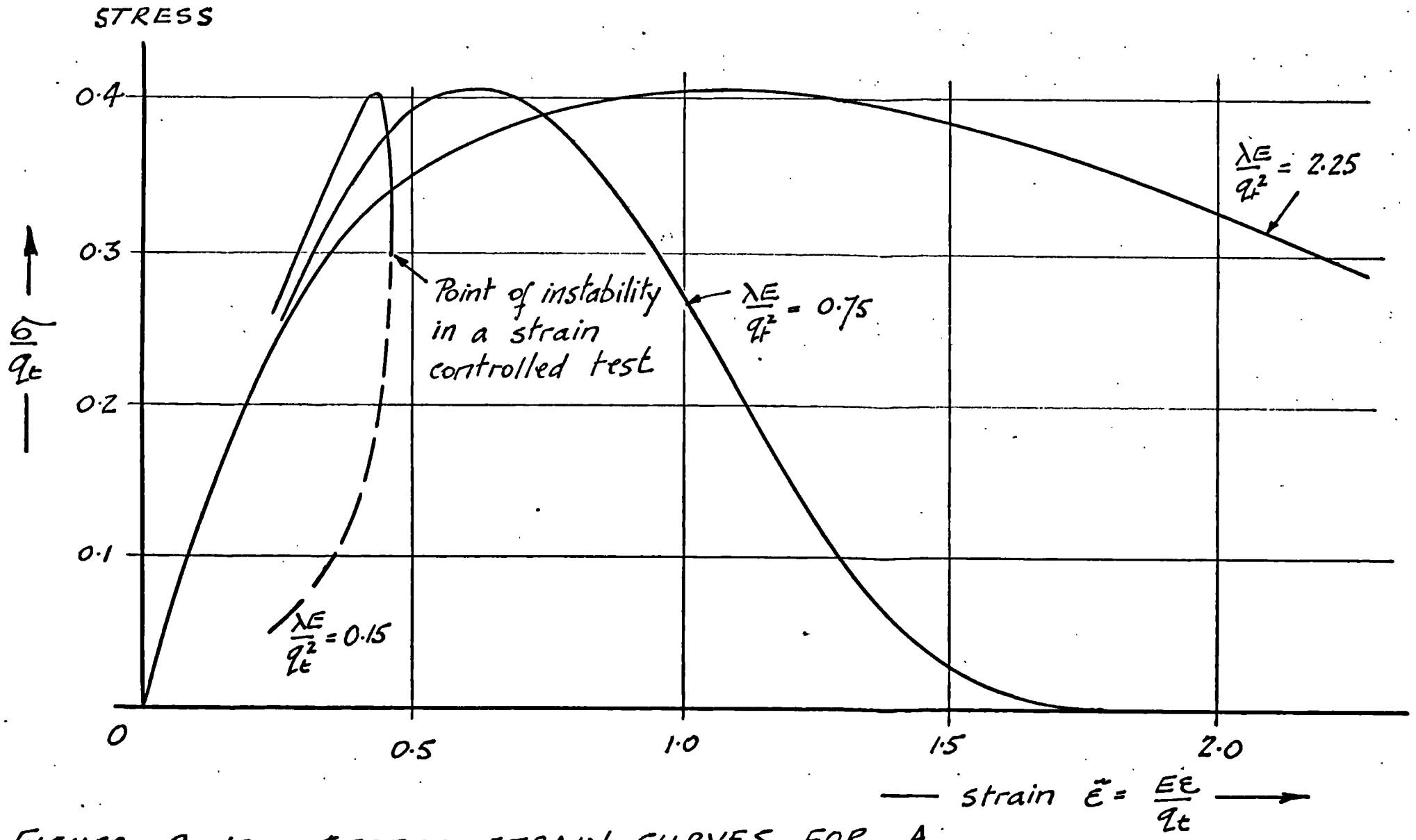


Figure 2-10 STRESS-STRAIN CURVES FOR A MATERIAL WITH $\alpha = 1$, IN TENSION, FOR VARIOUS VALUES $\frac{\lambda E}{q_t^2}$

that occur throughout a heterogeneous material rather than with effects that are local to a single abnormally large imperfection. This difference of approach is emphasised by the differing dimensions of λ and G_c.

Further analysis shows that instability can not occur under controlled strain conditions if $\lambda E/q_t^2$ is greater than 1/2. For lower values of λ, instability will occur somewhere in the decending branch of the stress-strain curve. In practical terms, the conditions for controlled deformation amount to those for the testing machine to be infinitely stiff ($K = \infty$ in section 2·3). In the more general case, in which the testing machine has finite stiffness, the rate of release of strain energy from the specimens will be augmented by that from the testing machine and instability will occur at a higher stress nearer to the peak value. Thus, in the general case, the conditions for failure can not be obtained by considering the behaviour of an isolated sample, but depend on the behaviour of the entire system. This is clearly a feature of the model material which it has in common with mortars and concretes. On the other hand, instability occurs very near to the peak stress for low values of λ and such a material behaves in a brittle manner, almost irrespective of the manner of loading. It seems probable that cement paste is such an intrinsically brittle material and, on this basis, it seems possible that the mathematical model may provide a single method of description for the whole family of materials that can be referred to as cement paste, mortar or concrete. At present this description can only be attempted in qualitative terms. However, even in this form (see Table 2·2) the results are interesting and suggestive.

Table 2·2 Qualitative view of the description of concrete systems afforded by the mathematical model.

Cement paste	Mortar	Concrete
← heterogeneity α →		
← peak tensile stress —		
— Flaw density, and toughness →		
← Likelihood of instability under similar test conditions —		

Note: the materials are assumed to have the same intrinsic strength q_t. The direction of the arrow indicates the manner in which a particular quantity increases within the range of materials described.

The model material is based on an assumption, concerning the manner in which redistribution of micro-stress occurs during progressive fracture, and a simplification, in which variations of the descriptive parameters throughout the body

of the material are ignored. These deficiencies in the theory imply that the model has the character of a mathematical idealisation which is used to define a range of ideal (and so possibly imaginary) materials. However, there are real materials that show qualitative agreement with the behaviour of the model and each of the controlling parameters has a definite physical meaning. This in itself suggests that further development of the model may be worthwhile. In particular, attention must be paid to behaviour under combined states of stress and to effects due to specimen size and stress gradient.

2·9 Size Effects

Size effects have already been the subject of much theoretical work as, besides being the starting point for fracture mechanics, Griffith's ideas stimulated development of statistical theories for the strength of brittle materials. These follow directly from the postulate that strength is determined by the nature of the flaws within the material. In general, no particular mechanism of fracture or form of imperfection is defined in a statistical theory and the term flaw can be applied to any local feature that affects the strength of the material. The most critical flaw is the one where fracture occurs first. In most theories it is assumed that the flaws are independent and that the material is ideally brittle so that the occurrence of fracture, at the most critical flaw, implies complete failure of a specimen irrespective of its size. Weakest link theories of this sort have been developed by Weibull (1939) and Frenkel and Kantorova (1943) (see Freudenthal 1950b) but the assumptions

used in these theories do not seem to be particularly suitable for concretes or mortars. Nevertheless, Weibull's theory forms the basis of some successful work to account for the effects of size on the flexural strength of concrete (Tucker 1941, Wright and Garwood 1952 and Nielsen 1954).

The purely statistical theories can provide no information on possible modes of failure, as there is no physical connection between the assumed flaw distribution and the mechanism of failure. Such a connection is included in the mathematical model described in the previous section but, as yet, this does not include statistical variables. However, it seems likely that the parameter λ, which depends on the flaw distribution, will vary throughout a large specimen indicating that the form of the stress-strain curve may be affected by size effects in addition to the peak stress. Clearly this type of phenomenon could not be investigated using the weakest link approach and it is interesting to note that such behaviour has already been recognised and studied, in qualitative terms, by Glucklich and Cohen (1967).

It seems that the problem of size effects in concrete and concrete structures has not yet been satisfactorily resolved. The available statistical theories are useful in correlating data obtained from different size test specimens. However, these theories are not sufficiently definitive from the physical standpoint for them to be used, with any confidence, to predict the performance of large mass concrete structures. Clearly there is the

possibility of a few very large cracks occurring in such structures. If the details of the cracks are known the fracture mechanics approach can be used to investigate the stability of the system. However, if the presence of the cracks is merely postulated for design purposes, the problem is a statistical one for which experience and data can not be obtained from tests on small specimens.

2·10 Comments on Criteria for Failure.

In the design or analysis of concrete structures it is necessary to have an appreciation of the conditions that correspond to the occurrence of failure. Because the objectives of design and analysis are essentially different, different concepts of failure are required for each of these processes. In design, we attempt to ensure the continued utility of a structure, that may be subject to any or all of a number of possible applied loadings, by a suitable arrangement of structural form and materials. On the other hand, analysis is the process by which the complete behaviour of an already defined structure is assessed for a particular history of loading.

Analysis may be complementary to design or may be used as a means of investigating the occurrence of a particular phenomenon, such as structural collapse. In these applications, criteria for failure provide the means by which the appearance of the phenomenon under examination is recognised in analytical terms. Thus, criteria for failure provide a link between the analytical model and physical phenomena. In Griffith's analysis, for example, the physical phenomenon is a sudden catastrophic disintegration of a sample of a brittle material. This

is recognised in the analysis as a mode of structural instability and the condition for instability is the criterion of failure.

In design the problem is rather more complicated and the criteria used become criteria for satisfactory performance rather than failure. Different criteria may be applied simultaneously to the structure as a whole, to individual elements of a structure or to small regions within a structural element. In this way the design of a building could be based on an allowable settlement for the structure as a whole, limits on the deflection and cracking of beams and slabs and permissible stresses in the materials used. With some structures, for which considerable experience of probable behaviour is available from the results of testing and analysis, this procedure can be improved. The proposed working load can be compared with the load that would be required to cause collapse of the structure. This leads to a direct indication of the available margin of strength in terms of a load factor. If this is considered adequate, the servicability of the structure at working load is assessed in terms of limiting deflections, cracking etc.

This approach, in which ultimate load theory is applied to design, can only be used for those structures whose behaviour, under all combinations of loading up to collapse, is relatively predictable. In general, an alternative approach is required for the major 'one-off' engineering structure as a full appreciation of possible structural behaviour and its implication is seldom available in these

exceptional cases. In this situation, it is customary to design structures to resist some loads without the occurrence of any significant damage. In addition, a design limit is put on the stresses that may be induced by any one of a number of prescribed abnormal loadings. In this way, servicability under working loads is coupled with a margin of safety against an occasional overload. This margin will not normally be known and, for this reason, the approach is inferior to the method based on Ultimate Load Theory.

Newman's (1964 and 1969 with Newman) concept of a discontinuity stress level is clearly relevant as a serviceability limit for working loads. Below this stress level, concrete may be considered to be a linear visco-elastic isotropic material (Hannant 1967), to a sufficient accuracy for design purposes, and the normal methods of analysis are available for checking a design. In addition, it is considered unlikely that a structure will collapse under an overload if the possibility of instability, accompanying the appearance of the decending portion of the stress-strain curve, is avoided. This is achieved by ensuring that the stresses under overload conditions are less than the peak values that would be obtained in a test under the relevant stress combination. Many tests have now been performed to obtain these values and the results can be represented by a surface, in principal stress space, giving the values of peak stress for any combination of principal stresses. Much effort has been devoted to deriving mathematical expressions to describe the form of this surface and these expressions are generally referred to as 'failure criteria'.

It is evident that the concept is useful but that the term is a misnomer. The early work in this field occurred as off shoots from main programs of research. In this way Richart et al (1928 and 1929) obtained a criterion for concrete strength in triaxial compression for use in the study of hooped columns. Similarly, Bresler and Pister's (1956 and 1957) criterion, for combined tensile and compressive stresses, was aimed at the problem of shear failure in beams. Also, Cowan (1952 and 1953) applied his criterion directly in his study of the effects of combined bending and torsion in beams. More recently, greater generality has been attempted in postulating failure criterion for use in the design of prestressed concrete pressure vessels. These include the criteria proposed by Rockenhauser (1968), Hannant and Frederick (1968), Brebbia and Frederick (1969) and Lewis and Carmichael (1969). It is clearly of interest to note how the occurrence of particular design problems has stimulated research in these directions.

2·11 The Present Problem

The present work is concerned with spalling. The objective is to examine the causes of spalling. In the broad sense, the approach must be analytical and any criteria adopted in this work are required in order to recognise the occurrence of spalling rather than to postulate conditions for satisfactory performance. In general, it appears that brittle catastrophic failure of materials can be regarded as a form of structural instability that may be influenced by local conditions or the entire structural system. Arguments have been presented to suggest that Griffith's

approach is unlikely to be satisfactory for concretes and that the conditions for stability should be obtained by considering the entire structural system. The most dangerous mode of spalling, general or destructive spalling (Table 1·3·1) is apparently a brittle catastrophic failure that occurs during fast heating. It is proposed to investigate the phenomenon by looking for the conditions of heating, loading and restraint that can cause structural instability in a member and so lead to violent failure. Before this can be done, additional information is required on the properties of concrete at high temperatures. These data are discussed in the next chapter.

Chapter 3

PROPERTIES OF CONCRETE AT ELEVATED TEMPERATURES.

3·1 Introduction

An analysis of structural behaviour during heating to high temperatures requires information on the thermal expansion and the relevant structural properties of concrete. In addition, the thermal properties that affect the rate of heat transmission within the concrete must be known. All these properties have been studied extensively during the last few years in connection with the analysis of prestressed concrete pressure vessels for nuclear reactors (Browne 1967, Tan 1968). The operating conditions in these structures are very different from those that obtain during a fire and attention has been focussed principally on behaviour over extended periods of time at only moderately elevated temperatures. (England and Ross 1962). Thus, many recent data concerning the behaviour of concrete at elevated temperatures have only limited relevance to fire conditions. However, besides these studies, there have been a number of investigations into the properties of concrete at the high temperatures that can be experienced in a fire. The results of this work are less complete than those for the lower temperature range and there are thus some uncertainties in applying the results in analysis. The areas of uncertainty will be made evident in the discussion that follows. The main aim, however, is to summaries information on concrete properties that may be useful in an analysis of behaviour under fire conditions.

3·2 Thermal Strains.

In dealing with thermal expansion, it is useful to consider separately the properties of hardened cement paste

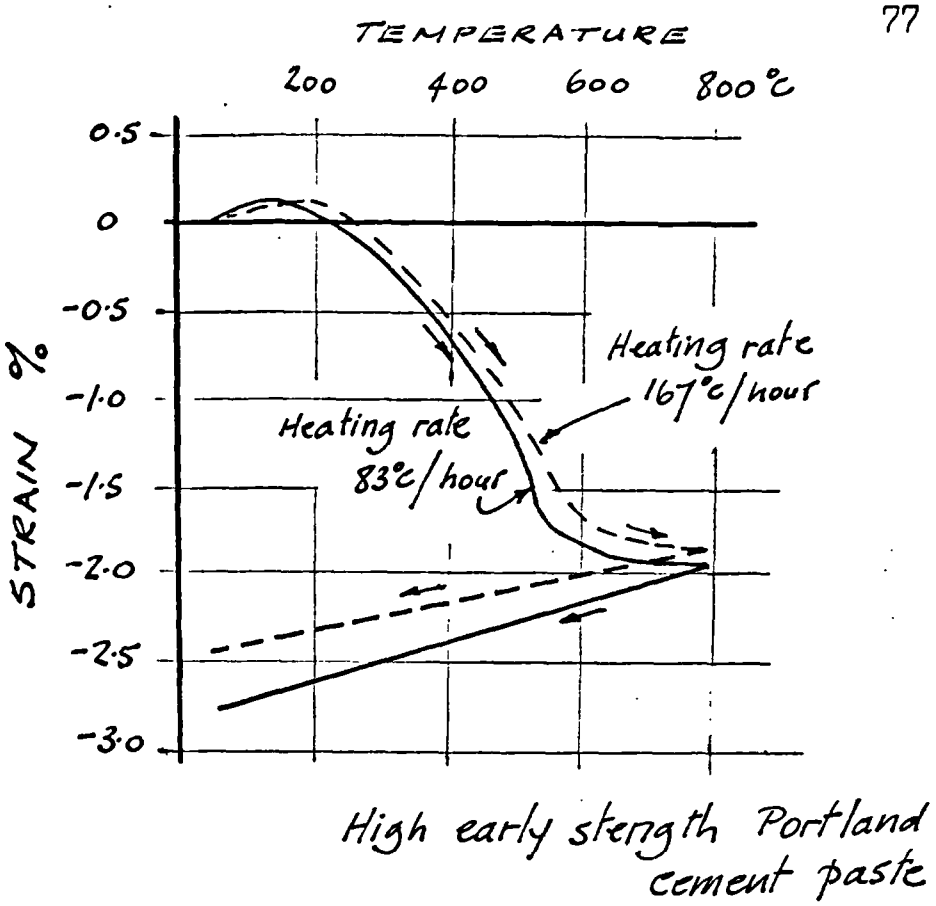
and the aggregate. This is because the thermal movements of these two materials can be taken to represent the two extremes of behaviour that can be obtained from a range of concretes of different composition.

Stradling (1920), Harada (1966) and Philleo (1958) have studied the thermal movement of ordinary Portland cement pastes. In these tests, the heating rate was either very slow (Philleo and Harada) or the specimen was maintained at constant temperature for sufficient time for the strain to become constant before a result was recorded. Dougill (1965[a]) and Marechal (1970) note that there are two main effects which contribute to the thermal movement of a cement paste. These are the thermal expansion of the solid phase of the paste structure and the shrinkage that accompanies desorption of moisture during heating. For a moderate rise in temperature, the shrinkage is small and the paste specimen shows a net expansion. At higher temperatures, the effect of shrinkage outweighs the effects of thermal expansion so that there is a net contraction of the specimens. Shrinkage continues with increasing temperature until all available moisture has been removed and the paste begins to expand once more. This behaviour is not reversible, as resorption does not occur during cooling from a high temperature. Thus, it is possible to consider the thermal movement of cement paste to be the sum of reversible and irreversible components which are respectively due to thermal expansion and moisture desorption. (Dougill 1965[a]).

Crowley (1956) measured the thermal movements of a

number of different cement pastes during heating with prescribed rates of temperature rise and subsequent cooling. The results, shown in figure 3-1 for an impure calcium aluminate paste and a high early strength Portland cement paste, illustrate the difference in behaviour during heating and cooling. These figures also show the effect of different rates of heating. Once past the initial stages, less shrinkage occurs at a particular temperature level for the faster rate of heating, so increasing the net expansion. This is to be expected in transient conditions, as desorption of moisture requires time and so lags behind the thermal expansion of the solid phase. This behaviour is similar to the time dependent deformations that Helmuth (1961) observed with thermal expansion at normal temperatures. He suggested that these were due to migration of water between the gel pores and the capillaries within the cement paste. Besides these effects, the thermal expansion at moderate temperatures is influenced by the relative vapour pressure within the cement paste. Thus, Mitchell (1953) has shown that, in the temperature range 0 - 20°C the coefficient of thermal expansion of oven-dried and saturated neat cement pastes are practically identical and that a higher coefficient is obtained at intermediate moisture contents. This increase is due to vapour pressure, which is absent from both the oven-dried and saturated specimens.

Many workers have measured the coefficients of thermal expansion of rocks at normal temperatures. At higher temperatures the problem is more complicated, as the coefficient cannot be taken as constant and may be



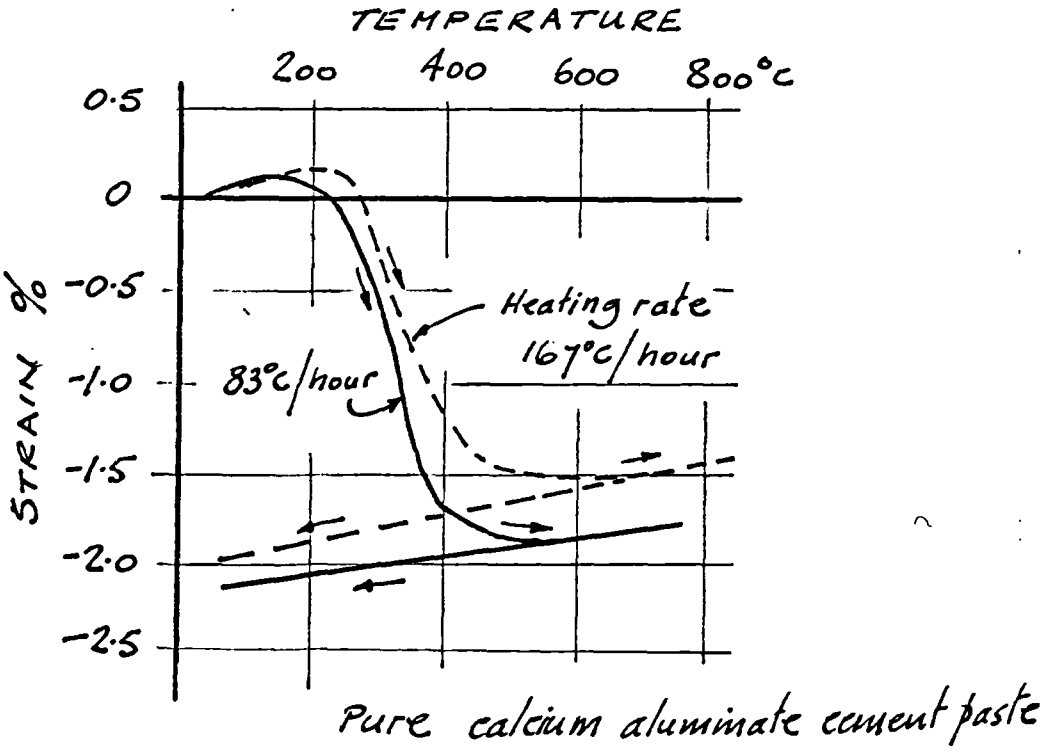


Figure 3-1 EFFECT OF HEATING RATE ON THE INITIAL THERMAL EXPANSION OF TWO CEMENT PASTES after CROWLEY 1956

influenced by phase changes or structural breakdown. In particular, aggregates made from crystalline rocks are liable to progressive disintegration at high temperatures because of thermal incompatibility within the aggregate itself. (Stradling and Brady 1927). The parent material is composed of a variety of closely packed minerals whose differences in thermal expansion can cause intercrystalline stresses and progressive failure. This process may be exacerbated by phase changes, in the constituent materials, especially if this is accompanied by a severe volume change.

In this country, many of the aggregates used are of a siliceous nature and contain a large proportion of quartz in their mineral composition. The expansion of quartz is complicated by a number of physical changes that take place at high temperature and are accompanied by volume change. These changes were studied by Fenner (1913) in his work on the stability of the silica minerals. Silica itself can exist as either quartz, tridymite or critobalite in the temperature range 0 - 1000°C and each of these three forms of silica has two allotropes, the α form occurring in nature. Fenner found the following transformations could occur during heating to high temperatures:-

α	Tridymite	⟶	β Tridymite	at 163°C
α	Cristobalite	⟶	β Cristobalite	at 220-275°C
α	Quartz	⟶	β Quartz	at 575°C
β	Quartz	⟶	β Tridymite	at 870°C
β	Tridymite	⟶	β Cristobalite	at 1470°C

The most important of the above changes is probably the α - β quartz transformation as this occurs at a temperature

that is easily achieved in fire conditions and is accompanied by a considerable increase in volume. Siliceous aggregates are notoriously unsatisfactory for use at high temperatures and the α - β quartz transformation is generally considered to have a marked influence on the behaviour of concrete exposed to high temperatures.

In contrast to siliceous aggregates, limestone neither changes its physical composition nor undergoes any sudden expansion during heating except at very high temperatures, when it is decomposed to form lime with the evolution of of carbon dioxide. This reaction is endothermic and so tends to retard the temperature rise in a concrete made with limestone aggregate that is exposed to fire. This extends the period of fire resistance, but deterioration is likely to occur on cooling when the free lime combines with atmospheric moisture to form calcium hydroxide (Ingberg 1929). This reaction is accompanied by an increase in volume which has a disruptive effect on the concrete.

Measurements of thermal expansion on samples of aggregate are not easy to perform because of difficulties in sample preparation. Some results were obtained by Endell (1929) for limestone and,more recently, Harada (1966) has measured the thermal expansion of a number of naturally occurring Japanese aggregates. These results, which are given in figure 3-2, are particularly interesting as Harada gives a brief description of the mineralogical composition of the aggregates. This information is summarised in Table 3·1. The aggregates A and B are both highly siliceous and show the expected rise in rate of expansion between 500 and 600°C.

Although aggregate G is also siliceous it has the lowest thermal expansion of all the rocks tested. This rock is volcanic however and it is most probable that the silica is present as tridymite (Blyth 1960), rather than quartz, and so remains stable up to 870°C. Note also that the limestone aggregate L has a high coefficient of exansion: this is not unusual.

Table 3-1 Description of Harada's (1966) Aggregates

Reference	From	Description
A	Midori River	Crushed fragments of hard sandstone, quartzite, metamorphic tuff etc.
B	Tama river	Crushed fragments of hard and soft sandstone and quartzite.
E	Shirakava	Dissociated product of pyroxene-andesite amphibolite, andesite.
F	Shimazki	Pyroxene-andesite containing about 80% plagioclase.
G	Mt. Asama	Siliceous volcanic rock: pumice.
L	Yatsushiro	Crushed limestone.

Harada (1953[a]) also measured the thermal expansion of concretes and mortars made with these aggregates. Some of the results he obtained using aggregates A, from the Midori river, are shown in figure 3-3. The thermal expansion of

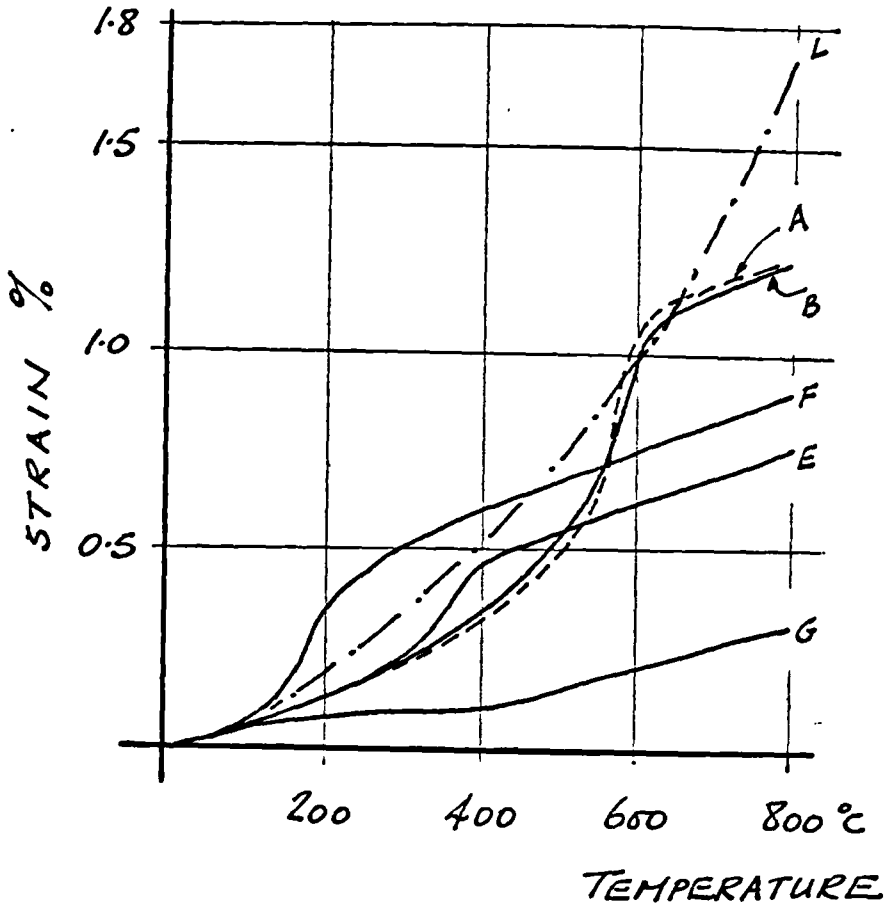


Figure 3-2 THERMAL EXPANSION OF A NUMBER OF JAPANESE ROCKS USED AS AGGREGATE IN CONCRETE after. HARADA 1953

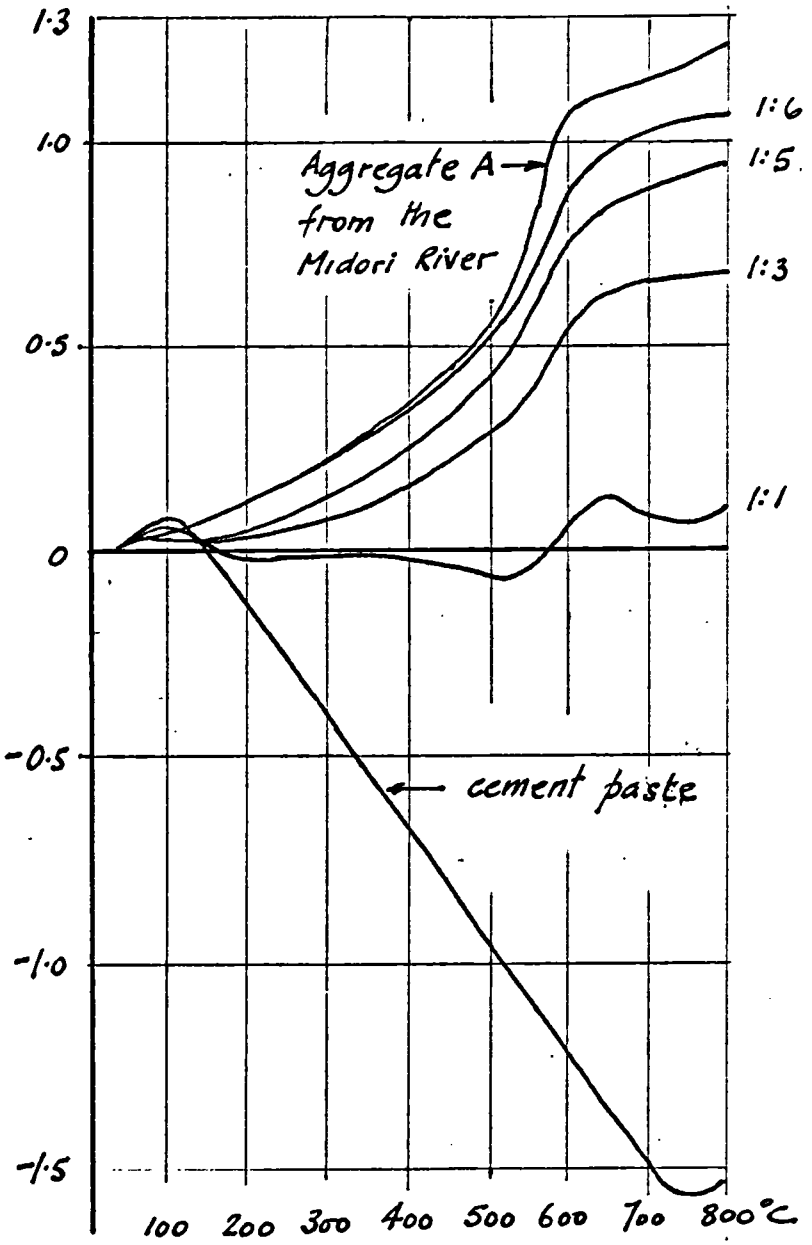


Figure 3-3 THERMAL EXPANSION OF VARIOUS CONCRETES MADE WITH THE SAME AGGREGATE after HARADA (1953[a])

the concrete is not much different from that of the aggregate itself. However, with smaller concentrations of aggregate the effect of shrinkage of the paste matrix becomes more significant so that the strains observed for the 1:1 mortar are quite small throughout the entire temperature range. Similar results are obtained with the other aggregates.

Figure 3-3 illustrates the composite nature of concrete, with the thermal expansion being bounded by the values for the two principal constituents and depending on their relative proportions. On this basis, it appears that a rise in temperature followed by cooling to the original temperature should cause a residual contraction in a concrete specimen, due to the shrinkage of the cement paste. This does occur, but only for concretes and mortars heated to moderate temperatures (typically less than 400°C). Cooling from higher temperatures leads to a residual expansion which is considered to be due to cracking within the paste or at the aggregate/paste interface (Marechal 1970). It is to be expected that this cracking will have some effect on the stiffness and strength, of concrete heated to high temperatures, as well as on thermal expansion.

3.3 Structural Properties.

A number of workers have attempted to measure the stress/strain curve for concrete, in compression, at high temperatures. In some of this work (Nekrassow 1961, Fischer 1970) strains were not recorded up to failure as the tests were designed primarily to obtain values of the initial tangent modulus of concrete. Harmathy and Berndt (1966) were interested in the condition at failure and took

measurements continuously during loading until the specimen collapsed at a strain not much greater than that corresponding to the peak stress. This may have occurred because the testing machine was 'soft' but was more probably attributable to the testing technique and an unsatisfactory method of specimen preparation+. In any case, it is almost certain that the full stress-strain curve was not obtained for the specimens tested. However information of this sort was obtained, in Japan, by Furumura working approximately concurrently with Harmathy and Berndt. The work was published in a series of three papers in Japanese and brief descriptions have subsequently appeared in English by Baldwin and North (1969) and Furumura himself (1970). This work appears to be of major importance.

Furumura (1966[a]) used cylindrical concrete specimens, of diameter 50mm and height 100mms, which he first heated and then maintained at temperature whilst the specimen was loaded in compression in a 1500kN universal testing machine. A heating rate of 60 - 90°C per hour was used to reach a particular test temperature, in the range 70°C- 700°C, which was held constant for a period of one to two hours before the start of heating. During loading, values of load and strain were recorded continuously by means of an X-Y plotter (Furumura (1966[b]). No details appear to be given of the strain rate used, but strain cycles were included in the test programme and it is possible that the loading test, at high temperatures, took an hour or more to perform.

Footnote +

Harmathy and Berndt noted that the ends of their specimens were not truly parallel. The specimens were not capped for the test and no ball seating was used in the testing machine.

In his first paper, Furumura presented extensive results for a low strength one year old concrete, made with a Japanese ordinary Portland cement and a siliceous river sand and gravel aggregate combined in the proportions 1:2:8:2:9 with a water cement ratio of 0·7. These results are shown in figure 3-4. It is clear from this figure that the general form of the stress-strain curve for concrete at normal temperatures (see figure 2-2 p.28) is unaltered at high temperatures, as postulated by Dougill (1966) in his study of the effects of restraint in columns. The results for the various temperature levels appear to differ only in scale and Baldwin and North (1969) have suggested that a useful generalisation of the results is obtained if the various stress-strain curves are normalised and expressed in the form,

$$\frac{\sigma}{\sigma_m} = f\left(\frac{\varepsilon}{\varepsilon_m}\right), \qquad (3\cdot3\cdot1)$$

where σ and ε represent stress and strain respectively and σ_m and ε_m are the particular values of stress and strain that correspond to the peak in the stress/strain curve. The quantities σ_m and ε_m are functions of temperature but Furumura's (1966[a]) results indicate that the suggested functional relationship (3·3·1) is relatively insensitive to temperature. Also, Baldwin and North found that a very reasonable fit to the combined experimental results is obtained with the expression:-

$$\frac{\sigma}{\sigma_m} = \frac{\varepsilon}{\varepsilon_m} e^{(1-\varepsilon/\varepsilon_m)} \qquad (3\cdot3\cdot2)$$

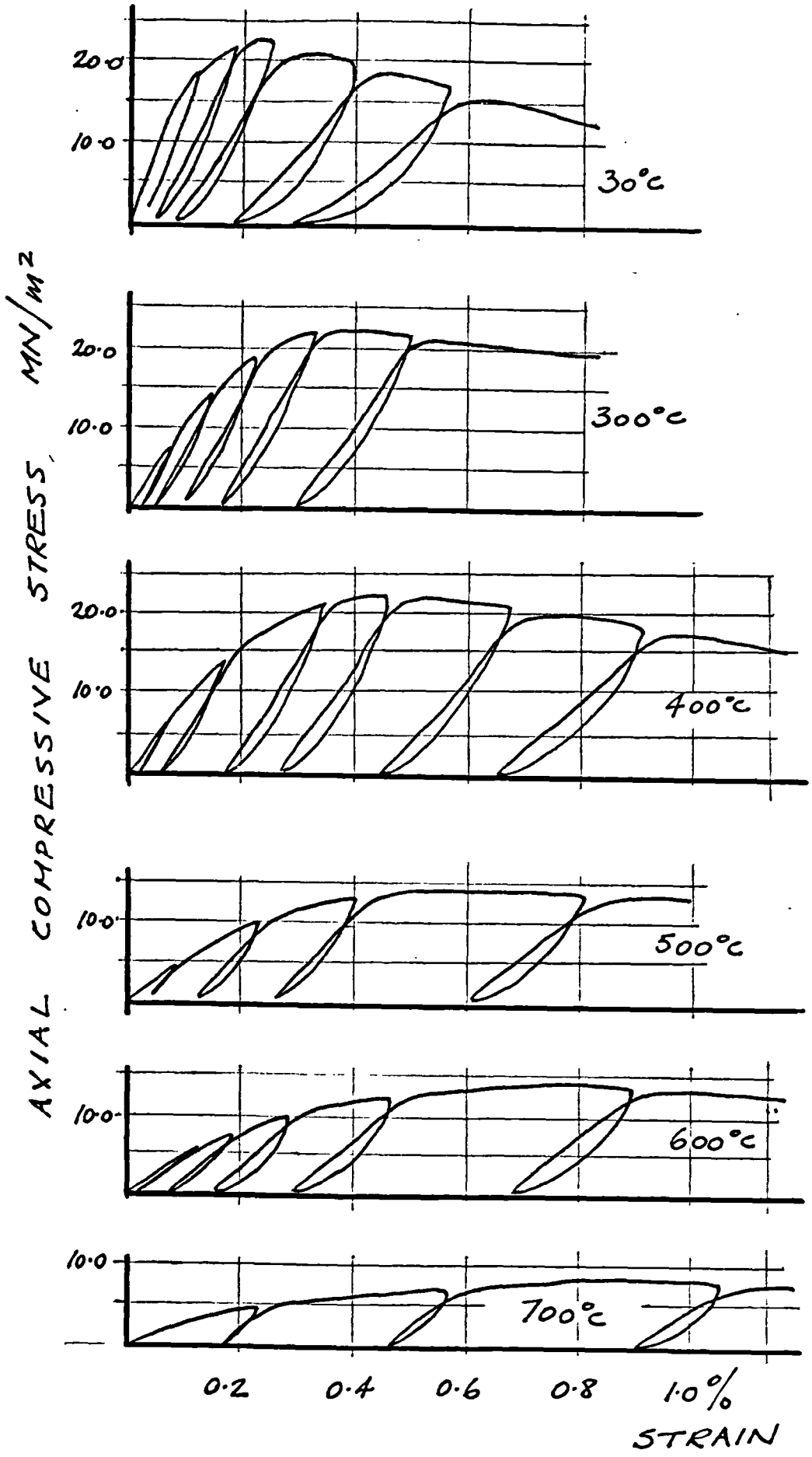


Figure 3-4 STRESS STRAIN CURVES FOR CONCRETE TESTED IN COMPRESSION AT HIGH TEMPERATURES after FURUMURA 1966[a]

A result of this form may not have universal application. Nevertheless, it is a compact description of observed behaviour which may be very useful in analysis.

Furumura's (1966[a]) choice of a very weak concrete for his test series helped to avoid any effect due to lack of stiffness in his testing machine. This may well have influenced the results of a later series of tests (Furumura 1966[c]) on a slightly richer and much stronger concrete made with similar materials and a water cement ratio of 0·45. However, the results from this second series of tests were of the same form as those shown in figure 3-4, for tests undertaken at temperatures greater than 300°C.

It appears that Furumura's results for the complete stress-strain curve of concrete in compression at high temperatures are the only available data of this kind. Before this, much work had been done to determine Young's modulus for heated concrete and the effects of heating on the peak stress, i.e. conventional strength, of concrete specimens. These data are still of considerable value, particularly if an equation of the form of 3·3·1 is found to be generally applicable.

3·4 Effects of heating on conventional strength, or peak stress, in compression.

Many different workers[+] have investigated the compressive strength of various concretes after heating to high temperatures and subsequent cooling and there is a fair measure of agreement on some aspects of this work. The results shown in figure 3-5, obtained by Grün and Beckman (1930), are typical of this work. In general the testing

+ see note at foot of page 89

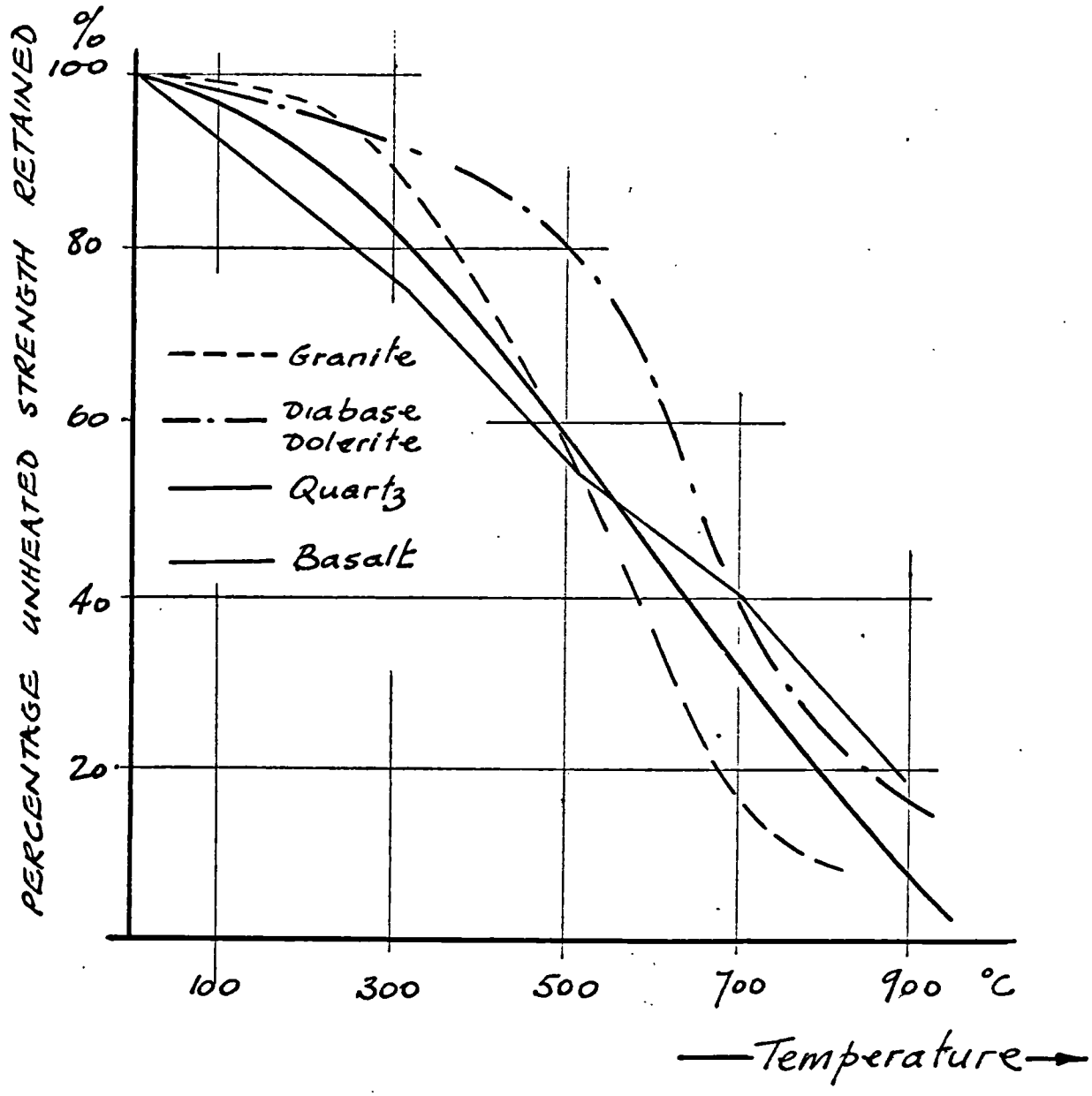


Figure 3-5 TEMPERATURE / STRENGTH RELATIONSHIPS FOR 1:3 O.P.C MORTARS MADE WITH VARIOUS AGGREGATES after GRÜN and BECKMAN 1930

procedure follows the following pattern. Mature concrete specimens are heated quite slowly to the selected temperature which is maintained for a period of hours. The specimens are then allowed to cool before being tested in compression.

There are considerable differences between the results from different workers for the temperature range up to 300°C. These variations appear to be caused by differences in the types of cement, curing conditions and specimen maturity at the time of test (Fischer 1970). In particular, it is clear that the hygral condition of the cement paste, within the concrete, is particularly important in this temperature range. As concrete is heated, moisture will be removed from the cement paste causing shrinkage of the gel and possibly an increase in strength due to an increase in the Van de Waal's forces. With further heating, a point is reached where removal of moisture causes some breakdown in the gel structure and consequential loss in strength. These variations in strength will be accompanied by dimensional changes in the paste that may induce an internal stress system in the concrete (Dougill 1965) or structural breakdown in the form of cracking. The load capacity of the

Footnote+

A bibliography would include Woolson (1905, 1906), Lea (1920), Lea and Stradling (1922), Miller and Faulkner (1927), Hirano (1927), Stradling and Brady (1927), Grün and Beckman (1930), Giles (1939), Harada (1953b and 1957), Watkeys (1955), Malhotra (1956), Saeman and Washa (1957), Protze (1957), Dougill (1960), Zoldners (1960), Weigler and Fischer (1964), Campbell-Allen et al (1965), Davis (1967), Campbell-Allen and Desai (1967), Abrams (1968) and Fischer (1970). The more important contributions are underlined.

entire specimen will be influenced by both the strength of the paste and the parasitic stresses and will therefore be very dependent on the moisture state of the specimen. There will also be an effect due to accelerated hydration in the less mature concretes. Clearly, depending on the moisture condition at the start of the test, a modest increase in temperature may cause either an increase or a decrease in load capacity. Both these effects have been observed.

The behaviour at temperatures greater than 300°C is rather more predictable. With a rise in temperature, there is an increase in the difference between the thermal movement of the concrete and those of the contituent materials (see figure 3-3). This strain incompatibility leads to internal stresses which are partially relieved by cracking at high temperatures. Thus, the connectivity of the concrete structure is progressively destroyed under increasing temperature and the corresponding reduction in strength reflects the increasing difference between the free thermal movements of the aggregate and the cement paste. Note also that the reduction in strength due to cracking is coupled with the influence of the internal stress system on the final load capacity. These effects of thermal incompatibility appear to have been first examined by Lea and Stradling (1922).

The residual strength of concrete depends on the conditions that obtain after cooling is complete as well as on the actual heat treatment. Thus a further reduction in strength after cooling has been observed for specimens

that have been maintained in a moist environment for a few days. Following Lea and Stradling (1922), Dougill (1961) suggested that this behaviour was due to swelling caused by reabsorption of moisture and his analysis indicated that this could eventually lead to a recovery of strength after the initial reduction. Such a recovery has been observed by Weigler and Fischer (1967), for specimens stored under water, and by Harada (1957) for specimens stored in a humid atmosphere. Harada's results are shown in figure 3-6. Although these recoveries are quite dramatic, they are still less than that obtained, by Crook and Murray (1970) for a pressed concrete block, by water immersion after heating to 620°C.

There is some disagreement on the effects of repeated cycles of heating to high temperature and subsequent cooling on the strength of concrete. Protze (1957), Davis (1967), Campbell-Allen and Desai (1967) all found that there was a reduction in strength with repeated heating and cooling but Dougill (1960) found that there was a lower temperature limit to this behaviour, for concrete made with Thames valley river gravel aggregate, and that no further reduction in strength occurred after the first cycle for temperatures below 400°C. This result is confirmed, to some extent, by Sullivan (1970)[+] who tested plain concrete beams in flexure at temperatures up to 400°C. Sullivan found that repeated

Footnote[+]

These tests were undertaken using the furnace and testing rig which was designed and constructed by the present author at Imperial College, London in the period 1961-1964.

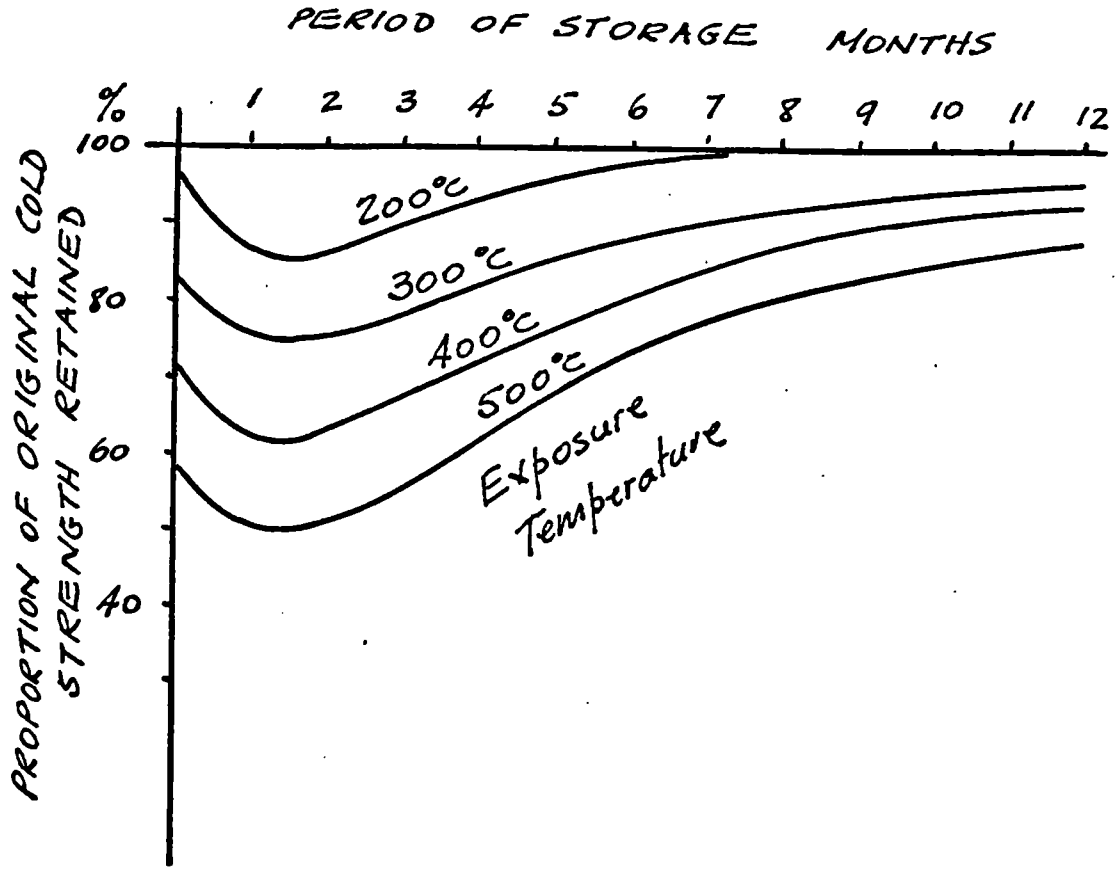


Figure 3-6 POST COOLING RECOVERY OF STRENGTH DURING COOLING IN HUMID CONDITION: after HARADA 1957

heating and cooling had no effect on the residual strength of his beams, provided that slow rates of heating and cooling were used and the load carried during heating was less than about half the breaking load at the temperature considered. It seems plausible that a lower temperature limit should exist and correspond to the temperature at which severe cracking is initiated on heating. Such a limit could be regarded as a 'temperature discontinuity' level for unrestrained concrete as this would have a similar significance to Newman's 'stress discontinuity' level for isothermal conditions.

This is fair agreement on the effects of mix proportions on strength after high temperature exposure. In an extensive series of tests on concrete made with river gravel aggregate, Malhotra (1956) found that variations in water cement ratio had a negligible effect on the proportional reduction in strength. On the other hand, variations in the aggregate/cement ratio were significant, the proportional reduction being smaller for lean mixes than rich ones. The type of cement used is also influential. Concrete made with Portland blast furnace cement retains a slightly greater proportion of its original strength than if ordinary Portland cement is used (Grün and Beckman (1930), Weigler and Fischer (1964). Also, concrete made with high alumina cement does not perform as well as an ordinary Portland cement concrete for temperatures below 650°C (Fire Research 1955). However, at higher temperatures, the behaviour of high alumina concrete.

heating and cooling had no effect on the residual strength of his beams, provided that slow rates of heating and cooling were used and the load carried during heating was less than about half the breaking load at the temperature considered. It seems plausible that a lower temperature limit should exist and correspond to the temperature at which severe cracking is initiated on heating. Such a limit could be regarded as a 'temperature discontinuity' level for unrestrained concrete as this would have a similar significance to Newman's 'stress discontinuity' level for isothermal conditions.

This is fair agreement on the effects of mix proportions on strength after high temperature exposure. In an extensive series of tests on concrete made with river gravel aggregate, Malhotra (1956) found that variations in water cement ratio had a negligible effect on the proportional reduction in strength. On the other hand, variations in the aggregate/cement ratio were significant, the proportional reduction being smaller for lean mixes than rich ones. The type of cement used is also influential. Concrete made with Portland blast furnace cement retains a slightly greater proportion of its original strength than if ordinary Portland cement is used (Grün and Beckman (1930), Weigler and Fischer (1964). Also, concrete made with high alumina cement does not perform as well as an ordinary Portland cement concrete for temperatures below 650°C (Fire Research 1955). However, at higher temperatures, the behaviour of high alumina concrete.

is superior, due to the development of a ceramic bond. (Protze 1957). Thus, high alumina cement is often employed in refractory concretes for use at temperatures around 1000°C.

So far, this discussion has dealt with the strength of concrete that has been obtained from specimens after they have been allowed to cool from high temperatures. Lea (1920), Malhotra (1956) and Abrams (1968) have shown that greater strengths are obtained if the specimens are tested hot and Dougill (1961) has suggested that this occurs because the difference in free thermal movements of the aggregate and the cement paste increases during cooling, so promoting further damage and loss in strength. Malhotra (1956) also showed that the load capacity of his specimens was further increased if they were maintained under load. This increase was appreciable, the total load capacity at 500°C being increased by about 20% when the specimens were heated under a stress of between 20 and 25% of the cold strength. Malhotra considered that the sustained load inhibited cracking during heating and so increased the total load capacity. This appears plausible when it is recognised that an overall uniaxial compressive stress induces a state of average triaxial compression in the matrix of a conventional concrete made with hard aggregate (Dougill 1970).

Following Malhotra, the effects of sustained load during heating were investigated further by Abrams (1968) and Fischer (1970). Abrams used sustained stresses of 25, 40 and 55% of the standard cylinder strength of the concrete, and tested concretes made with American Type I (i.e. ordinary Portland) cement and three different coarse aggregates,

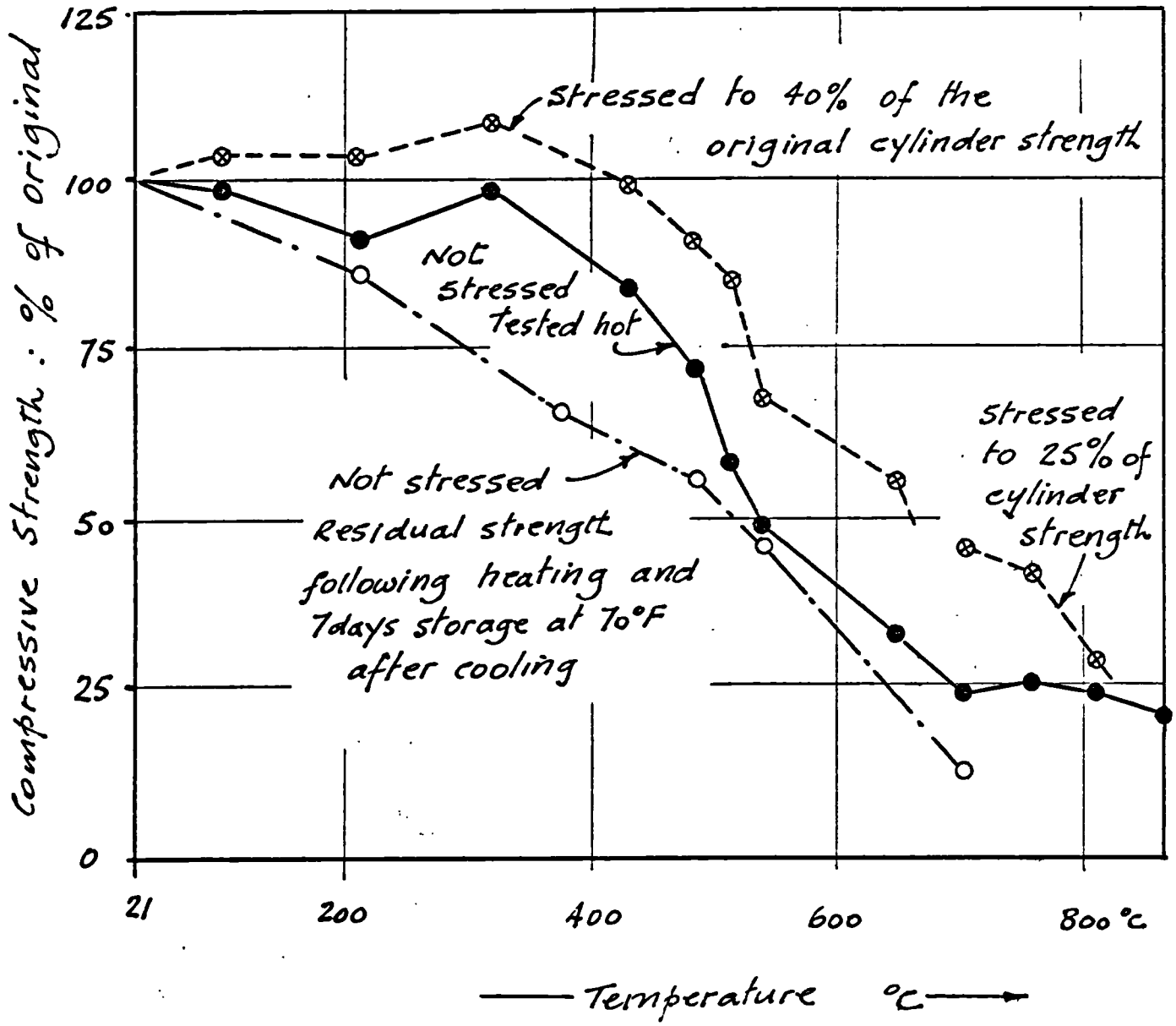


Figure 3.7 EFFECT OF TEMPERATURE ON THE COMPRESSIVE STRENGTH OF A SILICEOUS AGGREGATE CONCRETE after Abrams 1968

a siliceous gravel, a carbonate gravel and a lightweight expanded shale. A siliceous sand was used in each mix. There was no significant difference in the results of tests with the different levels of superimposed load but the presence of this load had a definite effect on the strength of the specimen. For the loaded carbonate aggregate concrete the hot strength was within $\pm$ 10% of the original cold strength for all temperatures up to 700°C. The results for the siliceous aggregate concrete are shown in figure 3-7. This gained strength on heating to 300°C and the strength was only reduced to its original value at around 400°C. At higher temperatures there was a relatively sharp drop in strength, which Abrams attributes to the α - β quartz transformation in the aggregate. The behaviour of the lightweight aggregate concrete was also interesting in that the superimposed load reduced the total load capacity for temperatures below 300°C but caused an increase at higher temperatures. This could be explained, on the basis of the average stresses in the mortar matrix, if the mortar was initially stiffer than the aggregate and this situation was reversed at high temperatures. This is quite likely, as an expanded shale experiences temperatures of around 1000°C, in a rotary kiln, during manufacture and so could be expected to have relatively stable high temperature properties.

3·5 Young's modulus for heated concrete.

Values of Young's modulus for concrete at high temperatures have been found by a number of different methods. Philleo (1958) measured the resonant frequency

of small concrete beams, Cruz (1962 and 1966) tested solid cylindrical specimens in torsion, Sullivan (1970) tested beams in flexure both at elevated temperatures and after cooling, and Harmathy and Berndt,(1966), Cruz (1968) Furumura (1970) and Weigler (1970) obtained their results from tests in compression. Other workers, including Harada (1954[a] and 1957), have measured Young's modulus after cooling. Harada also noted the occurrence of post cooling changes, including a partial recovery of stiffness during storage in a moist atmosphere.

The American results (Philleo and Cruz) are very similar and show sharp reduction in Young's modulus even for only a modest rise in temperature (see figure 3-8). There is general agreement that the proportional loss in stiffness at high temperatures tends to be greater than the proportional loss of strength. However, as with compressive strength, there are considerable differences between different workers results for temperatures below 300°C. Again these appear to arise from the variety of pre-conditioning procedures used prior to the test. Possibly more important than these, however, is the effect of a superimposed load during heating.

Fischer (1970) obtained the first part of the stress-strain curve, at high temperatures, for a quartz aggregate concrete made with ordinary Portland cement that had been subjected to stress during heating. Fischer found that heating to temperatures less than 450°C, with a superimposed load of one third the cold strength, had negligible effect on Young's modulus unless measurements were taken

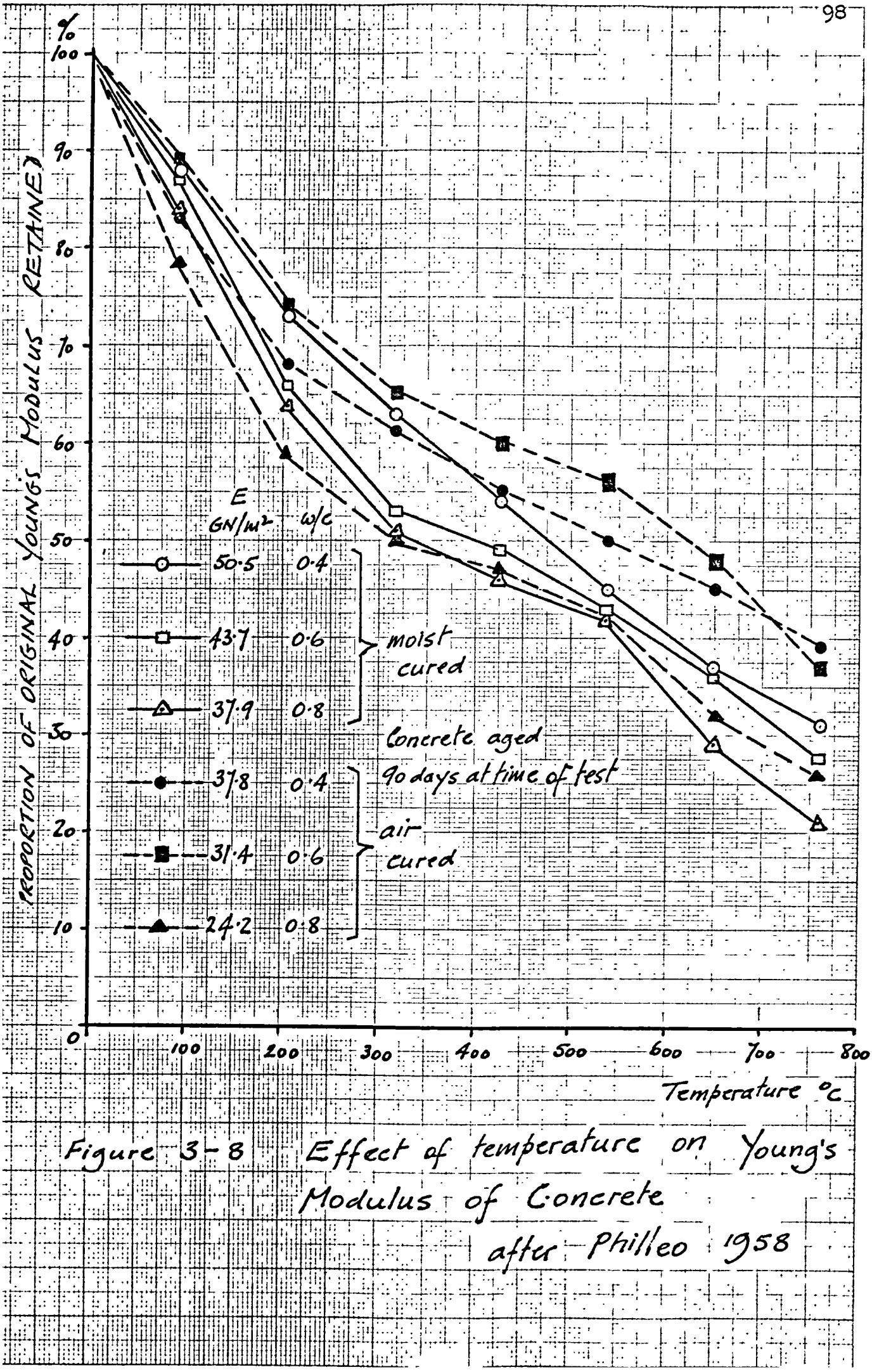


Figure 3-8 Effect of temperature on Young's Modulus of Concrete after Philleo 1958

after cooling, when some changes were observed. Significant reductions in modulus occurred at temperatures greater than 450°C. However, these reductions were much less than occurred without the load during heating; the loss in stiffness at 600°C being approximately halved by a superimposed load in the range 1/6 to 1/2 of the cold strength. Similar results were obtained with concretes using barytes aggregate and also blast-furnace Portland cement.

The observed effects of imposed load during heating on compressive strength and Young's modulus suggest that many of the available data concerning these quantities are not particularly relevant to fire conditions. The influence of load appears to be of major importance but this is neglected in most data. Also, besides ameliorating the effects of heat on stiffness and strength, an imposed load will cause additional strains, over a period of time, due to creep. It is known that creep is considerably accelerated by quite small rises in temperature above normal (England and Ross 1962) so that it is reasonable to suppose that creep could have very important effects at high temperatures.

3·6 Time dependent strains induced by loading - creep.

The effects of creep can be seen in the tests undertaken by Fischer (1970) in which the thermal movements of loaded concrete specimens were measured whilst the temperature was raised at a rate of 150°C/hour to 600°C and than reduced slowly back to normal. The concrete used was 7 months old and made with ordinary Portland cement, quartz sand and coarse aggregate combined in the proportions 1:1:5 with water cement ratio 0·6. The results of these tests are

shown in figure 3-9. The strains recorded represent the combined effects of thermal expansion, shrinkage and the strains due to stress including creep. The temperature was held steady at 600°C for 3 hours during which time the unloaded specimen continued to expand. The effects of creep can be seen in the way this expansion is inhibited or reversed in the specimens carrying load.

Cruz (1968) also measured the time dependent strains in concrete specimens maintained at high temperatures under load. A carbonate aggregate was used together with ordinary Portland cement and a water cement ratio of 0·56. The specimens were stored under water for 7 days and then in the laboratory air until they were tested, 28 days after casting when the compressive strength was about 28·3 MN/m^2. Each specimen was subjected to three cycles of loading to 12·5 MN/m^2, in order to determine an initial value of Young's modulus, and was then heated at about 330°C/hour to the required test temperature. This was maintained for an hour before the test load of 12·5 MN/m^2 was applied. No strains were measured during the period of heating and temperature stabilisation but strains were measured during loading in order to obtain a value of Young's modulus at the test temperature. Strains were then recorded for a period of five hours with the specimen in a steady state of temperature and load.

The results from Cruz's (1968) tests are shown in figure 3-10. The time dependent strains measured for the higher temperatures are very large compared with what

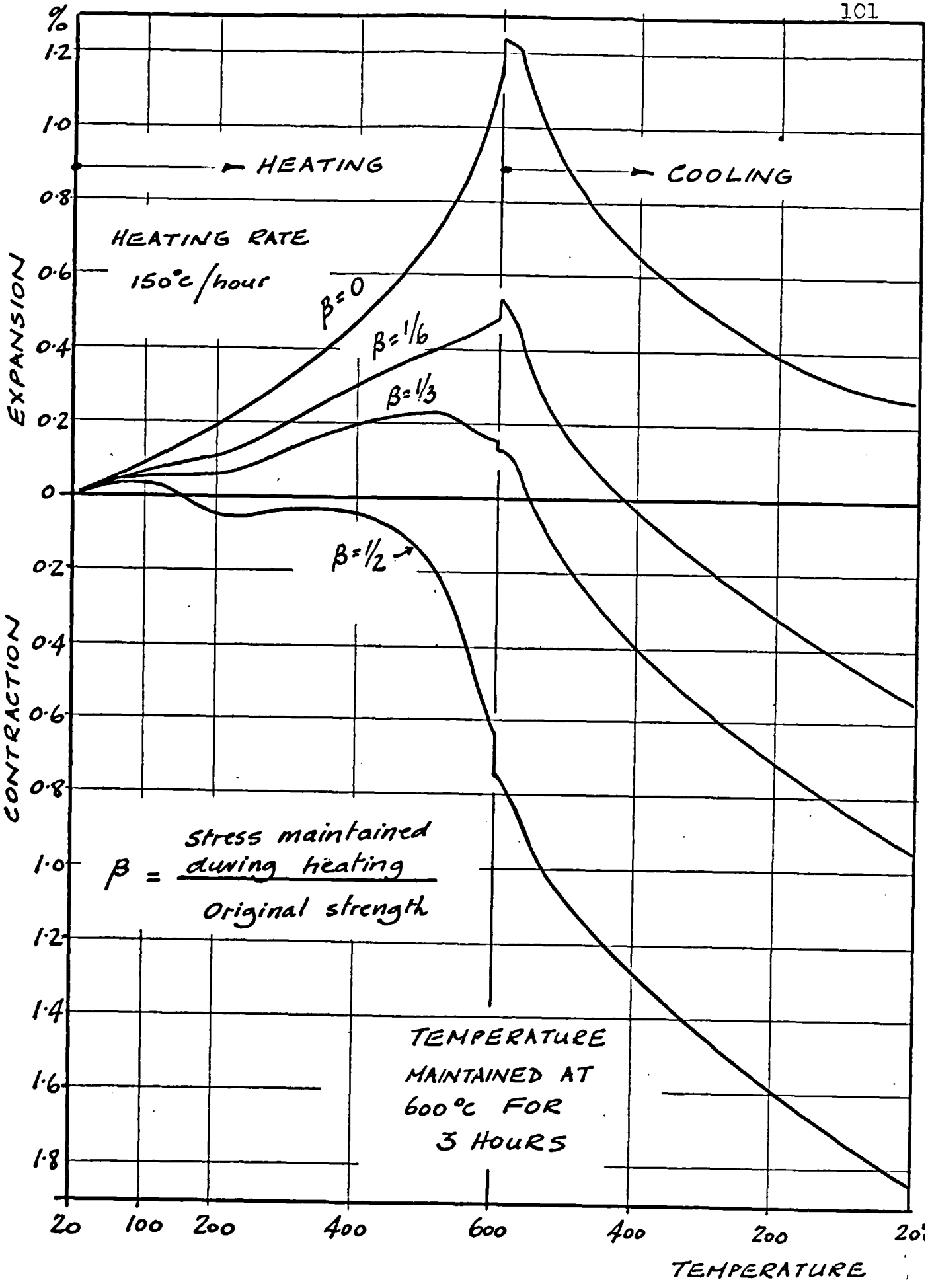


Figure 3-9 STRAINS MEASURED ON CONCRETE SPECIMENS HEATED AND COOLED UNDER LOAD after FISCHER 1970

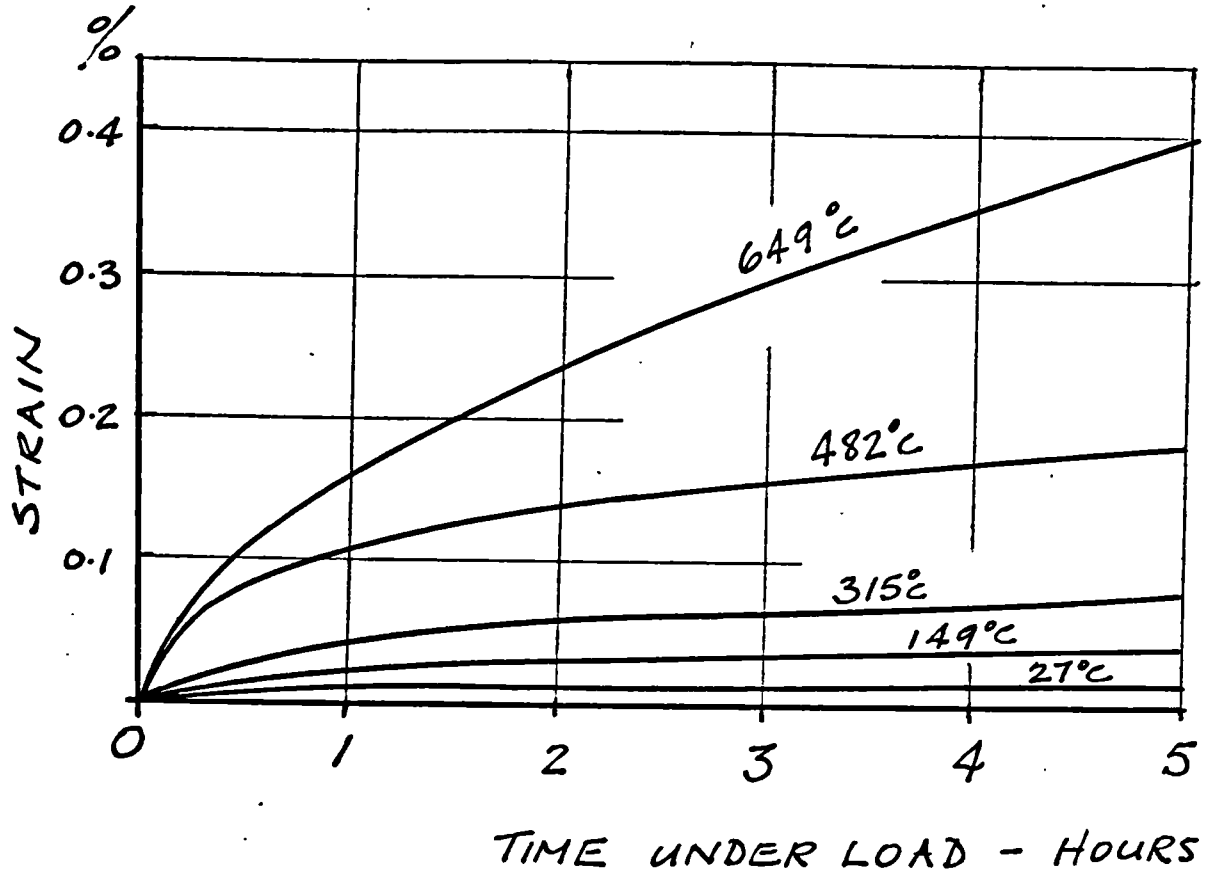


Figure 3-10 TIME DEPENDENT STRAINS IN CONCRETE MAINTAINED UNDER LOAD AT HIGH TEMPERATURES after CRUZ 1968
APPLIED STRESS 12·5 MN/M²

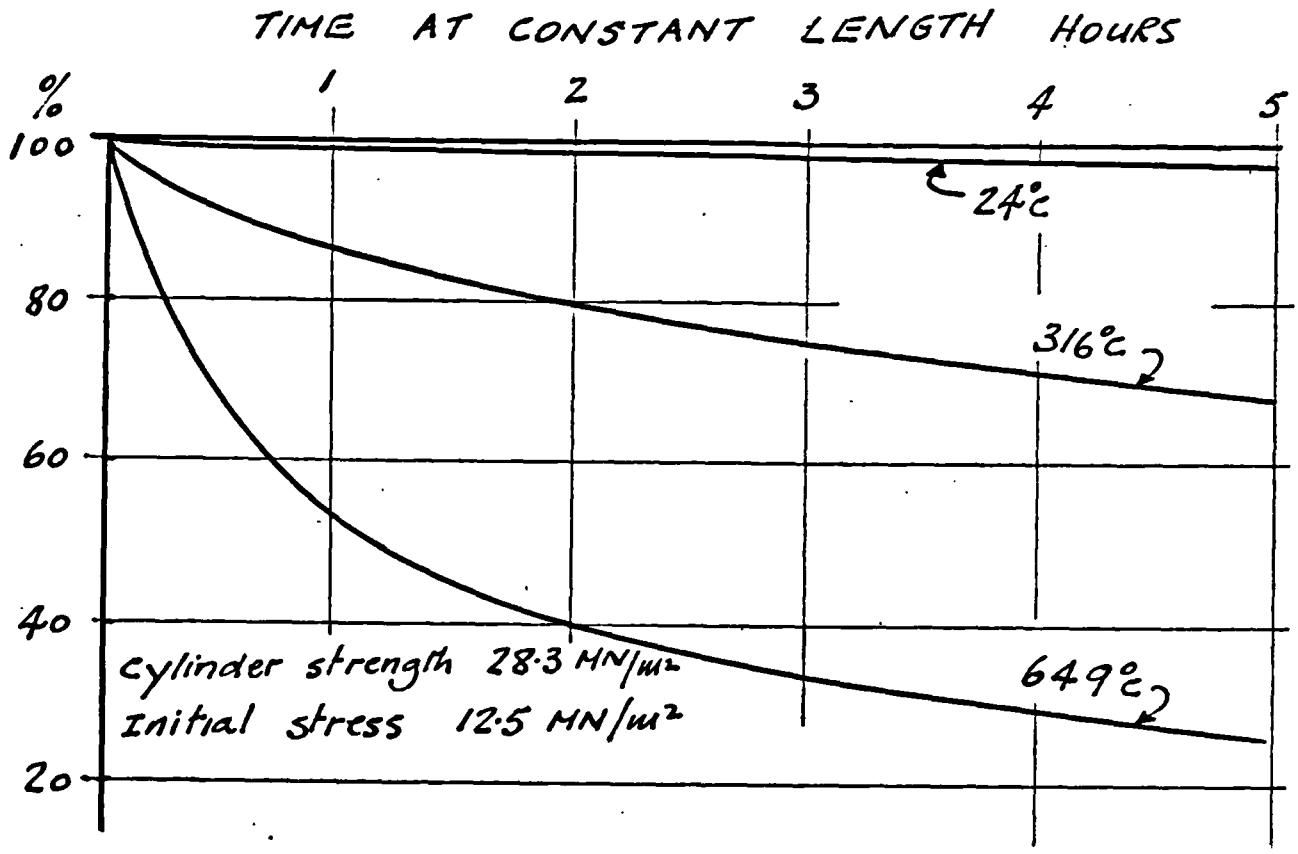


Figure 3-11 RELAXATION OF STRESS IN CONCRETE AT HIGH TEMPERATURES After CRUZ 1968

could reasonably be expected at normal temperatures[+]. Creep may increase the strains or cause relaxation of stress when deformation is restrained. Cruz also investigated this aspect in a series of relaxation tests, at high temperature, and the results indicate a very high rate of relaxation of initial stress at elevated temperatures (figure 3-11).

Sullivan (1970) also measured creep deflections in his tests on slender beams at temperatures up to 400°C. However, it is difficult to relate these results to fire conditions because of the extensive heat treatment and load cycling undertaken before the start of the creep test. A similar criticism can be made of Cruz's work and most other data discussed in this chapter. Clearly, some care is necessary in using the available experimental results in a study of fire induced phenomena.

3·7 Heat Transmission Properties - Introduction.

Although conditions in a fire change rapidly with time, the available data for structural properties and the thermal properties controlling heat transmission have generally been obtained under steady state conditions. For heat transmission within a concrete member the properties of interest are the specific heat c, the thermal conductivity λ and the thermal

Footnote [+]

The 'ultimate' specific creep for concrete at normal temperatures is around 150×10^{-6} per MN/m^2. Thus Cruz's specimens could be expected to achieve a strain of around 0·0015 after a year under load at normal temperatures.

diffusivity k. These quantities are related as $\lambda = k\rho c$ where ρ is the mass density. It is useful to note the dimensions and units of these quantities for easy reference. This is done in Table 3·2, which also gives typical values for the quantities under normal conditions. However, and in spite of using the word typical, it must be noted that there are wide variations in these values (particular for thermal conductivity) between different concretes at normal temperatures. (Campbell-Allen and Thorne 1963).

Table 3·2 Thermal Properties, Units and Dimensions

Properties	Dimension	Typical value at normal Temperature	
		Imperial Units	S.I.U.
Mass Density (ρ)	ML^{-3}	146 lb/ft^3	2340kg/m^3
Specific heat (c)	$HM^{-1}\varphi^{-1}$	0·23BTU/lb °F	960 J/kg°C
thermal conductivity (λ)	$HL^{-1}T^{-1}\varphi^{-1}$	1·40 BTU/fthr°F	2·41J/ms°C (= w/m°C)
thermal diffusivity (k)	L^2T^{-1}	0·0415 ft^2/hr	1·07mm^2/se

Symbols H: heat, φ: temperature, M: Mass, L: Length, T: Time. The numerical values are approximate typical values for a normal density concrete at normal temperature.

diffusivity k. These quantities are related as $\lambda = k\rho c$ where ρ is the mass density. It is useful to note the dimensions and units of these quantities for easy reference. This is done in Table 3·2, which also gives typical values for the quantities under normal conditions. However, and in spite of using the word typical, it must be noted that there are wide variations in these values (particular for thermal conductivity) between different concretes at normal temperatures. (Campbell-Allen and Thorne 1963).

Table 3·2 Thermal Properties, Units and Dimensions

Properties	Dimension	Typical value at normal Temperature	
		Imperial Units	S.I.U.
Mass Density (ρ)	ML^{-3}	146 lb/ft^3	2340kg/m^3
Specific heat (c)	$HM^{-1}\varphi^{-1}$	0·23BTU/lb °F	960 J/kg°
thermal conductivity (λ)	$HL^{-1}T^{-1}\varphi^{-1}$	1·40 BTU/fthr°F	2·41J/ms°((= w/m°C)
thermal diffusivity (k)	L^2T^{-1}	0·0415 ft^2/hr	1·07mm^2/s

Symbols H: heat, φ: temperature, M: Mass, L: Length, T: Time. The numerical values are approximate typical values for a normal density concrete at normal temperature.

3·8 Thermal Conductivity

Jakob (1949[a]) notes that, at normal temperatures, the thermal conductivity of most mineral based building materials is primarily dependent on the dry density and moisture content. Jakob gives average values for the thermal conductivity λ_o of bone dry building materials, as shown in figure 3-12, together with a multiplying factor f_w to account for the presence of moisture in the pores. Jakob does not regard the accuracy of these figures very highly and states that the error could be as high as $\pm$ 15% for some materials. However, Loudon and Stacy (1965) found that Jakob's values could be applied very satisfactorily to a wide range of concretes and brickwork if an additional multiplying factor f_m is introduced which refers to a particular material. Loudon and Stacy's values of f_m are given in Table 3·3 and using these, together with Jakob's values, an estimate of the thermal conductivity λ is obtained from

$$\lambda = f_w f_m \lambda_o \qquad (3·8·1)$$

When concrete is heated, moisture is lost and this may be the most significant single influence on the value of thermal conductivity at high temperatures. In order to investigate this idea, consider a fully hydrated cement paste with water cement ratio 0·475 that has been cured in a sealed condition. Neville (1963) has calculated the relative volumes of the hydration products for this paste. These calculations show that the density is 1860 kg/m^3 if the evaporable water in the gel and capillary pores is removed. The moisture

content is 31% by volume so that the effect of drying is to reduce the thermal conductivity of the paste by a factor of around 3 (i.e. $f_w \simeq 3$ from figure 3-12). If a similar paste is cured under water, the capillary pores are filled and the moisture content rises to 38·4%. Thus, the reduction in thermal conductivity, to be expected on drying, would be even greater.

Table 3·3 Values of 'material factor' f_m for use with equation 3·8·1. and figure 3·12 on p. 108

Material	Factor f_m
Concrete with aggregate of gravel, clinker expanded clay or sintered pulverised fuel ash pellets - Includes no fines concrete	1·1
Aerated concrete	0·90
Foamed slag, pumice or brick aggregate concrete	0·75
Brickwork	1·35

Table from Loudon and Stacy (1965)

Neville (1964) notes that the cement paste content for the more usual grades of structural concrete only varies

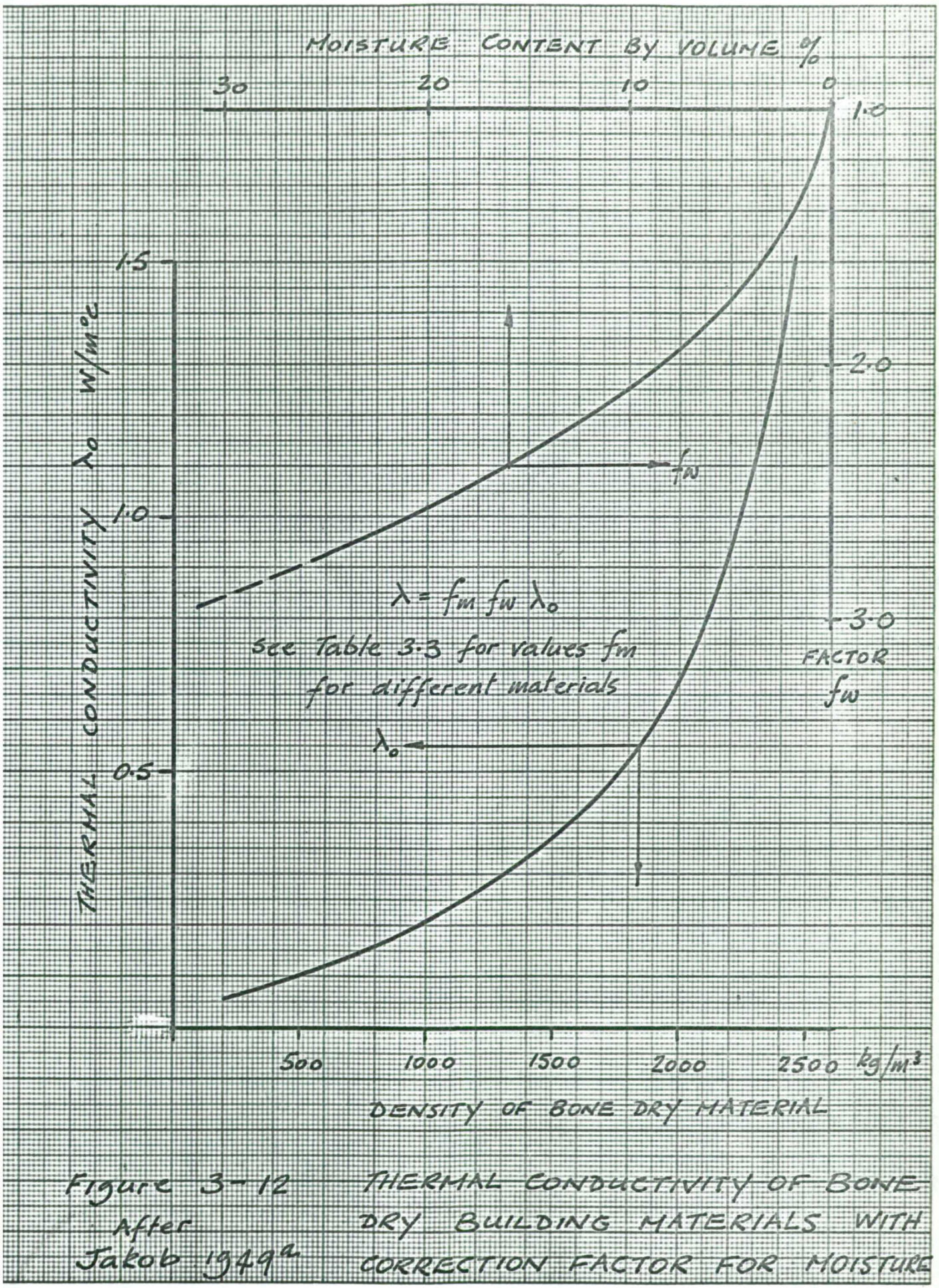


Figure 3-12 After Jakob 1949[a] THERMAL CONDUCTIVITY OF BONE DRY BUILDING MATERIALS WITH CORRECTION FACTOR FOR MOISTURE

between very narrow limits and calculates a range for three widely different mixes of from 24 - 29% to support his view. Rounding these figures, it seems that most mature structural concretes will have an aggregate content of between 70 and 75%, the remainder of the volume being cement paste containing around 40% of evaporable water. Thus, the proportion of evaporable water in concrete is typically between 10 and 12% by volume. Referring to figure 3-12, this suggests that the thermal conductivity of concrete may be reduced by a factor of around 2 by drying.

If concrete is heated, the reduction in thermal conductivity due to loss of moisture will be accompanied by changes due to the effects of heat on the constituents. In this respect, Jakob (1949[a]) notes that there is a fundamental difference between the behaviour of materials that are crystalline and those that are glassy or amorphous. The thermal conductivity of amorphous materials increases with temperature whereas the opposite trend is obtained with materials having a crystalline structure. Materials such as sulpher or silica have both amorphous and crystalline allotropes, each of which exhibits behaviour appropriate to its structure. Cement paste is composed of minute crystals that grow during the hydration process (Mills 1969) and, although the structure of cement paste is very small, it should be regarded as crystalline in the present context. On this basis, we expect that the thermal conductivity of cement paste will decrease with increasing temperature. No such generalisation can be made concerning the behaviour

of aggregates, although many of the most desirable hard aggregates are crystalline and Birch and Clark (1940) find the thermal conductivity of most rocks decreases with temperature rise.

These general ideas lead to the following qualitative account of the effect of heating on the thermal conductivity of concrete. A moderate rise in temperature causes removal of moisture from the capillary and gel pores and eventually leadsto a reduction in conductivity which is typically around 50%. The conductivity may be reduced further at higher temperatures due to the changing properties of the constituents. The results obtained by Marechal (1970) for two mature quartzite concretes, for the temperature range 20 - 400°C, follow this general pattern except that there is a significant increase in conductivity on heating to 60°C before the reduction, caused by drying, becomes effective. (figure 3-13)

There are few data giving measurements of thermal conductivity for concrete at high temperatures. Norton's (1913) results show very little change in thermal conductivity with temperature rise up to 500°C (if a single value for an 'untamped' concrete is ignored) and the average value of 0·91 W/m°C is reasonable for a concrete that has been dried. Surprisingly, Norton found higher values of conductivity at 1000°C and 1100°C. More recently, Harada (1954) has measured the thermal conductivity at high temperatures of a series of concrete materials including a cement paste and mortars and concretes made with a sandy river gravel aggregate.

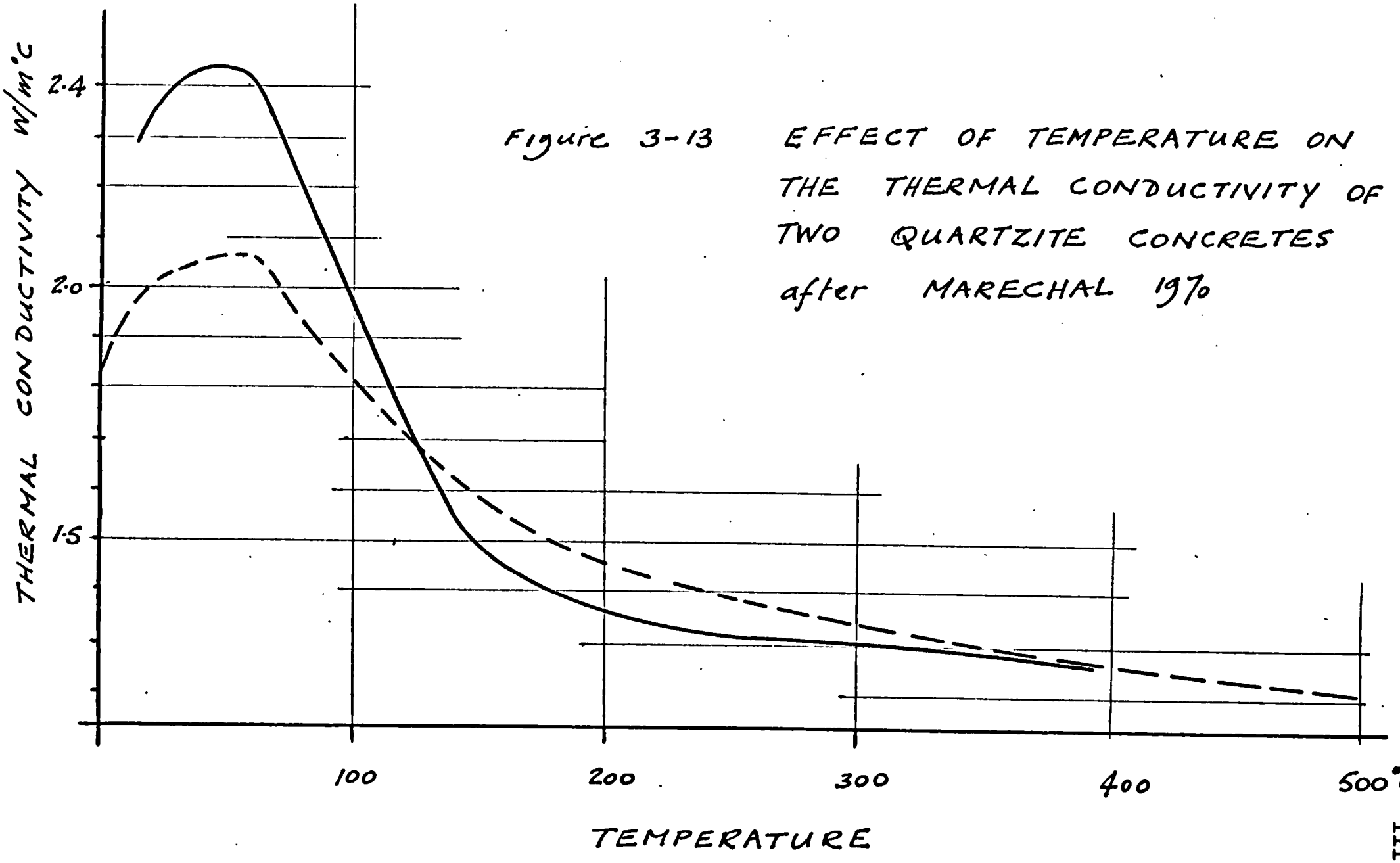


Figure 3-13 EFFECT OF TEMPERATURE ON THE THERMAL CONDUCTIVITY OF TWO QUARTZITE CONCRETES after MARECHAL 1970

He finds that the reduction in conductivity of the mortars and concretes is approximately directly proportional to the rise in temperature, for temperatures greater than 100°C, and that the reduction is around 50% over the temperature range 100-750°C. Zoldners (1960), does not find such severe reductions occurring in the temperature range 100-400°C, for concretes made with ordinary Portland cement and expanded slag, gravel or limestone aggregates but obtains similar reductions to Harada with a sandstone aggregate. Zoldners' results are given in Table 3·4. It is interesting that a modest increase in thermal conductivity is obtained with the heated limestone concrete.

Table 3·4 Values of Thermal Conductivity from Zoldners (1960)

Expanded Slag density 1545		Gravel 2320		Limestone 2300		Sandstone 2200 kg/m^3	
Mean Temp. °C	λ W/m°C	Mean Temp. °C	λ W/m°C	Mean Temp. °C	λ W/m°C	Mean Temp. °C	λ W/m°C
		100	1·53			95	2·28
182	0·505	164	1·53	164	0·971	167	2·27
398	0·478	402	1·29	393	1·090	406	1·54

Water/cement ratio 0·65 by weight, aggregate/cement ratio 7·3 ± 0·7 by volume.

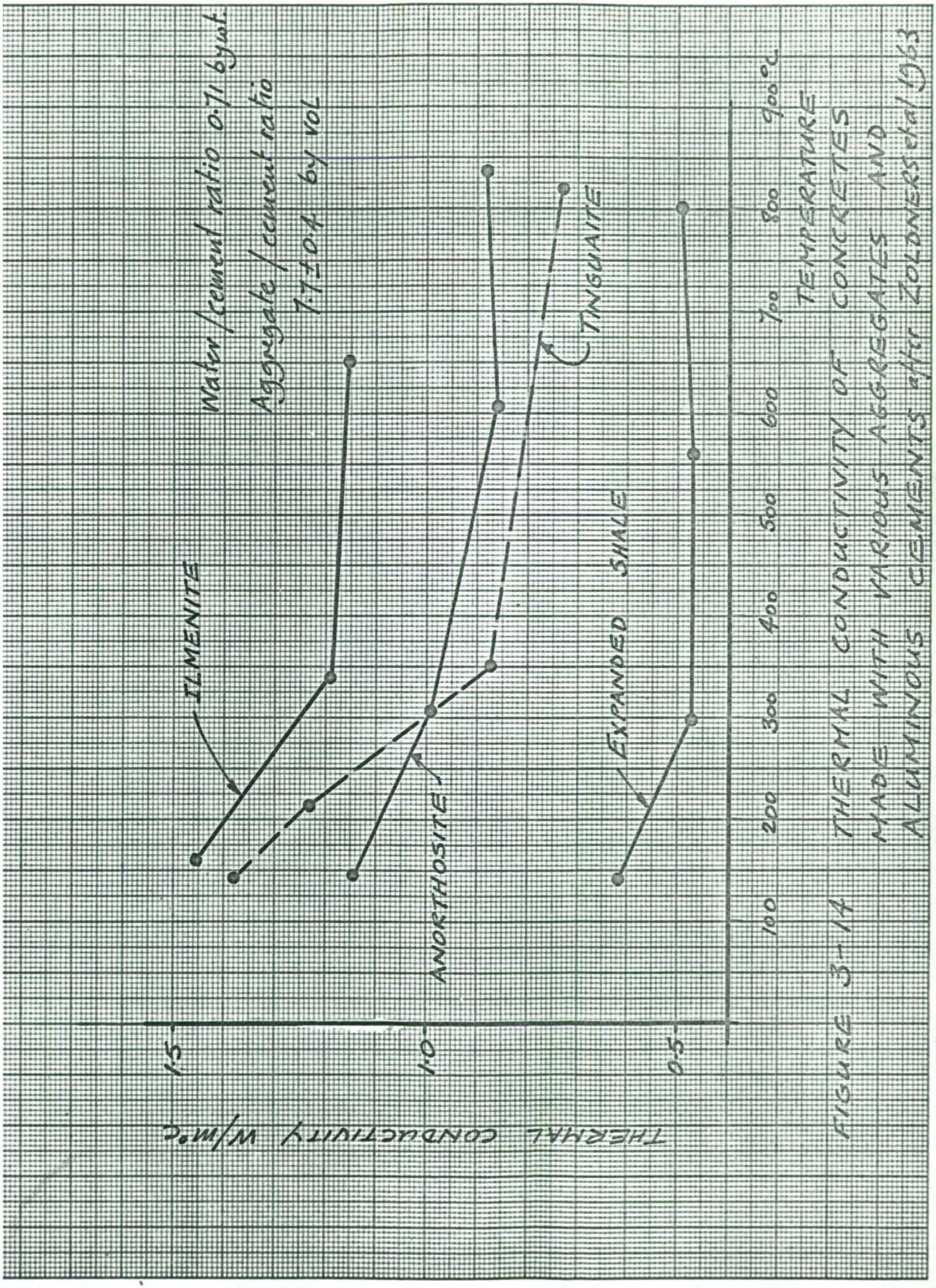


FIGURE 3-14. THERMAL CONDUCTIVITY OF CONCRETES MADE WITH VARIOUS AGGREGATES AND ALUMINOUS CEMENTS after Lotonen et al 1963

Besides this work, Zoldners et al (1963) have investigated the effects of heat on the thermal conductivity made of high alumina cement at temperatures up to 850°C and obtained the results shown in figure 3-14. In these it is interesting that there is a tendency for the thermal conductivity to increase at temperatures greater than 600°C, for the concretes made with expanded slag and anorthosite aggregates.

These sparse data tend to confirm the qualitative view of the effects of temperature on thermal conductivity developed in an earlier paragraph. However, it will be noted that all the results that have been discussed have been obtained from steady state tests and application of these results to transient conditions is open to question.

3·9 Specific Heat and thermal diffusivity

A fair amount of information on the specific heat of concrete is given by Klein et al (1962) and by the Bureau of Reclamation in their report on the concrete for the Boulder Dam. (U.S. Bureau of Reclamation 1940). The specific heat of concrete appears to lie within the range 800-1200 J/kg°C with most common aggregates having rather lower specific heats in the range 700-800 J/kg°C. There are few data concerning the effects of heating on the specific heats of mature concretes. Clearly some reduction below the initial value can be expected on account of drying but there will be increases around particular temperature levels corresponding to the thermal requirements of phase transformation in the aggregate and the cement paste. These will include the various quartz transformations and

calcination of limestone aggregates at temperatures greater than 700°C. In the cement paste, dehydration of calcium hydroxide occurs rather rapidly between 400 and 600°C and once desorption of the evaporable water is complete other dehydration reactions proceed up to temperatures of 800°C (Crook and Murray 1970)

Norton's (1913) results for specific heat are given in Table 3·5. The specimens were heated slowly in an electric furnace to the upper temperature before being transferred to the calorimeter. On this basis the heat measured does not include that for processes which are irreversible on cooling and so may be an underestimate of the average heat requirement for heating over any temperature range. In spite of this, Norton obtained significant increases in specific heat over the whole temperature range 22-80°C.

Table 3·5 Specific Heat of Concrete from Norton (1913) in J/kg °C.

Temp. range °C	1:2:5 Stone concrete	1:2:4 Stone concrete	1:2:4 Cinder concrete
22 - 100	638	644	
22 - 188	802	794	752
22 - 633	836	876	860
22 - 800	915	894	910

The effects of temperature on thermal diffusivity can be estimated once the specific heat, density and thermal conductivity are known. If Norton's data are typical, the

thermal diffusivity of dry concrete will be reduced rather more rapidly with increasing temperature than is the thermal conductivity. Also, there will be a significant reduction in thermal diffusivity caused by drying a moist concrete. Again there are few experimental data available and Harada (1958) appears to have undertaken the only comprehensive series of tests to determine thermal diffusivity at elevated temperatures. Harada tested concretes made with various aggregates including andesite, pumice, coal ash and a sandy river gravel as well as a number of mortars and a cement paste. The results for all these materials fall within the range shown in figure 3-15. The values of thermal diffusivity at normal temperatures ranged from 0·5 mm^2/sec for a neat cement paste with water cement ratio 0·3 up to 0·91 mm^2/sec for a 1:4:5 gravel aggregate concrete with water cement ratio 0·7. The value for the cement paste can be compared with the value of 0·41 mm^2/sec obtained by Hoyle (1954) for an unspecified cement paste. Also for comparison, Dougill (1960) obtained a value of 0·99 mm^2/sec for the thermal diffusivity of a 1:4:9 mixture of ordinary Portland cement and Thames valley river gravel with a water cement ratio of 0·475. This value was reduced by half on heating to 220°C and heating to higher temperatures had little effect. It appeared that with this aggregate the thermal diffusivity was relatively constant once drying was complete. However, this is a result from a very limited series of tests.

In concluding this section, we note that precise data

are rare but the general trends are established. The available information should be sufficient for analytical work of an exploratory nature although more tests would be required if this were required to be related to a particular concrete.

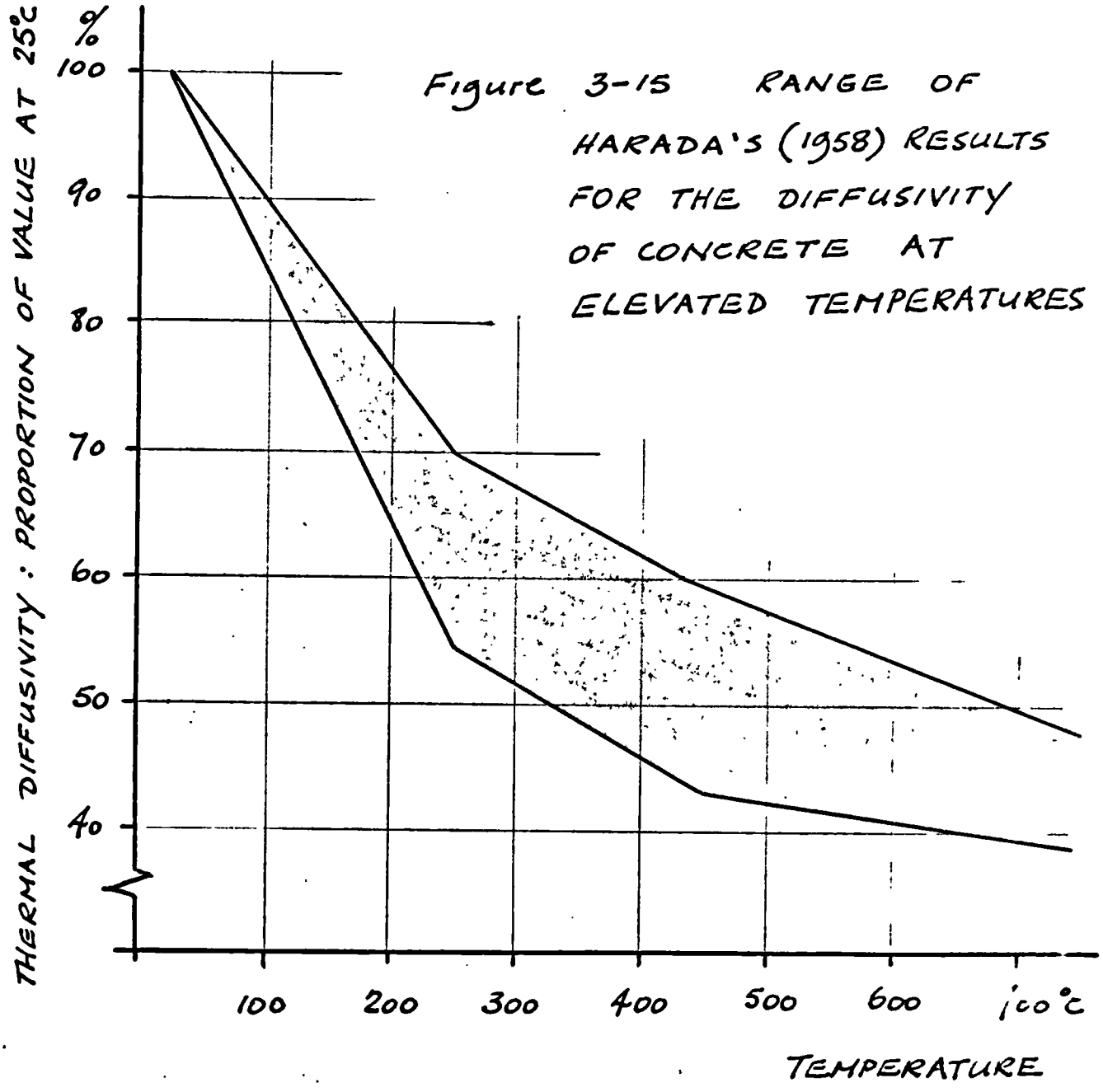


Figure 3-15 RANGE OF HARADA'S (1958) RESULTS FOR THE DIFFUSIVITY OF CONCRETE AT ELEVATED TEMPERATURES

Chapter 4

STRUCTURAL BEHAVIOUR IN FIRE TESTS AND STRUCTURES.

4·1 Introduction

It was noted, in Chapter 1, that tests for fire resistance are performed in a highly idealised manner in which a standardised exposure condition is used and structural elements are tested rather than complete structures. However, if the idea of fire resistance testing is to be useful, it is necessary that the performance required of an actual structure under fire conditions should be capable of being translated into an equivalent performance in the fire test. In this way, the behaviour of different types of structure can be assessed in terms of a single test and it becomes possible to specify the requirements for structural safety, in a fire, in terms of a particular period of endurance in a standard test.

Butcher et al. (1966) give a brief account of the background to the procedures used for grading buildings for fire resistance. This is a large subject in itself but, in essence, buildings are divided into classes, according to their size and usage, and a period of fire resistance is specified for each class of building. The various elements of construction that comprise a building are then required to provide this period of fire resistance under the standard test conditions. Thus, the requirements can be satisfied equally by different materials, or by alternative forms of construction, provided that they show similar endurance in the standard test.

It is clear that the standard test (i.e. in accordance with B.S. 476) plays a fundamental role in design for fire resistance. However, difficulties arise if the method of

test is such that a particular element of construction behaves differently in the test than it would do as part of a structure. If this occurs, the relevance of the test may be undermined and satisfaction of the test requirements may become an end in itself rather than the means of obtaining a structure of therequisite quality. It is therefore important to recognise the circumstances in which there may be a major discrepancy between the test result and real conditions.

It is known that the occurrence of spalling can have a major influence on the result of a fire test. However, it is not clear how far this result is relevant to the effects of spalling in structures. Also, it is clear that many reinforced concrete structures survive the effects of fire, in a condition that is amenable to reinstatement, even though extensive spalling has occurred (Green and Long 1971). Thus, it seems that there is the possibility that the effects of spalling may be unduly emphasised by the type of test used for fire resistance. It is therefore necessary to examine the form of test used for the most common types of structural element and compare the results with the sort of behaviour that could be expected in a fire in a structure. This comparison should give a guide to the relative importance of spalling in the test and the real situation. The discussion is divided into two parts, dealing with columns and flexural members respectively. The emphasis is on structural behaviour and little account is taken of the difference in thermal conditions that exists between a particular fire and the standard test. These are being

investigated in work being undertaken at the Fire Research Station and first reported by Butcher et al. (1966). However, it is felt that, although the quantitative results will depend on the thermal conditions, the mode of behaviour will be most affected by the structural parameters.

4·2 Fire Resistance of Reinforced Concrete Columns.

The fire resistance of reinforced concrete columns has been investigated at intervals from the earliest days of reinforced concrete construction (Bauschinger (1885), McFarland and Johnson (1906), Hull (1920),Ingberg et al. (1921), Thomas and Webster (1953)). Almost invariably, the procedure has been to heat axially loaded columns from all sides and to observe the time taken from the start of heating until collapse occurs under the applied load. The control of heating was poor in the early tests but in later work a standard ambient temperature exposure condition was used. In all these tests, the load on the column was maintained at a constant value during heating and this is the procedure used today, with the magnitude of the applied load being the same as the design working load on the column. It is of interest that both the current standard (B.S. 476, 1953) and the draft revision (1969) are ambiguous regarding the precise test conditions as they require that the load shall be maintained constant during the test period and that, as far as possible, the member shall be supported in a similar manner as it would be in service. For columns, these requirements are usually incompatible and the member is effectively tested with pinned ends but unrestrained in the axial direction.

In this country, the most recent data, on the fire resistance of reinforced concrete columns, are those obtained by Thomas and Webster (1953) in a comprehensive series of tests on unrestrained columns. These tests were on square sectioned columns with sides in the range 229 to 483mm (i.e. 9 to 19 inches). A number of different quality concretes were used and the proportion of mild steel reinforcement was also varied. In addition, temperatures were measured during the tests at points on the steel and throughout the concrete cross section. These measurements enabled Thomas and Webster to generalise their data and so put it into a form that is useful for prediction. The discussion that follows is based on their procedures.

According to Thomas and Webster, the maximum load capacity, P, of a reinforced concrete column at normal temperatures may be written

$$P = 0{\cdot}65\, u\, A_c + f_y\, A_{sc} \qquad (4{\cdot}2{\cdot}1)$$

where A_c and A_{sc} are the areas of concrete and steel in the cross section, f_y is the yield stress in the steel and u is the stress corresponding to the maximum load capacity of a standard concrete cube specimen.

In generalising their results, Thomas and Webster suggested that the load capacity P_T, of an axially load column tested at high tempertures, could be written,

$$P_T = 0{\cdot}65\, \lambda_c\, u\, A_c + \lambda_s\, f_y\, A_{sc} \qquad (4{\cdot}2{\cdot}2)$$

The second term of this expression represents the

reinforcement's contribution to the strength of the column and this was calculated, knowing the steel temperature, from F.C.Lea's (1920) results for the effects of heating on the yield stress of mild steel. The ultimate load of the column was known from the fire test and thus the contribution of the concrete to the strength of the column could be found together with the factor λ_c. It was found that this factor, λ_c, depended only on the average temperature in the column at failure and was independent of column size. Thomas and Webster's results for λ_c are shown in figure 4-1. Lea's (1920) results for λ_s, the proportion of the normal yield stress retained by the reinforcement at elevated temperatures, are shown in figure 4-2 together with some more recent results from Corson (1965) and Bannister (1968).

Figures 4-1 and 4-2 can be used to estimate the load capacity of a heated column if the original cube strength of the concrete and yield stress of the steel are known together with the average temperature in the column and the temperature of the steel. Using this approach, Thomas and Webster predicted the load capacities of their columns at failure with reasonable success.

Although the particular values of λ_c given in figure 4-1 apply to Thomas and Websters' tests only, the general form of the functions λ_c and λ_s is probably typical. This enables some general conclusions to be made concerning the behaviour of columns in a fire test.

If a load W is maintained on the column during heating, failure occurs when the load capacity P_T is reduced to the

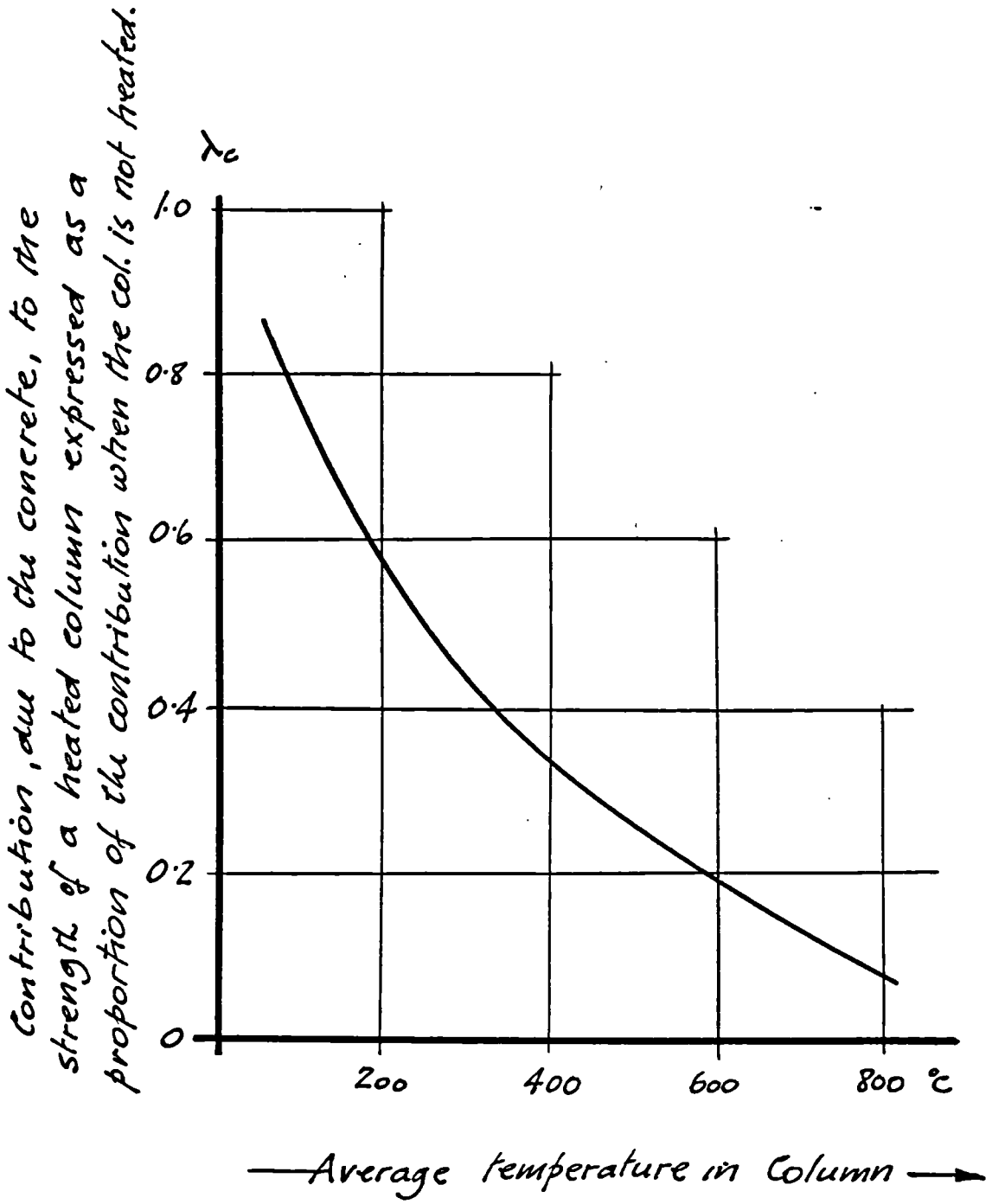


Figure 4-1 EFFECTIVE STRENGTH OF CONCRETE IN A COLUMN SUBJECTED TO THE STANDARD EXPOSURE CONDITIONS

after THOMAS and Webster 1953

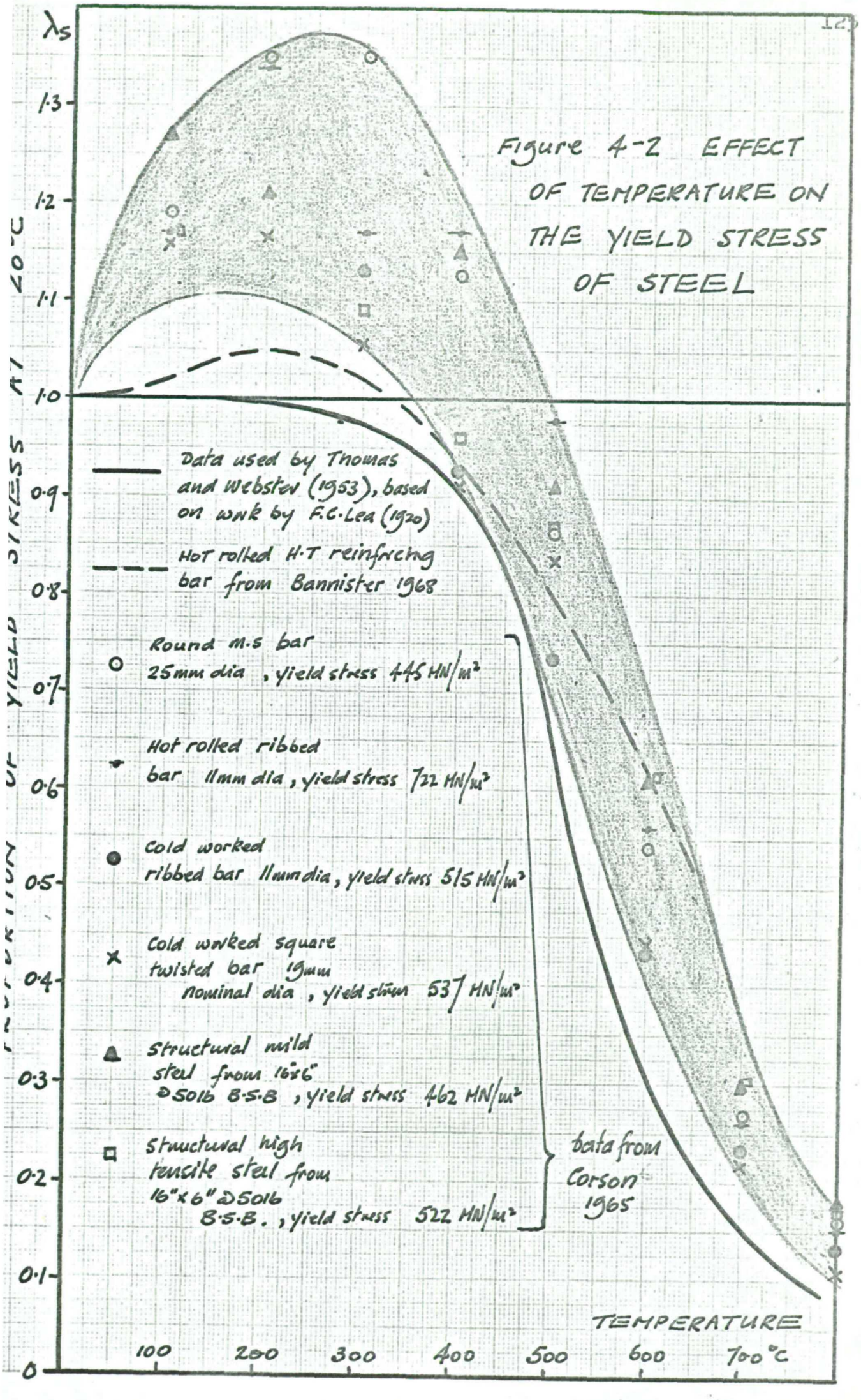


Figure 4-2 EFFECT OF TEMPERATURE ON THE YIELD STRESS OF STEEL

value W. Thus, the columns can support the applied load if,

$$P_T \geqslant W$$

or, introducing the load factor γ that existed before heating, if

$$\frac{\gamma P_T}{P} \geqslant 1$$

Thus, using equations 4·2·1 and 4·2·2, the column continues to carry the applied load if

$$\frac{(\lambda_c + p\lambda_s)\gamma}{1 + p} \geqslant 1 \quad , \quad \text{where } p = \frac{f_y A_{sc}}{0{\cdot}65\ u\ A_c} \qquad \cdot(4{\cdot}2{\cdot}3)$$

The equality in the condition 4·2·3 corresponds to a state of incipient collapse. The terms p and γ are constants for any particular column whilst the parameters λ_c and λ_s are reduced, from the initial values of unity, by the effects of heating.

If we consider a range of columns with different load factors it is clear that, as the load factor is increased, a greater reduction in the term $(\lambda_c + p\lambda_s)$ is required in order to achieve the equality in 4·2·3. This requires a longer period of heating so that the fire resistance is increased by an increase in the load factor. This conclusion is generally accepted and holds for timber columns (Malhotra and Rogowski 1969) and concrete encased steel stanchions (Malhotra and Stevens 1964) as well as reinforced concrete.

The effect of different proportions of reinforcement is rather more difficult to establish. An increase in the proportion of reinforcement, only increases the term on the left hand side of the condition 4·2·3 if λ_s is greater than λ_c. Thus the fire resistance for a given load factor is increased by an increase in p, if $\lambda_s > \lambda_c$ before collapse. However, the relative magnitudes of λ_s and λ_c depend on the column dimension, cover to the reinforcement and the time from the start of heating and it is difficult to arive at a general conclusion regarding fire resistance. On the other hand, it is clear that the load capacity of a column containing a high proportion of steel is more dependent on λ_s than is one that contains less steel. Thus, any influence that causes an abrupt reduction in λ_s will be most noticeable in columns that have a high p value. Spalling has such an effect, as removal of the cover exposes the steel, allowing the temperature to rise, and reduces λ_s. On this basis, spalling is likely to have most influence on the behaviour of columns containing a high proportion of reinforcement. The effect is worst if the column is small, as the reduction in the concrete cross section may also lead to a significant loss in load capacity in addition to that due to the steel. Thus, the fire resistance of small sectioned columns, containing a high proportion of reinforcement, is likely to be reduced considerably if spalling occurs during a fire test.

4·3 <u>The behaviour of columns when they are part of a structure</u>

<u>The Localised fire</u>

In the fire test, the load is maintained at a constant

value during heating. It seems improbable that this would occur if the column was part of a structure. In order to investigate this, Dougill (1966) considered the extreme case of a local fire, in which a single interior column in a large multi-storey building is subject to the effects of heating whilst the remainder of the structure remains cool. In these circumstances, the thermal expansion of the column is restrained by the surrounding structure and this causes further loads to be induced in the column during heating. The general details of the structure and the column are shown in figure 4·3.

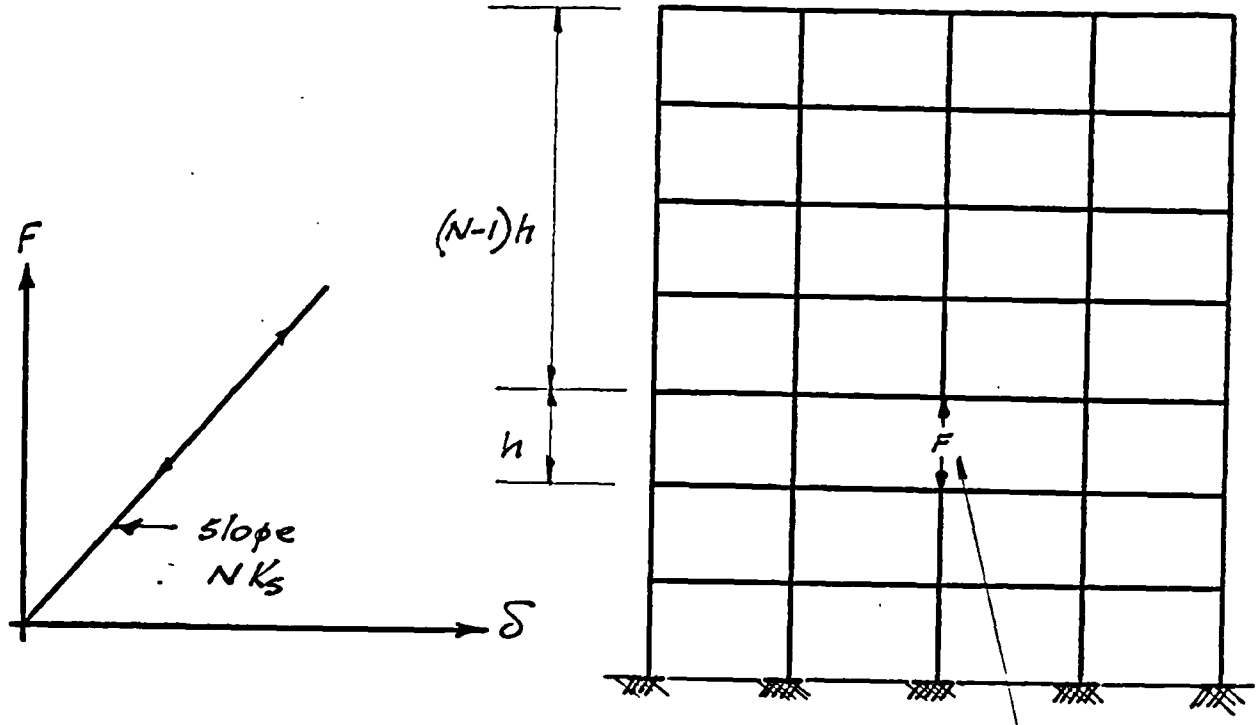
Consider the behaviour of the heated column as though it was separated from the building. Before the start of heating the column has stiffness K_c and carries an axial load F_o, due to the dead and superimposed loadings within the structure. Thus, the shortening δ_o due to the initial load is given by

$$\delta_o = F_o/K_c \qquad (4\cdot3\cdot1)$$

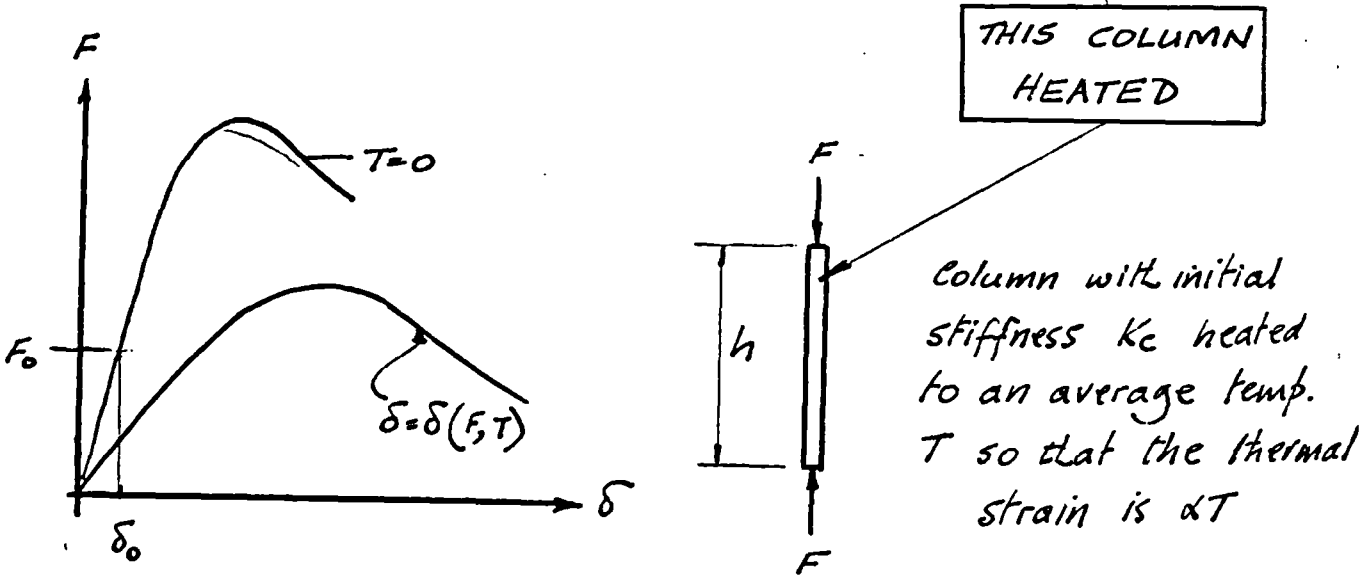
If the column was taken on its own and tested in compression at high temperatures the displacement δ due to load would depend on the average temperature rise T in the column so that,

$$\delta = \delta(F,T) \qquad (4\cdot3\cdot2)$$

In the building, the displacement due to load is accompanied by thermal expansion of an amount αTh where h is the column height and αT is the thermal strain for the average temperature T. Thus if Δ is the total expansion



FRAME DETAILS



COLUMN DETAILS

Figure 4-3 STRUCTURAL DETAILS OF THE BUILDING FRAME AND HEATED COLUMN

of the column during heating

$$\Delta = \alpha Th - \delta(F,T) + \delta_o \qquad (4\cdot3\cdot3)$$

Now consider the building frame. During heating, the frame above and below the column has been separated by a further distance Δ while the load, applied by the column to the frame, has increased from F_o to F. The force and displacement are related and, assuming linear behaviour of the frame, we write

$$\Delta = \frac{F - F_o}{NK_s} \qquad (4\cdot3\cdot4)$$

where K_s is the average stiffness of the structure per floor and N is the number of floors affected by the expansion of the column.

The condition for the displacements of the column and building frame to be compatible is obtained by equating the two values for Δ given by equations 4·3·3 and 4·3·4. Then, by using equation 4·3·1, the result can be put in the form,

$$\frac{\delta(F,T)}{\delta_o} + \frac{1}{R}\cdot\frac{F}{F_o} = 1 + \frac{1}{R} + \frac{\alpha Th}{\delta_o} \qquad (4\cdot3\cdot5)$$

where $R = NK_s/K_c$ and is a measure of the restraint offered to the column by the surrounding structure and will be termed the relative stiffness.

Before discussing the solution of this equation it is necessary to consider the form of the function $\delta(F,T)$. In this, it seems that the stiffness of the column will be very much dependent on the behaviour of the concrete and not much

influenced by the stiffness of the steel, as this is near the outside of the column and quickly raised to a high temperature. Thus, the relationship between the load F and the corresponding displacement δ could be expected to be very similar to the usual form of the stress-strain curve for concrete in compression. Also, following Furumura (1966[a]), it is expected that a rise in temperature of the column will cause a decrease in the peak load and an increase in the corresponding displacement as suggested by the curves shown in figure 4-4.

Once the form of the function δ(F,T) is known, the equation of compatibility 4·3·5 can be solved by means of the construction shown in figure 4-4. The separate terms of the equation are shown annotated on the figure with the term (1 + 1/R) being obtained from the load displacement curve for the unheated column. The construction is similar to one used by Sigvaldason (1964) in investigating the behaviour of a compression testing machine. This procedure can be used because the complete structural system, comprising the column and the frame, is analogous to a testing machine with the column and surrounding structure representing the specimen and test frame respectively and the load being applied by thermal expansion rather than by a hydraulic jack.

The behaviour of a compression testing machine has already been discussed (in Chapter 2, section 2·2) and it was noted that instability could occur if the machine did not possess sufficient stiffness. It appears that similar

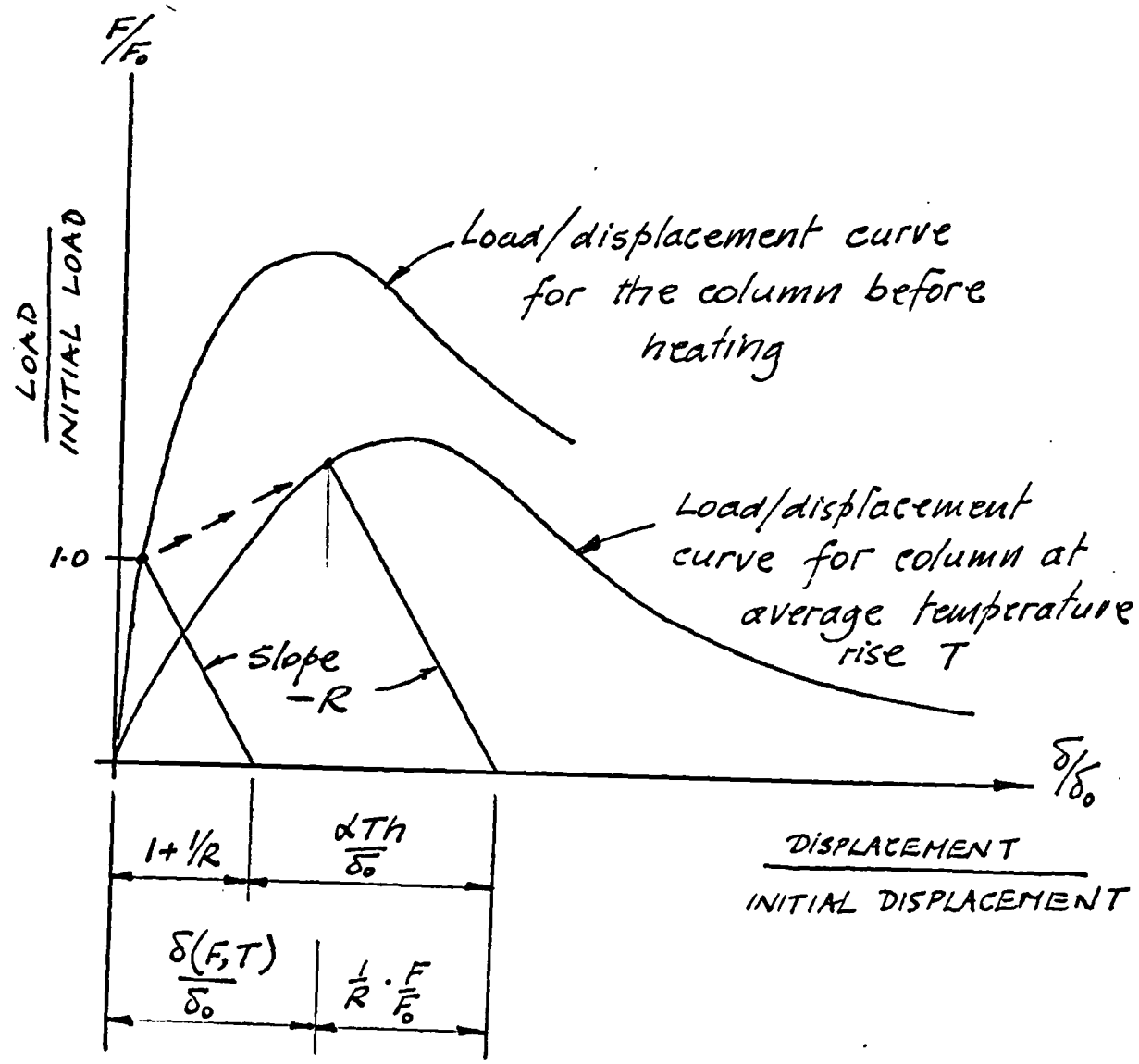


Figure 4-4 LOADS AND DISPLACEMENTS IN A HEATED COLUMN SHOWING THE SOLUTION OF THE EQUATION OF COMPATIBILITY 4.3.5

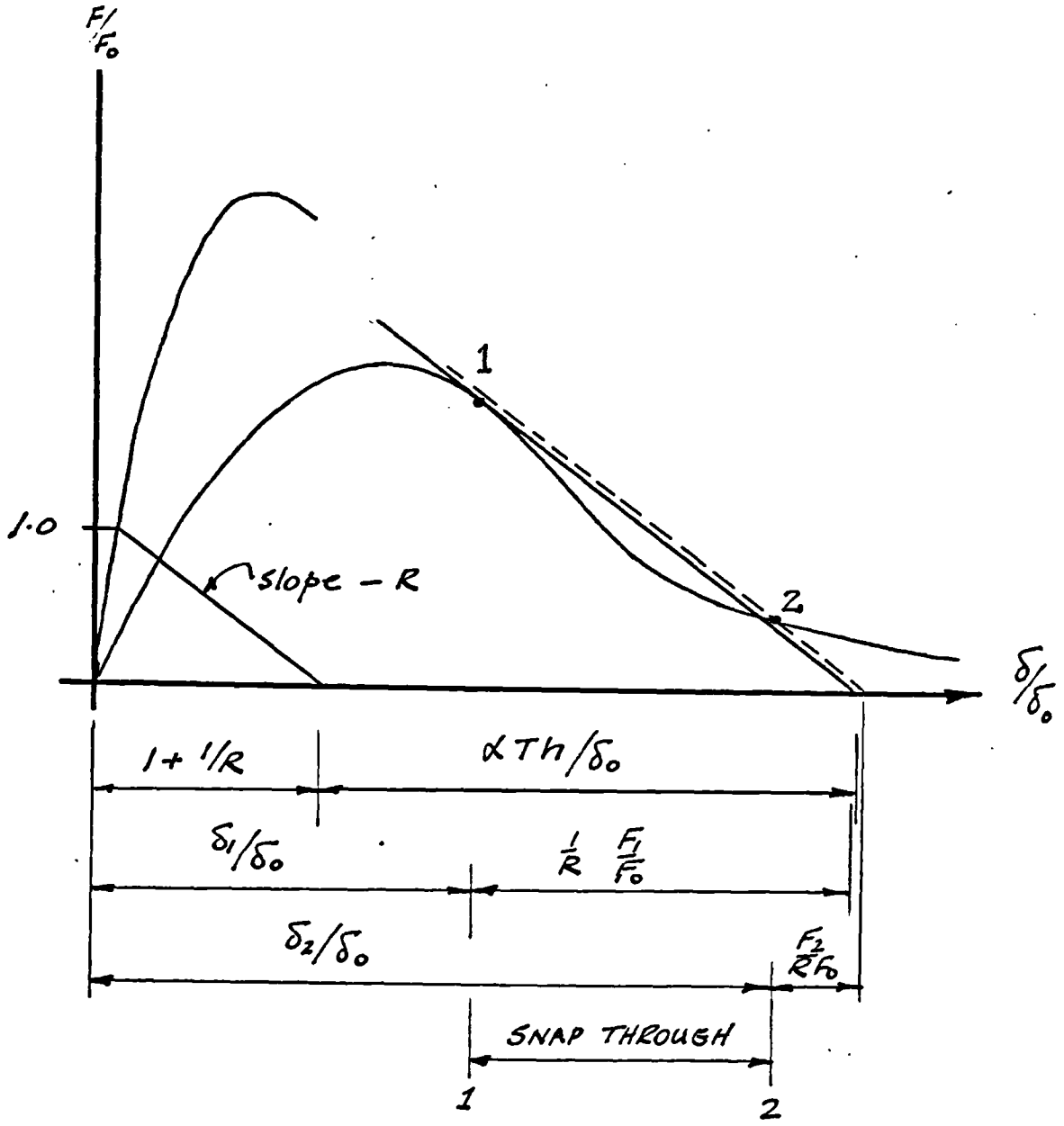


Figure 4-5 CONDITIONS FOR THE OCCURRENCE OF LONGITUDINAL INSTABILITY IN A HEATED COLUMN

behaviour could occur in a heated structure if the relative stiffness R is not sufficiently great. The conditions for such an instability to occur are illustrated in figure 4-5. Here, a slight increase in the thermal strain αT would mean a considerable sudden shortening of the column, and possible collapse, as it attempts to snap through between the equilibrium position marked 1 and 2 on the figure.

If longitudinal instability does occur, the behaviour is very similar to that observed when a single column is tested in the standard manner. In the test, the load F is maintained equal to F_o and this corresponds to the condition in a very flexible structure described by R = 0. However, if the relative stiffness is high, instability does not occur and the column remains intact, although considerable irrecoverable strains are induced during heating.

Approximate calculations suggest that multistorey structures of beam and slab construction will behave in a stiff manner for conditions of local heating. These results tend to lack conviction without further data on the behaviour of restrained columns under fire conditions. However, experience of fires suggests that collapse is very unlikely to result from a local fire in a reinforced concrete multi-storey structure that is constructed in-situ. The considerable stiffness of these structures is well known and there are instances where one or more columns have been removed in a particular storey and the stiffness of the structure has been sufficient to redistribute the loading to the surrounding columns. This has generally occurred as

the result of an explosion and Hamilton (1956), in his history of reinforced concrete, shows several photographs of structures remaining suitable for reinstatement even though a number of principal members have been severed or removed by the effects of bombing. It is not certain whether this behaviour could be expected from the more flexible flat-slab construction or from some of the modern 'system' built structures.

The continued performance of a member in a stiff structure during a fire depends on redistribution of load. Thus, the loads in members remote from the fire may be augmented during redistribution and this may cause damage away from the seat of the fire+. Also, the additional damage that occurs on cooling, due to the large irreversible strains induced during heating, will not necessarily be confined to the heated member. Thus the damage resulting from a local fire of long duration is not confined to the heated regions (Harada et al. c. 1960, Green and Long 1971). Also, some further deterioration occurs during the post cooling period of recovery in strength and stiffness. (Sanderson-Watts 1969)

Footnote +

If this damage is severe, equation 4·3·4 must be replaced by a non-linear expression to account for the loss in stiffness of the surrounding structure.

More general heating

So far the discussion has been confined to the extreme case in which only one column is affected by heating. At the other extreme there is the case in which all the columns in a particular storey height are heated equally, so that there is no restraint to expansion in that storey and the value of R is effectively reduced to zero. If more than one column is heated, the stiffness of the heated region is increased, at the expense of the surrounding structure, and the value of the effective relative stiffness is reduced. Thus, the effect of increasing the number of heated columns is the same as reducing the stiffness of the structure in the analysis of a single column. It follows that instability and collapse are more likely to occur as a result of an extensive fire than if the heating is local. However, it is considered that many fires in large buildings will be local in character, particularly if the buildings are properly divided by walls and partitions to delay or prevent the spread of fire.

Spalling

For flexible structures, the mode of behaviour is similar to that observed in the standard test. Here, the occurrence of spalling may have a significant effect on fire resistance especially if the member is slender or heavily reinforced. However, if the structure behaves in a stiff manner, the mode of behaviour is entirely different and spalling merely causes a reduction in the column stiffness and an increase in R. Thus, overall structural failure does not result

from spalling in a structure that remains stiff during heating. In these circumstances, experience from the standard tests tends to exaggerate the importance of spalling.

4·4 Simply supported flexural members

The Portland Cement Association has devoted considerable effort in research aimed at understanding the behaviour of flexural members under fire conditions. Some of this work deals with the simply supported beams and slabs that are the usual subject in tests for fire resistance, but the effects of restraint and continuity have also been investigated.

With simply supported beams and slabs, the cover to the steel has a decisive influence on fire resistance. Gustaferro and Selvaggio (1967) and Gustaferro (1970) have shown that the procedures used for the analysis of reinforced concrete sections at normal temperatures can be used to predict the ultimate moment of resistance of flexural members under fire conditions. For an under-reinforced beam heated from below, the ultimate moment is determined primarily by the amount and quality of the reinforcement and the lever arm, so that, at high temperatures, the ultimate moment of resistance M_T is given by:

$$M_T = \lambda_s \, a \, f_y \, A_{st} \qquad (4\cdot4\cdot1)$$

where A_{st} is the area of the tensile reinforcement, $\lambda_s f_y$ is the yield stress of the steel at high temperature and a is the lever arm.

On exposure to fire, the temperature in the steel rises and the factor λ_s is reduced below its original value of

unity. This reduction is accompanied by a small increase in the lever arm but the effect of this, on the moment of resistance, is relatively unimportant compared with the change in yield stress. On this basis the beam continues to support the applied load as long as

$$\gamma \lambda_s \geqslant 1 \qquad (4\cdot4\cdot2)$$

where γ is the original load factor and the condition is approximate because the variation in lever arm has not been considered. As with columns, the fire resistance is increased by an increase in load factor as a greater reduction in λ_s is then required in order to reach the condition for incipient collapse (i.e. $\lambda_s = 1/\gamma$). Also, the rate of reduction of λ_s can be reduced by increasing the cover to the reinforcement or by providing a protective insulating layer to the soffit of the beam or slab. Conversely, if spalling occurs, to remove part of the cover, it generally causes a significant reduction in fire resistance.

Because of their dependence on the yield stress of the reinforcement, results from simply supported members have often been interpreted in terms of a critical temperature for the steel. Thus, if beams are tested, that are reinforced with mild steel and have a load factor in the range 2 to 2·5, failure occurs when λ_s is in the range 0·4 to 0·5. It is seen, from figure 4-2, that this corresponds to a rather narrow range of temperatures around 550°C which suggests the idea of a critical steel temperature that determines fire resistance. This is apparently a useful

concept in deciding what depth of cover is required to the reinforcement. However, it will become apparent that the concept only applies to statically determinate members and that, the idea of a critical steel temperature has more relevance to the standard test than to real forms of construction.

Most tests on reinforced concrete beams and slabs have been undertaken on simply supported single span members. However, the effects of continuity have been examined in recent work (Ehm and von Postel 1965, Carlson and Gustaferro 1965) and it appears that the ideas of limit analysis, developed for use in the design of reinforced concrete at normal temperatures, can be used to account for behaviour under fire conditions.

As an example, consider an interior span, of length L and loaded with a uniformly distributed load W, of the continuous beam shown in figure 4-6. Before heating, the moment of resistance at the supports and mid-span are M_{so} and M_{co} respectively. Thus, on the basis of the collapse mechanism shown in figure 4-6,

$$M_{so} + M_{co} = \frac{\gamma WL}{8} \qquad (4\cdot4\cdot3)$$

where γ is the load factor.

At high temperatures, the moments of resistance are reduced to M_{sT} and M_{cT} so that the span does not collapse if

$$M_{sT} + M_{cT} \geqslant \frac{WL}{8} \qquad (4\cdot4\cdot4)$$

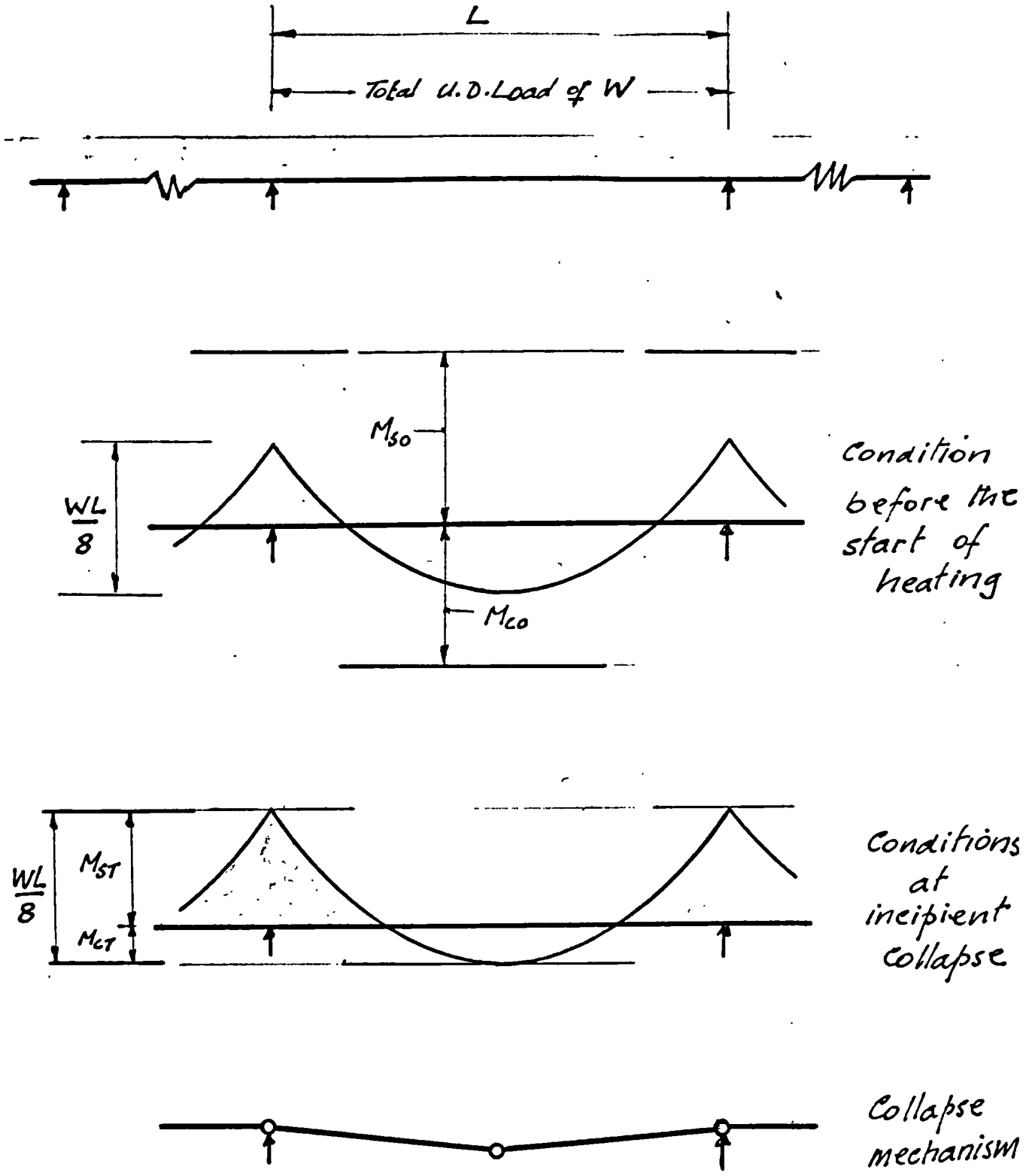


Figure 4-6 CONDITIONS LEADING TO COLLAPSE OF AN INTERIOR SPAN OF A CONTINUOUS BEAM

The moment of resistance at mid span depends principally on the yield stress in the reinforcement which is reduced by a factor λ_s by the effects of heating. Now, using the same approximation that lead to equation 4·4·2,

$$M_{cT} = \lambda_s M_{co}$$

where λ_s is found from the temperature of the reinforcement at mid span and figure 4-2. Using this result, the condition for the span to remain standing under the load W becomes

$$\gamma \lambda_s \geq \frac{1 - rM_{sT}/M_{so}}{1 - r/\gamma} \quad \text{where } r = \frac{8M_{so}}{WL} \qquad (4\cdot4\cdot5)$$

It will be noted that this condition reduces to that for simply supported beams (4·4·2) if $M_{so} = 0$. Also, it is clear that the fire resistance of the continuous beam is greater than that of a simply supported beam designed with the same load factor if

$$M_{sT}/M_{so} > 1/\gamma \qquad (4\cdot4\cdot6)$$

This condition is likely to be satisfied in practice, except for unusually shallow beams or beams with compression reinforcement at the support. It is expected that the reduction in moment capacity at the support will be small as the tensile reinforcement is well protected from the effects of heating and the change in resistance moment comes principally from the change in lever arm caused by the reduced strength of the concrete in the compression zone.

There is some support for this view. Carlson and Gustaferro (1965) found only a 10% reduction in a resistance moment at the support, of a 305mm by 458mm deep rectangular reinforced concrete balanced cantilever beam, after more than three hours exposure.

If the reduction in load capacity at the support is small, it is possible that the beam may survive the effects of heating indefinitely. This occurs if

$$r\, M_{sT}/M_{so} > 1 > r/\gamma \qquad (4\cdot4\cdot7)$$

It is significant that this condition can be satisfied by beams designed without particular regard to fire resistance. In design, it would be quite usual practice to proportion the reinforcement at the support to give $M_{so} = WL/10$. For such a design, $r = 0\cdot8$ and the condition 4·4·7 is satisfied for any reasonable value of load factor.

These results tend to explain the usually excellent performance of continuous reinforced concrete structures under fire conditions. Again the effects of spalling can be misinterpreted if only the results from tests on single span members are ccnsidered. In the usual test for fire resistance, spalling at mid span is a very serious occurrence and leads to a reduction in fire resistance. However, with continuous beams the behaviour at mid span is relatively unimportant. For these structures it is much more important to prevent spalling near the supports and so conserve the compression flange of the beam. This may be accomplished by using adequate binders, which will also

help to provide the ductility necessary for moment redistribution.

These arguments have been based entirely on the flexural behaviour of the member. The advantages of continuity may not be realised if the member fails in shear, or failure is initiated by breakdown of bond with the reinforcement. As yet, these aspects of the behaviour of reinforced concrete at high temperatures remain to be investigated and some caution is necessary in extending the results obtained from simply supported members to continuous construction.

4·5 Longitudinal Restraint

In structures, the conditions for simple supports are seldom realised and the structure offers some resistance to the extension or contraction of a beam or slab. During a fire, there is a tendency for forces to be induced which oppose the free thermal movements of the heated members. In this way, the member may be prestressed by the effects of heating and so behave in an entirely different way from a member that depends on the yield stress of the reinforcement for its load capacity. The induced prestress increases the load factor against flexural failure and so extends the period of fire resistance. However, there is the possibility that the restraint may be so great that some form of compression failure may result.

Gustaferro and Carlson (1962) were probably the first to consider the problem of longitudinal restraint. They suggested that the relation between restraint and fire resistance would be of the form shown in figure 4-7. Here,

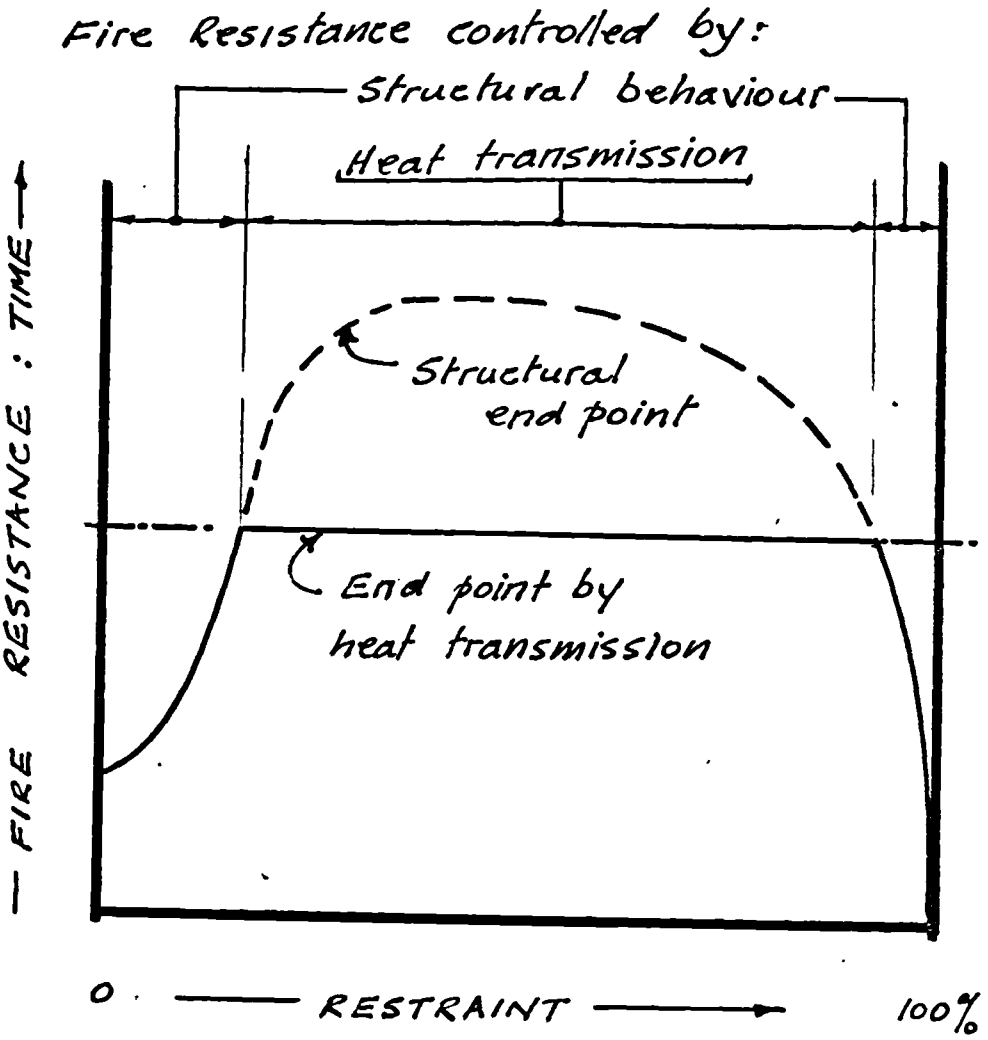


Figure 4-7 EFFECT OF RESTRAINT ON THE FIRE RESISTANCE OF CONCRETE MEMBERS

after GUSTAFERRO and CARLSON 1962 with additions

restraint is defined as the ratio of the induced longitudinal load to the load required to prevent extension or rotation of the member. This definition is not entirely satisfactory, as the effects of extension and rotation are not separated, but it does provide a convient parameter that is compatible with the idea that simply supported and built in beams should have zero restraint and 100% restraint respectively. Referring to figure 4-7. a small amount of restraint causes a considerable increase in fire resistance. Thus, only a modest amount of restraint is needed to increase the structural performance so that the fire resistance of slabs is determined on the basis of heat transmission and their ability to act as separating members. With high restraint, there is the possibility of compression failure and fire resistance is once more controlled by structural considerations.

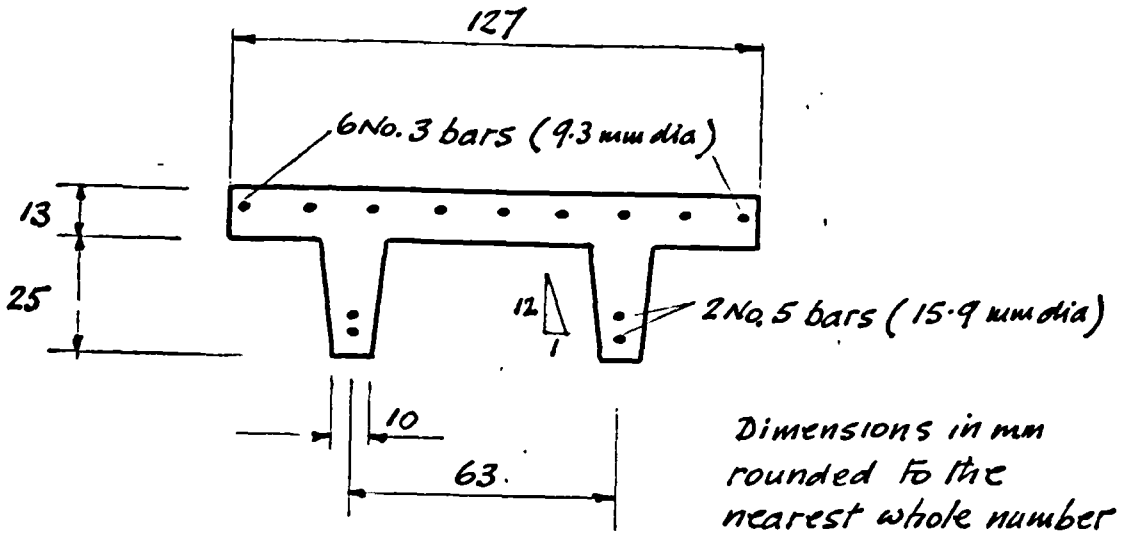
It is very difficult to arrange tests to investigate the effects of restraint on reasonable size members. However, a special furnace and loading frame was built in the P.C.A. laboratories and extensive data were obtained, during the period 1960-1968, concerning the magnitudes of the forces that could be induced during heating. (see Selvaggio and Carlson 1963 and 1966, Carlson et al 1965 and Issen et al 1970)

Most of the tests were undertaken on loaded beams with a length of 4·85m being exposed to heating from below in the furnace. A number of different cross sections were used and the procedure was to allow the beams to expand

freely through a given distance before imposing restraint against rotation and further expansion by means of hydraulic jacks which were constantly adjusted during the heating process. Some typical results, obtained on prestressed double T sections with allowed expansions of 1·3, 7·3 and 30·7mm, are shown in figure 4-8.

Referring to figure 4-8, it can be seen that, as soon as the 'allowed expansion' was taken up, longitudinal forces were induced by heating. In the early stages of heating these act well below the centroidal axis of the beam and so provide a bending moment of opposite sign to that due to the vertical loading. With further heating, the line of action of the prestressing force rises higher in the beam so that the eccentricity of the induced prestressing force is reduced. However, the magnitude of the longitudinal force continues to rise so that the section as a whole is maintained in compression. With high restraint (i.e. with small allowed expansion) it seems that creep and structural degradation combine to limit the magnitude of the induced load which, having achieved a maximum value, decreases gradually with time. Some further tests were undertaken on slabs which were restrained against expansion in the plane of the slab. Prelimimary tests indicated that this form of biaxial restraint is particularly effective in increasing the fire resistance of slab assemblies. However in one case, where almost full restraint was used, violent spalling occurred, very early in the test, and this lead to premature failure.

These results tend to support the general ideas on



DETAILS OF DOUBLE T SECTION

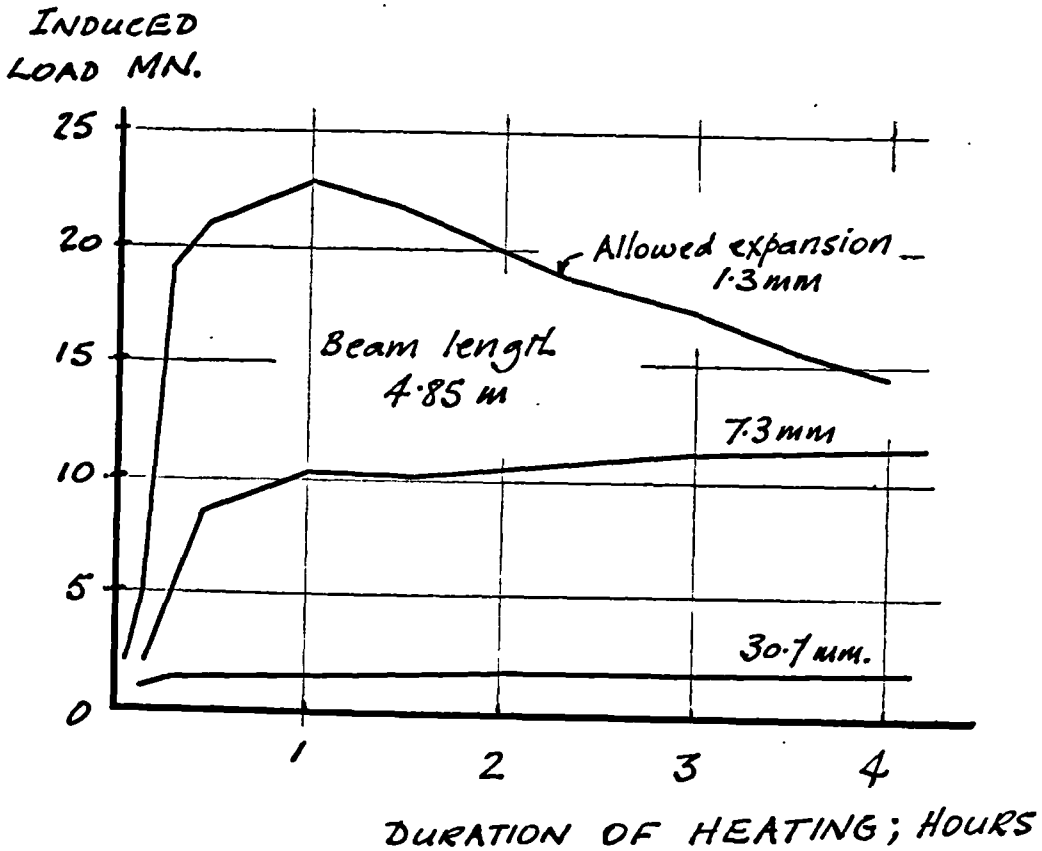


Figure 4-8 FORCES INDUCED IN A REINFORCED CONCRETE BEAM DUE TO RESTRAINED THERMAL EXPANSION after CARLSON et Al. 1965

restraint put forward by Gustaferro and Carlson (1962). The most significant conclusions are that only a small amount of restraint is necessary in order to extend the fire resistance period of a beam for several hours and that undesirable behaviour occurs only if the conditions for full restraint is approached. These conclusions are particularly important for slabs, as it can be expected that restraint will improve their structural performance, so that fire resistance will be determined by heat transmission rather than structural considerations, almost irrespective of the precise values of the loads induced. This is a considerable advantage which does not appear to be shared by protected structural steel assemblies unless these are adequately stiffened against buckling under high restraint forces.

Bletzacker (1966) has tested a number of restrained composite beams made up of a concrete flange with a steel web protected with a sprayed vermiculite-cement mixture. In most of these tests, the effect of restraint caused an increase of approximately 25% in fire endurance compared with unrestrained assemblies. However, there appeared to be a narrow range of restraint conditions when an optimum performance, giving an increase in fire resistance of around 50%, was approached. For higher amounts of restraint, failure occurred by buckling of the steel web and this must be prevented if satisfactory performance is to be obtained for a wide range of restraint conditions.

The results of the P.C.A. tests suggest that if sufficient restraint can be guaranteed, the amount of cover

provided to the reinforcing steel is no longer critical and the occurrence of spalling, with consequential exposure of the steel to the direct effects of fire need not be catastrophic. Again, this is a result whcih is not apparant from standard tests on simply-supported members and which suggests that the effects of spalling may be over-emphasised if the standard test is taken to be relevant to continuous construction.

The work on restraint has some very encouraging implications for concrete construction, However, there are one or two points that require further investigation. For instance, Dougill (1970[a]) has suggested that the early stages of heating may be critical for a lightly loaded beam heated under restraint. Here tensile stresses may be induced at the top of the beam, because of the large eccentricity of the thermally induced loading, which could lead to cracking and premature failure. Also. there seems to be a need to avoid very slender construction,as this could lead to sudden failure by buckling if high restraint forces can be developed.

4·6 Conclusions

When the effects of continuity and restraint are considered, it appears that the occurrence of spalling may not be such an overwhelming influence on fire resistance as might be thought from tests on simply supported unrestrained members. Situations where local spalling occurs to expose the reinforcement are improved by restraint and continuity. However, high restraint may lead to general or destructive spalling and if this happens it is

particularly serious as the destruction of a wall slab or floor panel allows the fire to spread to another region and increases the overall danger and difficulty in controlling the fire.

Chapter 5

OBJECT AND METHOD OF INVESTIGATION

5·1 Objective

The previous three chapters have contained reviews and discussions of the strength of concrete, the properties of concrete at elevated temperatures and the significance of spalling in structures and fire testing. The principal conclusions are set out below.

a) Sudden failure should be regarded as a form of instability. In general, this should be investigated by considering the equilibrium of the entire structural system, as was done with the testing machine and Dougill's (1971) model material, in chapter 2, and the restrained column in chapter 4. Particular cases can arise, where the conditions for stability can be established by considering local behaviour only. This was done by Griffith (1920) and subsequent workers in fracture mechanics. However, it appears that the first approach must be used in investigating fracture of concrete, except when the cracks and imperfections are abnormally large.

b) There are considerable data available concerning the properties of concrete at elevated temperatures. Most properties have been observed under steady-state or quasi-steady state conditions and it is not clear whether these data are relevant to conditions involving rapid heating or steep temperature gradients. Because of this, it will be necessary to assess the information that is available, to decide how it can be used in analysis and whether more relevant data

could be obtained by testing.

c) Of all the different forms of spalling described in Chapter I (Table 1·3·1), general or destructive spalling seems likely to have the most significant influence on the fire resistance of reinforced concrete structures. In its worst form, general spalling causes complete disintegration of a member. If this occurs, in a floor slab or wall panel, the fire can spread and cause further damage. It appears that high restraint can induce, or help to promote, general spalling but that statically indeterminate structures can sustain appreciable local spalling without collapse.

The last of these conclusions suggests that most practical benefit might result from this investigation if general spalling is regarded as the principal objective. The precise method of investigation to be employed requires further discussion.

5·2 General Method

One approach to the problem of general spalling would be to test a variety of slabs, with different degrees of restraint and thermal exposure, to determine the conditions, under which spalling occurs, in terms of particular combinations and values of the listed influential variables. The work undertaken by Meyer Ottens (1965), which was described in Chapter I Section I·4, was of this kind. However, a more comprehensive series of tests would be required if the conditions controlling spalling were to be established completely. The principal advantage, of this approach, is that no knowledge is required of the mechanism

of spalling or the manner in which heat is transferred within the slab and affects the properties of the materials involved. The main disadvantage is that many different combinations of variables have to be explored and each combination requires a separate test. Clearly, the method is only viable if sufficient resources can be brought to bear and thus, this approach has little appeal until other alternatives have been tried.

At the other extreme, a theoretical approach can be used to study the factors controlling spalling. There are difficulties in this, as a mechanism of spalling must be assumed and it is necessary to have a satisfactory understanding of the thermal and structural aspects of the problem. This requires more detailed knowledge, of the behaviour of concrete at high temperatures, than is currently available. Thus, the results of an anlysis must be checked by experiment or at least compared with experience from fires and fire tests.

Fortunately, it is possible to divide the investigation into two stages dealing with the thermal and structural aspects respectively. In this way, some of the effects of the uncertainties in the materials data are eliminated as the results of an anlysis of the thermal conditions can be tested directly by experiment. Thus, the first stage of the work comprises,

1) experiments in which temperatures are measured in typical slabs during heating in a prescribed manner

and 2) an analysis of the thermal conditions of the

tests and a comparison of the temperatures found by analysis and experiment.

The principal objective of this stage of the work is to produce a method of calculation that gives results for the temperature distribution that correspond reasonably well with those measured in slabs during heating. It would be an advantage if the physical processes of heat transfer were fully described in the analysis. This is not absolutely necessary, however, as the success of the structural investigation will depend more on the actual values of temperature than the method by which these are obtained.

Once a satisfactory solution to the thermal problem is available, the method of analysis can be used to provide the temperature distributions, as data, in an analysis of the structural conditions in typical slabs. In this way the investigation of general spalling is concluded by

3) developing a method of analysis for the structural behaviour of a floor slab or wall panel during the early stages of heating and

4) using the methods of analysis, for thermal and structural behaviour, to investigate the effects of the major controlling variables.

5·3 Choice of Variables

Before discussing the background to the analysis in more detail it is convenient to list the variables that need to be studied. These may be separated into three categories in the following manner

a) Slab Specification

Slab thickness

Reinforcement: quantity and disposition

Axial and Flexural Restraint

Edge Loading

Initial moisture distribution

Initial stress or strain

b) Materials Data

Individual properties of the concrete and reinforcement (i.e. thermal expansion, Young's Modulus etc.) and their variation with temperature.

c) Ambient conditions

Rate of rise of ambient temperature

General pattern of heating: heating on one or both faces.

Local variations in the heating pattern: effect of hot spots etc.

In this list, the form of the variables is determined by the type of investigation proposed in Section 5·2. Thus, the concrete materials data are expressed directly in terms of properties, rather than by specifying the constituent materials, mix proportions and curing conditions as might be done in a purely experimental investigation. This has the advantage that the influence of different properties can be studied separately although some care is necessary to ensure that any particular combination of variables is a possible combination for concrete.

Not all the variables in the list will be studied in detail. In particular, the effects of reinforcement will not be considered and the standard rate of ambient temperature rise specified in I.S.O. 834 will be adopted in the work to be described.

5·4 Status of the Analysis

The main point of the analysis is to identify a mode of instability that corresponds to general spalling and to investigate the influence of the controlling variables on the incidence of this instability. The main difficulty in this work follows from the uncertainity in interpreting the available experimental evidence, on the behaviour of concrete, and in extending these results to conditions of rapid heating.

Some of this uncertainty could be resolved by additional testing but some questions must remain because there are physical limitations to what can be measured in a material like concrete. This occurs because the properties of concrete must be found from tests on reasonably large samples in order that the test specimen is representative of the bulk material. The minimum representative volume is not necessarily the same for different properties (Brown 1965) but must be large when compared with the size of the aggregate. For example, it is generally assumed that the length of the sides of cubes or prisms, used for compression tests on concrete, should not be less than five times the maximum aggregate sizes. The size of specimen limits the rate of heating that can be employed in a test. If the

specimen is large, only a gradual rise in temperature can be tolerated, otherwise, high temperature gradients and stresses are developed and breakdown of the material occurs.[+] Thus, if tests are to be undertaken using fast heating rates, small specimens must be used. This is not possible with concrete and the minimum representative volume determines the maximum heating rate that can be used in the test. Inevitably this rate will be much slower than that experienced near the heated surface of a wall panel exposed to a fire. Thus it appears to be almost impossible to measure a bulk property of concrete when the rate of heating approaches that experienced in a fire. Also, even if such measurements were made, there would be no accepted way in which these results could be applied in the regions, where the temperature gradient is very steep, near the heated face of a heated member. These difficulties are fundamental to any investigation in which the composite nature of concrete is disregarded and the material is taken to be a continuum. However, it is considered than any alternative approach is likely to be impracticable at the present time.

Bearing these difficulties in mind, the results of the analysis will have to be treated with some reserve.

Footnote [+]

A dimensional analysis suggests that the stresses developed in geometrically similar specimens of the same material are proportional to the rate of heating and to the square of the linear dimensions.

However, it is anticipated that the theoretical approach will be capable of distinguishing between broad classes of behaviour, although the numerical results obtained may not be precise in all details. In addition, the availability of the theoretical approach enables conceptual experiments to be performed that may help to isolate the most critical variables and so suggest ways to lessen the problem of general spalling.

Chapter 6

FIRE TEST ON A CONCRETE WALL PANEL.

6·1 Introduction

The object of the work reported in this chapter was

1. to obtain temperature histories for a number of wall units heated under identical conditions

and 2. to observe qualitatively which concretes are most liable to breakdown or fracture under thermal stress.

In the event, little or no breakdown of the concrete occurred within the first half hour or so of heating and the damage, observable after cooling, comprised some minor surface disintegration, tesselated shrinkage cracks and considerable irrecoverable curvature. Thus the second objective could not be realised. However, a wide range of concrete compositions were used in the tests and it is considered that the temperatures recorded are typical and must include those thermal conditions under which spalling is possible.

6·2 Test and specimen details

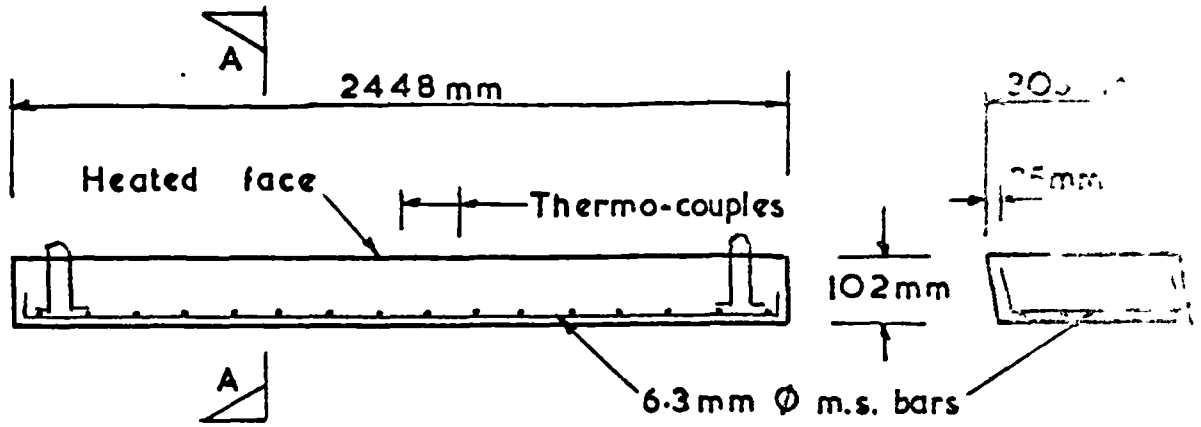
The test consisted of heating one side of a wall panel, comprising eight separate concrete planks arranged as shown in figure 6-1,in the wall furnace at the Fire Research Station, Boreham Wood, England. This figure also shows the details of the planks which were each 100mms (4 inches) thick, of a rhomboid section and containing six 26 S.W.G. chromel/ alumel thermo-couples. The rhomboid section was chosen to lessen the possibility of radiation, or passage of flame, through the longitudinal joints where the planks butted together. As an additional precaution, these joints were stuffed with asbestos rope. These measures were successful.

The planks contained no reinforcement in the heated face, which was uppermost during casting, but lifting hooks were provided together with nominal reinforcement near the cool face (cover 12mms,1/2 inch). The slabs were cast in timber formwork at Imperial College, London, and cured by storing under wet sacking for the first week after casting and in air thereafter. Details of the formwork are shown in figures 6-2 and 6-3. The slabs were cast during March and April 1962 and finally tested at the Fire Research Station on 27th July 1962.

The aggregate used was a 12mm down irregular river gravel of which approximately half was retained on a 5mm sieve. Details of the aggregate grading are given in Table 6·1. The mix proportions, age at test and strengths of the concrete used in each plank are given in Table 6·2.

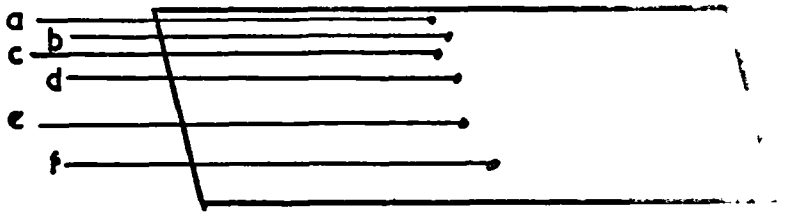
During the test, the temperature of the furnace was controlled by adjusting the gas supply so that the standard exposure condition was obtained, (i.e. to B.S. 476 Part I: 1953 - Fire Tests of Building Materials and Structures). This was clearly difficult to arrange during the first 10 - 15 minutes of heating and there was also a variation in temperature, between different points in the furnace, of around ± 50°C about the normal specified curve (see figure 6-4)

The temperatures within the planks were recorded using four 12 channel potentiometric pen recorders (two planks to each recorder). A few days after the test, an unsuccessful attempt was made to check the actual position of the thermo-couples, near to the surface, by chipping away the damaged concrete to expose the thermo-couple bead.



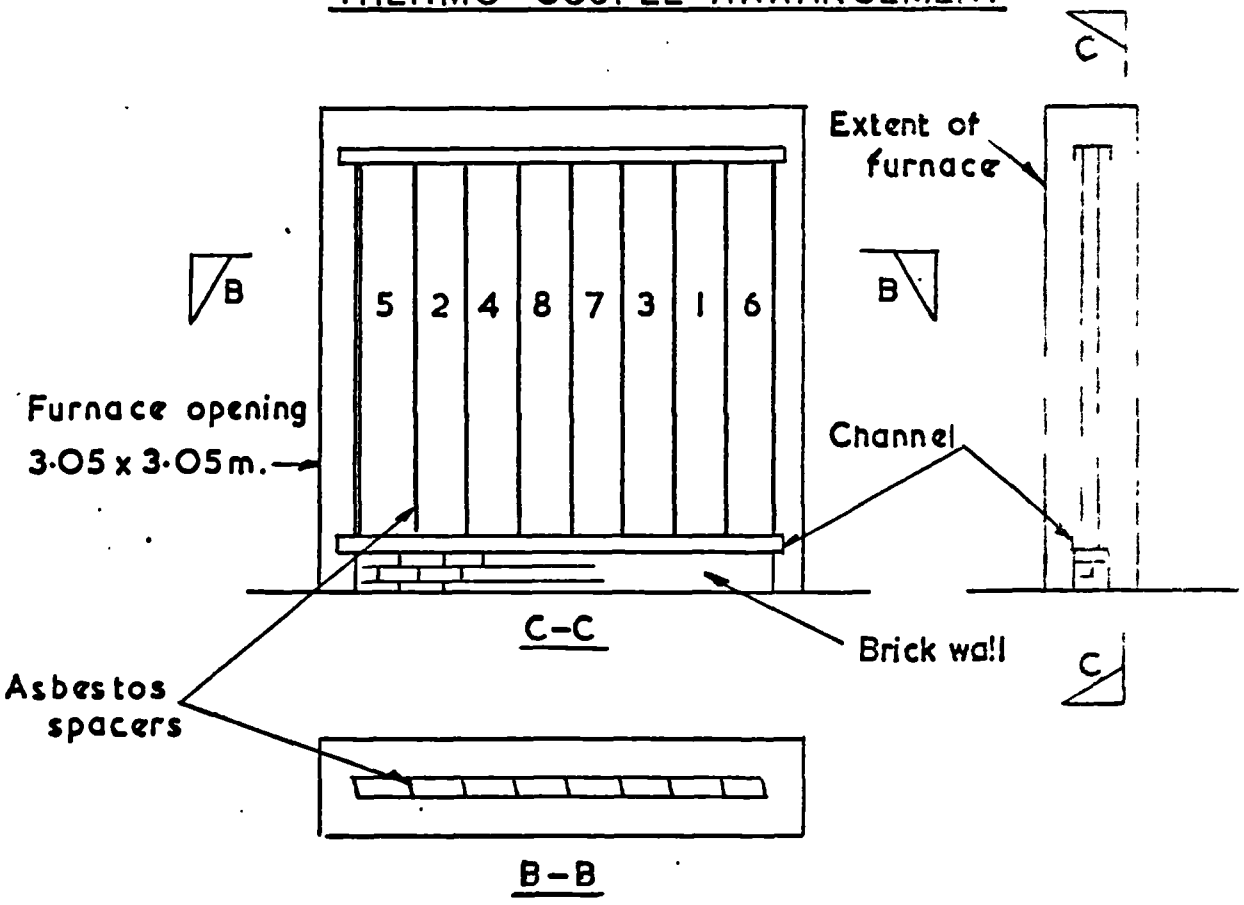
PLANK DETAILS

Thermo couple	Distance from hot face 1/8 in	mm
a	1	3
b	3	9.5
c	6	19
d	11	35.
e	18	57
f	26	82



Thermo couples from 26 s.w.g. chromel

THERMO COUPLE ARRANGEMENT



ARRANGEMENT OF UNITS

FIGURE 6-1 GENERAL DETAILS OF THE FIRE

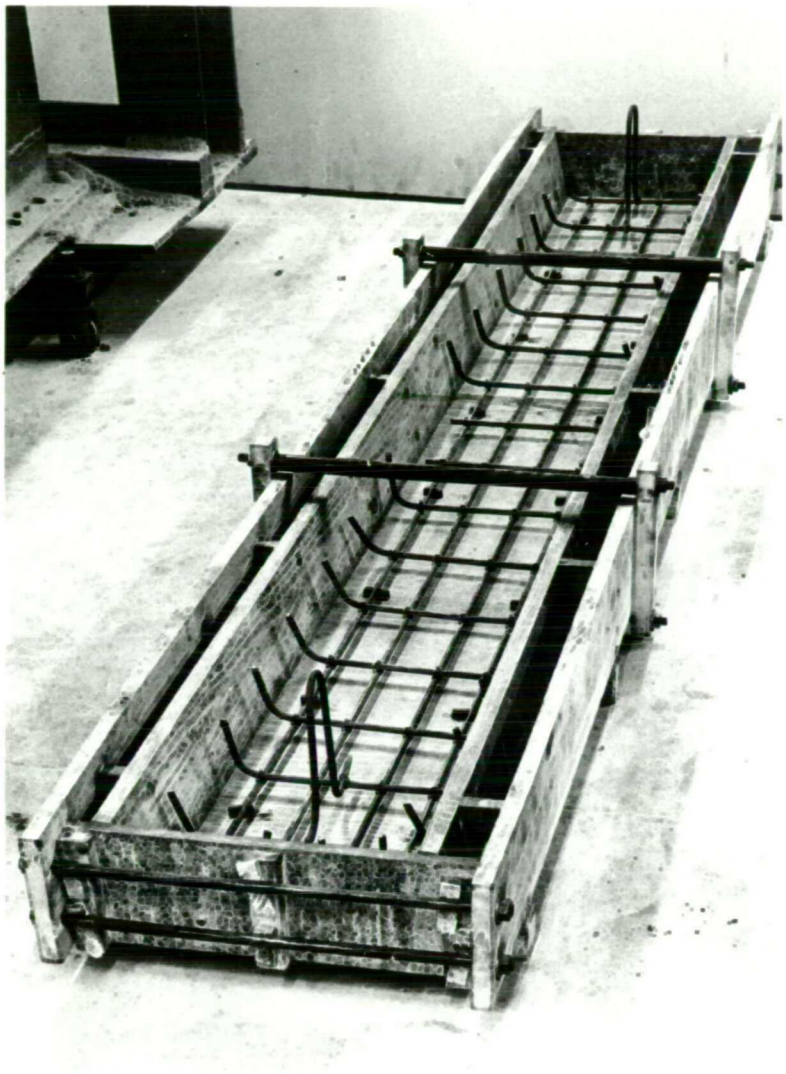


FIGURE 6-2 GENERAL VIEW OF THE FORMWORK AND REINFORCEMENT USED IN THE CONCRETE PANELS

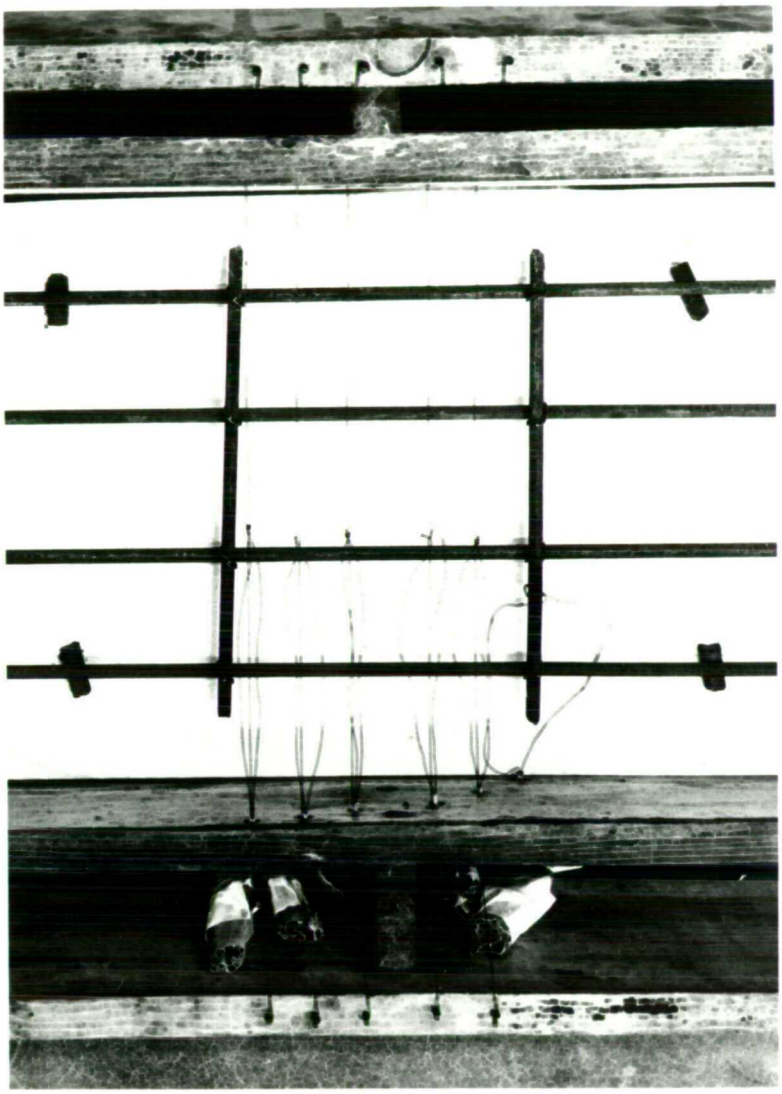


FIGURE 6—3 ARRANGEMENT OF THE THERMO-COUPLES USED IN EACH PLANK

NOTE : For the purpose of the photograph only, a piece of white paper has been placed in the bottom of the mould.

Table 6•1	Aggregate Grading								
B.S.Sieve	3/4	3/8	3/16	7	14	25	52	100	200
size in mm	19	9•5	5						
% Passing	100	93•4	55•4	40•7	29•4	20•0	5•0	0•8	0•2

Irregular river gravel in bone dry condition, Absorption 3%

Table 6·2 Concrete Mix Proportions

Slab	A/C	Total W/C	Age at test-days	Cube strength N/m^2
1	4·5	0·625	140	41·3
2	6·0	0·722	135	37·2
3	4·5	0·675	133	35·3
4	6·0	0·775	128	29·1
5	3·0	0·500	126	56·1
6	3·0	0·450	114	66·1
7	4·5	0·700	112	31·6
8	6·0	0·850	107	23·1

Aggregate/cement and water/cement ratios by weight. Cube strength from the average of four results from tests on 100mm (4 inch) cubes.

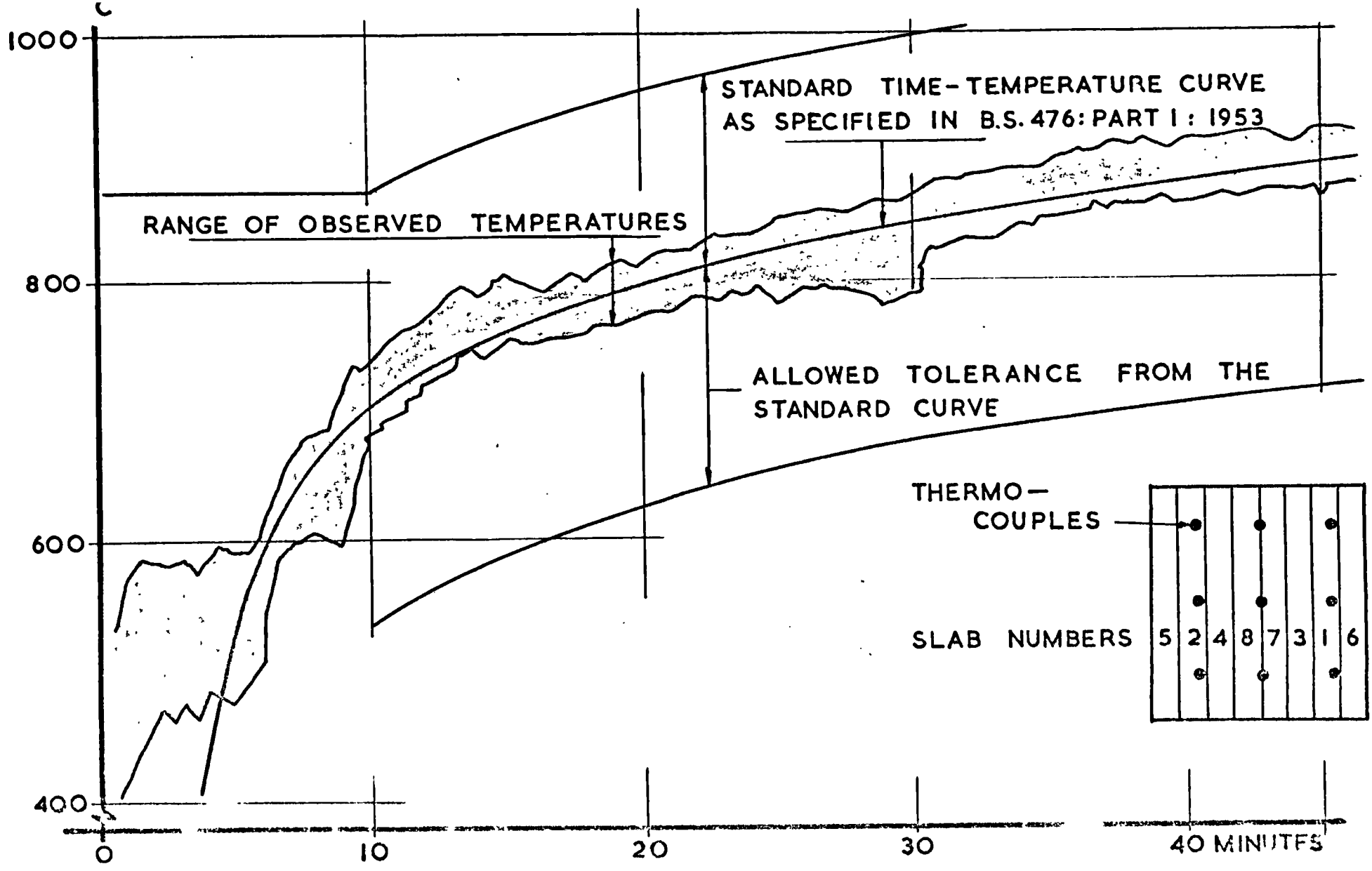


FIGURE 6.4 VARIATION IN FURNACE TEMPERATURE DURING THE FIRE TEST

6·3 Results and Observations

Figures 6-5 to 6-12 (pages 174 to 181) have been prepared from the original strip chart records to show the development of temperature in each slab during the first 40 minutes heating. The form of these results is the same for each of the slabs although the temperature rise recorded in slabs 1, 5 and 6 is appreciably less than in the remainder. It is seen from figure 6-1 that planks 5 and 6 were the two edge units in the assembled wall with plank 1 being placed next to 6. From this, it seems possible that there may have been some heat loss from the edges of these units and that the temperatures recorded are not truly representative of unidirectional heat flow conditions.

At any particular depth, the temperatures recorded in each of the remaining slabs are remarkably similar. This is shown in figure 6-13 which gives the range of values of temperature obtained at each depth for slabs 2,3,4,7 and 8. In some ways, this result could have been anticipated from the available information on thermal properties (Ch. 3 p. 10[illegible] et seq.) and it may be supposed that major changes, in the temperature distribution under standard conditions, will be obtained only if different aggregates or cements are used and that the effect of mix proportions is of secondary significance.

Again referring to figure 6-13, it will be noted that the greatest differences in temperature occur at the two points nearest to the heated surface. Here, the temperature gradient is very steep and any error in positioning the

thermo-couples, either in fixing, during casting or when finally 'finishing' the surface would have most effect on interpreting the thermo-couple results. It appears, from subsequent theoretical work, that an error of ± 1mm in the position of the thermo-couple near the surface could in itself provide a scatter of 50°C. From this, it appears that not too much significance must be attached to results obtained near the heated surface.

Little of a dramatic nature occurred during the test. After about 12 minutes, steam was emitted from the hot face. At 15 minutes from the start of heating, the unheated face was already warm to the touch and the planks showed noticeable curvature. Also at this time, there was some splitting and the appearance of a few blow holes in the hot face. Rather later, after 25 minutes heating, free water appeared at the cooler face and continued to be driven off for some while.

6·4 Consideration of Drying

The formation of steam within the concrete creates a dry zone next to the hot face and a wet zone of varying saturation throughout the remainder of the thickness. Vapourisation occurs at a temperature rather greater than 100°C at the interface between these zones which thus move away from the hot face. The rate of temperature rise is momentarily halted at the interface during vapourisation, thus giving rise to the steps, or gradually sloping ramps, in the temperature-time curves of figures 6-5 to 6-12. These features provide a means to obtain a crude indication

of the depth of the dried zone and the temperature at which vapourisation occurs. On this basis, it appears that the maximum temperature at the interface was around 150°C and that this occurred 19mm from the surface at about 15 minutes from the start of heating. At this temperature the pressure of saturated steam is 0·38 MN/m^2 above atmospheric, which must be considerably below the tensile strength of the concrete used.

6·5 Fire Resistance

All the eight slabs tested could be rated as having a two hour fire resistance period based on the temperature rise at the cooler face. This is a better performance than might have been expected: for instance, Abrams and Gustaferro (1968) find that a naturally dried 4 inch (100mm) thick slab using siliceous aggregate gave a fire endurance of only 1·3 hours.

6·6 Spalling and Conclusions

Very little surface deterioration occurred in the tests and there was no explosive spalling. The maximum size of the aggregate used was only 12mm and this may have contributed to the good performance of the slabs by reducing the occurrence of aggregate splitting (see Chapter 11 and Dougill 1965). Also, the concrete was comparatively young, in the context of fire resistance tests, and thus may have been more than usually permeable so preventing the generation of high pore pressures. However, the limited data available (Ruettgers et al 1935) suggest that the gross changes in permeability, that occur during the early

stages of hydration, were over and that the permeability would be at least comparable with that in a more mature concrete.

In comparing the performance of the planks with that of a slab or wall unit, it is clear that there are differences in the state of stress induced by heating and thus the conditions at failure. However, it is considered that these differences are not of major importance and that, in considering local phenomena at least, the behaviour of the slabs and a complete panel are directly comparable.

Although the same siliceous aggregate was used in making all eight planks a wide variety of mix proportions were used. These gave nominal compressive strengths ranging from those used in normal structural concrete to values higher than are generally used in prestressed concrete construction. In spite of these differences in concrete quality, the temperature distributions in different planks were remarkably similar. This is a useful result as it appears that it will be reasonable to adopt a single standard set of thermal properties in deriving data for use in the structural investigation. In this way the number of variables to be considered in assessing the causes of spalling, in concrete panels made with siliceous aggregates, is very much reduced.

6·7 <u>Acknowledgement</u>

The test described in this chapter could not have been performed without the help and co-operation of the

staff of the Fire Research Station. In this connection, the author is particularly grateful to Mr L.A.Ashton for making the facilities available and to Mr H.L.Malhotra, for his considerable help and guidance with the fire test.

FIG. 6-5

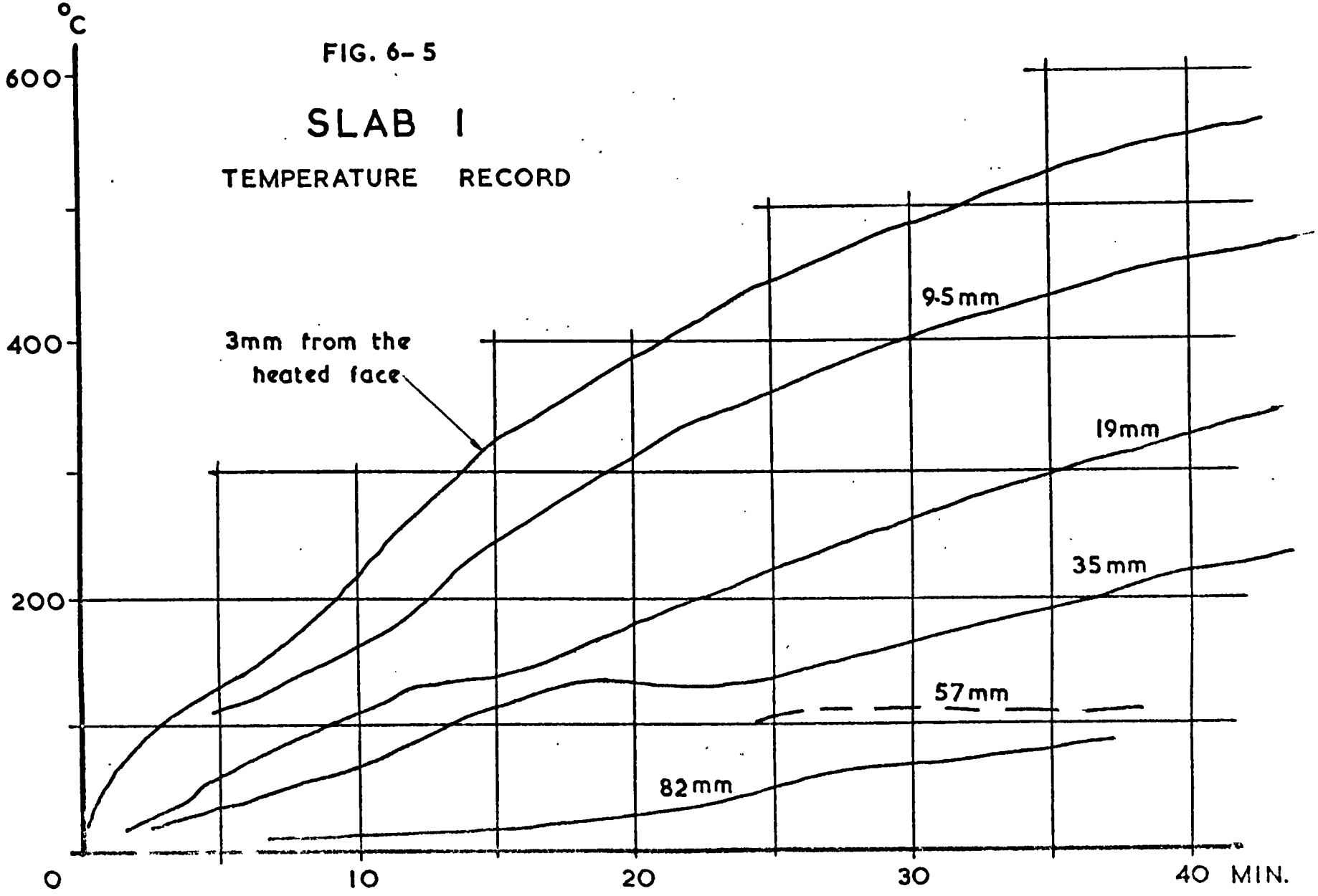

°C
600
400
200
0
10
20
30
40 MIN.
SLAB 1
TEMPERATURE RECORD
3mm from the heated face
9.5mm
19mm
35mm
57mm
82mm

FIG. 6-6

SLAB 2

TEMPERATURE RECORD

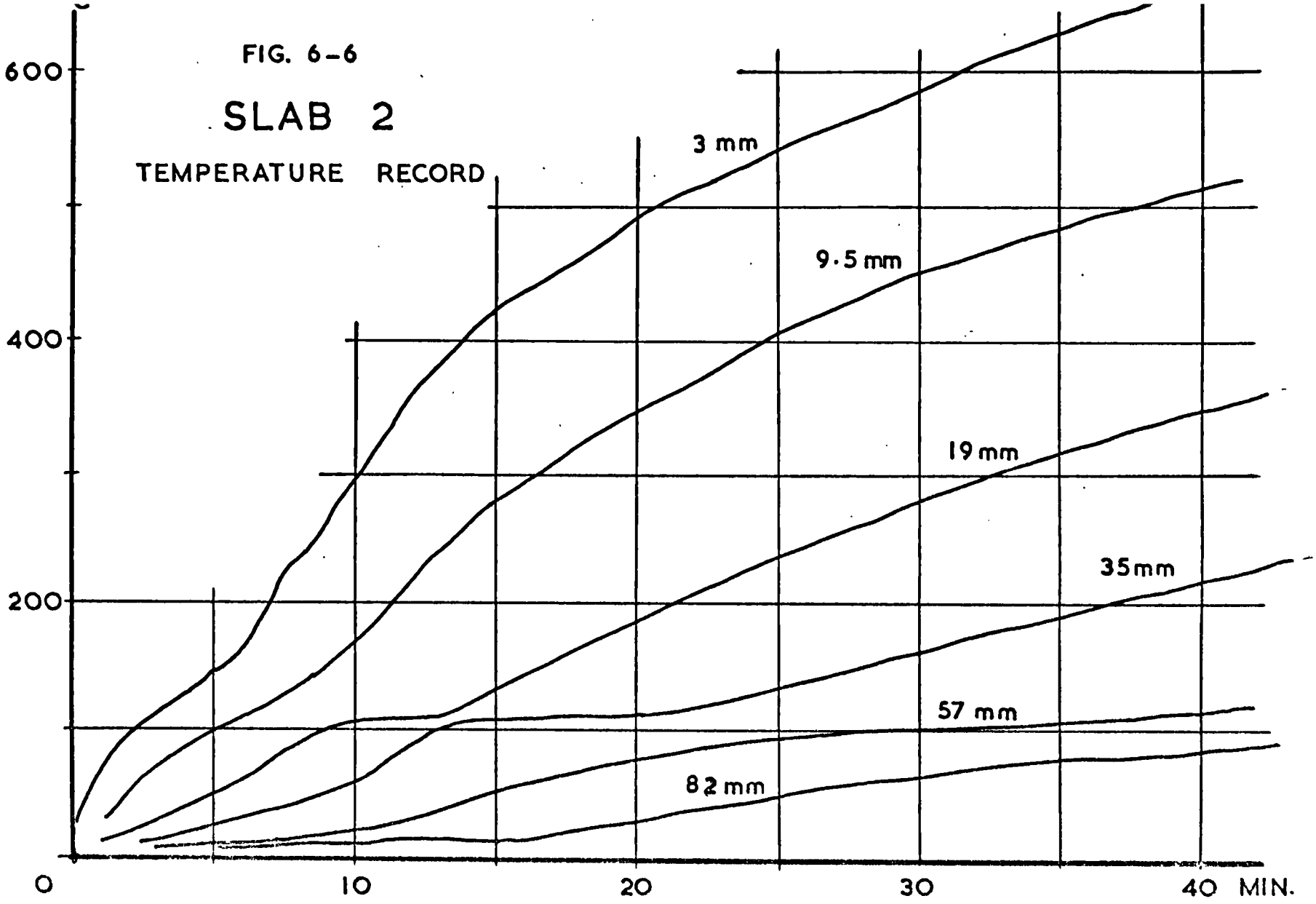
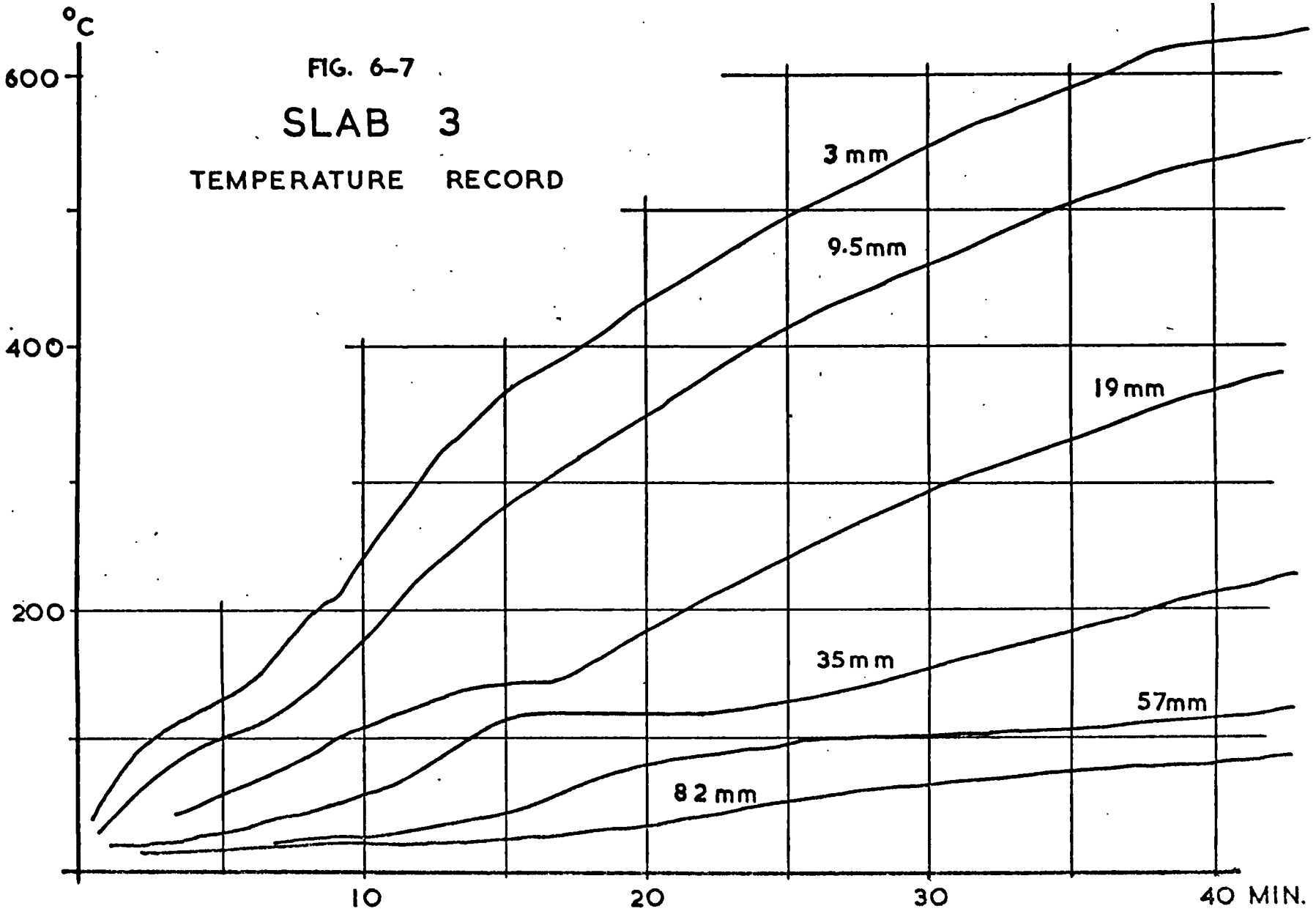


FIG. 6–7

SLAB 3

TEMPERATURE RECORD



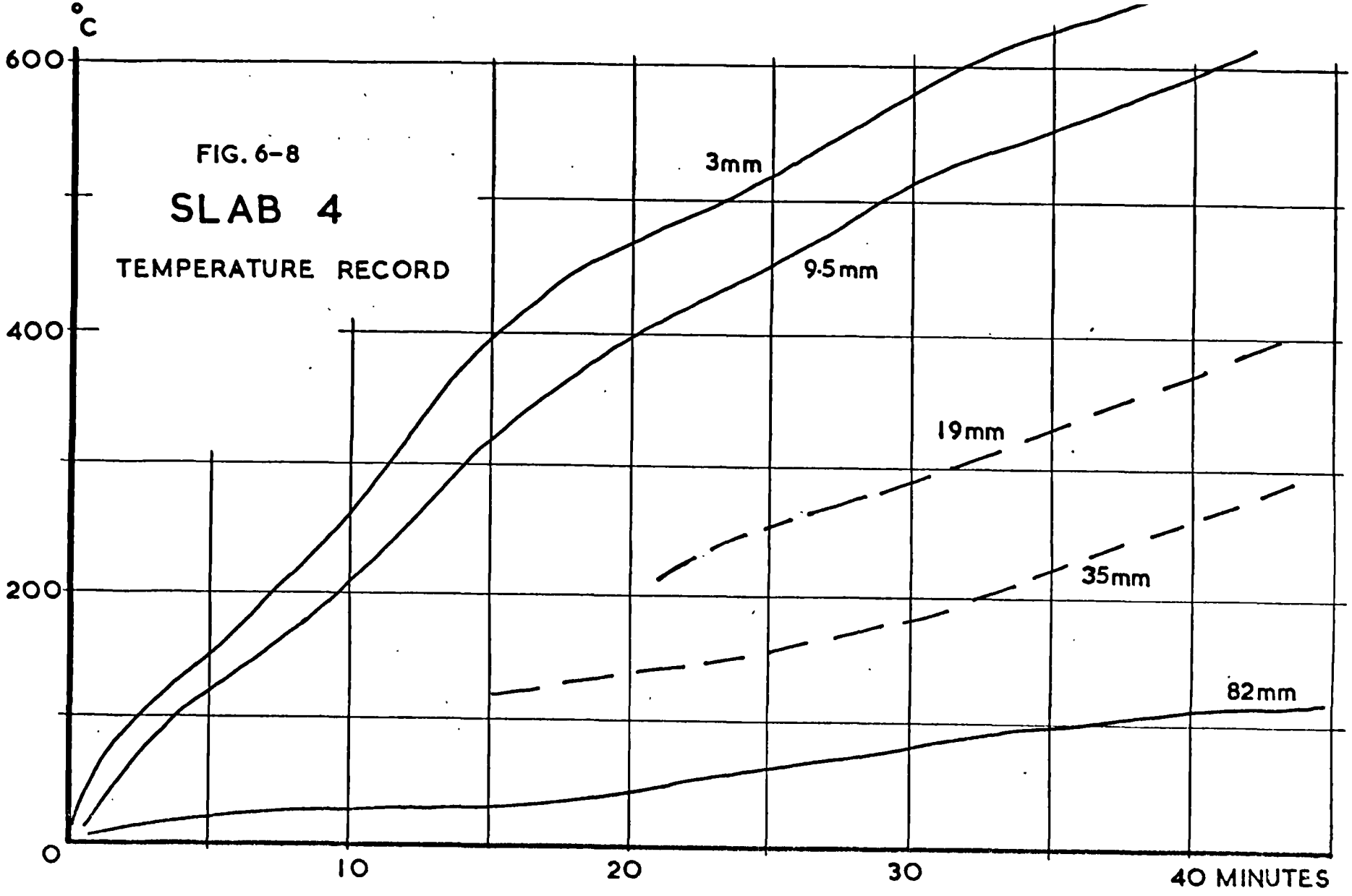


FIG. 6-8

SLAB 4

TEMPERATURE RECORD

FIG. 6–9

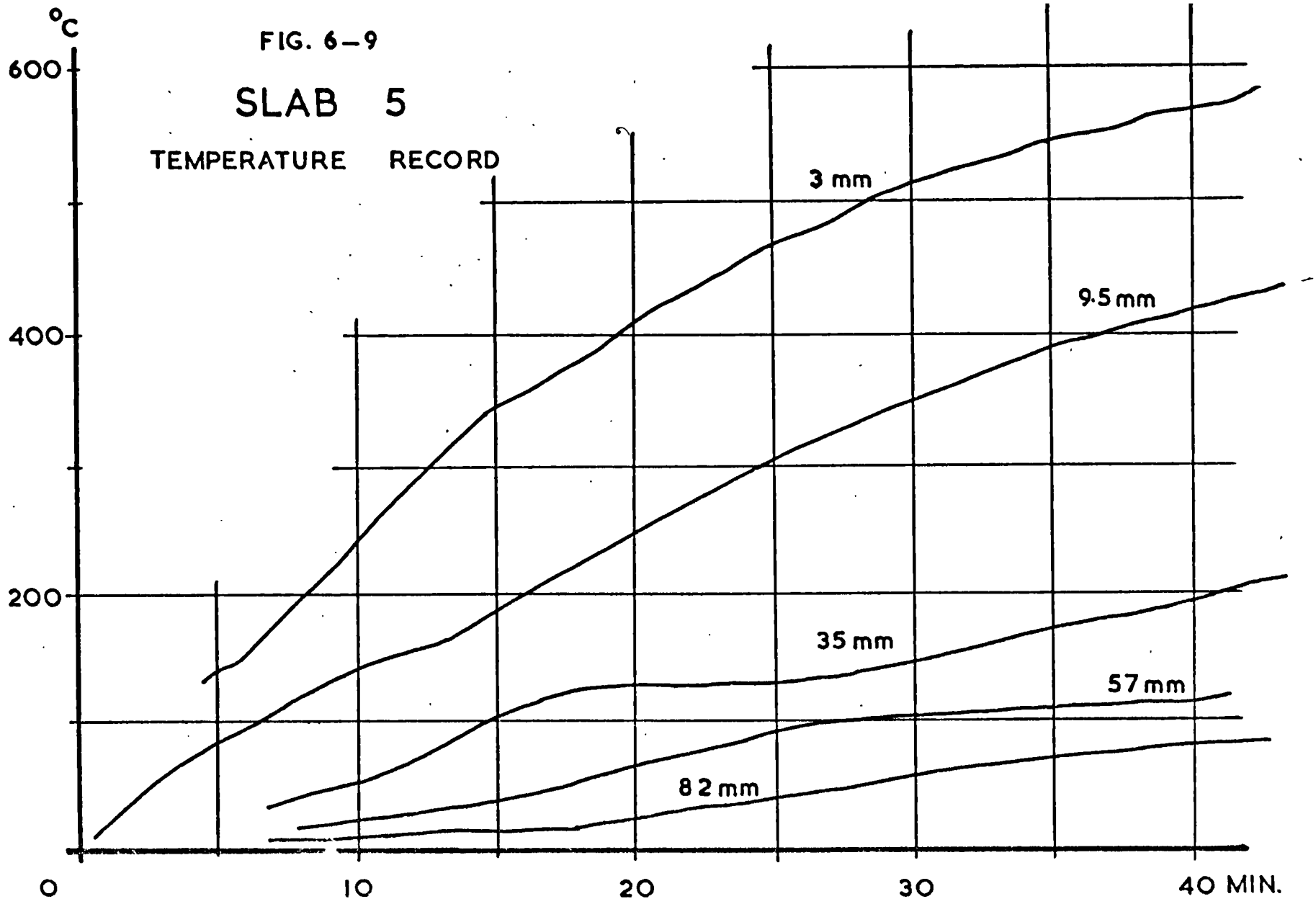
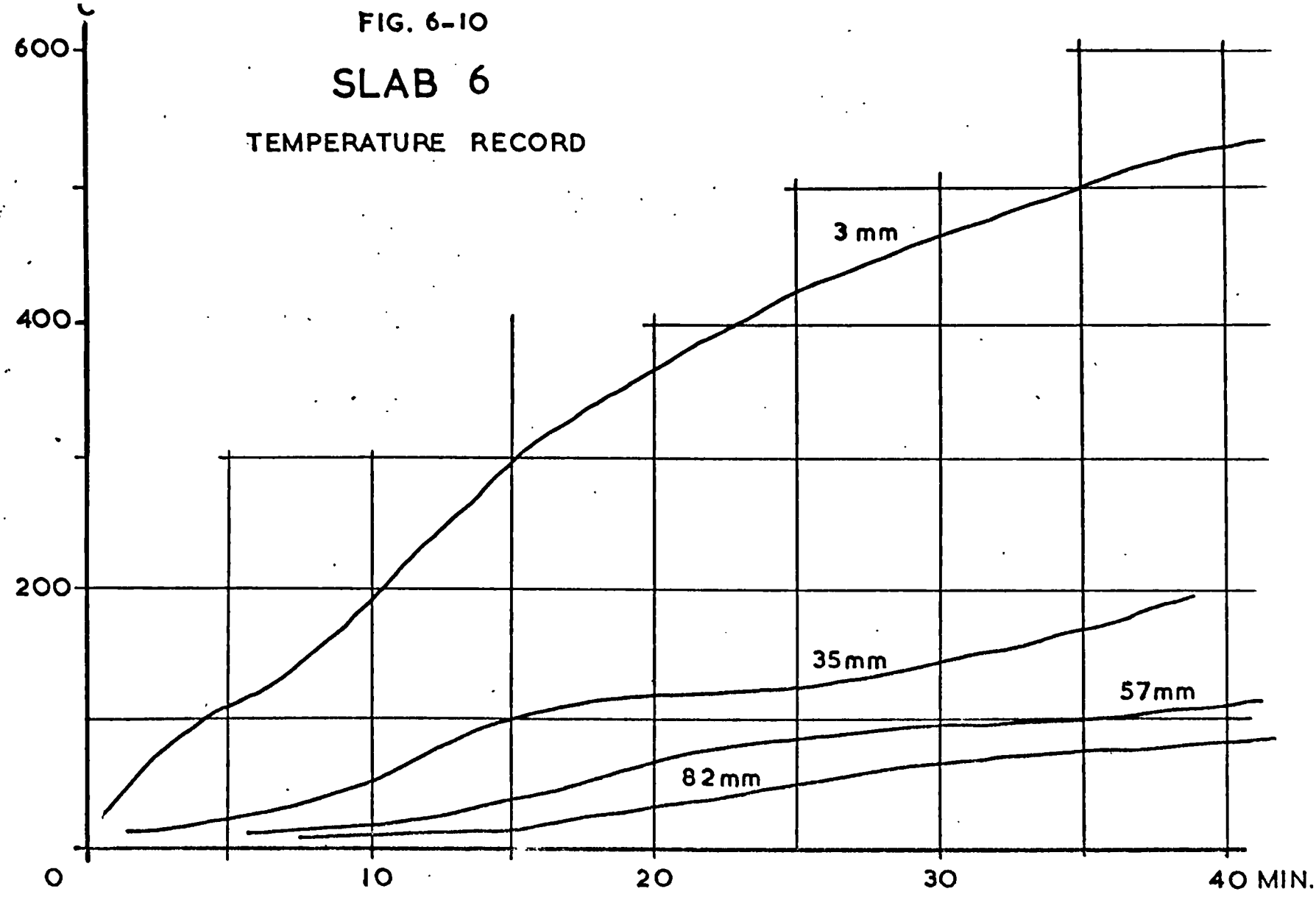

SLAB 5
TEMPERATURE RECORD
°C
600
400
200
0
10
20
30
40 MIN.
3 mm
9.5 mm
35 mm
57 mm
82 mm

FIG. 6-10

SLAB 6

TEMPERATURE RECORD



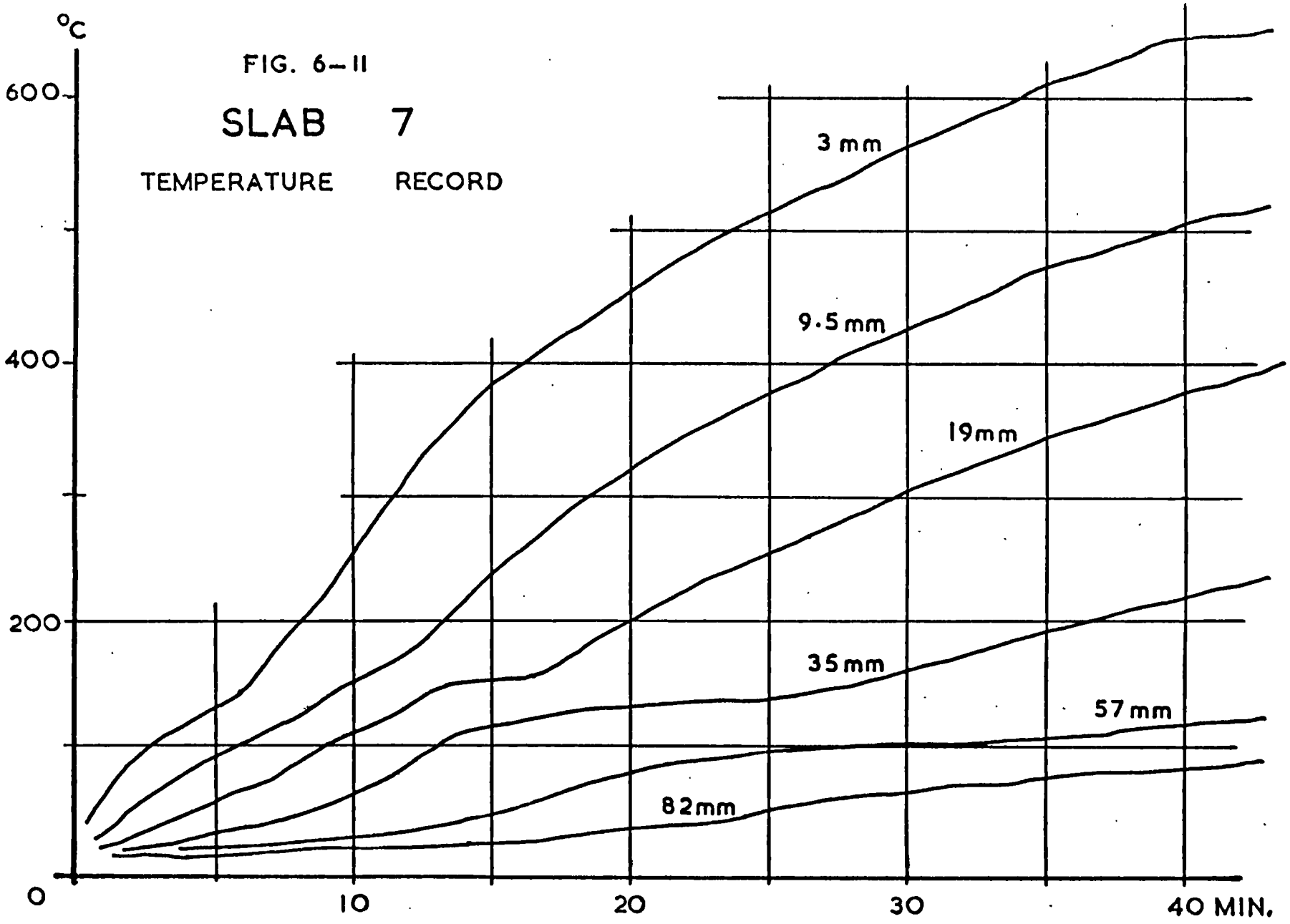


FIG. 6–11

SLAB 7

TEMPERATURE RECORD

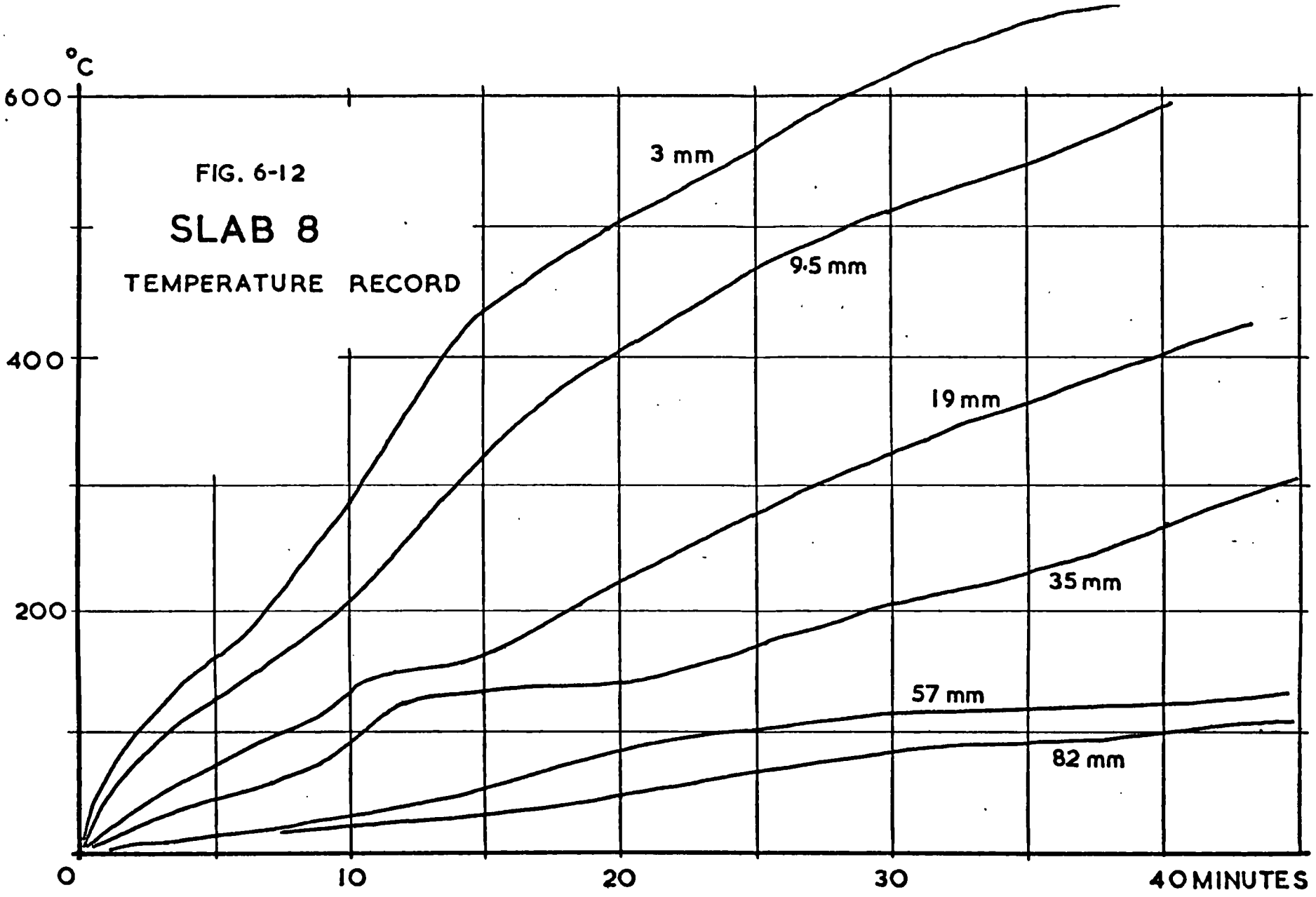


FIG. 6-12

SLAB 8

TEMPERATURE RECORD

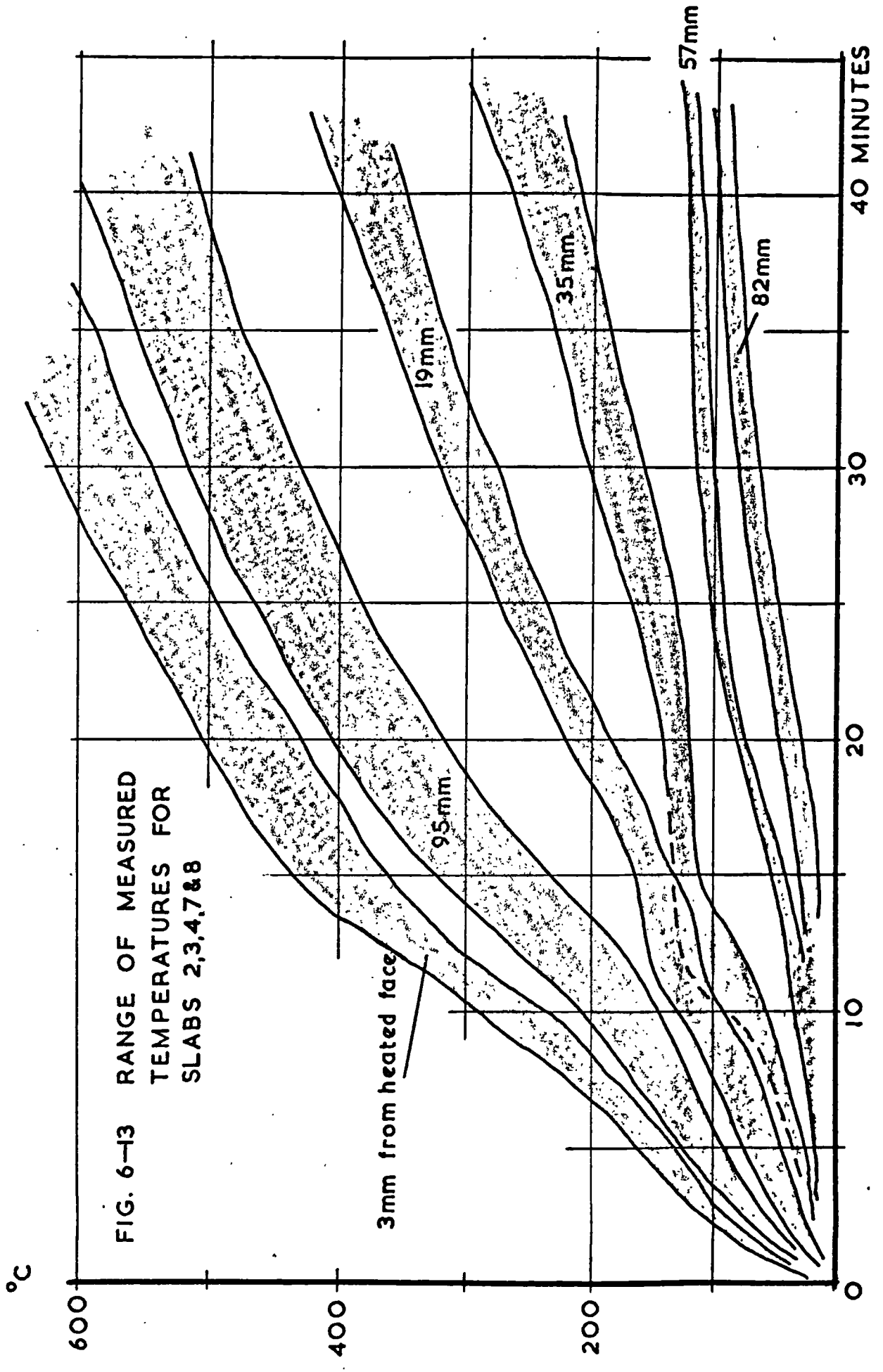


FIG. 6–13 RANGE OF MEASURED TEMPERATURES FOR SLABS 2,3,4,7&8

Chapter 7

THERMAL CONDITIONS: THEORETICAL CONSIDERATIONS

7·1 Introduction

The results of the experiments described in the previous Chapter provide a useful background to an investigation into the temperatures developed in concrete units during heating. However, the fire resistance test is inconvenient and interpretation of the results is difficult if the temperatures are obtained at only a few isolated points within the specimen. Thus, there are advantages to be gained if a theoretical approach to this problem can be developed. Such an approach would have a direct use in estimating the fire resistance of those separating members that remain structurally sound during heating and could also be used to investigate the effects of a whole range of variables in conditions different from those obtained experimentally with the equipment normally available in fire test laboratories.

The object of the work reported in this chapter is to develop a method for determining the temperatures developed in a plain concrete wall panel during heating. The results will be compared with the experimental results presented in the previous chapter.

7·2 Assessment of the Problem

The transfer of heat in concrete will generally be accompanied by movement of moisture, in some form, within the pore structure of the material. This process has been described in qualitative terms, when discussing moisture clog spalling (in chapter 1), and it is clear from this description that the problem of determining temperatures is a difficult one. The heat and moisture transfer

problems are connected by the heat required for vapourisation and the associated pore pressure gradients. In addition, the pore pressures developed will depend on the permeability of the material and this will be influenced by the state of stress and the possible occurrence of micro or macro-cracking in the concrete. Thus, the heat transfer, moisture transfer and structural problems should ideally be regarded as a single problem. This combined problem is very difficult and it is not clear how it could be formulated or solved. In these circumstances it is necessary to idealise the situation in some way in order to make it amenable to analysis.

The most sweeping idealisation is to neglect the effects of moisture entirely. Even on these terms the problem is not trivial, because of the difficult boundary conditions, and solutions are obtained only by using an electrical analogue (Lawson and McGuire 1953, Robertson and Gross 1958) or in numerical terms (Robertson and Genensky 1956). Such solutions may be useful in comparing the effects of different exposure conditions but the neglect of moisture means that only a rough estimate can be made, in this way, of the fire resistance of concrete members.

The problem has been treated in a more nearly satisfactory fashion by Harmathy (1961). Here the analysis is undertaken in numerical terms with due account being taken of the latent heat of vapourisation and the variation of the thermal properties of the concrete with temperature. The main idealisation occurs in the treatment

of vapourisation. This is simplified by ignoring any pore pressure gradients together with the possibility that vapour liberated at the interface with the dry zone may be readsorbed in the cooler regions. Vapourisation is assumed to occur at atmospheric pressure and the liberated vapour is assumed to have negligible heat capacity and to escape freely through the dry zone.

These assumptions seem reasonable. However, there are some details in Harmathy's numerical treatment that appear dubious and his results may not be as satisfactory as should be possible using these assumptions. The main difficulties occur in dealing with the hot face boundary condition and with the conditions at the moving interface. In the following sections, an attempt is made to resolve these difficulties in an improved treatment of the problem based on Harmathy's assumptions.

7·3 Problem specification

Consider the slab of thickness d shown in figure 7-1. We require to find the temperatures throughout the thickness of the slab when heat is supplied to the face $z = 0$. The rate of heating is described by a specified rise in ambient temperature outside the hot face and the initial temperatures are taken to be equal to the ambient temperature that obtains before the start of heating. The initial moisture distribution must be prescribed.

Some time after the start of heating the wall is divided into a dry zone and a wet zone. Vapourisation occurs at the interface, between these zones, which moves into the wall so increasing the size of the dry zone.

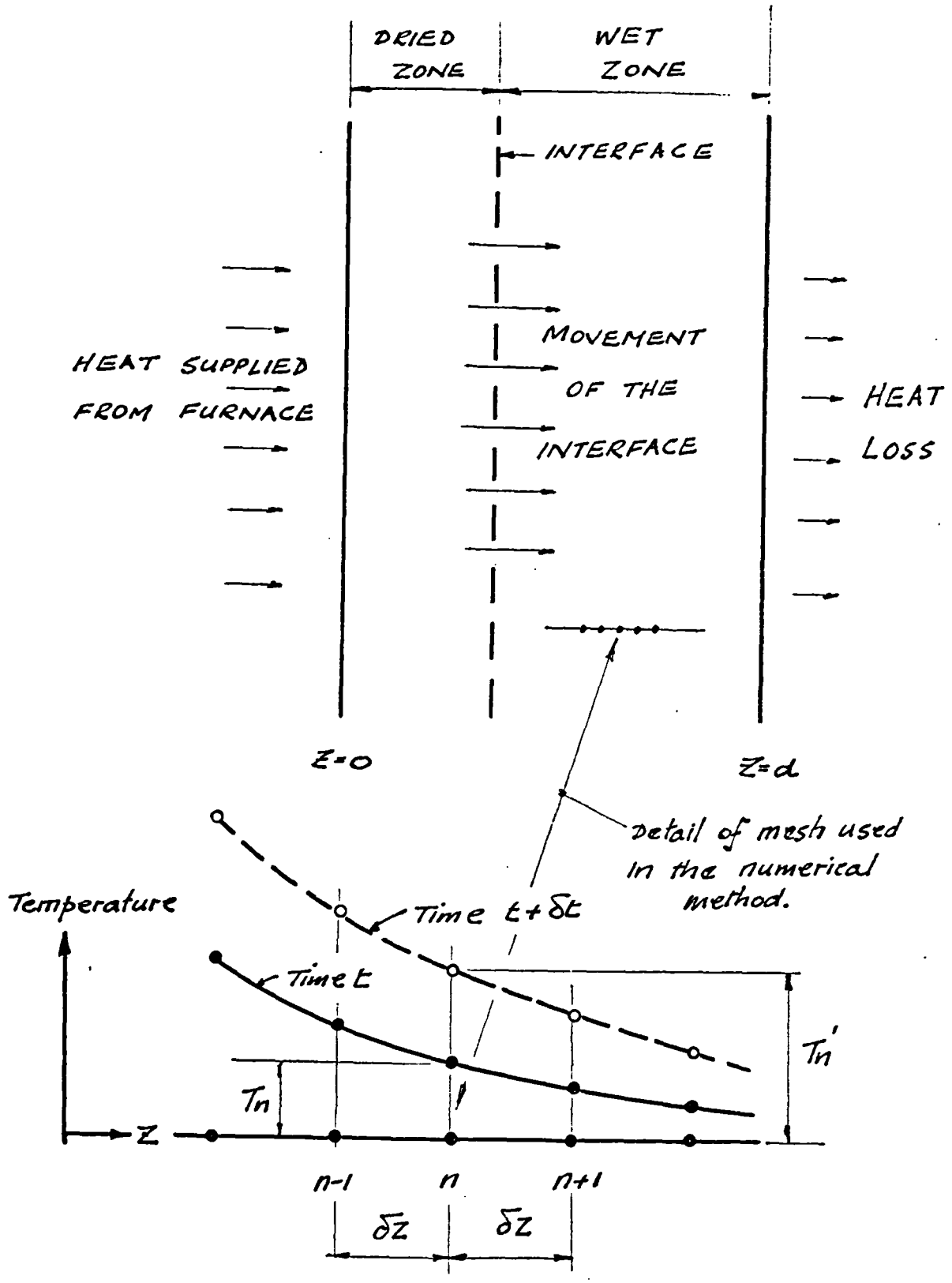


Figure 7-1 PRINCIPAL FEATURES OF THE HEAT TRANSFER PROBLEM

The temperature in the wet zone will generally be less than 100°C and, as the detailed mechanism of moisture transfer is to be ignored, it seems reasonable to adopt constant values for the thermal properties of the concrete in this zone. Constant values are also adopted for the properties of the concrete in the dry zone. In a more refined analysis, these properties would probably be taken to be functions of temperature but such precision seems hardly justified under the present assumptions, particularly when it is realised that drying penetrates to a depth of only a few inches, in most fire tests.

The above assumptions deal with heat transfer within the wall. The conditions at the boundaries are now considered.

Heat is transferred from the surroundings by both convection and radiation. In these circumstances, it is convenient to express the heat flux q entering the wall in the form

$$q = h_s (T_a - T_s) \qquad (7\cdot3\cdot1)$$

where T_a is the ambient temperature and T_s is the temperature of the surface. The quantity h is the surface heat transfer coefficient and this can be regarded as the sum of the individual coefficients, h_c and h_r, for convection and radiation respectively.

Equation 7·3·1 applies at both the heated and non-heated face, although the value of h used at each face will generally be different. At the cooler face, the surface

temperature will be greater than that of the surroundings and heat is lost from the slab.

For moderate differences in temperature between the surroundings and the surface, Fishenden and Saunders (1932) suggest that

$$h_c = 1{\cdot}77 \left(T_a - T_s \right)^{0{\cdot}25} \qquad (7{\cdot}3{\cdot}2)$$

for heat transfer by natural convection between air and a plane solid vertical surface. This equation is not entirely satisfactory when the difference $T_a - T_s$ becomes very large (see Jacob 1949[b] for instance) but, when this occurs in the present problem, radiation is the principal mechanism of heat transfer and some error can be tolerated in the expression for h_c.

The coefficient for heat transfer by radiation h_r follows from the Stefan-Boltzmann law and is given by Fishenden and Saunders as

$$h_r = SE \frac{K_a^4 - K_s^4}{T_a - T_s} \qquad (7{\cdot}3{\cdot}3)$$

where K_a and K_s are the absolute temperatures of the surroundings and surface respectively, S is the Stefan-Boltzmann constant ($5{\cdot}77 \times 10^{-8}$ W/m^2C^4) and E is the emissivity of the surface. In the analysis that follows E is taken to be 0·8. This is close to the value used by Harmathy (1961) and lies at the upper end of the range of values given by Fishenden and Saunders for the emissivity of refractories, ceramics, bricks and tiles.

The other boundary condition occurs at the interface between the dry and wet zones. In general it will be assumed that vapourisation occurs at atmospheric pressure, the latent heat of vapourisation being taken to be 2258 J/g of water. Some difficulty occurs in specifying the moisture content, as loss of moisture continues at temperatures much in excess of 100°C (Philleo 1958) and the total weight loss is greater than the true evaporable water content. This difficulty arises because water is taken to be liberated at the interface only. This simplification should give satisfactory results if the depth of the dry zone is not too great and if the initial moisture content is augmented, when setting up the calculations, to allow for the increased weight loss.

7·4 Numerical Analysis of Heat Conduction

When the thermal diffusivity k is constant the equation for heat conduction in one direction becomes (Carslaw and Jaeger 1947)

$$k \frac{\partial^2 T}{\partial z^2} = \frac{\partial T}{\partial z} \qquad (7\cdot4\cdot1)$$

This equation will be put into finite difference form so that the temperatures can be found at a number of discrete points throughout the thickness of the wall. Here, it is convenient to take these points to be equally spaced through the wall thickness, the points being separated by an amount δz and numbered 1 to R, starting at the hot face.

We consider the temperatures T_{n-1}, T_n and T_{n+1} that obtain at time t at three consecutive points that are either all in the dry zone, or in the wet zone. Some short time later, at time $t+\delta t$, these temperatures have become T'_{n-1}, T'_n, T'_{n+1}. We express equation 7·4·1 in finite difference form by writing,

$$\left(\frac{\partial^2 T}{\partial z^2}\right)_n = \frac{T_{n-1} - 2T_n + T_{n+1}}{\delta z^2} \qquad (7\cdot4\cdot2)$$

$$\text{and} \left(\frac{\partial T}{\partial t}\right)_n = \frac{T'_n - T_n}{\delta t} \qquad (7\cdot4\cdot3)$$

$$\text{to obtain} \quad T'_n = \frac{T_{n-1}}{M} + \frac{M-2}{M} T_n + \frac{T_{n+1}}{M} \qquad (7\cdot4\cdot4)$$

$$\text{where} \quad M = \frac{\delta z^2}{k\,\delta t} \qquad (7\cdot4\cdot5)$$

Equation 7·4·4 expresses the temperatures at a particular point at time $t+\delta t$ in terms of the temperatures that obtain at that point and its immediate neighbours one time interval, δt, previously. The equation thus enables temperatures to be calculated directly by stepping forward in time.

The approximation 7·4·4 has been used extensively by Dusinberre (1945, 1949) and is a generalisation of Schmidt's (1924) method, in which M is given a value of 2, that was used by Ross and Bray (1949) in their study of

the temperatures developed in mass concrete structures. The equation is only satisfactory if small time intervals are used and errors may accumulate in the solution if the value of M is too low. This is probably because the expression used for the time derivative is a better approximation at time t + δt/2 than at the time, t, for which the equation is written.

Carlson (1937) avoided this difficulty by taking

$$\left(\frac{\partial^2 T}{\partial z^2}\right)_n = \frac{1}{2}\left(\frac{T_{n-1} - 2T_n + T_{n+1}}{\delta z^2} + \frac{T'_{n-1} - 2T' + T'_{n+1}}{\delta z^2}\right) \qquad (7\cdot4\cdot6)$$

which can be regarded as the mean value of the space derivative over the time interval from t to t + δt. In this way, the following approximation for the governing equation at the n^{th} point and time t + δt/2 is obtained,

$$-T'_{n-1} + 2(M+1)\,T'_n - T'_{n+1} = T_{n-1} + 2(M-1)\,T_n + T_{n+1}, \qquad (7\cdot4\cdot7)$$

Here it will be noted that the simple forward integration technique, used in the Schmidt method, can no longer be used as a set of simultaneous linear equations have to be solved for the temperatures at each time interval. Carlson's method was developed, and used successfully, for calculating the temperatures developed in mass concrete dams. Later, the same approximation for the space derivative was used by Crank and Nicolson (1947) and this approach is now generally referred to as the Crank-Nicolson method (Crank 1956).

The choice between the Schmidt method and that of

Carlson, Crank and Nicolson is usually made on grounds of computational convenience. If the conditions for stability can be satisfied, the Schmidt method is very attractive as it is the simpler to use. This question of stability is taken up in the next section.

7·5 Stability of the Schmidt-Dusinberre method.

Suppose that the temperatures have been calculated at all points throughout a region at time t. Suppose also that each of these temperatures may be in error and that all these errors are in the range $\pm\ \delta$ where δ is small. Now consider the particular errors ε_{n-1}, ε_n, ε_{n+1} that occur at the n^{th} point and its immediate neighbours. These errors give rise to an error ε_n', at the point n, in a subsequent calculation for the temperatures at time $t + \delta t$. Clearly, errors can not accumulate if

$$\left|\varepsilon_n'\right| < \delta, \text{ for all } n, \qquad (7\cdot5\cdot1)$$

and the numerical method will be termed stable if this condition is satisfied.

Because the governing equation is linear, the consequential error, ε_n', in the temperature at the point n, can be obtained from equation 7·4·4, i.e.

$$\varepsilon_n' = \frac{\varepsilon_{n+1} + \varepsilon_{n-1}}{M} + \frac{M-2}{M}\varepsilon_n$$

Now, as $\left|\varepsilon_n\right| \leqslant \delta$ for all n, we obtain

$$\left|\varepsilon_n'\right| \leqslant \frac{2\delta}{M} + \left|\frac{M-2}{M}\right|\delta$$

Thus, for condition 7·5·1 to be satisfied,

$$\left| \frac{M-2}{M} \right| < \frac{M-2}{M}$$

which gives, for the stability condition,

$$M > 2 \qquad (7\cdot5\cdot2)$$

This condition merely ensures that the results of the numerical process will not be subject to a cumulative error. However, the accuracy of solution depends on the suitability of equation 7·4·4, as well as precision in the arithmetic. Thus, stability of the calculation does not, in itself, guarantee accuracy in the solution.

Jaeger (1950) has commented that the accuracy of a numerical method, which is based on a finite difference approximation, can only be demonstrated by comparing the results with those obtained from an analytical solution. Accordingly, he investigated the accuracy of the Schmidt method (M=2) by comparison with the fundamental solution for the instantaneous plane source in an infinite solid (Fourier, 1822, ch.9). In this way he showed that the basic Schmidt method gave temperatures at any particular point that oscillated about the true solution for successive time intervals. In addition, he showed that the bounding solutions, obtained by taking the results for the odd and even time increments separately, converged to the true solution with increasing time. This is an important result, as the solution for the instantaneous plane source can be used to generate solutions for a wide range of situations

by superposition in space and time, using the convolution theorem. Also, it is interesting to note that the oscillatory nature of the solution is not a disadvantage, as the results obtained for any point can be smoothed, in the time direction, to give a better approximation for the temperature than is given by the original computed values.

Jaeger's analysis was concerned with the particular case when M=2 but it seems reasonable to suppose that solutions using shorter time intervals (i.e. $M > 2$) will be at least as accurate as the basic Schmidt method. In general some increase in accuracy can be expected when using a higher value of M (Dusinberre 1961) but in many cases, satisfactory results are obtained when using the minimum value M for stability.

Jaeger's (1950) approach gives additional insight into the effects of minor numerical errors in the calculation. These have the same effect as the occurrence of a set of instantaneous sources and sinks at each of the mesh points. Thus, although there will be a tendency for errors to be distributed throughout a region, the possibility of a reduction in the total error in a particular problem will depend on the form of the boundary conditions. For instance, the effect of a single abnormally large arithmetic error will not be dissipated in subsequent calculations if the boundaries are insulated. In cases such as this, it is clearly worthwhile to supplement the stability condition and attempt to monitor the average cumulative error, by means of a heat balance for the whole region, at each

stage of the calculation.

Returning to the present problem; if M is chosen so that the stability condition 7·5·2 is satisfied, equation 7·4·4 can be used to calculate temperatures within the wall with the exception of those at the boundaries or at points adjacent to the vapourisation interface. The additional expressions required to take account of these discontinuities are discussed in the next sections.

7·6 Interface Temperatures

The conditions at the interface are shown in figure 7-2. Here the interface has penetrated a short distance $\alpha\delta z$ beyond the point p so that at the time considered it lies between the p^{th} and $p+1^{th}$ point. At any time, the temperatures at the interface and at the point p-1 can be expressed in terms of the temperature T_p and its derivatives with respect to z (at the point p) by means of Taylor's series. If the terms containing derivatives of order three and higher are neglected (as is done in the derivation of 7·4·2) two equations are obtained which may be solved to give

$$\left(\frac{\partial T}{\partial z}\right)_p = \frac{\bar{T} - (1-\alpha^2)T_p - \alpha^2(T_p-1)}{\alpha(1+\alpha)\ \delta z} \qquad (7\cdot6\cdot1)$$

$$\text{and } \left(\frac{\partial^2 T}{\partial z^2}\right)_p = \frac{2}{\alpha(1+\alpha)\delta z^2}\ (\alpha T_{p-1} - (1+\alpha)\ T_p + \bar{T}) \qquad (7\cdot6\cdot2)$$

where $\bar{T}$ is the temperature for vapourisation. This last result can be used with the forward difference approximation 7·4·3 to express the governing equation (7·4·1)

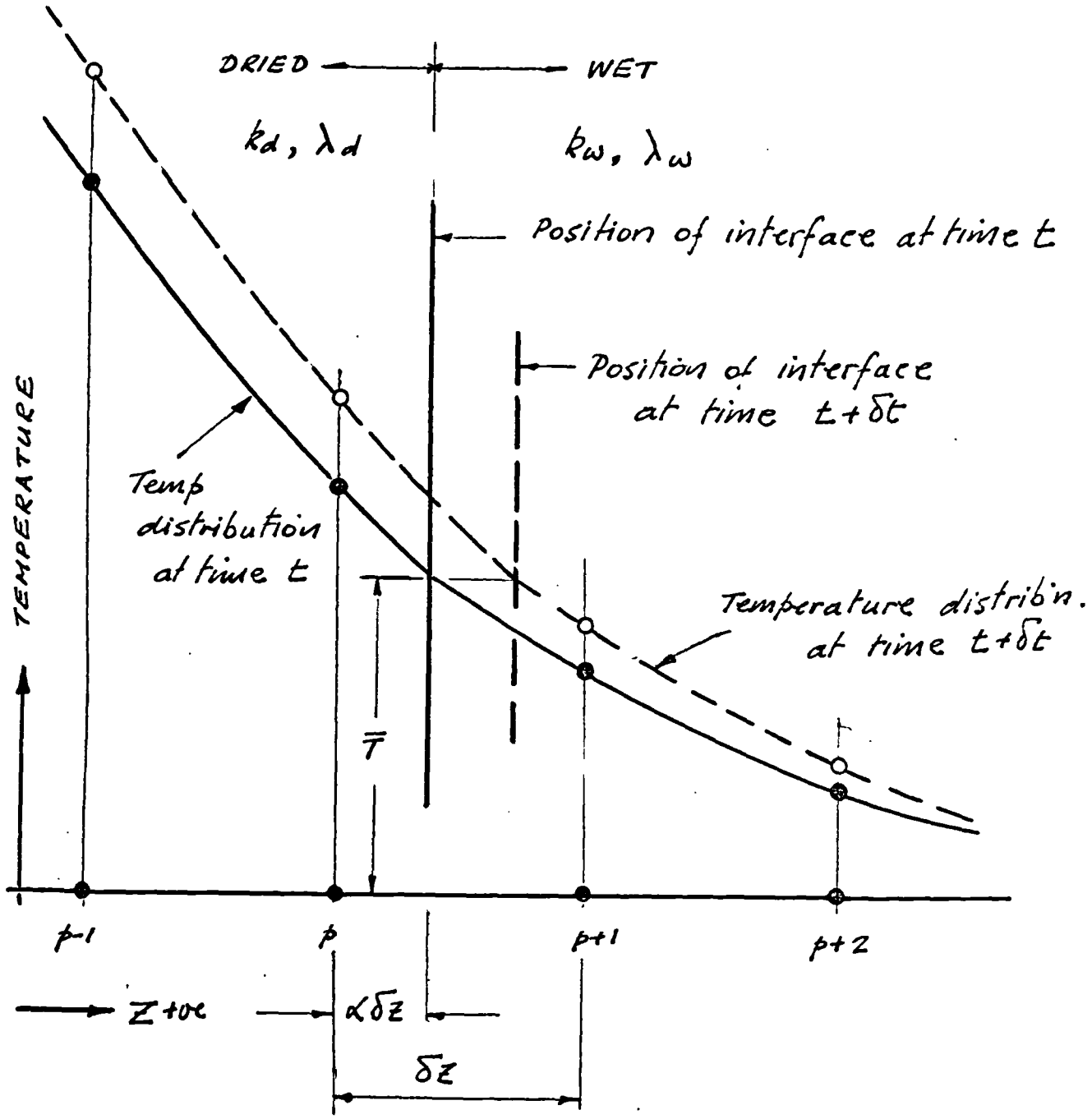


Figure 7-2 CONDITIONS IN THE VICINITY OF THE INTERFACE ILLUSTRATING THE NOTATION USED IN DERIVING EQUATIONS 7.6.3

NOTE THAT THE DEFINITION OF α IS LATER REVISED

see fig 7-4

in finite differences form to obtain -

$$T'_p = \frac{2}{(1+\alpha)M_d} T_{p-1} + \frac{(\alpha M_d - 2)}{\alpha M_d} T_p + \frac{2\bar{T}}{\alpha(1+\alpha)M_d} \quad (7\cdot6\cdot3a)$$

where M_d is the value of M (7·4·5), calculated using the thermal diffusivity appropriate to the dry zone. Similarly, we find that, after the time interval δt, the temperature at the $p+1^{th}$ point becomes -

$$T'_{p+1} = \frac{2\bar{T}}{(1-\alpha)(2-\alpha)M_w} + \frac{(1-\alpha)M_w - 2}{(1-\alpha)M_w} T_{p+1} + \frac{2}{(2-\alpha)M_w} T_{p+2}$$

(7·6·3b)

where M_w is the value of M appropriate to the wet zone.

These equations appear to be satisfactory in that they reduce to the form of equation 7·4·4 for particular values of α. However, it is clear that the equations would lead to computational difficulties as arguments, similar to those of section 7·5, suggest that the calculation is likely to be unstable unless

$$\alpha M_d \geqslant 2 \qquad \text{and} \quad (1-\alpha) M_w \geqslant 2$$

or unless $$\frac{2}{M_d} \leqslant \alpha \leqslant 1 - \frac{2}{M_w}$$

This condition is particularly restrictive and implies that very small time increments must be used if the interface is near either of the points p or p+1. This is not efficient and it seems advisable to avoid this approach

if at all possible.

Harmathy (1961) manages to avoid this difficulty by taking the interface to move in discrete steps from mesh point to mesh point. Thus, the interface is taken to remain at one of the numbered points until sufficient heat is absorbed at that point as would be required to vapourise all the moisture held in the material for a distance δz beyond the interface. When this occurs, the interface is moved to the next highest numbered point in the mesh.

A computer program was written on this basis to determine the temperatures in a wall, and some typical results are shown in figure 7-3. The procedure is straightforward, but the method gives a poor description of the movement of the interface unless very small space intervals are used. This suggests that the calculated temperature distribution may be somewhat distorted near the hot face. Errors of this sort were of no great concern to Harmathy, who was most interested in the temperature rise at the cooler face. In the present work, errors in the temperature distribution near the hot face could have significant effects on subsequent calculations for stresses and deformations. Thus, it is considered that a better description of the thermal conditions near the hot face must be obtained if the results are to be useful in a study of spalling.

As an alternative to Harmathy's method, an attempt can be made to use the Carlson, Crank-Nicolson method to determine the temperatures at the points p and p+1 by assuming that the interface remains stationary during the

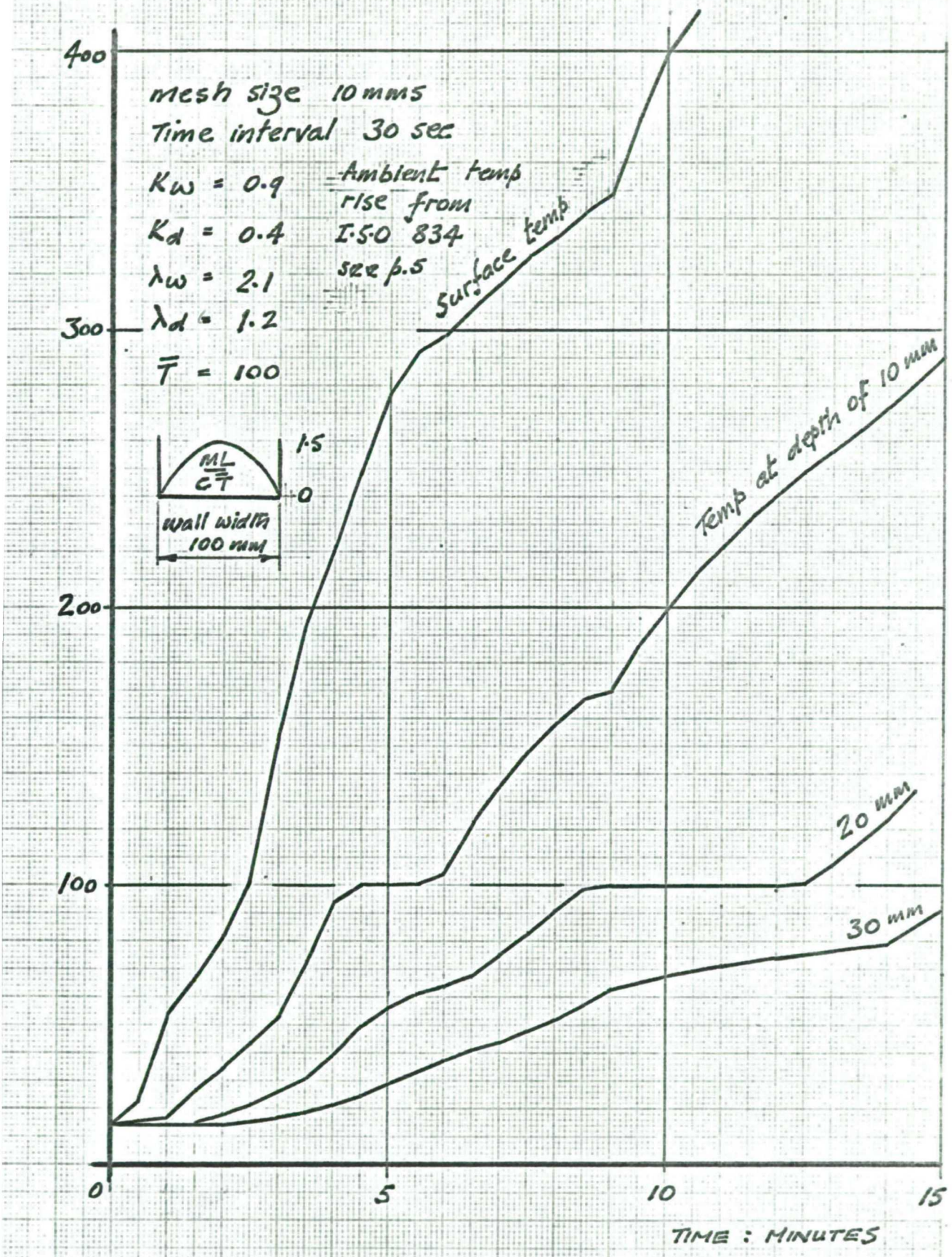


Fig 7-3 RESULTS FOR THE TEMPERATURES INDUCED IN A WALL DURING THE FIRST FIFTEEN MINUTES HEATING CALCULATED BY HARMATHY'S METHOD

time interval considered. Once the temperatures are known, the distance actually moved by the interface can be estimated by considering the heat apparently absorbed at the point where the interface was held during the previous time interval. However, this approach turns out to be unsatisfactory as it is complicated to program and runs into serious difficulties when the interface is moved from one element to the next. This occurs, as movement of the interface past the point p+1 (which is at a temperature lower than $\bar{T}$) effectively produces a spurious temperature gradient causing heat to flow towards the hot face. This temperature gradient can be very large and so leads to gross errors in the calculated temperatures. Although these errors may be reduced somewhat, by using different computional arrangements, the difficulty is fundamental to the method which has thus to be discarded.

The difficulties of the above method and those of equation 7·6·3 would be avoided if it could be arranged that the interface did not pass a mesh point. Clearly this is not possible, as the interface must be able to progress throughout the thickness of the wall. However, the desired effect is obtained if the temperature at the mesh point on one side of the interface is not used in setting up the governing equation for then the interface itself assumes the status of one of the mesh points. This situation is shown in figure 7-4, in which the interface occurs between the points p-1 and p+1 at a point a distance $\alpha\delta z$ from the point p-1. The temperatures at the points p-1 and p+1 can be found using Schmidt's method, if suitable

equations are derived in the manner of equation 7·6·3. These new expressions take the form,

$$T'_{p-1} = \frac{2}{(1+\alpha)M_d} T_{p-2} + \frac{\alpha M_d - 2}{\alpha M_d} T_{p-1} + \frac{2\bar{T}}{\alpha(1+\alpha)M_d}$$

and (7·6·4)

$$T'_{p+1} = \frac{2\bar{T}}{(2-\alpha)(3-\alpha)M_w} + \frac{(2-\alpha)M_w - 2}{(2-\alpha)M_w} T_{p+1} + \frac{2T_{p+2}}{(3-\alpha)M_w}$$

Note that no attempt is made to write an equation for T'_p, the new temperature at the point p. This can be found, by interpolating between the known temperatures at the interface and the points p-1 and p+1, once the movement of the interface has been determined.

Considering the stability of the process; arguments similar to those of section 7·5 suggest that the calculation is likely to be unstable unless,

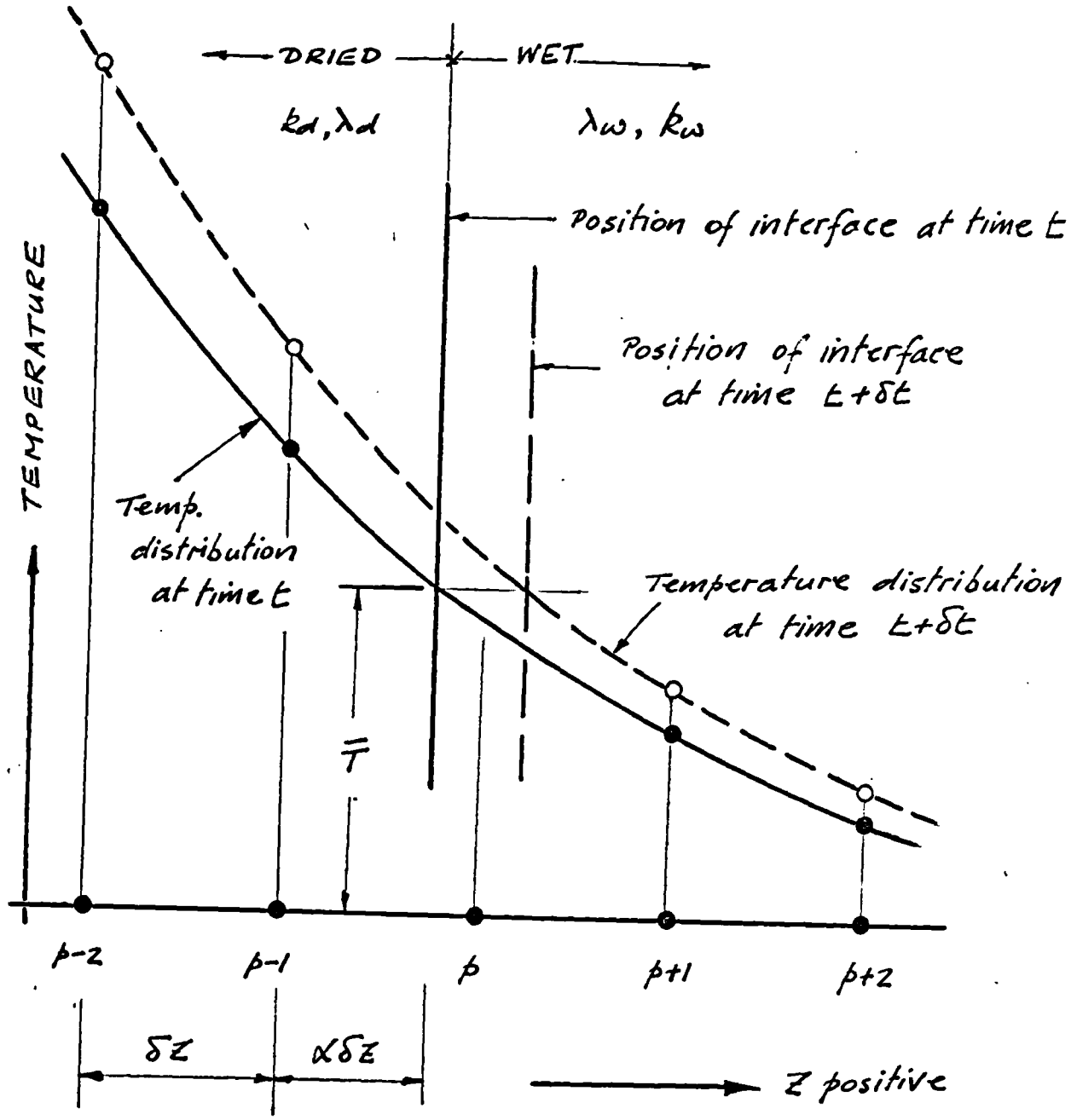
$$\alpha M_d \geqslant 2 \quad \text{and} \quad (2-\alpha)M_w \geqslant 2$$

In many cases M_d is approximately twice M_w. It follows that it is helpful to choose the point p so that α is in the range,

$$1/3 \leqslant \alpha < 4/3 \qquad (7·6·5)$$

This choice leads to the stability condition

$$M_w \geqslant 3 \quad \text{and} \quad M_d \geqslant 6, \qquad (7·6·6)$$



The point p is chosen so that $1/3 \leq \alpha < 4/3$ (7.6.5)

Figure 7-4 ARRANGEMENT OF MESH POINTS IN THE VICINITY OF THE INTERFACE FINALLY ADOPTED IN THE ANALYSIS

which is easily satisfied. Thus the equations 7·6·4 can be incorporated into the Schmidt method and merely require an assessment of which point (p) is to be omitted from the process at each stage. This is done using the criterion 7·6·5. In addition the complete solution requires the movement of the interface to be calculated and some consideration of the boundary conditions.

7·7 Boundary Conditions

The heat flux q supplied to the hot face at time t+δt is given by equation 7·3·1 i.e.

$$q = h_1 (T_f' - T_1')$$

Also, according to Fourier's (1822) law of heat conduction, the heat flux crossing any isothermal plane within the material is proportional to the temperature gradient normal to the isothermal. Thus, near the surface,

$$q = -\lambda_1 \left(\frac{\partial T}{\partial z}\right)_1$$

where λ_1 is the coefficient of thermal conductivity of the material adjacent to the heated surface. In this way the hot face boundary condition becomes

$$(T_f' - T_1') + \frac{\lambda_1}{h_1}\left(\frac{\partial T}{\partial z}\right)_1 = 0 \qquad (7·7·1)$$

This equation can be expressed in terms of the temperatures at the surface and interior points by using a suitable finite difference approximation for the

temperature gradient at the surface. Different forms for this approximation are most appropriate at different stages in the drying process. For instance for $T_1' < \bar{T}$ and $\lambda_1 = \lambda_w$, i.e. before drying starts

$$\left(\frac{\partial T}{\partial z}\right)_1 \doteq \frac{4T_2' - T_3' - 3T_1'}{2\delta z} \qquad (7\cdot7\cdot2)$$

which gives the boundary condition:-

$$T_1' = \frac{1}{3+2N}(2NT_f' + 4T_2' - T_3') \qquad (7\cdot7\cdot3a)$$

where $N = \dfrac{h_1 \delta z}{\lambda_1}$

The approximation 7·7·2 can also be used when the interface has moved into the wall and beyond the point 3. Thus, writing s for the depth of the dry zone, the boundary condition 7·7·3 can be used for

$$T_1' < \bar{T} \quad \text{with} \quad \lambda_1 = \lambda_w \qquad (7\cdot7\cdot3b)$$

and $s \geqslant 2\delta z \quad$ with $\lambda_1 = \lambda_d$

By using the same procedure that leads to equation 7·7·3, an expression for the boundary conditions that applies when

$$p = 3 \quad \text{and} \quad 4/3 < s/\delta z < 2$$

can also be found. This has the form

$$T'_1 = \frac{\alpha(1+\alpha)\, NT'_f + (1+\alpha)^2\, T'_2 - \bar{T}}{\alpha(2+\alpha+(1+\alpha)N)} \qquad (7\cdot7\cdot4)$$

which reduces to the condition 7·7·3a when $\alpha \to 1\cdot0$

Special consideration must be given to the occasion when drying first occurs at the heated surface and also when the depth of the dry zone is less than $4\delta z/3$. This point will be dealt with when drying is considered. Before this, we deal with the boundary conditions at the cooler face, i.e. at the point R. Here, the boundary conditions are mathematically similar to those at the hot face. Thus

$$(T'_R - T_a) + \frac{\lambda_R}{h_R}\left(\frac{\partial T}{\partial z}\right)_R = 0$$

where T_a is the ambient temperature. No consideration will be given to the possibility that drying may penetrate so far that the interface approaches the cool face as the main interest is in the early stages of heating when spalling is most likely to occur. With this restriction, the approximation for the temperature gradient at the cool face can be taken to be

$$\left(\frac{\partial T}{\partial z}\right)_R = \frac{3T_R - 4T_{R-1} + T_{R-2}}{2\delta z}$$

giving the boundary condition

$$T'_R = \frac{2NT'_a + 4T'_{R-1} - T'_{R-2}}{3+2N} \qquad (7\cdot7\cdot5)$$

for $s \leqslant (R-3)\,\delta z$

7·8 Drying within the wall or movement of the interface

In order for drying to proceed, heat must be absorbed at the interface between the dry and the wet zones. Suppose a quantity of heat δQ is absorbed at the interface in time δt. Then from Fourier's law,

$$\delta Q = \left[-\lambda_d\left(\frac{\partial T}{\partial z}\right)_d + \lambda_w\left(\frac{\partial T}{\partial z}\right)_w\right]\delta t \qquad (7\cdot8\cdot1)$$

Here the suffices d and w refer to the dry and wet zones respectively. Also, as the temperature gradient will not generally be continuous across the interface, the two values of the temperature gradient must be regarded as the gradients that exist at points very near to the interface, but in the dry and wet zones respectively.

Suppose now that, in the time interval δt, the process of vapourisation causes the interface to move a distance $(\alpha'-\alpha)\delta z$ towards the point p+1 as shown in figure 7-5. This vapourisation is effected by the amount of heat δQ, so that

$$\delta Q = m\rho L(\alpha'-\alpha)\delta z \qquad (7\cdot8\cdot2)$$

where m is the proportion of evaporable water present by weight, ρ is the mass density and L is the latent heat of vapourisation. The two expressions for δQ (7·8·1 and 7·8·2) are equated to find $\alpha'-\alpha$. A convenient form is obtained by noting that $M=\delta z^2\rho c/\delta t$, where c is the specific heat of the material i.e.

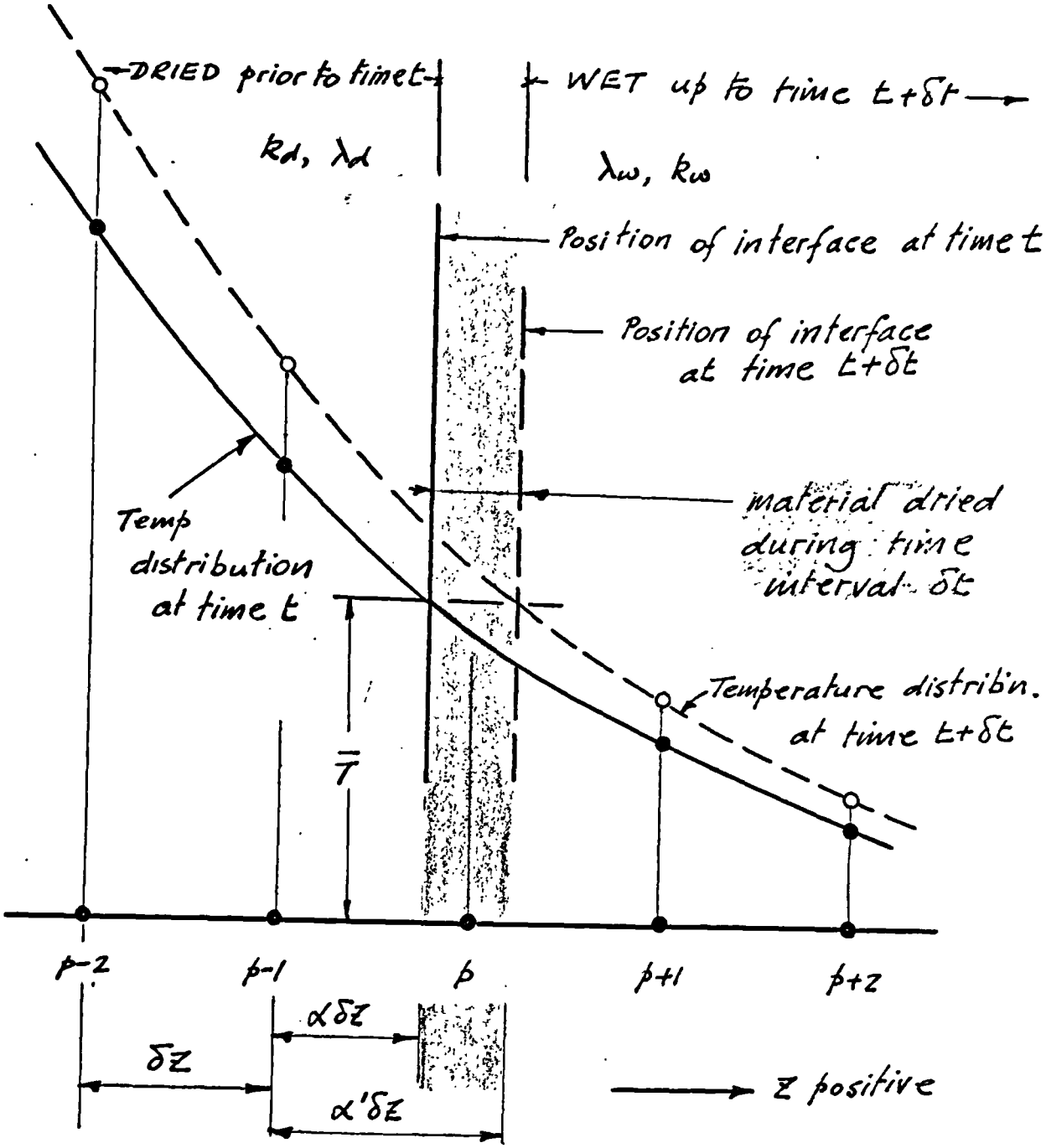


Figure 7-5 MOVEMENT OF THE INTERFACE

$$\alpha'-\alpha = \frac{c}{ML}\left(\frac{1}{M_w}\left(\frac{\partial T}{\partial z}\right)_w - \frac{\lambda_d k_w}{\lambda_w k_d}\ \frac{1}{M_d}\left(\frac{\partial T}{\partial z}\right)_d\right)\delta z$$

This equation will be written

$$\alpha'-\alpha = \frac{c\bar{T}}{ML}\left(\frac{\phi_w}{M_w} - \gamma\frac{\phi_d}{M_d}\right) \qquad (7\cdot8\cdot3)$$

where the ratio γ of the volumetric heat capacity of the material in the dry and wet regions is given by

$$\gamma = \frac{\lambda_d k_w}{\lambda_w k_d}$$

and $$\phi_d = \frac{1}{\bar{T}}\left(\frac{\partial T}{\partial z}\right)_d \delta z$$

In order to use equation 7·8·3, values are required for ϕ_w and ϕ_d. These follow from the appropriate finite difference approximations for the temperature gradients which, in the spirit of the Schmidt method, are given the values that obtain at the beginning of the time interval considered. Thus,

$$\left.\begin{aligned}\phi_d &= \frac{(1+2\alpha)\bar{T} - (1+\alpha)^2 T_{p-1} + \alpha^2 T_{p-2}}{\alpha(1+\alpha)\bar{T}} \\ \text{and } \phi_w &= \frac{-(5-2\alpha)\bar{T} + (3-\alpha)^2 T_{p+1} - (2-\alpha)^2 T_{p+2}}{(2-\alpha)(3-\alpha)\bar{T}}\end{aligned}\right\} \qquad (7\cdot8\cdot4)$$

These equations hold for $s \geqslant 4\delta z/3$, where s is the depth of the dry zone. For smaller values of s, the temperature gradient on the dry side of the interface is not well defined by the available values of temperature and an alternative procedure is required. This is discussed in the next section.

7·9 Initial Stages of Drying - drying near the heated surface

When vapourisation first occurs at the hot face it will be recognised in the calculation as occurring when the new surface temperature first exceeds the vapourisation temperature $\bar{T}$. At this stage no account has been taken of drying and the surface temperature has to be recalculated. A number of ways were tried to deal with drying near the hot face. The simplest approach is used in the present work. In this, Harmathy's method (as described in Section 7·6) is used for the first two elements during the period of time from the start of drying until the interface penetrates to a depth of $4\delta z/3$ when p=3. In order to avoid the basic difficulty of Harmathy's method and to obtain a fair description of the movement of the interface both the time interval δt and the distance δz between mesh points in the vicinity of the surface are subdivided as shown in figure 7-6. The calculation parameters M_D and M_W are unaffected by the change in mesh size and thus the calculation proceeds using equation 7·4·4. The only change concerns the particular mesh point (the i^{th}) where the interface is situated.

Here the quantity of heat required to dry a layer of thickness δz is $mL\rho\delta z$. In the absence of drying, this

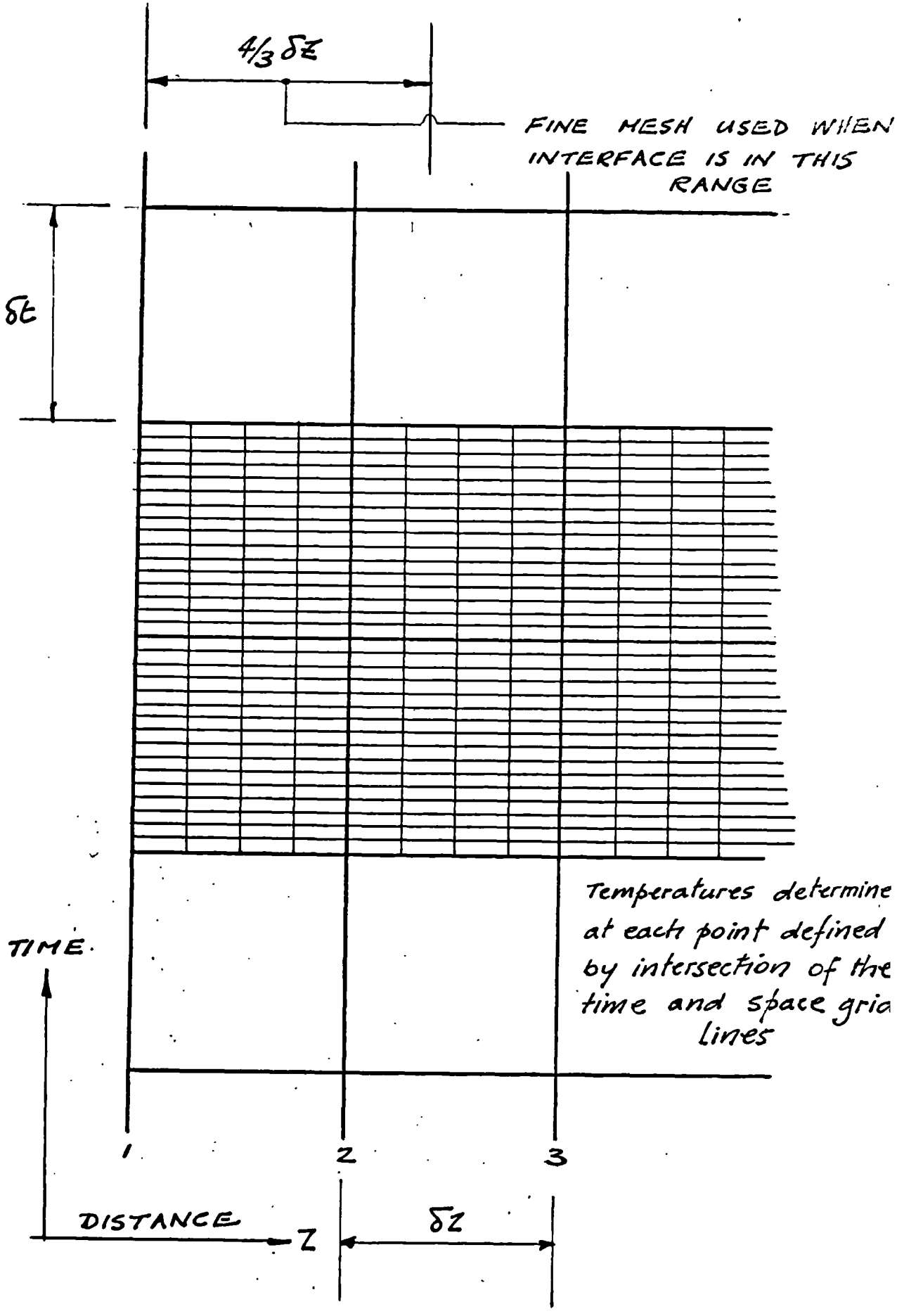


Figure 7-6 FINITE DIFFERENCE MESH USED WHEN CONSIDERING THE INITIAL STAGES OF DRYING

quantity of heat would be sufficient to raise the temperature of the layer by an amount $mL/c = T^*$. Harmathy's procedure for the interface is first to ignore vapourisation and calculate the new temperature T_i' where:-

$$T_i' = \gamma \frac{T_{i-1}}{M_d} + \left(1 - \frac{\gamma}{M_D} - \frac{1}{M_w}\right) T_i + \frac{T_{i+1}}{M_w} \qquad (7\cdot9\cdot1)$$

In this equation, T_i is equal to the vapourisation temperature $\bar{T}$. The value obtained for T_i' is fictitious, as the temperature at the i^{th} point remains at $\bar{T}$ during drying, and Harmathy takes the quantity $T_i' - \bar{T}$ to be a measure of the heat available for drying during the time interval δt considered. As this heat is used in drying, the temperature equivalent of the heat required to vapourise the moisture, in a layer of thickness δz adjacent to the interface, is reduced by $T_i' - \bar{T}$ in the time interval δt. Initially, the temperature equivalent of the heat for drying is T^*. This reduced in successive time intervals, by the amounts $T_i' - \bar{T}$, until it becomes zero and the interface is moved to the next point i.e. the $i + 1^{th}$.

The boundary conditions take the form of equation 7·7·3a (with the appropriate value of N) except when the interface is at the first point within the boundary. For the subdivided mesh, this occurs at a distance $\delta z/4$ from the hot face so that, at the boundary,

$$\frac{\partial T}{\partial z} = - \frac{4(T_1' - \bar{T})}{\delta z}$$

The boundary condition follows from this result and equation 7·7·1 i.e.

$$T_1' = \frac{NT_f' + \bar{T}}{(1+N)} \qquad (7\cdot9\cdot2)$$

where $N' = \frac{h\delta z}{4\lambda}$

All the equations required for the heat flow calculations are now available. Details of the computational arrangements are given in the next chapter together with an account of the development procedures and some results.

Chapter 8

CALCULATIONS AND RESULTS FOR TEMPERATURES IN WALLS

8·1 Introduction

A number of computer programs were written to undertake the step-by-step analysis, for the temperatures in a heated wall, described in the previous chapter. The principal features of these programs are given in Table 8·1. Only two programs, viz. THERMAL and TWOWARM, were required for the subsequent analysis of stresses in walls but the remainder were necessary in the development and checking of these two programs.

Ideally, the accuracy of a numerical method, based on finite differences, should be checked by comparison with an analytical solution (Jaeger 1950) of those available, the simplest solution that approaches the conditions of the present problem is that due to Neumann, which is described by Carlsaw and Jaeger (1947b). Neumann dealt with the problem of melting in a solid that initially occupies the semi-infinite region $z \geqslant 0$ and is subjected to a sudden rise in temperature at the boundary. The details of this analysis can be rephrased to deal with an endothermic process that occurs at a transition temperature other than zero. This is done in the next section, so that the results can be used to check the accuracy of the numerical method outlined in Chapter 7.

8·2 Neumann's solution

We consider a material that extends throughout the semi-infinite region $z \geqslant 0$. The surface $z = 0$ is maintained at a temperature T_s which is greater than the temperature $\bar{T}$ at which vapourisation of the evaporable moisture held in the

TABLE 8·1 PROGRAMS FOR CALCULATION OF TEMPERATURE IN HEATED WALL PANELS

Program Name	Exposure Condition	Heating Pattern	Basic Method
FRYFACE	Hot face temperature specified by a,b,c where $T_s=a+bt+ct^2$	One face heated the other maintained at a constant specified temperature	after Harmathy (1961)
TOASTER			
TWOWARM	Ambient temperature rise according to I.S.O. 834 as Figure 1·1	Ambient temperature raised equally outside both faces	As Chapter 7
THERMAL		Ambient temperature raised outside one face only. Heat loss to specified constant ambient temperature at the other.	
TIBORZH			after Harmathy (1961)

In all Programs the initial moisture distribution is prescribed in terms of a surface and centre value the variation being taken to be parabolic and symmetric about the centre.

All programs are written in FORTRAN 1V and were run on the University of London CDC 6600

material occurs. It is assumed that vapourisation occurs only at this transition temperature so that, at some time t, the material is separated into a dry region of depth s, in which the temperatures are T_d, and a wet region in which the temperatures are T_w.

In the dry region, the material has thermal conductivity λ_d and thermal diffusivity k_d so that the temperature T_d must satisfy the governing equation,

$$k_d \frac{\partial^2 T_d}{\partial z^2} = \frac{\partial T_d}{\partial t} \qquad \text{for } 0 \leqslant z < s \tag{8·2·1}$$

for the boundary condition

$$T_d = T_s \quad \text{at } z = 0 \tag{8·2·2}$$

Similarly, the temperature T_w of the material in the wet region must satisfy the equation

$$k_w \frac{\partial^2 T_w}{\partial z^2} = \frac{\partial T_w}{\partial t} \qquad \text{for } z > s \tag{8·2·3}$$

and the condition

$$T_w \to T_\infty \quad \text{as} \quad z \to \infty, \tag{8·2·4}$$

if it is assumed that the temperatures, at great depths into the slab, remain constant at the value T_∞.

There are additional boundary conditions that must be satisfied at the surface of separation between the dry and wet regions. Clearly,

$$T_d = T_w = \bar{T} \quad \text{at} \quad z = s \tag{8·2·5}$$

Also, the rate of heat adsorption at the interface must equal the rate required for drying. The quantity of heat needed to move the interface a distance δs is $mL\rho_w \delta s$, where L is the latent heat of vapourisation, m is the proportion of evaporable water by weight in the moist material and ρ_w is the density of the material in the wet zone. Thus, using Fourier's law of heat conduction, we obtain the condition

$$-\lambda_d \frac{\partial T_d}{\partial z} + \lambda_w \frac{\partial T_w}{\partial z} = mL\rho_w \frac{ds}{dt}, \quad \text{at } z = s$$

where λ_d and λ_w are the coefficients of thermal conductivity for the material in the dry and wet zones respectively. On introducing the specific heat, c_w, of the moist material, a more convenient form of this equation is obtained i.e.

$$-k_d \gamma \frac{\partial T_d}{\partial z} + k_w \frac{\partial T_w}{\partial z} = \frac{mL}{c_w} \frac{ds}{dt} \quad \text{at } z = s \qquad (8\cdot2\cdot6)$$

where

$$\gamma = \frac{\lambda_d}{\lambda_w} \frac{k_w}{k_d}$$ as defined in Chapter 7.

The statement of the problem is completed by noting that the equations 8·2·1 to 6 are to be solved for the following initial conditions.

$$\text{At } t=0, \quad s = 0 \quad \text{and} \quad T_w = T_\infty \quad \text{for } z > 0 \qquad (8\cdot2\cdot7)$$

Neumann arrived at a solution that satisfies these initial conditions by considering combinations of particular solutions of the governing equations, 8·2·1 and 8·2·3, that satisfy

the boundary conditions at time $t > 0$. Thus Neumann noted that equations 8·2·1 and 8·2·3 are satisfied by

$$T_d = T_s + A \ \mathrm{erf}\left(\frac{z^2}{4k_d t}\right)^{1/2} \qquad (8\cdot2\cdot8)^+$$

$$\text{and } T_w = T_\infty + B \ \mathrm{erfc}\left(\frac{z^2}{4k_w t}\right)^{1/2} \qquad (8\cdot2\cdot9)^+$$

where A and B are constants.

At the interface, between the dry and wet regions, $T_d = \bar{T} = T_w$ so that

$$T_s - \bar{T} = -A \ \mathrm{erf}\left(\frac{s^2}{4k_d t}\right)^{1/2} \qquad (8\cdot2\cdot10)$$

$$\text{and } \bar{T} - T_\infty = B \ \mathrm{erfc}\left(\frac{s^2}{4k_w t}\right)^{1/2}$$

In these expressions A, B, $T_s - \bar{T}$ and $\bar{T} - T_\infty$ are all constants so that the terms in parenthesis must be independent of time. Thus, we can introduce a parameter $\bar{k}$,

---

Footnote $^+$
The error function, $\mathrm{erf}(u) = \frac{2}{\sqrt{\pi}}\int_0^u e^{-x^2} dx$, The complement of the error function, 1-erf(u), is written erfc(u). A table of values of the error function is given by Gautschi (1964) who also provides rational approximations for use in numerical computation of the function.

having the same dimensions as thermal diffusivity, and write

$$s = \sqrt{4\bar{k}t} \qquad (8\cdot2\cdot11)$$

Expressions for the constants A and B can be obtained by substituting this value for s into equation 8·2·10. Following this, an equation for $\bar{k}$ can be obtained from the other condition at the interface (i.e. 8·2·6) in the form

$$Q(\bar{k}/k_d)\ (T_s-\bar{T})/\bar{T} - Q(\bar{k}/k_w)\ (T-T_\infty)/\bar{T} = \sqrt{\pi}\ mL/c\bar{T} \qquad (8\cdot2\cdot12)$$

where $Q(x) = 1/x^{1/2}e^x\ \mathrm{erf}(x^{1/2})$

Equation 8·2·12 must be solved for $\bar{k}$. Once this value is obtained the temperature T_d and T_w may be found from

$$T_d = T_s - \frac{T_s - \bar{T}}{\mathrm{erf}\left(\frac{\bar{k}}{k_d}\right)^{1/2}} \mathrm{erf}\left(\frac{z^2}{4k_d t}\right)^{1/2}, \quad z \leqslant s \qquad (8\cdot2\cdot13)$$

$$T_w = T_\infty + \frac{\bar{T} - T_\infty}{\mathrm{erfc}\left(\frac{\bar{k}}{k_w}\right)^{1/2}} \mathrm{erfc}\left(\frac{z^2}{4k_w t}\right)^{1/2}, \quad z > s$$

so far, the initial conditions have not been considered. However, it is clear that these are satisfied as s = 0 at t = 0, from 8·2·11, and $T_w = T_\infty$ at t = 0 for z > 0, from 8·2·13. The solution is thus seen to be satisfactory.

Equation 8·2·12 could be solved for $\bar{k}$ directly using a method of successive approximations. Rather than attempt this, a short computer program (NEUMANN) was written to calculate values of the surface temperature parameter $(T_s-\bar{T})/\bar{T}$ for any specified range of values of $\bar{k}/k_d$ and particular values of γ, k_w/k_d, $mL/c\bar{T}$ and $(\bar{T}-T_\infty)/\bar{T}$. This program was used to obtain data relevant to the problem of melting ice, for which Carslaw and Jaeger (1947[b]) have tabulated certain values. The agreement between the two sets of results was entirely satisfactory. Following this test, the program NEUMANN could be used with confidence to generate data with which to check the numerical method of analysis.

8·3 Development of TOASTER

A computer program (TOASTER) was written, to solve Neumann's problem, numerically, using the procedures developed in Chapter 7 but with the simpler boundary condition of prescribed temperature. The program was written for a wall of finite width with Harmathy's method[+] being used for the short period, following the start of heating, during which drying first penetrates into the slab. Following this initial stage, the more general method was used in

---

Footnote[+]

Harmathy's method was programmed separately as FRYFACE and this was given the status of a subroutine within TOASTER

which the position of the interface is not confined to a mesh point.

As an initial check on this program, results were obtained for a thick solid having constant thermal diffusivity k and in which no latent heat effects are present. If the initial temperature of this semi-infinite solid is T_∞, a sudden rise in boundary temperature, to a value T_s, induces temperatures T throughout the solid where

$$T - T_\infty = (T_s - T_\infty) \operatorname{erfc}\left(\frac{z^2}{4kt}\right)^{1/2} \qquad (8\cdot3\cdot1)$$

The results from this equation are compared with those from the computer program in figure 8-1. The differences are greatest for the first few minutes of heating and after this the agreement is excellent. This is reassuring but could be anticipated because no new procedures, that extend the range of application of the Schmidt-Dusinberre method, have been employed at this stage.

The program was next used to obtain the solution of Neumann's problem for a number of different values of surface temperature. The values of the thermal properties used were taken to correspond approximately with those of wet and dry concrete and these are shown, in Table 8-2, together with the other variables used in this investigation.

Some typical output from TOASTER is shown in figure 8-2. The program parameters are given as a heading together with the data and time. The results are then printed at specified times in the following manner.

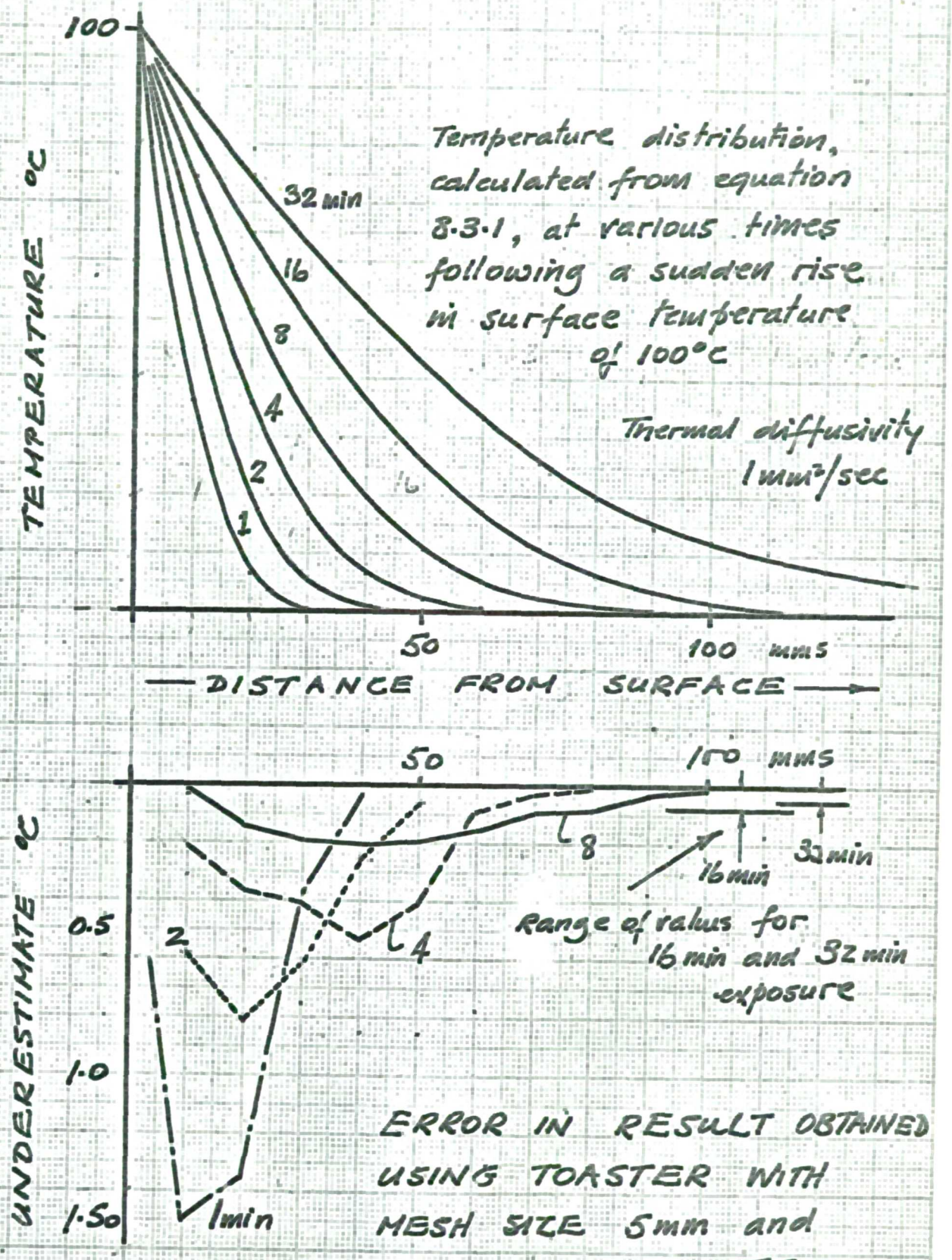


Figure 8-1 COMPARISON OF THE RESUTS OBTAINED FROM TOASTER WITH THOSE FROM AN ANALYTICAL SOLUTION.

```
TOASTER/DOUGILL      18/06/71      12.51.07.
WALL WIDTH  320.0/  SURF MOIST 1.600/  AMB TEMP  15.0/  WET DIFY  1.00/  WET COND  2.500/  TIME INC   7.50/
 MESH SIZE    5.0/  CENT MOIST 1.600/  VAP TEMP 100.0/  DRY DIFY   .50/  DRY COND  1.250/  MW = 3.33,  MD = 6.67/
                    TEMPERATURES PRINTED AT EVERY10.00MM FROM HOT FACE

-----------------------------------------------------------------------------------------------------------------

 1. 0      3.75    200.00   10.9545
           200.00     57.72     23.03     15.73     15.03     15.00     15.00     15.00     15.00     15.00
            15.00     15.00     15.00     15.00     15.00     15.00     15.00     15.00     15.00     15.00
            15.00     15.00     15.00     15.00     15.00     15.00     15.00     15.00     15.00     15.00
            15.00     15.00     15.00
 2. 0      5.00    200.00   15.4919
           200.00     75.17     37.99     21.19     16.15     15.15     15.01     15.00     15.00     15.00
            15.00     15.00     15.00     15.00     15.00     15.00     15.00     15.00     15.00     15.00
            15.00     15.00     15.00     15.00     15.00     15.00     15.00     15.00     15.00     15.00
            15.00     15.00     15.00
 3. 0      6.25    200.00   18.9737
           200.00     84.24     48.93     28.25     19.09     15.98     15.18     15.03     15.00     15.00
            15.00     15.00     15.00     15.00     15.00     15.00     15.00     15.00     15.00     15.00
            15.00     15.00     15.00     15.00     15.00     15.00     15.00     15.00     15.00     15.00
            15.00     15.00     15.00
 4. 0      7.72    200.00   21.9089
           200.00     91.37     56.88     34.83     22.90     17.62     15.72     15.16     15.03     15.00
            15.00     15.00     15.00     15.00     15.00     15.00     15.00     15.00     15.00     15.00
            15.00     15.00     15.00     15.00     15.00     15.00     15.00     15.00     15.00     15.00
            15.00     15.00     15.00
 5. 0      8.47    200.00   24.4949
           200.00     94.83     63.26     40.67     26.90     19.78     16.65     15.49     15.12     15.03
            15.00     15.00     15.00     15.00     15.00     15.00     15.00     15.00     15.00     15.00
            15.00     15.00     15.00     15.00     15.00     15.00     15.00     15.00     15.00     15.00
            15.00     15.00     15.00
```

FIG. 8–2 TYPICAL OUTPUT FROM TOASTER SHOWING RESULTS FOR FIRST FIVE MINUTES EXPOSURE

First line: Time in minutes and seconds, depth of dried zone in mms; Surface temperature and the quantity $\sqrt{4k_d t}$ in mms.

Subsequent lines: Temperatures at equally spaced points across the thickness of the wall given in groups of ten and read from left to right.

Table 8·2 DATA used in the numerical investigation of Neumann's Latent Heat Problem.

Material Properties		Dry zone	Wet zone
Thermal conductivity W/m°C		1·25	2·50
Thermal Diffusivity mm^2/sec		0·50	1·0
$\frac{mL}{c\bar{T}}$		Two values used 0·8 and 1·6	
Temperatures °C	Surface	In the range 200 - 800	
	Interface	100	
	Initial	15	

Calculations undertaken with a wall width of 320mms

δz = 2mm δt = 1sec

Equation 8·2·11 suggests that the depth of the dried zone should be proportional to the square root of time. This is borne out by the computed results, shown in figures 8-3 and 8-4, in which the depth of the dried zone is plotted to a base of $\sqrt{4k_d t}$ for each surface temperature investigated. The slopes of these lines give a value for $\sqrt{\bar{k}/k_d}$ which can be regarded as a measure of the depth of the dried zone when comparing the effects of different surface temperatures or moisture contents. The values of $\sqrt{\bar{k}/k_d} = s/\sqrt{4k_d t}$ are shown as points in figure 8-5. The lines on this figure represent the solution of equation 8·2·12, as computed using the program NEUMANN, for the data given in Table 8·1 with some additional values of moisture content. The agreement between the results obtained from the numerical step-by-step method and the analytical solution is very satisfactory.

The results shown in figures 8-3 to 8-5 have been obtained using very small time and space divisions. However, it is clear from Table 8·3 that very similar results can be obtained with a much coarser mesh. The Table also shows values for the temperatures obtained using the analytical result (i.e. equation 8·2·13) and again there is very good agreement.

To complete the development checks on the numerical method, the results were compared with those obtained using Harmathy's (1961) method. This is done in figure 8-6 from which it is seen that there is fair agreement between the two methods although Harmathy's approach tends to give a more uneven view of the temperature distribution in the vicinity of the interface.

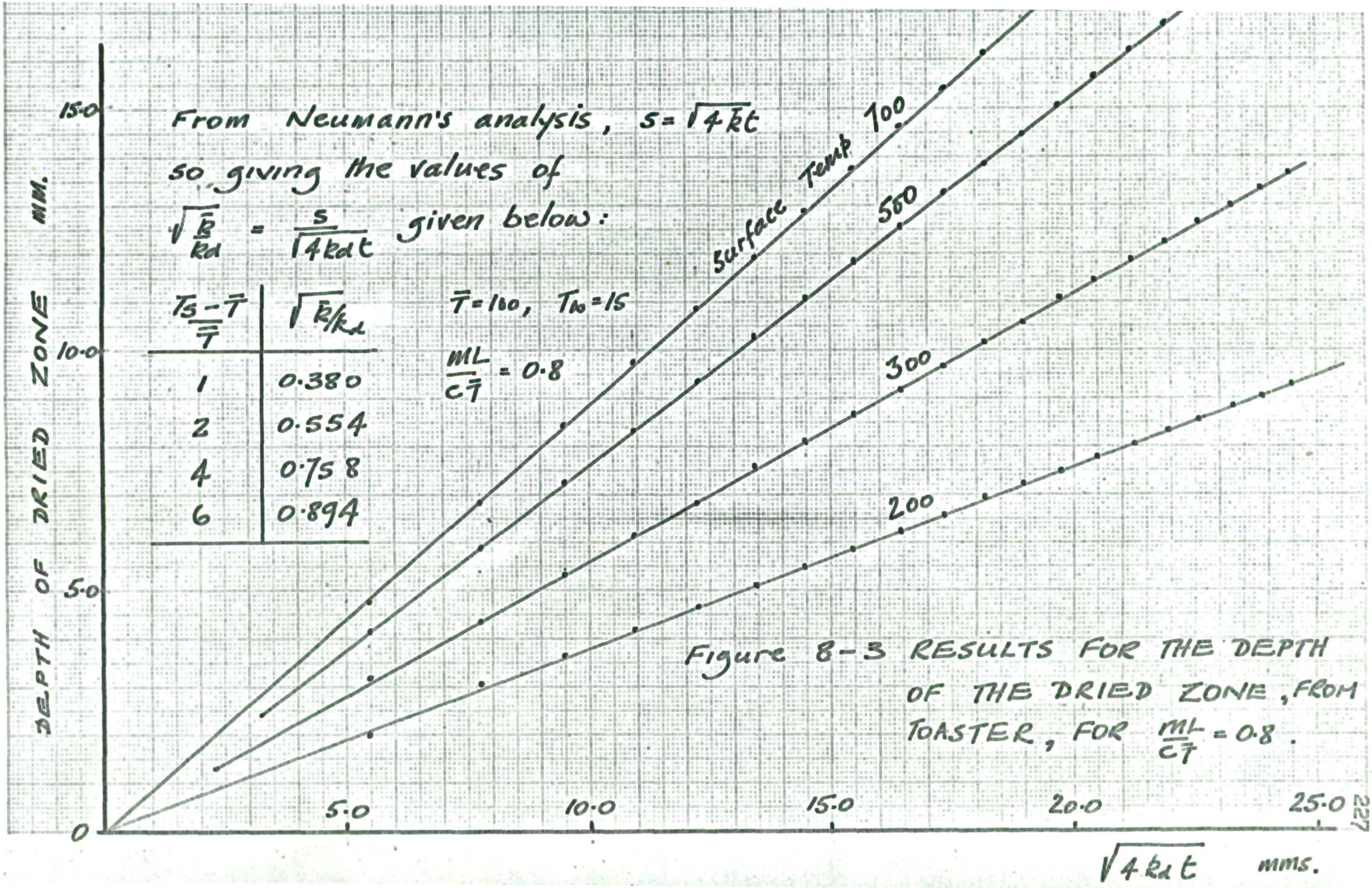
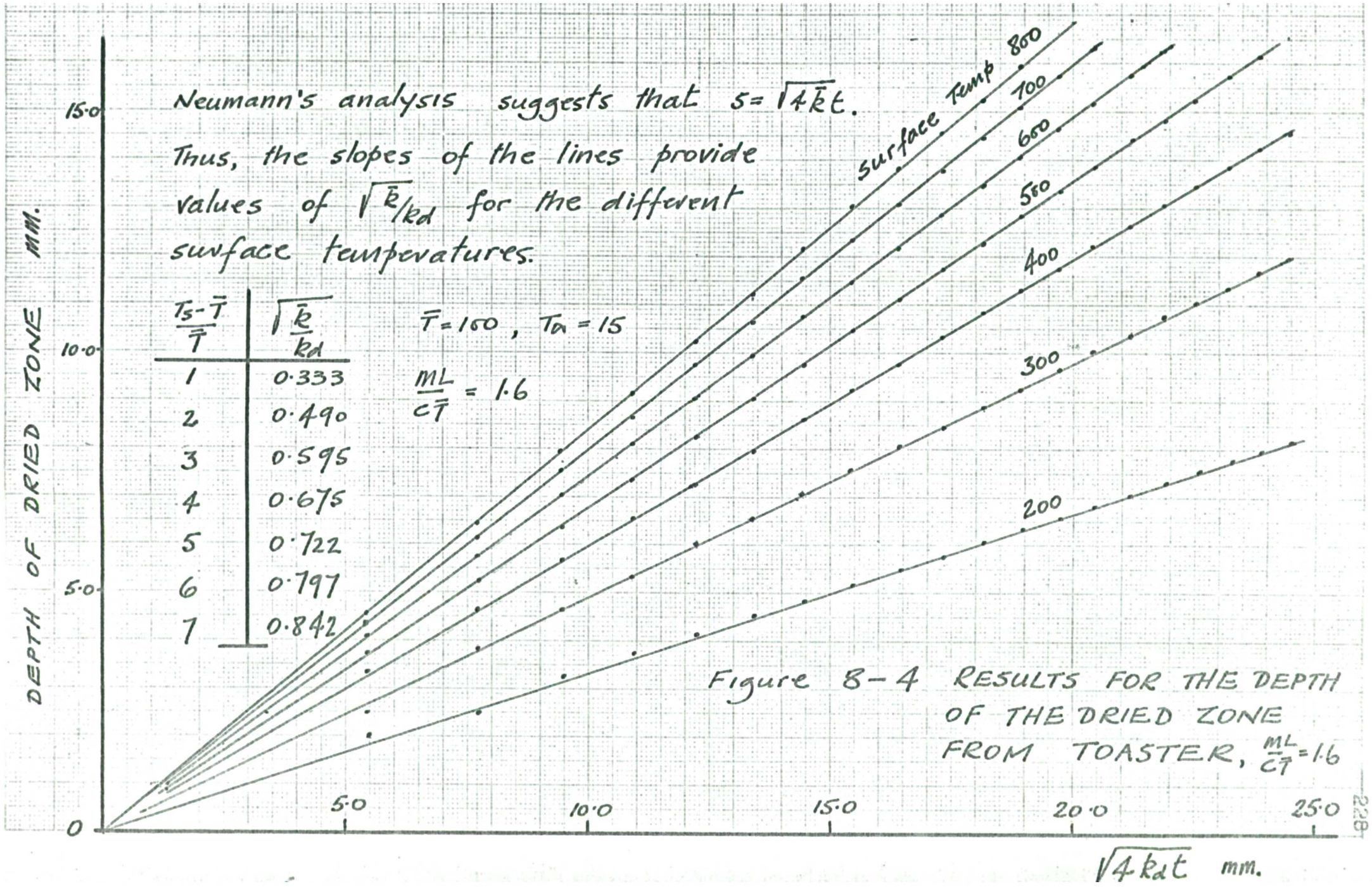


Figure 8-3 RESULTS FOR THE DEPTH OF THE DRIED ZONE, FROM TOASTER, FOR $\frac{ML}{C\bar{T}} = 0.8$.



$\frac{T_s - \bar{T}}{\bar{T}}$	$\sqrt{\frac{\bar{k}}{kd}}$
1	0·333
2	0·490
3	0·595
4	0·675
5	0·722
6	0·797
7	0·842

Figure 8-4 RESULTS FOR THE DEPTH OF THE DRIED ZONE FROM TOASTER, $\frac{ML}{c\bar{T}} = 1.6$

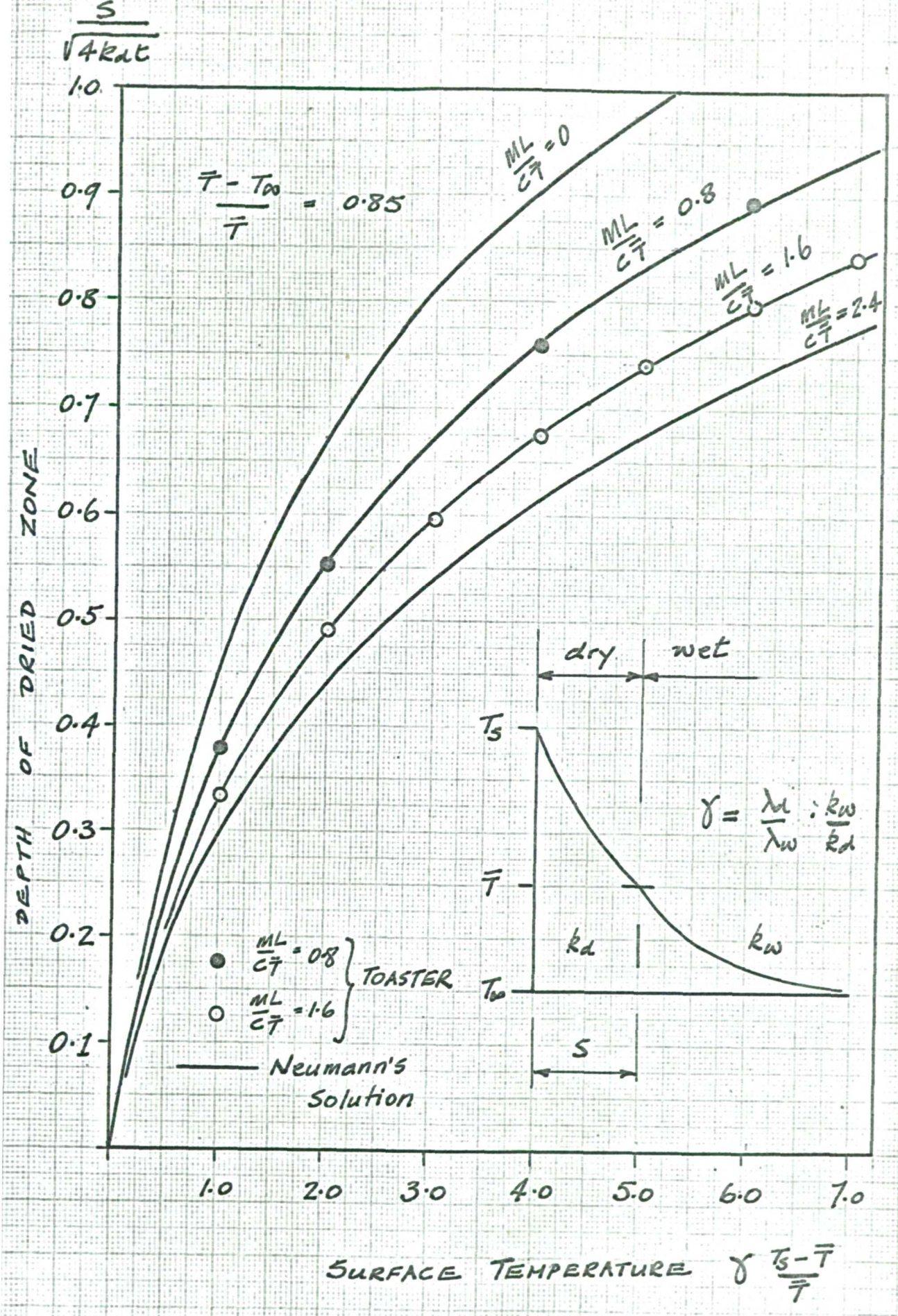


Figure 8-5 COMPARISON OF THE DEPTH OF THE DRIED ZONE OBTAINED BY ANALYSIS AND COMPUTATION

Table 8·3 Effect of mesh size on results from TOASTER for Neumann's problem

Neumann's Solution	Distance from hot face mms	Results from TOASTER δz = 2 δt = 1	5 7·5	10 30
235·66 (307·99)	10	235·9	236·3 (308·2)	242·5 (310·2)
85·46 (145·09)	20	85·6	85·6 (145·5)	89·9 (153·8)
52·54 (80·74)	30	52·6	52·8 (80·9)	54·6 (81·4)
32·43 (57·22)	40	32·4	32·6 (57·3)	32·4 (58·1)
17·43 (29·16)	60	17·4	17·4 (29·2)	17·4 (29·6)
16·53 (23·38)	Depth of Dried Zone mms	16·56	16·54 (23·42)	17·15 (23·44)

Data taken from Table 8·2 with T_s=500°C and $mL/c\bar{T}$ = 1·6. Values in parenthesis are those that obtain 10 minutes after the rise in surface temperature. The remainder are values after 5 minutes exposure.

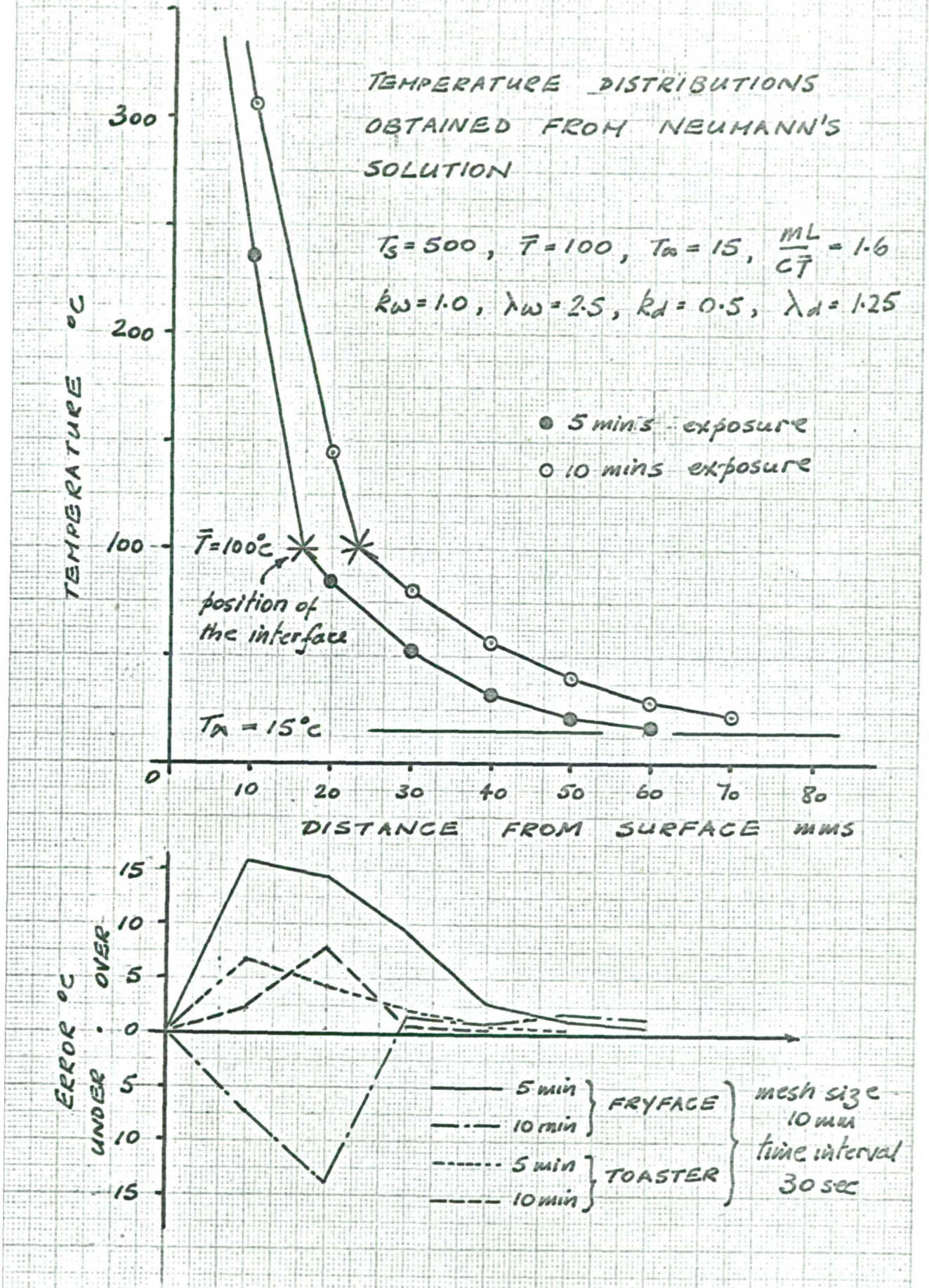


Fig 8.6 COMPARISON OF RESULTS OBTAINED FROM TOASTER WITH THOSE OBTAINED FROM NEUMANN'S ANALYTICAL SOLUTION

The various checks undertaken using Neumann's solution suggest that the numerical method used in TOASTER is satisfactory. This is a useful development, in itself, as a numerical treatment of this sort has possible applications, outside the range of the present work, in studying processes such as charring of timber and in certain problems in soil mechanics.

8·4 THERMAL

Returning to the present work, TOASTER has to be modified slightly to take account of the convection and radiation boundary conditions described in section 7·3 of Chapter 7. These modifications are included in the program THERMAL.

Boundary Conditions

The situation that obtains when calculating the surface temperature is shown diagramatically in figure 8-7. Here the heavy dots represent known values of temperature, at various times, and the open circles indicate values that are still to be determined. If the surface heat transfer coefficient is known, the surface temperature can be found directly from an equation of the form of 7·7·3a (p.205). This introduces a minor difficulty, as the value of this coefficient depends on the surface temperature, as shown in equations 7·3·1 to 7·3·3. Apparently, these non-linear equations have to be solved, with 7·7·3a, to find the surface temperature. However, it was found that this process is unnecessary if the surface heat transfer coefficient, to be used with the boundary condition, is first calculated from a reasonably close estimate of the surface temperature.

The procedure used in the program is as follows. The

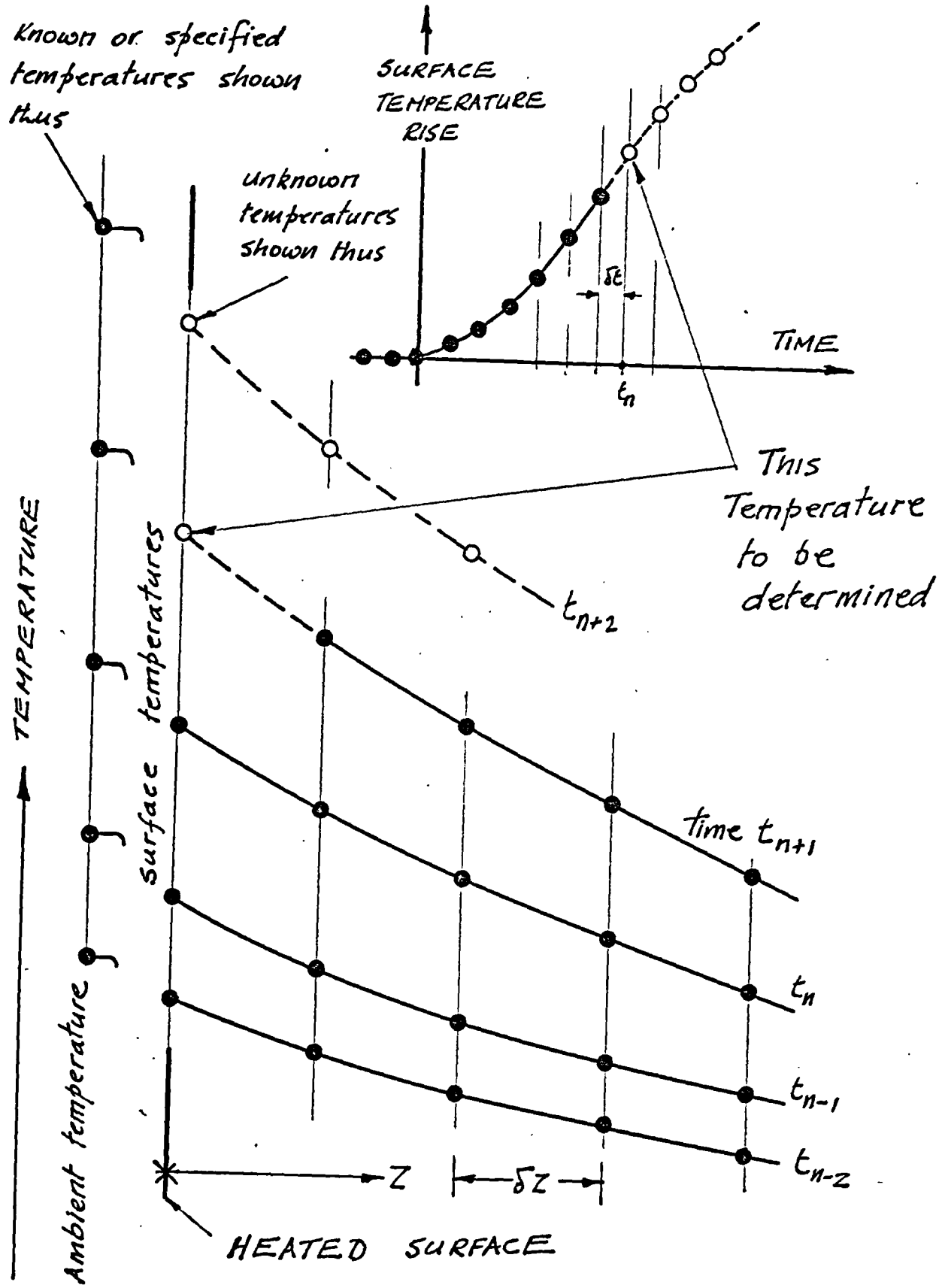


Figure 8-7 SITUATION IN THE COMPUTATION IMMEDIATELY PRIOR TO FINDING THE SURFACE TEMPERATURE AT TIME t_n

surface temperature at time t_{n+1} is estimated to be $T'_{s,n+1}$ where

$$T'_{s,n+1} = 3(T_{s,n} - T_{s,n-1}) + T_{s,n-2} \qquad (8\cdot4\cdot1)^{+}$$

and $T_{s,n}$, $T_{s,n-1}$ and $T_{s,n-2}$ are the surface temperatures that obtain after each of the three preceding time increments δt. The value of the surface temperature calculated from equation 8·4·1 are used with equations 7·3·2 and 7·3·3 to determine the surface heat transfer coefficient. This is then employed, with the boundary conditions, to obtain a new value of the surface temperature. The forward extrapolation procedure is clearly adequate, as the estimated and revised values of the surface temperature are practically identical for the time intervals most often used. Identical procedures are used at the hot and cool faces of the wall panel.

Heating Pattern

The program THERMAL is written for a wall panel in which the initial temperature equals the constant ambient temperature T_a outside the cool face. The temperature T_f outside the heated face is taken to rise in the manner

---

Footnote^{+} Equation 8·4·1 can be established by writing a Taylor's series for each of the temperatures that obtain at the previous three time intervals in terms of the surface temperature at time t_{n+1} and its derivatives with respect to time. If terms of order higher than 2 are ignored, the series provide three equations that can be solved for $T_{s,n+1}$.

specified in the I.S.O. standard 8·3·4 so that

$$T_f = T_s + 345 \ \mathrm{Log}_{10} (8t + 1) \qquad (8·4·2)$$

where the temperatures are in degrees Centigrade and the time t is in minutes. Clearly, the use of a functional form, such as 8·4·2, for the temperature rise is a convenience which assists in data preparation. Other forms of surface temperature rise could accommodated within the program.

Data

The data for each case to be studied using THERMAL comprises the initial details of the wall, the properties of the concrete, the computation parameters together with the output specification. Each set of data requires the preparation of five punched cards as shown in Table 8·4. The specified time interval δt is reduced by the program, if the stability condition 7·6·6 is not satisfied. Thus, some preliminary calculation is advisable if the results are required at predetermined time intervals. The output from THERMAL is obtained in a similar form to that of TOASTER, shown in figure 8-2, except that the estimated values of surface temperature, used in calculating the surface heat transfer coefficient are printed in the place of $\sqrt{4k_d t}$.

8·5 Results from THERMAL

Before considering concrete, it is helpful to study the behaviour of some other materials in order to obtain an idea of the way in which different thermal properties may affect

Table 8·4 Data preparation for THERMAL

CARD NUMBER	DATA	PUNCH IN COLUMNS
1	General Control Card punch TRUE	1-4
2	WALL Properties	
	Width, mms	1-10
	Surface value $mL/c\bar{T}$	11-20
	Centre value $mL/c\bar{T}$	21-30
	Initial temperature °C	31-40
	Surface emissivity	41-50
3	Concrete Data	
	Thermal conductivity of wet concrete W/m°C	1-10
	Thermal diffusivity of wet concrete mm^2/sec	11-20
	Vapourisation temperature °C	21-30
	Thermal conductivity of dry concrete W/m°C	31-40
	Thermal diffusivity of dry concrete mm^2/sec	41-50
4	Calculation Parameters	
	Number of mesh points; odd number only (RA)	1- 5
	Time interval, secs	6-15
5	Output Control	
	Overall Time minutes	1-10
	Print out interval (space) integer (RA)	11-12
	Print out interval (time) (RA)	13-14
	Form of output 1,2 or 3	15
CLOSURE	The above sequence of five cards in repeated for each set of data. After the last set a further card punched FALSE is required.	1-5

the temperature distribution and to demonstrate where concrete fits into the general pattern. The temperatures, obtained in a 100mm thick wall panel heated on one face, are shown in figure 8-8 for each of the three materials having the thermal properties shown in Table 8·5. These properties correspond reasonably closely to those of an aluminium alloy, a stainless steel and translucent fused silica and so range from those of an extremely good conductor to those of a typical dense ceramic. Referring to figure 8-8, it is seen that the temperature difference between the exposed and unheated faces of the aluminium panel is less than 30°C and that a substantial quantity of heat must be transferred through the panel to the surroundings. Also, the temperature rise near the heated face is less than for the two poorer conductors, as heat is removed rapidly form this region by conduction.

The thermal properties of the stainless steel are approximately an order of magnitude less than those of the aluminium alloy, but it is a reasonably good conductor and the temperature difference across the slab is only 170°C after 45 minutes exposure. However, greater differences in behaviour are obtained with the fused silica which has thermal properties about two orders of magnitude lower than those of the aluminium alloy. The silica is a relatively poor conductor of heat so that both the temperature rise at the heated face and the difference in temperature across the panel are high. Also, very little heat is lost to the surroundings; the temperature at the unheated face being only 84°C after 45 minutes exposure.

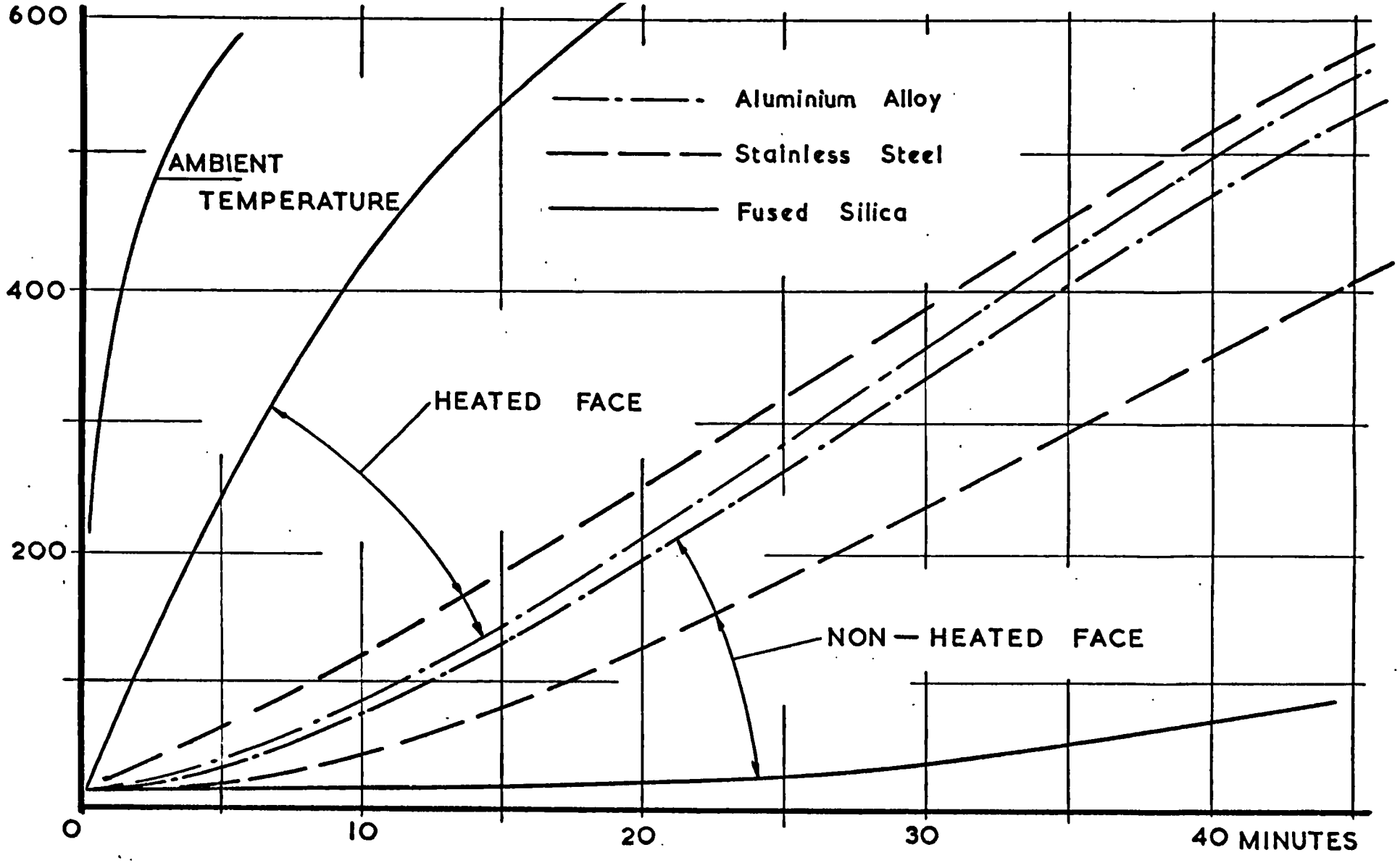


FIG. 8–8 RANGE OF TEMPERATURES IN THREE PANELS MADE OF MATERIALS WITH WIDELY DIFFERENT THERMAL PROPERTIES

Table 8·5 Thermal Properties of the materials compared in figure 8-8

Material	Thermal Conductivity W/m°C	Thermal Diffusivity mm^2/sec	Comment	Reference
Aluminium Alloy D.T.D. 683	162	67·2	Mean over range 20-400°C	Johns (1965)
Stainless Steel Jethete M160	22·5	7·75	Constant up to 400°C	Johns (1965)
Translucent fused silica	1·40	0·68	Approx. values for 20-500°C	Thermal Syndicat Ltd. re Vitreosi

The calculations were undertaken using an assumed constant value of Emissivity of 0·8. The standard rate (I.S.O. 834) of ambient temperature rise was used outside one face of the panel. The ambient temperature outside the unheated face was taken to remain constant at 15°C.

It will be noted that the differences in behaviour illustrated in figure 8·8 have been obtained only by considering materials with exceptionally large differences in thermal properties. Also, the thermal properties of normal density concretes are of the same order as those of fused silica and the variation with materials, mix proportions and moisture content is very small in comparison with the range of values used in obtaining the data of figure 8-8. In these circumstances, the narrow range of results obtained from the tests on concrete wall units (figure 6-13 p. 182) is readily understandable.

No consideration of drying was necessary in deriving the data shown in figure 8-8. However drying will occur in concrete and it is necessary to estimate values for the parameter $mL/c\bar{T}$ for use in the calculations. For a normal density concrete, containing between 10% and 12% of evaporable water by volume (see p. 109), the parameter will lie in the range 1·05 to 1·35, if vapourisation occurs at 100°C and at atmospheric pressure. This range has been broadened, to extend from 0·8 to 1·5, in obtaining the results shown in figure 8-9. This refers to a 100mm thick concrete wall panel heated on one side only. In the calculation it was assumed that the parameter $mL/c\bar{T}$ had a constant value across the width of the wall and the values of the thermal diffusivity and conductivity of the concrete were taken to be 1·0 mm^2/sec and 2·5 W/m°C before drying with half these values being used for the dried material. To help in assessing these data, the range of results

obtained in the tests on concrete panels, reported in Chapter 6, are also shown as background to the figure.[+] It is clear that there is fair agreement between the computed temperatures and the results of the tests, although the computed temperatures appear to be rather too high at points 10mm and 20mm from the hot face and too low at greater distances into the wall.

The effects of moisture movement have been very much simplified in the analysis and it would therefore be too much to expect exact agreement between the computed results and experiment. In spite of this, it seems possible that some improvement may be obtained if it is recognised that the escape of steam is restricted, in a real wall, and that the vapour is generally produced under a modest pressure at temperatures somewhat greater than 100°C. The results shown in figure 8-10 represent an attempt to include this effect in the calculations. Here, the vapourisation temperature has been increased to 120°C, for which value the parameter $mL/c\bar{T}$ could be expected to be in the range 0·9 to 1·1. Also, the insulating effect of the dried surface layer on the material remote from the heated face, has been reduced by increasing the values assumed for the thermal conductivity

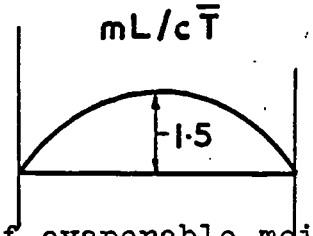
---

Footnote[+] This arrangement is used for the remaining figures of this section. The numerical data in the top left hand corner of each figure comprises the value of the major parameters used in the calculation. A key to these data is given in Table 8·6. Figure 8-9 appears on p. 243.

Table 8·6 KEY TO FIGURES 8-9 to 8-13

VARIABLES

These are displayed on the figures as shown below



Distribution of evaporable moisture across the width of the wall

	DRY	WET	
Thermal	0·90	2·10	Thermal conductivity
Diffusivity	0·40	1·20	

Thermal Properties

Constant Factors

Wall width	100 mm
Emissivity	0·8

NOTES

The figures are superimposed on a copy of figure 6-13 to provide an easy means of comparison with the range of results to be expected in an experiment.

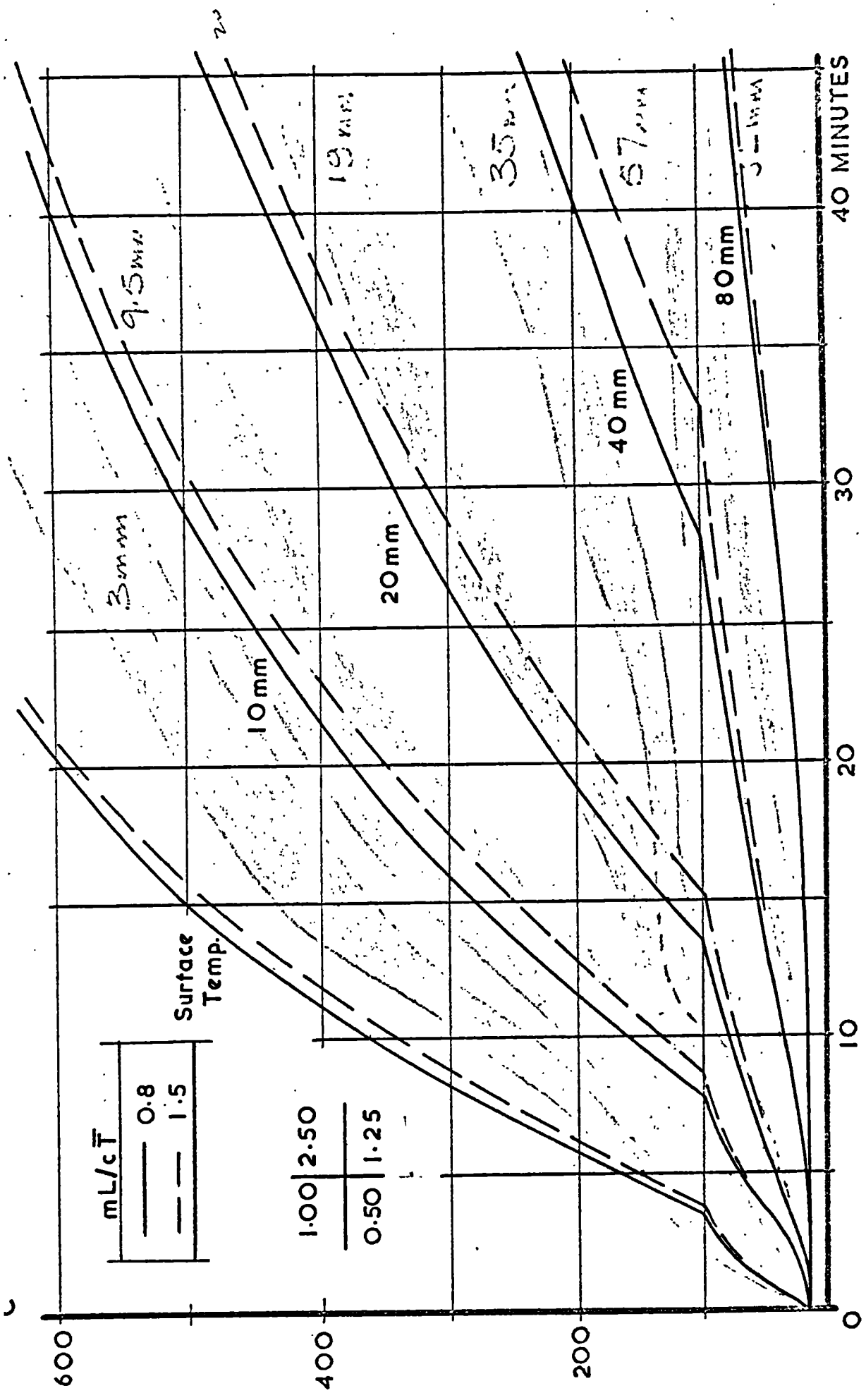


FIG. 8—9 TEMPERATURES CALCULATED FOR A CONCRETE WALL PANEL IN A FIRE TEST — TRANSITION TEMPERATURE 100°C — mL/cT̄ CONSTANT

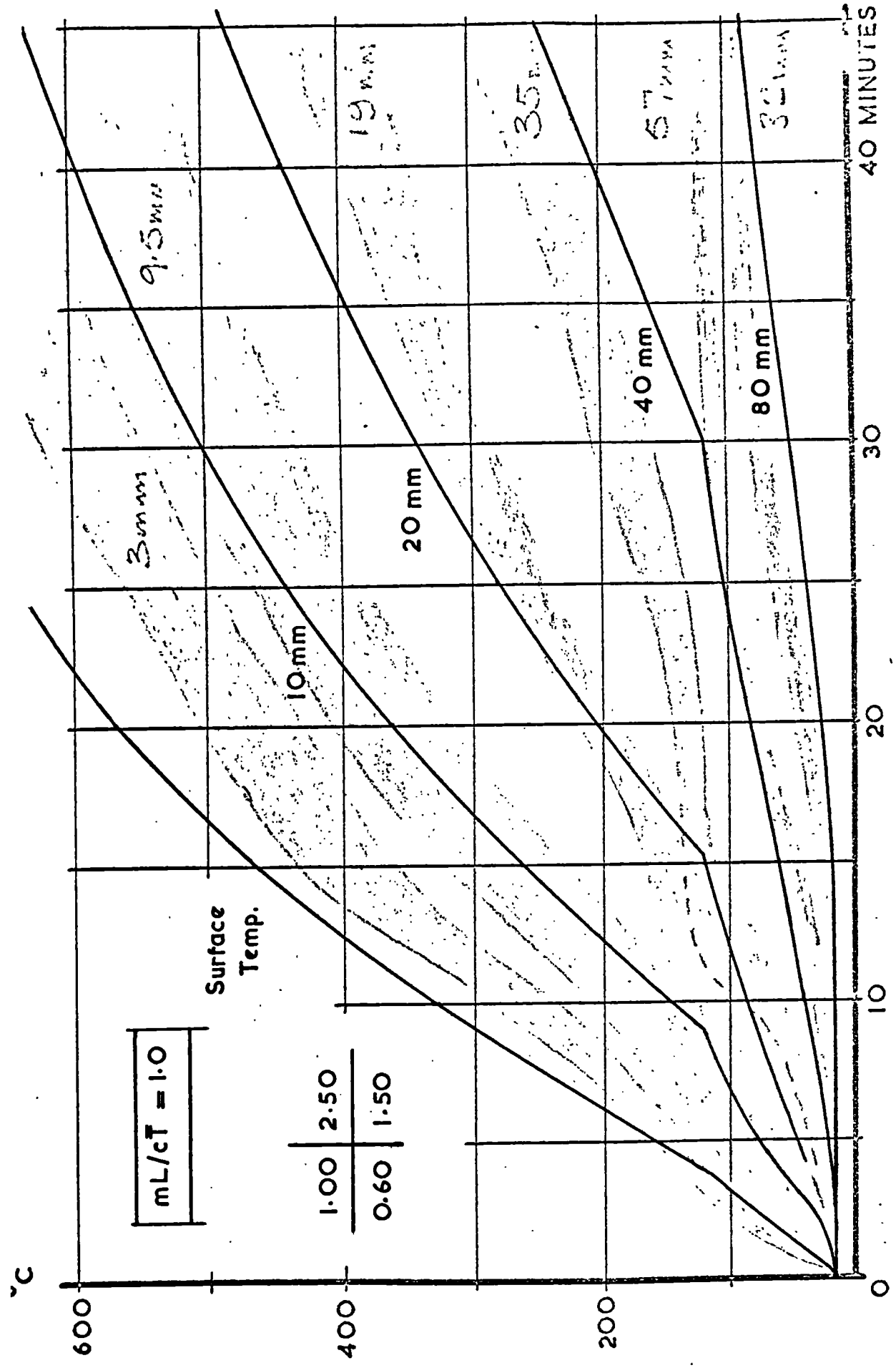


FIG. 8-10 TEMPERATURES CALCULATED FOR A CONCRETE WALL PANEL IN A FIRE TEST — TRANSITION TEMPERATURE 120°C — mL/cT̄ CONSTANT

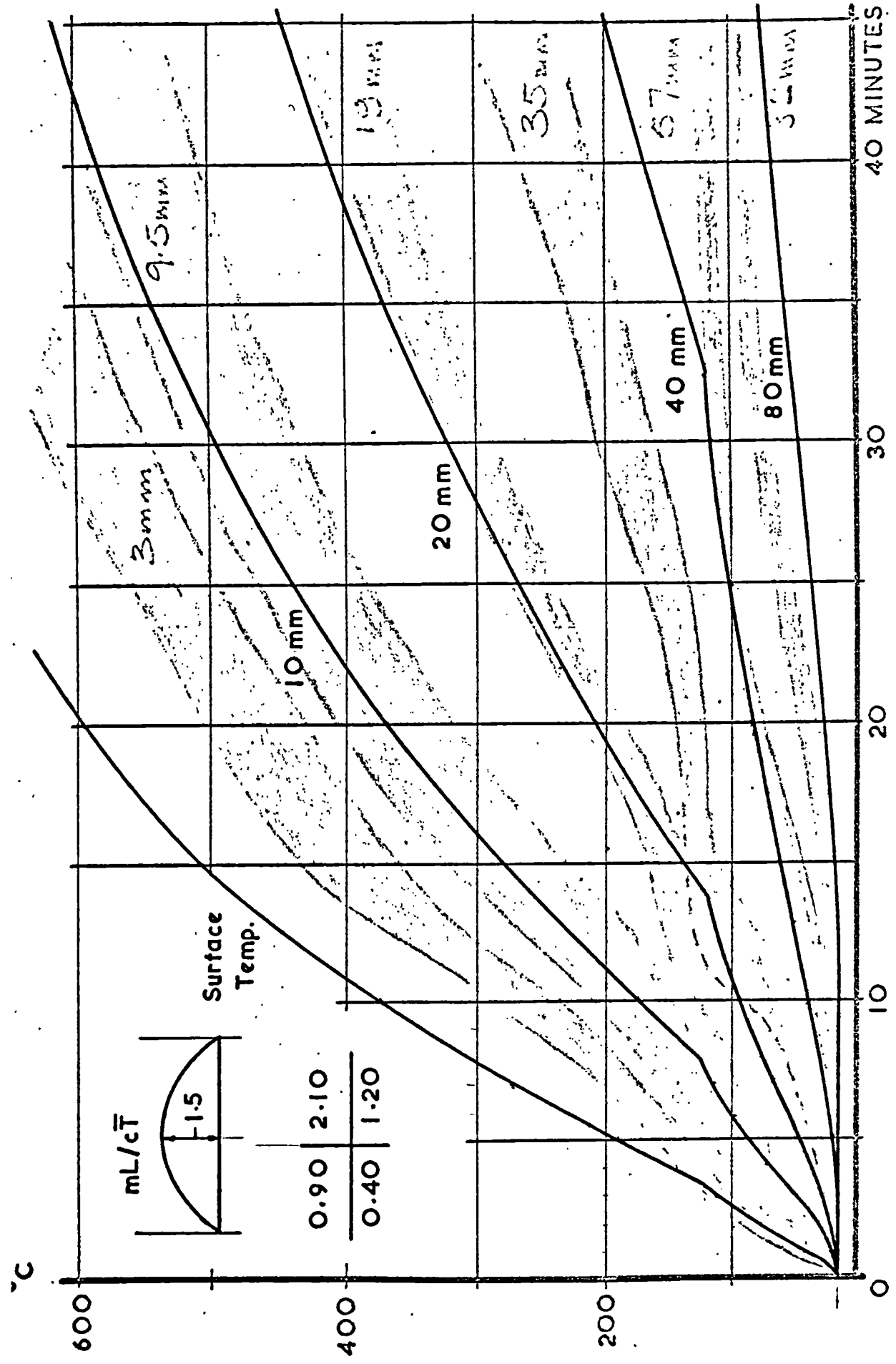


FIG. 8–11 TEMPERATURES CALCULATED FOR A CONCRETE WALL PANEL IN A FIRE TEST — TRANSITION TEMPERATURE 120°C.— mL/cT̄ PARABOLIC

and diffusivity of the dried material. The effect of these changes on the calculated temperatures is surprisingly small and no significant improvement in the overall result is obtained.

Slightly better agreement is obtained by using a parabolic distribution, for the moisture parameter $mL/c\bar{T}$, with a higher value at the centre of the wall than at the surface. This arrangement provides results of the form shown in figure 8-11 from which it is seen that, although the temperatures in the cooler regions are slightly under-estimated, there is reasonably good agreement in the vicinity of the heated face. The reason why the parabolic moisture distribution gives a slightly better result is not entirely clear. However, it is considered that the temperatures, obtained in this way, do provide a reasonable basis for an investigation of the structural behaviour of a heated panel. This topic is taken up in the next chapter. However, before doing this, it is convenient to discuss the results obtained for the thermal problem in greater detail.

8·6 Discussion

There are two major differences in the general form of the temperatures obtained by the numerical analysis and by experiment. The first of these has already been noted in that the numerical approach consistently underestimates the temperature in regions some distance away from the heated face. The second difference is most apparent when the results from THERMAL are compared with the test results from individual planks (figures 6-5 to 6-12, p. 172 et seq). In this way, it is seen that, for any particular point,

the change in slope of the temperature/time curve around the vapourisation temperature is much more marked in the computed results than in those found by experiment. In seeking reasons for these discrepancies, it must be realised that the analytical results are not greatly altered by changes in the values of the thermal properties used in the calculations, provided that these are kept within the narrow range appropriate to concrete. Because of this, it appears that the errors in the analytical solution must occur because of limitations imposed by the initial assumptions. These were most suspect in the treatment of vapourisation and in the neglect of heat transfer due to movement of the fluid phase.

The discontinuity in slope of the temperature/time graph in the analytical solution occurs because of the assumed difference in properties in the wet and dry zones. If drying occurred and had no effect on the thermal properties there would be no discontinuity in the slope of the individual temperature/time curves. This is demonstrated in figure 8-12 in which smooth occurs are obtained, in spite of vapourisation at 100°C, because the thermal properties in the dry and wet zones are identical. This result suggests that the assumption, that there is an abrupt division between the dry and wet zones, may be at fault and that there is really a smooth change in thermal properties with temperature during vapourisation. This appears reasonable, as vapourisation of the free water in the large capillary pores of the concrete will be followed by desorption of some of the more firmly bound water within the

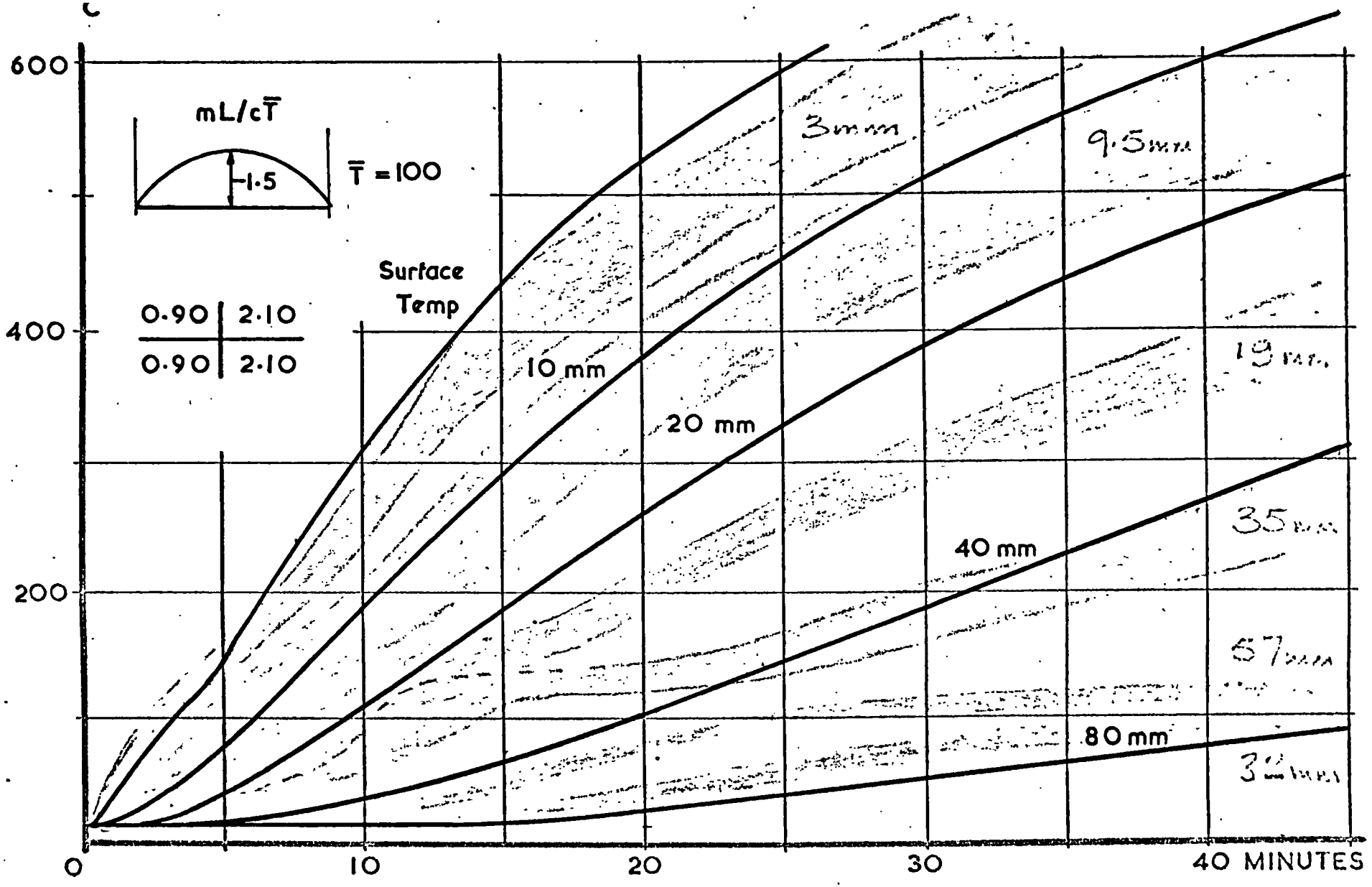


FIG. 8—12 TEMPERATURES CALCULATED TO ILLUSTRATE THE RESULT OF DRYING WITHOUT ANY CHANGE IN THERMAL PROPERTIES

nominally dry zone. Thus, vapourisation is likely to occur throughout a region rather than at an interface and the thermal properties at each point are likely to change continuously with temperature and moisture condition. More information on the effects of temperature and desorption of moisture on the thermal properties of concrete would used to be obtained and checked under transient conditions before these effects could be satisfactorily included in an analysis. However, it is felt that the effect of these refinements would be relatively slight at points some distance away from the zone in which vapourisation occurs and that the assumptions of a definite interface provides the most practical approach to the problem, even though this leads to some irregularity in the results near the assumed interface.

Rather than concentrate on behaviour in the vicinity of the interface it seems more important to consider effects due to movement of the fluid phase. In the early stages of heating, some of the vapour that is liberated by drying is expelled through the heated face but the remainder is driven in the direction of heat flow further into the wall where it condenses in the cooler regions. No account has been taken of this vapourisation-condensation cycle in the analysis but it seems that the heat transferred in this way may have a significant effect on the temperatures in the cooler regions.

Consider a wall panel of width d, that is heated on one side. After a certain period of time the wall has been dried to a depth s and the total quantity of heat used in

vapourisation is $mL\rho s$ per unit area of wall, where the symbols are as defined in section 8-2 of this Chapter. Now, suppose that the proportion of the vapour retained in the wall, by condensation in the cool regions, is F. Then the average rise in temperature ΔT_c of the material in the wet region, due to the heat available from condensation, is given by

$$\Delta T_c = F \frac{mL}{c\bar{T}} \frac{s}{(d-s)} \bar{T} \qquad (8\cdot6\cdot1)$$

As an example, consider a panel 100mms thick at a time when drying has already penetrated to a depth of 25mms from the heated face. Suppose the average value of the vapourisation temperature is 120°C, for which a realistic value for $mL/c\bar{T}$ is around unity. In these circumstances, it is necessary for only one half of the vapour liberated to be retained in the wall for the average temperature in the wet zone to be increased by about 20°C. In this calculation, the value of one half, taken for the fraction F, may be considerably in error. However, it seems significant that an increase of around 20°C, at point 80mms away from the heated face, would bring the computed temperatures very much more in line with the experimental results.

Consideration of the vapourisation-condensation cycle also provides an explanation for the improvement in the results calculated on the basis of a parabolic distribution of moisture content. The effect of the cycle is to move

moisture from the heated surface towards the centre of the panel which thus has a greater moisture content at the time when vapourisation occurs, than the region near the surface. Clearly, the parabolic distribution would not be appropriate in a calculation extending over a considerable time, in which the depth of drying exceeded half the depth of the slab. However, for short exposure times, or for symmetric heating from both sides, the use of the parabolic moisture distribution appears to provide some allowance for the effects of mass transfer. In a similar way, it may be possible to make an allowance, in the analysis, for the effects due to transfer of latent heat by using an artificially high value for the thermal diffusivity of the material in the wet zone. Some results of this sort are shown in figure 8-13. It is seen that the trend of the results is in the right direction but, a rational theory is required in order to establish the effective diffusivity for combined conduction and latent heat transfer before this modification can be used satisfactorily.

In fire tests on concrete elements, liquid water is often expelled from the heated face some time after the start of heating (Carlson and Abrams 1965). This occurred in the tests on 100mm thick concrete wall units, described in Chapter 6, after about 25 minutes heating. For this to occur, the material, in the relatively cool region near the unheated face, must be saturated and it must be supposed that the accumulation of condensate, in the cool region, forms a saturated zone within the wall. This zone will provide

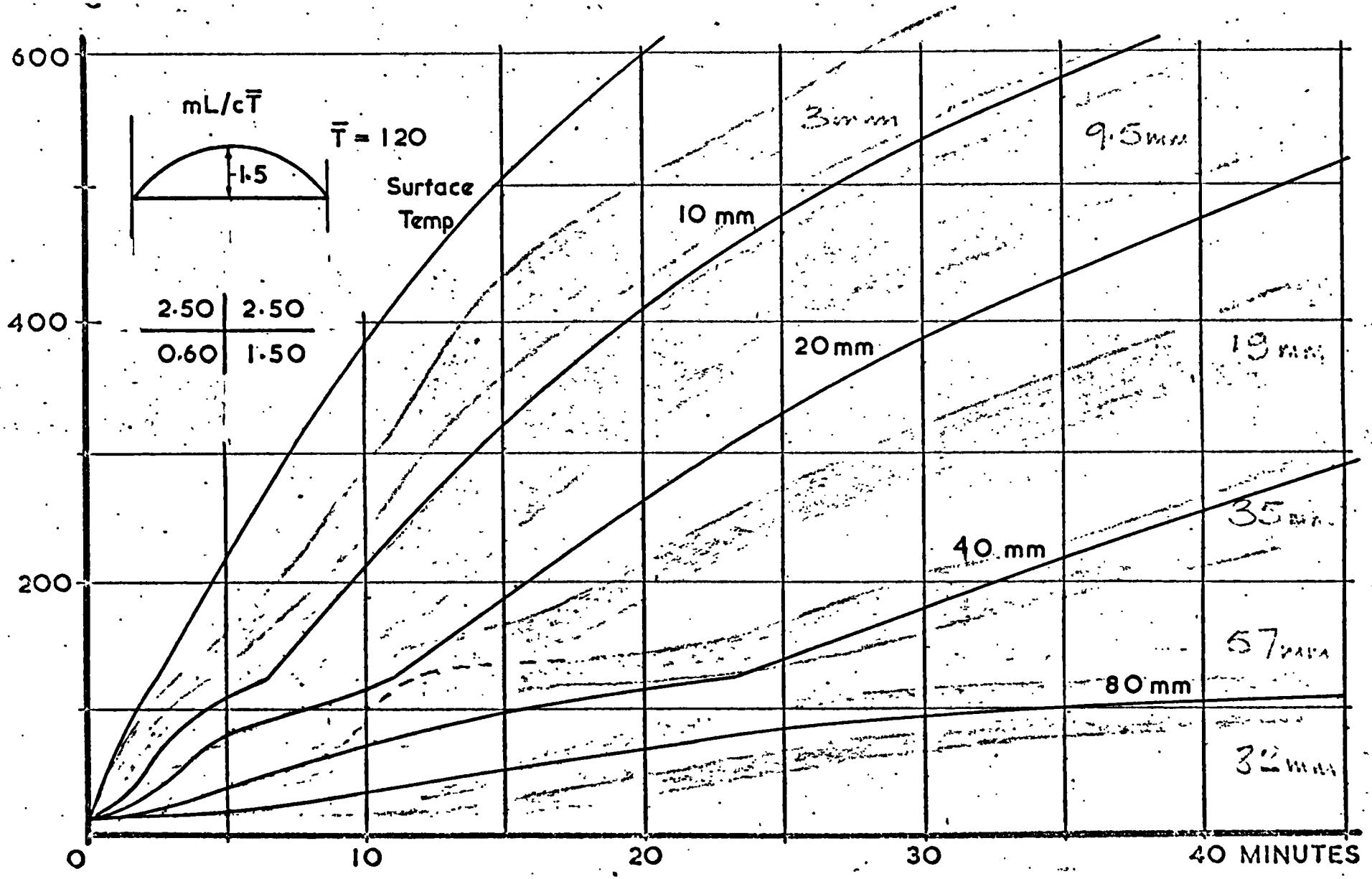


FIG 8—13 TEMPERATURES CALCULATED FOR A CONCRETE WALL PANEL ON THE BASIS OF AN ABNORMALLY HIGH WET ZONE DIFFUSIVITY

a barrier to the movement of vapour into the wall and so will inhibit the transfer of latent heat by vapourisation and condensation. On this basis, it appears that the effects of latent heat transfer will be most apparent in the early stages of heating, before a saturated zone is formed to restrict the movement of vapour. Once this occurs, the assumptions used in the analysis, described in this and the preceding chapter, should be adequate for the calculation of temperatures at succeeding time intervals.

8·7 Conclusions from the analysis of the Thermal Conditions

The main conclusions from this portion of the work may be summarised as follows

a) The results obtained from tests and analysis suggest that the effect of mix proportions on the temperature distribution is not very significant for the condition of rapid heating that obtains in a fire test.

b) The method of analysis used is subject to error which is mainly attributable to the neglect of the consequences of moisture movement within the pores of the concrete. These errors are most apparent during the initial stages of heating.

c) In spite of the limiting assumptions used in the analysis, the results obtained show reasonable agreement with the temperature measured in wall units during a fire test. It is considered that the agreement is sufficient, for the present purpose, and that the method can be used to produce the thermal data required in an investigation of possible modes of structural behaviour under fire conditions. This study is the subject of the following two chapters.

Chapter 9

STRUCTURAL BEHAVIOUR OF CONCRETE PANELS I

9·1 Introduction

The investigation described in the previous three chapters, of the thermal conditions that obtain in a fire test, provides a basis for examining the structural behaviour of a concrete wall or floor panel during heating. The results of this examination should indicate the conditions under which particular modes of general failure can occur in practice and should also provide information, concerning the average stresses in any region, which must be considered in a detailed study of local phenomena.

The structural behaviour is extremely complicated and some idealisations will have to be made for the purpose of analysis. Because of this, it is helpful to take an overall view of the situation before deciding on a particular analytical model so that the possible implications of any idealisation can be appreciated at the outset.

9·2 Analytical Preliminaries

Consider the slab of thickness d shown in figure 9-1. The slab extends indefinitely in the directions x and y so that effects that are local to the ends may be neglected. Suppose the surface $Z = 0$ is uniformly heated. The temperature within the slab is then a function of z only and, in these circumstances, the stresses will also be a function of Z only. Thus, from symmetry and for equilibrium within the slab,

$$\sigma_{xx} = \sigma_{yy} \quad \text{and} \quad \sigma_{zz} = \tau_{xy} = \tau_{yz} = \tau_{zx} = 0 \qquad (9\cdot2\cdot1)$$

This result is independent of any consideration of

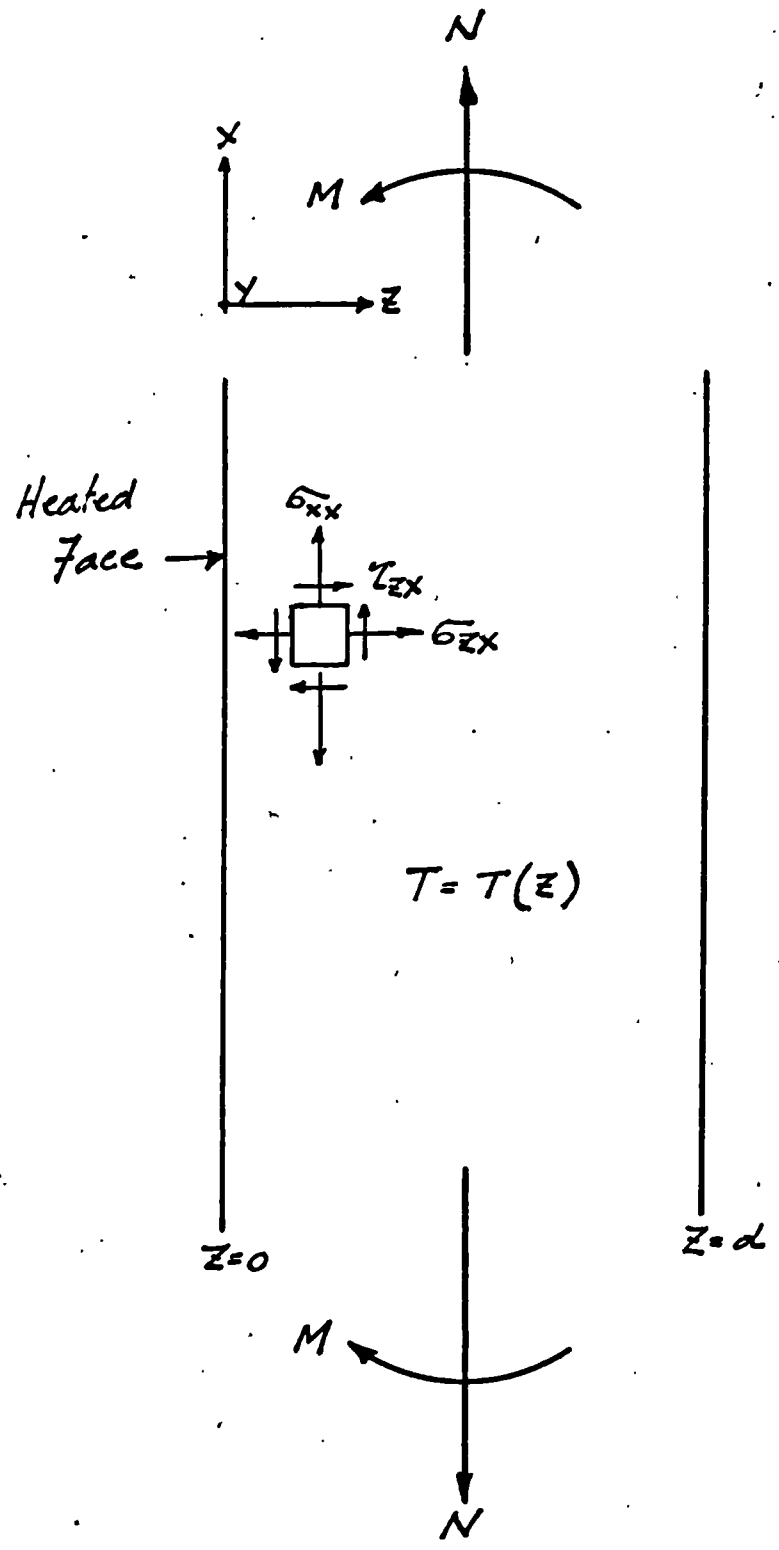


Figure 9-1 DETAIL OF THE WALL SHOWING NOTATION FOR STRESSES AND STRESS RESULTANTS

material behaviour other than the idealisation implied in the assumption of isotropy and homogeneity. The result is also restricted to situations where the curvature can be considered to be small.

The surface heating induces temperatures T and pore pressures u within the slab and it will be assumed that the effective stresses, for the calculation of deformation or strength of the material, are given by

$$\sigma'_{xx} = \sigma_{xx} + u = \sigma'_{yy} \quad , \qquad \sigma'_{zz} = u \qquad (9\cdot2\cdot2)$$

These equations follow from Terzaghi's effective stress concept which is an excellent approximation for most soils but not so good for concrete and rocks (Skempton 1960).

The curvature of the heated surface is constant and the strains are functions of z only. This implies that

$$\varepsilon_{xx} = \varepsilon_{yy} \qquad \text{and} \qquad \gamma_{xy} = \gamma_{yz} = \gamma_{zx} = 0 \qquad (9\cdot2\cdot3)$$

in which the equations of compatibility require that ε_{xx} and ε_{yy} be linear functions of z.

Equations 9·2·1, 9·2·2 and 9·2·3 are basic to any analysis of the overall structural behaviour of the slab. These equations must be supplemented by the relations between stress and strain for the heated material. In order to determine the range of stress and strain that must be covered by such a constitutive law, we examine a number of extreme cases.

9·3 The thick slab

First consider the slab to be very thick so that ε_{xx}

and ε_{yy} are both zero. Suppose also that the material is linear elastic and that the strain ε_{xx} can be regarded as the sum of the elastic strain, due to the effective stress components, the thermal strains αT and a creep strain C_{xx} i.e.

$$\varepsilon_{xx} = \sigma_{xx} \frac{(1 - \nu)}{E} + \frac{1 - 2\nu}{E} u + \alpha T + C_{xx} . \qquad (9\cdot3\cdot1)$$

Putting $\varepsilon_{xx} = 0$ gives the stresses

$$\sigma_{xx} = \sigma_{yy} = - \left(\frac{E (\alpha T + C_{xx})}{1 - \nu} + \frac{(1 - 2\nu)}{(1 - \nu)} u \right)$$

so that the effective stresses become

$$\sigma'_{xx} = \sigma'_{yy} = - \left(\frac{E(\alpha T + C_{xx})}{(1 - \nu)} - \frac{\nu}{(1 - \nu)} u \right) , \qquad (9\cdot3\cdot2)$$

with $\sigma'_{zz} = u$.

It is convenient to write

$$(\alpha T + C_{xx}) = (1 - R) \alpha T, \qquad (9\cdot3\cdot3)$$

Where R can be considered to be a measure of the relaxation of the thermal strain. In these terms the expressions for the effective stresses become

$$\sigma'_{zz} = u, \quad \sigma'_{xx} = \sigma'_{yy} = - \left(\frac{1 - R}{1 - \nu} E\alpha T - \frac{\nu}{(1 - \nu)} u \right) . \qquad (9\cdot3\cdot4)$$

It is interesting to use this analysis to find the temperature rise required to achieve the maximum possible compressive stress at the surface of a thick concrete slab. Clearly, this value is determined by the strength of the

material or, more correctly, the value of the peak stress obtained from the appropriate stress-strain curve, (here equal biaxial compression, as u = 0 at the surface). In order to obtain a feel for the problem,the following values are taken to be representative of a typical strong concrete.

Table 9·3·1 Typical Concrete Properties

Peak stress in biaxial compression	40·0 MN/m^2
Secant value of Young's Modulus	30·0 GN/m^2
Poisson's ratio, in the range	0·1 - 0·5
Coefficient of linear thermal expansion	10 x 10^{-6}/°C
Drying shrinkage accompanying the thermal expansion	200 x 10^{-6}
Relaxation parameter R, in the range	0 - 1

Based on these values, with Poisson's ratio 0·15, the temperature rise required to induce compressive stresses of 40·0 MN/m^2 at the surface of the slab can be found, for different values of the relaxation coefficient R. These data are given in Table 9·3·2

In considering spalling, interest is confined to the first half hour of heating, during which the surface temperature rises to around 600°C. Results obtained by Cruz (1968), from relaxation tests in uniaxial compression, suggest that the initially induced stress is reduced by less than 10% during half an hours heating at 316°C and by around

50% for a similar period of heating at 648°C. These data may not be entirely relevant to the present study, the initial stress in the tests being only 45% of the cylinder strength of the concrete used, with the specimens being heated for an hour at the test temperature before loading. However, it is considered that these results, taken together with Table 9·3·2 suggest that the peak stress would be reached at a surface temperature of only 130 - 150°C which could occur within the first five minutes of heating, during which the relaxation may be almost negligible.

Table 9·3·2 Temperature rise required to induce peak stress at the surface of a very thick slab

Relaxation Coefficient R	0	0·1	0·25	0·5	0·80
Temperature rise °C	133	146	171	246	585
Approx. heating time in the standard test	- - 5 - - - - - - -			10 - - - - -	

The values given in Table 9·3·1 are not universally representative but it seems reasonable to assume that the peak stress is likely to be achieved at the surface of a thick normal density concrete slab for a surface temperature less than 200°C. Two conclusions follow from this result.

a) The peak stress is likely to be achieved where large section members are subject to heating in the standard manner, and

b)) except during the first few minutes of heating, the behaviour of the material near to the heated surface is determined by the form of the 'descending branch' of the stress-strain curve.

Some workers (notably Saito 1965) have suggested that explosive spalling occurs when the compressive stress reaches a critical value corresponding to the strength of the material. The first conclusion tends to oppose this view, as it seems that the material near the surface of a concrete slab will generally be strained, to a point on the stress-strain curve, beyond the peak stress when spalling occurs. The second conclusion shows clearly that a linear analysis is inappropriate in an investigation of behaviour after the first few minutes heating and that the constitutive law used must include a description of the descending branch of the stress-strain curve.

9·4 Pore pressures

The analysis of the behaviour of the thick slab also suggests that pore pressure will have only a minor effect on the stresses or strains developed in the x and y directions. It is seen from equation 9·3·1 that a pore pressure u has a similar influence on the strain ε_{xx} as a temperature rise of $(1 - 2\nu)\, u/E\alpha$. If it is supposed that the pore pressure is that of saturated steam at temperature T_s the error in the strain ε_{xx}, caused by neglecting the pore pressure, is the same as that due to an error δ

temperatures around 150°C and it is clear, from the Table, that the pore pressures had little effect on the strains, in directions parallel to the surface of the wall, in these tests. It is considered that this result would be common to most tests of this sort.

It is seen, from equation 9·3·4, that the effect of pore pressure on the effective stresses σ'_{xx} and σ'_{yy} is less than on the corresponding strains if the effects are considered in terms of an equivalent temperature change. Thus, we can conclude that

c) the effect of pore pressure, on the stresses and strains in directions parallel to the heated surface, is of secondary importance to that of temperature rise and can be ignored in analysis. and

d) pore pressure induces a component of effective stress acting in a direction normal to the heated surface. This stress is almost unaffected by thermal strain and its effect on the mode of failure of the concrete in the vincinity of the hot face must be considered, at some stage.

9·5 The Thin slab symmetrically heated

As a second case study, consider a thin slab which is unrestrained in the longitudinal direction and heated on both sides in the same manner. The slab carries no net longitudinal load so that the stresses must satisfy the equilibrium condition

where $$\delta = \frac{(1-2\nu)\ u\ 100}{E\alpha T_s} \quad \%$$

in assessing the temperature within the wall. This value is shown in Table 9·4·1 for different values of the temperature T_s in the range 100 - 200°C. The values of pore pressure have been taken from steam tables and the results are shown for two values of $E\alpha/(1-2\nu)$. These have been chosen, using secant values for Young's Modulus, to be representative of the behaviour of concrete under increasing stress and at a high strain on the descending branch of the stress-strain curve.

Table 9·4·1 Percentage change in temperature equivalent to effect of pore pressure

Temperature °C	$E\alpha/(1-2\nu)$ MN/m^2 °C	
	0·5	0·1
100	0	0
125	0·2	1·1
150	0·5	2·5
175	0·9	4·6
200	1·5	7·5

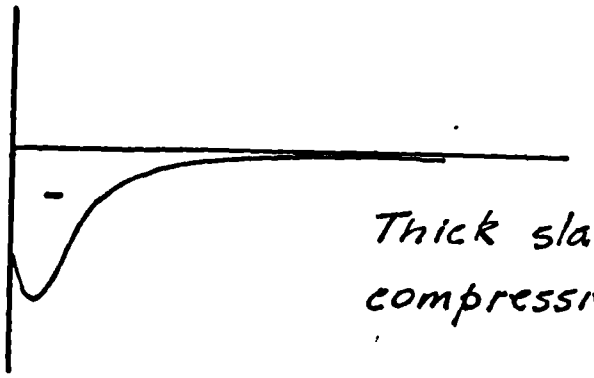
The experimental results given in Chapter 6 suggest that steam was produced in the tests at Boreham Wood at

$$\int_0^d \sigma_{xx}\, dz = 0 \qquad (9\cdot5\cdot1)$$

Because the longitudinal stresses must satisfy condition 9·5·1 any compressive stress induced in the outer layers of the concrete must be accompanied by tensile stresses in the central cooler regions. This is shown diagramatically in figure 9 - 2b. Here, heat has penetrated only a small distance into the wall when the stress distribution (1) is obtained and the tensile stresses within the wall are still modest. Some time later, more heat has been supplied and the surface temperature and depth affected by heating have both increased. At this time, the stress distribution could be similar to that marked (2) in the figure.

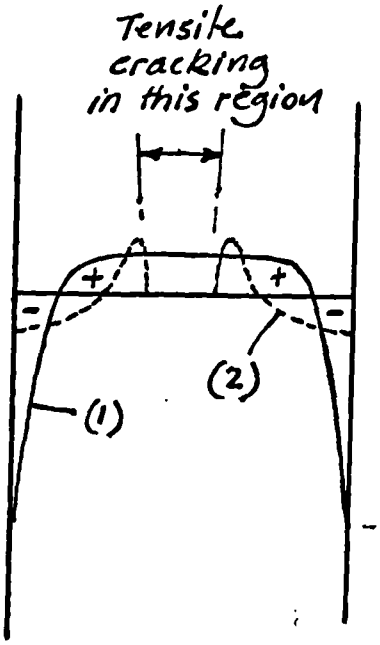
The magnitude of the tensile stresses developed will depend very much on the thickness of the wall. However, it is clear that there will be occasions when cracking occurs in the central regions and that this will inhibit the development of compressive stress in the hot outer layers. For very thin walls, it seems that such cracking could occur before the concrete in the outer layers has achieved the peak stress expected from the stress-strain curve in compression. Alternatively, for thicker walls in which the peak stress in compression has been reached, subsequent tensile cracking causes an increase in longitudinal strain and the behaviour during unloading, from a point on the decending branch of the stress-strain curve, becomes important in the analysis. Two further conclusions follow from these arguments. These are,

9-2a



Thick slab - stresses compressive throughout

9-2b

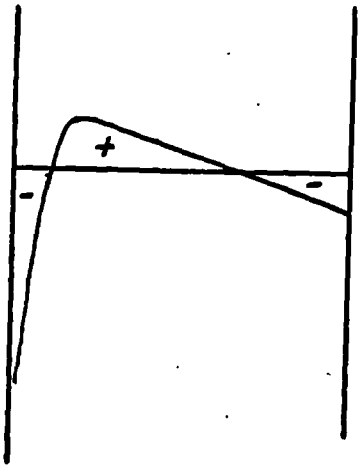


Thin slab heated from both sides

(1) Soon after exposure

(2) Later, when development of thermal stress is limited by cracking

9-2c



Thin slab heated from one side only showing effects of curvature on the stress distribution

Figure 9-2 Initial Qualitative View of the development of thermal stress in wall panels during a fire test

e) that behaviour in tension, including tensile cracking should be included in the analytical model and

f) that the description of the stress-strain curve for concrete used in the analysis must include effects due to reversals of the sense of deformation.

It is interesting to note that, following a reversal of the sense of deformation, a reversal of the sign of the stress could eventually occur at the outer face. The existance of this sort of behaviour has been established, for an elastic-perfectly plastic bar , by Parkes (1961) and, if similar behaviour is obtained with concrete, this could provide an explanation for the phenomenon of 'sloughing off' that sometimes occurs at a late stage of heating.

9·6 The thin slab heated on one side only

If the slab considered in the last section is heated on only one side, the symmetry condition is replaced by the equilibrium equation

$$\int_0^d \sigma_{xx} z dz = 0 \qquad (9\cdot6\cdot1)$$

which must be considered together with equation 9·5·1.

If the slab is thin, some curvature occurs even in the early stages of heating when the longitudinal stress distribution is of the form shown in figure 9 -2c. In this situation, the curvature of the slab induces compressive stresses in the concrete near to the cooler face so that relatively high tensile stresses may be developed within

the slab. Initially some cracking may occur, to limit the development of compressive stress, but it seems possible that some of these cracks will be closed as heat penetrates further into the wall and, eventually, the fractured surfaces may be required to carry compressive stress. No attempt is made to follow this behaviour in the figure. However, we conclude that

g) besides tensile cracking, crack closure and subsequent behaviour in tension should be included in the analytical model.

9·7 Creep

At the present time there is little information available on the effects of creep at very high temperatures. However, it is clear from the work done by Cruz (1968) that the rate of creep is much greater at high temperatures than at moderately elevated or normal temperatures so that creep could have a profound effect on the stresses induced in a member during heating to high temperatures. On the other hand, a test for fire resistance is of relatively short duration and, in a study of spalling, the behaviour of most interest occurs within the first 30 minutes or so from the start of the test. Thus, it seems probable that the effects of even a high rate of creep may not be of major importance in investigating the stress distribution at times when the occurrence of spalling is most possible.

This last view is supported, to some extent, by the results of tests, undertaken at the P.C.A. laboratories and reported by Issen et al (1970), on beams heated under

restraint in the standard manner. Very large axial forces were induced during heating. In one test for example, on a 4·85m long reinforced concrete double T section (see figure 4-8), the beam was allowed to expand 3·4mm freely before being restrained against axial movement. The restraining system became effective after about 15 minutes heating and the maximum thrust of 2·17MN was obtained after 90 minutes heating, the thrust reducing to 1·47MN as the test was continued for a further 2 hours 40m. The maximum axial force that the section could withstand in a uniaxial compression test under normal temperature conditions can be calculated to be 8·2MN and this load capacity must be reduced considerably by heating because of the relatively thin webs and flange+. The recorded axial thrusts are thus an appreciable proportion of the load capacity of the heated section. It appears therefore, that although some relaxation of the thermal stress must have occurred, this was not sufficient to affect the structural behaviour of the beam to any great extent.

In the analysis that follows effects due to creep are ignored. In spite of the arguments presented here, it is realised that this may be a serious omission. However, it is considered that an analysis ignoring creep can provide

---

+ Merely for comparison; Thomas and Websters (1953) results suggest that the strength of a 450mm square lightly reinforced concrete column would be reduced by 40% after $1\frac{1}{2}$ hours heating and possibly 70% after 4 hours. The cross sectional area and heated perimeter of the column are comparable to those of the double T section.

information that is useful and relevant to the early stages of heating.

9·8 Method of Analysis

We consider the slab shown in figure 9-1 for which we require to find the stress distribution at all times from the start of heating. The equations of equilibrium and compatibility lead to

$$\int_0^d \sigma dz = N \qquad (9\cdot8\cdot1)$$

$$\int_0^d \sigma\,(z - d/2)\,dz = M \qquad (9\cdot8\cdot2)$$

$$\text{and} \quad \varepsilon = \bar{\varepsilon} + \chi(z - d/2) \qquad (9\cdot8\cdot3)$$

where $\bar{\varepsilon}$ is the longitudinal strain at the mid plane of the slab, χ is the curvature and the suffices $_{xx}$ and $_{yy}$ have been omitted from the symbols for the components of stress and strain (cf. equations 9·5·1 and 9·6·1)

At any point, the longitudinal strain ε can be considered to be the sum of the thermal strain ε_T and the strain, ε_s, due to the stress at the point considered. Thus,

$$\varepsilon = \varepsilon_s + \varepsilon_T \qquad (9\cdot8\cdot4)$$

If creep were to be considered, the creep strain (being due to stress) would be included in the component ε_s. Also, the term thermal strain will be taken to include

both linear expansion and any concomitant drying shrinkage.

It will be assumed that for, any temperature T, a relationship between the stress σ and the strain component ε_s has been established. At any stage, this relationship depends on the state of the material H. This will depend on a wide range of parameters (such as the extent of cracking, the sign of the stress, the sense of deformation etc.) which themselves reflect the previous history of loading and temperature change. Thus the relationship between stress and strain is a function of the temperature and state of the material i.e.

$$\sigma\ (\varepsilon_s) = \sigma\ (\varepsilon_s, T, H) \qquad (9{\cdot}8{\cdot}5)$$

The form of this relationship and the definition of H will be discussed in the next chapter which will deal with the details of the analysis and the assumed material behaviour. Before this, it is convenient to discuss the method of analysis in general terms.

It is clear, from the arguments developed in earlier sections of this chapter, that there will be appreciable changes in the structure and stiffness of the slab during heating. In problems such as this, the most satisfactory method of solution is to work in small increments of real, or parametric, time and solve a series of linear problems for the various increments of stress and strain. In general, each of these linear problems requires an iterative solution as the relevant linear properties can only be estimated at first and then improved once a solution over the time interval is obtained. Procedures

of this sort have been used successfully in non-linear elasticity (Clough 1965), plasticity (Mendelson 1968) and other branches of mechanics. The main difficulty lies in achieving convergence for the particular model of material behaviour used in the analysis.

By adopting the incremental procedure, the present problem can be expressed in the following terms. At time t, the temperature T, stress σ, strains ε, ε_s and ε_T are known throughout the thickness of the wall together with the state of the material, H, at any point. A short time later, at time $t' = t + \delta t$, the temperature T' and the thermal strain ε'_T are both known and we require to find the stress σ', strain ε' and material state H'. Once these are known, a further time interval can be considered.

Estimates can be made of the strain and material state, at time t', from the data known at time t. Let these estimates be ε^* and H^*. These values lead to an estimate for the strain, ε_s^*, due to stress (from equation 9·8·4 and an estimate of the stress σ^*, from the functional relationship 9·8·5 in the form,

$$\sigma^* (\varepsilon_s^*) = \sigma^* (\varepsilon_s^*, T', H^*)$$

The estimated stress σ^* will be different from the true solution by an amount $\delta\sigma$ i.e.

$$\sigma' = \sigma^* + \delta\sigma \qquad (9·8·6)$$

or, proceeding formally,

$$\sigma' = \sigma^* + \left(\frac{\partial\sigma}{\partial\varepsilon_s}\right)^* \delta\varepsilon_s + \left(\frac{\partial\sigma}{\partial H}\right)^* \delta H \quad , \qquad (9\cdot8\cdot7)$$

where $\delta\varepsilon_s$ and δH are the changes in strain and material state due to a stress increment $\delta\sigma$ at temperature T'. In the present problem, the last term in equation 9·8·7 must be regarded as symbolic, having a logical rather mathematical significance. The inherent difficulty of this concept is avoided by assuming, in the first instance, that H^* is a good estimate for the state of the material at time t', so that δH is taken to be zero. Then,

$$\sigma' = \sigma^* + c^* \delta\varepsilon_s \quad , \qquad (9\cdot8\cdot8)$$

where c^* is the estimated value for the slope of the stress-strain curve at temperature T' for the estimated state of the material. We write,

$$\delta\varepsilon_s = \delta\bar{f} + \delta\chi\,(z - d/2), \qquad (9\cdot8\cdot9)$$

where $\delta\chi$ and $\delta\bar{f}$ are the changes in curvature and strain corresponding to $\delta\varepsilon_s$. Now this equation can be used together with 9·8·8, to express the equilibrium equations in the form,

$$\begin{bmatrix} k_{11} & k_{12} \\ k_{21} & k_{22} \end{bmatrix} \begin{bmatrix} \delta\bar{f} \\ \delta\chi \end{bmatrix} = \begin{bmatrix} \delta N \\ \delta M \end{bmatrix} \qquad (9\cdot8\cdot10)$$

The square matrix, in this equation, is the stiffness matrix for the slab for small changes in load from those corresponding to the estimated stresses. The stiffness

matrix contains the terms

$$k_{11} = \int_0^d c^* dz \ , \ k_{12} = k_{21} = \int_0^d c^* (z - d/2)dz$$

$$\text{and} \quad k_{22} = \int_0^d c^* (z - d/2)^2 \, dz \qquad (9\cdot8\cdot11)$$

On the right hand side of equation 9·8·10 the equivalent loading terms for the interval considered are given by

$$\delta N = N - \int_0^d \sigma^* dz$$

and (9·8·12)

$$\delta M = M - \int_0^d \sigma^* (z - d/2)dz$$

Equation 9·8·10 is solved to find the increments of strain and curvature and from these a revised estimate ε_s^* of the strain ε_s is obtained. This also leads to a new value for H^* so that the procedure can be repeated until the equivalent loads in equation 10 and the increments of strain and curvature are acceptably small. At this stage, the estimated stress σ^* is sufficiently close to the true solution σ'. The calculation can then be repeated in a similar manner for all subsequent time intervals.

9·9 Instability

The criteria adopted for assessing the convergence of

the iterative process will be discussed in the next chapter. However, it is important to realise that convergence difficulties may not necessarily be due to peculiarities of the numerical method but can be due to real instability in the behaviour of the slab. This occurs if the stiffness matrix becomes singular.

The solution of equation 9·8·10 takes the form

$$\begin{bmatrix} \delta\zeta \\ \delta\chi \end{bmatrix} = \frac{1}{D} \begin{bmatrix} k_{22} & -k_{21} \\ -k_{12} & k_{11} \end{bmatrix} \begin{bmatrix} \delta N \\ \delta M \end{bmatrix} \qquad (9\cdot9\cdot1)$$

where D is the determinant of the array making up the stiffness matrix i.e.

$$D = k_{11}k_{22} - k_{12}^2 \,. \qquad (9\cdot9\cdot2)$$

Clearly, the slab is unstable if D approaches zero as the values of $\delta\zeta$ and $\delta\chi$ approach infinity for finite δN and δM.

The determinant D can approach zero if the compliance c^* becomes zero throughout the thickness of the slab. Such a situation implies structural failure following the propagation of cracks across the whole thickness.

A more interesting situation could develop if the compliance c^* was negative over part of the thickness and greater than, or equal to, zero over the remainder. This could occur when some of the material has been strained to a point, on the stress-strain curve, beyond the peak stress.

The mode of failure would then be one of longitudinal instability, similar to that described by Whitney (1943) and many others, for a compression specimen in a flexible testing machine, or that postulated by Dougill (1966) for a single heated column in a flexible structure.

This form of longitudinal instability could result in a violent failure. Thus the question arises; is it possible for the conditions, that are necessary for this form of instability, to occur in practice? This question provides the main incentive to undertake the analysis described in the next chapter.

Chapter 10

STRUCTURAL BEHAVIOUR OF CONCRETE PANELS 11

10·1 Introduction

In applying the method of analysis described in the previous chapter to concrete wall panels, some assumptions have to be made concerning the state of the material and how this is affected by stress and temperature. These assumptions are dealt with in the first few sections of this chapter which lead to a brief description of the computer program, that was written to undertake the stress calculations. Following this, some results of these calculations are given with the work being mainly directed to demonstrating the causes of instability and the circumstances under which sudden failure can occur.

10·2 Representation of concrete behaviour at normal temperatures

In arranging the details of the numerical analysis, it is helpful to adopt a convenient function to describe the relationship between uniaxial stress and strain for concrete. Following an extensive experimental investigation on eccentrically loaded concrete prisms, Hognestad et al (1955) proposed a polynomial expression to describe the complete stress-strain curve of concrete in uniaxial compression under monotonically increasing strain. Later Sinha et al (1964) extended this approach to include behaviour during unloading and reloading so that the conditions that obtain during cyclic loading could be studied. The resulting function involves nine separate descriptive parameters that need to be evaluated from tests on the material. Although this provides a good approximation to true material behaviour, it was felt

that this precision could not be justified in the present work when the uncertainties accompanying the inclusion of temperature dependent properties were considered.

A simpler function involving only three descriptive parameters has been used by Liebenberg (1962) and Bresler and Selna (1964). This expresses the compression stress/strain curve in the form

$$\sigma = A\varepsilon - B\varepsilon^{m} \qquad (10\cdot2\cdot1)$$

where the parameters A, B and m are found from the initial Young's modulus E_o, the peak stress $\bar{\sigma}$ and the strain corresponding to the peak stress $\bar{\varepsilon}$. This expression provides a good approximation to behaviour under increasing compressive stress but does not give a good account of the shape of the stress-strain curve beyond the peak stress. This could be a disadvantage in the present work as it appears, from the standpoint developed in the previous chapter (in Section 9·9 page 273), that the form of the decending branch could have a major influence on the occurrence of instability.

In the present work, the relation between stress and strain for concrete in compression, is taken in the form

$$\sigma = E_o \left(\bar{\varepsilon} + m(\varepsilon - \bar{\varepsilon})\right) e^{-\left(\bar{\varepsilon} + m(\varepsilon-\bar{\varepsilon})\right)/\bar{\varepsilon}} \qquad (10\cdot2\cdot2)$$

where $m=1$ for $\varepsilon/\bar{\varepsilon} \leq 1$

This equation is not so general as equation 10·2·1 and it is implicity assumed that there is a fixed relationship

between E_o, $\bar{\varepsilon}$ and the peak stress $\bar{\sigma}$ of the form $\bar{\varepsilon} = e\bar{\sigma}/E_o$. Clearly this is not universally true and the expression generally tends to over-estimate the slope of the stress-strain curve at low stresses and strains, if the curve is arranged to pass through the point $\bar{\sigma}$, $\bar{\varepsilon}$. This discrepancy is considered to be of little account in the present work. With m=1, equation 10·2·2 becomes identical to that used by Baldwin and North (1969) to describe Furamura's stress - strain data obtained in experiments on concrete at different temperatures in the range 20°C to 700°C (see Section 3·3 pages 84-87). The parameter m only affects the form of the decending branch of the stress-strain curve, as shown in figure 10-1. A value of m=0 would correspond to deformation at a constant stress, equal to the peak value $\bar{\sigma}$, whilst a value of $m=\infty$ gives an infinitely steep decending branch. Concrete is unlikely to behave in either of these extreme fashions and a value of m=1 can be regarded as typical. However, it is known that the form of the decending branch is affected by the strain rate (Rusch 1960) and that there is a significant effect of aggregate size (Hughes and Chapman 1966). Also, it appears that some lightweight aggregate concretes exhibit a very steep decending branch, even in compression (Polivka et al 1967, Grimer and Hewitt 1969). It is thought that some idea of these effects can be obtained by using an appropriate value of m in the calculations.

It was shown, in the previous chapter, that the material description must include behaviour during unloading and in tension and must make provision for the occurrence of

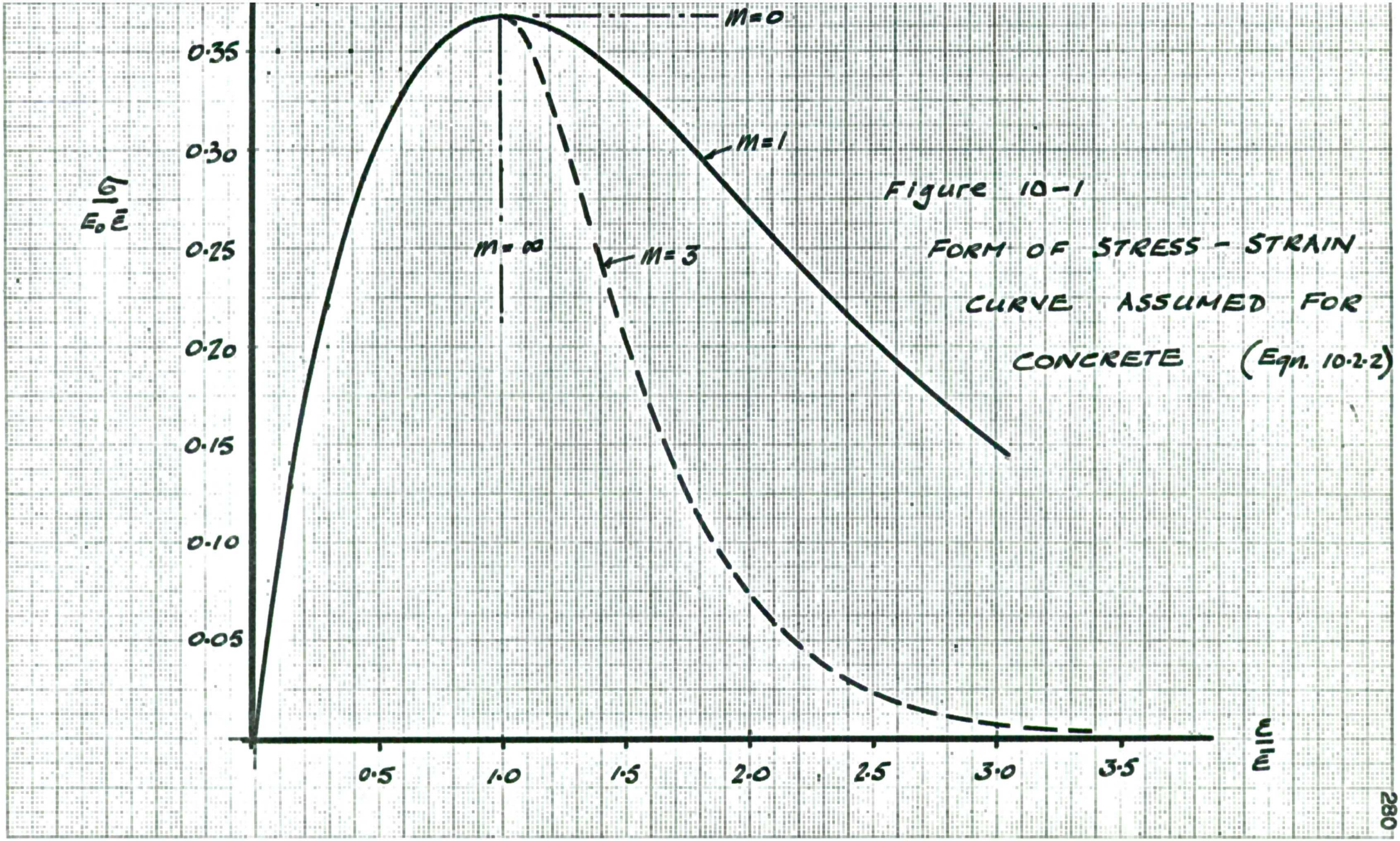


Figure 10-1
FORM OF STRESS - STRAIN
CURVE ASSUMED FOR
CONCRETE (Eqn. 10.2.2)

cracking and the possibility of crack closure. To do this we make the following four assumptions.

1) Behaviour in tension, before the occurrence of cracking, and during loading and unloading is linear with $d\sigma/d\varepsilon=E_o$, the initial Young's modulus.

11) Cracking occurs if the tensile stress reaches a critical value equal to the tensile strength of the concrete.

111) Immediately following the occurrence of cracking in any region, the stiffness of the concrete in tension in that region is reduced to zero.

1V) The occurrence of cracking in any region has no effect on subsequent performance in compression.

When these assumptions are taken together with the stress strain relationship 10·2·2 they lead to behaviour of the sort shown in figure 10-2. This is not an exact representation of the behaviour of concrete as, besides the limitations of equation 10·2·2, each of the assumptions listed represents an idealisation of material behaviour. The most serious departure from reality probably arises from assumption 1 as it is clear, from the available experimental results, that this leads to an over-estimate of stiffness during unloading (see figure 2-2 on page 28 and figure 3-4 on page 86). This may need to be borne in mind in considering the results obtained from the calculations.

The remaining assumptions idealise the occurrence and effect of cracking. This is taken to be an ideal, but localised, brittle failure so that no consideration is given to the occurrence of cracking before the peak stress is

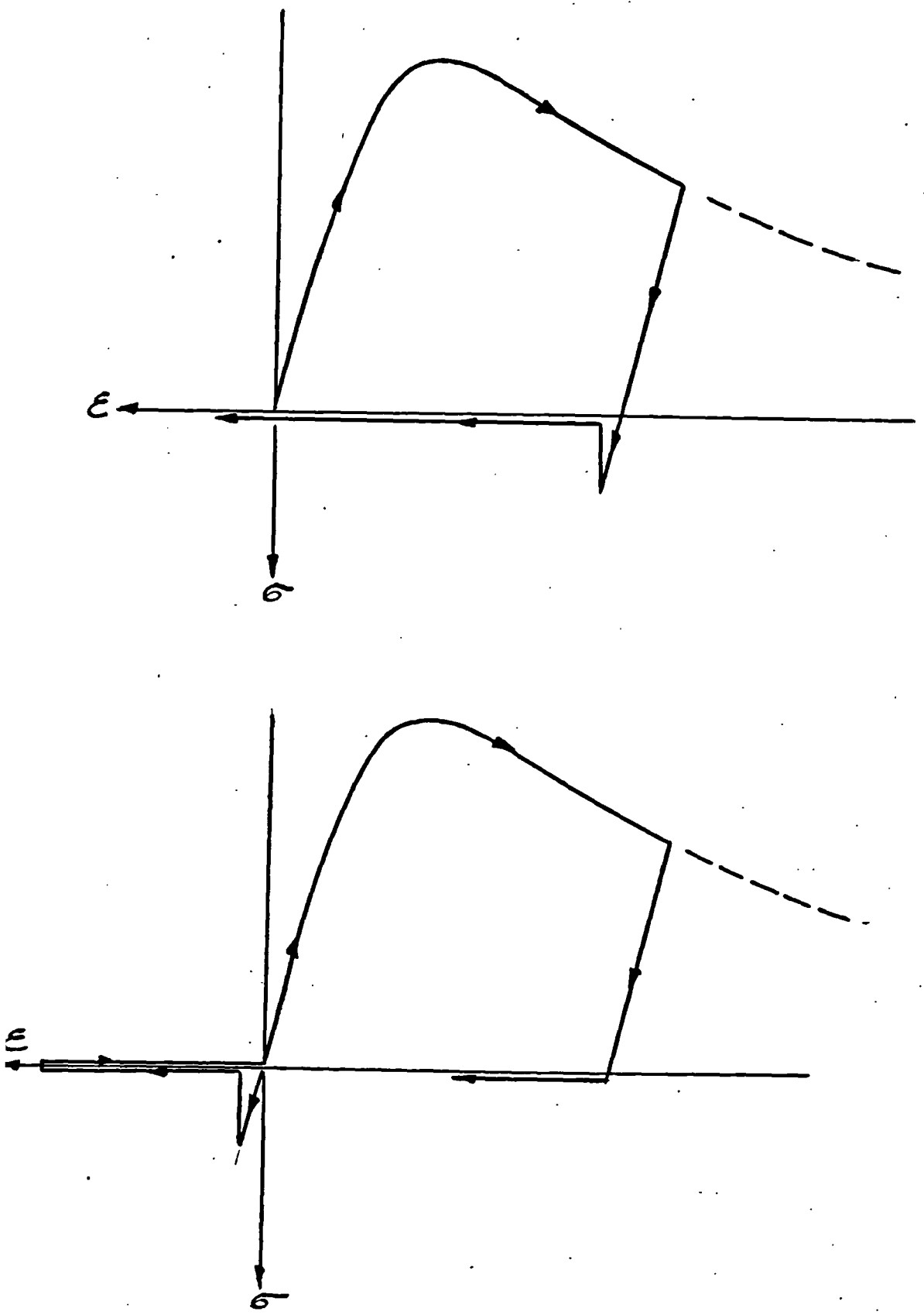


FIG. 10.2 TWO EXAMPLES OF MATERIAL BEHAVIOUR IN ACCORDANCE WITH THE ASSUMPTIONS GIVEN ON PAGE 281

achieved or to the precise form of the decending branch of the stress-strain curve in tension. In addition the process of crack closure has been idealised, by ignoring any form of autogenous heating or the wedging effects of debris within the cracks.

10·3 Behaviour at elevated temperatures

Following Baldwin and North (1969), we assume that the stress-strain curve in compression can be represented by equation 10·2·2 if E_o and $\bar{\varepsilon}$ are taken to be functions of the temperature T. Thus, rewriting equation 10·2·2

$$\sigma = E_o(\bar{\varepsilon} + m(\varepsilon_s - \bar{\varepsilon}))\, e^{-(\bar{\varepsilon} + m(\varepsilon_s - \bar{\varepsilon})) / \bar{\varepsilon}} \qquad (10·3·1)$$

where $m = 1$ for $\varepsilon_s/\bar{\varepsilon} \leqslant 1$ and ε_s is the strain due to stress. This equation gives good agreement with the results obtained by Furamura in 1966, but really applies to constant temperature conditions and so requires further interpretation before it can be used in situations where the temperature varies. Accordingly, we make the following assumptions, in addition to points 1 to 1V of Section 10·2.

V The total observable strain ε is the sum of the thermal strain ε_T and the strain due to stress ε_s, where ε_s is found from equation 10·3·1.

$$\varepsilon = \varepsilon_s + \varepsilon_T \qquad (10·3·2)$$

which has been brought forward from Section 9·8, page 269

Vl The strain due to stress, ε_s, can be regarded as the sum of a reversible component ε_R and an irreversible component ε_D, as shown in figure 10-3, i.e.

$$\varepsilon_s = \varepsilon_R + \varepsilon_D \qquad (10·3·3)$$

VII A change of stress or temperature cannot reduce the numerical value[+] of the irreversible component of strain ε_R that exists before the change occurs.

VIII The ratio, of the tensile strength of the concrete to the peak stress in compression, is independent of temperature.

These assumptions provide a consistent model of material behaviour which can be used as a basis for analysis. Inevitably these assumptions go beyond the limits of the available experimental data for concrete discussed in chapter 2 and also involve an extreme simplicication in the neglect of time dependendent behaviour. However, it is thought that this is permissible in discussing phenomena occurring during a very limited period of heating.

The concept of dividing the strain due to stress into a reversible and an irreversible component is identical to that used in the Theory of Plasticity (Prager and Hodge 1951). For short term loading, the irreversible strain in concrete will be principally due to micro-cracking and breakdown of bond between the aggregate and the cement paste. The irreversible strain ε_D can thus be regarded as a measure of damage and the postulate, that this can not be reduced

---

Footnote[+]

The irreversible strain ε_R will be a contraction and so has a negative value with the present sign convention.

---

by a change in load or temperature, provides a criterion for deciding whether a particular change causes 'loading' or 'unloading' of the material. These terms have been defined by Sinha et al (1964) and are used in the same spirit as when applied to strain hardening materials in the Theory of Plasticity (see Mendelson 1968 for instance). Thus, considering a history of strain $\varepsilon_s(\tau)$ defined with respect to a continuous measure τ of the sequence of straining, we have for loading in compression,

$$\frac{d\varepsilon_s}{d\tau} < 0 \,, \quad \frac{d\varepsilon_D}{d\tau} < 0 \quad \text{and} \quad \sigma = \sigma(\varepsilon_s)$$

and, for unloading or reloading (10·3·4)+

$$\frac{d\varepsilon_D}{d\tau} = 0 \,, \quad \frac{d\sigma}{d\varepsilon_s} = E_o \quad \text{and} \quad \sigma > \sigma(\varepsilon_s)$$

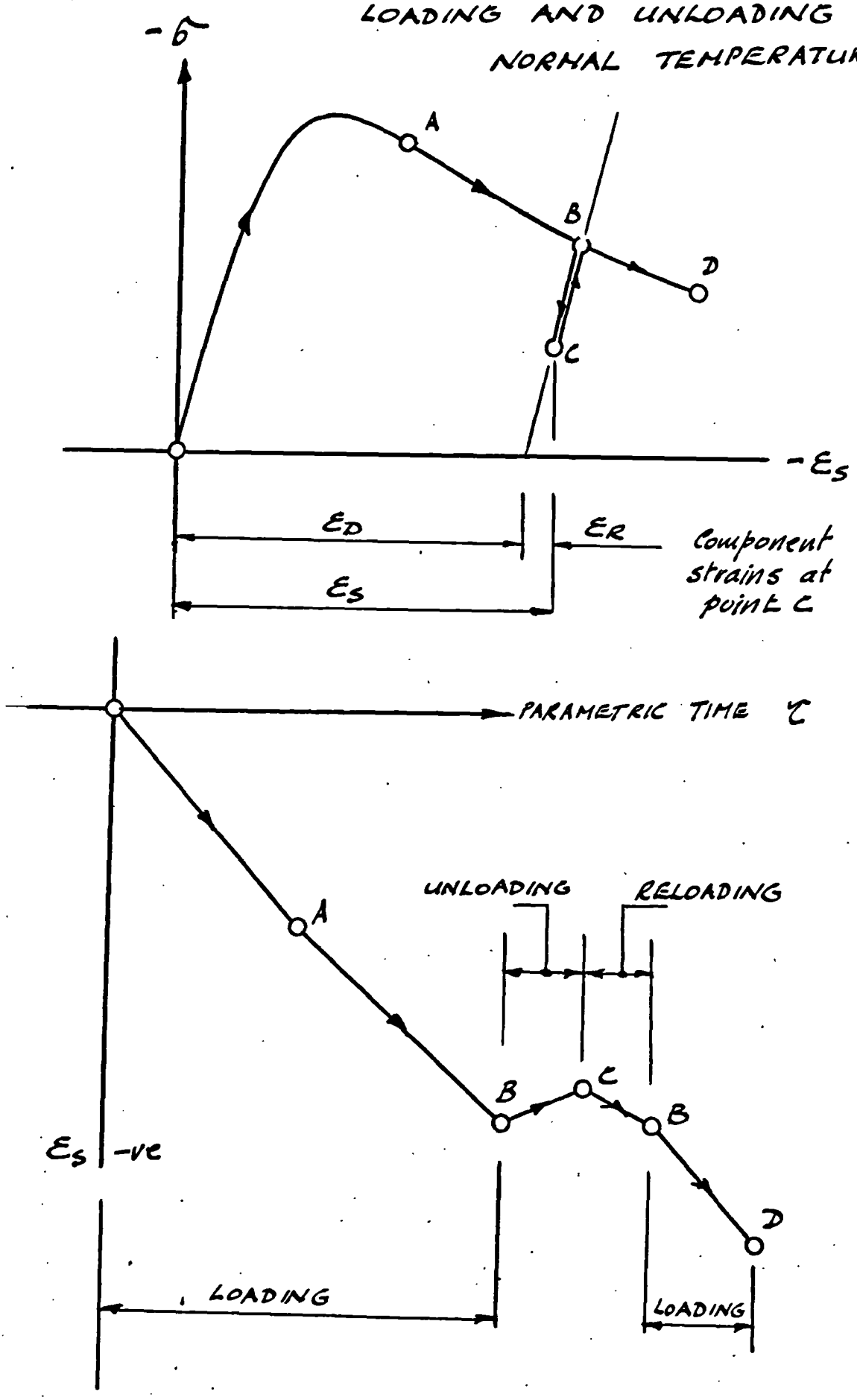
These definitions are illustrated in figure 10-3 from which it is seen that at constant temperature the condition that unloading occurs with no change in the irreversible strain component corresponds to assumption 1 of Section 2. However, the main use of the concept is in assessing the affects of changes in temperature.

As an example, consider a sample of concrete at three

Footnote+

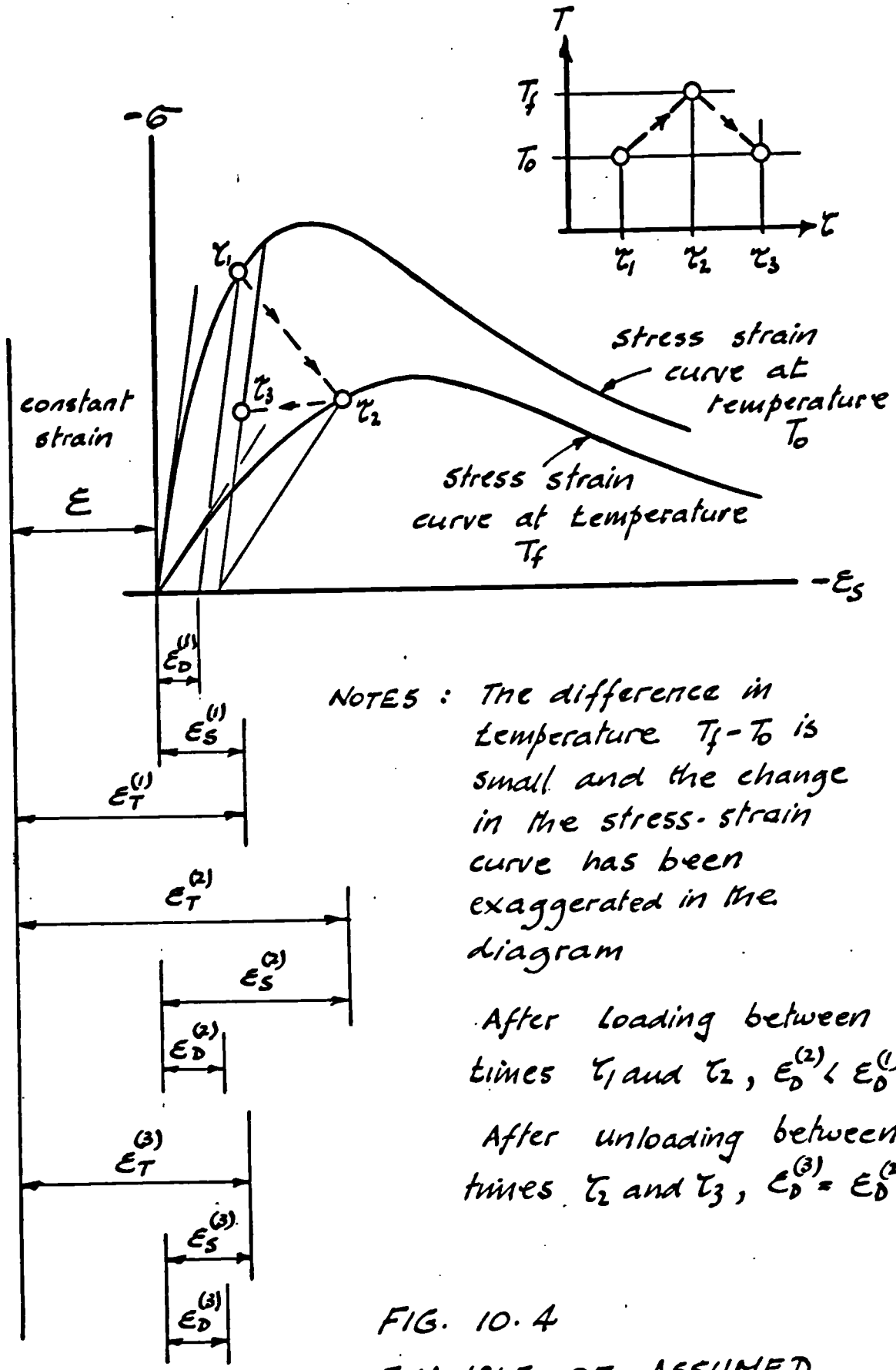
The present problem is concerned with the effects of transient heating and thus it is convenient to use time t for the parameter τ. Also in the present work, the function $\sigma=\sigma(\varepsilon_s)$ is equivalent to equation 10·3·1.

FIG. 10-3 BEHAVIOUR DURING LOADING AND UNLOADING AT NORMAL TEMPERATURES



successive times τ_1, τ_2 and τ_3. The initial state is taken to be one in which the specimen has already been loaded to a point on the stress-strain curve corresponding to the initial temperature T_o. Following this the temperature is raised by a small amount to a new value T_f, with the overall strain being kept constant. Finally, the temperature is reduced to T_o again keeping the strain constant. This situation is shown in figure 10-4 which is annotated to show the various strain components at the three stages of straining, the superior suffix indicating the time τ_1, τ_2 or τ_3. With a rise in temperature, it is not possible for the irreversible strain to remain constant so that there must be an increase in damage and the stress is found from the loading portion of the stress-strain curve. On the other hand, when the temperature is lowered to T_o a return to the appropriate loading curve would require a decrease in damage, which is not permitted, and the unloading curve must be used. The chosen example thus suggests that a temperature rise induces loading in a restrained specimen whilst a drop in temperature causes unloading. This seems reasonable and could be expected on intuitive grounds alone.

The assumed behaviour is consistent with the assumptions commonly used for isothermal conditions (Sinha et al 1964 Bresler and Selna 1964) and the extension to consider the effects of temperature gives results that appear realistic. However, the consideration of damage is very much idealised and in reality there may be a more complicated relationship, between the effects of heating and loading, in concrete.



NOTES : The difference in temperature $T_f - T_0$ is small and the change in the stress-strain curve has been exaggerated in the diagram

After loading between times τ_1 and τ_2, $\varepsilon_D^{(2)} < \varepsilon_D^{(1)}$

After unloading between times τ_2 and τ_3, $\varepsilon_D^{(3)} = \varepsilon_D^{(2)}$

FIG. 10.4

EXAMPLE OF ASSUMED MATERIAL BEHAVIOUR

Involving temperature changes at constant total strain

Thus, the postulated behaviour should be regarded as defining an ideal material and caution must be used in applying the results, obtained on this basis, to deduce the behaviour of concrete. In spite of these reservations, it is felt that the assumptions are reasonable, and likely to give a fair picture of the broad aspects of the behaviour of concrete under short term changes in stress and temperature, and so will lead to a satisfactory indication of possible modes of failure. This is all that is required in the present work but, if more precision were needed, the correspondence between the ideal material and the behaviour of concrete itself would need to be fully investigated[+]. This is beyond the scope of the present work.

10·4 Material State

In the previous Chapter the concept of the state of the material H was introduced in order to specify the incremental stiffness of the material under particular conditions of strain and temperature. The assumptions adopted in this chapter provide four categories of behaviour, or separate states, corresponding to loading or unloading in compression and behaviour in tension before and after cracking. These states are illustrated in figure 10-5 where a further

---

Footnote[+]

Matters of this sort are the subject of a separate experimental investigation which is now in progress at King's College London, under the supervision of the author.

distinction has been made between behaviour occurring in the accending and decending portions of the stress-strain curve for loading in compression. These five types of behaviour will each be referred to, in subsequent work, by the initial letter of their description i.e.

A Accending branch in compression

D Decending branch in compression

U Unloading in compression (also reloading)

T Tension

C Cracked, with cracks remaining open.

The method of analysis presented in Section 9·8 requires that an estimate be made of the state of the material H that corresponds to an estimate, ε, of the total strain. A flow diagram for this process is given in figure 10-6.

10·5 Arrangements for computation SLOADED

A computer program, SLOADED, was written to calculate the stresses in a wall panel heated from one side. This program uses the incremental method of analysis described in chapter 9 and is based on the material behaviour postulated in this chapter. The calculation of the temperature distribution is undertaken using the program THERMAL (described in Section 8·4 page 232) which is thus incorporated within SLOADED. The broad features of SLOADED are shown in the macro-flow diagram given in figure 10-7. This links the different operations involved in each stage of the incremental process and so illustrates the main part of the program. The remainder of the program is mainly organisational and deals with input of data, the initial conditions and the output of results. These matters will

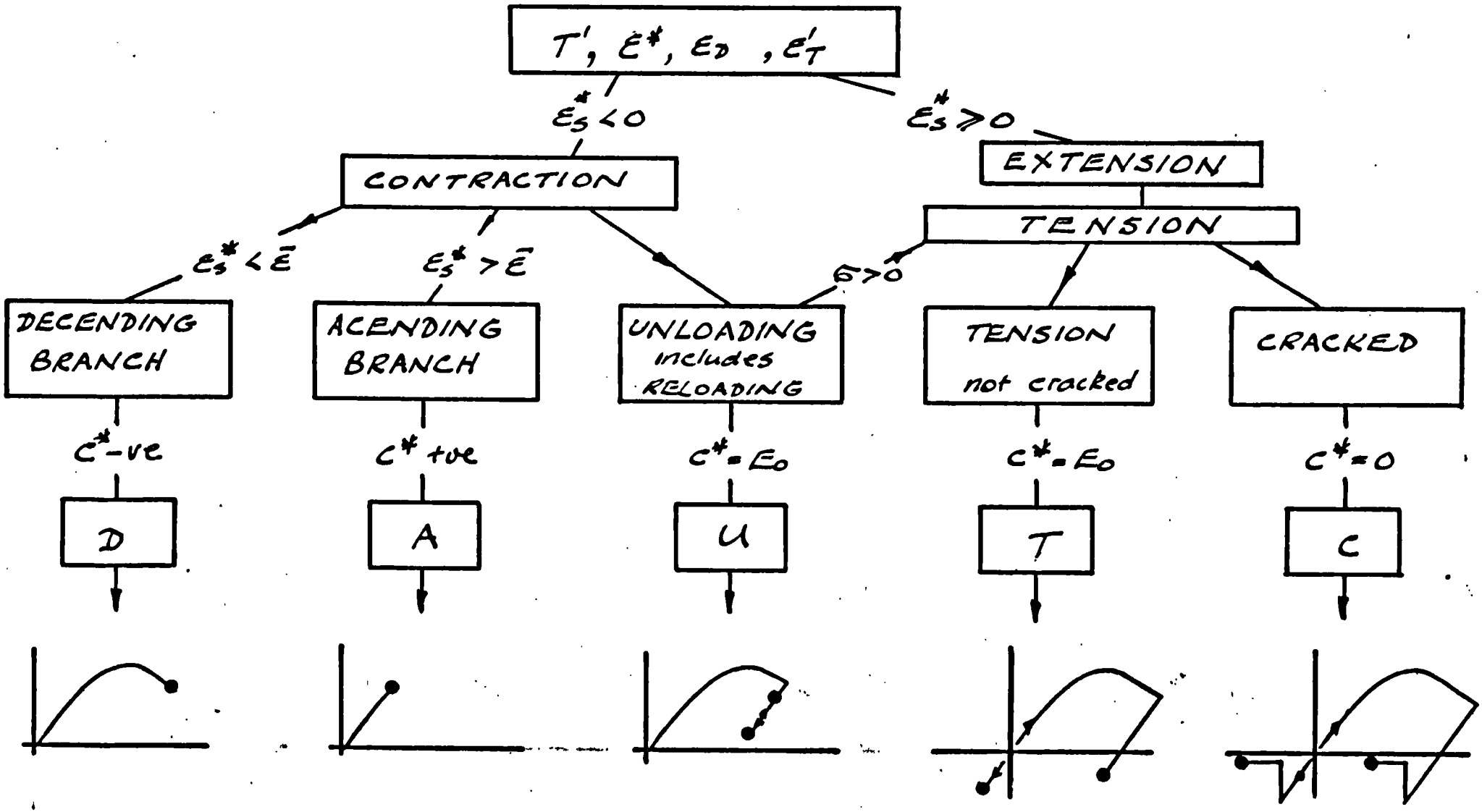


FIGURE 10.5 CATEGORIES OF MATERIAL BEHAVIOUR

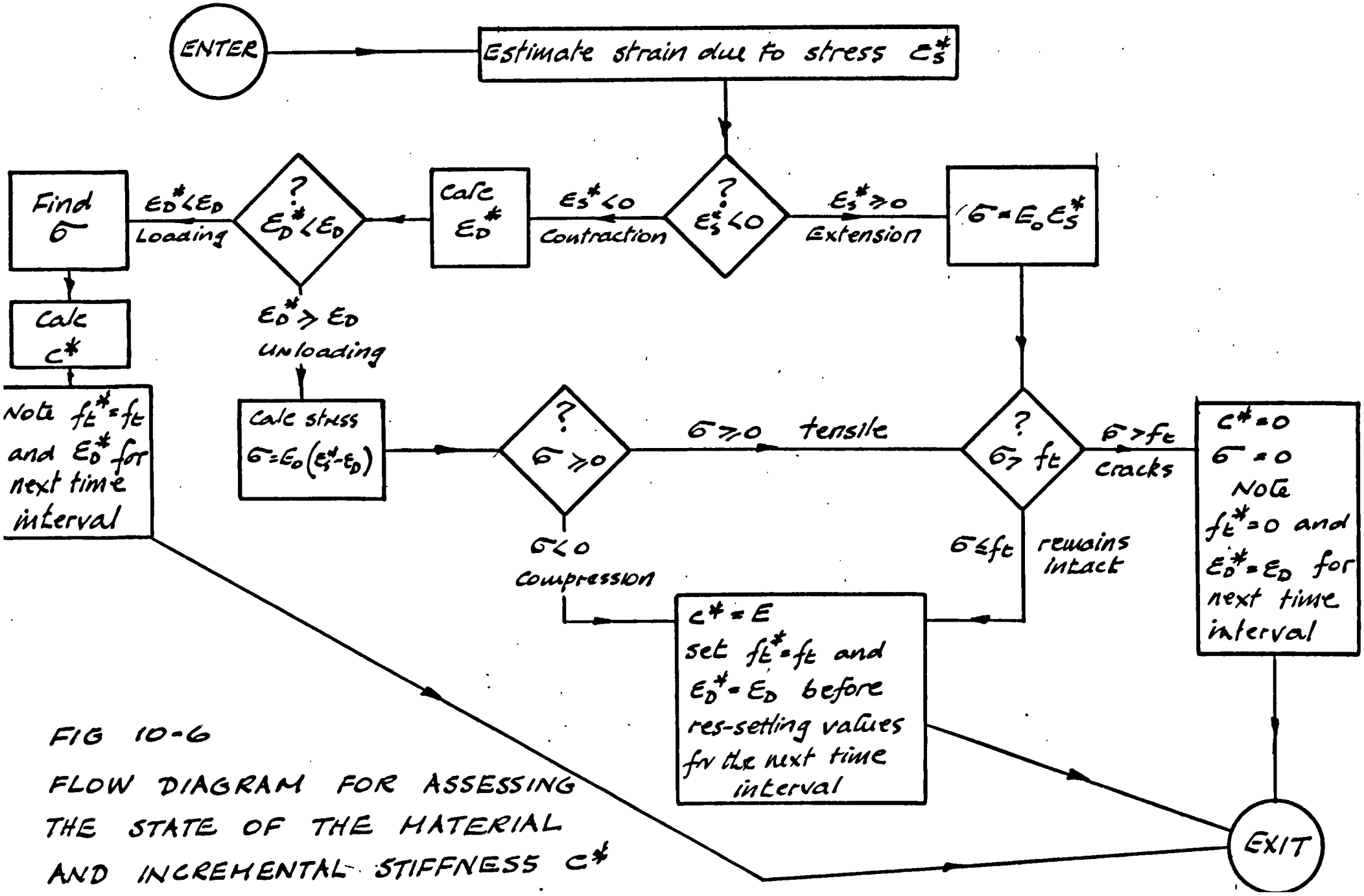


FIG 10-6

FLOW DIAGRAM FOR ASSESSING THE STATE OF THE MATERIAL AND INCREMENTAL STIFFNESS c^*

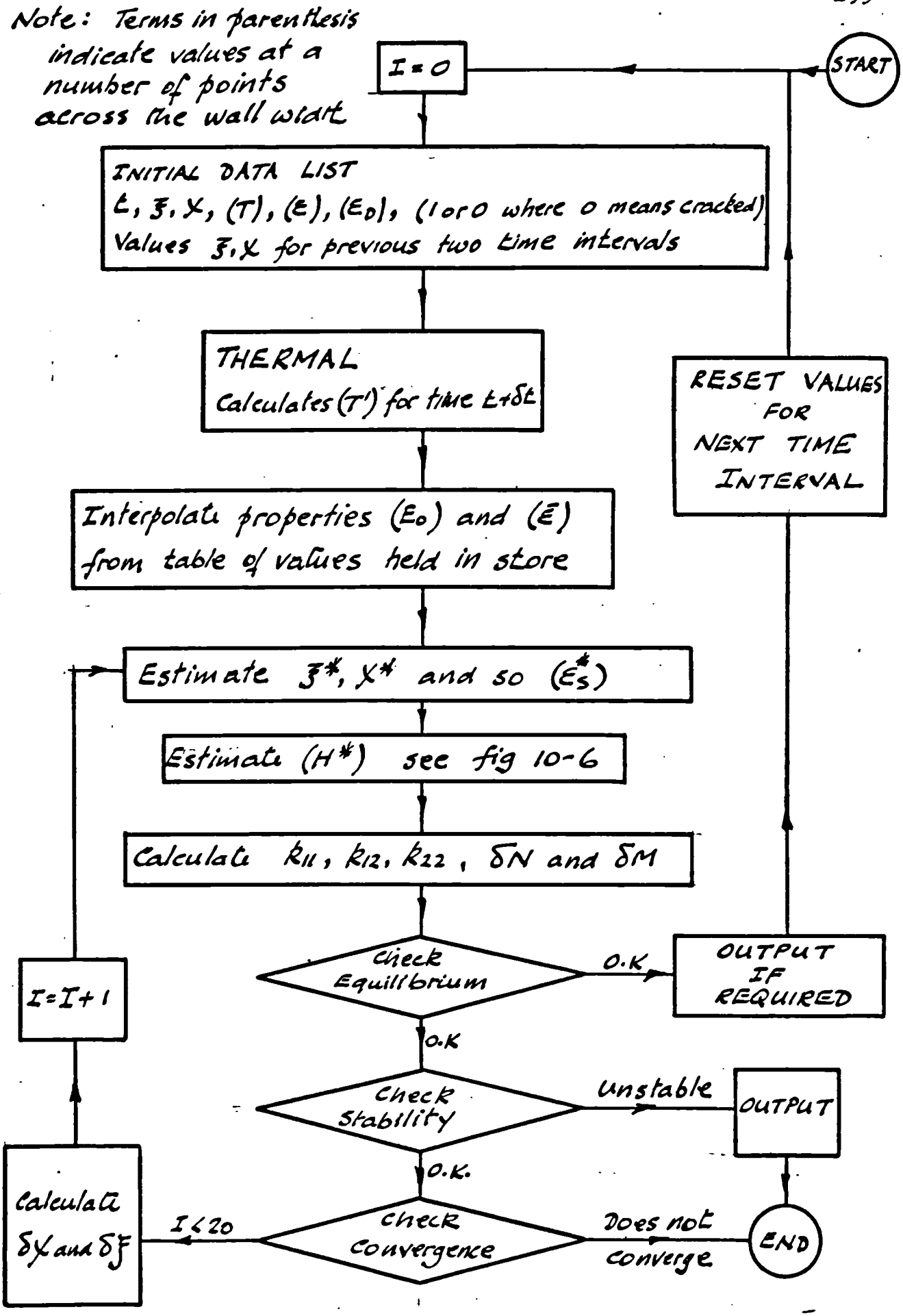


FIG. 10-7 MACRO. FLOW DIAGRAM FOR SLOADED

not be described in detail but some comment is necessary on the tests employed for equilibrium, stability and convergence and the method used to estimate the strain at each time interval. In the discussion that follows the notation is identical to that of Chapter 9.

Forward estimate of the average strain $\bar{\varepsilon}$ and curvature χ

In most cases, an initial estimate of the average strain and curvature, at any time, is found from the values that obtain at the previous three time intervals. The same procedure is adopted as is used in estimating the surface temperature in THERMAL, the expression for the new value of strain or curvature being of the same form as equation 8·4·1 on page 234. The initial estimates are then modified by the correction terms $d\bar{\varepsilon}$ and $d\chi$ found at each iteration.

This approach can not be used for the first three time increments or if the estimates of strain and curvature result in a situation in which the panel is cracked throughout its width and thus has zero stiffness. In these circumstances the values of $\bar{\varepsilon}$ and χ found for the previous time interval are used as the initial estimates to start the iterative process.

Equilibrium

The conditions for equilibrium are taken to be satisfied if the generalised forces δN and δM (in equations 9·8·12 page 273), that are required in order to restore equilibrium are acceptably small. In order to apply this condition, two quantities $\bar{N}$ and $\bar{M}$ are introduced to provide measures of the magnitudes of δN and δM. These quanties are defined

by

$$\bar{N} = \int_0^d \left|\sigma_{xx}\right| dZ \quad \text{and} \quad \bar{M} = \int_0^d \left|\sigma_{xx}(z-d/2)\right| dZ \qquad (10\cdot5\cdot1)$$

On this basis, the equilibrium condition is satisfied

$$\text{if} \quad \left|\frac{\delta N}{\bar{N}}\right| < 0\cdot01 \qquad \text{and} \qquad \left|\frac{\delta M}{\bar{M}}\right| < 0\cdot01 \qquad (10\cdot5\cdot2)$$

Stability

As suggested in Section 9·9 the structure becomes unstable if the determinant of the stiffness matrix becomes equal to zero, as this would imply infinite strains in the material. However, as the calculation is performed at discrete points in time it would be an exceptional coincidence if the calculation actually gave a value of zero for the determinant. Because of this, a different criterion for stability must be used and the most convenient is to regard the panel as unstable if the increment of axial strain $\delta\zeta$ or curvature $\delta\chi$ is exceptionally large in any time interval. Thus, the panel is taken to be unstable if

$$\left|\delta\zeta\right| \geq 1 \quad \text{or} \quad \left|\delta\chi\right| \geq 2/d \qquad (10\cdot5\cdot3)$$

Convergence

In most cases there was no difficulty with convergence with the time and space divisions commonly used in the calculation. However, it was clear that the equilibrium conditions would become unnecessarily precise if the magnitudes of the stresses σ_{xx} were low at all points within the panel. This could occur if the section was extensively cracked, so that the values of $\bar{N}$ and $\bar{M}$ became

very low. When this occurs, the calculated change in stress is small and the absolute values of the generalised forces δN and δM are also very low. Thus, although the panel approaches a state of instability it does so very gradually with reductions in both stiffness and the out of balance forces. In these circumstances, it seemed most economic, in computer time, to recognise that this could occur and place a limit of 20 iterations on the extent of the calculation at any time. If this limit is reached the analysis is terminated.

Restraint

The method of analysis presented in Chapter 9 dealt with a panel loaded with an axial load N and a couple M at its ends. These loads were taken to remain constant during heating. This situation is changed if the panel is partially restrained against expansion or rotation, as the loads induced during heating are dependent on the deformations of the panel. This type of behaviour is of considerable practical interest, as a heated panel will generally be subject to restraint from the surrounding structure. The analysis may be extended to treat this effects by writing

$$N = -K_n \xi \qquad \text{and} \quad M = -K_m \chi \qquad (10{\cdot}5{\cdot}4)$$

where the stiffness K_n and K_m are properties of the structure providing restraint to the panel.

On including these expressions for N and M in the analysis, the elements of the stiffness matrix 9·8·10 become

$$k_{11} = K_n + \int_0^d c^* dz$$

$$k_{12} = k_{21} = \int_0^d c^*(z-d/2)\, dz \qquad (10\cdot5\cdot5^+)$$

$$k_{22} = K_m + \int_0^d c^*(z-d/2)^2\, dz$$

which may be compared with equation 9·8·11. In a similar way, the equivalent loading terms given in equation 9·8·12 become

$$\delta N = -(K_n \delta \zeta^* + \int_0^d \sigma^* dz)$$

$$\delta M = -(K_m \delta \chi^* + \int_0^d \sigma^*(z-d/2)^2 dz) \qquad (10\cdot5\cdot6^+)$$

and the analysis continues in the same way as in Section 9·8.

In some structures, restraint may be combined with some form of prescribed loading. Accordingly, the program SLOADED was written so that any of the four possible combinations of load and restraint could be dealt with.

Footnote$^+$

Note that, as in Chapter 9, the superior asterisk refers to estimated quantities. Also δN and δM approach zero as the estimates approach the correct values

---

10·6 Input and Output

The data for SLOADED is prepared in the form given in Table 10·1. Within the program, the materials data for any particular temperature is found by linear interpolation, between the values given on cards 6, 7 and 8, with the thermal strain ε_T being obtained after subtracting the value corresponding to the initial temperature. The values for $\bar{\varepsilon}$ and E_o given for 0°C do not necessarily reflect the true behaviour of the material at the freezing point of water but are chosen so that interpolation between 0°C and 100°C gives the correct values at normal temperature. The restraint parameters are prescribed in dimensionless form with values being given for K'_n and K'_m where

$$K'_n = K_n/E_o d$$
$$K'_m = 12K_m/E_o d^3 \qquad (10·6·1)$$

In these expressions, d is the width of the wall and the value for the initial Young's modulus E_o is that specified for 0°C.

Some typical output from SLOADED is shown in figure 10-8. The first line gives the program name together with the date, time and run number. Following this, the various input and control data are 'echo printed' above the dashed line, with the values of $\bar{\varepsilon}$ and thermal expansion being given in micro-strain. The results of the calculation are then given below the dashed line, in the form described in Table 10·2 and 10·3.

TABLE 10·1 DATA preparation for SLOADED

CARD NUMBER	DATA	PUNCH IN COLUMNS
1 - 5	Data as for THERMAL and described in Table 8·4 page 236	
	The following three cards give the additional materials data at 100°C intervals in the range 0°C - 1200°C i.e. 13 values punched with 5 cols/value	
6	% age thermal strain as if heated from 0°C	1 - 65
7	Initial Young's Modulus GN/m^2	1 - 65
8	% age strain corresponding to peak stress stress in compression - positive value given	1 - 65
	Ratio of Peak stress in compression to the tensile strength - single value	66 - 70
9	Loading Conditions	
	Axial Load/unit length N/mm	1 - 10
	End Couple/unit length N	11 - 20
	Axial Restraint factor dimensionless	31 - 40
	Flexural restraint factor dimensionless	41 - 50
	m - parameter defining decending branch	61 - 65
	Run reference number - integer (RA).	66 - 70
10	Closure	
	As for THERMAL, punch FALSE	1 - 5

```
SLOADED/DOUGILL      19/07/71        15.41.50.      RUN   3
WALL WIDTH   .50./  SURF MOIST 0.000/  AMB TEMP  15.0/  WET DIFY   .90/  WET COND  2.100/  TIME INC   1.00/
 MESH SIZE   2.0/  CENT MOIST 1.500/  VAP TEMP 100.0/  DRY DIFY   .40/  DRY COND  1.200/  Mw = 4.44,  MD =10.00/
          CONCRETE PROPERTIES GIVEN AT INTERVALS OF 100/C IN RANGE 0-1200/C
THM EXP        0.   1000.   2000.   3000.   4000.   5000.   6000.   7000.   8000.   9000.  10000.  11000.  12000.
YS MOD     30.00   30.00   30.00   30.00   30.00   30.00   30.00   30.00   30.00   30.00   30.00   30.00   30.00
STRAIN     2000.   2000.   2000.   2000.   2000.   2000.   2000.   2000.   2000.   2000.   2000.   2000.   2000.
AXIAL LOAD     -0.00/END COUPLE      -0.00/AXIAL RESTRAINT -0.000/FLEXURAL RESTRAINT100.000/SLOPE MOD  1.000/
              TEMPERATURES AND STRESSES PRINTED AT EVERY 4.00MM FROM HOT FACE

---------------------------------------------------------------------------------------------------------------

 1. 0      0.00     344.21      39.27     15.00
             39.27      26.77      20.21      17.09      15.75      15.24      15.07      15.02      15.00      15.00
             15.00      15.00      15.00
           24.         -1.          .9701      .0029   100.9248     97.908962     2   -.1613696E-05     .3722834E-05
            AAAAAATTTTTTTTTTTTT  TTTTTT
             -5.87      -2.67      -.82        .10        .50        .65        .70        .71        .71        .71
              .71        .71        .70
 2. 0      0.00     439.50      72.51     15.01
             72.51      50.15      35.54      26.44      21.06      18.05      16.45      15.65      15.28      15.11
             15.04      15.02      15.01
          343.           -0           .1467    -.2171   100.3243     14.667104     2    .1136868E-14    -.1091394E-14
            UUTTCCCCCCCCCCCCCCC  CCCCCC
             -3.94       .68        0.00       0.00       0.00       0.00       0.00       0.00       0.00       0.00
              0.00       0.00       0.00
 3. 0       .50     497.29     107.65     15.12
            107.65      77.75      56.27      41.14      31.05      24.54      20.47      18.03      16.62      15.83
             15.42      15.21      15.13
          725.           -0           .0667    -.1081   100.1754      6.666680     2   -.2842171E-14     .9276846E-14
            UTCCCCCCCCCCCCCCCC  CCCCCC
             -3.01       0.00       0.00       0.00       0.00       0.00       0.00       0.00       0.00       0.00
              0.00       0.00       0.00
FAILS TO CONVERGE
```

FIG. 10–8 OUTPUT FROM SLOADED FOR A FLEXURALLY RESTRAINED SLAB

TABLE 10·2 Results given by SLOADED at the end of each time interval - see figure 10-8

Line	Result
1	Time : mins and seconds Depth of dried zone : mm furnace temperature : °C Estimate for hot face temperature : °C Estimate for cool face temperature : °C
2 and 3	Temperatures at equally spaced points across the wall thickness : °C
4	Axial strain ξ micro strain χ' 10^{-6}units $k'_{11}, k'_{12}, k'_{22}, D'$ dimensionless Number of iterations $\delta N', \delta M'$
5	Structural State of the material of the wall described by symbol A,D,U,T, or C as shown in figure 10-5 page 291.
6 and 7	Stresses in MN/m^2 at equally spaced points across the wall thickness : tension positive.
Note	The primed quantities in line four are dimensionless values related to χ, k_{11}, k_{12}, k_{22}, D, δN and δM as described in Table 10·3

TABLE 10·3 Dimensionless variables used in Input and Output to SLOADED

$K'_n = K_n/E_o d$ $K'_m = 12k_m/E_o d^3$	K_n and K_m defined by equations 10·5·4
$k'_{11} = k_{11}/E_o d$ $k'_{12} = \sqrt{12}\, k_{12}/E_o d^2$ $k'_{22} = 12k_{22}/E_o d^3$ $D' = 12D/E_o^2 d^4$	Elements of stiffness matrix: defined in equation 9·8·10 and 9·8·11 Determinant of stiffness matrix equation 9·9·2
$\delta N' = \delta N/d$ $\delta M' = 6\delta M/d^2$	δN and δM defined by equations 9·8·12 MN/m^2 units
$\chi' = \chi d$	χ is curvature

Note d is the width of the wall and E_o is the value of the initial Young's modulus specified for 0°C

THERMAL DATA

The same thermal data as shown in fig.10-8 is used throughout the structural investigation described in this Chapter.

The results shown in figure 10-8 were obtained for a thin slab subject to high flexural restraint. The slab becomes extensively cracked soon after the start of heating and the calculation is terminated using the convergence criteria described on page 295. The effects of cracking on the stress distribution and panel stiffness can be easily seen from the results shown. After one minutes heating, there is still no cracking and the non-dimensionalised determinant of the stiffness matrix is near its original value ($D' = 97{\cdot}9$). A considerable amount of cracking occurs, during the next one minute of heating, to cause unloading of the concrete in compression next to the heated face and a reduction in D' to $14{\cdot}7$. During the next time interval, there is some additional cracking and D' is reduced to $6{\cdot}7$. Following this, cracking becomes so extensive that a situation is approached where thermal stresses can not be developed within the panel.

In considering the results from SLOADED, it was soon found that the qualitative information contained in the material state description was extremely useful in providing a compact guide to the overall performance. Accordingly, it was arranged that the letter symbols comprising the material-state description could be printed out line-by-line in a separate block following the detailed results. The control for this is punched in card 5 (Table 8·4 page 236). Some examples of this form of output will be used in discussing the results obtained from SLOADED (i.e. figure 10-14).

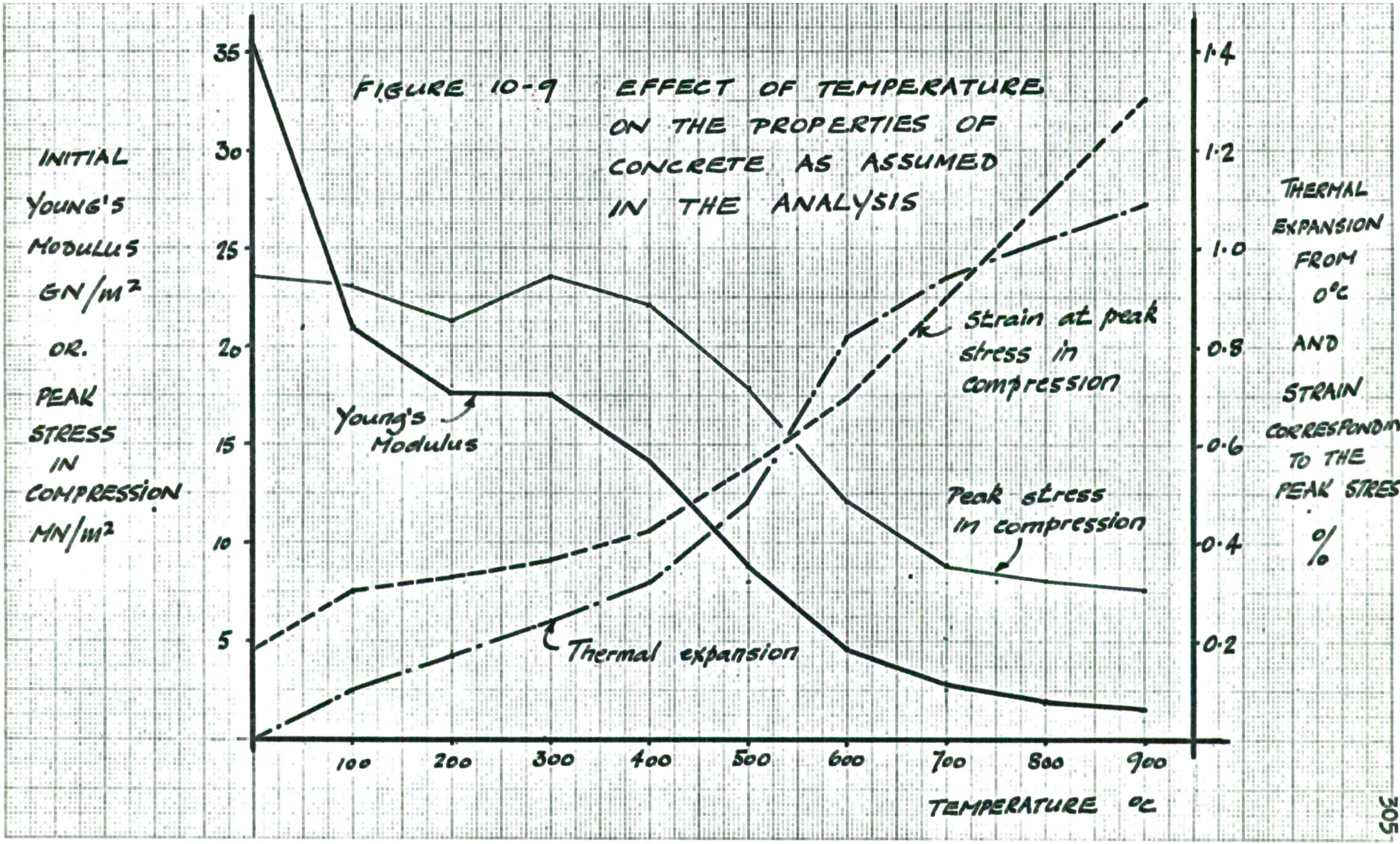
10·7 Data for use with SLOADED

The program SLOADED was used to investigate the behaviour

of a large number of different thickness panels with a variety of combinations of loading and restraint. It was soon found that structural failure occurred much earlier in thin panels than with thicker members. Thus, in order to economise in computer time and achieve a reasonable turn-round in program use, the work was mainly directed to examining the behaviour of a 50mm thick panel.

In some of the work, two sets of data describing the material properties were used in an effort to prescribe bounds to the true behaviour. The first set was based on Furamura's (1966[a]) results, for the stress-strain curve of concrete in compression at temperatures up to 700°C, and the general form of Harada's (1953[a]) results for thermal expansion. These data are shown in figure 10-9. For the other set of data, it was assumed that the properties of concrete were not affected by heating and had the constant values shown in Table 10·4. In both cases a value of 10 was taken for the ratio of the peak compressive stress to the tensile strength of the concrete. This is a reasonable value for a normal density concrete but tends to over-estimate the tensile strength of high strength concretes and vice-versa (Newman 1964[a])

The data shown in figure 10-9 exhibit some peculiarities that require comment. After an initial steep reduction with rising temperature, the value of Young's modulus remains practically constant for temperatures between 200 and 300°C. Such behaviour was not observed by Philleo (1958), in obtaining the results shown in figure 3-8, but has been found, in flexural tests at elevated temperatures, by


FIGURE 10-9 EFFECT OF TEMPERATURE ON THE PROPERTIES OF CONCRETE AS ASSUMED IN THE ANALYSIS
INITIAL YOUNG'S MODULUS GN/M² OR. PEAK STRESS IN COMPRESSION MN/M²
THERMAL EXPANSION FROM 0°C AND STRAIN CORRESPONDING TO THE PEAK STRESS %
Young's Modulus
Strain at peak stress in compression
Peak stress in compression
Thermal expansion
TEMPERATURE °C
35
30
25
20
15
10
5
1·4
1·2
1·0
0·8
0·6
0·4
0·2
100
200
300
400
500
600
700
800
900

Sullivan and Poucher (1968). The peak stress in compression, shown in figure 10-9, has been calculated from the values of initial Young's modulus and $\bar{\varepsilon}$, using equation 10·3·1. The results are rather uneven, for temperatures up to 400°C, but it is recognised that this is quite usual. Moreover, the data obtained in this way are rather similar to Abrams (1968) results shown in figure 3-7.

TABLE 10·4 Alternative Material Properties used in the Stress Analysis.

Young's Modulus	30·0 GN/m^2
Strain corresponding to peak stress in compression	0·20%
Peak stress in compression (approx)	22·1 MN/m^2
Coefficient of thermal expansion	10×10^{-6}/°C

In looking at the results presented in the following sections it will become clear that failures that occur soon after the start of heating are very much dependent on the form of the stress-strain curve and, in particular, on the gradient of the descending portion of the stress-strain curve in compression. In investigating this effect, most attention was given to the two cases, shown in figure 10-1, corresponding to m=1 and m=3. The second of these cases

may be slightly exceptional but stress-strain curves, with a steep decending branch in compression, have been obtained for a concrete using Leca lightweight aggregate (Grimer and Hewitt 1969) and normal density concretes using small sized aggregate (Hughes and Chapman 1966). Also, there are indications that the steepness of the decending branch increases with the rate of loading and concrete strength (Rusch 1960, Hognestadt et al 1955 and Smith and Young 1956)

At present there is no way of being certain of the manner in which the form of the stress-strain curve of concrete is affected by temperature during the early stages of heating. The only available data on the form of the complete stress-strain curve for concrete in compression at elevated temperatures have been obtained only after the unloaded specimens had been exposed to high temperature for a considerable time (Furamura 1966[a]). During this initial period the specimens must have been extensively damaged by cracking due to thermal incompatibility of the constituents. As noted in Chapter 3, both Fischer (1970) and Abrams (1968) have suggested that the development of these cracks is inhibited by the presence of a load during the heating period and their experiments show that such a load tends to maintain the stiffness and peak stress of a normal density concrete at a high value. More particularly, it appears that there is no significant reduction in strength or stiffness, caused by heating a siliceous aggregate concrete to temperatures as high as 400°C, provided that the specimens are maintained under a modest load during heating.

In the situation considered in the present work, the concrete is heated rapidly and is generally under stress, caused by restrained thermal expansion or an applied load. Here, Furamura's data are not really relevant but Fischer's and Abram's results suggest that the change in structural properties of the material will be small, provided it remains in compression. Thus, in considering behaviour that occurs shortly after the start of heating, it seems reasonable to ignore the effects of temperature on the material properties and use the data given in Table 10·4. This is the view taken in the present work.

This completes the discussion of the assumptions and data used in the analysis of panel behaviour. The results of a number of calculations undertaken on this basis are presented in the next Sections. Here no attempt is made to examine all the possible situations that can arise. Instead, attention is concentrated on the various modes of failure in an attempt to obtain a qualitative understanding of the manner in which these are influenced by loading and restraint.

10·8 Results from SLOADED : Axially loaded Panels

The affect of axial load on the performance of an unrestrained 50mm thick panel heated from one side is shown in figures 10-10 and 10-11. Here, the material properties are taken to be dependent on temperature with m=1 (figures 10-1 and 10-9). Results are shown for an unloaded panel and for three values of applied stress, equivalent to 23%, 47% and 70% of the peak stress of the concrete in compression before heating.

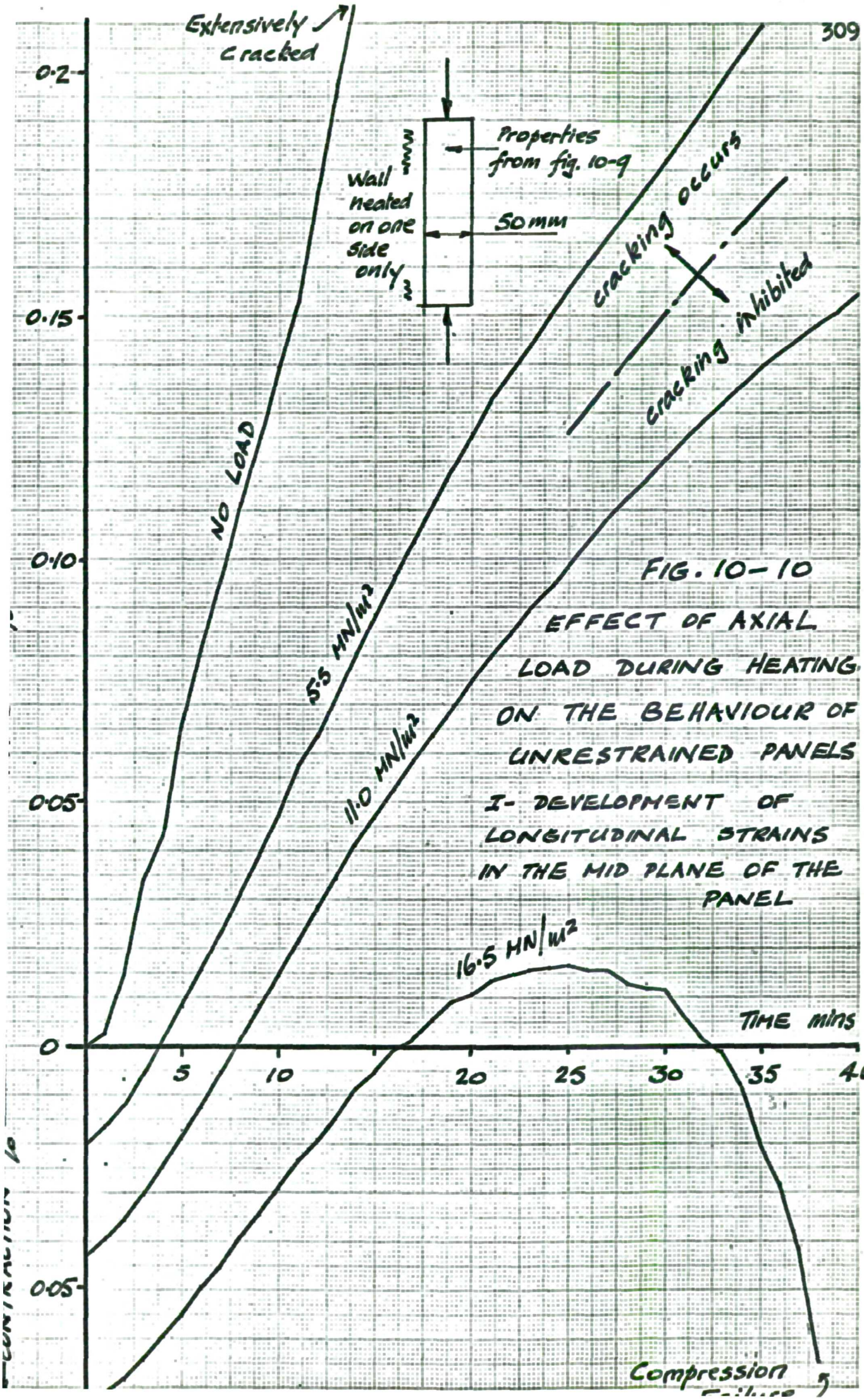


FIG. 10-10

EFFECT OF AXIAL LOAD DURING HEATING ON THE BEHAVIOUR OF UNRESTRAINED PANELS

I- DEVELOPMENT OF LONGITUDINAL STRAINS IN THE MID PLANE OF THE PANEL

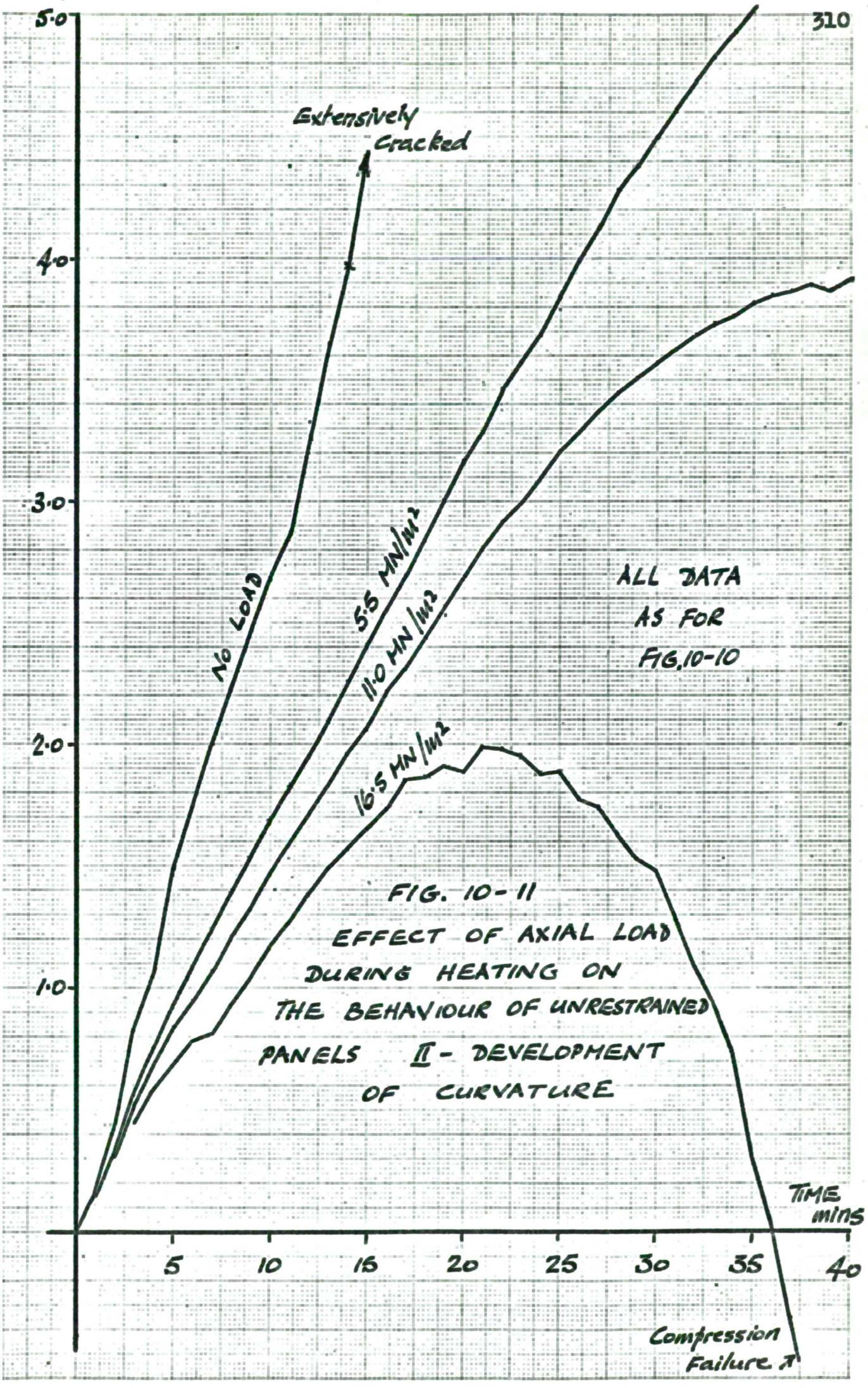


FIG. 10-11
EFFECT OF AXIAL LOAD DURING HEATING ON THE BEHAVIOUR OF UNRESTRAINED PANELS II - DEVELOPMENT OF CURVATURE

Cracking occurs within the central regions of the unloaded panel within the first two minutes heating. These cracks extend rapidly, so that the stiffness of the panel approaches zero after only 14 minutes exposure and the calculation fails to converge. It seems unlikely that a progressive failure of this sort will be violent and it seems that the panel may continue to act as a thermal barrier for some time, even though it has been effectively destroyed as a load bearing structure. In practise, this may be a case where very light reinforcement could be used, to retain the panel in position after extensive cracking.

An applied compressive load tends to inhibit cracking and so leads to better endurance provided that failure in compression is avoided. Thus, an improved performance is obtained with an applied stress of 5·5 MN/m^2, for which a small amount of tensile cracking occurs, and also with a stress of 11·0 MN/m^2 which is enough to maintain the whole section in compression. However, higher loads can lead to failure in compression as occurs after 38 minutes heating with a load of 16·5 MN/m^2.

Although there are differences in procedure and time scale, the results shown in figure 10-10 have the same general form as those obtained by Fischer (1970, figure 3-9 page 101) in tests on concrete specimens heated under load. Agreement of this sort is reassuring in the present work and suggests that, even though some time dependent phenomena, involving creep, have been ignored in the analysis, the qualitative conclusions concerning modes of behaviour are probably satisfactory.

Considering the occurrence of compression failure, the load capacity of a heated panel is determined by the maximum stress that can be carried in each region and the way in which the stresses within the panel are redistributed to take advantage of the strength of the material. With perfectly plastic materials (m=0 in figure 10-1) considerable redistribution of stress can occur and, with symmetric heating at least, the full potential strength of the section is realised. On the other hand, no stress redistribution is possible in a brittle material ($m=\infty$) and failure occurs, in the manner assumed by Saito (1965), as soon as the peak stress is reached at any point. The behaviour of a strain softening material, like concrete, lies between these two extremes with the ability to redistribute stress being determined by the form of the decending branch of the stress-strain curve. If the load capacity of such a material is calculated on the basis of perfect plasticity the collapse load is over-estimated[+] and the correct result can only be obtained in an analysis in which strain compatibility and the form of the decending branch of the stress-strain curve are considered.

The result obtained for the panel loaded with a stress of 16·5 MN/m^2 is due to both strain softening and the

---

Footnote[+]

It is interesting that an over-estimate of this sort was obtained by Thomas and Webster (1953) in attempting to estimate the load capacity of concrete columns from the results of tests on small samples. The source of the error does not appear to have been appreciated.

reduction in strength due to heating. In this case, it appears that the strength reductions had most influence, as calculations using the properties given in Table 10·4 (which are not dependent on temperature) show more rapid and extensive cracking under moderate loads but better performance at the high stress levels. This situation does not always obtain as the occurrence of failure may be very much influenced by the steepness of the decending branch and the time to failure may be less for a material with properties that are unaffected by heating than for one with the properties shown in figure 10-9. These matters are discussed in the latter part of the next section.

10·9 Flexurally restrained panels with axial load

In the previous section, the applied loading did not vary during the heating period. This situation may be contrived, for the purpose of a fire test, but is unlikely to occur if the panel is part of a structure. Generally a panel must be joined to the remainder of a structure in some way and, with this in mind, it is possible to imagine a practical situation, such as that shown in figure 10-12, in which a panel is restrained against rotation but also carries axial load.

The results shown in figure 10-13 have been obtained for a 50mm thick panel of a material with the properties given in Table 10·4 and with m=1. The panel has been almost completely restrained against rotation by setting $K'_m = 100$.

In the absence of a longitudinal load (N=0), the heavy flexural restraint leads to the development of tensile stresses across most of the section and an early loss of stiffness, as shown in figure 10-8. The presence of an

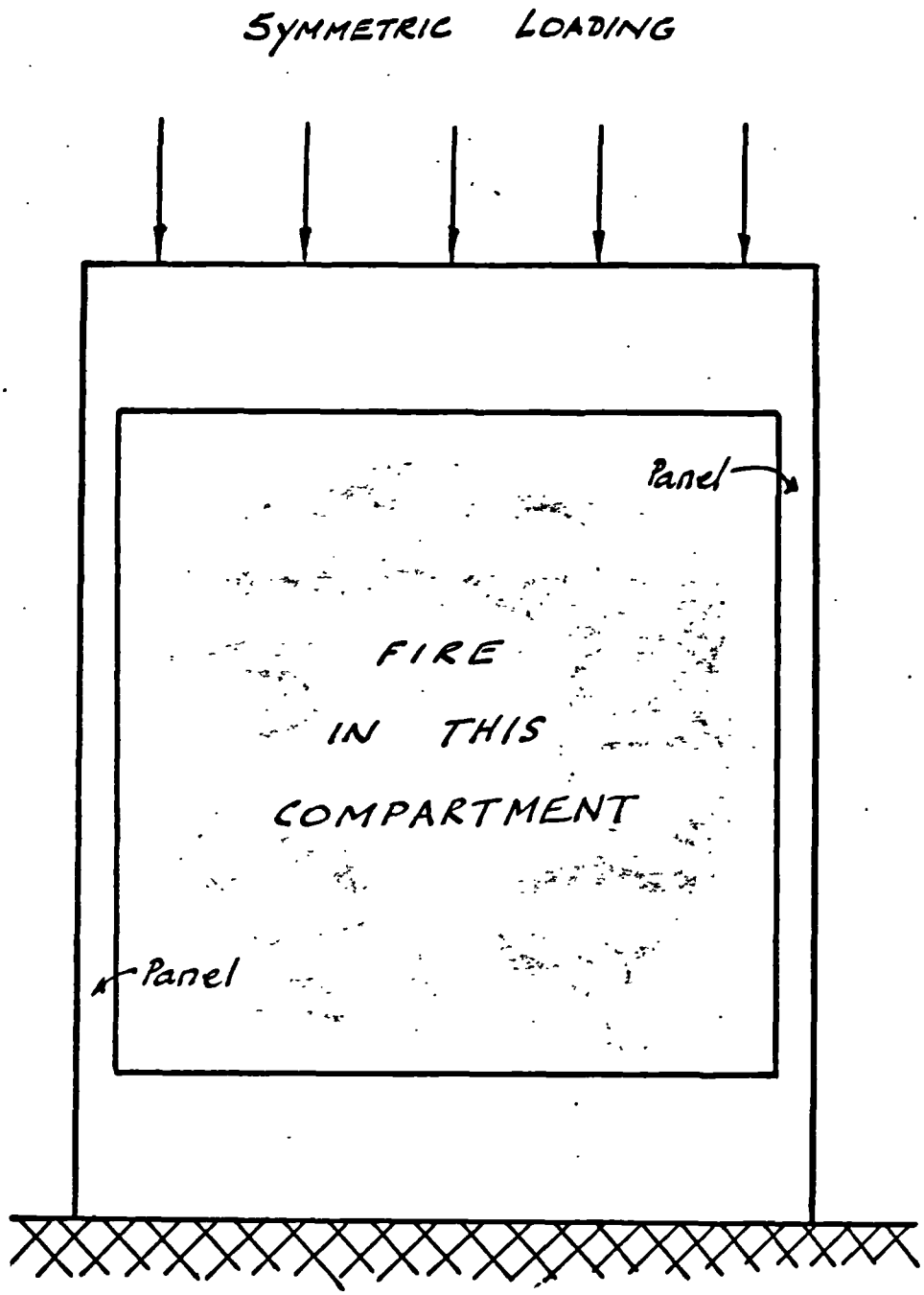
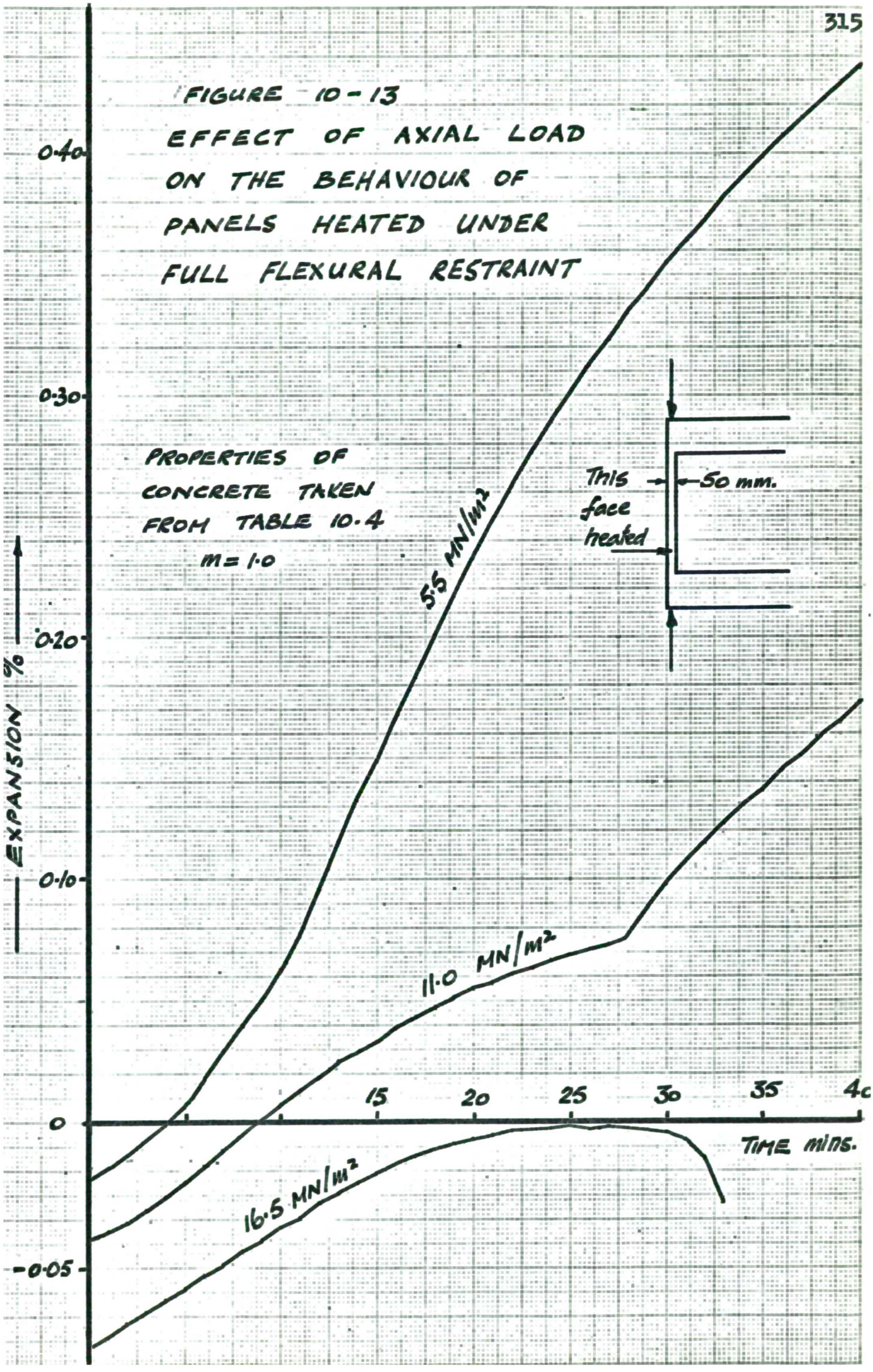


FIGURE 10-12 IDEALISED STRUCTURAL ARRANGEMENT PROVIDING A COMBINATION OF LOAD AND FLEXURAL RESTRAINT TO A PANEL SUBJECT TO FIRE

FIGURE 10-13

EFFECT OF AXIAL LOAD ON THE BEHAVIOUR OF PANELS HEATED UNDER FULL FLEXURAL RESTRAINT



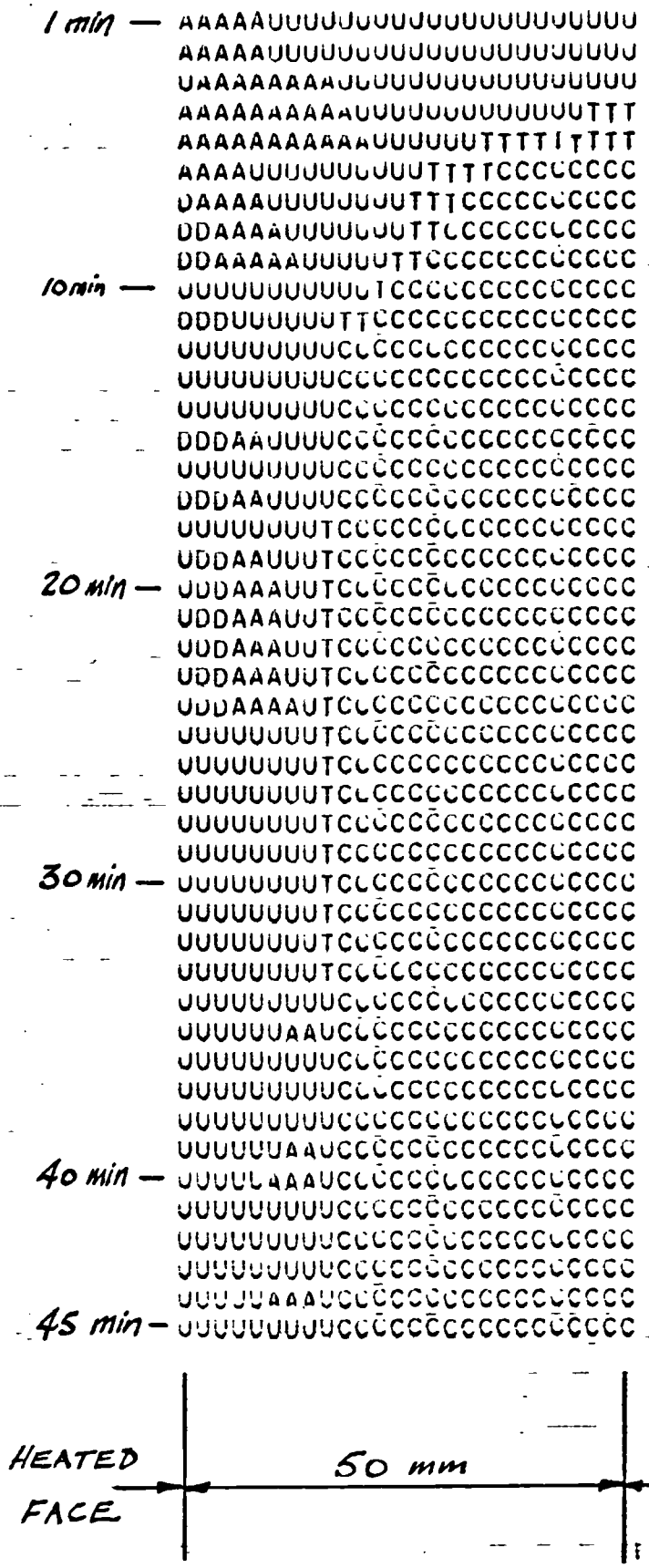


FIG. 10-14 MATERIAL STATE DESCRIPTION FOR PANEL UNDER FULL FLEXURAL RESTRAINT AND AXIAL LOAD OF 5·5 MN/m²

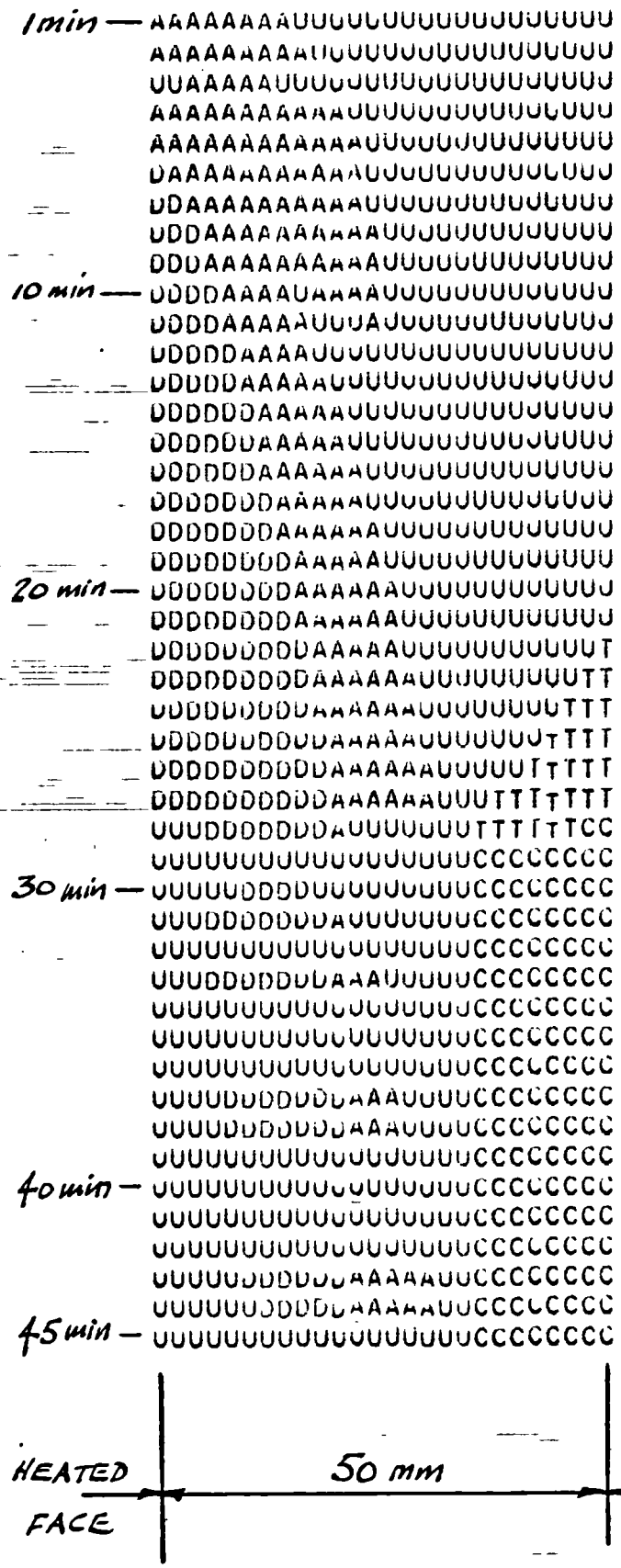
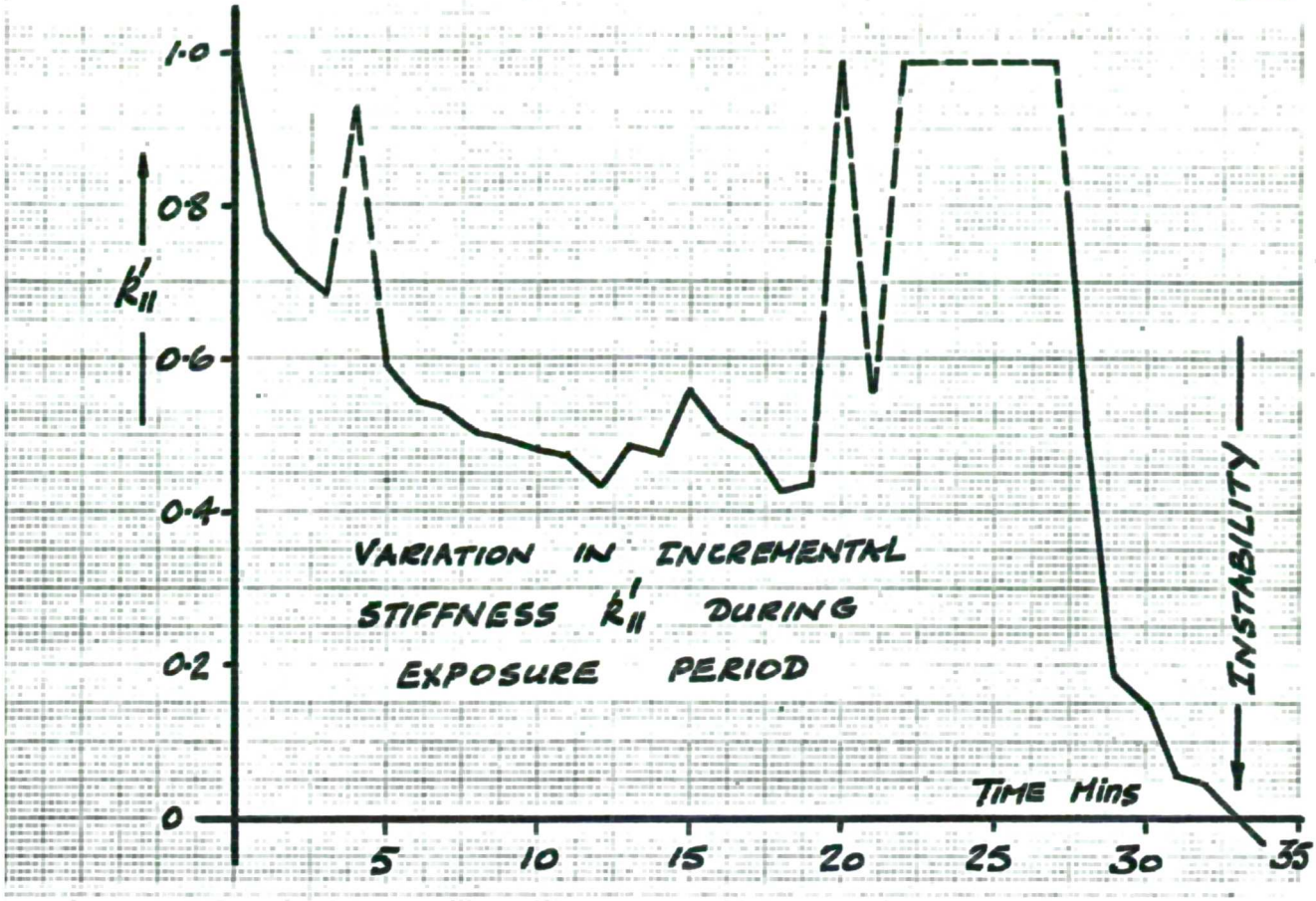


FIG. 10-15 MATERIAL STATE DESCRIPTION FOR A PANEL UNDER FULL FLEXURAL RESTRAINT AND AXIAL LOAD OF 11.0 MN/m²



FIG. 10-16 MATERIAL STATE DESCRIPTION FOR A PANEL UNDER FULL FLEXURAL RESTRAINT AND AXIAL LOAD OF 16.5 MN/m².



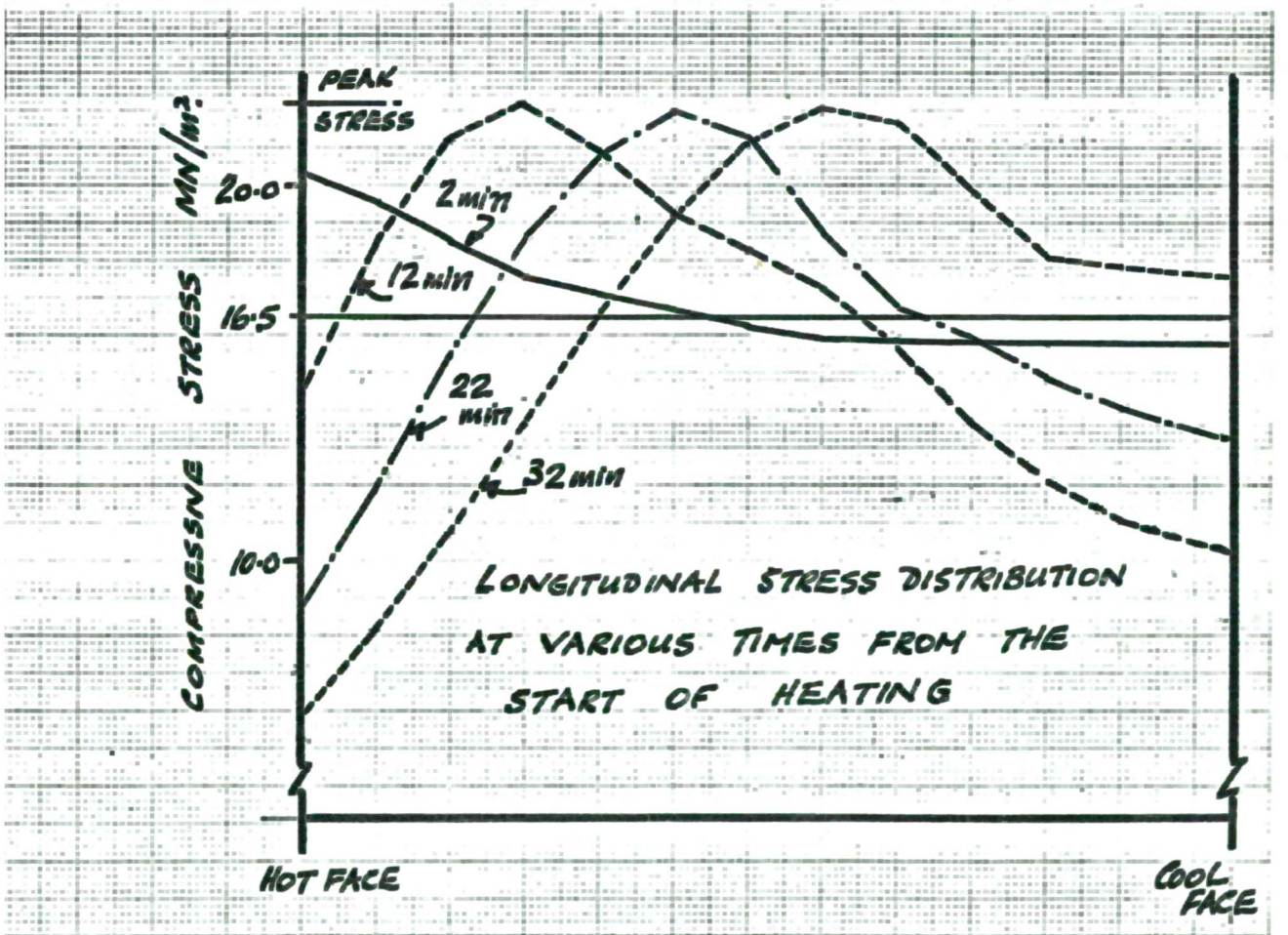


FIG. 10-17 VARIATION IN STIFFNESS AND STRESS IN A FLEXURALLY RESTRAINED PANEL CARRYING AN AXIAL LOAD (See also figs 10-13 / 10-16)

axial load delays or inhibits the development of cracking, as can be seen from the material state descriptions given in figures 10-14, 15 and 16. With the highest axial load (16·5 MN/m^2), the section is always in compression and instability occurs in the expected manner with a proportion of the section being loaded beyond the peak stress (marked D in figure 10-16) and the component k_{11} of the stiffness matrix approaching zero. Thus, a compression failure occurs in spite of the external restraint, which maintains the flexural stiffness k_{22} at a high value.

The manner in which the stiffness k'_{11} changes during the exposure period is shown in figure 10-17. This result suggests that unloading, within the section, leads to an increase in stiffness. However, it is considered that this increase is probably exaggerated because of the simplified treatment of unloading used in the calculations (assumption 1 page 281). Figure 10-17 shows the rapid reduction in stiffness, of the most heavily loaded panel, during the final few minutes heating. A failure of this sort is relatively sudden and appears to have all the characteristics of general or destructive spalling described in Table 1·3·1 on page 11.

There are some points of interest in the description of the panel loaded with 11 MN/m^2 given in figure 10-15. Before the start of heating, the section is entirely in compression and the initial effect of restraint is to cause further loading in the vicinity of the heated face (A) and unloading (U) throughout the remainder of the section. After 6 minutes exposure, the material near the heated face is

strained beyond the peak stress and the region contributing to instability (marked D in the figure) increases in size during the next few minutes heating. At this stage, the overall behaviour is very similar to that of the more heavily loaded panel (figure 10-16) and it would be tempting to suppose that the panel would eventually fail in the same way. However this does not occur, as tensile stresses are developed near the unheated face after 22 minutes exposure and these increase and lead to cracking, after a further 6 minutes heating. This cracking is beneficial, as it allows the section to unload and so avoid the conditions necessary for instability. The onset of cracking has a marked effect on the expansion of the panel. As seen from figure 10-13, the two most heavily loaded panels expand in a similar manner, during the early stages of heating, but this similarity ceases abruptly, with the occurrence of cracking after 28 minutes exposure, in the panel carrying 11·0 MN/m^2.

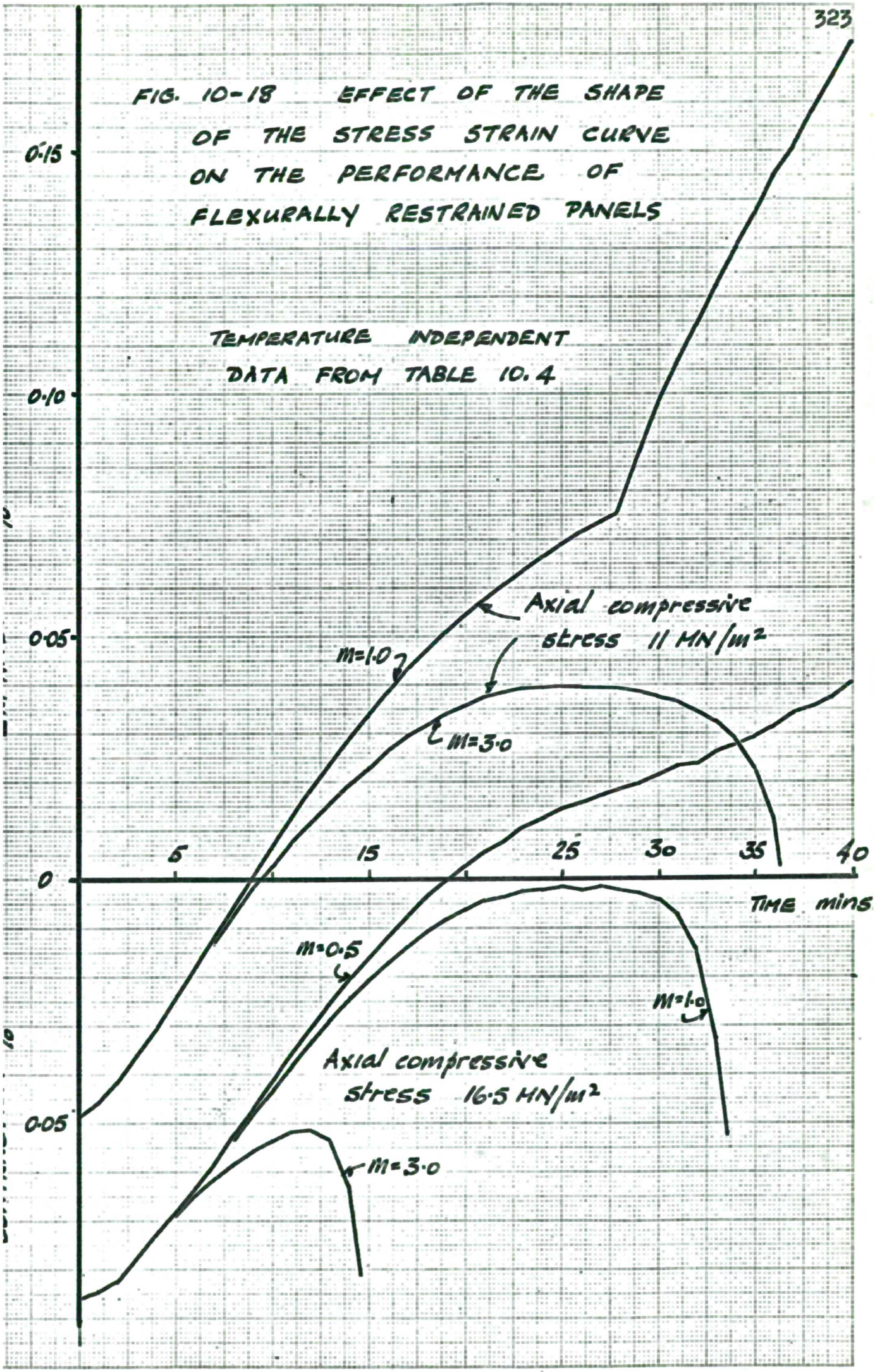
It is clear that the panel carrying 11·0 MN/m^2 survives because cracking provides some relief from the effects of restraint. Thus, it appears that this is a case where the presence of reinforcement could have a particularly damaging effect on performance. The steel would effectively increase the tensile strength of the section and so enable the process of loading, of the material near the heated face, to continue beyond the stage when cracking occurs in an unreinforced panel. In this way, the presence of an appreciable quantity of steel in the section could promote instability and so lead to a sudden failure.

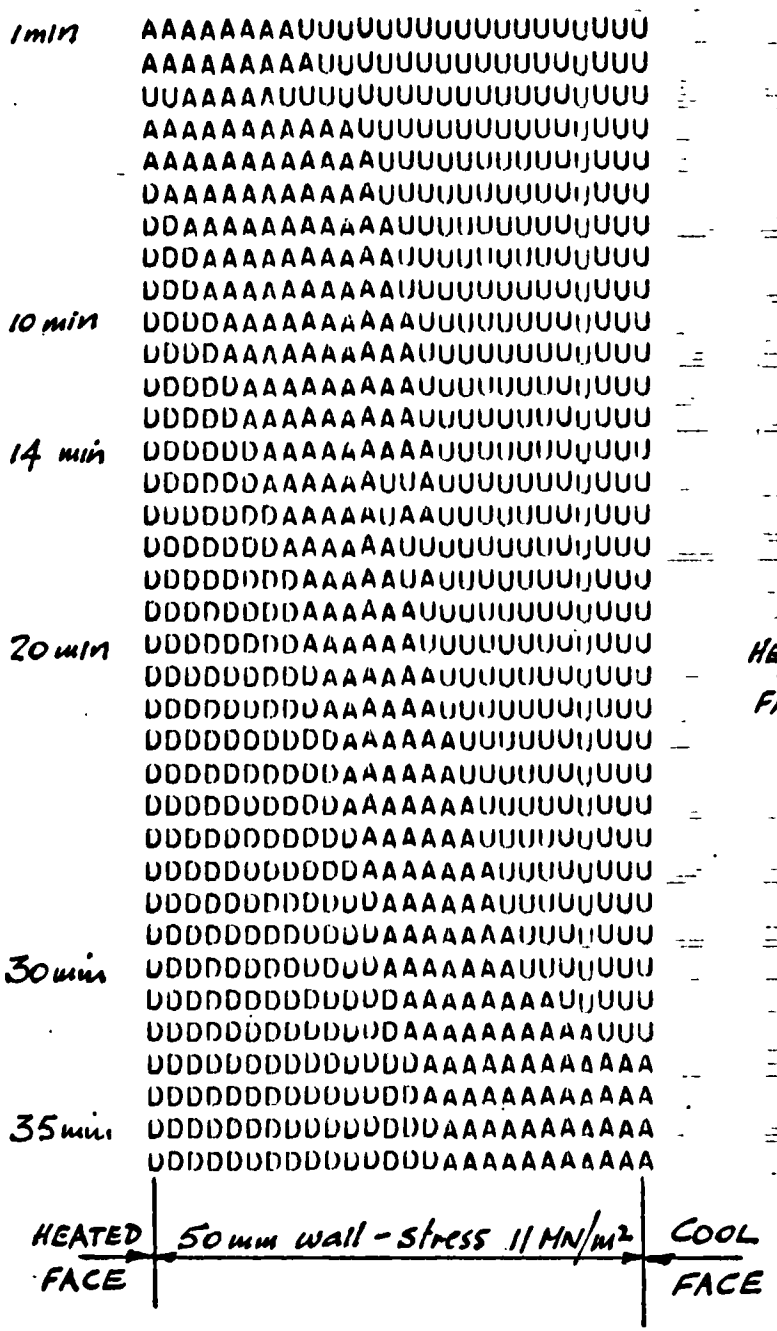
The results given in figure 10-13 refer to a panel of a material with properties that are not affected by changes in temperature. Thus, the mode of failure in compression is entirely dependent on the shape of the stress-strain curve and not at all due to changes, in the available peak compressive stress, caused by rising temperature. In this case, the form of the decending branch seems to be particularly important and calculations undertaken with the temperature dependent properties (given in figure 10-9) gave a rather better performance with compression failure of the panel loaded with 16·5 MN/m^2 not occurring until after more than 45 minutes exposure. It appears that this improvement can be attributed to the reduction in (negative) slope of the decending branch of the stress-strain curve, with temperature rise, and this leads to less brittle behaviour and greater use of the potential compressive strength of the entire section.

In the present work, failures that occur soon after the start of heating are of particular interest. It seems that these are most likely to occur, and be most catastrophic, if the decending branch of the stress-strain curve is steep. This is shown in figure 10-18, in which the data from figure 10-13, for the two most heavily loaded panels, is supplemented with results of calculations using alternative values of m.

It is seen that the form of the decending branch has a considerable effect on the behaviour of the panel carrying 11 MN/m^2 and that the occurrence of instability is no

FIG. 10-18 EFFECT OF THE SHAPE OF THE STRESS STRAIN CURVE ON THE PERFORMANCE OF FLEXURALLY RESTRAINED PANELS





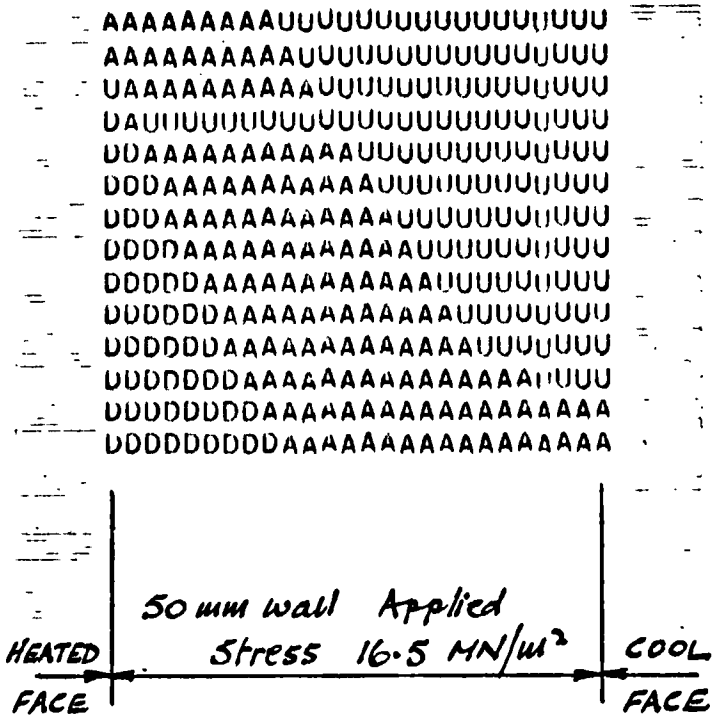


FIGURE 10-19 MATERIAL STATE DESCRIPTION FOR TWO PANELS UNDER FULL FLEXURAL RESTRAINT

STRESS STRAIN CURVE OF FIG. 10-1 WITH M = 3·0

longer prevented by cracking, when m=3 and the material has a steeper decending branch to the stress-strain curve. Increasing the value of m also affects the behaviour of the other panel, with instability occurring after only 14 minutes heating when m=3. The material state descriptions for the two cases with m=3 are given in figure 10-19.

10·10 Panels with less than Full Restraint

In the last section the panels were taken to be fully restrained against rotation. This is an extreme case and, in practice, cases of partial restraint with K'_m ∞ will be much more frequent.

In providing examples of this behaviour, the effects of temperature on the structural properties of concrete are ignored and it is assumed that there is a fairly steep decending branch to the stressMstrain curve (i.e. m=3). This is done, bearing the results of the previous section in mind, in order to set up the conditions under which sudden, apparently brittle failures are likely to occur.

Some results, for a 50mm panel loaded with an axial stress of 11 MN/m^2 and subject to different degrees of restraint, are shown in figure 10-20. For low values of the restraint parameter K'_m the behaviour is very much influenced by cracking. For the unrestrained slab, cracking occurs in the central regions of the panel and this postpones the development of instability in the manner discussed in section 10-8. With small values of applied restraint ($K'_m <$ 0·175 in figure 10-20) the effect of restraint is to reduce the extent of cracking and this correspondingly reduces the

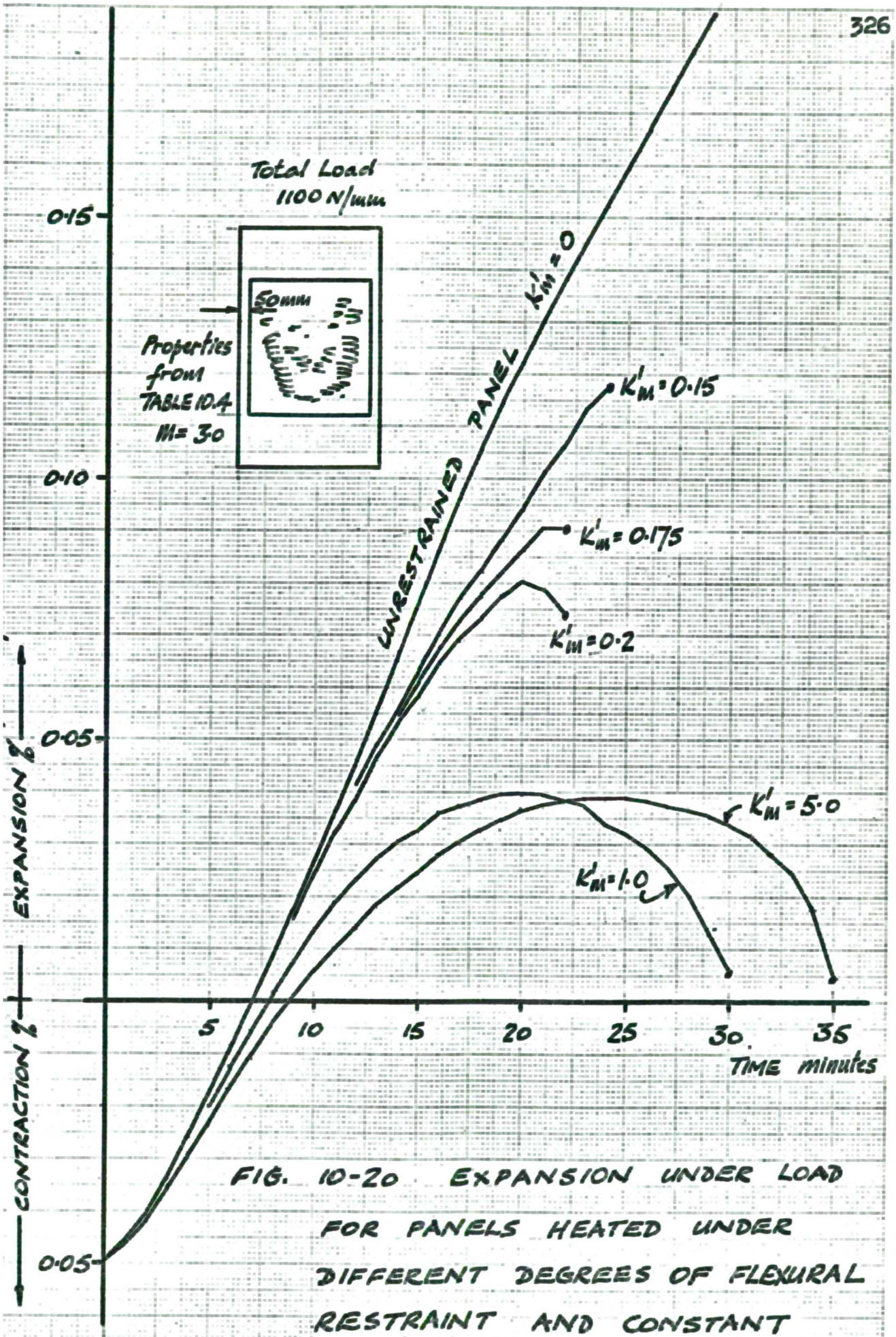


FIG. 10-20 EXPANSION UNDER LOAD FOR PANELS HEATED UNDER DIFFERENT DEGREES OF FLEXURAL RESTRAINT AND CONSTANT AXIAL LOAD

period of exposure necessary for the occurrence of instability. Higher values of restraint maintain the section in compression and, once this state is achieved, an increase in flexural restraint leads to an increase in the time required to cause failure.

Although the qualitative pattern will remain the same, some difference in results can be expected for different loadings and panel thickness. With greater applied loads, cracking could be avoided entirely and the effects of restraint would always be benefical, in the sense of extending the endurance period. With lower loads, the overall behaviour may be dominated by cracking and flexural restraint will lead to poorer performance. This is illustrated by the results for an unloaded panel given in figures 10-8 and 10-10. These suggest that the unrestrained panel survives for 14 minutes, before failure occurs due to extensive cracking, whereas a similar panel under full restraint only lasts 3 minutes.

Some results for thicker walls are shown in figure 10-21. The same material properties have been used as were adopted in deriving the results for the 50mm thick panel and the loading is again equivalent to half the peak stress in compression. The main difference in the results occurs because a smaller proportion of the panel width is subject to the effects of heating at any particular time. Because of this, the tensile stresses caused by heating are small and differences in behaviour caused by modifications to the extent of cracking are not so important. On this basis, it would appear that the effect of flexural restraint should

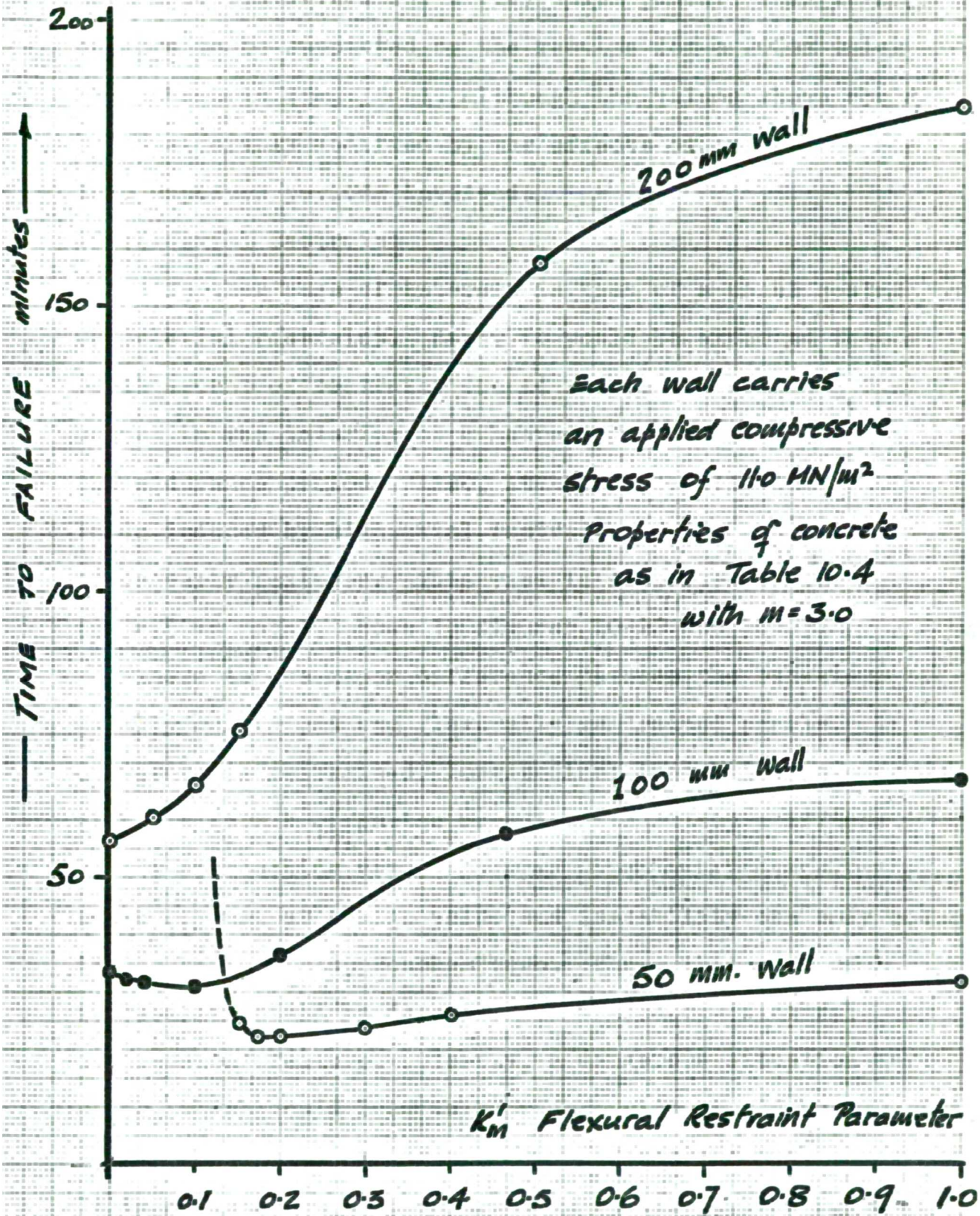


FIG. 10-21 EFFECT OF FLEXURAL RESTRAINT ON THE ENDURANCE OF WALLS OF DIFFERENT THICKNESS

always be beneficial for a very thick panel. This idea appears to be supported by the results for a 200mm thick slab shown in fig. 10-21, although the values shown could be considerably modified by the effects of creep over the long exposure periods involved.

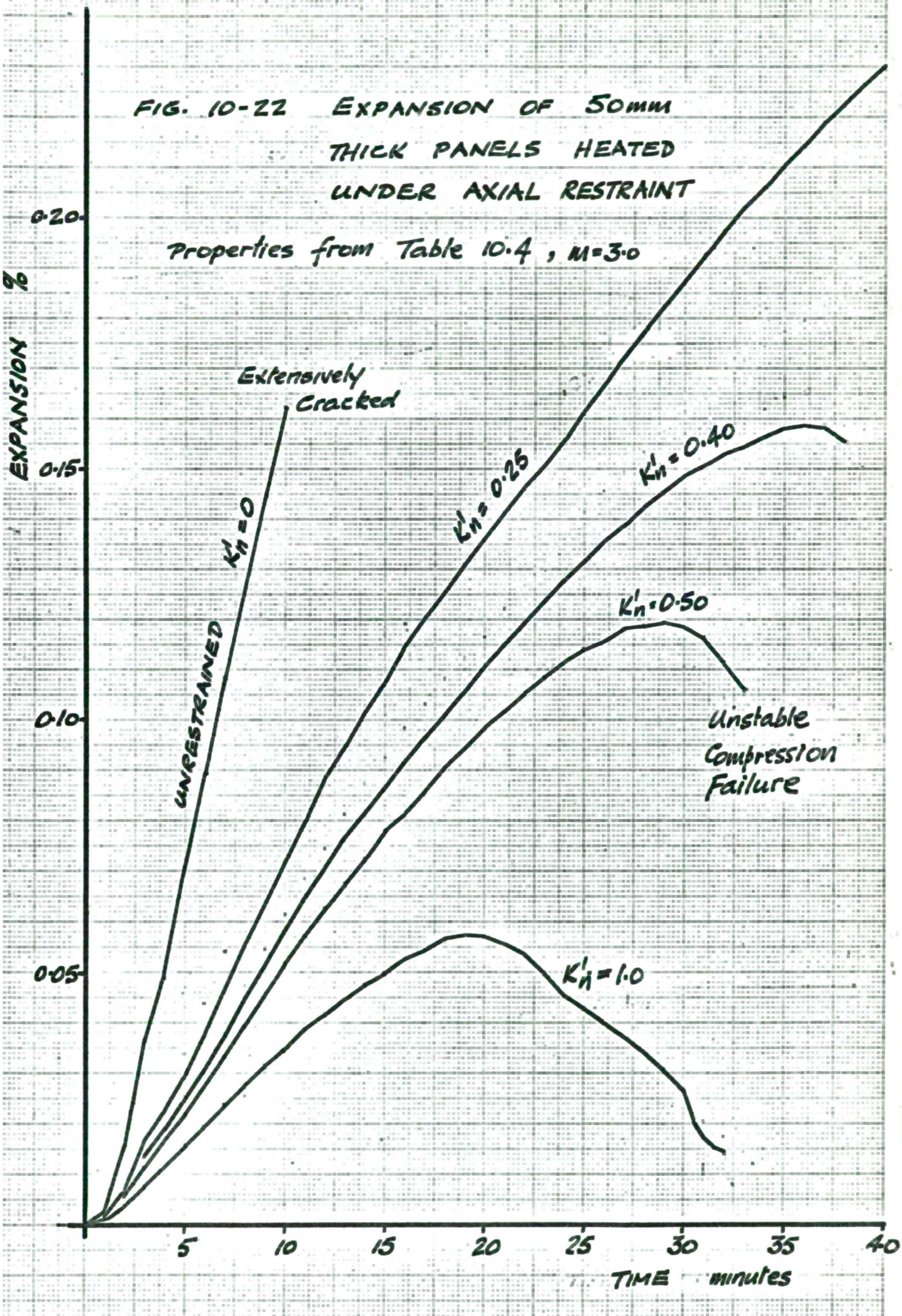
10·11 Axial Restraint

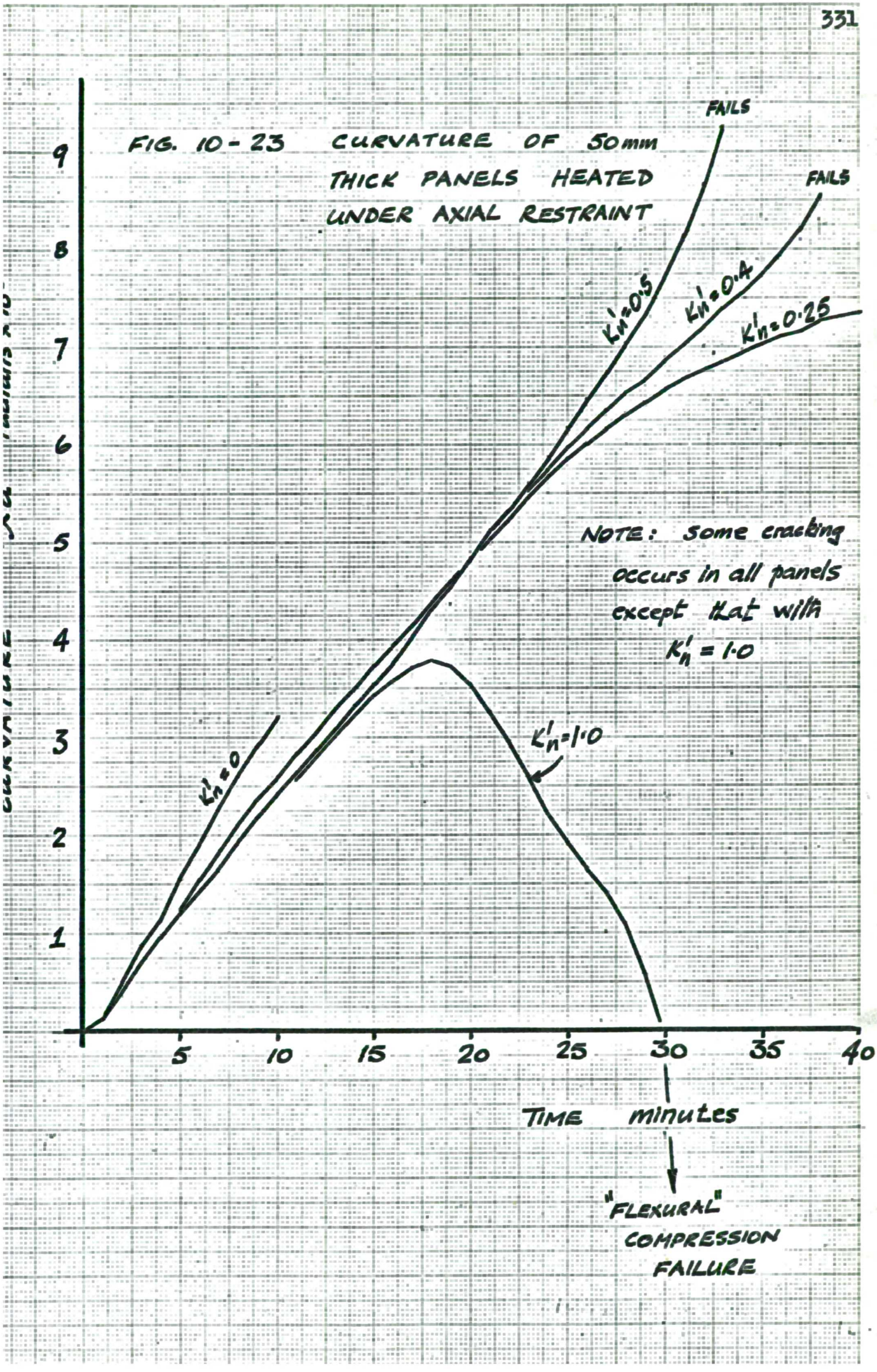
A further case of interest is that of a panel heated under axial restraint. Here, it would be expected that a small amount of restraint should reduce the cracking that occurs in the interior of a heated panel and so increase the endurance period. Also, it seems possible that the loads induced by high axial restraint may be such as to cause early failures. This view is supported by the results, for a 50mm panel, shown in figures 10-22 and 10-23.

There is one major difference between the behaviour of axially restrained and flexurally restrained panels. If curvature is restrained, longitudinal instability occurs with the term k'_{11} in the non-dimensionalised stiffness matrix approaching zero. However, high axial restraint keeps the k'_{11} term at a high value and instability can only occur if the k'_{22} term approaches zero. Thus, this mode of instability could be described as a kind of 'flexural compression' failure. Clearly, a dangerous situation may arise, which could lead to a sudden collapse, if heavy axial restraint is present together with a constant applied couple. It is of interest that destructive spalling, leading to complete destruction of a floor slab, has been observed in these particular circumstances (Carlson and Abrams 1965).

FIG. 10-22 EXPANSION OF 50mm THICK PANELS HEATED UNDER AXIAL RESTRAINT

Properties from Table 10.4, M=3.0




FIG. 10-23 CURVATURE OF 50mm THICK PANELS HEATED UNDER AXIAL RESTRAINT
FAILS
FAILS
$K_n' = 0.5$
$K_n' = 0.4$
$K_n' = 0.25$
NOTE: Some cracking occurs in all panels except that with $K_n' = 1.0$
$K_n' = 0$
$K_n' = 1.0$
CURVATURE
1
2
3
4
5
6
7
8
9
5
10
15
20
25
30
35
40
TIME minutes
"FLEXURAL" COMPRESSION FAILURE

10·12 Discussion

The calculations that have been undertaken have been based on an idealised model of material behaviour and it is doubtful whether the numerical values obtained have any great significance in themselves. Because of this the commentary on the results has been conducted mainly in qualitative terms and aimed at understanding modes of behaviour.

There are two main influences that affect the form of failure that might occur soon after the start of heating. These influences are the extent of cracking and the form of the stress-strain curve in compression.

Considering first the effect of cracking, it appears that this is often beneficial as it limits the development of thermal stress and so leads to good performance under fire conditions. However, cracking may be very extensive in thin panels that carry little load and, in such members, cracking must be controlled if the structure is to remain intact. It is considered that this could be done by using a very small quantity of reinforcement in the panel with the object of holding the fractured material in place and distributing the cracks throughout the panel. This would prevent the formation of holes that could allow the passage of flame and so limit the effectiveness of the panel as a thermal barrier.

The use of reinforcement in a panel may limit the development of cracking and may thus cause higher compressive stresses to be developed than could be achieved without the tensile reinforcement. In this way, the use of

a large quantity of steel may transform a situation from one where failure is progressive, and controlled by cracking, to one where failure occurs in compression and may be relatively violent.

The occurrence of compression failure, in panels during the early stages of heating, appears to depend primarily on the form of the stress-strain curve. It is not possible to induce a compression failure by heating a panel of a perfectly plastic material, that has temperature independent properties, no matter what initial conditions of load or restraint are involved. However instabilities can arise in a strain softening material, like concrete, and these are more likely to occur when the slope of the descending branch of the stress-strain curve is steep.

The possibility that instabilities could occur in wall panels during heating was first recognised from the form of the stiffness matrix developed, for a typical panel, in Chapter 9. This recognition did not depend on the assumptions made earlier in this Chapter concerning material behaviour but these have affected the detailed results obtained using SLOADED.

At present the assumptions used in the analysis are not fully supported by experimental evidence and much more testing is required in order to assess the full effects of simultaneous changes in stress and temperature and to study the effects of creep. In spite of this, the results obtained, taking account of temperature dependent properties, appear to be reasonable and in line with the few available experimental data. In addition to this, the assumptions

used in the analysis are only in the nature of simplifications, if the effects of temperature on the properties of the material can be ignored. As explained in Section 10·7 this seems to be a reasonable approximation to the conditions that must obtain during the early stages of heating of a section that is maintained in compression. Fortunately these are the circumstances under which instability in compression seems to occur.

In discussing the results, it has been implicitly assumed that a compression failure induced by heating would have the appearance of destructive or general spalling. This view seems to be unexceptionable, even though some modes of overall failure have been ignored. In particular, it appears that there may be some circumstances where lateral stability should be considered.

Some of the factors affecting the form of the stress-strain curve have already been discussed in Section 10·7. However, in addition to these factors, it is clear that the slope of the decending branch is affected by the state of stress and it may be necessary to take some account of the effects of pore pressure as mentioned in Section 9·4 page 261. Referring again to Richart et al's (1928) results, shown in figure 2-5 on page 35, it is clear that an all round confining pressure inhibits the development of cracking and reduces the steepness of the decending branch of the axial stress-axial strain curve. In a wall panel, the micro-cracking caused by a predominantly biaxial compressive stress field may be exacerbated by a small effective tensile stress, due to pore pressure, acting in

a direction normal to the heated surface. In this way, the existence of a modest pore pressure within the wall could steepen the decending branch of the stress-strain curve and so significantly affect the occurrence of destructive spalling.

Even ignoring possible effects of pore pressure, the results from SLOADED appear to give a comprehensive explanation for the occurrence of destructive spalling. The results obtained are most relevant to the early stages of heating, before changes in material properties, with temperature rise, and creep of the concrete have any great effect. It is considered that both these influences will tend to prevent spalling, by reducing the slope of the stress-strain curve and by allowing relaxation of the thermal strains induced by heating. Because of this, the conditions for general spalling are likely to occur only during the early stages of heating.

In recognising that general spalling is a type of compression failure, there is a distinct similarity between the present approach and that used by Saito (1965) and discussed in Chapter 1 (page 16 et seq.). However, some of the anomalies in Saito's work are avoided when spalling is treated as an instability, rather than by assuming a limiting value of compressive stress. In a way, Saito's approach can be regarded as a particular case of the present method with the value of m being set to ∞. However, such an approach ignores the strain softening behaviour of concrete and leads to the anomalous result that failure should occur even when both the axial and flexural restraint parameters have high values. In qualitative terms, this anomaly was

the most serious deficiency in Saito's results, which were further suspect due to the clear lack of correspondence between the assumed material behaviour and that of concrete. It is considered that both the anomaly in the results and the deficiency in the material description have been overcome in the present work.

Chapter 11

MECHANISMS OF LOCAL SPALLING

11·1 Introduction

The conditions that lead to general structural failure of a heated wall panel were considered in the previous chapter. The analysis suggested that the process of failure is gradual in many cases, but that there are circumstances where sudden major changes in stiffness occur which may lead to the more violent form of behaviour associated with destructive spalling. In this chapter, attention is focussed on possible mechanisms for the forms of local spalling given in Table 1·3·1 (page 11). Here, the term local is used to suggest that these forms of failure are either initiated or occur in relatively small regions and that the mechanism involves localised breakdown rather than the occurrence of instability in the entire structural member. However, it should be noted that local spalling may be quite extensive, in practice, and so can promote general structural failure of a complete member.

11·2 Aggregate Splitting

It seems that one form of surface breakdown in concrete members may be due to splitting of the aggregate during the early stages of heating. When this occurs in a wall panel, or floor slab, the aggregate particles near the heated surface are split in a plane approximately parallel to the heated face. This behaviour can be seen quite clearly in the photograph, in figure 11-1, which was taken following the fire that occurred during construction of the Rathbone Place Sorting Office in London in 1962. In this case, surface breakdown may have been influenced by

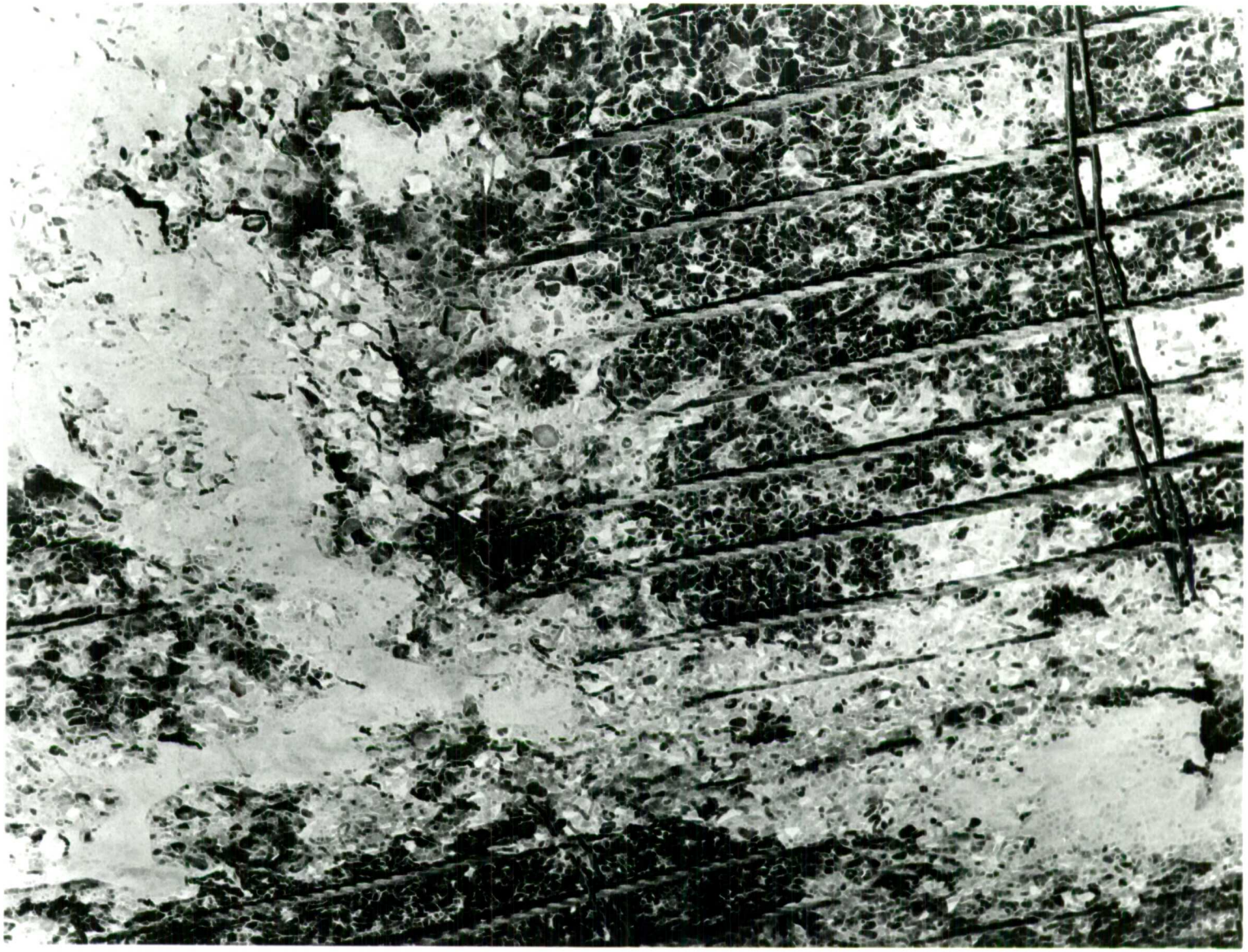


FIG. II-1 FIRE DAMAGE TO THE SOFFIT OF A FLOOR SLAB SHOWING SURFACE SPALLING WITH AGGREGATE SPLITTING

the presence of the reinforcement although it is felt that the region affected would have been smaller if the usual amount of distribution steel had been employed. In any case, it is clear that splitting of the aggregate has been accompanied by removal of material from the surface and that the steel has been exposed to the direct effect of fire. This could have serious consequences and it is clear that a method is required to assess the probable behaviour of any particular aggregate at high temperatures so that those aggregates likely to disintegrate in a structure exposed to fire can be rejected.

Kingery (1955) has shown how the ability of a single material to resist sudden changes in temperature can be expressed in terms of a Thermal Stress Resistance Factor. For example, consider a sphere of linear elastic material, with Young's modulus E and Poisson's ratio ν, throughout which the temperature is initially uniform. The surface temperature is now raised instantaneously by an amount T_s and maintained at this new value. A state of hydrostatic tension is induced, at the centre of the sphere which eventually reaches a maximum value of

$$\sigma_r = \sigma_t = 0{\cdot}386\, E\alpha T_s / (1 - \nu) \qquad (11{\cdot}2{\cdot}1)^{+}$$

Footnote $^{+}$

This result was obtained by Grünberg (1925)

---

where α is the coefficient of thermal expansion for the material of the sphere.

If the maximum value of equal triaxial tensile stress that the material can withstand is f, the rise of surface temperature T_f that will cause a cleavage failure is found from,

$$T_f = \frac{1-\nu}{E\alpha} \frac{f}{0{\cdot}386} \qquad (11{\cdot}2{\cdot}2)$$

Now, we define a Thermal Stress Resistance Factor F by

$$F = \frac{(1-\nu)\, f}{E\alpha} \qquad (11{\cdot}2{\cdot}3)$$

so that

$$T_f = FS \qquad (11{\cdot}2{\cdot}4)$$

where S is a non-dimensional factor often referred to on the shape factor.

The factor F embodies all the material properties that influence fracture and it is clear that the higher the value of this factor the better is the resistance of the material to thermal shock. The concept of a stress resistance factor is quite general although the application of the principle has been considerably simplified by assuming linear elastic behaviour with constant material properties. In addition the influence of Poisson's ratio is probably not correctly represented in equations 11·2·3 and 11·2·4 for shapes other than spheres, if the shape factor is to be independent of

material properties. In spite of these limitations, thermal stress resistance factors have found considerable application in refractory technology in selecting the most appropriate material for a particular situation.

For different exposure conditions, additional material properties such as thermal conductivity, specific heat, density and also the surface heat transfer coefficient may affect the magnitude of the stresses developed and these must be included in the Thermal Stress Resistance Factor if this is to be relevant. These matters are discussed in detail by Kingery (1955) and White (1958) but will not be taken further in the present work, which will be aimed more particularly at the thermal stress resistance of aggregate particles in concrete. In order to do this, an idealised situation will be considered in an attempt to derive a factor which will include most of the material properties involved in aggregate splitting.

11·3 A Thermal Stress Resistance Factor for Aggregate Splitting

Consider a spherical aggregate particle of radius R, Young's modulus E_a and Poisson's ratio ν_a that is surrounded by a large quantity of concrete which, in this case, will be regarded as a linear elastic material with Young's modulus E_c and Poisson's ratio ν_c. This situation is illustrated in figure 11-2. The temperature distribution throughout the aggregate particle and the surrounding material is assumed to be a function of time t and the radius r with the temperature T_R, at the interface r = R rising at constant rate ϕ.

Within the concrete, the temperature distribution is such as to cause an outward radial displacement of $n\alpha_c RT_R$ at the surface $r = R$, if the aggregate particle has negligible stiffness or is replaced by a void. In this expression α_c is the coefficient of linear thermal expansion of the concrete and the quantity n serves to represent the influence of the temperature distribution in the concrete. Thus, n would be unity if the temperature was uniform throughout the concrete mass but would be greater than unity if the temperature increases with radius.

When a stiff aggregate particle is present, the radial displacement of the interface is modified due to the effect of the radial stress ($\sigma_r = -p$) at the interface. Thus, using Lamé's solution for a very thick spherical container under internal pressure as given by Timoshenko and Goodier (1951[a]), the conditions at the boundary of the aggregate particle become

$$\left.\begin{aligned} T &= \phi t, \\ \sigma_r &= -p, \\ \text{and} \quad u &= n\alpha_c R\, t + \frac{pR}{2}\left(\frac{1+\nu_c}{E_c}\right) \end{aligned}\right\} \quad \text{at } r = R \qquad (11\cdot3\cdot1)$$

Within the aggregate particle, the temperature satisfies the equation of heat conduction

$$k\left(\frac{\partial^2 T}{\partial r^2} + \frac{2}{r}\frac{\partial T}{\partial r}\right) = \frac{\partial T}{\partial t} \qquad (11\cdot3\cdot2)$$

Where k is the thermal diffusivity of the aggregate

material. In the special case considered, in which the temperature at the boundary rises at a constant rate ϕ, a situation is approached, some time after the start of heating, in which the temperature at all points within the sphere rises at the same rate. In this way, a quasi-static temperature distribution is established relative to the surface temperature. This asymptotic solution is obtained by integrating equation 11·3·2, after replacing $\partial T/\partial t$ by ϕ, to give

$$T = \phi t \left[1 - \frac{R^2 - r^2}{6kt} \right] \qquad (11\cdot3\cdot3)$$

It will be noted that this solution satisfies the conditions at the interface but does not provide the correct temperature within the aggregate at time t = 0. However, comparison with the complete solution, obtained by Williamson and Adams (1919) and shown in figure 11-3, suggests that the true temperatures are within 10% of those given by equation 11·3·3 for $kt/R^2 > 0{\cdot}25$. Thus, the asymptotic solution becomes satisfactory for all normal size aggregate particles after only a few minutes heating.

Timoshenko and Goodier (1951[b]) give a general solution for thermal stress in a symmetrically heated sphere and this solution can be easily adapted to satisfy the boundary conditions 11·3·1. For the temperature distribution 11·3·3 the maximum tensile stress occurs at the centre of the sphere, where

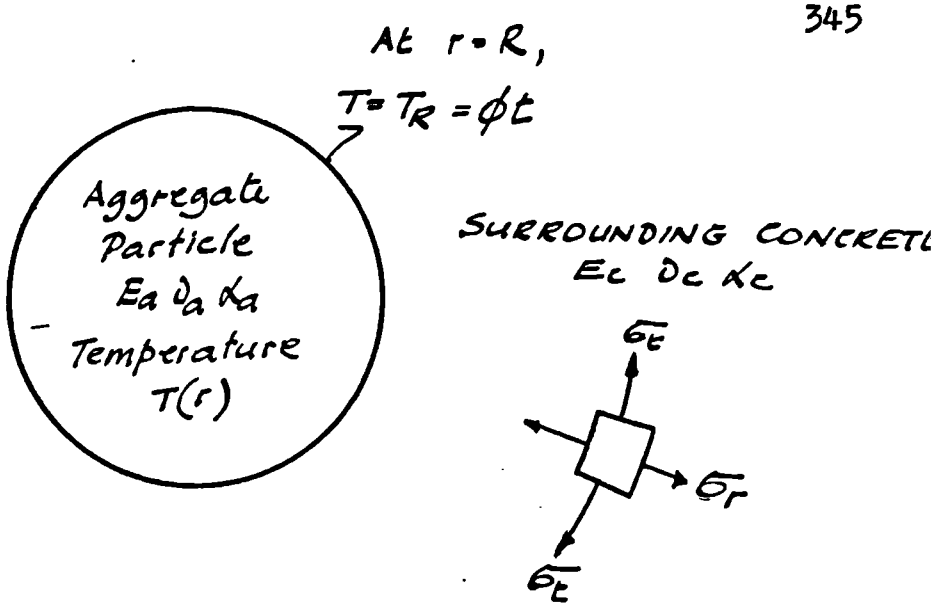


FIG. 11-2 IDEALISATION USED IN CONSIDERING AGGREGATE SPLITTING

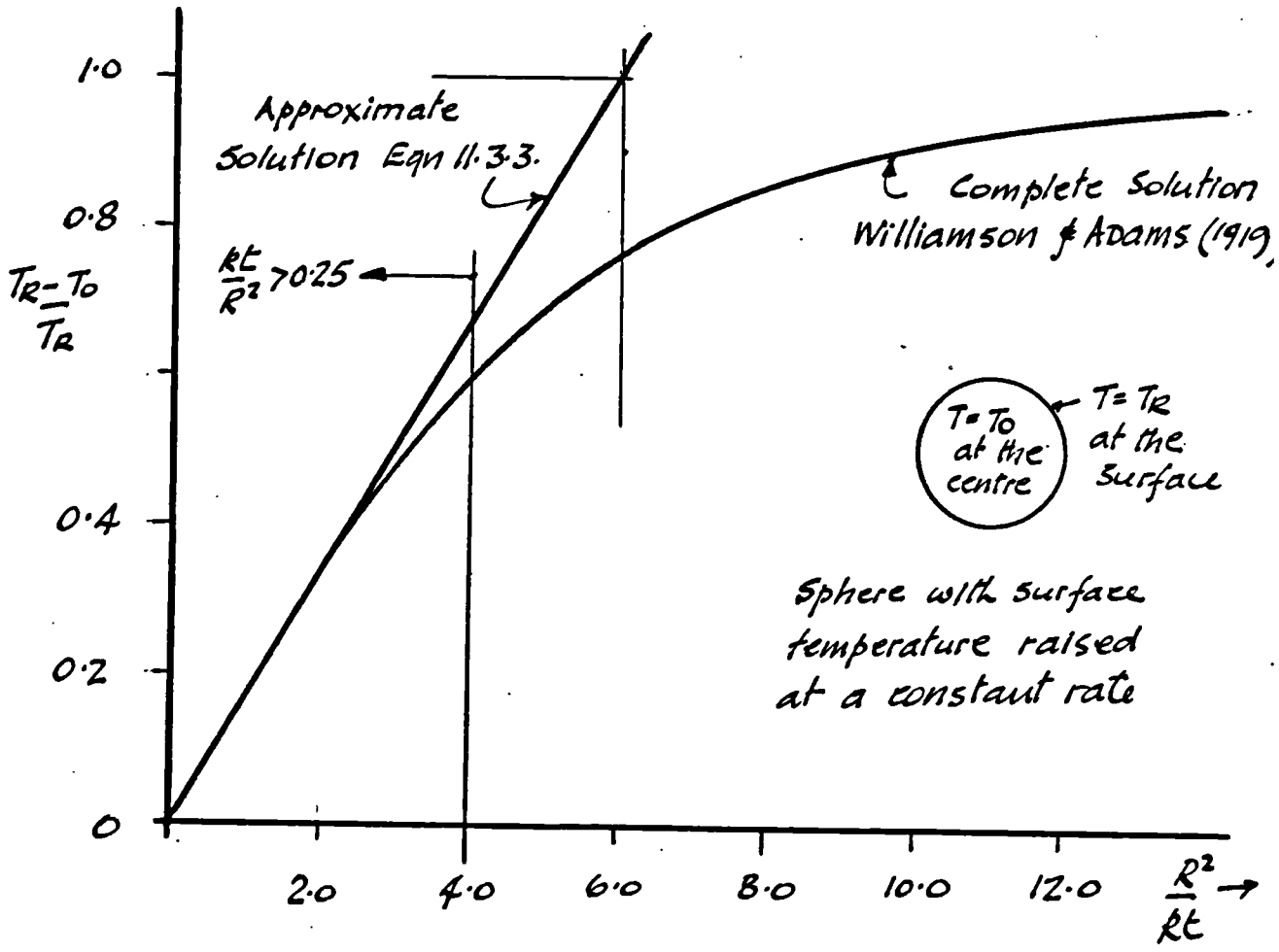


Fig. 11-3 SOLUTIONS FOR THE TEMPERATURE IN A SPHERE WITH A CONSTANT RATE OF TEMPERATURE RISE AT THE SURFACE

$$\sigma_r = \sigma_t = \frac{2E_a\alpha_a}{1-\nu_a}\left[\frac{R^2}{30k}(M+5) + \left(\frac{n\alpha_c}{\alpha_a} - 1\right)\phi t\right] \Big/ (M+3)$$

(11·3·4)

where $$M = \frac{1+\nu_a}{1-\nu_a}\left(\frac{1+\nu_c}{1+\nu_a}\frac{E_a}{E_c} - 1\right).$$

Failure occurs by splitting of the aggregate when $\sigma_r = f$, the maximum tensile stress that the aggregate can withstand. In this way, the condition for failure can be written

$$\left(\frac{M+5}{M+3}\right)\frac{\phi}{\phi_f} + \frac{5\cdot17}{(M+3)}\left(\frac{n\alpha_c-\alpha_a}{\alpha_a}\right)\frac{T_R}{T_f} = 1 \qquad (11\cdot3\cdot5)$$

where $T_R = \phi t$,

$$T_f = \frac{(1-\nu_a)\, f}{0\cdot386\, E_a\alpha_a}$$

and $$\phi_f = \frac{15\,(1-\nu_a)\, k\, f}{E_a\alpha_a R^2}$$

The terms ϕ_f and T_f are themselves thermal stress resistance factors for the aggregate particle. ϕ_f is the heating rate required to cause fracture in a sphere of aggregate of radius R heated at a constant rate and T_f is the temperature that would cause failure if the aggregate particle was suddenly exposed to heating with the boundary being maintained at constant temperature. The expression for T_f follows from equation 11·2·2 and ϕ_f is found from equation 11·3·5 by putting σ_r equal to f and letting M approach infinity. Although it is difficult to obtain

representative values of the properties of single pieces of aggregate, the order of magnitude of the factors ϕ_f and T_f may be demonstrated by using assumed values for the material properties. Thus, based on the properties given in Table 11·1, T_f has a value of 22°C and the critical heating rate ϕ_f is 39°C/ minute for a 20mm diameter piece of aggregate.

TABLE 11·1 Properties of aggregate used in calculating values of T_f and ϕ_f.

Young's Modulus	70 GN/m^2
Poisson's ratio	0·2
Maximum tensile stress	7·5 MN/m^2
Coefficient of thermal expansion	10 x 10^{-6}/°C
Thermal diffusivity	0·5 mm^2/sec

Returning to equation 11·3·5, two separate cases must be considered depending on the relative magnitudes of the thermal expansion of the aggregate and the surrounding concrete. If α_a is greater than α_c the second term of the equation is negative and splitting tends to be inhibited by increasing temperature and time. If failure is to occur under these conditions it must do so early so that, even

admitting the possibility of failure at the start of heating, aggregate splitting cannot occur if,

$$\phi < \left(\frac{M+3}{M+5}\right)\phi_f \qquad \text{for } \alpha_a \geqslant n\alpha_c \qquad (11\cdot3\cdot6)$$

If the effective thermal expansion of the concrete is greater than that of the aggregate ($n\alpha_c > \alpha_a$) the radial stress at the interface is tensile and so helps to promote splitting, providing that bond is maintained at the interface. The second term in the square brackets of equation 11·3·4 represents the effect of radial stress at the boundary between the aggregate and the surrounding concrete. This stress is tensile if $n\alpha_c$ is greater than α_a and increases with time, so that, if aggregate splitting does not occur, the radial stress at the interface will eventually become equal to the maximum tensile bond strength f_b and separation will occur at the interface. On this basis, aggregate splitting can not occur when $n\alpha_c > \alpha_a$ if

$$\phi < \left(1-\frac{f_b}{f}\right)\left(\frac{M+3}{M+5}\right)\phi_f \qquad (11\cdot3\cdot7)$$

before bond failure or

$$\phi < \phi_f \qquad (11\cdot3\cdot8)$$

once separation has occurred.

Although the analysis has been based on a very idealised model, it seems reasonable to use the results to deduce qualitative information on the behaviour of aggregate in concrete members exposed to fire. It is known that the coefficient of thermal expansion of different samples of natural aggregate may vary widely, even when these are obtained from the same source ; Bonnell and Harper (1951), Lerch (1957). Thus, it appears that, if different aggregate particles are considered, the thermal expansion of the aggregate may be greater or less than the effective expansion of the concrete and thus the different forms of aggregate splitting may occur in the same member. The main factors influencing the conditions 11·3·6 to 11·3·8 are summarised in Table 11-2. From this it appears that splitting is most likely to occur in concretes with a strong, stiff mortar matrix and that the best approach, to reduce aggregate splitting, is to reduce the maximum size of aggregate used in the concrete mix. In any case, if aggregate splitting is likely to occur, it seems desirable to use a smaller sized aggregate than usual, as experimental results by Tomita and Taylor (1961) suggest that the thermal stress resistance of natural aggregate particles deceases with an increase in particle size. Some further experiments on the effect of aggregate size are described in the next section.

TABLE 11•2 Factors Influencing Aggregate Splitting

ϕ_f	Depends on the properties of the aggregate particle and also on its size. ϕ_f is inversely proportional to the square of the aggregate diameter.
$\left(\frac{M+3}{M+5}\right)$	Increases with M and so tends to decrease with increasing strength or stiffness of the surrounding concrete.
$\left(1-f_b/f\right)$	Controlled by the tensile strength of the particle and its bond strength with the matrix. The factor decreases with increasing matrix strength
ϕ	The rate of temperature rise depends on the exposure conditions and the concrete quality. The experimental results given in Chapter 6 suggest that ϕ will not be significantly affected by changes in mix proportions.

11·4 Experiments concerned with aggregate splitting[+]

In order to investigate the effect of particle size on aggregate splitting, various samples of aggregate were heated in a furnace so that the proportion of material surviving this treatment could be compared.

The aggregate sample comprised a known weight of material passing one B.S. sieve and retained on the next smaller size. Generally around 200 grams of material were used, although no attempt was made to standardise the sample. The sample was resieved, following the heating test, and the weight of material retained within the original size range was taken as a measure of the quantity surviving. The materials used consisted of a Dungeness beach gravel (mainly flint), barytes and limestone.

In the test, the aggregate samples were heated in a wire basket and placed in a furnace heated to the required temperature. This temperature was maintained for one hour before the closed furnace, containing the sample, was allowed to cool gradually, to the laboratory temperature, over a period of several hours. It is thought that little damage occurred during this cooling period as the crackling noise, accompanying the splitting of the aggregate, was heard only

---

Footnote [+]

These tests formed part of an undergraduate project undertaken at King's College London by Mr R.S.Stone, working under the direct supervision of the author. His help in this work is gratefully acknowledged.

---

whilst the furnace was at, or near, the test temperature.

Some results, for the beach gravel aggregate, are shown in figure 11-4. Few tests were undertaken on the other aggregates although these were sufficient to indicate similar trends to those shown in the figure. The size effect is clearly demonstrated, considerable damage occurring in the largest sizes of aggregate for only a small increase in temperature above a 'threshold' value of around 285°C. This threshold value (corresponding to the maximum temperature that the sample can withstand without appreciable damage) appears to be relatively insensitive to aggregate size and may be a useful means of comparing the quality of different types of aggregate. On this basis, we can compare the performance of the beach gravel (285°C) with that of the limestone (around 500°C) and Barytes (having a threshold value of about 640°C).

In order to see if these size effects were reproduced in concrete, a number of 50mm diameter, 300mm long cylindrical specimens were made. The mix was proportioned by volume with one part of cement to three parts siliceous sand to four parts of the aggregate under test. A water cement ratio of 0·45 by weight was used. These specimens were tested at 500°C in the same manner as the aggregate samples. Little damage occurred with the smallest size aggregates (between the 3/16 inch and the Number 7 B.S. sieves, i.e. 5-3mm) but more damage was apparent in the specimens with each succeedingly larger size of stone. The consequences of splitting of the largest pieces of

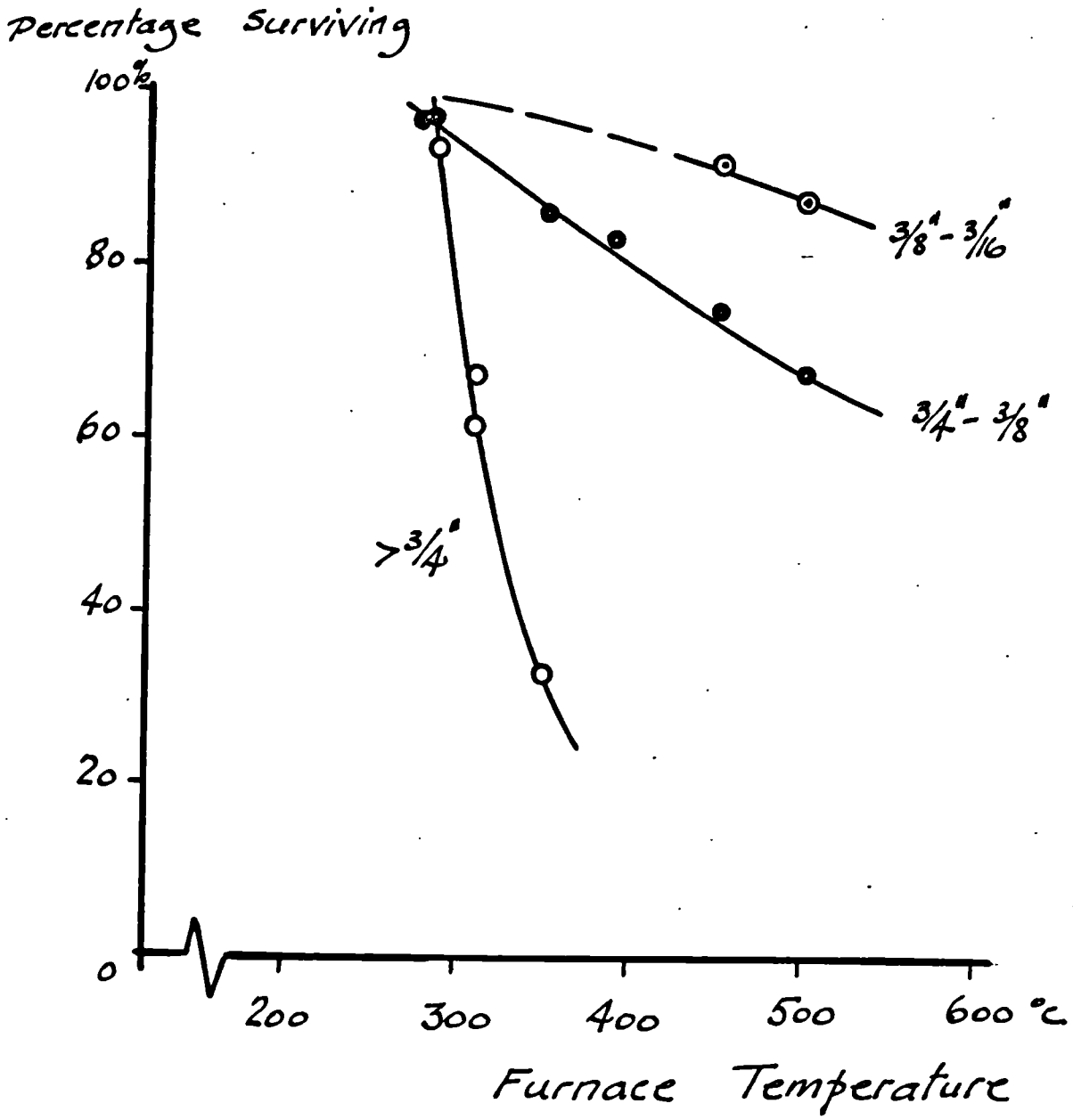


Figure 11-4. PROPORTION OF AGGREGATE SAMPLE SURVIVING EXPOSURE TO HIGH TEMPERATURE

aggregate was particularly noticeable, as the occurrence of aggregate splitting appears to promote the removal of an appreciable quantity of the matrix surrounding the pieces of stone.

The experimental conditions are such that it may be difficult to reproduce the quantitative results precisely if a different type of furnace or form of specimen was used. If the test were to be used as a means of comparing aggregate quality, a standard form of furnace would be needed with a standard test procedure. However, it is considered that the results described illustrate trends that may be significant in practice and show the need to develop a standard form of test for aggregate splitting.

Aggregate splitting is a form of cleavage failure that is caused by thermal stress. It seems likely that corner failures are also of this type although fracture takes place within the concrete as a whole rather than preferentially within a single phase.

11·5 Corner Failures

Loss of material by the removal of external corners is a common occurrence in ceramics exposed to high temperatures. Norton (1931) has noted corner splitting of the form shown in figure 11-5 in the bricks used in furnace linings where it appears that this form of failure is of particular importance (Howie 1945).

In concrete structures, separation often occurs at the corners of rectangular or square columns or at the arrisses of rectangular beams. This last form of breakdown is shown

in figures 11-6 and 11-7 which were again taken following the fire in the Rathbone Place Sorting Office. Here, the presence of the reinforcement may have had some influence on the extent of splitting but it is thought that the experience with unreinforced ceramics suggests that the principal cause of failure is the development of high thermal stress in the concrete.

If the thermal stresses induced by heating the surface of a long circular column are considered, it is found that the radial stress component is tensile near the surface where the longitudinal and tangential components are both compressive. As early as 1922, Lees recognised that these stresses could cause failure and suggested that the spalling of concrete, that had been observed during fire tests on cylindrical columns (by Hull, 1920 for example), was due to tangential cracking caused by the radial tensile stress.

It is clear that a similar situation must obtain at an external corner. Figure 11-8 shows the probable distribution of temperature and radial stress in the plane that bisects the surfaces of a heated corner of infinite extent. The stress must be zero at the boundary and must increase to a peak tensile value before decreasing to zero at large distances from the apex. The distribution of the tangential stress component σ_ϕ follows from the radial stress in accordance with the equation of equilibrium.+

Footnote+

$$\frac{\partial \sigma_r}{\partial r} + \frac{\sigma_r - \sigma_\phi}{r} = 0$$ Timoshenko and Goodier (1951)

Thus σ_ϕ is compressive at the surface but becomes tensile some distance away from the apex and is equal to the radial stress where this has its maximum value.

Because of the rapid variation of stress with distance from the apex and the changing nature of the system of combined stress, it is difficult to decide which is the critical section at which failure will occur. However, if it is assumed that the tensile strength of concrete is reduced monotonically with increasing temperature, it is clear that failure will be initiated at a point some distance in from the apex rather than at the surface. The conditions immediately prior to this type of failure are illustrated in figure 11-8.

Corner splitting depends on the thermal stress resistance of the concrete itself and thus concretes having a high value of the factor F, given in equation 11·2·3, are more likely to perform satisfactorily than those with a low value. Also, it is to be expected that the use of a surface insulating layer would be beneficial, as this would reduce the rate of temperature rise and allow more time for the thermal stresses to be relaxed by creep in the concrete.

In practice, it seems necessary to allow for the occurrence of corner separation in all members made of normal density concrete. Thus, it is advisable to use a quantity of supplementary reinforcement to hold the fractured material in position and so protect the main reinforcement from the direct effects of fire.

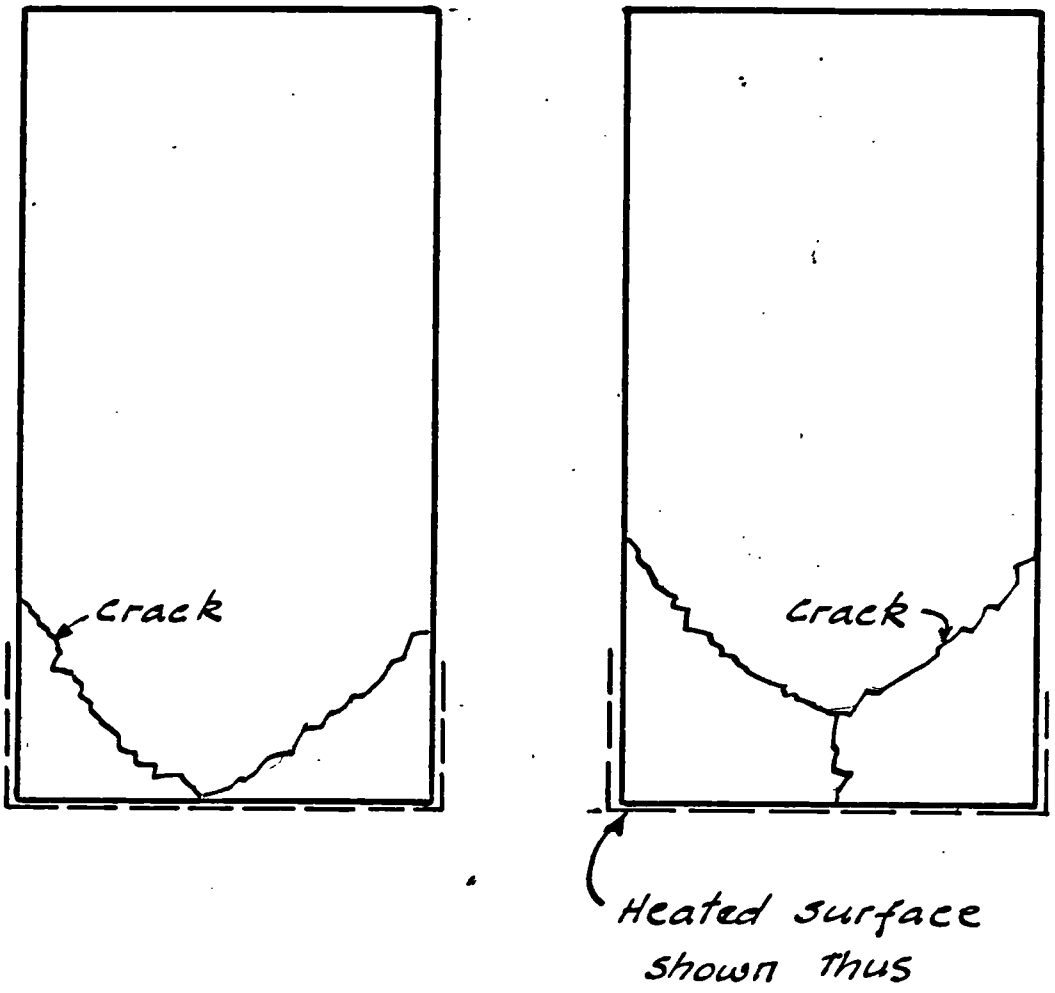


Figure 11-5 TYPICAL FORMS OF DAMAGE OBSERVED IN FURNACE BRICKS IN SERVICE - after NORTON (1931)

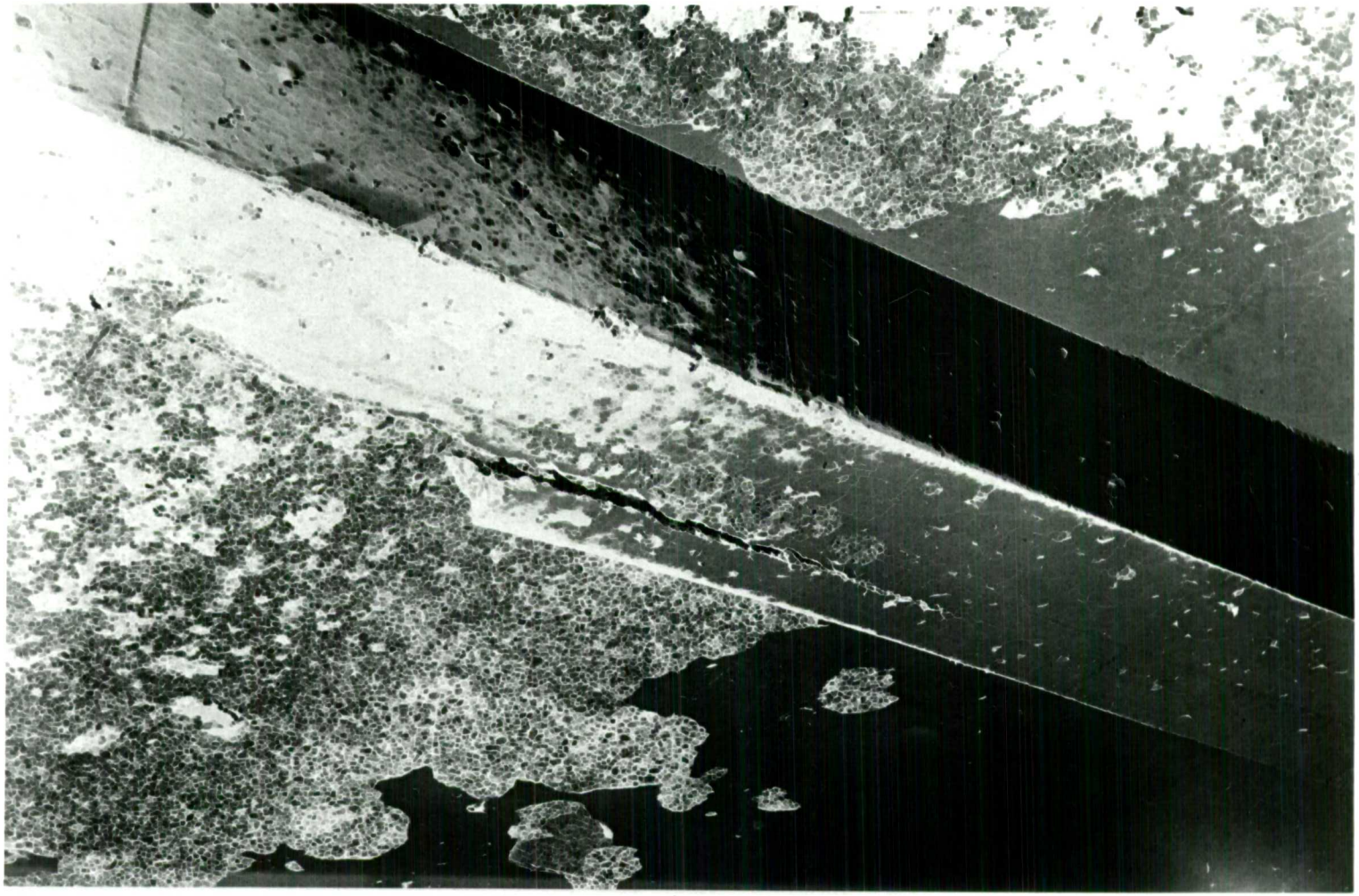


FIG. II-6 FIRE DAMAGE AT RATHBONE PLACE — FLOOR BEAM SHOWING CORNER SEPARATION



FIG. II–7 CORNER SEPARATION IN A FLOOR BEAM AT RATHBONE PLACE IN 1962

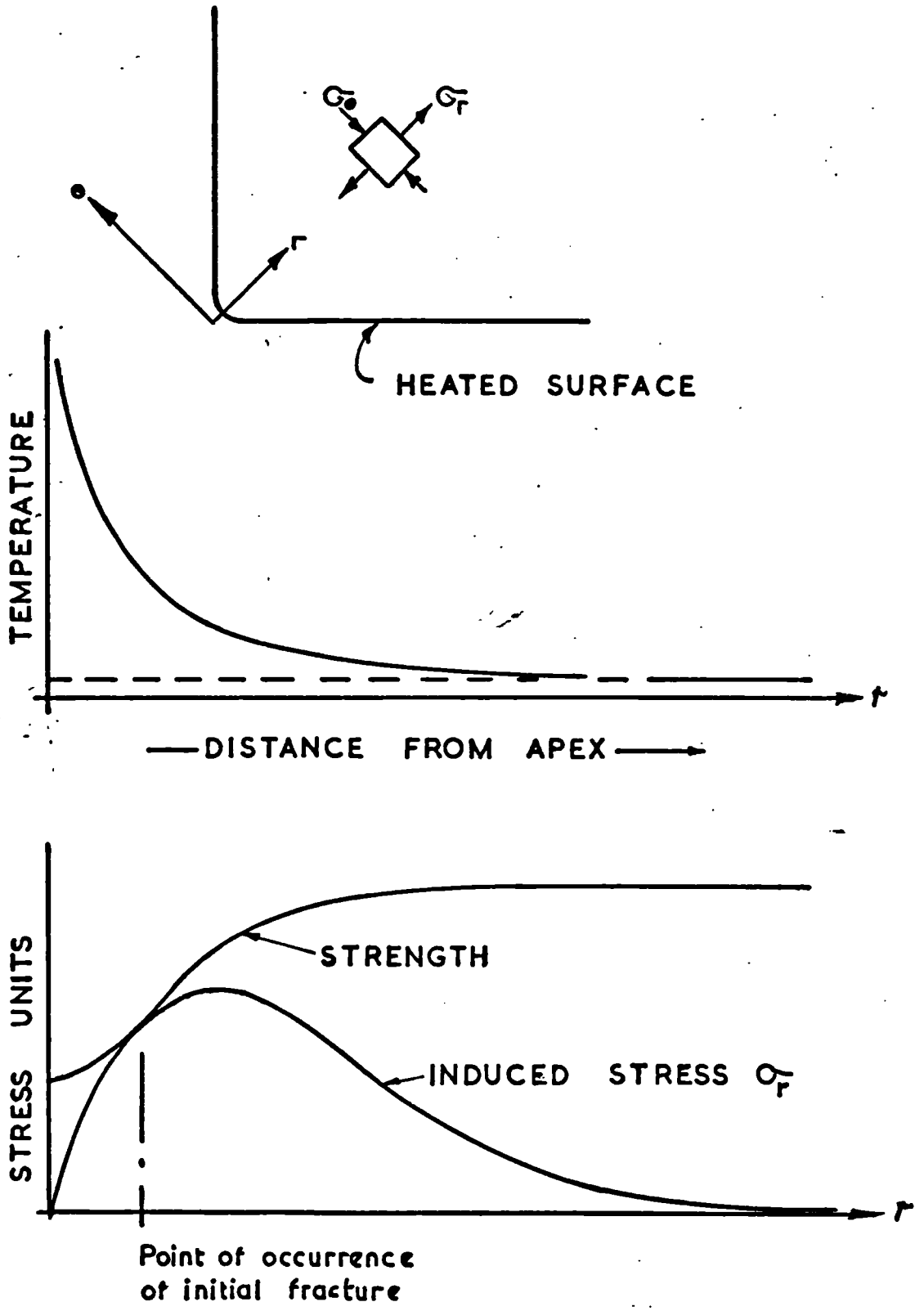


FIG. II-8 MECHANISM OF CORNER SEPARATION

11·6 Surface Spalling: Introduction

With both aggregate splitting and corner separation the primary cause of failure is the development of tensile stress during heating. Accordingly, it seems reasonable to start a study of failures, that occur near the surface of heated floor slabs or wall panels, by looking for situations in which a tensile stress component can be developed in a direction normal to the heated surface. This can only occur when there are departures from the ideal conditions assumed in the analysis described in chapters 9 and 10. Here, it was assumed that the material in the wall was initially homogeneous, the heating was uniform and the curvature was small. However, in real walls, there may be local inhomogeneities, due to the presence of reinforcement, together with variations in the heating pattern that lead to hot and cool spots in the heated surface. Also, the curvature may be appreciable in thin panels heated from one side. The effects of these factors will now be discussed in more detail.

11·7 Effects of Large Curvature

Consider the section of a wall panel shown in figure 11-9 that is uniformally heated at the surface z = 0. Here the stresses and strains are functions of z only and, if the effects of curvature are neglected, the stresses σ_{xx} are found using the appropriate constitutive equation and the equilibrium equations

$$\int_0^d \sigma_{xx} dz = 0 \quad \text{and} \quad \int_0^d \sigma_{xx} z dz = 0 \,. \qquad (11\cdot7\cdot1)^+$$

Footnote +

These are equations 9·5·1 and 9·6·1 brought together for easy reference.

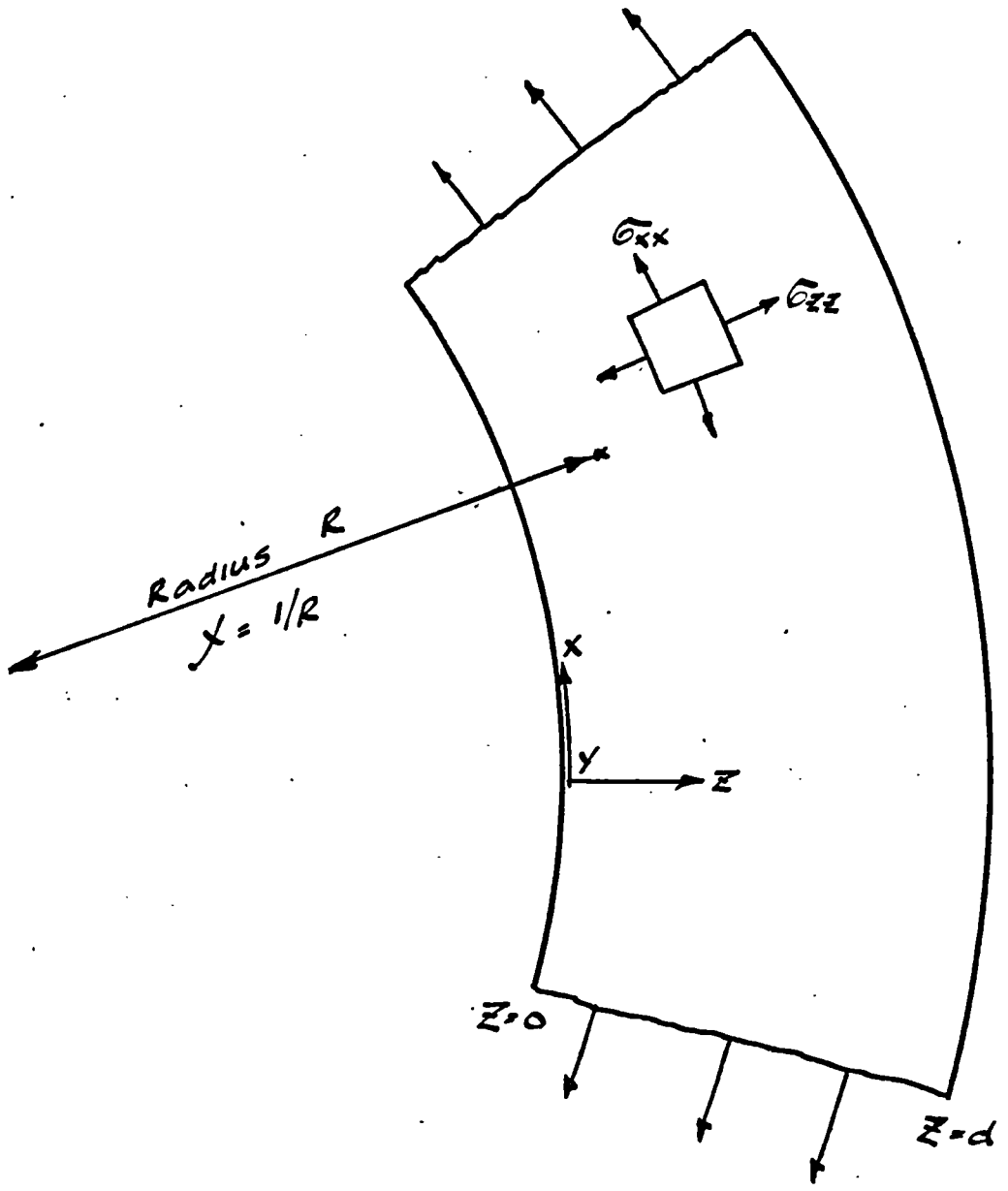


Figure 11-9 NOTATION USED IN CONSIDERING THE EFFECTS OF CURVATURE

Note

The analysis given in Section 11 is undertaken as though the panel was narrow so that only bending about the y axis need be considered. For a wide panel, the second term in equation 11·7·2 should be doubled.

If the curvature is significantly large, equilibrium in the radial direction must also be considered. Thus

$$\frac{d}{dz}\sigma_{zz} + \chi(\sigma_{zz} - \sigma_{xx}) = 0 \qquad (11\cdot7\cdot2)$$

where χ is the curvature and the slab is sufficiently then for the variation in χ, across the thickness, to be ignored. In most cases, χ is so small that the second term can be omitted so leading to the result that σ_{zz} is a constant, that must be zero in order to satisfy the boundary conditions. This may not necessarily be so with thin slabs and it is of interest to determine an approximate value for the radial stresses σ_{zz} introduced by curvature.

In attempting this approxiamate solution, we assume that the stresses σ_{xx} and σ_{yy} can be found satisfactorily by ignoring the effects of curvature. This means that equations 11·7·2 can be taken to be linear and so solved directly for σ_{zz}. This procedure is not entirely correct as this method of solution only allows the boundary conditions at one face of the slab to be satisfied exactly. However, it will be seen later that if a solution is obtained that gives $\sigma_{zz}=0$ at z=0 the corresponding stress at z=d is negligible and the solution may thus be considered to be satisfactory.

Integrating equation 11·7·2 and putting $\sigma_{zz}=0$ at z=0 gives the solution,

$$\sigma_{zz} = e^{-\chi z}\int_0^z e^{\chi z}\,\sigma_{xx}\,dz \qquad (11\cdot7\cdot3)$$

At z=d, the boundary conditions require that $\sigma_{zz} = 0$

which is not provided by equation 11·7·3. However, the expression for σ_{zz} at the unheated face can be expanded to give

$$(\sigma_{zz})_{z=d} = \chi e^{-\chi d}\left[\int_o^d \sigma_{xx}dz + \int_o^d \sigma_{xx}zdz + \int_o^d \sigma_{xx}\left(\frac{\chi^2 z^2}{2!} + \frac{\chi^3 z^3}{3!} + \cdots\right)dz\right]$$

in which the first two integrals are each zero from the conditions 11·7·1. Thus, the value of the stress normal to the boundary at z=d depends on terms involving the curvature raised to the power three, and higher, and so must be negligible in any practical situation.

This approximate analysis has been undertaken for a panel that is unrestrained at its ends and carries no end loading. With different boundary conditions, additional non-linear effects may become important and equation 11·7·3 is not then such a good approximation to the stress σ_{zz}. A routine to calculate equation 11·7·3 was written and included in the program SLOADED described in the previous chapter. For slabs that are unrestrained and without end load the stresses due to curvature are very small, as the stresses in the longitudinal direction are limited by extensive cracking very soon after the start of heating. In general, it is thought that the stresses normal to the heated face due to curvature will be very small and will play an insignificant part in cracking or local spalling.

11·8 Effect of local variations in the heating pattern

Consider a small spherical region of radius 'a' within a large mass of linear elastic material, of Young's modulus E and Poisson's ratio ν, that is heated so that the temperature T is given by

$$\begin{aligned} T &= T_o\,(1 - r/a) \qquad \text{for } r \leqslant a \\ T &= 0 \qquad\qquad\quad \text{for } r > a \end{aligned} \qquad (11\cdot8\cdot1)$$

It follows from the known results for a heated sphere (Timoshenko and Goodier 1951[b]) that the radial and tangential stresses (σ_r and σ_t) that correspond to these temperatures are :-

$$\left.\begin{aligned} \sigma_r &= -P\left(1 - \frac{3r}{4a}\right) \\ \sigma_t &= -P\left(1 - \frac{9r}{8a}\right) \end{aligned}\right\} \qquad (11\cdot8\cdot2^a)$$

in the region $r \leqslant a$ and

$$\left.\begin{aligned} \sigma_r &= -\frac{P}{4}\,(a/r)^3 \\ \sigma_t &= \frac{P}{8}\,(a/r)^3 \end{aligned}\right\} \qquad (11\cdot8\cdot2^b)$$

outside the heated region

where $P = \frac{2}{3}\,\frac{E\alpha T_o}{1-\nu}$ and α in the coefficient of linear thermal expansion for the material.

Suppose the material is now divided by a plane passing through the centre of the sphere (r=0). The region to one

side of this plane comprises a semi-infinite solid with a hemi-spherical thermal inclusion at the surface. This arrangement will be regarded as a reasonable idealisation of the situation that obtains during local heating at the surface of a large thick slab.

In deriving the solution for this case, it is noted that there is no normal stress at the surface. Thus, the stresses given by equations 11·8·2 must be modified by superposing the stress system produced by a normal surface traction equal to $-\sigma_r$, where σ_r is given by equation 11·8·2. This second stress system can be found by integrating solutions of the type obtained by Boussinesq[+] for the stresses due to a uniformly distributed load applied to a circular region at the surface of a semi-infinite solid. The result is most conveniently obtained by working with cylindrical polar co-ordinates r, z and θ, the stress system 11·8·2 being transformed to these co-ordinates before the complete solution is obtained by superposition.

Some results, obtained in this way, are shown in figure 11-10. These data refer to the stresses at points along a line normal to the surface and through the centre of the heated region (i.e. along the z axis). For the case considered, of

---

Footnote[+]

The solution is given in some detail by Timoshenko and Goodier (1951[a])

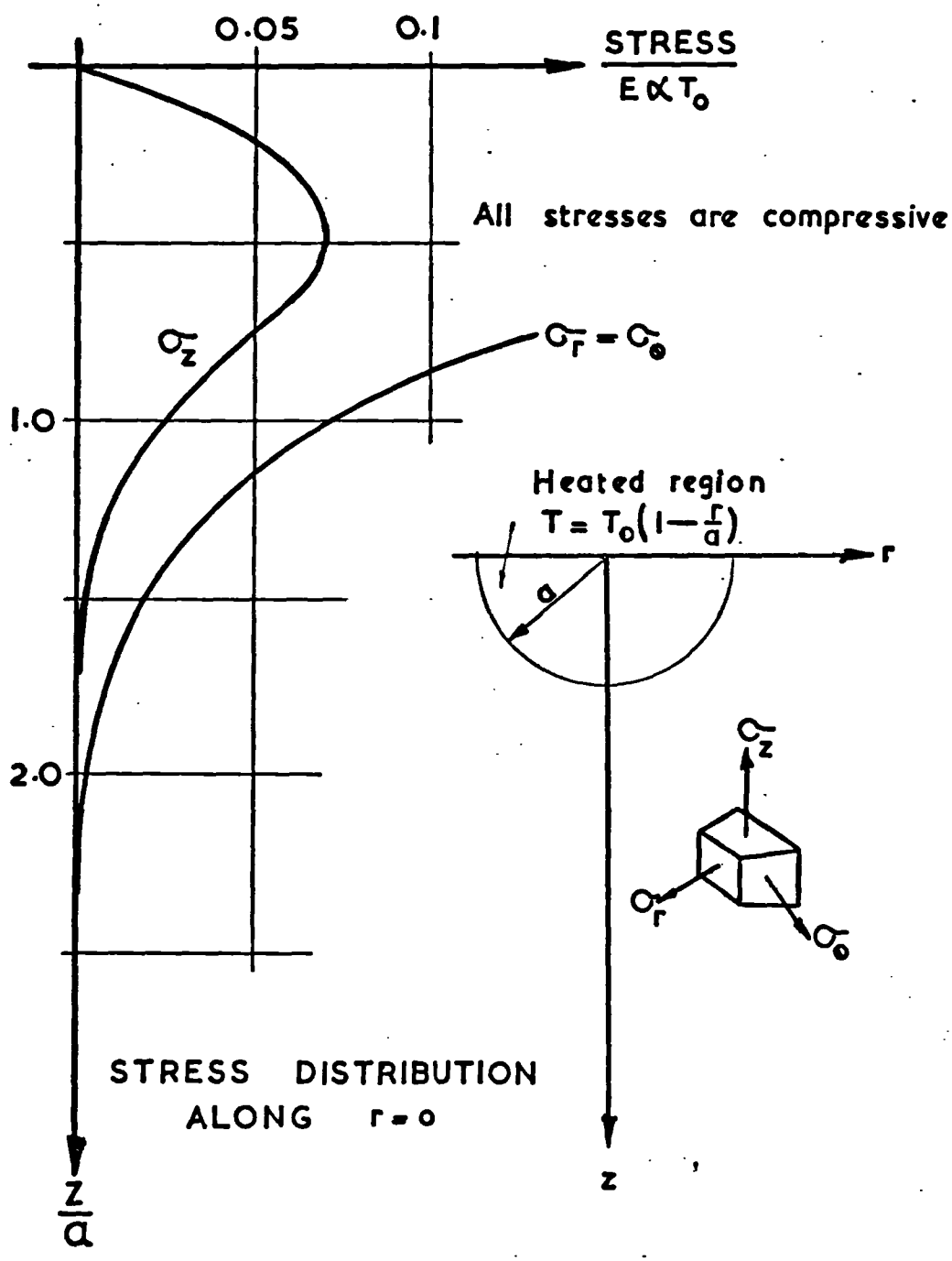


FIGURE 11-10
LOCAL STRESSES CAUSED BY
SURFACE HOT SPOT

local heating, the stress σ_{zz} is compressive and achieves a maximum value some distance below the heated surface. However, if the local temperature is below that of the remainder of the solid, σ_{zz} is tensile and there is the possibility of cleavage failure being initiated within the solid and parallel to the heated surface. This occurs in a similar manner to corner separation, the stress distributions controlling these two forms of breakdown being very much alike (ef. figures 11-10 and 11-8).

The analysis has been based on a convenient idealisation but it is thought that the same form of result would be obtained if the analysis were undertaken with a more representative type of thermal inclusion. There is some support for this view, as Sadowsky (1955) has idealised the present problem, by considering a thin circular disc of heated material embedded into the surface of the solid, and obtained results of the same general form as those shown in figure 11-10. Also, it is considered that the results obtained for the stresses normal to the heated surface are a reasonable indication of the distribution that would obtain when the local variation in temperature is combined with more uniform general heating. In this way, it is concluded that local cool spots in the overall heating pattern may lead to sub-surface cracking in directions parallel to the heated face. The effect of these cracks in relation to surface spalling is discussed in a later section.

11·9 Local effects due to the presence of reinforcement

If a reinforcing bar is surrounded by a mass of concrete, it is clear that thermal incompatibility can lead to cracking if there is a sufficiently large rise in temperature. With constant temperature throughout the assembly, the behaviour will depend on the relative values of the unrestrained thermal expansion of the steel and the concrete. If the concrete expands away from the steel, bond failure is likely to occur followed by separation at the bar surface. This may have serious consequences for the anchorage of the reinforcement but is not likely to cause local damage. On the other hand, if the coefficient of thermal expansion of the steel is greater than that of the concrete, tangential tensile stresses are induced in the concrete which could cause radial cracking.

The situation in a heated concrete member is usually more complicated than that described, as the reinforcing bars are often near the surface and in a region of high thermal gradient. The local stresses induced by a thermal gradient have been examined analytically by Dundurs and Zienkiewicz (1964) who considered a cylindrical inclusion in a large elastic solid within which the temperature gradient was constant. Based on assumed typical values for the material properties, this analysis provided the results shown in figure 11-11 for the special case of a steel bar in concrete. The other results shown in the figure are for the local stresses caused by a thermal gradient around a cavity.

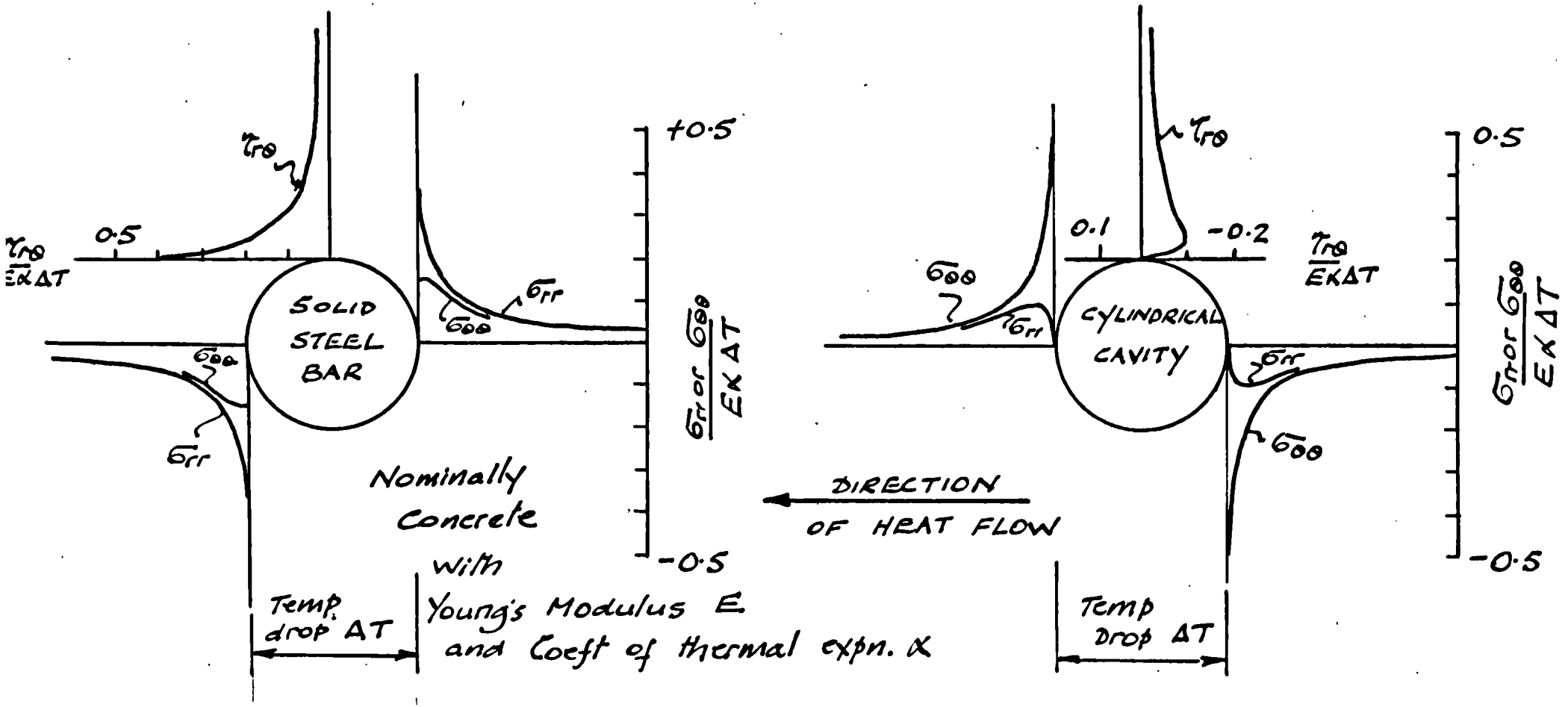


FIGURE II–11 STRESSES AROUND A SOLID INCLUSION AND A CYLINDRICAL CAVITY IN A REGION WITH A CONSTANT TEMPERATURE GRADIENT after DUNDURS & ZIENKIEWICZ (1964)

For the steel bar in concrete, the maximum tensile stress is in the radial direction at the hottest point of the interface and thus cracking may be initiated at this point in a direction parallel to the isothermal planes. The stresses are proportional to the temperature drop across the diameter of the bar so that cracking is most likely to occur with the larger diameter bars. Cracking may also be promoted by the presence of a cavity, but, in this case, the maximum tensile stress is in the tangential direction and occurs at the coolest point on the circumference so that the cracks would be expected to propagate in the direction of heat flow. However, the main conclusion to be borne in mind, in considering local spalling, is that the presence of reinforcing bars in a region of high temperature gradient can induce cracking in directions perpendicular to the direction of heat flow. It will be assumed that this conclusion remains valid even if the bars are comparatively near the surface of the concrete so that it appears that the presence of reinforcement promotes sub-surface cracking similar to that caused by local cool spots in the overall heating pattern.

11-10 Pore Pressure

In addition to the factors already mentioned, pore pressure within the capillaries of the concrete will induce tensile stresses within the material. At present, there is no comprehensive theory for the combined problem of heat transfer accompanied by moisture migration

and phase changes. However, various estimates have been made of the pressure developed in the pore structure of the concrete due to the formation of steam during heating.

The most straightforward approach is to assume that the pore pressure developed is equal to the presure of saturated steam at the vapourisation temperature. However, Shorter and Harmathy (1961) note that the temperature at which the steam is liberated must be considerably in excess of 100°C if the pressure is to be sufficient to fracture the concrete. This does not seem likely to occur in many practical situations, as the results from the tests described in Chapter 6. and also from Meyer Ottens (1965) experiments, suggest that, in fire tests, steam is generally formed at temperatures less than 150°C. It has already been noted (in Section 6·4 p 170) that the pressure of saturated steam at this temperature is only 0·38MN/m^2 above atmospheric, which can only be 15-20% of the tensile strength of concrete at normal temperatures.

A different approach was used by Waubke (1965 and 1966) who considered the drag forces opposing the movement of vapour in the capillary pores of a concrete. These forces induced tensile stresses in the concrete but again these are small; Waubke suggesting that they could be as high as 10% of the tensile strength of unheated concrete. Clearly stresses of this magnitude are not going to have a primary role in the occurrence of spalling. On the other hand, there is evidence that both fire resistance and the occurrence of spalling are affected by moisture content (Harmathy 1965, Gatenby 1961). Also, it is clear that there will be some

circumstances where the escape of vapour, liberated within the concrete during heating, is particularly restricted and high internal pressures will develop. One such situation follows from the moisture clog concept developed by Harmathy (1965) and described in Section 1·5 (page 17 et seq.)

If a wall panel is heated from one side, a zone saturated with liquid water is formed within the wall shortly after the start of heating. Steam is produced under pressure at the edge of this zone so that a 'clog' of water is pushed away from the heated face into the cooler regions of the slab. This is the most usual situation but in some cases thin slab-like members (the web of an I beam for example) are exposed to heating on both sides. Dougill (1969[b]) has suggested that this can lead to a dangerous situation in which spalling is likely to occur.

Figure 11-12 shows the form of the distribution of temperature and pore pressure that can be expected to exist, some time after the start of heating, in a slab exposed to heating on both sides. The saturated zones tend to migrate towards the centre and, in a thin slab, may coalesce to form a single saturated zone in the central region. When this occurs, the vapour produced by desorption at the interfaces between the dry and saturated zones can only escape towards the heated face and the pore pressure must increase rapidly with further increase in temperature.

Behaviour of this sort may have had some influence on the exposive failures that have been reported by Akhtaruzzaman and Sullivan (1970) following a series of

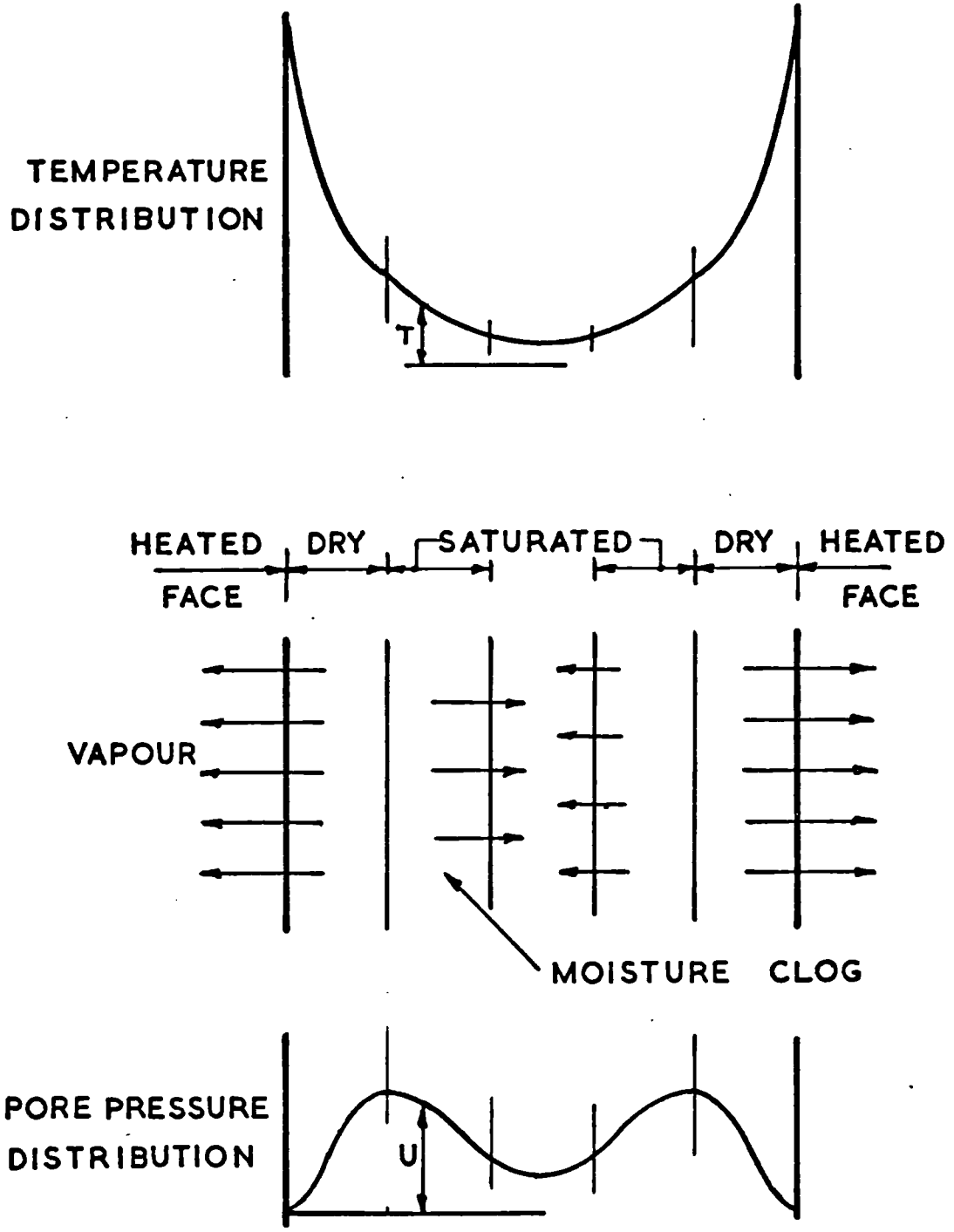


FIGURE 11—12

SLAB HEATED FROM BOTH SIDES

pilot tests in which a number of small concrete beams were heated at moderately fast rates in the electric furnace at Imperial College. The beams were 50x75x840mm long, made of ordinary Portland cement and Thames Valley aggregate with a 10mm (3/8 in) maximum sized aggregate. After making allowance for absorption of water by the aggregates during mixing, the effective water cement ratio was 0·58 and the specimens were either moist cured under hessian or wet cured under water for six days before testing at ages up to 28 days. The conditions causing explosive failure are outlined in Table 11·3. An interesting feature of these results is that there is apparently an upper age limit for each combination of curing and heating conditions above which explosive failures can not occur. It may well be worth investigating this further with more mature concretes and faster rates of heating.

Akhtaruzzaman and Sullivan measured the weight of the specimen and the concrete temperature during heating in each of their tests. As usually occurs, there was a halt in the rise in temperature within the specimen during the period when the free water was driven off. This occurred at a specimen temperature of between 100°C and 120°C depending on the curing conditions. A similar halt in the rise in temperature within the specimen occurred between 165°C and 198°C and it was in this temperature range that the explosive failures occurred. Akhtaruzzaman et al. assume this second pause in the temperature rise is caused by water being removed from the gel pores of the concrete structure. This explanation may not be complete, as the weight loss is

not confined to the periods when the temperature rise is halted and desorption of moisture must occur continuously during heating. Clearly there are other alternatives that need to be examined, including the possible occurrence of a solid phase transformation or vapourisation of the free water that has collected as a central moisture clog.

Table 11·3 Results from Akhtarzzaman and Sullivan (1970)

Heating Rate	Curing	Upper Age Limit days	Furnace temp. °C	Time to Failure mins.	Concrete temp. °C
H - H	w.c	28	380	31	In the range 165 to 198
	m.c	10	421	38	
H - L	w.c	10	390	45	
	m.c	3	378	42	
H - 0	w.c.	18	380	47	
	m.c.	5	378	46	

Irrespective of these considerations, the pressure of saturated steam in the temperature range 165°C to 198°C is around 0·6 to 1·4 MN/m^2 above atmospheric. This pressure may be enough to fracture a concrete only three days old

but is probably not enough, on its own, to produce failure in more mature concretes, even at temperatures as high as 200°C. This is the view taken by Akhtarzzaman and Sullivan, who concluded that the observed explosive failures were due to the combined effects of pore pressure and thermal gradient.

In Akhtarzzaman and Sullivan's tests, very small specimens were used and these were heated from all sides, so that there was little opportunity for dissipation of pore pressure This is an exceptional situation which is unlikely to arise in practice with members heated from one side only or with members of a reasonable size. Although it is accepted that the moisture conditions have a significant role in the occurrence of spalling, it is thought that the effects of pore pressure can not be assessed in isolation but must be considered together with the overall structural conditions. Thus, the problem is to determine the structural mechanism by which a modest pore pressure can cause local surface spalling.

11·11 Mechanism of Surface Spalling

Before heating, a slab or wall panel may already contain some shrinkage cracks orientated at right angles to the surface. These cracks can be expected to form a tesselated pattern with the crack spacing being somewhat greater than the maximum size of the aggregate used in the concrete. Also, shrinkage cracks of this sort will be closed by thermal expansion very soon after the start of heating.

With continued heating, it has been shown that both local

cool spots and the presence of reinforcement may cause cracking in planes parallel to the heated surface. These effects will be increased by high pore pressure within the concrete. There is also a tendency for cracks to form parallel to the heated face, when the concrete is strained beyond the discontinuity point or past the peak stress and into the decending region of the stress-strain curve. The extent of these cracks will depend on the condition of loading and restraint, for the peak stress can not be achieved if extensive cracking occurs to reduce the stiffness of the panel during the early stages of heating. Typically then, the conditions that obtain, in the region near to the heated face, during the period shortly after the start of heating are

a) the region is in a state of biaxial compression in the plane parallel to the heated surface. In addition there may be a small effective tensile stress in the direction normal to the heated surface.
b) The pre-existing shrinkage cracks have been closed by thermal expansion, and
c) there are a number of cracks of different sizes that have been formed in planes approximately parallel to the heated surface.

Considering this typical situation, two types of failure seem possible. In the first, Dougill (1964[a]), the material outside a crack becomes unstable under increasing thermal strain and end load, so causing blistering or breakdown of the surface. In the other, Dougill (1970), some of the

cracks become filled with vapour under sufficient pressure to punch out the pellet of material between the crack and the surface.

An example of blistering can be seen in figure 11-13, again taken after the fire in Rathbone Place. Here blistering is confined to a very thin surface layer and the photograph shows an area containing a broken blister and other regions where the surface layer is crimped due to high compression. It is interesting that a similar mechanism has been proposed by Uppal and Kemp (1971) to account for the form of local failure observed in compression tests on specimens containing a neck to give a longitudinal stress gradient. Again, but at a different dimensional level, there appear to be similarities between these forms of surface instability and the phenomenon of blow-ups in concrete road slabs. (Stott and Brook 1968)

In considering the other mechanism of surface spalling it is suggested that the process of cracking must produce a situation, such as that shown in figure 11-14, where the material between the heated surface and the crack may be regarded as a potential spall. Failure occurs when the forces due to the pore pressure on the spall is sufficient to overcome the shear resistance at the edges. Thus, for a circular spall of diameter D and depth S, failure occurs for

$$u \geqslant 4\left(\frac{S}{D}\right)\tau \qquad (11\cdot11\cdot1)$$

where τ is the maximum possible average shear stress that can be developed along the edge.



FIG. 11–13 SURFACE DAMAGE SHOWING BLISTERING, CRIMPING AND SOME AGGREGATE SPLITTING

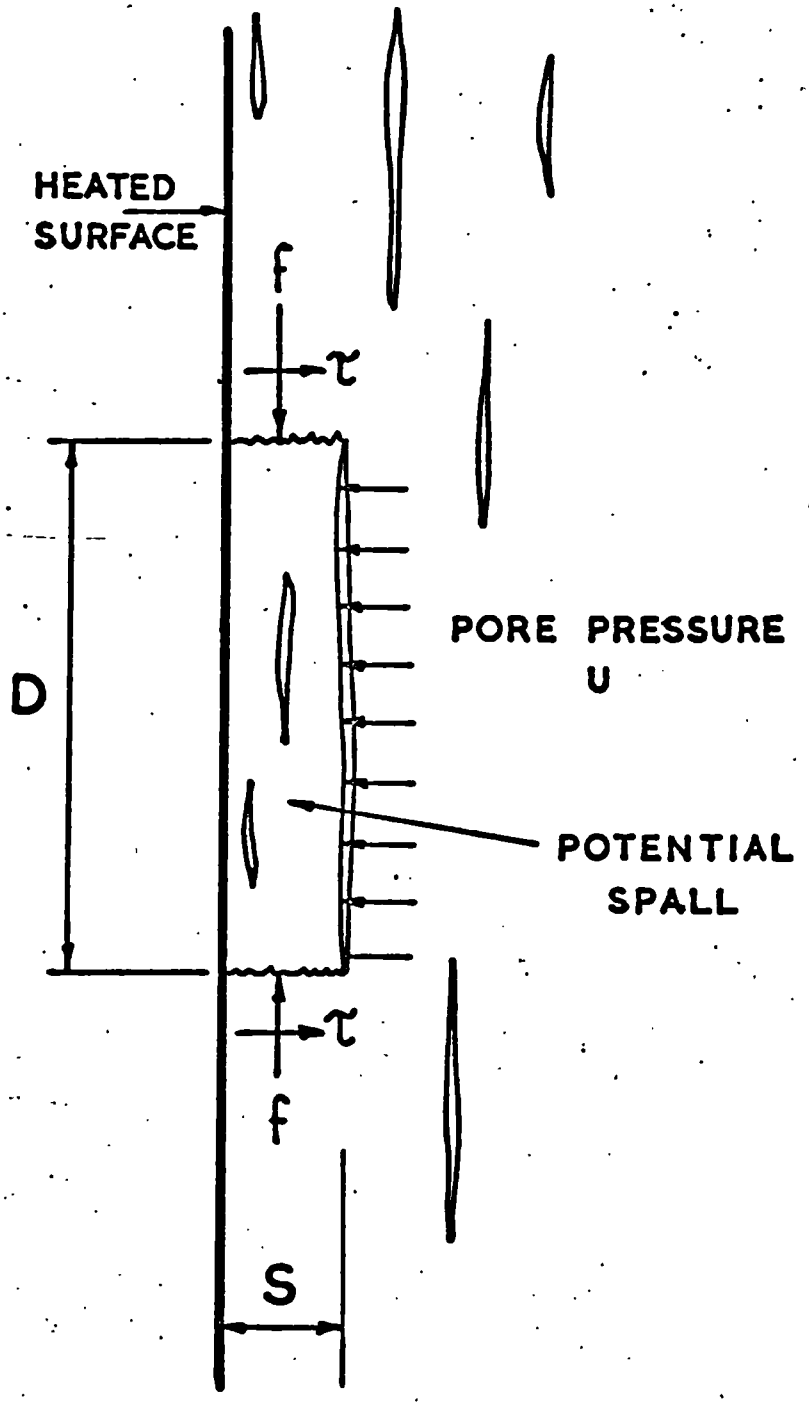


FIGURE II—14

STRESSES ACTING ON A POTENTIAL SPALL

Alexander has made an extensive study of the shear bond strength that exists between cement paste and steel, various aggregates and cement paste itself. His results (Alexander et al. 1965) show that the shear stress required to cause slip is due to adhesion and friction and that the total shear stress may be calculated from the Mohr-Coulomb theory,

$$\tau_s = c + f \tan \phi \qquad (11{\cdot}11{\cdot}2)$$

where c represents the contribution due to adhesion and ϕ is the angle of friction.

If the normal stress is low, the process of shear failure is one in which the adhesive bond is broken. Thus the shear stress required to propagate the failure decreases with continuing slip and finally attains a constant value less than that required to initiate the shear failure.

With higher values of the normal stress, junction formation will occur during slip to restore some of the adhesive bond. (see Bowden and Tabor 1954 and Alexander 1969) Here, higher values of shear stress are required to induce and propagate slip. Alexander has also shown that, if the normal stress is sufficiently high, the shear stress required to cause slip may increase above the initial value before decreasing to a constant value for large relative movements.

The important feature that is common to both these modes of behaviour is that there is a peak value of shear stress and that slip can continue under much reduced values of shear stress, once this maximum has been attained. Thus, if the spall shown in figure 11-14 were to be pushed out under a

constant pressure u, corresponding to that required to overcome the shear stress, an unstable situation would develop. Only part of the work done by the applied pressure would be required to propagate slip and most of the remainder would appear as the kinetic energy of the moving spall. Failure would be explosive.

This mechanism is slightly idealised as there may be a reduction in pore pressure during the expulsion of the spall which could stop the process prematurely. This stabilising effect would be opposed by reductions in the width of the loaded edge S and the normal stress f. Clearly the explosive nature of spalling will depend on which of these opposing effects is the more dominant. If the drop in pore pressure during slip is significant, movement of the spall may be intermittent with the pore pressure being repeatedly built up to induce successive increments of slip. Alternatively, with little drop in pore pressure or considerable reduction of the normal stress, explosive spalling will occur when the peak shear stress is first reached. It is considered that both these mechanisms are possible in concrete.

Equation 11·11·1 shows that the pore pressure required to cause spalling, to a depth S, is inversely proportional to the crack length D. The proposed mechanism requires the presence of these cracks and, if these are sufficiently long, only a modest pore pressure is required to initiate failure. The equation also suggests that this mode of failure is confined to the surface regions where both the pore pressure and the extent of cracking may be appreciable. Clearly,

this form of explosive spalling can be avoided by preventing the propagation of cracks or by allowing the pore pressure to be dissipated. Alternatively, the occurrence of explosive spalling is made more likely by fast rates of heating, which lead to higher pore pressures, or any action that promotes the formation of cracks within the material parallel to the heated surface.

11·12 Discussion

In this chapter the occurrence of aggregate splitting and corner failures have been examined and mechanisms have been proposed to account for the occurrence of surface failures.

The analysis of aggregate splitting is based on a very idealised model. However, the results appear to be reasonable and the conclusion that aggregate splitting can be alleviated, by reducing the maximum aggregate size in the concrete mix, is of practical importance.

Corner separation seems to be a mode of failure that is difficult to avoid in conventional reinforced concrete. One approach to this problem is to use an insulating surface layer to reduce the temperature rise in the concrete and so lessen the thermal stresses. Alternatively, a 'stronger' concrete with a better thermal stress resistance could be used. However, both these approaches have their disadvantages. The surface layer may itself be spalled away early during heating and the use of a stronger material may postpone local failure but make the occurrence more dangerous when it finally occurs. The ideal solution would be to provide the concrete with some ductility in tension so that the

thermal stresses may be accommodated without fracture. It is possible that this requirement may eventually be satisfied in practice by using steel or glass fibre reinforced cementitous materials for permanent shuttering to columns and beams.

The discussion of surface failures is, to some extent, speculative. The main uncertainty concerns the magnitude of the pore pressure developed in concrete during heating. This uncertainty will not be resolved until a comprehensive theory for combined heat and mass transfer is available or alternatively measurements are taken of the pore pressure and internal stress developed in concrete structures during fire tests.

In spite of the lack of background, the proposed mechanisms for surface spalling are of interest and appear to be possible in practice. In particular, the mechanism for explosive spalling suggests the way in which pore pressure can produce a violent failure from an otherwise stable situation. It seems likely that pore pressure could exacerbate corner separation in a similar way and may also lead to pop-out of isolated aggregate particles in the manner studied by Bache and Isen (1968).

Acknowledgement

The photographs of the fire damage at Rathbone Place were taken, at the author's direction, by Miss J.Gurr of Imperial College, London.

Chapter 12

DISCUSSION AND CONCLUSIONS

12·1 General Discussion

The work described in the previous chapters comprises an attempt to understand the effects of heating on the strength of concrete and concrete structures and, in particular, to explain the occurrence of spalling. In this, a broad treatment has been used and some aspects of the problem remain to be investigated in detail.

The conventional idea of strength is derived from materials testing, and strength is usually taken to correspond to the value of a particular stress or combination of stresses causing failure. This concept is useful, in comparing the properties of different materials under conditions of uniform stress, but can be misleading if the concept is extended to provide a criterion for failure of the material within a structure. With strain softening materials, the conditions corresponding to overall failure of a structure can not be recognised from the values of stress achieved at any particular point and the conventional idea of material strength is not relevant in analysis.

The classification of spalling given in Chapter 1 is an important component of the work. In particular, recognition that spalling could be a general structural failure,or alternatively localised within a member, suggested separate approaches to these problems. These provided an explanation of the mode of general spalling, based on the occurrence of instability due to strain softening, and mechanisms for the various forms of local spalling.

The review of structural behaviour given in Chapter 4 suggests that the effects of local spalling may not be

nearly so damaging in real structures as might appear from the results of fire tests. These arguments are based on the effects of continuity on the behaviour of reinforced concrete structures. Only behaviour in flexure was considered although it is realised that there may be some situations where the behaviour of continuous structures may be very much influenced by shear (Bobrowski 1969). However, it appears that in most practical cases of reinforced concrete beams and slabs the only additional requirement to ensure satisfactory performance in a fire is that the concrete in compression, in the vicinity of the supports, should remain intact.

The conclusion that reinforced concrete structures can sustain appreciable local damage, without the occurrence of collapse, is particularly important because some of the measures that could be adopted to prevent local spalling may themselves help to promote general failure. Thus, if reinforcement is used to hold the spalled material in position and if small sized aggregate is used to prevent splitting, the amount of local spalling may be reduced and the possibility of a catastrophic failure through instability is increased.

From the design point of view, it is clearly important to avoid general destructive spalling, as this can lead to the rapid spread of fire and possible collapse of a structure. Rather than risk this, it is better to accept the occurrence of a certain amount of local spalling and only provide protection where it is necessary for the survival of the structure. If this is done and the critical regions of a structure are protected, the occurrence of local

spalling could be beneficial in providing increased flexibility to accommodate the thermal strains. However, before this procedure can be adopted with confidence, more work is required to investigate the true mode of behaviour of continuous structures at high temperatures in order to recognise the critical regions. For the present, it is clear that the use of slender sections and situations involving high axial restraint should be avoided.

In concrete and reinforced concrete, micro-cracking and cracking serve as the means of redistributing stress under overload conditions. The idea, that the occurrence of local spalling may sometimes be beneficial in preventing a more serious mode of failure seems to be in line with this behaviour. In the previous Chapter, it was shown that cracking may be necessary to ensure the stability of some wall panels or floor slabs during heating. Clearly, if reinforcement is used to control the cracking, care must be taken to avoid stiffening the section unduly and so promoting overall failure.

A practical example of the benefits to be obtained from cracking is shown in figure 12-1. Here, two thin mortar slabs were heated using oxy-acetylene flames. The slabs were approximately 300mms in diameter and cast within a brass restraining ring. With one slab, the heating was concentrated in a small area near the centre and in the other the heating was more general. With localised heating, tangential tensile stresses develop in the cooler regions and these cause radial cracking as shown in the figure.

This appears to be beneficial, as heating was continued until the temperature within the hot spot exceeded 1250°C which was enough to cause vitrification of the heated material. With more general heating,a violent failure occurs of the form shown in the figure. Here the restraining ring prevents the development of tangential tensile stresses and the relief that could be afforded by cracking.

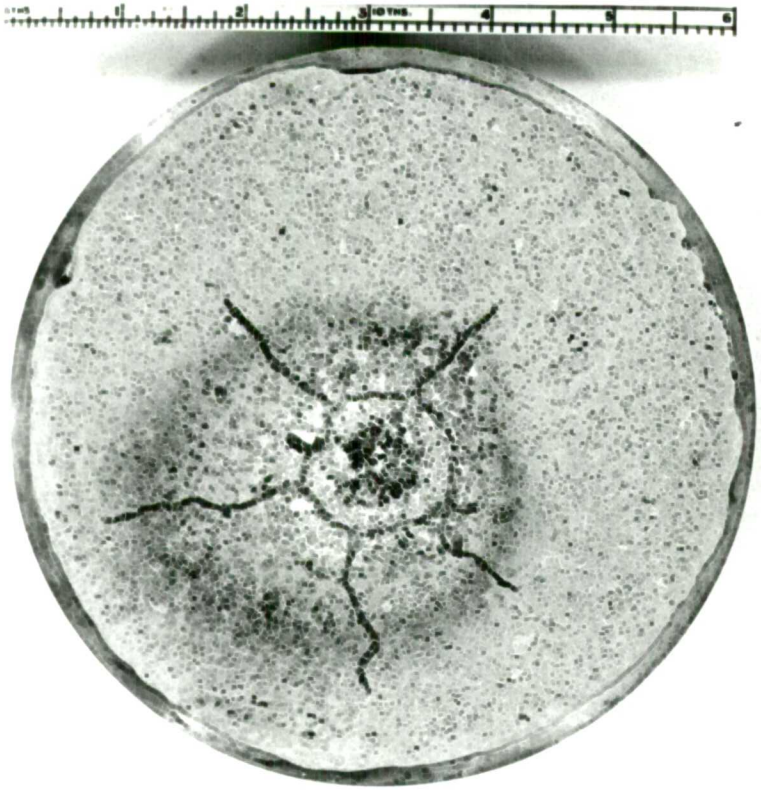
The test[+] illustrated in figure 12-1 should be regarded as a pilot test and, as yet, the mechanics of the failure process are not fully understood More work is being undertaken on this particular problem of local heating but again, it seems better to accept the occurrence of local damage rather than risk the stability of the structure in an attempt to minimise cracking. This conclusion seems to be of general application and should form part of a philosophy of design of structures for survival in a fire.

12·2 Conclusions

The principal conclusions relating to spalling are summarised in this Section under the following headings: Classification, Effect, Influences and Design Philosophy. Suggestions for further work are incorporated with the conclusions where these are appropriate.

Footnote[+]

This test was performed, as part of an undergraduate project undertaken at King's College London, by Mr M.L.French working under the direct supervision of the author. His help is gratefully acknowledged.



Local Heating



More General Heating

FIG. 12-1 DAMAGE IN SMALL RESTRAINED MORTAR SLABS HEATED TO HIGH TEMPERATURE

Classification (see Chapter 1)

1) Spalling may be general and completely destructive or essentially local in occurrence. This distinction is important in developing an understanding of the mechanisms of spalling and also in design.

2) The classification of spalling proposed in Table 1·3·1 on page 11 appears to be useful and it would be helpful if this terminology were adopted in describing phenomena observed in fire tests.

Effect (see Chapter 4)

3) The occurrence of local spalling in continuous structures does not generally have the same overwhelming influence on fire resistance that it does in fire tests on simply supported structures. It appears that the destructive effects of local spalling have been exaggerated in real structures and it is possible that, on occasions, the occurrence of local spalling may be beneficial.

4) The effects of general spalling are always undesirable. Elimination of a member may lead to complete structural collapse, in a progressive manner, or allow the fire to spread so increasing the danger and difficulty in dealing with the outbreak.

5) More experimental work is required to investigate the behaviour of continuous structures under fire conditions. Particularly necessary are studies on the behaviour of joints and on the effects of shear on modes of failure at high temperatures.

Influences

General Spalling (see Chapter 10)

6) General spalling occurs as a form of instability in the behaviour of a complete structural member. It is a form of compression failure that is a fundamental characteristic of strain softening materials. The use of materials with a steep descending branch to the stress-strain curve in compression is a principal cause of general spalling.

7) The occurrence of general spalling is affected by the size of the member and the conditions of loading and restraint. High axial loading or restraint can promote general spalling.

8) General spalling can not occur in large section members or under conditions where the section is restrained against rotation and expansion.

9) The presence of flexural restraint may induce compression failures in thin panels heated from one side. However if the section is maintained in compression by an applied load, or if the panel is sufficiently thick, the effect of flexural restraint is to increase the heating time required to cause collapse.

10) The presence of steam generated within the concrete may have some influence on the occurrence of general spalling through its effect on the shape of the stress-strain curve. This effect needs to be demonstrated experimentally.

11) Further studies are necessary to investigate the behaviour of concrete under conditions of changing stress and temperature. In addition, the present analytical work needs extending so that the effects of reinforcement, on the occurrence of general spalling, can be examined.

Modes of Local Spalling (See Chapter 11)

12) Aggregate splitting is most likely to occur under conditions of fast heating and when large size aggregates are used in a strong stiff matrix.

13) Corner Separation occurs as a cleavage fracture in which external corners of beams or columns are removed, sometimes violently. In practice, it seems necessary to allow for the probable occurrence of corner separation in all members made of normal density concrete.

14) The conditions for the occurrence of surface failures require that tensile stresses are developed in a direction normal to the heated face or planar cracks are formed parallel to the heated face.

15) It seems that surface failures could occur in either of the following ways

a) The material outside a crack becomes unstable under increasing thermal strain and end load so causing blistering or breakdown of the surface

or b) Some of the cracks become filled with vapour under sufficient pressure to punch out the material between the crack and the surface.

16) The presence of high axial load or restraint, reinforcement or cool spots in the general heating pattern may assist in the development of the conditions required for surface spalling by inducing planar cracks, parallel to the heated surface.

17) In addition to the modes of behaviour already outlined, violent surface failure may occur in concrete if the pressure of steam generated within the pores approaches the tensile strength of the material. This seems unlikely to occur in most practical situations but more work is required to study the development of pore pressures in concrete heated rapidly to high temperatures.

Design (see Chapter 12)

18) In designing structures to resist the effects of fire, the primary objective should be to avoid general spalling and the collapse of a member.

19) Avoidance of general spalling may imply acceptance of local damage in the form of spalling or cracking.

20) More work, of the type mentioned in paragraph 5.is necessary in order to appreciate where protection against spalling is necessary for satisfactory structural performance.

REFERENCES

In addition to the usual abbreviations used in referring to the names of well known Journals, the following descriptions are used to refer to the Proceedings of four recent Conferences.

Braunschweig Symposium: Fire resistance of prestressed concrete. Proceedings of a Symposium held at Braunschweig, Germany in June 1965. Bauverlag GmbH 1966

London Conference: The Structure of Concrete and its behaviour under Load: Proceedings of an International Conference, London. Sept. 1965, Cement and Concrete Association 1968.

Pressure Vessel Conference: Proceedings of a Conference on Prestressed Concrete Pressure Vessels. London, March 1967, The Institution of Civil Engineers, London 1968.

Southampton Conference: International Conference on Structure, Solid Mechanics and Engineering Design in Civil Engineering Materials. Southampton University, April 1969. Proceedings to be published, J.Wiley.

Papers. by the present author, marked + in the list of references are included with the Subsidiary Material.

Abrams M.S. (1968) Compressive strength of concrete at temperatures to 1600°F. Paper presented at the A.C.I. Symposium on the 'Effect of Temperature on Concrete' Fall Meeting 1968 Later published in A.C.I. SP-25 1970.

Abrams M.S. and Gustaferro A.H. (1968) Fire endurance of Concrete Slabs as influenced by Thickness, Aggregate Type and Moisture. Journal of the P.C.A. R. and D. Labs. Vol.10 No.2 pp.9-24.

Akhtaruzzaman A.A. and Sullivan P.J.E. (1970) Explosive spalling of concrete exposed to high temperature. Concrete Structures and Technology Report CSTR 70/2 Imperial College, Civil Eng. Dept. pp.24.

Alexander K.M., Wardlaw J. and Gilbert D.J. (1965) Aggregate-cement bond, cement paste strength and the strength of concrete. London Conference 1965 pp.59-81.

Alexander K.M. and Wardlaw J. (1965) Discussion of the paper by Taylor and Broms (1964) Proc. A.C.I. Vol.62 No.3 pp 1705-1710.

Alexander K.M. (1969) The mechanism of shear failure at the steel-cement and aggregate-cement interface. Paper 32 Southampton Conference 1969.

Anson M. (1964) An investigation into a hypothetical deformatio and failure mechanism for concrete. M.C.R. Vol.16 No.47 pp.73-82.

Anson M. and Newman K. (1966) The effect of mix proportions and method of testing on Poisson's ratio for mortars and concretes. M.C.R. Vol.18 No.56 pp.115-130.

Ashton L.A. (1951) The Fire Resistance of Prestressed Concrete Floors. Civ. Eng'g and P.Wks. Rev. Vol.46 pp.843-845 and 940-943.

Ashton L.A. (1965) Effects of restraint of longitudinal deformation or rotation. Braunschweig Symposium pp 15-19.

Ashton L.A. and Bate S.C.C. (1961) Reply to contribution to the discussion of their own paper Proc. I.C.E. Vol.20 pp.305-320.

Bache H.H. and Isen J.C.(1968) Modal determination of concrete Resistance to Popout Formation. Proc. A.C.I. Vol.65 No.6 pp.445-450.

Baker A.L.L. (1956) The Ultimate load Theory Applied to the design of reinforced and prestressed concrete frames. Concrete Publications Ltd., 1956.

Baker A.L.L. (1959) An analysis of deformation and failure characteristics of concrete. M.C.R. Vol.11 No.33 pp.119-128.

Baker A.L.L. (1970) A criterion of concrete failure. Proc. I.C.E. Vol.47 pp.285-295.

Baldwin R. and North M.A. (1969) Stress-strain curves of concrete at high temperature - a review Fire Research Note No.785, J.F.R.O. Fire Research Station Boreham Wood pp.12.

Bannister J. (1968) Steel reinforcement and tendons for structural concrete Part 1: Steel for reinforced concrete. Concrete Vol.2 No.7 pp.295-306.

Barends J.F.B. (1965) Abplatzungen und plotzlicher Bruch Braunschweig Symposium p.58.

Bauschinger J. (1885) Mitt. Mech. Tech. Lab. D.K. Tech. Hochschule, Munchen, Vol.12 (1885) Vol15(1887) Reported by Singleton-Green (1923).

Birch F. and Clark H. (1940) Thermal conductivity of rocks and its dependence on temperature and composition. Am.Journal of Science Vol.238 pp.529 and 613.

Blakey F.A. and Beresford F.D. (1962) Discussion of a paper by Kaplan (1961) Proc. A.C.I. Vol.58 pp.919-923.

Bletzacker R.W. (1966) Effect of Structural Restraint on the Fire Resistance of Protected Steel Beam Floor and Roof Assemblies. Building Research Lab. Final Report EES 246/266 Engineering Experiment Station Ohio State University, Columbus. Ohio.

Blyth F.G.H. (1960) Geology for Engineers 4th Edition, Arnold Ch.3. Rock forming minerials p.59-85.

Bobrowski J. and Bardhan-Roy B.K. (1969) A method of calculating the Ultimate Strength of reinforced and prestressed concrete beams in combined flexure and shear. The Structural Engineer Vol.47 No.5 pp.197-209.

Bonnell D.G.R. and Harper F.C. (1951) The thermal expansion of concrete. National Building Studies Technical Paper No.7 H.M.S.O.

Bowden F.P. and Tabor D. (1950) The Friction and Lubrication of Solids Clarenden Press Oxford.

Brace W.F. (1969) Micromechanics in Rock Systems Paper 18 Southampton Conference.

Brebbia C.A. and Frederick C.O. (1969) A Failure Surface for Concrete C.E.R.L. Laboratory Note RD/L/N9/69

Bresler B. and Pister K.S. (1956) Strength of concrete under combined stress. Structures and Material Research Division of Civil Eng., Report Series 100 Issue 1 Institute of Engineering Research, University of California Berkeley Nov.1956.

Bresler B. and Pister K.S. (1957) Failure of plain concrete under combined stresses. Trans. A.S.C.E. Vol.122 pp.1049-1059.

Bresler B. and Selna L. (1964) Analysis of time dependent behaviour of reinforced concrete structures. Symposium on creep A.C.I. Special Publication SP9, 1964 pp.115-128.

Brown C.B. (1965) Minimum volume to ensure homogeneity in certain conglomerates. Journal of the Franklin Institute Vol.279 No.3 pp.189-199.

Browne R.D. (1967) Properties of concrete in reactor vessels. Pressure Vessel Conference pp.131-151.

Butcher E.G.,Chitty T.B. and Ashton L.A. (1966) The temperature attained by steel in building fires. Min. of Technology and Fire Officers' Cttee Joint Fire Research Organisation London H.M.S.O. pp.V1,37.

Campbell-Allen D and Desai P.M. (1967) The influence of aggregate on the behaviour of concrete at elevated temperatures. Nuclear Eng. and Design Vol.6 pp.65-77.

Campbell-Allen D.,Low E.W.E. and Roper H. (1965) An investigation on the effect of elevated temperatures on concrete for reactor vessls. Nuclear Structural Engineering Vol.2 pp.382-388.

Campbell-Allen D and Thorne C.P. (1963) The thermal conductivity of concrete M.C.R. Vol.15 No.43 pp.39-48.

Carlson C.C. and Abrams M.S. (1965) Discussion of a paper by T.Z.Harmathy A.S.T.M. Special Publication No.385 pp.94-95

Carlson C.C. and Gustaferro A.H. (1965) A review of studies of the effects of restraint on the fire resistance of prestressed concrete. Braunschweig Symposium pp.32-42 also available as P.C.A. R.and D. Lab. Bulletin 206.

Carlson C.C., Selvaggio S.L. and Gustaferro A.H. (1965) A review of studies of the effect of restraint on the Fire Resistance of Prestressed Concrete P.C.A. R. and D. Labs Bulletin 206.

Carlson R.W. (1937) A simple method for the computation of temperatures in concrete structures. Proc. A.C.I. Vol.34 p.89-102

Carslaw H.S. and Jaeger J.C. (1947[a]) Conduction of heat in solids Chapter 1 General Theory pp.1-32 Oxford.

Carslaw H.S. and Jaeger J.C. (1947[b]) Locus cit Article 31 Problems of Melting and solidification pp.71-74.

Chinn J. and Zimmermann R. (1965) Behaviour of plain concrete under various high triaxial compression loading conditions. U.S. Air Force Weapons Lab. Tech. Rep. WL-TR 64-163

Clough R.W. (1965) The Finite Element Method in structural mechanics Ch.7 in Stress Analysis ed O.C.Zienkiewicz and G.S.Holister Wiley 1965 pp.85-119.

Corson R.H. (1965) The effect of elevated temperatures on the strength of steel reinforcement for concrete Building Research Station Internal Note IN 110/65 from the Structural Engineering Division.

Cowan H.J. (1952) Strength of Concrete under the action of Combined Stresses and the representation of the criterion of Failure by a Space Model Nature Vol.169 p.663.

Cowan H.J. (1953) The strength of plain, reinforced and prestressed concrete under the action of combined stresses M.C.R. Vol.5 No.14 pp.75-86.

Crank J. and Nicolson P. (1947) A practical method for numerical evaluation of solutions of partial differential equations of the heat conduction type Proc. Camb. Phil. Soc. Vol.43 pp.50-67.

Crank J. (1956) The mathematics of Diffusion Oxford ppVl 347.

Crook D.N. and Murray M.J. (1970) Regain of strength after firing of concrete M.C.R. Vol.22 No.72 pp.149-154.

Crowley M.S. (1956) Initial thermal expansion characteristics of insulating refactory concretes. Bulletin of the Am. Ceramic Soc. Vol.35 No.12 Dec.1956 pp.465-468.

Cruz C.R. (1962) An optical method for determining the elastic constants of concrete. Journal P.C.A. R.and D. Labs. Vol.4 No.2 pp.24-32 P.C.A. Research Bulletin No.144.

Cruz C.R. (1966) Elastic properties of concrete at high temperature Journal of the P.C.A. R. and D. Labs Vol.8 No.1 pp.37-45.

Cruz C.R. (1968) Apparatus for measuring creep of concrete at high temperatures. Journal P.C.A. R. and D. Labs Vol.10 No.3 pp.36-42.

Dantu P. (1958) Study of the stresses in heterogeneous materials Application to concrete, Annales de l'Institut Technique du Bâtiment et des Travaux Publics Vol.11 Serie Essais et Mesures (40) No.121 pp.55-77.

Davies J.D. (1968) A modified splitting test for concrete specimens M.C.R. Vol.20 No.64 pp.183-186.

Davies J.D. and Nath P. (1967) Complete Load-Deformation curves for plain concrete beams Building Science Vol.2 No.3 pp.215-221.

Davis H.S. (1967) Effects of High Temperature Exposure on Concrete Materials Research and Standards Vol.7 No.10 pp.452-459.

Dixon J.R. and Pook L.P. (1969) Stress Intensity Factors calculated generally by the Finite Element Technique Nature Vol.224 No.5215 pp.166-167 Oct.11th 1969.

Dougill J.W. (1960) An investigation into the residual compressive strength of concrete after exposure to high temperatures Thesis presented to the University of London for the degree of M.Sc.(Eng).

+ Dougill J.W. (1961) The effects of thermal incompatibility and shrinkage on the strength of concrete. M.C.R. Vol.13 No.39 pp.119-124.

Dougill J.W. (1962) Contribution to a paper by Hirsch (1962) Proc A.C.I. Vol.59 No.9 pp.1363-1365.

Dougill J.W. (1964[a]) Contribution to the Discussion of a paper by H.L.Malhotra and R.F.Stevens (1964) Proc I.C.E. Vol.29 pp.451-2.

Dougill J.W. (1964[b]) A Thermal stress resistance factor for aggregate splitting in concrete exposed to fire. Unpublished note, circulated to the Fire Research Station, England.

+ Dougill J.W. (1965) Some effects of thermal volume changes on the properties and behaviour of concrete. London Conference pp.499-513.

+ Dougill J.W. (1966) The relevance of the established method of structural fire testing to reinforced concrete. Applied Materials Research Vol.5 No.4 Oct 1966 pp.235-240.

+ Dougill J.W. (1967) A mathematical model for the failure of cement paste and mortars. M.C.R. Vol.19 No.60 pp.135-142.

+ Dougill J.W. (1969[a]) An approximate assessment of the effects of heterogeneity on the strength and mode of failure of concrete systems. Southampton Conference to be published.

Dougill J.W. (1969[b]) Some Aspects of Spalling of Concrete Caused by Exposure to High Temperatures. Report submitted to the Fire Research Station.

Dougill J.W. (1970[a]) Discussion of a paper by Issen et al (1970) Fire Test Performance A.S.T.M. STP 464 pp.180-182.

+ Dougill J.W. (1970) Some results for the average stresses induced in the principal components of concrete M.C.R. Vol.22 No.72 pp.133-142.

+ Dougill J.W. (1971) Further consideration of a mathematical model for progressive fracture of a heterogeneous material. M.C.R. Vol.23 No.74 pp.5-10.

Dundurs J. and Zienkiewicz O.C. (1964) Stresses around circular inclusions due to thermal gradients with particular reference to reinforced concrete. Proc. A.C.I. Vol.61 No.12 pp.1523-32.

Dusinberre G.M. (1945) Numerical Methods for Transient Heat Flow Trans A.S.M.E. Vol.67 pp.703-712.

Dusinberre G.M. (1961) Heat Transfer Calculations by Finite Differences International Texbook Co (Pennsylvania)

Ehm H. and von Postel R. (1965) Versuche an stahlbetonkonstruktionen mit Durch-laufwirkung unter Feuerangriff. Braunschweig Symposium pp.24-31.

Endell K. (1929) Versuche uber Langen-und Gefugeanderungen von Betonzuschlagstoffen und Zementmorteln unter Einwirkung von Temperaturen bis 1200°C Deutscher Ausschuss Fur Stahlbeton Heft 60.

England G.L. and Ross A.D. (1962) Reinforced concrete under thermal gradients. M.C.R. Vol.14 No.40 pp.5-12.

Evans R.H. and Marathe M.S. (1967) Stress concentration in prestressed concrete. Paper 47 Pressure Vessel Conference 1968. pp.549 - 553.

Fenner C.N. (1913) The stability relations of the silica minerals Am. Journal of Science 4th Series Vol.36 No.214 p.331.

Fischer R. (1970) Über das Verhalten von Zementmortel und Beton bei hoheren Temperaturen Deutscher Ausschuss Fur Stahlbeton Heft 214 Berlin 1970 pp.60-128 Some of this work is described by Weigler (1970))

Fishenden M. and Saunders O.A. (1932) The calculation of heat transmission H.M.S.O. London pp.Xll 280.

Fourier J.B.J. (1822) Theorie analytique de la chaleur Paris 1822 (comprising some of his papers since 1807) English translation by Freeman, Cambridge 1878 and reprinted by Dover publications 1955 pp.XXlll, 466.

Freudenthal A.M. (1950[a]) The inelastic behaviour of engineering materials and structures pp.527 et seq Ch.18 Significance of Mechanical Testing J.Wiley 1950.

Freudenthal A.M. (1950[b]) Locus cit Ch.11 Article 55, Theories of Brittle Fracture pp.357-368.

Furumura F. (1966[a]) The Stress Strain Curve of Concrete at High Temperature No.1 Report for meeting of Architectural Institute of Japan Fire Research Station Reference Library No.D17CTF67/23.

Furumura F. (1966[b]) Testing Equipment for Compressive Strain of Concrete at High Temperature Report for meeting of Architectural Institute of Japan Fire Research Station Reference Library

Furumura F. (1966[c]) The Stress strain curve of concrete at high temperatures Report for meeting of Architectural Institute of Japan. Fire Research Station Reference Library No. CIB/CTF67/23(J)

Furumura F. (1970) Strength and Elasticities of Concretes at Elevated Temperatures. Part lV of Harada et al (1970)

Gatenby D.C. (1961) Contribution to the discussion of a paper by L.A.Ashton and S.C.C.Bate. I.C.E. Proc. Vol.20 pp.315-316.

Gautschi W. (1964) Error function and Fresnel Integrals Ch.7 of Handbook of Mathematical Functions Edited by M.Abromowitz and I.A.Stegun New York Dover 1965 pp.297-309 Previously published by the National Bureau of Standards 1964.

Giles R.T. (1939) What heat will concrete withstand without deterioration Proc A.C.I. Vol.35 p.417.

Glucklich J. (1963) Fracture of Plain Concrete. Proc of the A.S.C.E. Vol.89 No.EM6 pp.127-138 Dec. 1963.

Glucklich J. (1965) Static and Fatigue Fractures of Portland Cement Mortar in Flexure. Paper C19 Proc. of the First International Conference on Fracture Vol.3 pp.1343-1382 Japanese Soc. for Strength and Fracture of Materials 1966.

Glucklich J. (1967) Long term compressive strength of concrete Proc. Pressure Vessel Conference Group C Paper 18 pp.193-198.

Glucklich J. and Cohen L.J. (1967) Size as a factor in the Brittle-Ductile Transition and the strength of some Materials. International Journal of Fracture Mechanics Vol.3 No.4 pp.278-289.

Green J.K. and Long W.B. (1971) Gunite Repairs to fire-damaged concrete structures Concrete Vol.5 No.4 pp.118-122 see also pp.115-117 report of a meeting on The reinstatement of concrete construction after a fire. arranged by the Concrete Society Working Party on Fire Resistance Oct. 1970.

Griffith A.A. (1920) The phenomena of rupture and flow in solids Phil. Trans. Roy. Soc. London A221 pp.163-198.

Grimer F.J. and Hewitt R.E. (1969) The Form of the Stress-Strain curve of concrete interpreted with a diphase concept of material behaviour Paper 63 Southampton Conference

Grün R. and Beckman H. (1930) The behaviour of cement, aggregates and concrete at high temperatures. Cement and Cement Manufacture Vol.3 No.3 March 1930 pp.430-442.

Grünberg G. (1925) Uber die in einer isotropen Kugel durch ungleichforige Erwarmung erregten Spannungszustande. Z. Physik Vol.35 p.548.

Gustaferro A.H. (1970) Temperature criteria at failure A.S.T.M. Special Publication S.T.P.464 Fire Test Performance A.S.T.M. 1970 pp.68-84.

Gustaferro A.H. and Selvaggio S.L. (1967) Fire Endurance of Simply supported Prestressed concrete slabs. Journal of the Prestressed Concrete Institute Vol.12 No.1 pp.37-53 Also available as P.C.A. R. and D. Lab. Bulletin No.212.

Hamilton S.B. (1956) A note on the History of Reinforced Concrete in Buildings National Building Studies Special Report No.24 H.M.S.O. 1956 pp.30.

Hannant D.J. (1967) Strain behaviour of concrete up to 95°C under compressive stresses. Proc. Pressure Vessels Conference Group C Paper 17 pp.177-191.

Hannant D.J. and Frederick C.O. (1968) Failure criteria for concrete in compression. M.C.R. Vol.20 No.64 pp.137-144.

Hansen T.C. (1958) Creep of Concrete- a discussion of some fundamental problems. Bulletin No.33 Swedish Cement and Concrete Research Institute pp.1-48.

Harada T. (1953[a]) Thermal expansion of Concrete at high Temperatures. Trans. A.I.J. No.46 pp.1-10.

Harada T. (1953[b]) Variation of strength and elasticity of concrete under high temperature Part 1 Concrete strength at 28 days. Trans. A.I.J. No.47 pp.11-18.

Harada T. (1954[a]) Variation of strength and elasticity of concrete under high temperatures, Part 11 Tensile strength and Elasticity of Concrete at age of 28 days. Trans. A.I.J. No.48 pp.1-9.

Harada T. (1954[b]) The change in Thermal conductivity of cement mortar and concrete at high temperature. Trans A.I.J. No.49 pp.1-8.

Harada T. (1957) Variation of strength and elasticity of concrete under high temperatures Part 111 Natural recovery of strength and Elasticity. Trans A.I.J. No.56 pp.1-7

Harada T. (1958) Variation in Thermal diffusivity of cement-mortar and concrete at high temperatures. Trans A.I.J. No.58 pp.7-13.

Harada T.,Migita K.,Shiire T. and Shiina K. (c.1960) The thermal stress of reinforced concrete frame at fire of the Yokohana Bridge Stone tyre Company. Undated paper accompanying Harada (1966).

Harada T. (1966) Personal Communication which included a copy of the booklet Thermal expansion of concrete at high temperatures and a note Thermal character of concrete both in English but undated.

Harada T.,Takeda J.,Yamane S. and Furumura F. (1970) Strength, elasticity and thermal properties of concrete subjected to elevated temperatures. A group of five papers presented at the A.C.I. Seminar on Concrete for Nuclear Reactors West Berlin, Oct. 1970.

Harmathy T.Z. (1961) A Treatise on theoretical fire endurance rating A.S.T.M. Special Technical Publication No.301 pp.10-40 Research Paper No.153 Divn of Building Research N.R.C. of Canada April 1962.

Harmathy T.Z. (1965) Effect of moisture on the fire endurance of building elements A.S.T.M. Special Technical Publ'n 385 pp.74-94 Research Paper No.270 Divn of Building Research National Research Council of Canada Aug. 1965.

Harmathy T.Z. and Berndt J.E. (1966) Hydrated Portland Cement and Lightweight concrete at elevated temperatures. Proc. A.C.I. Vol.63 pp.93-112.

Hast N. (1945) Measuring stresses and deformations in solid materials Ingeniorsvetenskapsakademienshandlingar Nr 178 Roy. Swedish Inst for Eng. Research, Stockholm pp.164.

Hayden H.W.,Moffatt W.G. and Wulff J. (1965) Fracture - Ch.7 The Structure and Properties of Materials Vol.111 Mechanical Behavior John Wiley pp.143-167.

Helmuth R.A. (1961) Dimensional changes of hardened Portland Cement pastes caused by temperature changes. Proc. Highway Research Board Vol.40 1961 pp.315-336.

Hill A.W. (1965) The Fire Resistance of Prestressed Concrete Members. Also, Final comments on the Discussion Braunschweig Symposium pp.7-11 and p.155.

Hirano M. (1927) Effects of Temperature and Humidity on the Properties of Cement and Mixture. Memoirs of the College of Engineering Kyoto Imperial University Vol.1V No.5 p.261.

Hirsch T.J. (1962) Modulus of elasticity of concrete affected by elastic moduli of cement paste matrix and aggregate. Journal A.C.I. Proc. Vol.59 No.3 pp.427-452.

Hognestad E.,Hansen N.W. and McHenry D. (1955) Concrete stress Distribution in Ultimate Strength Design. Proc. A.C.I. Vol.52 No.4 Dec.1955 pp.455-480.

Howie T.W. (1945) Spalling of Silica Bricks. Trans. of the British Ceramic Soc. Vol.45 pp.45-61.

Hoyle R. (1954) The thermal diffusivity of hardened cement paste. M.C.R. Vol.6 No.16 pp.33-36.

Hsu T.T.C. (1963) Mathematical analysis of shrinkage stresses in a model of hardened concrete. Proc. A.C.I. Vol.60 pp.371 -390.

Hsu T.C.,Slate F.O.,Sturman G.M. and Winter G. (1963) Microcracking of plain concrete and the shape of the stress -strain curve. Proc. A.C.I. Vol.60 No.2 pp.209-224.

Hughes B.P. and Chapman G.P. (1966) The Complete stress-strain curve for concrete in direct tension. RILEM Bulletin No.30 (New Series) pp.95-97.

Hughes B.P. and Chapman G.P. (1966) The deformation of concrete and micro-concrete in compression and tension with particular reference to aggregate size. M.C.R. Vol.17 No.54 pp.19-24.

Hughes B.P. and Ash J.E. (1968) Short term loading and deformatio of concrete in uniaxial tension and pure torsion. M.C.R. Vol.20 No.64 pp.145-154.

Hull W.A. (1920) The behaviour of R.C. columns under fire test. Concrete and Constructional Eng. Vol.15 p.187 and 262 A fuller account of this work is given in Proc.A.C.I. Vol. 16 p.20.

Ingberg S.H.,Griffin H.K.,Robinson W.C. and Wilson R.E. (1921) Fire Tests of building columns. U.S. Dept. of Commerce, Bureau of Standards Technologic Paper No.184 Washington 1921.

Ingberg S.H. (1929) Influence of mineral composition of aggregates on the fire resistance of concrete. Proc. A.S.T.M. Vol.29 Part 2 p.824.

Irwin G.R. (1948) Fracture Dynamics. Fracturing of metals. Cleveland, Am.Society for Metals. pp.147-166.

Irwin G.R. and Kies J.A. (1952) Fracturing and Fracture Dynamics. Welding Journal Vol.31 pp.95-105.

Issen L.A. Gustaferro A.H. and Carlson C.C. (1970) Fire Tests of Concrete Members: An improved method for estimating thermal restraint forces. A.S.T.M. Special Publication S.T.P. 464 Fire Test Performance A.S.T.M. 1970 pp.153-185.

Jaeger J.C. (1950) Conduction of Heat in a Solid with a Power Law of Heat Transfer at its surface. Proc. Camb. Phil. Soc. Vol.46 pp.634-641.

Jakob M. (1949[a]) Heat Transfer, Volume 1 Ch.6 Thermal Conductivity. Sections 6-7 and 6-8 pp.91-98 John Wiley New York pp.XXX, 758.

Jakob M. (1949[b]) Locus cit. Ch.25, Section 25-2 Free Convection on Vertical and Horizontal surfaces. pp.526-534.

Johns D.J. (1965) Thermal Stress Analysis. Table A.3 p.189 Pergamon Press.

Johnson R.P. and Low P.G. (1969) Behaviour of concrete under biaxial and triaxial stress. Paper presented to The Southampton Conference 1969 To be published.

Jones R. (1952) A method of studying the formation of cracks in a material subjected to stress. British Journal of Applied Physics. Vol.3 No.7 pp.229-232.

Kaplan M.F. (1961) Crack propagation and the fracture of concrete. Proc.A.C.I. Vol.58 No.5 pp.591-610.

Kaplan M.F. (1965) The application of fracture mechanics to concrete. London Conference pp.169-175.

Kingery W.D. (1955) Factors affecting the Thermal Stress Resistance of Ceramic Materials. Journal of the Am. Ceramic Soc. Vol.38 No.1 pp.3-15.

Kordina K. (1965) Der Einflub von Abplatzungen, Schutzschichten und des Spannsystems auf die Feurerwiderstandsdauer. and final discussion on spalling. Braunschweig Symposium pp.51-56 and p.111.

Kordina K. (1966) Report of the F.I.P. Commission on Fire Resistance of Prestressed Concrete - Chairman K.Kordina Proc. of the Fifth Congress of F.I.P. Paris 1966, C.A.C.A. 1967 pp.61-66.

Kupfer H.,Hilsdorf H.K. and Rusch H. (1969) Behaviour of concrete under biaxial stresses. Proc. A.C.I. Vol.66 pp.656-666.

Lawson D.I. and McGuire J.H. (1953) The solution of transient heat flow problems by analogous electrical networks. Proc. Inst. Mech. Eng. Vol.A167 p.275.

Lea F.C. (1920) The effect of temperature on some of the properties of materials. Engineering Vol.110 No.2852 pp.293-298.

Lea F.C. and Stradling R.E. (1922) The resistance to fire of concrete and reinforced concrete. Engineering Vol.114 No.2959 pp.341-344 and No.2960 pp.380-382.

Lees C.H. (1922) Thermal stresses in solid and hollow circular cylinders concentrically heated. Proc. Roy. Soc. Series A Vol.101 pp.411-430.

Lerch W. (1957) Thermal coefficient of expansion of concrete aggregates. A.S.T.M. Bulletin No.219 p.36.

Lewis D.J. and Carmichael D.G.T. (1969) A Multiaxial Failure Diagram for concrete. C.E.G.B. R. and D. Dept. Note RD/B/N1355.

Liebenberg A.C. (1962) A stress-strain function for concrete subjected to short term loading. M.C.R. Vol.14 No.41 pp.85-90.

Lott J.L. and Kesler C.E. (1964) Crack propagation in plain concrete. University of Illinois T. and A.M. Report No.648 Urbana 1964.

Loudon A.G. and Stacy E.F. (1965) The thermal and acoustic properties of lightweight concretes. Ministry of Technology Building Research Station Note EN75/65

Malhotra H.L. (1956) The effect of temperature on the compressive strength of concrete. M.C.R. Vol.8 No.23 pp.85-94.

Malhotra H.L. and Stevens R.F. (1964) Fire resistance of encased steel stanchions. Proc. I.C.E. Vol.27 pp.77-98.

Malhotra H.L. and Rogowski B.F.W. (1967) Fire-resistance of laminated Timber Columns. Paper 3 pp.17-49 J.F.R.O. Symposium No.3 Fire and structural use of timber in buildings. H.M.S.O. 1970.

Marechal J.C. (1970) Thermal conductivity and thermal expansion coefficients of concrete as a function of temperature and humidity. Paper presented at the A.C.I. Seminar Concrete for Nuclear Reactors. Berlin Oct. 1970 to be published.

McClintock F.A. (1968) A criterion for ductile fracture by growth of holes. Journal of Applied Mechanics. Vol.35 Series E pp.363-371.

McCreath D.R.,Newman J.B. and Newman K. (1969) The influence of aggregate particles on the local strain distribution and fracture mechanism of cement paste during drying shrinkage and loading to failure. RILEM- Materials and Structures Vol.2 No.7 pp.73-84.

McFarland J. (1906) Tests of the Effects of Heat on Reinforced Concrete Columns. Engineering News Vol.56 p.316

Mendelson A. (1968) Plasticity: Theory and Application. Macmillan 1968 Ch.9 The method of successive elastic solutions pp.164-212.

Meyer-Ottens C. (1965) Abplatzungversuche. Braunschweig Symposium pp.59-66.

Miller A.L. and Faulkner A.F. (1927) A comparison of the effect of high temperatures on the concrete of High Aluminium and Ordinary Portland Cement. Bulletin No.43 University of Washington Experimental Stn.

Mills R.H. (1969) Collapse of Structure and Creep in Concrete. Paper presented to the Southampton Conference.

Mitchell L.J. (1953) Thermal expansion tests on aggregates, neat cements and concretes. Proc. A.S.T.M. Vol.53 p.963.

Murrell S.A.F. (1964) The Theory of the Propagation of elliptical Griffith cracks under various conditions of plane strain or plane stress. British Journal of Applied Physics. Vol.15 pp.1195-1223.

Nekrassow K.D. (1961) Hitzebestandiger Beton. Bauverlag Wiesbaden Berlin 1961.

Neville A.M. (1956) The influence of size of concrete test cubes on mean strength and standard deviation. M.C.R. Vol.8 No.23 pp.101-110.

Neville A.M. (1959) Some Aspects of the Strength of Concrete. Civil Engineering and Public Works Review. Vol.54 No.639 pp.1153-1156, No.640 pp.1308-1310 and No.641 pp.1435-1439.

Neville A.M. (1963) Properties of Concrete. Ch.1, Portland Cement: section on Structure of hydrated cement pp.22-32. Sir Isaac Pitman and Sons Ltd.,London pp.Xl 532.

Neville A.M. (1964) Creep of concrete as a function of its cement paste content. M.C.R. Vol.16 No.46 pp.21-30.

Newman K. (1964) The structure and engineering properties of concrete. in J.R.Rydzewski (Ed) Theory of Arch Dams Pergamon 1965 pp.683-712.

Newman K. and La chance L. (1964) The testing of brittle materials under uniform uniaxial compressive stress. Proc. A.S.T.M. pp.1044-1067. Vol. 64.

Newman K. and Newman J.B. (1969) Failure Theories and Design Criteria for Plain Concrete. Paper presented to the Southampton Conference. To be published.

Nielsen K.E.C. (1954) Effect of various factors on the flexural strength of concrete test beams. M.C.R. Vol.5 No.15 pp.105 -114.

Nielsen K.E.C. (1957) Internal Stresses in Concrete. Paper presented at the RILEM Symposium at Munich. RILEM Bulletin No.1 new Series 1959.

Norton C.L. (1913) Some thermal properties of concrete. Journal of the A.S.M.E. Vol.35 Part 1 pp.1011-1021.

Norton F.H. (1931) Refractories. Ch.12 Spalling 1st Edition McGraw Hill pp.339-368.

Orowan E. (1948) Fracture and strength of solids. Report in Progress in Physics Vol.12 1948-49 pp.185-232.

Philleo R.E. (1958) Some physical properties of concrete at high temperatures. Proc. A.C.I. Vol.54 pp.857-864.

Philleo R.E. (1967) Introductory remarks to a discussion on 'Thermal and Freezing - Thawing Behaviour' Conference on the Matrix of Concrete, Allerton Park, Illinois. T. and A.M. Report No.313 University of Illinois, Urbana. Illinois 1968.

Pickett G. (1956) Effect of Aggregate on Shrinkage of Concrete and a Hypothesis concerning Shrinkage. Proc. A.C.I. Vol.52 No.5 pp.581-590.

Polivka M.,Pirtz D. and Capanoglu C. (1967) Influence of rate of loading on strength and elastic properties of Structural Lightweight Concretes. Proc. R.I.L.E.M. Symposium on Lightweight Aggregate Concretes. Budapest pp.649-666.

Prager W. and Hodge P.G. (1951) Theory of Perfectly Plastic Solids. John Wiley.

Protze H.G. (1957) Structural Refractory Concrete. Proc. A.C.I. Vol.53 p.871.

Reinius E. (1955) A theory of the deformation and failure of concrete. Betong No.1 pp.15-43. C.A.C.A. Lib. Trans. Cj 63 pp.31.

Richart F.E.,Brandtzaeg A. and Brown R.L. (1928) A study of the failure of concrete under combined compressive stress. University of Illinois Engineering Experimental Station. Bulletin No.185 pp.102.

Richart F.E.,Brandtzaeg A.and Brown R.L. (1929) The failure of plain and spirally reinforced concrete in compression. University of Illinois Engineering Experimental Station. Bulletin No.190.

Robertson A.F. and Genensky S.M. (1956) Theoretical heat transfer scaling relationships for fire endurance of reinforced concrete. Nat. Bureau of Standards Report 4854 (not published)

Robertson A.F. and Gross D. (1958) An electrical analogue method for transient heat flow analysis. Journal of Research Nat.Bureau of Standards Vol.61 p.105.

Robinson G.S. (1965) The influence of micro-cracking and state of stress on the elastic behaviour and discontinuity of concrete. J.R.Rydzewski (Ed) Theory of Arch Dams 1965 Pergamon pp.713-721.

Robinson G.S. (1967) Behaviour of concrete in biaxial compression. Journal of the Structural Divn. Proc. A.S.C.E. Vol.93 No.ST1 pp.71-86.

Rockenhauser W. (1968) Structural Design Criteria for Primary Containment Structures. Lecture 5. Prestressed Concrete Nuclear Reactor Structures. Engineering Extension Course. The College of Engineering, University of California at Berkeley. March 1968.

Romualdi J.P. and Batson G.B. (1963) Mechanics of crack arrest in concrete. Proc. A.S.C.E. Vol.89 No.EM3 pp.147-168.

Ross A.D. and Bray J.W. (1949) The prediction of temperature in mass concrete by numerical computation. M.C.R. Vol.1 No.1 pp.9-20.

Ruettgers A.,Vidal E.N. and Wing S.P. (1935) An investigation of the Permeability of Mass Concrete with Particular Reference to Boulder Dam. Proc.A.C.I. Vol.31 pp.382-416. Discussion, Vol.32 (1936) pp.378-389.

Rusch H. (1959) Physical problems in the testing of concrete. Zement -Kalk-Gips Vol.12 pp.1-9.

Rusch H. (1960) Researches towards a general flexural theory for structural concrete. Proc. A.C.I. Vol.57 pp.1-28.

Sadowsky M.A. (1955) Thermal Shock on a Circular Surface of Exposure of an Elastic Half Space. Journal of Applied Mechanics Vol.22 pp.177-182.

Saemann J.C. and Washa G.W. (1957) Variations of Mortar and Concrete Properties with temperature. Proc. A.C.I. Vol.54 p.385.

Saito H. (1965) Explosive spalling of prestressed concrete in fire. Japanese Government, Ministry of Construction, Building Research Institute Occasional Report No.22 pp.18 reprinted in the Braunschweig Symposium pp.80-91.

Sanderson-Watts (1969) Concrete framed buildings: fire damage, repair and reconstruction. Lecture to the N.W.Region Concrete Society, Liverpool Sept. 1969

Schmidt E. (1924) On the application of the calculus of finite differences to technical heating and cooling problems in Festschrift zum siebzigsten Geburtstag, August Foepps J.Springer Berlin p.179 Reference form Jakob (1949)

Schumann H. (1965) Petrographische Untersuchungen von Abplatzungen an Zementkorpern Spezieller Herkunft. Braunschweig Symposium pp.92-93.

Sell R. (1958) Investigation into the strength of concrete under sustained load. R.I.L.E.M. Colloquium on The influence of time upon the strength and deformation of concrete. Munich 1958 R.I.L.E.M. Bulletin New Series No.4 1959 pp.5-17.

Selvaggio S.L. and Carlson C.C. (1963) Effect of restraint on the fire resistance of prestressed concrete. A.S.T.M. Symposium on Fire Test Methods S.T.P. No.344 pp.1-25 Also available as P.C.A. R.and D. Bulletin 164.

Selvaggio S.L. and Carlson C.C. (1966) Restraint in Fire Tests of Concrete Floors and Roofs. A.S.T.M. Symposium on Fire Test Methods- Restraint and Smoke 1966 STP 422 pp.21-39 (1967) A.S.T.M. Also available as P.C.A. R. and D. Lab. Bulletin No.220.

Shah S.P. and Winter G. (1966) Inelastic Behaviour and Fracture of Concrete. Proc. A.C.I. Vol.63. No.9 pp.925-930.

Shorter G.W. and Harmathy T.Z. (1961) Contribution to the Discussion of a paper by L.A.Ashton and S.C.C.Bate Proc. I.C.E. Vol.20 pp.313-315.

Sigvaldason O.T. (1964) The influence of the testing machine on the compressive strength of concrete. Symposium on Concrete Quality Nov. 1964. C.A.C.A.

Singleton-Green J. (1923) Reinforced Concrete and Fire Resistance. Part V. Concrete and Constructional Eng'g Vol.18 p.75.

Sinha B.P.,Gerstle K.H. and Tulin L.G. (1964) Stress strain relations for concrete under cyclic loading. Proc. A.C.I. Vol.61 No.2 pp.195-211.

Skempton A.W. (1960) Effective stress in soils, concrete and rocks. Proc. of a Conference on Pore Pressure and Suction in soils. Butterworth 1961 pp.4-16.

Slate F.O. and Olsefski S. (1963) X-rays for study of internal structure and micro-cracking of concrete. Proc. A.C.I. Vol.60 No.5 pp.575-588.

Smith G.M. and Young L.E. (1956) Ultimate flexural analysis based on stress strain curves of cylinders. Proc. A.C.I. Vol.53 No.6 pp.597-610.

Stott J.P. and Brook K.M. (1968) Report on a visit to U.S.A. to study blow-ups in concrete roads. Road Research Lab. Report LR 128 R.R. Lab. Ministry of Transport.

Stradling R.E. (1920) The resistance to fire of concrete and reinforced concrete. Ph.D. Thesis University of Birmingham.

Stradling R.E. and Brady F.L. (1927) Fire Resistant Construction Building Research Special Report No.8 London H.M.S.O. pp.57.

Sullivan P.J. and Poucher M.P. (1968) The Influence of Temperature on the Physical Properties of Concrete and Mortar in the range 20°C to 400°C. Paper presented at the A.C.I. Symposium on the Effect of Temperature on Concrete. Fall Meeting 1968 Later published in A.C.I. SP-25 pp.103-135.

Sullivan P.J.E. (1970) The structural behaviour of concrete at elevated temperature. Ph.D. Thesis University of London.

Tan C.P. (1968) Prestressed concrete in nuclear pressure vessels. A critical review of current literature. Prepared by the Franklin Institute Research Labs. under contract 2721 for the Oak Ridge National Lab. Ref. ORNL-4227 pp.409.

Taylor M.A. (1970) Ph.D.Thesis Div'n S.E.S.M. University of California at Berkeley.

Taylor M.A. and Broms B.B. (1964) Shear bond strength between coarse aggregate and cement paste or mortar. Proc. A.C.I. Vol.61 pp.939-956.

Timoshenko S. and Goodier J.N. (1951[a]) Theory of Elasticity 2nd Edition McGraw Hill Ch.13 Axially Symmetrical Stress Distribution in a Solid of Revolution pp.343-398.

Timoshenko S. and Goodier J.N. (1951[b]) ibid ch.14 Thermal Stress pp.399-437.

Thomas F.G. and Webster C.T. (1953) Investigations on Building Fires Part Vl. National Building Studies Research Paper No.18 H.M.S.O. London pp.80.

Tomita H. and Taylor D.D. (1961) Effect of aggregate size on thermal shock resistance. U.S. Naval Civil Eng. Lab. Technical Report R-170 Port Hueme Cal.

Tucker J. (1941) Statistical Theory of the effect of dimensions and of method of loading upon the modulus of rupture of beams. Proc. A.S.T.M. Vol.41 pp.1072-1088.

U.S.Bureau of Reclamation (1940) Thermal Properties of Concrete. Final Reports Boulder Canyon Project Part Vll Cement and Concrete Investigation Bulletin 1 U.S.B.R. 1940 pp.154.

Uppal J.Y. and Kemp K.O. (1971) The effect of longitudinal gradients of compressive stress upon the failure of concrete. M.C.R. Vol.23 No.74 pp.11-22.

Vile G.W.D. (1965) The strength of concrete under short term static biaxial stress. Proc. of the London Conference pp.275-288.

Watkeys D.G. (1955) Non destructive testing of concrete subject to fire attack. M.Sc. (Eng) Thesis University of London.

Waubke N.V. (1965) Uber den Einflub von Wasserdampf auf die inneren Spannungen von Beton im Feuer. Braunschweig Symposium pp.94 and 95.

Waubke N.V. (1966) Transportphanomene in Betonporen. Heft 6 Institut fur Baustoffkunde und Stahlbetonbau der Technischen Hochschule Braunschweig pp.76.

Wawersik W.R. (1968) Detailed analysis of rock failure in laboratory compression tests. A Thesis submitted to the Faculty of the Graduate School of the University of Minnesota in partial fulfillment of the requirements for the degree of Ph.D. pp.165 and Appendix.

Weibull W. (1939) A statistical theory for the strength of materials. Ingeniorsvetenskapsakademien. Handlingar 1939 Vol.146-153 No.151 pp.45.

Weigler H. (1970) Influence of high temperatures on strength and deformation of concrete. Paper presented at the A.C.I. Seminar on Concrete for Nuclear Reactors. W.Berlin.

Weigler H. and Fischer R. (1964) Verhalten von Beton bei hohen Temperaturen. Deutscher Ausschuss fur Stahlbeton. Heft 164 Berlin 1964 pp.1-18 (some of this work is described by Weigler (1970))

Welch G.B. and Haisman B. (1968) The Application of Fracture Mechanics to Concrete. UNICIV Report Nol 12 pp.15+ 2 University of New South Wales.

Welch G.B. and Haisman B. (1969) Fracture Toughness Measurements of Concrete. UNICIV Report No R.42 pp.17+13 University of New South Wales.

Wells A.A. (1966) The application of fracture mechanics to yielding materials. Proc. Roy. Soc. Series A Vol.285 pp.34-45.

Wells A.A. (1967) Fracture in Engineering Design. Strength of Materials. Taylor and Francis 1968 pp.75-87 Reprinted from Contempory Physics Vol.8 1967.

Wells A.A. (1969) Failure Theories and Design Criteria in Polycrystalline Systems. Paper 77 Southampton Conference.

White J. (1958) Some general considerations on thermal shock, Trans. of the British Ceramic Soc. Vol.57 pp.591-616.

Whitney C.S. (1943) in discussion of a paper by V.P.Jensen Proc. A.C.I. Vol.39 pp.584-2-6.

Williams M.L. (1969) The continuum Interpretation for Fracture and Adhesion. Journal of Applied Polymer Science Vol.13 pp.29-40.

Williamson E.D. and Adams L.H. (1919) Temperature Distribution in Solids during heating and cooling. Physical Review Vol.14 p.19.

Woolson I.H. (1905) Investigation of the effect of heat on the crushing strength and the elastic properties of concrete. Proc. A.S.T.M. Vol.5 p.335.

Woolson I.H. (1907) Investigation of the Thermal Conductivity of Different Concrete Mixtures and the effect of heat upon the strength and elastic properties. Proc. A.S.T.M. Vol.7 p.404.

Wright P.J.F. and Garwood F. (1952) The effect of method of test on the flexural strength of concrete. M.C.R. Vol.4 No.11 pp.67-76.

Wright W. and Byrne J.G. (1964) Stress concentration in concrete. Nature Vol.203 No.4952 pp.1374-1375.

Zoldners N.G. (1960) Effect of high temperatures on concretes incorporating different aggregates. Proc,A.S.T.M. Vol.60 pp.1087-1108.

Zoldners N.G.,Malhotra V.M. and Wilson H.S. (1963) High temperature behaviour of aluminous cement concrete containing different aggregates. Proc. A.S.T.M. vol.63

Zoldners N.G. and Malhotra V.M. (1964) Discussion of the paper by Campbell-Allen and Thorne. Campbell-Allen and Thorne (1963) M.C.R. Vol.16 No.49 pp.233-234.

Addenda

Klein A.,Pirtz D.,and Adams R.F. (1962) Thermal Properties of Mass Concrete during adiabatic curing. Paper 10 A.C.I. Symposium on Mass Concrete, Denver. A.C.I. Special Pub'n SP-6, 1963 pp.199-218.

Newman K. (1964[a]) Concrete control tests as a measure of the properties of concrete. Symposium on Concrete Quality C.A.C.A.

SUBSIDIARY MATERIAL

Besides the seven papers already noted in the list of references, the subsidiary material also includes the paper 'An experiment to determine the elastic constants of a transversely isotropic material.' Bulletin of Mechanical Engineering Education, Vol.6 1967 pp.325-331.

UDC 620.192 : 536.49

The effects of thermal incompatibility and shrinkage on the strength of concrete

by J. W. Dougill, M.Sc.(Eng.), D.I.C.

UNIVERSITY OF LONDON: KING'S COLLEGE*

SUMMARY

The effect of shrinkage of the mortar on the strength of a concrete specimen is demonstrated by means of a lattice analogy for concrete. The strains due to the thermal incomptability of the cement paste and the aggregate in a concrete heated to high temperatures are taken as a particular example and it is shown that the results deduced from the lattice agree closely with those obtained experimentally by other workers.

The limitations of the lattice approach are discussed: it is emphasized that the method is qualitative and that any extension to give quantitative results would be most unlikely to be successful.

Introduction

Since the earliest days of reinforced concrete construction, many workers have studied the effect of high temperatures on concrete with particular reference to fire resistance. However, in spite of this research, the manner in which heat affects the strength of concrete has not yet been fully explained.

Lea and Stradling[1] considered that the deterioration of concrete on heating is due to the thermal incompatibility of the cement paste and the aggregate, and to the decomposition of the calcium hydroxide in the hardened cement paste. They tried to estimate the magnitude of the stresses developed in a piece of concrete from the first of these causes, by examining analytically the effect of heating a single spherical sand grain surrounded by a shell of cement paste. The cement paste and the aggregate inclusion were assumed to behave elastically and the stresses in the shell were found by considering the tendency for the cement paste to shrink with respect to the aggregate.

Although this approach does not give any indication of the distribution of the internal stresses set up in a specimen and is based on a number of gross simplifying assumptions, it seems that the basic argument is correct and that the change in strength of a mature concrete on heating is partly determined by the stresses caused by the differing thermal movements of the cement paste and the aggregate. These internal stresses (referred to later as parasitic thermal stresses) act as a prestressing system which modifies the load that the concrete specimen can carry.

Besides being subject to the effects of thermal incompatibility, the strength of concrete is affected by the chemical changes that take place in the cement paste and the aggregate. Many workers (following Lea and Stradling) have suggested that the reaction having the greatest effect on strength is that in which the calcium hydroxide in the cement paste is decomposed. This reaction does not normally occur below 500°C and it may be assumed that chemical effects are of secondary significance below this temperature.

Another cause contributing to variations in strength on heating to high temperatures is the sudden expansion accompanying the α to β quartz transformation when a siliceous aggregate is used. This occurs at about 575°C, however, and it can therefore be assumed that any variations in the strength of a mature concrete heated to temperatures below 500°C must be principally caused by the occurrence of stresses due to thermal incompatibility.

As it is particularly difficult to measure the magnitude and distribution of stresses in concrete, an investigation of the occurrence and effect of parasitic thermal stresses must be primarily analytical, the results of such an analysis being later confirmed by the " circumstantial evidence " of experimental results.

*Mr Dougill is now a Research Assistant in the Concrete Structures and Technology Section of the Civil Engineering Department at the Imperial College of Science and Technology, University of London.

A formal analysis using the usual methods of elasticity and taking into account the heterogeneous nature of the concrete would be laborious and of little value, until the mechanism of failure of concrete is fully understood. Thus a simplified approach is required.

The lattice analogy

Recently Baker[2] suggested that the structure of a well compacted concrete could be represented by means of a pin-jointed frame made up of separate elements representing the aggregate thrusts and the bonding action of the mortar. This concept of an analogous lattice is based on the hypothesis that load is transmitted through a concrete specimen by the interaction of the aggregate particles and by direct thrust in the mortar between them. The aggregate thrusts form a " thrust ring " which is stabilized by tension developed in the mortar. The action of the lattice is shown diagrammatically in Figure 1 in which the inclined members represent the aggregate thrusts and the horizontal and vertical members the mortar bonds. In his original presentation, Baker gives expressions from which the relative stiffnesses of members and the form of the lattice can be chosen so that the deformation characteristics of a particular concrete are simulated.

A piece of concrete is represented by a large number of these elements joined together to form a lattice as seen in Figure 2. The normal criterion for failure under load is the development of excessive tension in any one of the mortar bonds. On the basis of this criterion, the cleavage planes and crack patterns at failure in compression tests, with and without end restraint, have been predicted satisfactorily. However, it is possible that, in some circumstances, other types of failure may occur with a correspondingly different representation in the lattice.

A concrete made with a strong mortar and weak aggregate may fail by crushing or splitting of the aggregate particles: this would be shown in the lattice by a failure of one of the aggregate bonds. Alternatively, it appears possible that concrete could fail by a compression failure (or powdering) of the mortar, if the aggregate were extremely strong and the specimen were tested in triaxial compression. Very high stresses would be involved in a failure of this type which is therefore likely to be relatively infrequent when compared with the more usual break-down of a mortar bond under excess tension.

The strength of concrete in triaxial compression has been investigated by Akroyd[3] whose results are reproduced in Figure 3. As this method of presenting the information tends to over-emphasize the suitability of applying Mohr's criterion for failure to the concrete as a whole, as opposed to considering the break-down of the individual constituents, the results are shown re-plotted in non-dimensional form in Figure 4 together with the results obtained by Bresler and Pister[4]

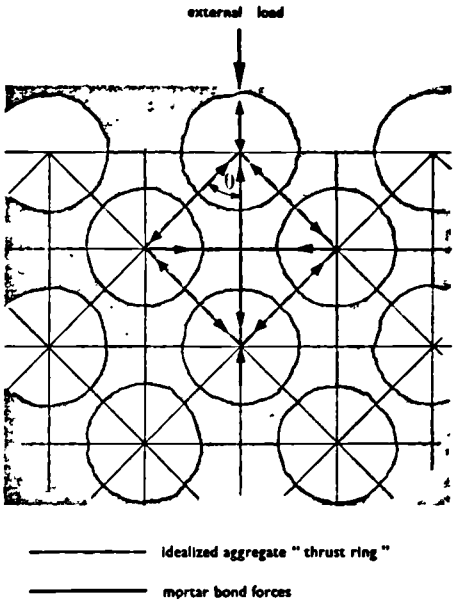


Figure 1: Lattice action of concrete under load.

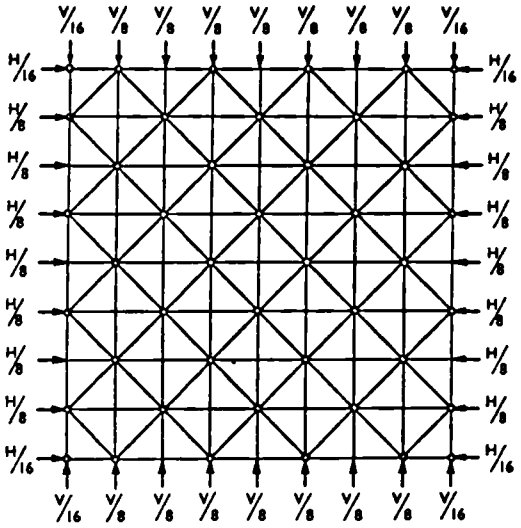


Figure 2: Typical lattice analogue for a concrete test specimen.

TABLE 1: **Properties of lattice members.**

Member	Extensional rigidity E_a	Length
Mortar bonds	1·0	1·0
Single aggregate bond	0·25	$1/\sqrt{2}$
Internal aggregate bonds	0·50	$1/\sqrt{2}$

Poisson's ratio = 0·15, σ = 45°.

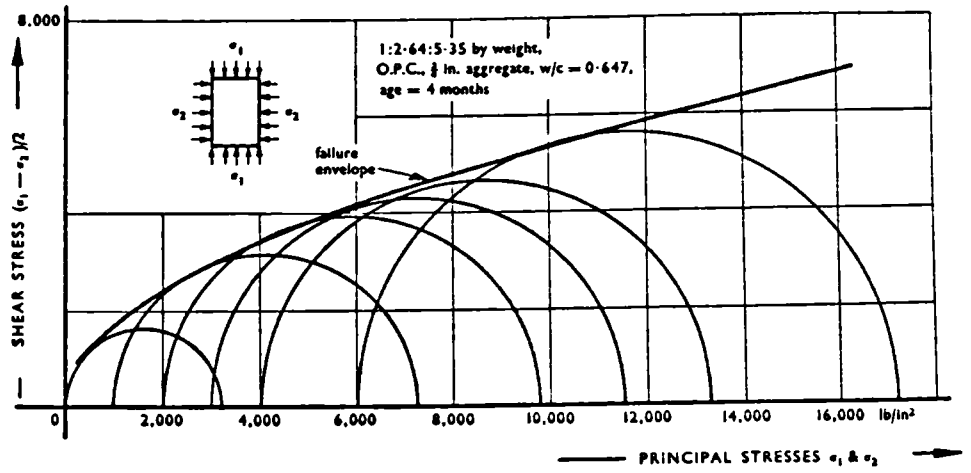


Figure 3: Results of triaxial compression tests on concrete (after T. N. W. Akroyd).

for combined tension and compression.

Similar results to these can be predicted from the behaviour of the analogous lattice under load. A lattice of the form shown in Figure 2 was used: the properties of the member being given in Table 1. The loads in the members were determined for different combinations of the 'H' and 'V' loads and, if failure is assumed to occur when a tensile load of a particular magnitude is reached in any mortar bond, the failure envelope shown in Figure 5 is obtained.

The effect of shrinkage

The effect of shrinkage of the mortar on the strength of the concrete specimen represented by the lattice was next investigated by calculating the loads in the members caused by an equal " lack of fit ", or shrinkage strain, in each of the mortar bonds in the frame. The additional values of the 'V' and 'H' loads required to increase the tensile load in any mortar bond to the value at failure could then be determined. These values are also shown in Figure 5 for different values of the non-dimensional mortar shrinkage k. A value of k equal to zero indicates that no shrinkage strains are present when the specimen is tested, whilst k equal to unity represents a spontaneous failure, due to the shrinkage of the mortar, similar to those observed by Pickett[5]. These results appear to suggest the possibility of manufacturing a concrete of greater tensile strength, if an expanding cement could be developed.

Thermal effects

When a cement paste is heated, it first expands until all the capillary moisture is removed. Continued heating causes shrinkage while the combined water is driven off from the hydration compounds in the cement gel until, at a temperature determined by the rate of heating, the total strain is again zero. Shrinkage continues until all the hydrated compounds are decomposed and then the cement paste begins, once more, to expand.

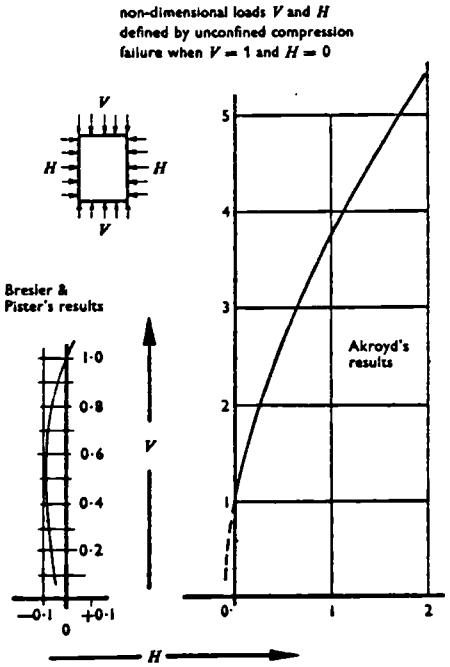


Figure 4: Results of triaxial tests on concrete.

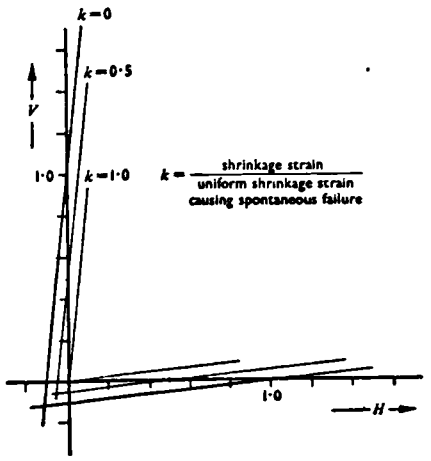


Figure 5: Strength of concrete under combined stress and uniform shrinkage loads, as predicted by the lattice analogue.

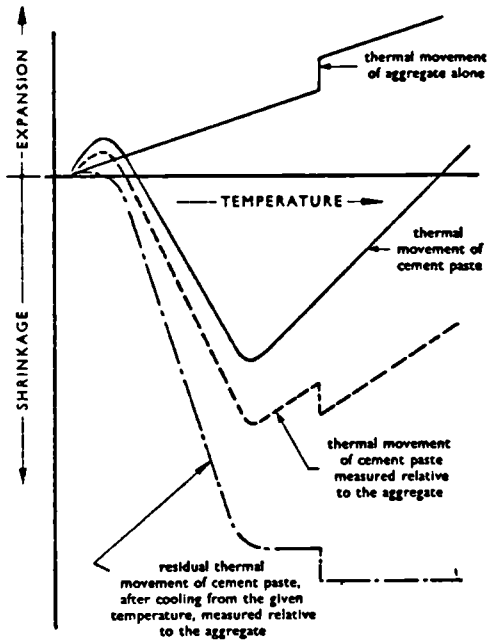


Figure 6: The thermal movements of a cement paste measured relative to a typical siliceous aggregate.

Crowley[6] studied the thermal movements of neat cement pastes which were repeatedly heated and cooled, in the temperature range 20–815°C. The most important conclusion to be drawn from his results is that, when a cement paste is cooled from a high temperature, the operative value of the coefficient of expansion is approximately the same as that in the final expansive stage during heating. This implies that a cement paste that is heated above a certain temperature and then cooled will have a residual shrinkage strain greater than any that occurs during heating. It is the magnitude of these residual strains which largely determines the load capacity of a specimen tested cold after cooling from high temperatures.

The thermal movements during continuous heating of a cement paste, measured relative to a typical siliceous aggregate, are shown diagrammatically in Figure 6. The step in the graph represents the volume change accompanying the α to β quartz transformation referred to previously. The curve for the residual thermal movement after cooling has been derived from the others and is based upon the constant final value of the coefficient of expansion of the cement paste reached during heating.

It is seen that this derived curve has the same form as those obtained by Malhotra[7] and others for the variation in residual compressive strength of concrete with temperature. At the lower temperatures, there are only small residual strains, causing very little change in the strength of the concrete. At higher temperatures, the large shrinkage of the cement paste causes considerable reductions in ultimate strength whilst, at still higher temperatures, the residual shrinkage of the cement paste reaches its maximum value and an increase in temperature has less effect on strength.

Figure 6 also shows that, if the reversible component of the thermal movement of the cement paste is greater than that of the aggregate, the shrinkage of the cement paste, measured relative to the aggregate, is greater after cooling than when the concrete is hot. This condition is usually satisfied and the internal stresses that are set up on heating increase on cooling as the cement paste and mortar continue to shrink, thus causing further reductions in the ultimate strength of the specimen. This is in direct agreement with Lea[8] and Malhotra who found that the strength of a concrete specimen was greater when tested hot than after cooling.

The effect of varying the constituents of the concrete can also be appreciated if it is accepted that thermal incompatibility is the cause of the variations in strength that occur on heating. The shrinkage of the mortar is determined by the amount of cement in the mix as well as by the exposure conditions: rich mixes shrink more than lean ones. This agrees with both Watkeys[9] and Malhotra, who found that rich mixes lost a greater proportion of their strength on heating than did leaner ones. If the role of the aggregate is considered, it is seen from Figure 6 that, if an aggregate with a higher coefficient of thermal expansion were to be used, the relative shrinkage of the cement paste would be increased. This would increase the reductions in strength expected at high temperatures and thus it appears that such reductions will be greatest for a concrete with a rich mix and an aggregate having a high coefficient of thermal expansion.

So far the shrinkage strains in the mortar have been assumed to be equal at every point throughout the concrete. In practice this could only occur after the concrete had been kept at a constant temperature for a considerable period. When a concrete specimen is heated, the outside becomes hot, moisture is driven off, and the concrete shrinks. As heating is continued, the shrinkage spreads further into the specimen until all the water has been removed and possibly the cement paste decomposed.

In order to illustrate the effect of the length of time of heating on the strength of a concrete cylinder, tested by the standard compression test, it is assumed that the distribution of shrinkage in the mortar bonds, at various times from the start of heating, is as shown in Figure 7a. These simplified initial data have been sketched without the use of mathematics or experimental results, but serve to demonstrate the manner in which the shrinkage strains in the mortar diffuse into the specimen during heating. When, finally, the temperature is maintained at a constant value, the shrinkage strains eventually become equal throughout. Figure 7b shows the idealized loading, adopted to

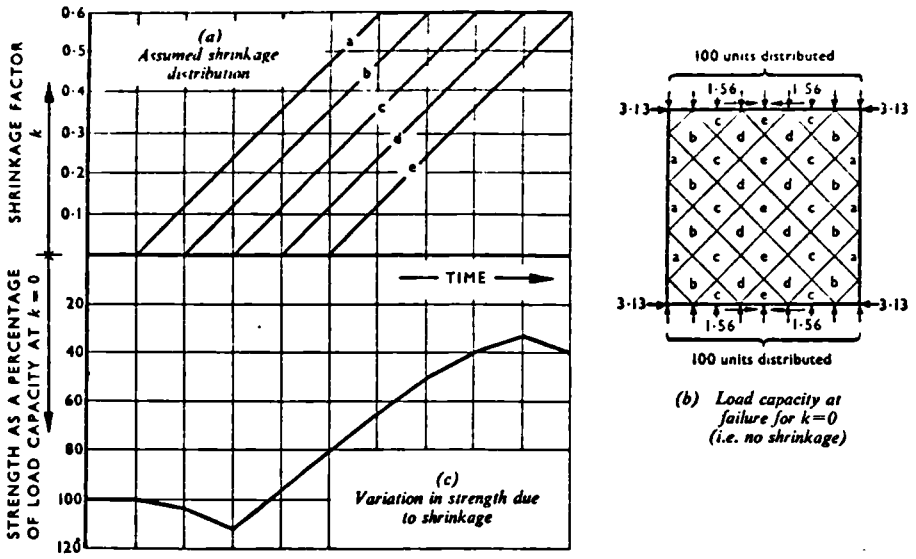


Figure 7

simulate the standard compression test on the specimen, represented again by the lattice shown in Figure 2.

The results (see Figure 7c) show that the ultimate strength is first slightly increased by shrinkage of the mortar bonds near to the surface, but is reduced as shrinkage spreads further into the concrete. A number of workers have recorded such an increase in strength but have generally attributed it to experimental error or to an ageing effect similar to that achieved by steam-curing an immature concrete.

Lea and Stradling observed that, if a concrete was heated to high temperatures and allowed to cool, it continued to lose strength after cooling, when stored in a humid atmosphere. In these conditions, the cement paste will expand, owing to swelling of the capillaries or the re-formation of calcium hydroxide, as moisture is absorbed. At first this appears to contradict the results obtained from the analogous lattice, as a general expansion of the mortar bonds should increase the strength measured by the standard compression test. However, complete absorption of moisture takes a considerable time and, at first, only the concrete near to the surface of the specimen is affected by the humid conditions. It is seen from Figure 7c that shrinkage of the outermost mortar bonds causes an increase in strength: expansion has the opposite effect, the ultimate load being reduced. The analogous lattice thus shows that the strength of a heat-treated specimen will first be reduced, by storing in humid conditions, and should then increase with time as moisture is absorbed further into the concrete. It is unlikely, however, that the original strength of the concrete can ever be regained, as the stiffness and strength of the concrete constituents are, almost certainly, reduced by temperature.

Limitations of lattice technique

The lattice analogy has been used to demonstrate the manner in which shrinkage of the mortar influences the strength of a concrete. The occurrence of these shrinkage strains has been illustrated by considering the strains induced when a concrete specimen is heated to high temperatures. The variations in strength due to these strains and the induced parasitic thermal stresses, predicted from consideration of the pin-jointed analogue, are always in fair agreement with the experimental results reported by previous workers. However, it is unlikely that this approach can be successfully extended to give precise quantitative results owing to the limitations of the simple lattice as a representation of the complete behaviour of a concrete specimen.

In the lattice, a plane frame has been used to represent the behaviour of a three-dimensional system and the relative stiffnesses of the members have been assumed to remain constant at all times. If only simple symmetrical specimens are studied, it is a reasonable assumption that this form of frame will give results in good qualitative agreement with results that could be obtained if a space frame were used. The major inaccuracy, however, is that the lattice is assumed to behave elastically, thus neglecting the effects of creep and plastic flow in the mortar on the behaviour of concrete at failure. When the effects due to heating are considered, there is the additional complication of the variation of the basic properties of the concrete constituents with exposure to high temperature. The basic strength of a mortar bond will be reduced by heating, but this will not upset most qualitative deductions of failure as this loss in strength will generally serve to emphasize the effect of shrinkage in the mortar.

It is seen from the foregoing that qualitative trends may be deduced with some confidence from the lattice, but that any attempt to obtain numerical results by this method is almost certain to fail. If these limita-

tions are recognized there is no reason why the analogous lattice should not prove to be a most useful tool in the study of the stress distribution and mechanism of failure in concrete.

Conclusion

Although the problem implied by an investigation into the effects of shrinkage on the strength of concrete has been very much simplified in order to obtain a solution, the correspondence between experimental results and the trends predicted from the lattice is undeniable. Important omissions have been made, particularly when the effects of shrinkage caused by heating have been considered. It is known that there is chemical activity, even at comparatively low temperatures, when concrete is heated, and these reactions must influence the basic strength of the constituents and the strength of the bond between them. It seems likely, however, that these effects are of secondary significance below 500°C and that, at these temperatures, the principal cause of variations in strength of a mature concrete are the parasitic thermal stresses set up by the thermal incompatibility of the cement paste and the aggregate. The effect of these internal stresses has been effectively demonstrated by means of the lattice analogue.

The results of this investigation into the effect of shrinkage on the strength of concrete are perfectly general and do not necessarily refer only to shrinkage caused by heating. The approach can clearly be used to study the effects of incompatibility on the strength of concrete at low temperatures, or in any other circumstance where internal stresses are set up by shrinkage, or expansion, of the cement paste with respect to the aggregate.

ACKNOWLEDGEMENTS

The work described in the paper formed part of a programme of research undertaken by the author in the Department of Civil Engineering, King's College, London. The author is particularly grateful to Professor A. D. Ross for his kind help and guidance during the course of this work.

The author also enjoyed the facilities of the University of London Computer Unit in the analysis of the lattice analogue.

REFERENCES

1. LEA, F. C. and STRADLING, R. E. The resistance to fire of concrete and reinforced concrete. *Engineering*. Vol. 114. No. 2959. 15 September 1922. pp. 341–344. No. 2960. 22 September 1922. pp. 380–382.
2. BAKER, A. L. L. An analysis of deformation and failure characteristics of concrete. *Magazine of Concrete Research*. Vol. 11, No. 33. November 1959. pp. 119–128.
3. AKROYD, T. N. W. Ultimate loads in rock and concrete. *Engineering*. Vol. 189, No. 4908. 13 May 1960. pp. 672–673.
4. BRESLER, B. and PISTER, K. S. Failure of plain concrete under combined stresses. *Proceedings of the American Society of Civil Engineers*. Vol. 81. April 1955. pp. 17. Separate No. 674.
5. PICKETT, G. Shrinkage stresses in concrete. *Proceedings of the American Concrete Institute*. Vol. 42. 1946. pp. 165–194 and 361–398.
6. CROWLEY, M. S. Initial thermal expansion characteristics of insulating refractory concretes. *Bulletin of the American Ceramic Society*. Vol. 35, No. 12. December 1956. p. 465.
7. MALHOTRA, H. L. The effect of temperature on the compressive strength of concrete. *Magazine of Concrete Research*. Vol. 8, No. 23. August 1956. pp. 85–94.
8. LEA, F. C. The effect of temperature on some of the properties of materials. *Engineering*. Vol. 110, No. 2852. 27 August 1920. pp. 293–298.
9. WATKEYS, D. G. *Non-destructive testing of concrete subject to fire attack*. Thesis submitted to the University of London for the degree of M.Sc.(Eng.), 1955. pp. 137.

APPENDIX

The strength envelope for an isolated lattice element

It is interesting to study the various types of failure that can occur in concrete by observing the behaviour of the single lattice element shown in Figure 8. It can be shown that the

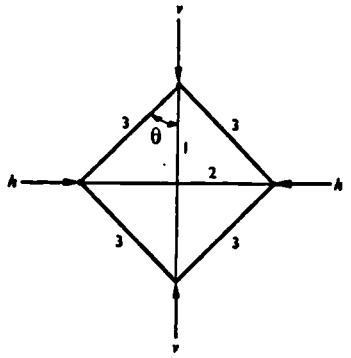


Figure 8: Symmetrical lattice element. ($\theta = 45°$. Extensional rigidities of mortar bonds are equal, i.e. $E_1a_1 = E_2a_2$)

tensile forces induced in the members of the frame by the loads v and h are as follows:

$$\frac{h}{R+1} - \frac{Rv}{R+1} \quad \text{in mortar bond 1}$$

$$\frac{v}{R+1} - \frac{Rh}{R+1} \quad \text{in mortar bond 2}$$

$$-\frac{v+h}{\sqrt{2}(R+1)} \quad \text{in the aggregate bonds}$$

where $1/R$ = Poisson's ratio

i.e. $R = \dfrac{\text{compressive strain in mortar bond 2}}{\text{tensile strain in mortar bond 1}}$

when $h > 0$ and $v = 0$.

Let m_t be the strength of a mortar bond in tension
m_c be the strength of a mortar bond in compression
a_t be the strength of an aggregate bond in tension
a_c be the strength of an aggregate bond in compression.

Then failure occurs in mortar bond 1

$$\text{if } m_t \leqslant \frac{h}{R+1} - \frac{Rv}{R+1} \leqslant -m_c$$

and failure occurs in mortar bond 2

$$\text{if } m_t \leqslant \frac{v}{R+1} - \frac{Rh}{R+1} \leqslant -m_c$$

and failure occurs in the aggregate bonds

$$\text{if } a_c \leqslant \frac{v+h}{\sqrt{2}(R+1)} \leqslant -a_t$$

If we write

$$V = \frac{v}{(R+1)m_t} \text{ and } H = \frac{h}{(R+1)m_t}$$

the " safe zone " for the lattice element is defined by the following six straight lines.

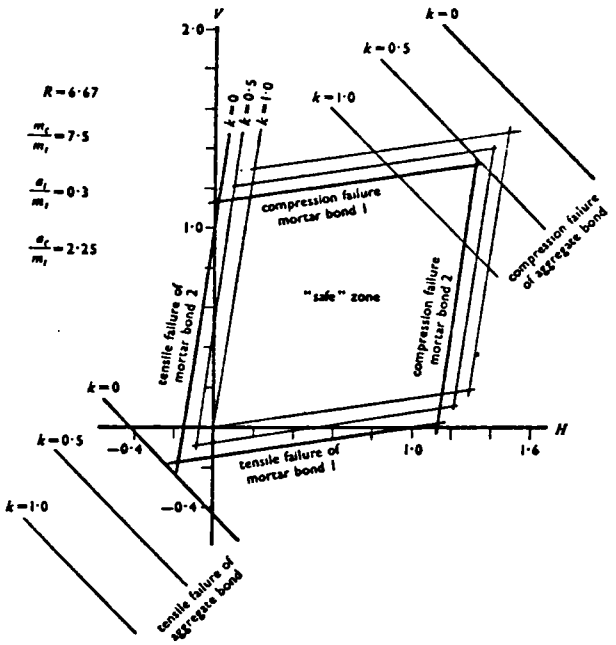


Figure 9: Strength envelopes for a single lattice element subject to varying degrees of shrinkage strain.

$$\left.\begin{aligned} V &= \frac{H}{R} - \frac{1}{R} \\ V &= \frac{H}{R} + \frac{m_c}{Rm_t} \end{aligned}\right\} \text{ Failure of mortar bond 1 in tension and compression.}$$

$$\left.\begin{aligned} V &= RH + 1 \\ V &= RH - \frac{m_c}{m_t} \end{aligned}\right\} \text{ Failure of mortar bond 2 in tension and compression.}$$

$$\left.\begin{aligned} V &= -\left(\frac{\sqrt{2}a_t}{m_t} + H\right) \\ V &= \left(\frac{\sqrt{2}a_c}{m_t} - H\right) \end{aligned}\right\} \text{ Failure of aggregate bonds in tension and compression.}$$

The safe zone (Figure 9) is the area enclosed by the above lines. The zone gives all possible combinations of the non-dimensional loads V and H which may occur without failure resulting. If the effect of shrinkage of the mortar is to be considered, the equations are modified as follows.

$$\left.\begin{aligned} V &= \frac{H}{R} - \frac{1-k}{R} \\ V &= \frac{H}{R} + \frac{m_c + m_t k}{m_t R} \end{aligned}\right\} \text{ Failure of mortar bond 1.}$$

$$\left.\begin{aligned} V &= RH + 1 - k \\ V &= RH - \frac{m_c + m_t k}{m_t} \end{aligned}\right\} \text{ Failure of mortar bond 2.}$$

$$\left.\begin{aligned} V &= -\left(\frac{\sqrt{2}a_t}{m_t} + H + k\right) \\ V &= \left(\frac{\sqrt{2}a_c}{m_t} - H - k\right) \end{aligned}\right\} \text{ Failure of aggregate bond.}$$

where $k = \dfrac{\text{lack of fit in mortar bonds}}{\text{lack of fit causing spontaneous failure}}$

It is seen from Figure 9 that, if the aggregate does not fail, the effect of shrinkage is to shift the safe zone along its axis of symmetry and further into the positive quadrant. It is interesting to note that the over-all size of the zone is unaltered by shrinkage. The prestressing action of the shrinkage strains is clearly shown by the Figure, the lattice being capable of sustaining higher compressive loads at the expense of its strength in tension.

The strength envelope for the isolated lattice shows the various possible types of failure that can occur in concrete. It is clear that a general theory using some stress combination as the criterion for failure cannot take these various break-downs into account unless expressed in terms of the stresses that occur in the individual constituents of the concrete. The main attraction of the lattice analogue is the implied consideration of the separate effects of the cement paste and the aggregate in the concrete.

Contributions discussing the above paper should be in the hands of the Editor not later than 31 January 1962.

Some effects of thermal volume changes on the properties and behaviour of concrete

INTERNATIONAL CONFERENCE ON THE STRUCTURE OF CONCRETE 1965

John W. Dougill

PAPER 12

Introduction

In considering the effects of changes in temperature, a new dimension is added to the study of the properties of concrete. Ideally the performance of concrete at elevated temperatures should be determined by repeating the types of test already undertaken at normal temperatures for a variety of thermal conditions. The number of possible combinations of tests and exposure conditions would be immense, especially when it is realized that thermal effects can not generally be isolated from time-dependent phenomena. In addition there are a number of pressing problems ranging from long-term thermal loading at moderate temperatures, as in pressure vessels for nuclear reactors, to the high transient stresses associated with thermal spalling of concrete exposed to fire. As yet few experimental data are available on such problems. It is therefore both tempting and necessary to hypothesize—to extrapolate the data and theories used to predict the behaviour of concrete at normal temperatures—in order to explain behaviour under different thermal conditions. If useful theories are to be established, concrete must be treated as a composite material with separate consideration being given to the constituent phases, each of which reacts differently to changes in temperature and applied stress.

If a small representative piece of concrete situated within a heated specimen is considered, the total stresses due to the applied stress and thermal effects acting at the boundaries of this element can be taken to be those that can be calculated on the assumption that the concrete is homogeneous and isotropic. These conventionally determined stresses constitute the loading on the element of concrete. Within this small volume, this loading causes certain stresses in the aggregate and cement paste on which are superposed the stresses caused by thermal incompatibility of the concrete materials. Conventionally, strength is a measurable property of the concrete as a whole and criteria for discontinuity and failure[1] are expressed in terms of the conventionally determined stresses or, in the case of the elemental volume, the loading. If the maximum possible loading is determined by the magnitudes of the total interparticle stresses, it is clear that the strength of the concrete will be partly dependent on the interparticle stresses causes by thermal incompatibility. The same situation arises at normal temperatures at which it has been suggested[2] that separate consideration of the loading and the stresses due to incompatibility is necessary in assessing the effect of shrinkage on the behaviour of concrete.

Thermal movement of concrete

Under short-term thermal loading, the stresses in a concrete body can be calculated for any prescribed temperature distribution if values of the elastic moduli and the coefficient of thermal expansion are known. No definite data are available on the variation of Poisson's ratio with temperature but it is established[3, 4] that Young's modulus for concrete is very much reduced at high temperatures.

The thermal expansion of concrete is a

function of the free thermal movements* of the cement paste and aggregate and their relative proportions and stiffnesses. As with Young's modulus, the thermal movement of a concrete may be found from the proportions and properties of the constituent materials. In general, a model is used in which the distribution of the two phases, aggregate and mortar or cement paste, is idealized for ease of solution. The simplest models are those used by Hansen[5] in which the two phases are arranged either in series or parallel. These arrangements are similar to the Maxwell and Kelvin bodies which are often used as analogies to visco-elastic behaviour. In the latter models, however, one of the phases is viscous rather than elastic and is thus represented by a dashpot instead of a spring in the model.

Hansen's models give the following two expressions for the thermal strains in the concrete, α_c.

For the series model:

$$\alpha_c = g\alpha_a + (1-g)\alpha_p \quad . \quad . \quad . \quad (1)$$

For the parallel model:

$$\alpha_c = \frac{mg\alpha_a + (1-g)\alpha_p}{mg + (1-g)} \quad . \quad . \quad (2)$$

where α_a and α_p are the free thermal strains of the aggregate and cement paste at the temperature considered, m is the ratio of the Young's modulus of the aggregate, E_a, to that of the cement paste, E_p, and g is the volumetric fraction of aggregate in the concrete. L'Hermite[6] has suggested equation 2 and Kingery[7] has shown that the values predicted by this expression agree closely with experimental results of thermal expansion in metal-ceramic composite systems. When the modular ratio m is not large, as occurs when the second phase is taken to be the mortar rather than the cement paste, the first expression is quite a reasonable approximation as can be seen from the results, shown in Figure 1, obtained by Walker, Bloem and Mullen.[8]

* The term thermal movement, α, is used to mean the total strain, due to thermal expansion and shrinkage, occurring in one material at any particular temperature, v. Equations such as 1 and 2, containing expressions for the thermal movements of more than one constituent, apply only at this temperature and the appropriate values of the elastic constants must be used. When the rate of change of thermal movement with temperature is constant, a coefficient expansion, $\bar{\alpha}$, can be defined by $\bar{\alpha} = d\alpha/dv$.

The model suggested by Dougill[9] following Hirsch's analysis[10] gives the mean of the two values obtained from the Hansen model, i.e.

$$\alpha_c = \frac{g\alpha_a + (1-g)\alpha_p}{2} + \frac{mg\alpha_a + (1-g)\alpha_p}{2mg + 2(1-g)} \quad (3)$$

This model provides excellent predictions of Young's modulus for concretes containing normal aggregates. In some ways this is analogous to the Burger's model (i.e. a Maxwell and a Kelvin body connected in series) which, although not completely satisfactory, has been extensively used in studies of creep of concrete.[11] It therefore seems reasonable to suppose that equation 3 is likely to give a very good estimate of the thermal strain α_c.

Another possible approach is provided by Pickett's work[12] in which he derived the following expression for the shrinkage strain in a concrete S_c in terms of that of the cement paste S_p:

$$S_c = S_p(1-g)^n \quad . \quad . \quad . \quad (4)$$

where n is a constant which depends on the elastic properties of the aggregate and the cement paste. If the thermal strains of the concrete and cement paste are measured relative to those of the aggregate, the structural problem is identical with that studied by Pickett and the following expression is obtained:

$$(\alpha_c - \alpha_a) = (\alpha_p - \alpha_a)(1-g)^n \quad . \quad . \quad (5)$$

In his analysis Pickett obtained an expression for n which contained the elastic properties of the concrete rather than those of the cement paste. Thus, although he assumed n to be constant in his analysis, he observed that n is likely to be a function of the volumetric composition, g, as well as the relative stiffness of the two phases. Recently, Hansen and Nielsen[13] have repeated Pickett's analysis, but this time using the expressions for the elastic modulus of concrete derived from Hansen's model. In fact, this approach seems hardly necessary as experimental results indicate that Pickett's assumption, that n is independent of g, is excellent. This can be seen when the results of Walker et al. are plotted in the logarithmic form shown in Figure 2. Each set of results for different mixtures of a particular aggregate with the same cement paste or mortar can be represented by a straight line,

the slope of which gives the appropriate value of n.

Pickett freely admitted that his analysis contained many approximations and it would therefore appear that his expression for n should be ignored and equation 4 regarded more as the mathematical expression of an experimental "law". If this view is taken, it is possible to show that equation 4 follows from the application of a more general postulate stating that the strain ϵ_c, in a concrete under a particular system of stress, is related to the strain ϵ_p, in a similar specimen of the cement paste loaded by the same stress system, by the expression:

$$\epsilon_c = \epsilon_p(1-g)^n \quad . \quad . \quad . \quad (6)$$

where the exponent n depends on the relative properties of the aggregate and cement paste, the loading system and the type of strain measured.

At first, this appears to be a very drastic generalization but a few examples soon show that, even if there is not yet sufficient evidence available to enable the postulate to be accepted unreservedly, it is worth consideration.

Apply equation 6, for example, to the strains caused by unit stress acting on a concrete or on its cement paste. For strains measured parallel to the direction of the applied stress, equation 6 gives:

$$\frac{1}{E_c} = \frac{1}{E_p}(1-g)^p \quad . \quad . \quad . \quad (7)$$

For strains at right-angles to the direction of the applied stress, it gives:

$$-\frac{\nu_c}{E_c} = -\frac{\nu_p}{E_p}(1-g)^q \quad . \quad . \quad . \quad (8)$$

where ν_c and ν_p are the values of Poisson's ratio for the concrete and cement paste respectively, and p and q are exponents which are not necessarily equal.

For small concentrations of aggregate, equation 7 may be simplified to give:

$$E_c = E_p(1+pg) \quad . \quad . \quad . \quad (9)$$

This is in the form of Einstein's equation which Ishai[14, 15] has successfully applied to concrete. The values of p found by Ishai are a function of the modular ratio m and are shown in Figure 3.

On dividing equation 8 by equation 7, an expression for Poisson's ratio is obtained:

$$\nu_c = \nu_p(1-g)^{(q-p)} \quad . \quad . \quad . \quad (10)$$

Newman[16] correlated Anson's[17] experimental values of Poisson's ratio by means of this equation in which the total exponent $(q-p)$ had a value 0·42.

Returning now to derive Pickett's expression, consider a concrete specimen which is heated uniformly but which is partially restrained by an applied stress so that the total observed strain equals the unrestrained thermal expansion of the aggregate alone. In these circumstances the total restraining stress on the specimen is $K_c(\alpha_a - \alpha_c)$ and the average stress in the cement paste is $K_p(\alpha_a - \alpha_p)$ where K_c and K_p are the bulk moduli for the concrete and cement paste respectively. The average stress in the aggregate particles will be zero.

Now equate the strain energy stored in the concrete to the total energy stored in the individual constituents, i.e.

$$K_c\frac{(\alpha_a-\alpha_c)^2}{2} = (1-g)K_p\frac{(\alpha_a-\alpha_p)^2}{2} + g(\text{zero})$$

But from the postulate 6

$$K_p = K_c(1-g)^r$$

and thus

$$(\alpha_c-\alpha_a) = (\alpha_p-\alpha_a)(1-g)^{(r+1)/2} \quad . \quad (11)$$

which is in the form of Pickett's equation as given in 5.

The postulate has also been used implicitly by Neville,[18] in his study of the effect of cement paste content on the creep of concrete, and it appears probable that equation 6 can be applied in many instances where concrete behaviour is controlled by variations in the aggregate composition. The most important use, however, may be as a means to step down the level of investigation and to determine the average stresses in the cement paste in terms of the total stress acting on the concrete. This will be apparent when the strength of concrete at high temperatures is discussed, but first, separate consideration must be given to the causes of thermal incompatibility, namely the individual thermal movement of the cement paste and aggregates.

Thermal movement of aggregate and cement paste

Although the coefficient of thermal expansion of the aggregate may be taken as constant for small thermal changes, this is not

possible for the extreme conditions obtained on exposure to very high temperatures. Aggregates produced from crystalline rocks may be liable to progressive distintegration at high temperatures[19] because of thermal incompatibility within the aggregate itself. The parent material is composed of a variety of closely packed minerals whose differences in thermal expansion can cause intercrystalline stresses and progressive failure. This process may be exacerbated by phase changes in the constituent materials, particularly when these are accompanied by sudden expansion. One such change is the α to β quartz transformation[20] which occurs at about 575°C and is accompanied by a considerable increase in volume. These volumetric changes are not reversed on cooling: Mellor and Cambell[21] found that the residual deformation of a specimen of quartz increased rapidly with repeated heating to 1,300°C until, after twelve cycles of heating, there was a 14% increase in volume. Not all this increase can be attributed to the α to β quartz transformation, however, as there is also a large expansion accompanying the formation of cristobalite above 1,000°C.[22]

The sudden expansion at 575°C is a feature of all siliceous aggregates and must have a damaging effect on the strength of concretes made with this material and exposed to high temperatures. However, this is clearly not the only important effect, since Malhotra[23] has shown that concrete made with river-gravel aggregate may lose as much as 70% of its strength on heating to temperatures less than 500°C, when the α to β quartz transformation has still to occur.

In contrast to siliceous aggregates, limestone neither changes its physical composition nor undergoes any sudden expansion during heating except at very high temperatures, when it is decomposed to form lime with the evolution of carbon dioxide. This reaction is endothermic and tends to retard the temperature rise in a concrete made with limestone aggregate that is exposed to fire. This extends the period of fire resistance, but deterioration is likely to occur on cooling[24] when the free lime combines with atmospheric moisture to form calcium hydroxide. This reaction is accompanied by an increase in volume which has a disruptive effect on the concrete.

Most of the work that has been undertaken on the thermal movements of cement paste and concretes has been to determine the coefficient of expansion at normal temperatures. Even under these conditions the coefficient is not a constant, as it depends on the relative vapour pressure of the moisture within the cement paste. Mitchell[25] has shown that, in the temperature range 0–20 C, the coefficient of expansion of oven-dried and saturated neat cement pastes are practically identical (see Figure 4) and that a higher coefficient is obtained at intermediate moisture contents. This increase is due to water vapour pressure, which is absent from both the oven-dried and the saturated specimens. There is also a time-dependent deformation caused by migration of water between the gel pores and capillaries[26] as the temperature of the cement paste is changed. In concretes, there are likely to be further time-dependent strains as the interparticle stresses due to the restraining influence of the aggregate are relieved by creep in the cement paste. It is clear that there are considerable difficulties in any attempt to separate strains due to creep, shrinkage and thermal expansion at temperatures only slightly above normal. The present paper, however, is more concerned with the gross thermal movements that occur when concretes or cement pastes are heated to very high temperatures.

When a cement paste is heated, it first expands until all the free moisture is removed. Further heating leads to the removal of adsorbed water from the gel pores with accompanying shrinkage until the total strain is again zero. Shrinkage continues until most of the adsorbed water is removed and some of the hydration products decomposed and then the cement paste begins to expand once more. The rate of removal of moisture is dependent on the rate of heating and the temperature at which a particular strain is obtained increases as the rate of heating is increased.[27]

Crowley[27] studied the thermal movement of neat cement pastes which were repeatedly heated and cooled in the temperature range 20–815°C. Although this work is mostly concerned with refractory cements, it is thought that similar results would be obtained with pastes made of ordinary Portland cement. It will be seen from these results (Figure 5) that

the coefficient of expansion obtained during cooling is approximately the same as that obtained during the final expansive stage of heating and that the residual shrinkage strains obtained after cooling from high temperatures will be greater than any that occur during heating. This work suggests that the thermal movement of cement paste may be considered to be the sum of a reversible and an irreversible component as shown in Figure 6. It is interesting to compare the form of the curve representing the irreversible component of thermal movement with that obtained by Philleo[3] for weight loss during heating. The connexion between shrinkage and weight loss due to removal of moisture appears to be clearly demonstrated (Figure 7).

Strength of concrete

When a specimen of concrete is heated uniformly so that the stresses calculated by conventional analysis are zero, the interparticle stresses are some function of the difference in free thermal movements of the aggregate and cement paste. These "parasitic thermal stresses" will be tensile in the cement paste if it shrinks with respect to the aggregate. Thus, if the ultimate strength of a concrete specimen is dependent on the tensile strength of its cement paste, the measured strength will be reduced. This reduction has been effectively demonstrated[28] by using Baker's[29] pin-jointed lattice analogy for the structure of concrete.

If idealized data are taken for the thermal movements of a cement paste and a siliceous aggregate, the general manner in which the strain difference due to incompatibility varies with temperature can be found. This is shown in Figure 8, from which it can be seen that at first these differential strains will induce a small compressive stress in the cement paste but that with increasing temperature this is reduced and changes to a much larger tensile stress. The residual strains obtained after cooling are also shown in this Figure. These determine the load capacity of a specimen tested cold after cooling from high temperatures.

The curves in Figure 8 may be compared with the ultimate strength results obtained by Malhotra and shown in Figure 9. Malhotra[23] tested small cylindrical specimens of concrete in uniaxial compression at high temperatures and after cooling. His results show fair qualitative agreement with the trends to be expected from consideration of the strains due to incompatibility. At first the effects of heating are not great but, as shrinkage of the cement paste occurs, the measured strength is greatly reduced. Finally a stage is reached when most of the moisture has been removed, and further heating has less effect. In particular, it will be seen that the strengths obtained by crushing specimens which had been allowed to cool are lower than those of specimens tested hot, which is to be expected, as the residual shrinkage strains due to incompatibility are greater than those that occur during heating.

Malhotra's is probably the most extensive experimental study undertaken of the effects of high temperature on the compressive strength of concrete made with river-gravel aggregates. Besides confirming the differences in hot strength and residual strength found by Lea,[30] he found that variations in water/cement ratio had negligible effect upon the proportional reduction in strength. On the other hand, variations in the aggregate/cement ratio were significant, the proportional reduction being smaller for lean mixes than rich ones. He also found that, if a stress of between 20 and 25% of the cold strength is maintained on a specimen during heating, the total load capacity is increased by as much as 20% at 500°C.

One aspect not covered by Malhotra's work is the reduction in strength that occurs after a specimen has been allowed to cool and is then stored in humid conditions. This effect, shown in Figure 10,[31] was first observed by Lea and Stradling,[32] who attributed these variations in strength to the volume changes accompanying the rehydration of the free lime formed when the calcium hydroxide in the cement paste is decomposed during heating. This occurs in concretes heated above a temperature of about 500°C. For concretes heated to lower temperatures, the post-cooling strength variations are caused by swelling due to moisture absorption, without chemical change. The lattice analogy[28] can again be used to illustrate the manner in which expansion due to absorption of moisture into the surface layers of a specimen can

cause a continued reduction in strength. Use of the analogy also suggests that a small recovery in strength may eventually occur as the moisture diffuses further into the specimen. This gradual change has still to be confirmed by experiment, although some recovery of strength has been recorded[19] for heat-resistant concretes stored under water for seven days.

Before Malhotra's work, many workers had investigated the residual compressive strength of concrete obtained after cooling from high temperatures. Miller and Faulkner[33] compared the performance of concretes made with ordinary Portland and high alumina cements and found that, whilst the concrete made with high alumina cement lost strength at a greater rate than did the ordinary Portland concrete at moderate temperatures, it retained a greater proportion of its strength at temperatures greater than 700°C.

Most work,[34-36] however, has been to compare the performance of concretes made with different types of aggregate as a guide to the selection of materials for concrete in structures where fire resistance is important. This form of test is not necessarily the best guide to the behaviour of concrete in a fire, as the aggregate properties affect not only the strength but also the rate of heat transmission and the temperature gradients achieved in the concrete. On the basis of experience gained from full-scale testing, Ingberg[24] suggested a classification of concrete aggregates with regard to fire resistance. He divided aggregates into four groups of which the first, comprising calcareous material, contains the aggregates which behave best in a fire but are liable to deterioration on cooling. If this is to be avoided, the aggregates in the second group give the best performance. These are feldspathic aggregates consisting of fine-grained igneous rocks but also including such artificial aggregates as broken brick, hard clinker etc., in which the sudden volume changes accompanying phase transformations have already occurred during their manufacture. The third group comprises the coarse-grained igneous and sedimentary rocks which can occasionally lead to cracking and spalling in concrete exposed to fire, whilst the fourth group contains siliceous aggregates, such as quartz, chert and flint, which generally behave badly during fire tests. It can be seen from the discussion in the previous section that this classification is directly related to the dimensional stability of the aggregate at high temperatures.

Aggregates in Ingberg's second group are suitable for use in structural refractory concrete,[37] especially when used with high alumina cement. Such concretes can maintain up to 50% of their cold strength after heating to 1,200°C. Stradling and Brady[19] also used aggregates of this type successfully in an earlier attempt to manufacture heat-resistant concrete. In addition, they tried to reduce shrinkage of the cement paste and minimize post-cooling strength variations by eliminating the calcium hydroxide in the cement paste. This was done by including sufficient pozzolanic material with the cement, so that hydrated compounds of lime, silica and alumina were formed during hardening instead of calcium hydroxide. Although these compounds are decomposed on heating, they do not recombine readily with water on cooling. In general, these concretes behaved well, often showing an increase in strength for temperatures below 600°C and recovering some of the strength lost on heating to 800°C and 1,000°C after immersion in water for 7 days.

Strength of concrete under combined stresses at elevated temperatures

All the experimental results referred to so far have been concerned with the ultimate strength of a specimen under nominally uniaxial compression. It is of great interest to know how these results may be applied to other states of stress likely to occur in heated structures. In particular, definite information is required concerning the effects of high temperature on strength in biaxial compression, as this state of stress is induced at the surface of a wall panel or floor slab in the early stages of heating and is presumably responsible for one form of thermal spalling. Unfortunately this information is not available and, in fact, it is only recently that the form of the strength envelope in the biaxial compression zone[17, 38] has been satisfactorily confirmed at normal temperatures; even then there are still considerable differences of opinion as to the form of criteria for discontinuity and failure of concrete under

different states of stress. It is unlikely that complete criteria for failure at elevated temperatures can be established before the problem is solved for normal conditions. However, it is necessary that some hypothesis should be advanced in order to try to explain phenomena occurring at high temperatures and to form the basis of planned, rather than ad hoc, experiments.

It will be assumed that some criterion for failure of cement paste has been established in terms of the average stresses acting on a paste specimen, i.e.

$$f(\sigma_1', \sigma_2', \sigma_3') \neq 0 \text{ before failure} \quad . (12)$$

where σ_1' etc. are the stresses in the cement paste, compression being positive.

If, in considering a concrete, failure is assumed to occur within the cement paste, the problem remains of finding the average stresses σ_1', σ_2' and σ_3' in the cement paste in terms of the stresses σ_1, σ_2 and σ_3 applied to the concrete. For very small volume concentrations of aggregate, the average strain in the cement paste can be taken to equal the strain in the concrete as a whole. For these conditions, the stresses in the cement paste caused by stresses applied to the concrete can be found from:

$$\begin{bmatrix}\sigma_1' \\ \sigma_2' \\ \sigma_3'\end{bmatrix} = A\begin{bmatrix}1 & B & B \\ B & 1 & B \\ B & B & 1\end{bmatrix}\begin{bmatrix}\sigma_1 \\ \sigma_2 \\ \sigma_3\end{bmatrix} \quad . . (13)$$

where

$$A = \left(1 + \frac{2\nu_p(\nu_p - \nu_c)}{(1+\nu_p)(1-2\nu_p)}\right)\frac{E_p}{E_c}$$

and

$$B = \frac{\nu_p - \nu_c}{1 - \nu_p - 2\nu_p\nu_c}$$

It is seen from the diagonal terms (1) that the inclusion of a small quantity of aggregate causes the stresses in the paste to be reduced approximately in the ratio E_p/E_c. However, the off-diagonal terms (B) indicate that the stress in the cement paste is not merely some proportion of that acting on the concrete but consists of a different combination of principal stresses. For instance, if the concrete is stressed in uniaxial compression, equation 13 shows that the cement paste will be in triaxial compression, provided that the Poisson's ratio of the cement paste is greater than that of the concrete. This fact had previously been deduced by Anson[16] from his own experimental results.

The strain in the cement paste again being assumed to be the same as that in the concrete as a whole, the stresses in the cement paste σ_v' due to thermal incompatibility can be found to be:

$$\sigma_{v1}' = \sigma_{v2}' = \sigma_{v3}' = (\alpha_c - \alpha_p)\frac{E_p}{1-2\nu_p} \quad . (14)$$

where the thermal strains are positive for shrinkage.

These stresses are the parasitic thermal stresses which must be added to the stresses σ_1' etc. in the cement paste due to the applied loading to give the total stresses in the cement paste to be used in the failure criterion. The effect of the parasitic stresses is that of adding an equal volumetric or triaxial stress $\sigma v'$ to the cement paste or alternatively a triaxial stress σ_v to the concrete as a whole, where:

$$\sigma_v = \frac{\sigma_v'}{A(1+2B)} \quad . . . (15)$$

The assumption concerning the distribution of strain is only valid for low aggregate concentrations. For higher concentrations, the assumption of an admissible displacement field leads to an upper-bound approximation to the stresses at failure.

So far, no consideration has been given to the basic criterion for failure within the cement paste. Previous analytical work in this field[28] was based on the use of a two-dimensional lattice analogy for concrete and, although the concept has been extended to three dimensions,[16] it is still unlikely to be suitable for all states of stress. This is because the properties of the members in the lattice are chosen to simulate the deformation of the concrete and, if failure is assumed to occur when the load in a member reaches a particular value, this must be interpreted as the assumption of a limiting strain criterion for failure of the concrete. Such a criterion provides a reasonable working relationship for qualitative deductions of strengths under combined compressive and tensile stresses and possibly triaxial compression, but is clearly incorrect in biaxial compression.

Further consideration of the precise form of the criterion for failure of the cement paste is beyond the scope of this paper. However,

suppose, for example only, that the required criterion depended only upon the values of the maximum and minimum principal stresses and could be expressed in the form:

$$\sigma'_{max} - R\sigma'_{min} \not> C \quad . \quad . \quad . \quad (16)$$

where C is the uniaxial compressive strength and R is the ratio of uniaxial compressive to uniaxial tensile strengths of the cement paste.

Equation 16 is one form of the Coulomb-Mohr criterion and can be expressed in terms of the stresses acting on the concrete using equation 13. Thus, for $\sigma_1 \geqslant \sigma_2 \geqslant \sigma_3$,

$$(1-RB)\sigma_1 - B(R-1)\sigma_2 - (R-B)\sigma_3 \not> (1-k)C/A \quad (17)$$

where

$$k = -\frac{(R-1)\sigma_v'}{C} = -\frac{A}{C}(1+2B)(R-1)\sigma_v$$

The non-dimensional parameter k is a measure of the parasitic thermal stresses which are zero when $k=0$. As k increases, the stresses that can be applied to the concrete before failure are gradually reduced. When $k=1$, spontaneous failure occurs in triaxial tension as a result of the parasitic thermal stresses alone.

Equation 17 shows that the proportional reduction in strength due to parasitic thermal stresses will be the same for all states of stress. This can be seen in Figure 11, which shows the strength envelope for a biaxial stress regime obtained from equation 17. Although this conclusion may not be valid for all possible forms of criteria which may be applied to the concrete or the cement paste, it will apply to some which have already been used[39, 40] and in particular those expressing the condition that some function of the shear stress is to be related to the mean normal stress at failure. The conclusion requires one further qualification as it is based on the assumption that a single function can describe the complete failure envelope for concrete. This is unlikely.

Another point of interest is that equation 17 is a failure criterion for concrete involving all three principal stresses even though it has been derived from an assumed criterion for failure of the cement paste (equation 16) which is independent of the intermediate principal stress. This is because of the nature of equation 13 and, although no great weight can be placed on the actual expressions for A and B obtained by such a simplified method, the general form appears to be correct. Thus, for the assumed criterion, the inclusion of additional aggregate causes the intermediate stress to have greater effect because of the increase in B.

Local failures due to thermal effects—aggregate splitting

Besides general loss in strength due to the development of parasitic thermal stresses and the effects of heating on the properties of the cement paste and the aggregate, premature failures may occur on the surface of concrete in the form of thermal spalling. This can occur in several ways,[41] of which one of the most common is splitting of the aggregate near the heated surface of a concrete member during the early stages of heating. This is particularly serious if the member is reinforced, as any removal of the surface layer of concrete causes the temperature of the steel to rise more than if the layer were present, so leading to early failure. The occurrence of aggregate splitting thus leads to reduced periods of fire resistance. It is clear that a method is required to assess the probable behaviour of any particular aggregate at high temperatures, so that those aggregates likely to disintegrate in a structure exposed to fire can be rejected.

Kingery[42] has shown how the ability of a single material to resist changes in temperature or thermal shock can be expressed in terms of a thermal stress resistance factor. The concept may be applied to other loading conditions and can be illustrated by considering the ability of concrete to withstand shrinkage stresses. Thus, if a partially restrained specimen of concrete is subject to a shrinkage strain ϵ_s, the stresses σ induced are:

$$\sigma = -\frac{E_c\epsilon_s}{1-2\nu_c}\frac{1}{s} \quad . \quad . \quad . \quad (18)$$

where s is a shape factor accounting for geometry and restraint.

If the failure stress is f_t, the load factor against failure is λ where

$$\lambda = \left(\frac{1-2\nu_c}{E_c\epsilon_s}f_t\right)s = Rs \quad . \quad . \quad (19)$$

The terms in brackets in the above expression ($=R$) can be considered to be a "shrinkage stress resistance factor" as they contain all the material properties influencing failure by shrinkage. It is clear that the factor is a measure of the ability of a concrete to resist shrinkage stresses and provides a means by which the relative performance of different materials can be assessed. Some such factor is required so that the likelihood of splitting of different aggregates can be compared.

Although thermal stress resistance factors could be derived for individual pieces of aggregate exposed to heating, it is clear that these would not necessarily be a satisfactory guide to the relative performance of different aggregates when used in concrete. Here, each piece of aggregate is surrounded by a material which usually has a different coefficient of expansion from the aggregate. With a change in temperature, stresses will be induced in the aggregate in addition to those caused in an unrestrained particle. The magnitudes of the stresses developed at a given temperature are thus dependent upon the properties and thermal volume changes of the surrounding material as well as those of the aggregate.

Consider a spherical particle of aggregate radius R within a large mass of material which is assumed to have infinite conductivity. The aggregate has Young's modulus E_a, Poisson's ratio ν_a, tensile strength f_t, thermal diffusivity h^2 and a coefficient of thermal expansion $\bar{\alpha}_a$. The surrounding material which is assumed to have the properties of concrete has Young's modulus E_c, Poisson's ratio ν_c and coefficient of thermal expansion $\bar{\alpha}_c$.

If the temperature in the surrounding material is raised at a constant rate φ, it can be shown[43] that failure due to tensile splitting will occur after a time T'' where

$$T''=0{\cdot}19\left[\frac{\frac{1}{\varphi}-\frac{1}{\varphi_f}\cdot\frac{M+5}{M+3}}{\bar{\alpha}_c/\bar{\alpha}_a-1}\right](M+3)v_f \quad (20)$$

in which

$$M=\frac{1+\nu_a}{1-\nu_a}\left(\frac{1+\nu_c}{1+\nu_a}\frac{E_a}{E_c}-1\right) \quad . (21)$$

$$\varphi_f=30f_t\frac{h^2}{R^2}\frac{1-\nu_a}{2E_a\bar{\alpha}_a} \quad (22)$$

and

$$v_f=\frac{1-\nu_a}{E_a\bar{\alpha}_a}\frac{f_t}{0{\cdot}386} \quad . (23)$$

In this expression φ_f and v_f may be regarded as thermal stress resistance factors for the aggregate alone; φ_f is the heating rate required to cause fracture in a sphere of aggregate of radius R heated at a constant rate but without any enveloping concrete and v_f is the temperature of a well-stirred bath of fluid, just sufficiently hot to cause fracture if an aggregate particle is suddenly immersed in the bath.

It is suggested that this quantity T'' may be suitable for use as a thermal stress resistance factor by which the relative performance of different aggregates may be assessed. By this, it is not suggested that the expression gives the actual time of heating required to cause splitting of the aggregate in a concrete member, but that the influence of the various quantities involved will be much the same as in the simplified analysis.

The parameter M will commonly have a value in the range 1–5. Variations in M in the term $(M+5)/(M+3)$ will thus have only minor significance and this term can be put equal to unity. The effect of Poisson's ratio on the quantity M is also an unnecessary refinement in an expression to be used to give an approximate guide to the relative performance of different aggregates. Thus, a new thermal stress resistance factor T' may be written:

$$T'=\left(\frac{1}{\varphi}-\frac{1}{\varphi_f}\right)\left[\frac{\bar{\alpha}_a}{\bar{\alpha}_c-\bar{\alpha}_a}\left(\frac{E_a}{E_c}+2\right)\right]v_f \quad . (24)$$

The terms not included in the square brackets in equation 24 should be found from tests on samples of aggregate: v_f represents the thermal stress resistance of the aggregate alone whilst the term $(1/\varphi-1/\varphi_f)$ shows the effect of heating rate and of particle size. It is seen from equation 22 that, as the size of the aggregate particle is increased, the rate of heating for failure is reduced, consequently reducing the thermal stress resistance factor T'. This suggests that one way in which the occurrence of aggregate splitting may be reduced is to use a smaller maximum size of aggregate in the concrete mix. This also explains why fine-grained aggregates behave better than coarse-grained materials, as suggested by Ingberg's classification.

The thermal stress resistance factor can be expressed in the form

$$T' = \left(\frac{1}{\varphi} - \frac{1}{\varphi_f}\right)\left(\frac{\bar{\alpha}_a}{\bar{\alpha}_p - \bar{\alpha}_a}\right) v_f \, F(g, m) \quad . \quad (25)$$

where the suffix p refers to the cement paste and the last term indicates some function of the volume concentration of aggregate and the modular ratio E_a E_p. This function can be evaluated by using equation 3 and Hirsch's[10] equation for the Young's modulus of concrete. This analysis gives the values shown in Figure 12. It is seen that, as the stiffness of the cement paste is increased in relation to that of the aggregate, the factor T is reduced, showing that the tendency towards splitting is increased. Also, it is possible that splitting may be prevented if the thermal expansion of the cement paste is less than that of the aggregate. This suggests that aggregate splitting is most likely to occur in strong rich mixes, rather than in weaker concretes which would have a high E_a/E_p ratio and considerable drying shrinkage to inhibit splitting. Splitting will also be confined to the early stages of heating when the cement paste has lost little of its combined water and is still expanding.

Conclusion

It has been shown that the individual thermal movements of the cement paste and the aggregate affect the properties and behaviour of concrete in a number of ways. The over-all thermal movement of the concrete determines the magnitude of the thermal stress component of the applied loading, whilst the difference in thermal movements of the constituent materials gives rise to parasitic thermal stresses which, together with any change in the properties of the material on heating, determine the strength of the concrete.

The effect of the parasitic thermal stresses is identical with that caused by an additional hydrostatic loading applied to the concrete, which is tensile when the cement paste shrinks with respect to the aggregate. Thus shrinkage of the cement paste relative to the aggregate causes a reduction in strength under all states of stress. It appears possible that the proportional reduction in strength will be the same for all combinations of stress which cause failure by the same mechanism.

Although expansion of the cement paste in relation to the aggregate can cause an increase in strength if the aggregate-paste bond strength is not exceeded, it does also induce tensile stresses in the aggregate particles. These stresses are additional to those caused by the thermal gradient and rate of heating and may lead to failure by splitting of the aggregate. Consideration of a form of thermal stress resistance factor shows that this tendency is increased by an increase in the rate of heating, the stiffness or thermal expansion of the cement paste, or the maximum size of the aggregate particles. This suggests that the most generally acceptable method of reducing aggregate splitting is to use a smaller size of aggregate in the concrete mix. All other methods lead to a concrete with a low strength or low modulus of elasticity, either of which may be structurally undesirable.

Acknowledgements

The author is indebted to Professor A. D. Ross of University of London, King's College, Professor A. L. L. Baker of University of London, Imperial College, and the Fire Service Research and Training Trust for their help, encouragement and support.

Summary

An attempt is made to review the manner in which thermal volume changes affect the properties of concrete with particular reference to its behaviour at high temperatures. The influence of these changes on thermal expansion and strength of concrete is discussed. In addition, a thermal stress resistance factor is proposed as a means of assessing the relative performance of different aggregates in concrete used at high temperatures or in a fire.

References

1. NEWMAN, K. The structure and engineering properties of concrete. Symposium on the Theory of Arch Dams, Southampton, April 1964.
2. DOUGILL, J. W. Contribution to discussion on a paper by L. C. Snowdon and A. G. Edwards. *Magazine of Concrete Research.* Vol. 16, No. 48. September 1964. pp. 169–170.
3. PHILLEO, R. Some physical properties of concrete at high temperatures. *Journal of the American Concrete Institute. Proceedings* Vol. 54, No. 10. April 1958. pp. 857–864.
4. CRUZ, C. R. An optical method for determining the elastic constants of concrete. *Journal of the PCA Research and Development Laboratories.* Vol. 4, No. 2. May 1962. pp. 24–32.
5. HANSEN, T. C. Creep of concrete—a discussion of some fundamental problems. Bulletin. Swedish Cement and Concrete Research Institute. No. 33. September 1958. pp. 1–48.
6. L'HERMITE, R. Volume changes of concrete. *Proceedings of the Fourth International Symposium on the Chemistry of Cement, Washington, 1960.* Washington, National Bureau of Standards, 1962. Vol. 2. pp. 659–694. Monograph No. 43.
7. KINGERY, W. D. Note on thermal expansion and microstresses in two phase compositions. *Journal of the American Ceramic Society.* Vol. 40, No. 10. October 1957. pp. 351–352.
8. WALKER, S., BLOEM, D. L. and MULLEN, W. G. Effects of temperature changes on concrete as influenced by aggregates. *Journal of the American Concrete Institute. Proceedings* Vol. 48, No. 8. April 1952. pp. 661–680.
9. DOUGILL, J. W. Contribution to the discussion of reference 10. *Journal of the American Concrete Institute. Proceedings* Vol. 59, No. 9. September 1962. p. 1363.
10. HIRSCH, T. J. Modulus of elasticity of concrete affected by elastic moduli of cement paste matrix and aggregate. *Journal of the American Concrete Institute. Proceedings* Vol. 59, No. 3. March 1962. pp. 427–452.
11. ROSS, A. D. The elasticity, creep and shrinkage of concrete. *Proceedings of Conference on the Mechanical Properties of Non-metallic Brittle Materials, London, April,* 1958. London, Butterworths Scientific Publications, 1958. pp. 157–174.
12. PICKETT, G. Effect of aggregate on shrinkage of concrete and a hypothesis concerning shrinkage. *Journal of the American Concrete Institute. Proceedings* Vol. 52, No. 5. January 1956. pp. 581–590.
13. HANSEN, T. C. and NIELSEN, K. E. C. Influence of aggregate properties on concrete shrinkage. *Journal of the American Concrete Institute. Proceedings* Vol. 62, No. 7. July 1965. pp. 783–794.
14. ISHAI, O. Contribution to the discussion of reference 10. *Journal of the American Concrete Institute. Proceedings* Vol. 59, No. 9. September 1962. p. 1365.
15. ISHAI, O. Influence of sand concentrations on deformations of mortar beams under low stresses. *Journal of the American Concrete Institute. Proceedings* Vol. 58, No. 5. November 1961. pp. 611–623.
16. NEWMAN, K. Chapter 8 in *Complex and Meteorophase Materials.* Ed. L. Holliday. Elsevier Publishing Company, 1965. (To be published.)
17. ANSON, M. An investigation into a hypothetical deformation and failure mechanism for concrete. *Magazine of Concrete Research.* Vol. 16, No. 47. June 1964. pp. 73–82.
18. NEVILLE, A. M. Creep of concrete as a function of its cement paste content. *Magazine of Concrete Research.* Vol. 16, No. 46. March 1964. pp. 21–30.
19. STRADLING, R. E. and BRADY, F. L. *Fire resistant construction.* London, H.M.S.O., 1927. Building Research Special Report No. 8. pp. 57.
20. FENNER, C. N. The stability relations of the silica minerals. *American Journal of Science.* 4th Series. Vol. 36, No. 214. 1913. p. 331.
21. MELLOR, J. W. and CAMBELL, A. J. Studies on flint and quartz. *Transactions of the English Ceramic Society.* Vol. 15. 1915–16. p. 80.
22. DAY, A. L., SOSMAN, R. B. and HOSTETTER, J. C. The determination of mineral and rock densities at high temperatures. *American Journal of Science.* 4th Series. Vol. 37. No. 217. 1914. p. 1.
23. MALHOTRA, H. L. The effect of temperature on the compressive strength of concrete. *Magazine of Concrete Research.* Vol. 8, No. 23. August 1956. pp. 85–94.
24. INGBERG, S. H. Influence of mineral composition of aggregates on the fire resistance of concrete. *Proceedings of the American Society for Testing and Materials.* Vol. 29, Part 2. 1929. p. 824.
25. MITCHELL, L. J. Thermal expansion tests on aggregates, neat cements and concretes. *Proceedings of the American Society for Testing and Materials.* Vol. 53. 1953. p. 963.
26. HELMUTH, R. A. Dimensional changes of hardened portland cement pastes caused by temperature changes. *Proceedings of the Highway Research Board.* Vol. 40. 1961. pp. 315–336. Reprinted as P.C.A. Research Department Bulletin No. 129.
27. CROWLEY, M. S. Initial thermal expansion characteristics of insulating refractory concretes. *Bulletin of the American Ceramic Society.* Vol. 35, No. 12. December 1956. pp. 465–468.
28. DOUGILL, J. W. The effects of thermal incompatibility and shrinkage on the strength

of concrete. *Magazine of Concrete Research.* Vol. 13, No. 39. November 1961. pp. 119–124.

29. BAKER, A. L. L. An analysis of deformation and failure characteristics of concrete. *Magazine of Concrete Research.* Vol. 11, No. 33. November 1959. pp. 119–128.
30. LEA, F. C. The effect of temperature on some of the properties of materials. *Engineering.* Vol. 110, No. 2852. 27 August 1920. pp. 293–298.
31. DOUGILL, J. W. *An investigation into the residual compressive strength of concrete after exposure to high temperature.* Thesis presented to the University of London for the degree of M.Sc. (Eng.). 1960.
32. LEA, F. C. and STRADLING, R. E. The resistance to fire of concrete and reinforced concrete. *Engineering.* Vol. 114. No. 2959. 15 September 1922. pp. 341–344. No. 2960. 22 September 1922. pp. 380–382.
33. MILLER, A. L. and FAULKNER, A. F. *A comparison of the effect of high temperature on the concrete of high aluminium and ordinary portland cement.* University of Washington, 1927. Experimental Station Bulletin No. 43.
34. GRUN, R. and BECKMAN, H. The behaviour of cement aggregates and concrete at high temperature. *Cement and Cement Manufacture.* Vol. 3, No. 3. March 1930. pp. 430–442.
35. WOOLSON, I. H. Investigation of the effect of heat on the crushing strength and elastic properties of concrete. *Proceedings of the American Society for Testing and Materials.* Vol. 5. 1905. p. 335.
36. WOOLSON, I. H. Investigation of the thermal conductivity of concrete and the effect of heat on its strength and elastic properties. *Proceedings of the American Society for Testing and Materials.* Vol. 6. 1906. p. 433.
37. PROTZE, H. G. Structural refractory concrete. *Journal of the American Concrete Institute. Proceedings* Vol. 53, No. 9. March 1957. pp. 871–888.
38. VILE, G. W. D. and SIGVALDASON, O. T. Contribution to the discussion of a paper by K. T. Sundara Raja Iyengar, K. Chandrashekhara and R. T. Krishnaswamy which appeared in *Journal of the American Concrete Institute. Proceedings.* Vol. 62, No. 5. February 1965. (To be published.)
39. MCHENRY, D. and KARNI, J. Strength of concrete under combined tensile and compressive stress. *Journal of the American Concrete Institute. Proceedings* Vol. 54, No. 10. April 1958. pp. 829–840.
40. BRESLER, B. and PISTER, K. S. Strength of concrete under combined stresses. *Journal of the American Concrete Institute. Proceedings* Vol. 55, No. 3. September 1958. pp. 321–345.
41. DOUGILL, J. W. Contribution to the discussion of a paper by H. L. Malhotra and R. F. Stevens. *Proceedings of the Institution of Civil Engineers.* Vol. 29. October 1964. pp. 451–452.
42. KINGERY, W. D. Factors affecting thermal stress resistance of ceramic materials. *Journal of the American Ceramic Society.* Vol. 38, No. 1. January 1955. pp. 3–15.
43. DOUGILL, J. W. *A thermal stress resistance factor for aggregate splitting in concrete exposed to fire.* Unpublished note circulated to the Fire Research Station, England, October 1964.

Printed in Great Britain by William Clowes and Sons, Limited, London and Beccles, and published by the Cement and Concrete Association, London.

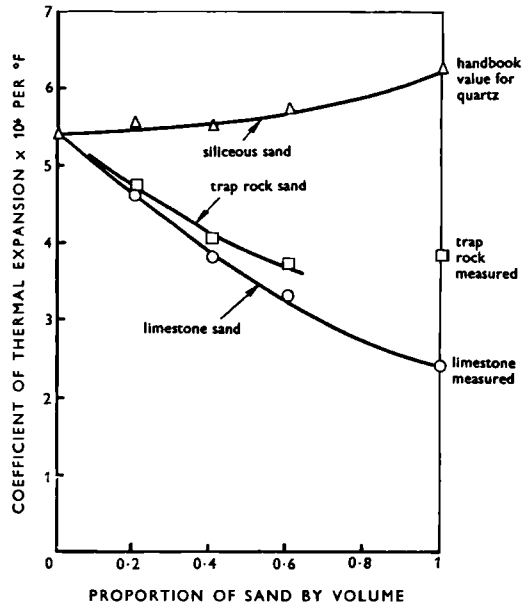


Figure 1a: Relationship between coefficient of thermal expansion of saturated mortar specimens and the proportion of fine aggregate. Water/cement ratio 0·4 by weight. (After Walker et al.[8])

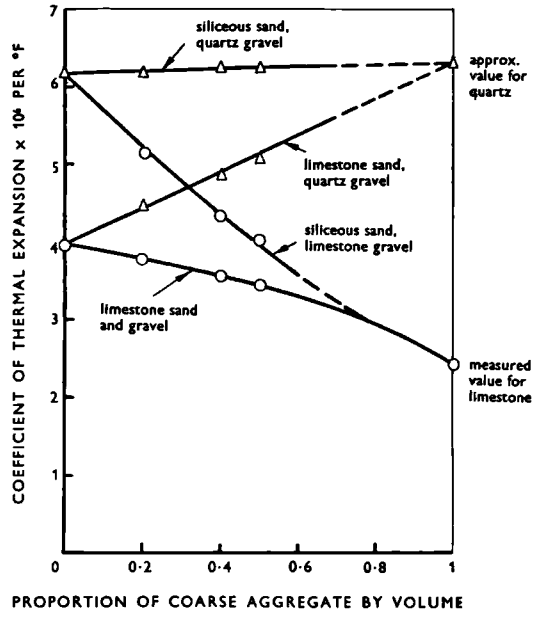


Figure 1b: Relationship between coefficient of thermal expansion of saturated concrete and proportion of coarse aggregate. (After Walker et al.[8])

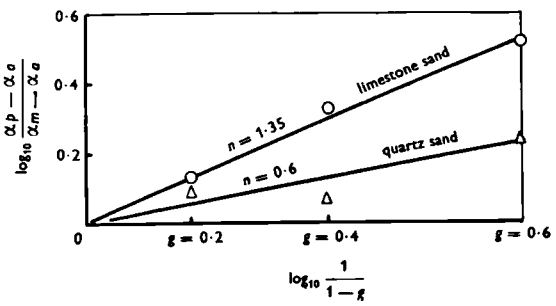


Figure 2a: Pickett plot for coefficient of expansion of mortars made with limestone and quartz sands. Line for trap rock not shown because value of α is uncertain. (After Walker et al.[8])

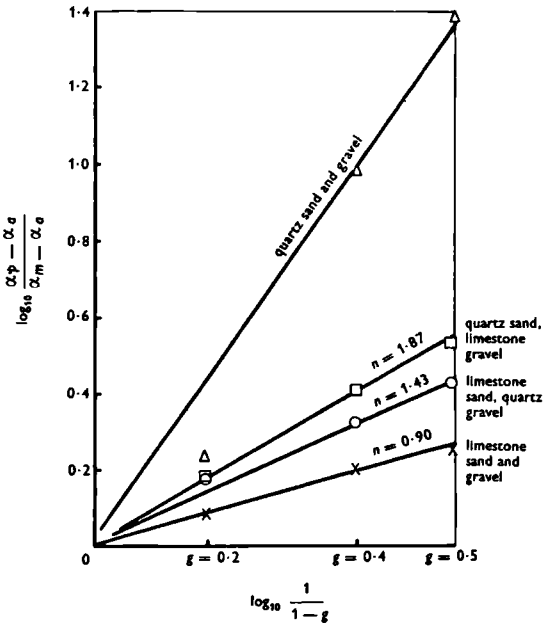


Figure 2b: Pickett plot for coefficient of expansion of oven-dried concretes. (After Walker et al.[8])

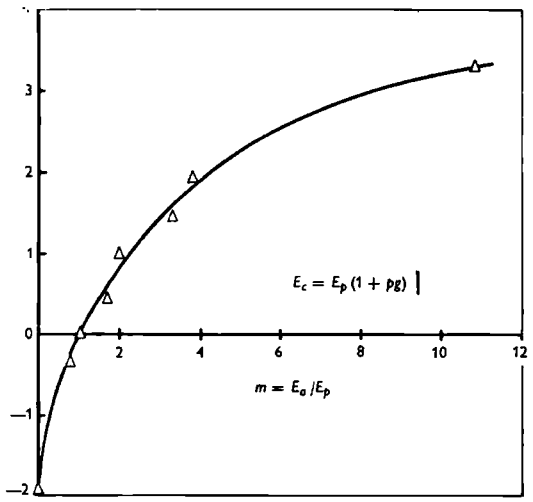


Figure 3: Relationship between Young's modulus of concrete and that of cement paste. $E_c = E_p\ (1+pg)$. *(After Ishai.*[14]*)*

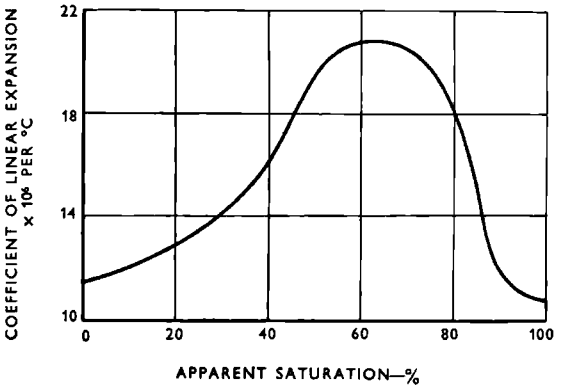


Figure 4: Variation of coefficient of thermal expansion of neat cement paste with moisture content. (After Mitchell.[25]*)*

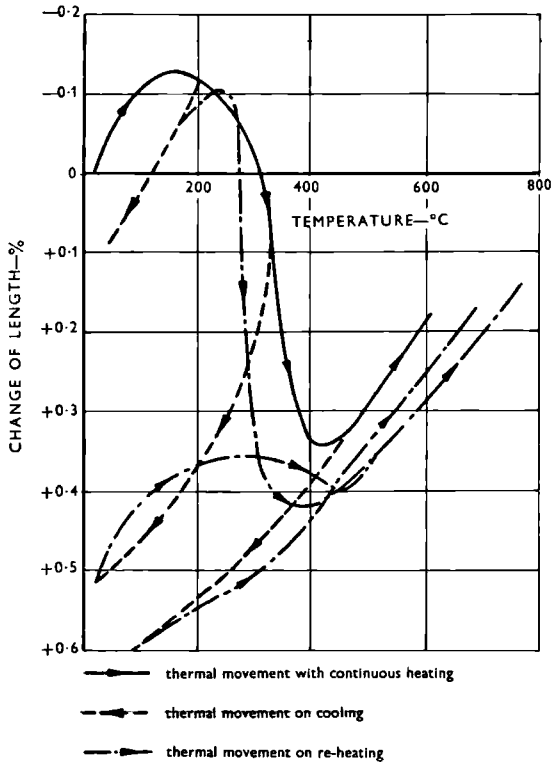
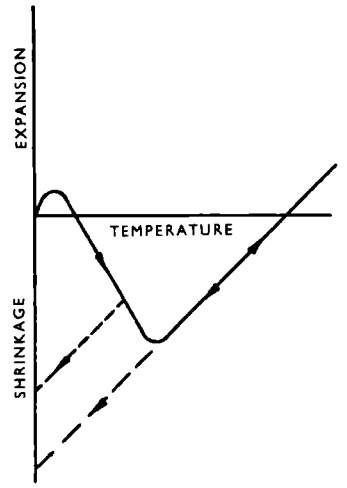
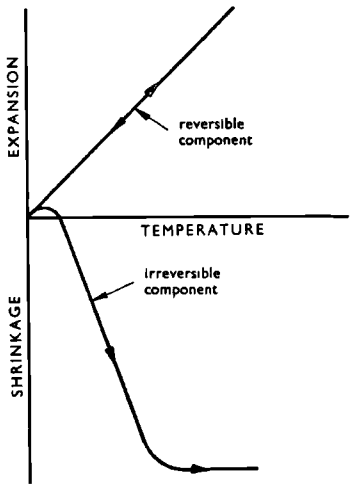


Figure 5: Thermal movements of neat cement pastes during repeated heating and cooling. (After Crowley.[27]*)*



(a) *Total thermal movement*



(b) *Component strains. Irreversible component is curve showing residual strains after cooling from any particular temperature.*

Figure 6: Reversible and irreversible components of the thermal movement of a cement paste.

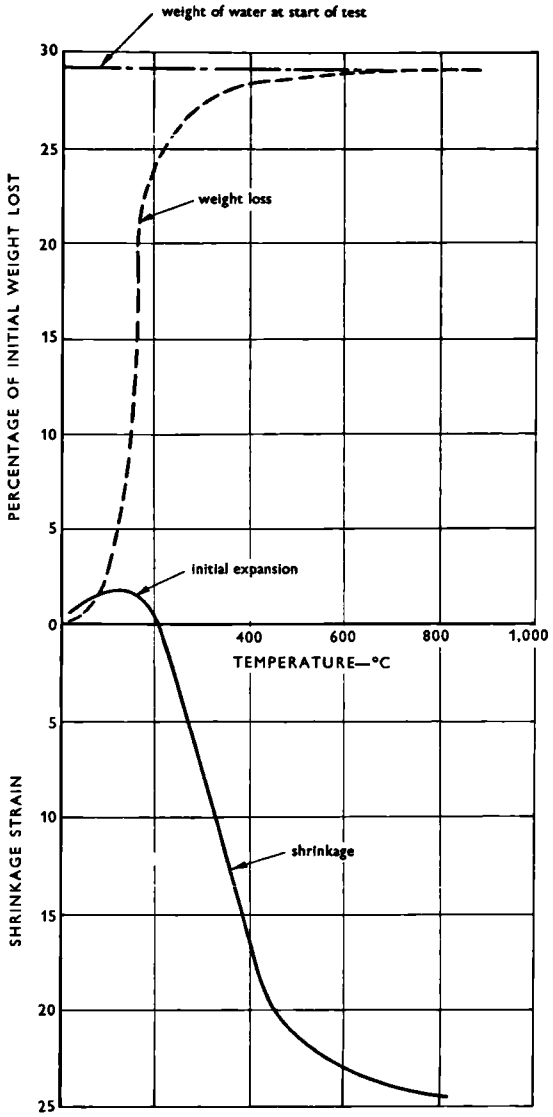


Figure 7: Thermal movement and weight loss during heating for a cement-paste specimen. Water/cement ratio 0·4, cement paste moist-cured tested at 28 days. (After Philleo.[3])

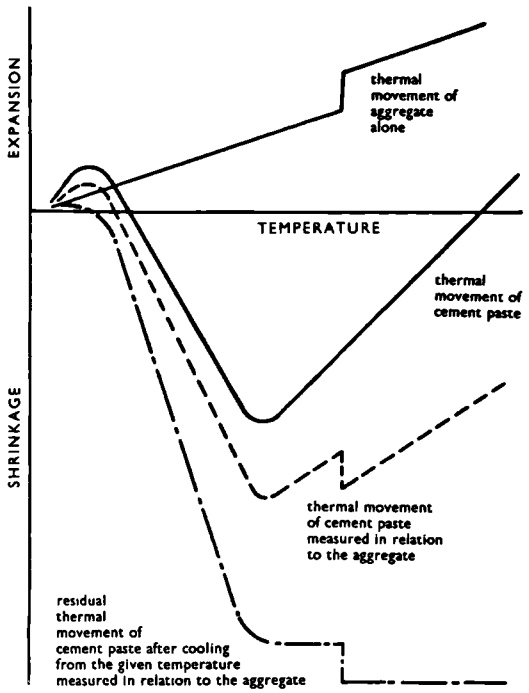


Figure 8: The thermal movements of a cement paste measured relative to a typical siliceous aggregate.

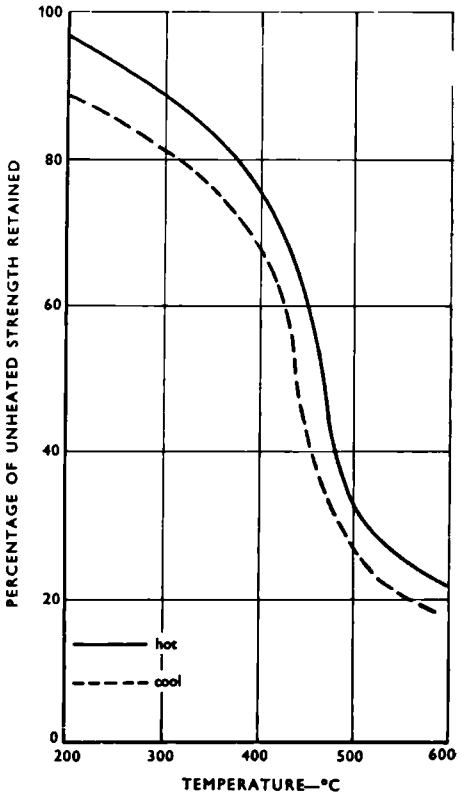


Figure 9: Relationship between strength and temperature for 1:3 concretes made with ordinary Portland cement and crushed when hot and after cooling. (After Malhotra.[23])

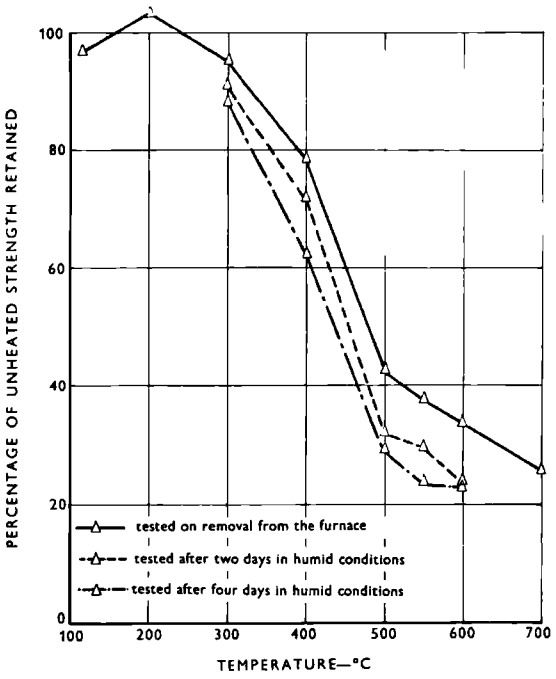


Figure 10: Relationship between strength and temperature for concrete two months old, showing post-cooling losses for cubes stored in a humid atmosphere.[31]

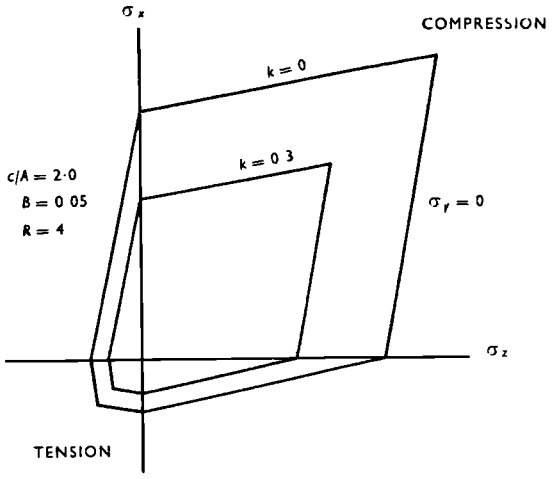


Figure 11: Biaxial strength envelopes derived from equation 17 showing influence of shrinkage on strength. $c/A = 2{\cdot}0$, $B = 0{\cdot}05$, $R = 4$.

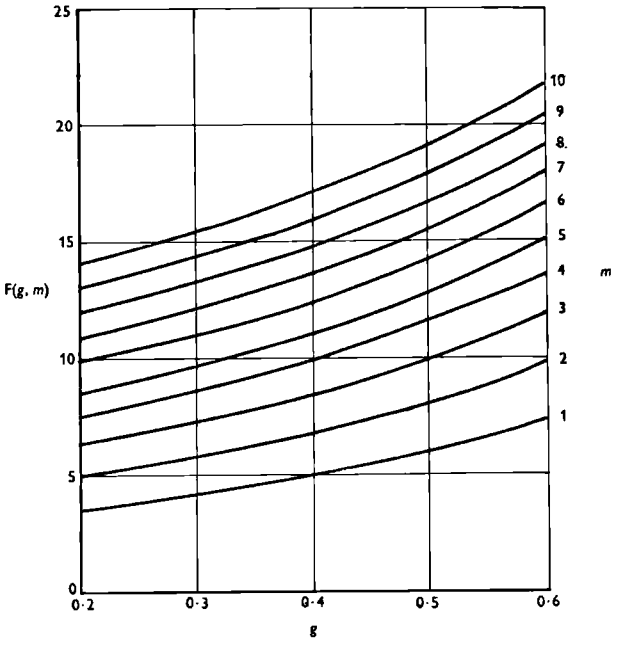


Figure 12: Calculated values of F (g, m) *in equation 25.*

THE RELEVANCE OF THE ESTABLISHED METHOD OF STRUCTURAL FIRE TESTING TO REINFORCED CONCRETE

J. W. DOUGILL

King's College, University of London, U.K.

Received 14 June 1966

IN the early days of reinforced concrete construction, concrete was often considered to be 'fire-proof'. In fact, it was soon apparent that concrete is affected by heating in a similar manner to all other building materials and that some allowance should be made in the design of structures for the possible occurrence of fire.

In general, buildings are designed and constructed to withstand certain specified loadings for an indefinitely long period. This philosophy of design is questionable, even when applied to specified working loads, as it is possible that economies could be made if the design was based on a specified 'useful life' of the structure. However, it is realized that it would be uneconomic to design a building to resist the continued and possibly repeated effects of fire over an indefinite period. The treatment of the influence of fire on a structure is thus fundamentally different from the usual treatment of other loadings. The view is taken that the occurrence of a fire in a building is so unlikely that it is better to insure against the possible financial loss rather than to build the structure to withstand the whole effects of fire. However, some consideration must still be given, in design, to the effects of fire, as it is necessary that the spread of fire should be limited and that any occupants should have enough time to escape before the building collapses.

In practice, these requirements are met by specifying a certain period of fire resistance for each element of the structure. To provide a basis for this approach, the concept of a standard exposure condition has been introduced in the form of a time versus ambient temperature curve.[1] The 'fire resistance' of a structural element is the time during which it continues to perform its function satisfactorily, when heated in this specified manner, in a laboratory test.

† This paper is based on a Lecture presented to the Materials and Testing Group of the Institute of Physics and the Physical Society at the one-day meeting on 'The Physics of Testing Concrete' at the Institution of Civil Engineers on 28 January 1966.

The standard exposure condition is used in all tests for fire resistance, but the type of test and the criterion of satisfactory performance depend on the function of the member in the structure during a fire. This function may be to prevent the spread of fire by dividing the structure into compartments or to carry the dead and superimposed loadings. In this paper only the 'structural fire resistance' of load bearing members is considered and no further attention is given to the thermal fire resistance of separating members, such as wall panels, etc.

Standard fire resistance tests are performed on full size structural elements carrying a load corresponding to the maximum working load on the element in the structure. This loading is maintained constant throughout the test, and the time from the start of heating to final collapse of the member is taken to be the fire resistance.

It is clear that, in its present form, the test has a number of disadvantages. The test is cumbersome, expensive, and requires large specialist apparatus. Also, even if it is assumed that the thermal conditions used in the test are similar to those likely to occur in an actual fire, the application of the results to monolithic construction is entirely artificial and may even be irrelevant. The purpose of this paper is to investigate the relevance of the test for structural fire resistance to the actual behaviour of reinforced concrete structures.

Criteria for assessing the relevance of tests for structural fire resistance

It is clear that the concept of fire resistance is necessary in the design of structures. However, it is not possible to reproduce, in a standard test, all the possible exposure conditions that might occur in an actual fire and thus the results of such a test cannot be considered to be absolute values of fire resistance for a structure. The most that could reasonably be expected is that the results from the standard test should give a quantitative comparison of the behaviour of

different forms of construction exposed to fire. If the test does not provide a true comparison, it is not a suitable basis for structural design.

If the behaviour of different forms of construction is to be compared, it is clear that each individual element should be tested under conditions of restraint which are identical to those offered to the element when this is used as a member in a structure. This is recognized in the Standard[1] which requires that the restraint applied to the test element shall be similar to that applied to the element in service. In direct contradiction, to this however, the Standard also requires that the applied loading shall be kept constant during the test, and it is this condition which is usually satisfied. In general then, the effects of continuity are ignored and the structural element is tested as though it were unrestrained in service. This approach appears to be particularly inappropriate to reinforced concrete with its capacity for large local deformations and the ability to redistribute forces and bending moments within a continuous structure. It is these properties of reinforced concrete that suggest that it is necessary to examine the relevance of the fire resistance test to actual structural behaviour.

u: Cube strength of concrete at normal temperature
f_{sy}: Yield stress of steel at normal temperature
A_{sc}: Area of steel in compression

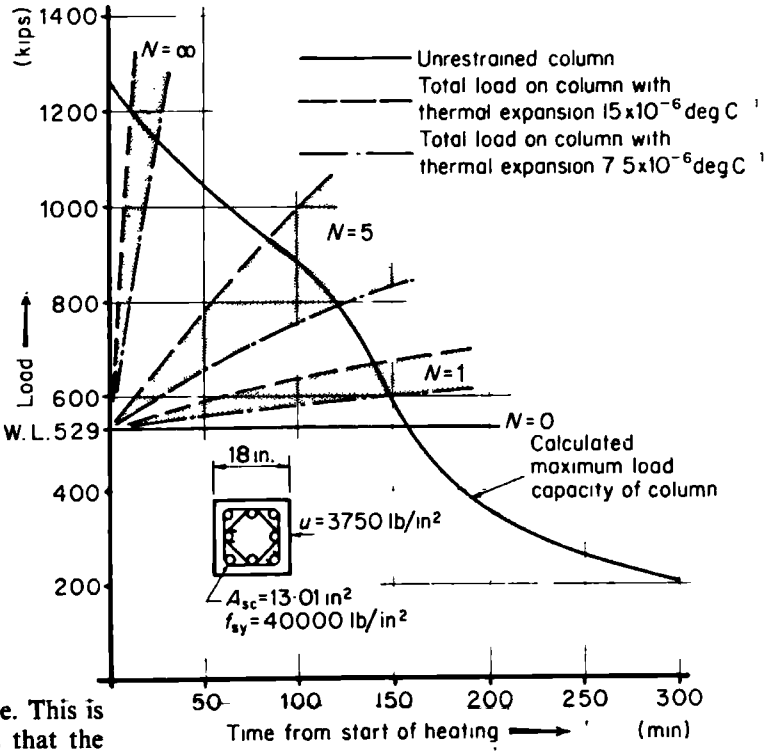


Figure 1. Loads induced in a restrained reinforced concrete column heated according to the standard exposure condition

Structural behaviour of a heated column

One of the few structural elements whose function is purely load bearing and which is invariably continuous is the reinforced concrete column. Consider such a column in a building which is subjected to a local fire in one storey so that only the column is heated and the remainder of the structure is unaffected by heating. The thermal expansion of the column is partially resisted by the axial restraint afforded to the column by the surrounding structure and this causes a load to be induced in the column which is additional to the load carried before heating. This increase in load is not reproduced in the fire resistance test and it is therefore interesting to take a particular example to determine the probable order of magnitude of this additional loading.

Figure 1 shows the loads induced in an 18 in. × 18 in. column, for various degrees of restraint, when this is heated in the standard manner. The column is one of many supporting a beam and slab structure, forming a 20 ft square grid, which is repeated at every floor level in a multi-storey building. The beams are 18 in. square below the 6 in. slab and the storey height is 9·5 ft. The member considered is an internal column reinforced with a large proportion of mild steel and it is assumed that it carries only axial load. The restraint to the column is mainly due to the stiffness of the beams and floors and therefore increases with the number of floors N above the heated column.

The average temperature rise in the column has been estimated from the results obtained by Thomas and Webster[2] in their series of tests on reinforced concrete columns. The loads induced in the column have been calculated assuming linear elastic behaviour of the whole structure. It was also assumed that the stiffness of the column is linearly dependent on temperature and that the stiffness is reduced to half its normal value when the average temperature reaches 460° C. This simple relationship fits the data obtained by Philleo[3] and Cruz[4] for the effect of heating on

Young's modulus of concrete moderately well and is sufficiently precise for the present purpose. The loads have been calculated for two values of the coefficient of thermal expansion (7·5 and 15 $\times$ 10^{-6} deg C^{-1}) for the concrete. Results obtained by Endell[5] suggest that the thermal expansion of most concretes will be between these limits below 450° C and that at higher temperatures the upper value is only likely to be exceeded in a concrete made with a highly siliceous aggregate.

Returning now to consider Figure 1 in more detail, it is seen that the increase in column load can be quite substantial. The restraining effect of five floors above the heated column is sufficient to increase the load to a value 50 per cent greater than the original working load. represented by the line $N = 0$, after less than 2 h heating. It is easier to assess the significance of these increased loadings if they are compared with the maximum load capacity of the column. This is shown in the Figure and has been obtained using the method proposed by Thomas and Webster[2] from the results of their investigation. It can be seen from this result that if failure occurs when the total load on the column equals its maximum load capacity the fire resistance of the column could be seriously reduced by restraint effects.

Although this analysis is quite interesting, it is considered that reinforced concrete structures do not necessarily behave in this way. Failure of reinforced concrete is usually taken to occur when a particular value of ultimate compressive strain is attained in the concrete. This concept is used in reinforced concrete design at normal temperatures, and would be expected to apply at elevated temperatures; the values of the ultimate strain being dependent on temperature. It is thus necessary to revise the analysis, leading to the results outlined in Figure 1, to include the behaviour of the column after the maximum load capacity has been equalled by the total imposed loading and until the ultimate concrete strain is achieved.

In order to do this it is necessary to assume the form of the stress–strain curve for a reinforced concrete column under a compressive load at high temperatures. The assumed relationship is shown in Figure 2. The form of the curve comprising initial approximately linear behaviour, attainment of a maximum stress, and a descending portion is well known at normal temperatures, although the slope of the descending portion may be much reduced for loadings applied slowly and over a considerable period. At higher temperatures both the modulus of elasticity[3, 4] and the maximum compressive stress[6, 8] are known to be reduced and it appears reasonable to assume that the stress–strain curves would have the same form as that obtained at a lower temperature, if the effect of thermal expansion is excluded from the total strain. At present there are few experimental data available to test this assumption. Harada[9] has obtained the stress–strain curve for concrete in compression after cooling the specimens from high temperatures. The form of the curves obtained are similar to those shown, although no information could be obtained for strains beyond that corresponding to the maximum compressive stress. Recently Harmathy and Berndt[10] have published some results for the complete stress–strain curves of a hydrated cement paste and a lightweight expanded shale aggregate concrete for temperatures up to 760° C. These results indicate that there is an increase in deformation at fracture with increase in temperature, the curves showing only a gradual descent with increasing strain. However, it is difficult to know to what extent these last results are applicable to normal concrete, especially in those portions of the stress–strain curve which are influenced by cracking and failure. In spite of this, it is felt that the assumed curves gain some support from these results.

Consider a single heated column in the building frame shown in Figure 3. The structure surrounding the column is unaffected by heating and is assumed to behave linearly with respect to a load applied at the position and in the direction of the column. The column carries a load P_v when the average temperature in the column is $\bar{v}$ and the strain in the column is the sum of the free thermal expansion $\alpha\bar{v}$ and the compressive strain ε due to the load P_v. Before heating, the column carries a load P_0, the corresponding strain being ε_0. The condition for the displacements of the column and the surrounding structure to be compatible can be put in the form

$$\left(1 + \frac{1}{R}\right) + \frac{\alpha\bar{v}}{\varepsilon_0} = \frac{\varepsilon}{\varepsilon_0} + \frac{P_v}{RP_0} \qquad \ldots (1)$$

where R is the ratio of the loads required, at the position and in the line of the column, to induce unit deflection of the surrounding structure and the unheated column when these are considered separately and disconnected. The ratio R is thus a measure of the restraint offered to the column by the rest of the structure and will be termed the relative stiffness of the surrounding structure.

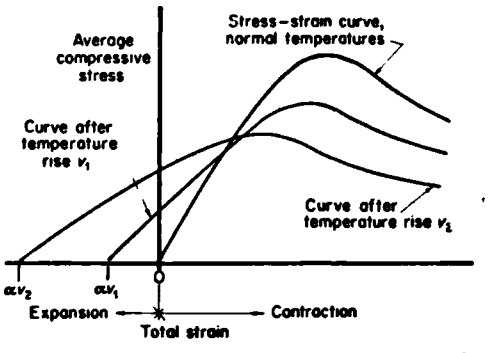


Figure 2. Probable form of stress—strain curves for a reinforced concrete column tested in compression at various temperature levels

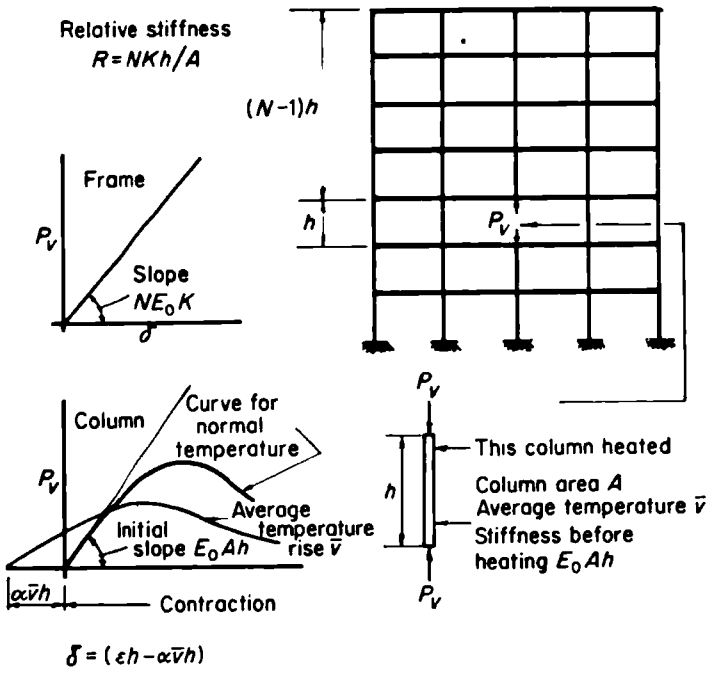


Figure 3. Structural arrangement of building frame and heated column

The equation of compatibility can be solved by means of the graphical construction shown in Figure 4. The separate terms of equation (1) are shown in the Figure, the term $(1 + 1/R)$ being obtained from the load deformation curve for the unheated column. This construction is similar to that used by Sigvaldason[11] to explain the behaviour of a conventional testing machine and, on consideration, it is clear that the complete structural system behaves in the same way as an analogous testing machine in which the machine frame represents the surrounding structure, the test specimen represents the column, and the load is applied by thermal expansion instead of the usual hydraulic ram. One of the peculiarities of a compression testing machine is the possibility that the machine components may not have sufficient stiffness, compared with that of the specimen, to enable the ultimate strain to be reached. Similar behaviour may be expected in the structure considered, so that it is unlikely that the ultimate strain of the column can be reached when there is little restraint: that is, for low values of the relative stiffness R.

Effects of restraint on mode of failure

In Figure 5, the loads and strains at failure are shown when the ultimate strain has been reached. In this case, the analogous testing machine would be termed 'hard'[12] as it has sufficient stiffness to enable the specimen to reach its ultimate strain ε_u. The term 'stiff' will be used to describe the structure which is similarly hard. Now consider Figure 6. It is clear that the line representing the load–deformation relationship for the surrounding structure (i.e. the line with slope $-R$) cannot intersect that for the column if the temperature is increased, no matter how small the increase. Thus, the column and the surrounding structure cannot remain compatible at higher temperatures and failure occurs immediately after the last possible equilibrium position. The structure will be termed 'flexible' when the relative stiffness R is less than the value indicated. The lower limit of a flexible structure ($R = 0$) applies to an unrestrained column.

The stiff structure has a single equilibrium position for each temperature, until the ultimate strain is reached. It is not possible to find an equilibrium position for a flexible structure above a certain value of thermal strain, even though the limiting strain is not exceeded. With an intermediate structure, more than one possible equilibrium position exists and the column is unstable between them. Here, the load-deformation curve for the structure intersects the descending portion of the curve for the column in more than one point. The range of relative stiffness for the three possible grades of structure is illustrated in Figure 7. It will be noted that a structure which is 'flexible' at low temperatures may become 'stiff' as the temperature is increased. The terms are relative and depend on a comparison between the initial stiffness of the structure and the stiffness of the column at the relevant temperature.

A column in a flexible structure will fail at a load not very much below the maximum load capacity of the column. It is, therefore, a reasonable approximation to assume that failure occurs when the total load on a column equals its maximum load capacity, if the column is part of a flexible structure. In these circum-

stances, the results for the effects of induced loading on fire resistance shown in Figure 1 adequately represent actual structural behaviour.

On the other hand, for the assumed conditions of local heating, the load at failure on a column in a stiff structure will be small, as the surrounding structure will relieve the column of much of its load. The

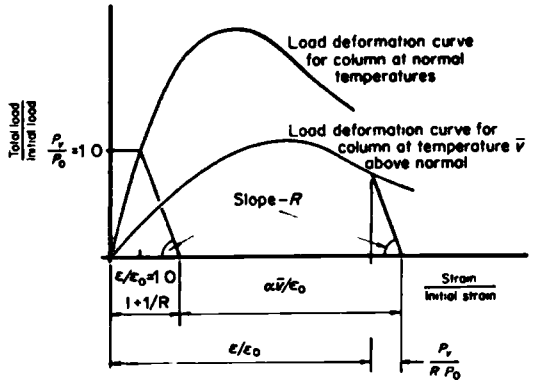


Figure 4. Loads and strains in a heated column

criterion for ultimate collapse is one of limiting strain and it is seen from the relevant figure (Figure 5) that if the relative stiffness R is increased the thermal strain ($\alpha\bar{v}$) at failure must also increase. This strain is a measure of temperature and time of exposure and it is therefore considered extremely probable that a column in a stiff structure will have a longer period of fire resistance than a similar column in a structure which is less stiff.

Effect of more general heating

So far the discussion has been confined to the case in which only one column in the entire structure is affected by heating. This is clearly an extreme case and as such is unlikely to occur in practice. The other possible extreme is obtained when all the columns in any one storey height are heated equally, so that there is no restraint to expansion in that storey. It is clear that this condition is also not likely to occur in practice and that the most likely distribution of heating

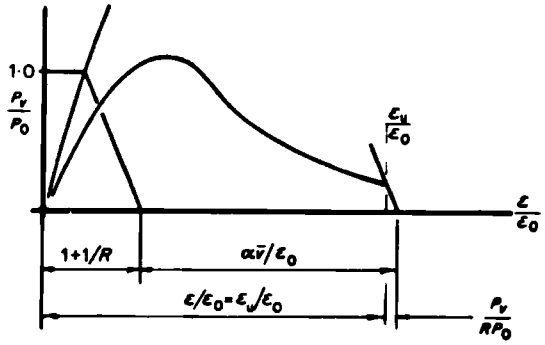


Figure 5. Loads and strains at failure of a column in a stiff structure

will be somewhere between these two extremes. It is thought that the distribution of heating in a large building is more likely to be effectively local in character due to the time required for the fire to spread from place to place. This is even more likely if the building is divided by walls and partitions which delay, or prevent, the spread of fire.

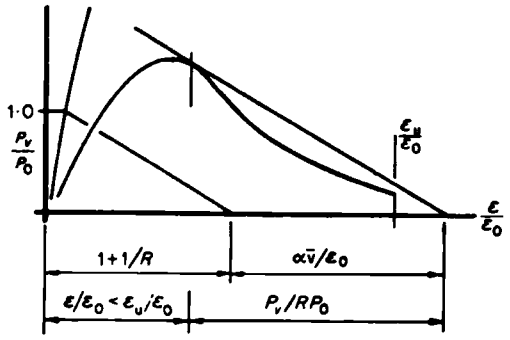


Figure 6. Loads and strains at failure of a column in a flexible structure

If more than one column is heated the combined stiffness of the heated columns is increased at the expense of that of the surrounding structure and the value of the effective relative stiffness R is reduced. The effect of increasing the number of heated columns is thus the same as reducing the stiffness of the structure in the analysis of any single column.

Relevance of tests for structural fire resistance

It is seen from the previous discussion that columns which are heated in a structure which behaves in a flexible manner eventually fail by the same mechanism of longitudinal instability as do the unrestrained columns in the standard fire test. However, the standard test does not include the effects of local heating which can induce additional loads in a column and a corresponding reduction in fire resistance. This would not be a serious disadvantage if enough was known of the material properties of concrete and steel at high temperatures to establish criteria in order to determine whether a structure would behave as 'flexible' or 'stiff' when heated in a given manner. If such criteria existed, and it was known that the struc-

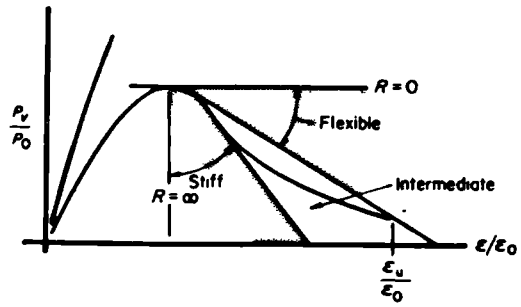


Figure 7. Limiting values of relative stiffness for different modes of structural behaviour

ture was flexible at high temperatures, an estimate of the reduction in fire resistance due to restraint could easily be made using existing test data.

The standard test for structural fire resistance is clearly relevant to flexible structures. However, it is suggested that most heavily loaded columns in multi-storey buildings form part of a very stiff structure. Here the results of tests on unrestrained columns are completely irrelevant. The mode of failure and the load on the columns during heating is different and direct application of the results of fire tests on columns free to expand to columns under considerable restraint is not justified and may be considerably in error. As yet, the data required for a quantitative assessment of the behaviour of a member which is heated in a stiff structure are not available and cannot be obtained by the usual test procedure.

It is also apparent that the standard test does not necessarily provide a valid comparison between different forms of construction. These could have widely differing stiffnesses which would affect their behaviour as part of a structural system but have no influence on the result from the standard test. Comparisons based on the standard test between structural elements which have the same function but are made from fundamentally different materials could also be very misleading.

Conclusion

Although the problems associated with interpreting the results of structural fire tests have been covered in some detail, the discussion must necessarily be inconclusive due to the present lack of data on the material properties of concrete at high temperatures. It is clear, however, that the usual tests for structural fire resistance have only limited relevance to monolithic construction such as reinforced concrete. This, in itself, is an important conclusion, as the general character of the basic tests for fire resistance has remained unchanged since the earliest days of reinforced concrete construction[13] and most of our knowledge of the effects of fire on reinforced concrete has been obtained from such tests.

REFERENCES

1. British Standards Institution. 'Fire tests on buildi g materials and structures.' Part 1, *BS4 76:1953* (B.S ', London)
2. THOMAS, F. G., and WEBSTER, C. T. 'Investigations on building fires. Part VI.' *National Building Studies Research Paper* **18** (H M.S.O., London, 1953)
3. PHILLEO, R. 'Some physical properties of Concrete at high temperatures.' *A.C.I. Journ. Proc.* **54**, 857 (1958)
4. CRUZ, C. R. 'An optical method for determining the elastic constants of concrete.' *Journ. P.C.A. Res. Dev. Lab.* **4**, No. 2, 24 (1962)
5. ENDELL, K. 'Determination of the extension and structure of concrete materials and cement mortars under the influence of heating to 1200 C.' *Deutscher Ausschuss fur Stahlbeton*, Vol. 60 (Berlin, 1929)
6. LEA, F. C. 'The effect of temperature on some of the properties of materials.' *Engineering* **110**, 293 (1920).
7. GRUN, R., and BECKMAN, H. 'The behaviour of cement aggregates and concrete at high temperatures.' *Cement & Cement Manuf.* 3, 430 (1930)
8. MALHOTRA, H L. 'The effect of temperature on the compressive strength of concrete. *Mag. Concrete Res.* **8**, No. 23, 85 (1956)
9. HARADA, T 'Variation in strength and elasticity of concrete heated to high temperatures.' *Trans. archit. Inst. Japan* No. 47, 11 (Sept. 1953); No. 48, 1 (March 1954); No. 56, 1 (June 1957)
10. HARMATHY, T. Z., and BERNDT, J. E. 'Hydrated Portland cement and lightweight concrete at elevated temperatures.' *Proc. A.C.I.* 63, 93 (1966)
11. SIGVALDASON, Q. T. 'The influence of the testing machine on the compressive strength of concrete.' Paper presented to the Symposium on Concrete Quality organized by the Cement and Concrete Association in London, Nov. 1964. To be published.
12. FREUDENTHAL, A. M. *The Inelastic Behaviour of Engineering Materials and Structures*, 1st Ed., p. 530 (Wiley, New York, 1950)
13. BAUSCHINGER, J. *Mitt. Mech. Tech. Lab. D.K. Tech. Hochschule, München*, Vol. 12 (1885). Vol. 15 (1887). Reported by Singleton-Green, J. 'Reinforced Concrete and Fire Resistance. Part V.' *Concrete and construction. Engng* **18**, 75 (1923)

Bull. Mech. Engng Educ. Vol. 6, pp. 325-331. Pergamon Press 1967. Printed in Great Britain

AN EXPERIMENT TO DETERMINE THE ELASTIC CONSTANTS OF A TRANSVERSELY ISOTROPIC MATERIAL

J. W. DOUGILL*

(*Received* 26 *May* 1967)

Abstract—The paper describes an experiment to determine the five independent elastic constants of a linear elastic transversely isotropic material comprising a silicone rubber/Perspex laminate. In addition an outline of the basic theory is given as well as details of the method used to manufacture the laminated specimens.

ALTHOUGH most undergraduate courses in strength of materials or stress analysis are principally concerned with isotropic materials the student's appreciation of the basic assumptions in the theory and of mechanical behaviour can be broadened by suitable laboratory tests on an aeolotropic material. Possibly the simplest of these is the transversely isotropic material. This Note describes an experiment to determine the five independent elastic constants required to define the stress v. strain relationship for a linear elastic transversely isotropic material. Although the experiment described has some deficiencies, it has been performed by both Civil and Mechanical engineering students for the past two years with reasonable success. An elementary derivation of the form of the generalised Hooke's Law for a transversely isotropic material is outlined in Appendix A.

The specimens used in the experiment are shown in Fig. 1 and comprise 4 in. cubes of a Perspex/silicone-rubber laminate. Two forms of specimen are used, one with the plane of laminations parallel to one pair of sides of the cube and the other having the laminations inclined at an angle of 45° to two pairs of sides and at right angles to the third. The method of manufacture of these specimens is outlined in Appendix B.

The experiment consists of three separate tests with the different arrangements of specimens shown in Fig. 2. In the first test, three specimens are loaded in compression in a direction parallel to the laminations. Strains are measured by means of a 2 in. gauge length demountable gauge (Demec by W. H. Mayes and Son) in the directions x, y, z (shown in the figure) on all accessible faces of the central cube. This test is then repeated with the specimens arranged so that the loading is applied in the direction z, i.e. perpendicular to the laminations.

Typical results from these first two tests are shown in Figs. 3 and 4. Using these results it is possible to obtain the elastic constants connecting direct stress and direct strain in the material. Noting that the direction z is normal to the plane of the laminations, the statement of Hooke's Law takes the form:

$$\begin{bmatrix} \epsilon_{xx} \\ \epsilon_{yy} \\ \epsilon_{zz} \\ \gamma_{xy} \\ \gamma_{yz} \\ \gamma_{zx} \end{bmatrix} = \begin{bmatrix} P & P-R/2 & S & 0 & 0 & 0 \\ P-R/2 & P & S & 0 & 0 & 0 \\ S & S & Q & 0 & 0 & 0 \\ 0 & 0 & 0 & R & 0 & 0 \\ 0 & 0 & 0 & 0 & T & 0 \\ 0 & 0 & 0 & 0 & 0 & T \end{bmatrix} \begin{bmatrix} \sigma_{xx} \\ \sigma_{yy} \\ \sigma_{zz} \\ \tau_{xy} \\ \tau_{yz} \\ \tau_{zx} \end{bmatrix}$$

* University of London King's College Department of Civil Engineering.

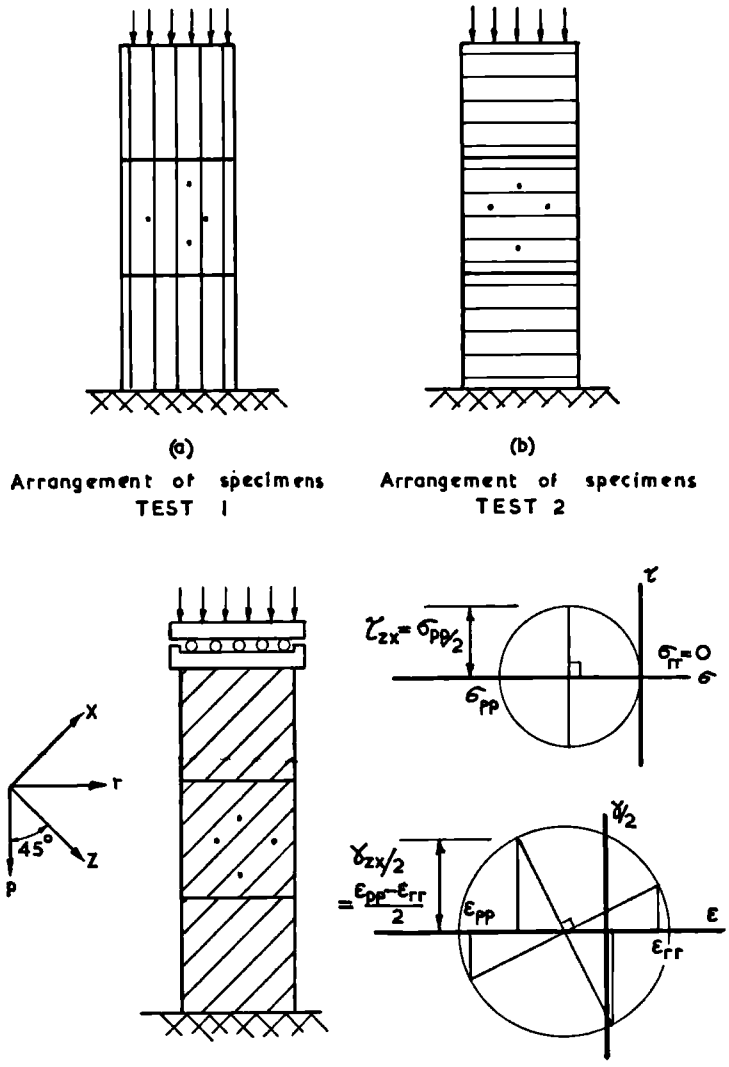


FIG. 2. Arrangement of specimens for each test.

Considering the results of the first test, in which σ_{zz} is the only stress acting on the specimen, we find:

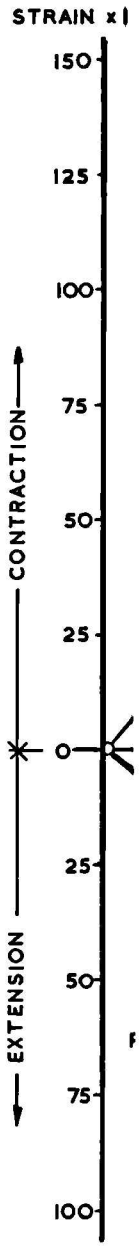
$\frac{1}{P}$ = the effective Young's Modulus for loading in the x or y directions = $2{\cdot}46 \times 10^5$ lb/in.^{2}

Also $(P\text{-}R/2) = -2{\cdot}82 \times 10^{-6}$ in.^{2}/lb so that

$\frac{1}{R}$ = effective shear modulus for the xy plane = $0{\cdot}73 \times 10^5$ lb/in.^{2}

$\frac{1}{S} = -3{\cdot}9 \times 10^5$ lb/in.^{2}

$-\epsilon_{zz}/\epsilon_{xx}$ = An effective Poisson's Ratio for loading in the x or y direction = 0·63.



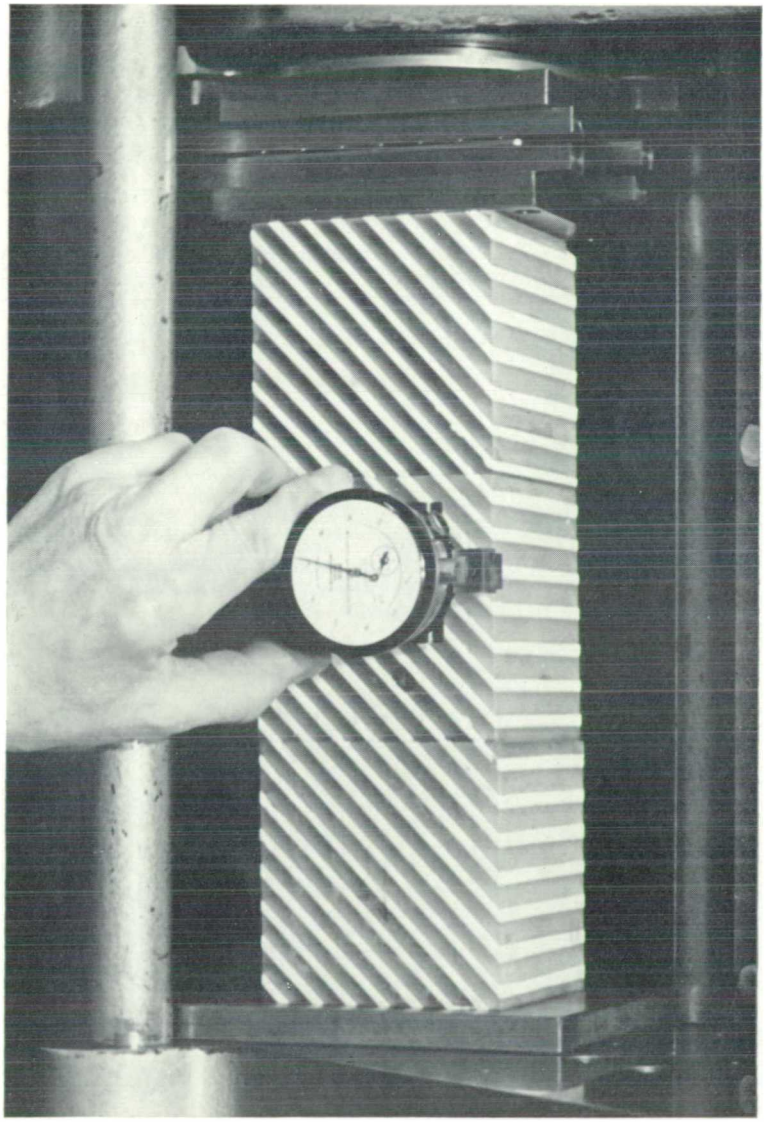


FIG. 1.

This last result i
the behaviour of th
have a value of Poi
that the material mu
condition for the tr

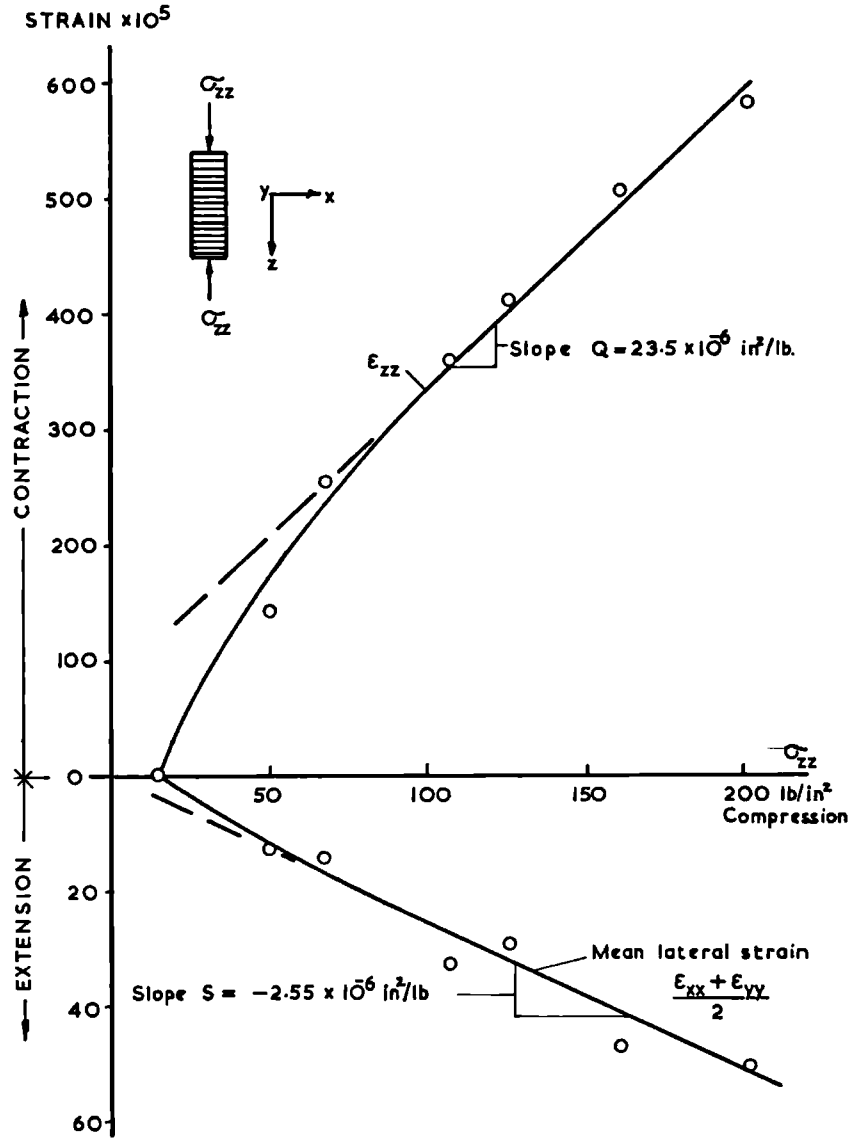


FIG. 4. Results of Test 2—The initial non-linear, apparently strain hardening, portion of the curves is probably due to the end faces of the cubes not being truly parallel. Accordingly, this portion is neglected in assessing the values of the constants.

From the results of the second test in which σ_{zz} is the only stress acting it is found that $1/S = -3{\cdot}9 \times 10^5$ lb/in.^{2} and $\frac{1}{Q} = 0{\cdot}43 \times 10^5$ lb/in.^{2}. Here, the approximate agreement between the values of S from the two tests is a direct demonstration of the Reciprocal Theorem. Also, the low value of the effective Young's Modulus for loading applied normal to the laminations could be expected from elementary structural considerations.

The third test was devised in order that the shear modulus $1/T$ could be determined

from observations in a simple compression test. In this way the same testing machine is conveniently used for all three tests. In this third test, the specimens are arranged as shown in Fig. 2c and are loaded in a vertical direction at 45° to the plane of the laminations. If the applied vertical stress is σ_r the shear stress τ_{zx} equals $\frac{1}{2}\sigma_r$. The shear strain γ_{zx} is most easily obtained as the difference between the direct strains measured in the vertical and horizontal directions (i.e. directions r and p respectively in the figure).

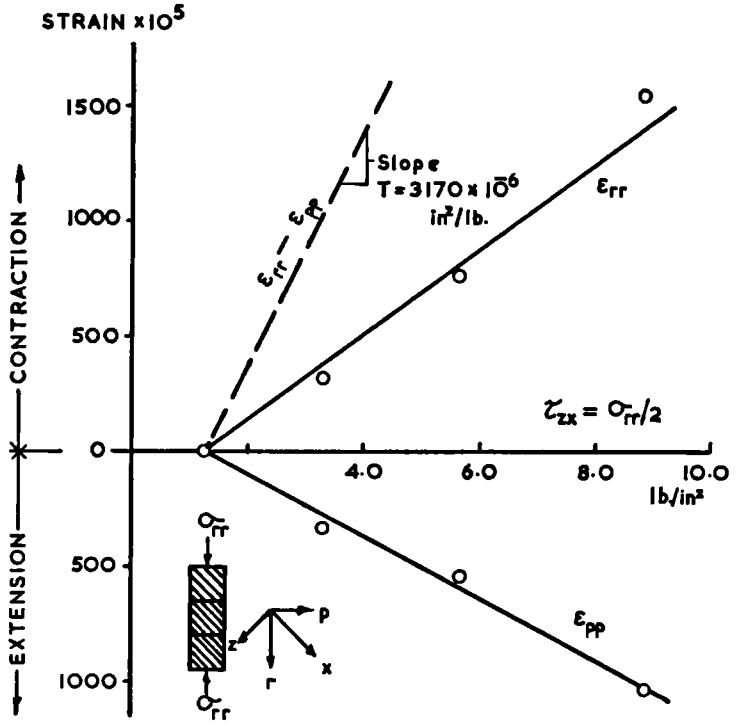


FIG. 5. Results of Test 3.

Because of the low shear modulus of the silicone rubber the shear strains are comparatively large for only small values of the applied load and it becomes important to ensure that the deformation is not restrained by the testing machine platen. This is done by loading the specimen through a platen mounted on roller bearings which thus allows free lateral displacement of the end of the composite test specimen. The results of this test are shown in Fig. 5 from which a value of the shear modulus $1/T$ is found to be 316 lb/in.^{2}. All five independent elastic constants of the material are thus determined.

The experiment could probably be improved by using a more sophisticated method of strain measurement, as some unavoidable scatter of results is obtained by students using the demountable gauge on a relatively soft specimen. However, the variations in reading caused by different "holding pressures" do not obscure the general trend. A more fundamental disadvantage of the present arrangement is that the specimens are far from homogeneous and that the thickness of the laminations, $\frac{1}{4}$ in. and $\frac{1}{8}$ in. for the Perspex and rubber respectively, is not insignificant compared with the 2 in. gauge length used. Also the gauge points for the demountable gauge can only be accommodated in the Perspex and

REPRINTED FROM *MAGAZINE OF CONCRETE RESEARCH*. VOL. 19, No. 60. SEPTEMBER 1967. pp. 135-142

UDC 666.94: 666.971.001.57: 624.043

MCR
145
REPRINT

A mathematical model for the failure of cement paste and mortars

by John W. Dougill, MSc(Eng), DIC, AMICE

UNIVERSITY OF LONDON: KING'S COLLEGE

SUMMARY

It is suggested that structural models have only a limited use in a study of failure and an alternative mathematical model is proposed which behaves, in many ways, like hardened cement paste or mortar. The model is similar to Volkov's normal micro-inhomogeneous material, the major difference being in the failure criteria used at the microscopic level. The behaviour of the model material in simple tension is studied and it is shown that progressive fracture, or micro-cracking, occurs during all stages of loading. The mode of failure depends upon the method of test because either the material fails when the maximum stress is reached or progressive fracture continues with increased deformation and a reduction in applied stress. In addition, a ductile mode of failure is investigated and it appears that, in contrast to brittle fracture, the ultimate strength may be almost unaffected by micro-inhomogeneity.

Introduction

Although there has been a large number of investigations to determine the mechanism of failure in concrete, many problems still remain, amongst which is that of determining a satisfactory criterion for the strength of concrete subject to a completely general stress system. The term 'concrete' describes a whole family of materials with widely different properties and varying degrees of heterogeneity, depending upon the proportions and grading of the aggregate in the mix. Ideally, any theory of failure or failure criterion should describe the behaviour of the whole range of possible materials. Clearly an experimental solution leading to purely empirical criteria is always possible but, because concrete comprises a continuous range of different materials, it seems essential that there should be some unified theory to complement the experimental work.

The same difficulty occurs in other branches of concrete research, for example in studies of the modulus of elasticity of concrete or of its time-dependent deformation under load. In these, it has been possible to develop a unified theory by considering the behaviour of models with an idealized structure and composition, and remarkably good agreement has been obtained between observed strains and predictions from model analysis, even when quite different structural arrangements are used.[1, 2] This is extremely useful, but it suggests that the model approach is only successful because the total deformation of concrete is relatively insensitive to changes in structural form, provided the relative proportions of the constituents remain unchanged. Failure, however, is likely to be particularly sensitive to structural form, because the occurrence of a brittle mode will depend upon the magnitude and distribution of local stresses in the material and not directly upon their cumulative effect throughout the volume. Thus, it is clear that simple structural models can have only a limited use in a study of failure.

Despite these limitations, models have been used successfully to explain and demonstrate particular aspects of deformation and failure[3]. Thus, Reinius's model[4] was developed as an idealization of the structure of cement paste, whereas Baker's lattice[5] is a simplified analogue for concrete which demonstrates the general effect of the hard aggregate particles upon the stress distribution. However, a comprehensive model would need to include all these characteristics, and many more besides, and would almost certainly become unmanageable.

Although the concept of a structural model has to be discarded, it is still necessary to make a number of assumptions and idealizations if a theoretical treatment is to be used. In a sense, these assumptions define the relevant properties of an artificial, but imaginary, material which may be examined theoretically to obtain results which may then be compared with experimental values obtained with real materials. This is the

approach used by Brandtzaeg[6] in developing what must still be regarded as the most complete theory for the deformation and failure of concrete. The purpose of this paper is to develop an alternative mathematical model, particularly designed to illustrate the effects of heterogeneity in the cement paste and concrete structure. The present paper is principally concerned with the behaviour of cement paste and mortar under simple stress conditions. The extension to concrete and combined stresses will be the subject of a separate paper.

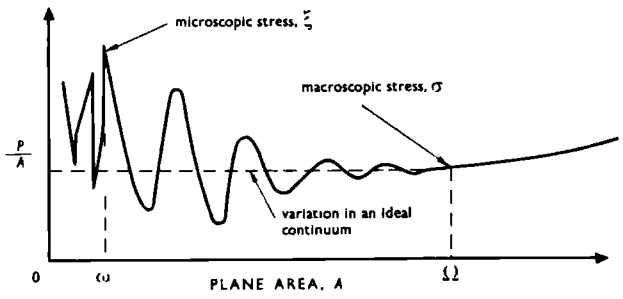


Figure 1: Definitions of stress.

The micro-inhomogeneous material

In defining stress in a continuum, the following procedure is generally used. The internal forces acting on one side of a plane area, A, containing the point where the stress is to be determined, are considered. The resultant of these forces is P. Then, the limiting value of P/A found as the area is made infinitely small is the value of the stress at the point about which the area has been made to vanish. This definition is not necessarily satisfactory for real materials, as it requires the internal forces to be continuously distributed throughout the material.

Figure 1 illustrates the general result obtained when an attempt is made to approach a limiting value for stress in a heterogeneous material whose structural components are all of microscopic dimensions. As the area A is reduced from a reasonably large value, the quantity P/A first changes monotonically and appears to be approaching a limiting value. However, as the area considered is reduced below some rather indeterminate value Ω, the effects of local variations in structure assume greater importance and the variation in P/A is both more rapid and less predictable. As the area considered is further reduced, the range and rate of variation of P/A increase until the area considered approaches a value ω corresponding to the smallest region in which it is permissible to treat the material as being continuous.

Following Volkov[7], we define a macroscopic stress σ by the value of P/A obtained when A equals Ω. In most practical circumstances, in which Ω and the stress gradients are both small, the value of the macroscopic stress will be very close to the value conventionally regarded as stress at a point.

The material of the mathematical model is assumed to be made up of a large number of identical elements, each having linear dimensions of order $\sqrt{\Omega}$, which are small in comparison with the over-all dimensions of the body. Each of these elements is itself regarded as being composed of a large number of microscopic elements, each of which is subjected to a microscopic stress ξ given by the value of P/A when the area is reduced to ω. The sizes of the two types of element are so chosen that Ω is very much larger than ω and it is permissible to represent the range of values of micro-stress, in any major element, by a continuous function for the relative frequency density. It is also evident that σ is the mean value of ξ throughout a major element.

It now remains to specify the distribution of micro-stress in any major element and adopt a criterion for failure at the microscopic level in such a way that the model may be representative of real materials. No information is available on the distribution of micro-stresses, although Volkov[7] quotes a number of Russian sources who claim to have obtained an approximately normal distribution of surface strain at the microscopic level. Recent work by Esin and Jones,[8] using a replica technique on aluminium samples, tends to confirm these results. However, this may not be conclusive if the effective gauge length is not small enough, because a real departure from the normal distribution may be obscured according to the central limit theorem. Despite this lack of information, the micro-stresses will be taken to be normally distributed on any plane within a major volume element.

There are also difficulties involved in specifying a suitable criterion for failure of the microscopic elements if the model is to represent a material like hardened cement paste. Here, the material contains a vast number of gel and capillary pores of various dimensions, and it would seem unreasonable to adopt a criterion which depended upon the onset of instability[9] or the rupture of molecular bonds[10] at the boundary of any single flaw. A maximum tensile stress criterion is adopted for the model so that any microscopic element fails when the direct stress ξ reaches a value q_t, the intrinsic tensile strength of the material. It is assumed that q_t is constant, although a more realistic model would require the intrinsic strength to vary from region to region throughout a major element and throughout the entire volume of the body. Because of this limiting assumption, a number of phenomena attributable to 'size effects' are excluded from this study.

Brittle failure in simple tension

Consider a specimen of the micro-inhomogeneous material (viz. cement paste) which is uniformly loaded in tension so that the macroscopic stress has a value σ

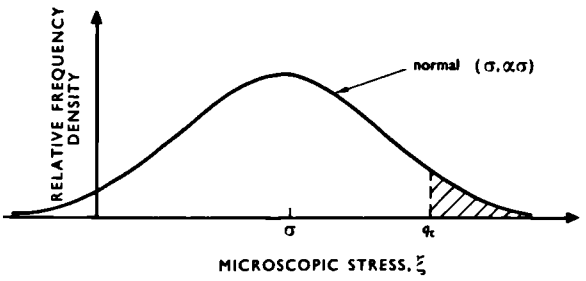


Figure 2: Normal distribution of micro-stress without redistribution.

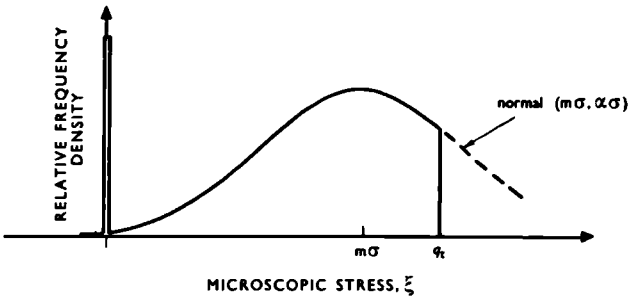


Figure 3: Assumed distribution of micro-stress during propagation of brittle failure.

everywhere. Then, if linear behaviour of the elemental structure of the model is specified, the distribution of the normal component of micro-stress, on any plane at right-angles to the direction of the applied loading, is normal with mean σ and standard deviation $\alpha\sigma$, where α is a property of the material.

This distribution (i.e. normal σ, $\alpha\sigma$) is shown in Figure 2, from which it is clear that the micro-stress ξ exceeds the intrinsic strength q_t in some parts of the cross-section, where failure must occur. The proportion of the total area of the cross-section in which failure occurs is given by the shaded area under the normal curve between $\xi = q_t$ and $\xi = +\infty$. Denoting this proportion by p, we have

$$p = \frac{1}{\sqrt{2\pi}} \int_{\frac{q_t - \sigma}{\alpha\sigma}}^{\infty} e^{-T^2/} \, dT \ldots\ldots\ldots (1)$$

where $T = \dfrac{\xi - \sigma}{\alpha\sigma}$

A similar expression is obtained by Volkov, who regards this value as the proportion of the material which contains 'micro-fissures' and suggests that failure of the material as a whole does not occur until some critical proportion of the cross-section has failed in this way. As the proportion containing micro-fissures is uniquely determined by the lower limit of the integral in equation 1, Volkov's criterion becomes:

$$\left.\begin{array}{lll} & \dfrac{q_t - \sigma}{\alpha\sigma} = -\chi & \text{at failure} \\ \text{or} & & \\ & \sigma \leqslant q_t + \chi(\alpha\sigma) & \text{before failure} \end{array}\right\} \ldots (2)$$

where χ may be regarded as a property of the material and the negative sign merely implies that more than half of the material contains micro-fissures at failure, when χ is positive.

This approach does not appear to be entirely satisfactory as some individual elements of the structure are required to sustain a stress which is far greater than the intrinsic strength. For brittle materials, it appears more reasonable to assume that a microscopic element (area ω) can carry no load after it has failed and that there must be progressive redistribution of micro-stress with increasing load in order that over-all equilibrium is maintained. This introduces a major difficulty which cannot be resolved without some sweeping assumption, unless the structural behaviour of the material is considered in greater detail at the microscopic level. Clearly, such a study would also involve approximations and it seems better to provide the model with a single eccentric, but convenient, property rather than indulge in unfounded analysis. It is therefore assumed that failure in some elements induces a uniform additional micro-stress in the remaining undamaged elements.

This process of redistribution of micro-stress is illustrated in Figure 3. Here, the stress in each undamaged microscopic element has been increased by $(m-1)\sigma$, and thus the form of the frequency distribution is identical with the normal distribution ($m\sigma$, $\alpha\sigma$) for $\xi \leqslant q_t$. The parameter m increases from unity with progressive failure and is thus a measure of the extent of stress redistribution or micro-cracking. The value of m is found from the condition that the material must be in equilibrium under the applied stress σ and that the mean value of micro-stress must remain σ after redistribution, i.e.

$$\sigma = \frac{1}{\alpha\sigma\sqrt{2\pi}} \int_{-\infty}^{q_t} \xi e^{-\frac{1}{2}\left(\frac{\xi - m\sigma}{\alpha\sigma}\right)^2} \, d\xi$$

We write $\sigma = q_t/r$ and $u = (r-m)/\alpha$ and thus, after standardizing the integral by the substitution $t = (\xi - m\sigma)/\alpha\sigma$, we obtain:

$$1 = \frac{1}{\sqrt{2\pi}} \int_{-\infty}^{u} (\alpha t + m) e^{-t^2/2} \, dt$$

This may be written:

$$\frac{1}{\alpha} = \frac{m}{\alpha} \frac{1}{\sqrt{2\pi}} \int_{-\infty}^{u} e^{-t^2/2} \, dt - \frac{1}{\sqrt{2\pi}} e^{-u^2/2}$$

or

$$\frac{1}{\alpha} = \frac{m}{\alpha} P(u) - Z(u) \ldots\ldots\ldots\ldots\ldots (3)$$

which is a particularly convenient form of the equilibrium condition as tabulated values of the normal probability function $P(u)$ and its derivative $Z(u)$ are readily available[11].

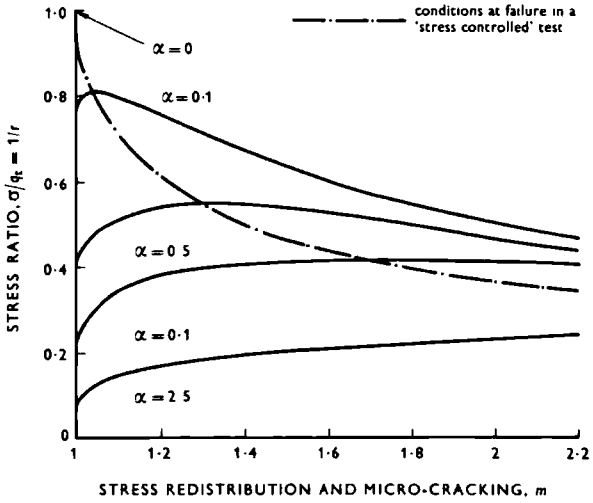


Figure 4: Stress redistribution during brittle behaviour.

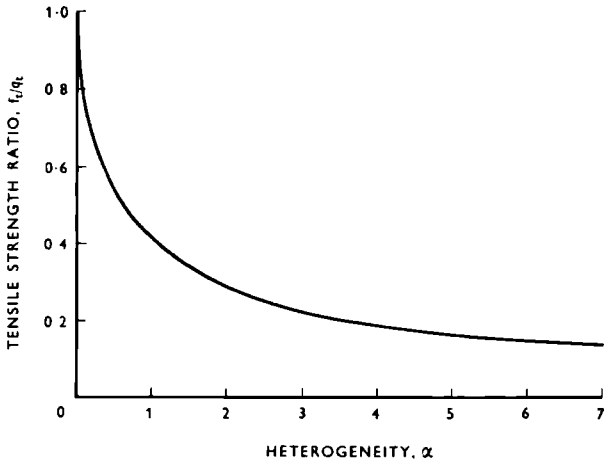


Figure 5: Reduction in tensile strength with increasing heterogeneity.

Equation 3 may be solved numerically to give a relationship between m and r for any particular value of α. The relationship is shown in Figure 4, from which it is seen that there is an increase in micro-cracking as the applied stress, represented by the non-dimensional ordinate $1/r$, increases from zero to a maximum value before decreasing, eventually to become zero when the entire section has failed ($m = \infty$). This result demonstrates that the manner of over-all failure of the material depends upon the method of loading. In a 'stress controlled' test, in which the load is increased monotonically, an unstable condition is reached and failure occurs when $1/r$ is a maximum and the micro-cracking is not complete. However, if the material is tested in such a way that the applied stress is relaxed, as micro-cracking proceeds beyond the critical value, no such instability occurs. In these circumstances, a criterion of failure cannot be expressed in terms of stress, and some other quantity, such as an ultimate strain, must be used.

Although this behaviour has not been observed in cement pastes, it is very similar to that obtained by Hughes and Chapman[12] when testing concretes and mortars in tension. This similarity is more remarkable when it is realized that the curves of Figure 4 must follow the general trend of the stress-strain curve for the material, as progressive micro-cracking causes a loss of stiffness in a specimen and increased deformations for any given loading.

Because failure in concrete is progressive and depends upon the test method employed, there has been considerable discussion[13] as to how failure should be defined. In practice, the definition should depend upon the use made of the material, but in laboratory testing it is most usual to record the maximum value of stress obtained. This corresponds to the maximum value of $1/r$ obtained with the model material and it is clearly of interest to determine the conditions for which $1/r$ is a maximum. This condition is the same as that which makes r assume a minimum value.

We differentiate equation 3 with respect to m:

$$\frac{1}{\alpha}\mathrm{P}(u) + \left(\frac{m}{\alpha} + u\right)\frac{\mathrm{d}u}{\mathrm{d}m}\,\mathrm{Z}(u) = 0$$

substitute:

$$\frac{r}{\alpha} = \frac{m}{\alpha} + u \quad \text{and} \quad \frac{1}{\alpha}\left(\frac{\mathrm{d}r}{\mathrm{d}m} - 1\right) = \frac{\mathrm{d}u}{\mathrm{d}m}$$

and obtain:

$$\mathrm{P}(u) + \frac{r}{\alpha}\left(\frac{\mathrm{d}r}{\mathrm{d}m} - 1\right)\mathrm{Z}(u) = 0$$

Now, for r to be a maximum or a minimum, $\mathrm{d}r/\mathrm{d}m = 0$ and

$$\mathrm{P}(u) - \frac{r}{\alpha}\mathrm{Z}(u) = 0 \qquad \ldots\ldots(4)$$

Equations 3 and 4 give the relation between m and r when the maximum stress is reached. It is important to realize that a unique solution is obtained for each value of α and that, for any specified degree of heterogeneity, the maximum stress is reached for a particular value of m, r and thus u. Denoting these particular values by $\bar{m}$, $\bar{r}$ and $\bar{u}$ we have, at failure:

$$\bar{u} = \frac{q_t - \bar{m}\sigma}{\alpha\sigma}$$

or, writing $q_t/\bar{m} = \bar{q}_t$ and $\bar{u}/\bar{m} = -\bar{\chi}$,

$$\left.\begin{array}{ll} \dfrac{\bar{q}_t - \sigma}{\alpha\sigma} = -\bar{\chi} & \text{at failure} \\ \text{or} & \\ \sigma \leqslant \bar{q}_t + \bar{\chi}(\alpha\sigma) & \text{before failure} \end{array}\right\} \ldots\ldots(5)$$

This expression is of the same form as Volkov's criterion (equation 2). Now, however, $\bar{q}_t$ is the apparent intrinsic strength of the material which is reduced with

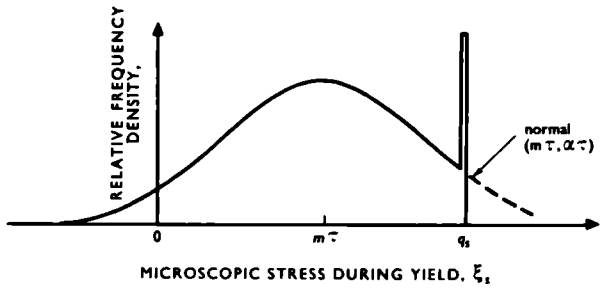


Figure 6: Assumed distribution of micro-stress during progressive yield.

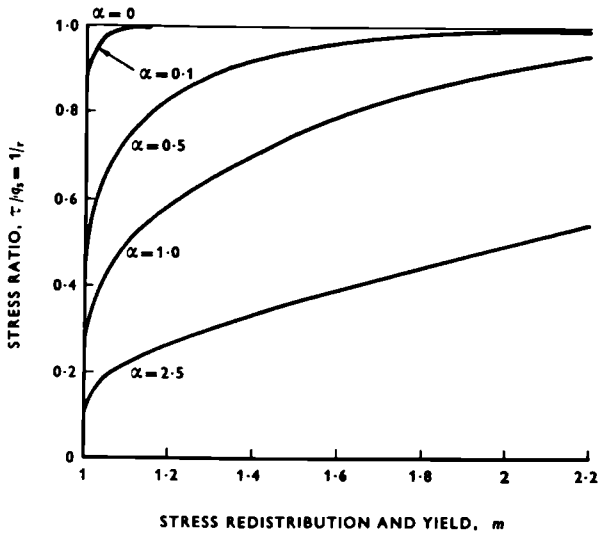


Figure 7: Stress redistribution during ductile behaviour.

increasing heterogeneity. $\bar{\chi}$ is also affected by heterogeneity and increases with increasing α.

The effect of increasing heterogeneity upon the maximum observed values of tensile stress is shown in Figure 5. This quantity is conventionally regarded as the tensile strength of the material (f_t) and it is seen that it is reduced by increasing heterogeneity. This conclusion gains some experimental support from recent work by Hughes and Chapman[12], who showed that the tensile strength of concretes and mortars depends upon aggregate size and that an increase in aggregate size causes a decrease in tensile strength.

Ductile failure in shear

So far, only a brittle mode of failure has been considered. It is interesting to compare these results with the behaviour that could occur if yield of the microscopic elements occurred rather than fracture.

It will be assumed that the occurrence of yield is determined by the values of the shear component of micro-stress, ξ_s, on the failure plane and is independent of the normal stress. Considering the failure plane, there is a macroscopic shear stress τ which is the mean of the values ξ_s on the same plane through a major element. These micro-stresses will be assumed to be normally distributed (τ, $\alpha\tau$); the parameter α may not necessarily have the same values as that used in the discussion of brittle failure. The material yields when the micro-stress in any element becomes equal to the intrinsic shear strength, q_s, and continues to carry this stress after yield. The process of progressive yield under increasing load requires redistribution of micro-stress in the same way as in brittle fracture, and again the assumption is made that redistribution is accompanied by a uniform increase in micro-stress in the regions where yield has not occurred.

The distribution of micro-stress is shown in Figure 6. Some redistribution has occurred and the values of micro-stress have been increased by $(m-1)\tau$ in the region where $\xi_s < q_s$. The resulting distribution is identical with the normal distribution ($m\tau$, $\alpha\tau$) for $\xi_s < q_s$.

The value of m is again found from the condition that the mean value of micro-stress must be equal to the macroscopic stress τ, i.e.:

$$\tau = \frac{1}{\alpha\tau\sqrt{2\pi}} \int_{-\infty}^{q_s} \xi_s \, e^{-\frac{1}{2}\left(\frac{\xi_s - m\tau}{\alpha\tau}\right)^2} d\xi_s + \frac{q_s}{\alpha\tau\sqrt{2\pi}} \int_{q_s}^{\infty} e^{-\frac{1}{2}\left(\frac{\xi_s - m\tau}{\alpha\tau}\right)^2} d\xi_s$$

We standardize the integrals by means of the substitution $(\xi_s - m\tau)/\alpha\tau = t$ and then write $\tau = q_s/r$ and $u = (r-m)/\alpha$ so that we obtain:

$$1 = \frac{1}{\sqrt{2\pi}} \int_{-\infty}^{u} (\alpha t + m) e^{-t^2/2} \, dt + \frac{r}{\sqrt{2\pi}} \int_{u}^{\infty} e^{-t^2/2} \, dt$$

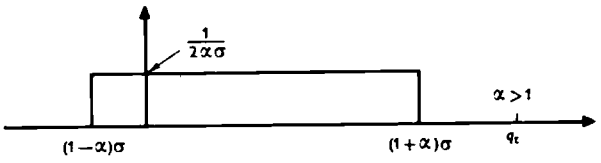
This may be written:

$$\frac{r-m}{\alpha} \frac{1}{\sqrt{2\pi}} \int_{-\infty}^{u} e^{-t^2/2} \, dt + \frac{1}{\sqrt{2\pi}} e^{-u^2/2} = \frac{r-1}{\alpha}$$

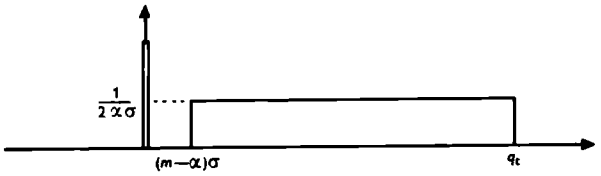
from which we obtain the equilibrium condition:

$$uP(u) + Z(u) = \frac{r-1}{\alpha} \quad \ldots\ldots\ldots\ldots (6)$$

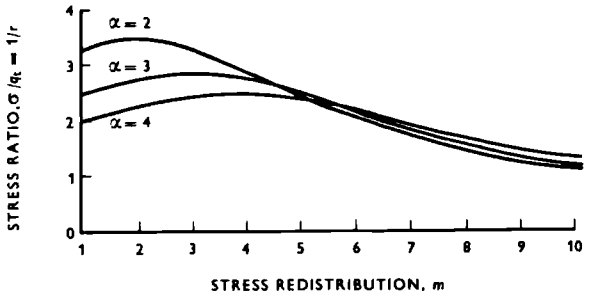
The values of m and r which are obtained from equation 6 for various values of α are shown in Figure 7. It is seen that progressive yield occurs as the applied stress, represented by $1/r$, is increased. In a load-controlled test, instability and failure occur when the applied stress becomes equal to the intrinsic yield stress.



(a) *Assumed distribution of micro-stress before micro-cracking.*



(b) *Distribution of micro-stress during progressive fracture.*



(c) *Stress redistribution during progressive failure.*

Figure 8

On the other hand, in a strain-controlled test, progressive yield occurs with continued straining and the macroscopic stress approaches the intrinsic yield stress asymptotically.

Although this result might appear obvious, it is interesting because, in contrast to brittle materials, it appears that micro-inhomogeneity has no effect upon the ultimate yield stress of purely ductile materials, although it probably affects the shape of the stress-strain curve. Experience suggests that this result has little relevance to cement paste or concrete in tensile stress regimes. However, it is well known that there are many materials which are nominally brittle under moderate stresses but which are effectively ductile under high triaxial compression (Nadai gives a number of examples[14]) or elevated temperature[15]. Clearly, it is possible that a shearing mode can occur in cement paste or concrete in these circumstances, and this possibility must be considered in extending the present work to general stress systems. The result, illustrated in Figure 7, which suggests that, in a ductile mode of failure, the ultimate strength is unaffected by micro-inhomogeneity, is probably applicable to more general states of stress than the one examined. However, strength in a tensile mode of failure is likely to be affected by inhomogeneity under all stress combinations.

General discussion

The mathematical model that has been used in this discussion is designed to represent cement paste and possibly mortars. However, there are still considerable differences between the idealized material and its real counterparts and these should be borne in mind in interpreting the results of the model and defining its range of application.

One of the major differences arises from the assumption that the intrinsic strength of the material does not vary from place to place although differences in stiffness, or lack of continuity, between the structural elements cause a variation in micro-stress. At first this appears illogical, but it is possible that the variation in micro-stress may be far greater than the variation in intrinsic strength in any major element. This is because a local variation in strength is entirely due to the quality of the material in that same locality, whereas a local change in material properties can produce a variation in stress throughout the whole volume. If this is so, the emphasis on stress in the model is justified.

It is interesting to note that most statistical studies of the occurrence of failure in concrete are based upon some postulated distribution of flaw size or intrinsic strength (Neville reviews a number of such theories[16]) and ignore micro-stress. In fact, this approach can be regarded as complementary to the present work if the established statistical theories are taken to apply at the macroscopic level. The postulated distribution in strength then refers to differences between major elements (size Ω) which are small in comparison with the over-all dimensions of the specimen. These differences have been ignored in the present work.

The most interesting feature of the model is the manner in which failure occurs by progressive propagation of fracture or yield at the microscopic level. This property is absent in any theory based upon a weakest link concept but depends upon the specified distribution of micro-stress and the rule of stress redistribution. The rule which has been used can only be justified on the grounds of mathematical convenience. However, the same trends can be obtained with quite different distributions of micro-stress, which suggests that the behaviour of the model must at least show some qualitative correspondence with real materials. An example of the results obtained by using an alternative distribution of micro-stress is shown in Figure 8.

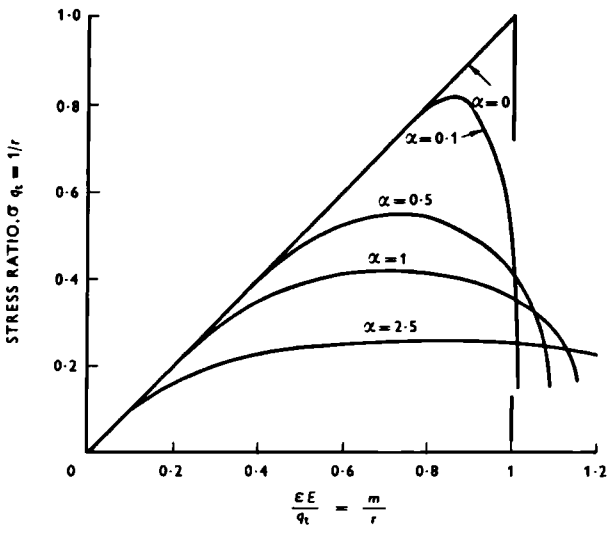


Figure 9: Stress-strain curves in tension.

In considering brittle fracture, it was suggested that the relationship between the stress ratio $1/r$ and the micro-cracking parameter m can be interpreted in terms of the macroscopic stress-strain curve for the material. This can be demonstrated if each microscopic element is taken to be linear elastic with Young's modulus, E, and it is assumed that the microscopic strains are normally distributed even after some breakdown has occurred. In these circumstances, the macroscopic strain is $m\sigma/E$ which corresponds to the modal value of micro-stress. A number of stress-strain curves have been calculated from this result, for various values of α, and are shown, in Figure 9, in non-dimensional form. It is seen that there is reasonable agreement with the experimental trends obtained by Hughes and Chapman[12], in that heterogeneity reduces strength and also the strain at which the maximum stress occurs. However, as far as strain is concerned, the analytical problem has been considerably over-simplified and this correspondence may not be so significant.

In considering possible applications of the model, the structure of the relevant real material must be considered. The structure and size of the individual constituents in hardened cement paste change with time as hydration progresses. The individual grains of partially hydrated cement will generally be larger than any other single constituent and have linear dimensions in the range from 10 to 100 microns. It is suggested that this may indicate the order of magnitude of the microscopic elements in the model and the size of the larger elements should be at least one order of magnitude greater than this. Thus a representative macroscopic element of hardened cement paste could have linear dimensions of the order of 1 mm.

In view of the sizes of test specimen most generally used, it is possible that the model could also be applied to represent mortars containing only fine sand. However, apart from the effects of size alone, the introduction of a large proportion of hard aggregate forms a number of dispersed regions in which the strength is very different from that of the cement paste matrix and where failure is unlikely to occur. In these circumstances it may only be possible to use the model, in its present form, as a representation of the cement paste or mortar matrix within the concrete.

In conclusion, it must be said that a detailed assessment of the value of the model must be suspended until more of its properties are demonstrated, such as its strength under general stress systems. However, the model material shows considerable promise and reasonable qualitative agreement has been obtained with important behaviour of real materials.

Notation

σ macroscopic direct stress component
τ macroscopic shear stress component
ξ component of microscopic stress
q_t intrinsic tensile strength of the model material
f_t maximum tensile stress which can be applied to the material (regarded conventionally, or by definition, as the tensile strength of the material)
q_s intrinsic shear strength of the model material
α stress variation or heterogeneity parameter
m stress redistribution or micro-cracking parameter
$1/r$ non-dimensional applied stress ($1/r = \sigma/q_t$ for tensile loading, or in shear $1/r = \tau/q_s$)
$u = \dfrac{r - m}{\alpha}$
$P(u)$ normal probability function
$Z(u)$ derivative of the normal probability function
ω microscopic element of area
Ω macroscopic element of area

REFERENCES

1. HIRSCH, T. J. Modulus of elasticity of concrete affected by elastic moduli of cement paste matrix and aggregate. *Journal of the American Concrete Institute. Proceedings* Vol. 59, No. 3. March 1962. pp. 427–452.
2. COUNTO, U. J. The effect of the elastic modulus of the aggregate on the elastic modulus, creep and creep recovery of concrete. *Magazine of Concrete Research.* Vol. 16, No. 48. September 1964. pp. 129–138.
3. DOUGILL, J. W. The effects of thermal incompatibility and shrinkage on the strength of concrete. *Magazine of Concrete Research.* Vol. 13, No. 39. November 1961. pp. 119–126.
4. REINIUS, E. A theory of the deformation and failure of concrete. *Betong.* No. 1. 1955. pp. 15–43. Cement and Concrete Association Library Translation Cj.63. pp. 31.
5. BAKER, A. L. L. An analysis of deformation and failure characteristics of concrete. *Magazine of Concrete Research.* Vol. 11, No. 33. November 1959. pp. 119–128.
6. BRANDTZAEG, A. Failure of a material composed on non-isotropic elements. *Det Kongelige Norske Videnskabers Selskags Skrifter.* No. 2. 1927. pp. 68.

7. VOLKOV, S. D. *Statistical strength theory.* (Translated from the Russian.) New York, Gordon and Breach, 1962. pp. 267. Russian Monographs and Texts on Advanced Mathematics and Physics.
8. ESIN, A. and JONES, W. J. D. A statistical approach to microplastic strain in metals. *The Journal of Strain Analysis.* Vol. 1, No. 5. October 1966. pp. 415–421.
9. GRIFFITHS, A. A. The phenomena of rupture and flow in solids. *Philosophical Transactions of the Royal Society.* Series A. Vol. 221. 1920. pp. 163–198.
10. OROWAN, E. Fracture and strength of solids. *Report on Progress in Physics.* Vol. 12. 1948 9. pp. 185–232.
11. ZELEN, M. and SEVERO, N. C. Probability functions. Ch. 26 of *Handbook of Mathematical Functions.* Edited by M. ABRAMOWITZ and I. A. STEGUN. New York, Dover Publications, 1965. pp. 925–995. Previously published by the National Bureau of Standards, 1964.
12. HUGHES, B. P. and CHAPMAN, G. P. The deformation of concrete and micro-concrete in compression and tension with particular reference to aggregate size. *Magazine of Concrete Research.* Vol. 17, No. 54. March 1966. pp. 19–24.
13. NEWMAN, K. Criteria for the behaviour of plain concrete under complex states of stress. *The Structure of Concrete and its behaviour under load: Proceedings of an International Conference, London, 1965.* Cement and Concrete Association, 1967. (To be published.)
14. NADAI, A. *Theory of flow and fracture of solids.* Vol. 1. Second edition. New York, McGraw Hill Book Company Inc., 1950. pp. 572.
15. HEARD, H. C. Transition from brittle fracture to ductile flow in Solenhofen limestone as a function of temperature, confining pressure and interstitial fluid pressure. Ch. 7 of *Rock Deformation.* Edited by D. GRIGGS and J. HANDIN. The Geological Society of America, 1960. *Memoir 79.* pp. 193–226.
16. NEVILLE, A. M. Some aspects of the strength of concrete. *Civil Engineering and Public Works Review.* Vol. 54. No. 639. October 1959. pp. 1153–1156. No. 640. November 1959. pp. 1308–1310. No. 641. December 1959. pp. 1435–1439.

Printed by the Cement and Concrete Association
52 Grosvenor Gardens, London S.W.1

87

AN APPROXIMATE ASSESSMENT OF THE EFFECTS OF HETEROGENEITY ON THE STRENGTH AND MODE OF FAILURE OF CONCRETE SYSTEMS

JOHN W. DOUGILL
Lecturer in Civil Engineering University of London King's College

SUMMARY

A mathematical model is developed to illustrate the effects of heterogeneity on the strength of hardened cement paste under general stress conditions. The possibility of failure by cleavage or in shear is considered and it is shown that the mode of failure under certain stress combinations may be either by cleavage or shear, depending upon the heterogeneity of the material.

An attempt is made to extend the results to mortars and concretes, by considering the effect of strong inclusions and the manner in which they modify the stresses in the matrix. The results for mortars are encouraging but there are difficulties, still to be resolved, in the application to concrete.

1. INTRODUCTION

In recent years there have been many investigations concerned with the mechanism of failure of concrete systems. This work has provided much valuable empirical data and has led to a better understanding of the mechanisms that may contribute to the failure process. However, no comprehensive theory has emerged from this work either to explain how the composition of the concrete influences strength or to provide failure criteria that are valid for all possible states of stress. Clearly some such theory would be useful in the design of engineering structures in concrete and also in the design of the material itself.

In the theoretical study of failure of materials under short term loading, most success has been achieved with materials that are nearly homogeneous. In these, the local variations in stress, due to widely dispersed imperfections of various kinds (cracks, impurities, dislocation pile-up, etc.), may often be calculated, so that it is possible to obtain criteria for local instability in a manner similar to that first used by Griffiths (1920) and later developed under the heading of fracture mechanics. If the imperfections are so numerous that they cannot be considered in isolation, or if the material is grossly heterogeneous, the formal approach, using fracture mechanics, can only be used if the geometry of the flaws and the structural arrangement of the material can be specified precisely. Although this may be possible for some types of composite, it will rarely be possible for concrete systems as these contain a large proportion of randomly distributed discrete particles held within a matrix of another material. This matrix may be homogeneous or, as in conventional concretes, comprise a separate heterogeneous sub-system.

This difficulty, of describing the material, is avoided if it can be regarded as a homogeneous continuum, but studies with this basis must be limited to an examination of the stability of cracks of an appreciable size compared with the structure of the concrete. Kaplan (1961) has achieved some success with this approach, but in general such a simplification cannot be made. Thus, theoretical studies have generally been based on idealized structural arrangements (such as those used by Brandtzaeg, 1927; Reinius, 1955; or Baker, 1959) and although these have been useful in demonstrating or explaining certain aspects of deformation and failure, no model has yet been devised that leads to an entirely satisfactory failure theory or accounts for the effects of composition on strength.

The crux of the problem is to establish a satisfactory means of describing the structure of concrete. The difficulties arise from the random geometry of this structure and also from the wide range of materials obtained by merely changing the mix proportions in any one concrete system. It is thought that a direct description of the material using a structural model must be so idealized that some phenomena are unavoidably excluded and it seems desirable, therefore, to attempt to devise

some other means of description. Some preliminary work of this nature was reported in an earlier paper (Dougill, 1967). This work was encouraging in that the description adopted for cement paste and mortars leads directly to an explanation of the manner in which heterogeneity could affect tensile strength, a phenomenon observed experimentally for mortars and concretes by Hughes and Chapman (1966). The description used is implicit, in that geometrical considerations are excluded, and only the effect of the structure on the distribution of stress within the material is specified. The object of the present paper is to extend the application of this mathematical model to general states of stress in cement paste and then in concrete. The initial developments are concerned only with the matrix of the concrete system and its description by means of the mathematical model, termed the micro-inhomogeneous material after Volkov (1962).

2. THE MICRO-INHOMOGENEOUS MATERIAL

The description of the material used to represent the matrix in the concrete system follows the form given in the previous paper. The material is considered to be composed of a large number of representative macro-elements in which the average stress is approximately equal to the stress in the material as a whole. These average stress conditions are defined by the three principal stresses σ_1, σ_2 and σ_3, the directions 1, 2 and 3 being chosen so that $\sigma_1 \geqslant \sigma_2 \geqslant \sigma_3$, with tensile stresses being taken as positive. Each macro-element is subdivided into many much smaller micro-elements within each of which the average stress (micro-stress) will be denoted by ξ_{ij}.

An individual micro-element is assumed to fracture when the normal stress on any plane reaches a value q_t, the intrinsic tensile strength of the material. Subsequently, the element cannot sustain any direct stress in the direction of the stress causing failure. Alternatively, the micro-elements are assumed to yield if the shear stress on any plane reaches the value q_s, the intrinsic shear strength of the material, and once yield has occurred the shear stress on the plane containing the yield surface remains equal to q_s. These criteria for the behaviour of the micro-elements are similar to the dual criteria proposed by Cowan (1952) for concrete and Paul (1961) for cast iron, except that any effect of normal stress on shear strength is here ignored. If it were possible to test a single micro-element under different combinations of principal stresses ξ_x, ξ_y and ξ_z, envelopes showing the combinations of micro-stress causing fracture or yield would be obtained in the form shown in Figure 1.

The micro-stresses are assumed to have a normal distribution on any plane within a macro-element until redistribution of stress occurs following fracture or yield. The underlying normal distribution on any plane is taken to be a function of all three principal stresses so that the distribution of the normal component of micro-stress ξ_{11}, acting in the direction 1, is normal with mean σ_1 and standard deviation

$$[\alpha^2\sigma_1^2 + \beta^2\sigma_2^2 + \beta^2\sigma_3^2]^{\frac{1}{2}}$$

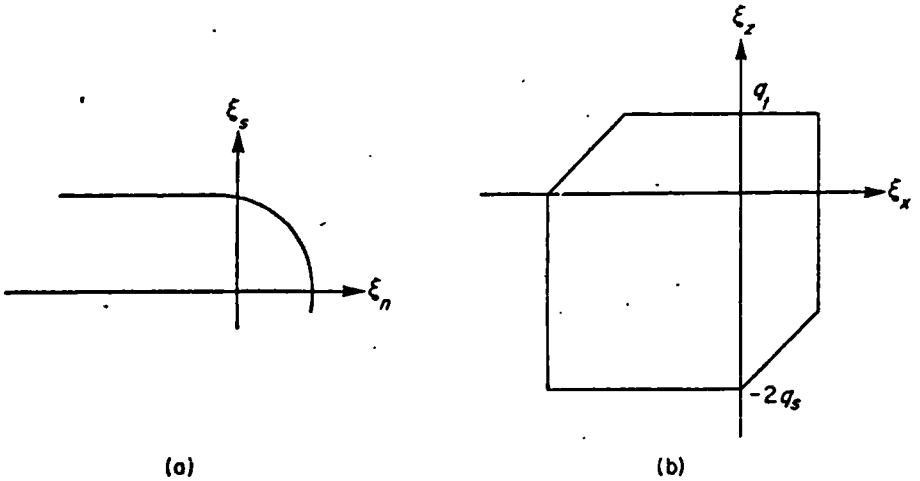


Figure 1. Conditions at yield or fracture of a single micro-element

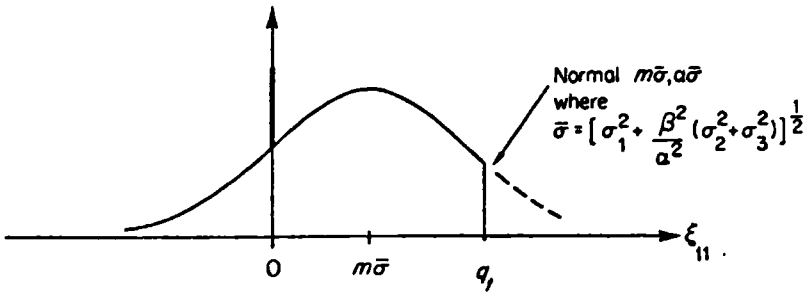


Figure 2. Assumed distribution of micro-stress on planes normal to the direction 1

The quantities α and β are properties of the material that describe heterogeneity through its effect on the stress distribution. For a completely homogeneous material α and β would both be zero and the stresses in all the micro-elements would be the same. The parameter α describes the irregularity in the stress field, normal to the direction 1, under the action of σ_1 alone, while the parameter β indicates the extent to which these stresses are affected by loading in the other direction. This last effect formed the basis of the 'scatter stress' theory used by Terzaghi (1945), following the earlier work of Rõs and Eichinger (1928), to explain the brittle mode of failure of concrete and rocks. It is plainly a possible result of structural irregularities, and the lattice analogue for concrete developed by Baker (1959) demonstrates one way in which this effect could occur. Under increasing stress, fracture or yield of some of the micro-elements causes some redistribution of micro-stress within the macro-element. Here a major simplification is made, in defining the mathematical model, by postulating that the process of redistribution is one in which failure of some elements introduces a uniform additional micro-stress in the remaining undamaged elements. The resulting distribution of the component ξ_{11} is shown in Figure 2. Here, the parameter m may be considered to be a measure of the extent of stress redistribution that is necessary for equilibrium to be established under a given stress system.

3. FAILURE BY PROGRESSIVE FRACTURE

Consider a plane normal to the direction 1 and carrying stresses distributed as shown in Figure 2. The extent of the stress redistribution, that occurs under increasing stress, is found from the condition that the material must be in equilibrium under the applied stress σ_1 and that the mean value of the micro-stress must remain σ_1 after redistribution, i.e.

$$\sigma_1 = \frac{1}{\alpha\bar{\sigma}\sqrt{(2\pi)}} \int_{-\infty}^{q_t} \xi_{11}\, e^{-\frac{1}{2}(\xi_{11}-m\bar{\sigma}/\alpha\bar{\sigma})}\, d\xi_{11}$$

where

$$\bar{\sigma} = [\sigma_1^2 + \beta^2/\alpha^2(\sigma_2^2 + \sigma_3^2)]^{\frac{1}{2}}$$

Now, by writing

$$\frac{q_t}{\bar{\sigma}} = r\,,\quad u = \frac{r-m}{\alpha}$$

and

$$\frac{\sigma_1}{\bar{\sigma}} = N$$

we obtain the equilibrium equation, in a manner similar to that in the previous paper (Dougill, 1967) in the form:

$$\frac{N}{\alpha} = \frac{m}{\alpha} P(u) - Z(u) \qquad (1)$$

Where $P(u)$ is the normal probability integral evaluated over the range $-\infty$ to u and $Z(u)$ is its derivative.

The equilibrium equation (1) can be solved numerically to give a relationship between m and r (and thus u) for any particular degree of heterogeneity or state of stress. This result is shown in Figure 3 for uniaxial tension ($N = 1$). It is seen that during progressive fracture the applied stress, represented by $1/r$, increases to a maximum value before finally decreasing, eventually to become zero when the entire section is fractured. In a load controlled test, the specimen as a whole would fail when the applied stress reached the peak value shown in the Figure, as behaviour beyond this point is only possible if the applied load can be relaxed during continued micro-cracking. The peak

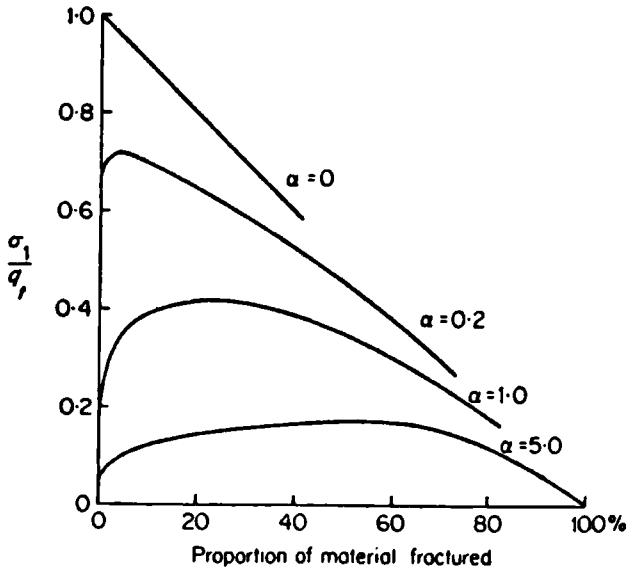


Figure 3. Progressive fracture in uniaxial tension, $N = 1$

value thus corresponds to the stress most often used to represent the 'strength' of a material under short term loading. The conditions at failure, i.e. instability in a load controlled test, are found from the equilibrium equation together with the requirement for $1/r$ to be a maximum. This can only occur (cf. Dougill, 1967) if $N > 0$ and when

$$P(u) - \frac{r}{\alpha} Z(u) = 0 \qquad (2)$$

The restriction on N implies that at least one of the principal stresses must be tensile if instability is to occur. The results (equations 1 and 2) can be applied to completely general stress systems if it is assumed that overall failure can occur, by progressive fracture, only on planes normal to the maximum principal stress. The criteria for failure are summarized in Figure 4 which shows the effect of heterogeneity on the strength of the model material under various combinations of the principal stresses defined by the quantity N. The range of N is from unity to zero, these values corresponding to uniaxial tension and uniaxial or biaxial compression respectively. A decrease in the value of N is accompanied by an increase in the proportion of material fractured before instability occurs. Thus, supposing that micro-cracking and stress redistribution are accompanied by a loss in stiffness of the material, it seems probable that the strains at failure will be greater, the less the value N.

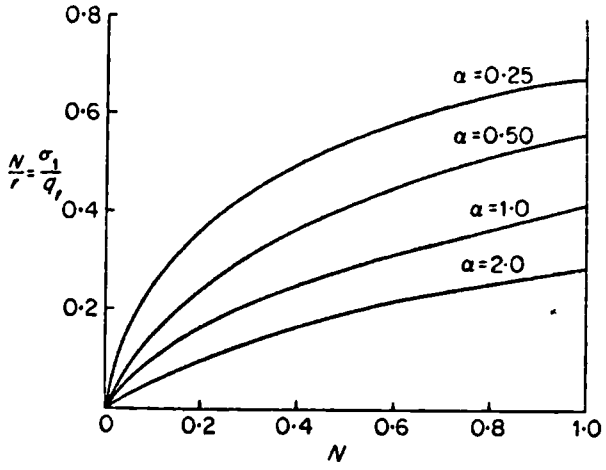


Figure 4. Fracture criteria for the micro-inhomogeneous material

Before considering other modes of failure, it is interesting to compare the present approach with that used by Griffiths (1920). In this he assumed a certain geometry for an imperfection in the material and then, by considering virtual changes in this geometry and using the theorem of minimum potential energy, he determined whether the original configuration was in stable equilibrium. In this present work, the energy approach is not available, as geometrical considerations have been ignored in defining the model, and criteria for instability are obtained by direct examination of the equilibrium of the system.

4. FAILURE IN SHEAR

Each micro-element may fail by yielding under a constant shear stress rather than by fracture. Consideration of this mode of behaviour (Dougill, 1967) suggests that instability does not occur, during the stress redistribution accompanying local yield, and that the ultimate strength of a material failing in shear is unlikely to be affected by micro-inhomogeneity. The criterion for overall shear failure may thus be assumed to be the same as for failure of the micro-elements.

5. ALTERNATIVE MODES OF FAILURE —DUAL CRITERIA

It is assumed that the separate processes of fracture or yield can proceed independently. The conditions at failure for these two distinct modes can be represented by a 'fracture surface' and

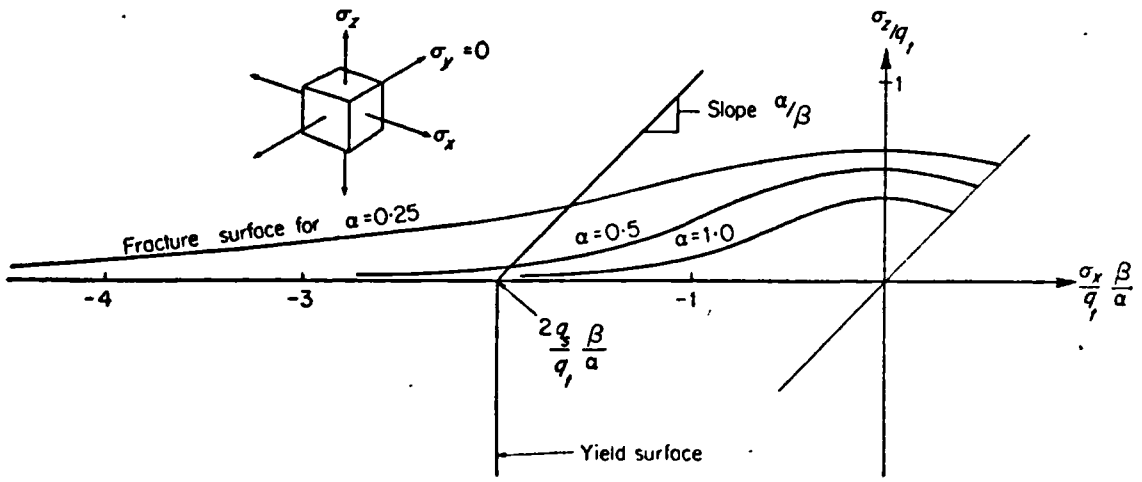


Figure 5. Yield and fracture surfaces for the micro-inhomogeneous material under biaxial states of stress

'yield surface' in principal stress space. Consider a vector (representing a particular stress combination) from the origin of these coordinates, that intersects the fracture and yield surfaces at distances R_T and R_S from the origin respectively. The principle of independence thus implies that fracture occurs if

$$R_T \leqslant R_S \tag{3}$$

or the failure is by shear if

$$R_S < R_T$$

These dual criteria are illustrated for biaxial states of stress in Figure 5. This result gains some support from Vile's (1965) tests on mortars in biaxial compression although there is an apparent shift of the envelope with respect to the stress axes in his results.

It can be seen from the figure that the effect of increasing heterogeneity (α) is to reduce the fracture strength of the material under all states of stress. The shape of the curves is affected by both the heterogeneity parameter α and the ratio β/α, a reduction in either of these quantities causing the surface to be stretched in a direction corresponding to negative values of the minor and intermediate principal stresses.

It will be noted that the fracture surfaces are asymptotic to the orthogonal planes $\sigma_1 = 0$, showing that fracture cannot occur unless one of the stresses is tensile. This feature is due to the assumed distribution of micro-stress, in which the stress in a few elements approaches $-\infty$. Clearly this is not possible, although very high values of compressive stress may occur. The assumed distribution could be truncated to allow for this, but there would be negligible resulting changes in the strength values, if the cut-off came at a reasonably high value of compressive stress.

6. EXTENSION TO CONCRETE SYSTEMS —MORTARS

So far, both the intrinsic tensile and shear strengths have been assumed to be constants. However, this assumption is unsuitable for mortars or concretes as these contain a large proportion of aggregate particles that form regions in which the strength is very different from that of the matrix. Thus the theory in its present form cannot be applied to a complete concrete system.

The separate mechanisms that can contribute to failure of concrete are breakdown of the aggregate, slip or separation at the aggregate/matrix interface and failure of the matrix by shear or cleavage. Almost certainly, all these mechanisms act simultaneously during the failure process. However, as the matrix is the only continuous phase in the concrete system, failure of the system as a whole must be accompanied by failure of the matrix. Looked at in this way, the strength of a concrete system is determined by the strength of the matrix, although the presence of the aggregate and the behaviour of the interface may have an important effect on the stress distribution in the matrix. Failure may be progressive, as stresses are induced by the applied loads and redistributed following bond slip and microcracking, until instability occurs in the

matrix. Alternatively, separation at the interfaces or, more probably, fracture of some of the aggregate particles may require a sudden comprehensive redistribution of stress in the matrix, if equilibrium is to be maintained. This may not be physically possible and so failure of the matrix occurs.

The 'triggered' mode of failure is likely if both the aggregate and matrix are highly stressed, relative to their respective strengths, at the time fracture of the aggregate occurs. Thus, it is a possible mode of behaviour for some lightweight aggregate concretes and for high strength concretes using natural aggregates in a very strong matrix. In more usual concretes, natural aggregates are not a major source of weakness and mostly remain intact during progressive failure. If the stresses in the matrix of these concretes can be expressed in terms of the applied loading, the failure criteria derived for the matrix alone can be used in an assessment of strength.

Leaving aside, for the moment, the difficulty of determining the stress distribution, there are some difficulties in applying the criteria to the matrix in concrete. Equations (1) and (2) were obtained for conditions of proportional loading and uniform macroscopic stress and neither of these conditions is likely to be satisfied within the matrix as failure is approached. The question of load history is avoided if the criteria are established for the material at incipient failure under a given combination of stresses, by considering a small virtual increase in the amount of fractured material and noting whether this leads to an increase, or decrease, in the value of N/r. In many ways this is a better approach, as the stress distribution under examination (Figure 2) can be considered to be independent of the rule of stress redistribution used to test stability. However, this suggests the possibility that α and β may need to be regarded as stress dependent material properties. The condition of uniform macroscopic stress can only be obtained by increasing the size of the macro-element to include all variation in micro-stress in the matrix. Again this implies a change in the heterogeneity parameters α and β. The manner of the change is indeterminate. For instance α is increased if aggregate is used in an otherwise homogeneous matrix but may be reduced if the matrix itself is grossly heterogeneous. These uncertainties concerning the effects of stress and aggregate concentration on the heterogeneity parameters imply that any application of the criteria to concrete must be regarded as approximate or exploratory.

In order to apply the criteria, the average stresses in the matrix σ' must be expressed in terms of the average stresses in the concrete as a whole. Thus the transformation matrix T must be known in the expression

$$\sigma' = [T]\sigma \tag{4}$$

Dantu (1958) has established the form of the matrix T for linear elastic behaviour of both phases and the composite, giving a relation between the average principal stresses in the matrix and those in the concrete as a whole in the form where A and B are functions of the aggregate content and the elastic properties of the aggregate, the matrix and the concrete.

$$\begin{bmatrix}\sigma'_1\\ \sigma'_2\\ \sigma'_3\end{bmatrix} = A\begin{bmatrix}1 & B & B\\ B & 1 & B\\ B & B & 1\end{bmatrix}\begin{bmatrix}\sigma_1\\ \sigma_2\\ \sigma_3\end{bmatrix} \tag{5}$$

The term A decreases with increasing aggregate content whilst B depends upon differences in values of Poisson's ratio of the constituents and the composite itself. This dependence on Poisson's ratio makes Dantu's expressions difficult to evaluate, but some idea of the magnitude of the terms A and B can be obtained by an elastic analysis in which the strain in the matrix is assumed to equal the strain in the composite solid. On this basis (Dougill, 1955)

$$\left.\begin{aligned} A &= \frac{E_m}{E_c}\left[1 + \frac{2\nu_m(\nu_m - \nu_c)}{(1+\nu_m)(1-2\nu_m)}\right]\\ B &= \frac{\nu_m - \nu_c}{(1 - \nu_m - 2\nu_m\nu_c)} \end{aligned}\right\} \tag{6}$$

Where E_m and E_c are Young's moduli for the matrix and the concrete and ν_m and ν_c are their respective Poisson's ratios. This analysis is approximate, being only suitable for low volume concentrations of aggregate and ignores any non-linear behaviour of the material. However, providing that there is very little stress redistribution before failure, the matrix stresses can be obtained from equation (5) and the strength assessed using equations (1) and (2) and the criteria for yield. Clearly, this procedure can only be applied to a very restricted class of concrete systems containing a small proportion of aggregate in a nearly homogeneous matrix and in which failure occurs in the

matrix only. It is thought that some mortars may approach this specification. For these materials, B is typically in the range 0·05 to 0·10 and the resulting failure surfaces are approximately similar to those for the matrix (see Figure 5). The yield surface is precisely similar, with the strengths increased by a factor of $1/A\ (1 - B)$ under all states of stress. The fracture strength is also increased, but the surface is now asymptotic to the pyramid, formed by the planes $\sigma_1 + B\ (\sigma_2 + \sigma_3) = 0$, at high negative values of the intermediate and minor principal stresses.

An interesting feature of these results is their similarity to those obtained experimentally by Mair (1968) for samples of flake graphite cast iron. Vile (1965) has already remarked upon the structural similarities between mortar and cast iron in comparing his own results for mortars with those for cast iron (as presented by Paul, 1961). It seems probable, therefore, that the proposed mathematical model can be considered to provide a valid description of such a material, particularly if the steel-like matrix is sufficiently embrittled by the presence of voids. Also, applications to other quasi-brittle fine grained heterogeneous materials are clearly possible.

6.1. Concrete

The approach described in the previous section is limited to materials in which stress redistribution, due to causes other than the basic heterogeneity of the matrix itself, can be ignored. Although mortars may behave in this way, it is thought that the limited approach is not applicable to more general systems in which interfacial phenomena, or breakdown of the aggregate itself, may lead to considerable changes in the state of stress in the matrix. Thus, there is a convenient distinction to be made between the behaviour of 'mortars' and 'concretes'; although the terms here refer to two extremes of behaviour and their use to classify any intermediate material must be rather arbitrary. In 'concrete', the distribution of micro-stress in the matrix is considerably influenced by changes in the macroscopic structure of the composite during loading, in addition to the effects due to the heterogeneity of the matrix itself. In these circumstances, the form of the transformation matrix T will depend on the manner in which failure occurs and thus on the overall state of stress.

The value of T required is that at incipient overall failure, at which stage the structure of the concrete may have been modified by extensive bond failure and micro-cracking within the matrix. In these circumstances, considerable reliance must be placed on empirical evidence in assessing the appropriate form of T for a particular stress combination.

Consider, for example, uniaxial compression. There is little change in the material properties under increasing load until the occurrence of 'discontinuity' (the term is Newman's 1964), when rapid growth of pre-existent or stress-induced micro-cracks first occurs. Alexander, Wardlaw and Gilbert (1965) and Jones (1965) all consider that the root cause of discontinuity is breakdown at the aggregate cement paste interface, and Shah and Winter (1966) have shown, by tests on isolated interfaces, that the effect of loss of adhesion at these boundaries is to induce tensile stresses in the matrix and to cause cracking parallel to the direction of the applied compressive load. This result is confirmed by Jones' (1952) tests on concrete, using the ultrasonic pulse technique to detect cracking, and also by the general appearance of tall specimens after compression testing. Thus, at incipient failure the average maximum principal stress in the matrix is tensile. A similar effect could occur in uniaxial tension as separation of the matrix from the aggregate boundaries would distort the stress trajectories around the inclusions so that the regions between stones would be in lateral compression. Thus, as a crude approximation, it seems possible that equation (5) could be used for certain states of biaxial stress if B is a small negative number.

Figure 6 has been prepared on this basis. The fracture surface is again asymptotic to the planes $A(\sigma q + B\sigma_3) = 0$, which are now in the compression/compression quadrant of the figure. The result appears reasonably satisfactory for the compression-tension region for which experimental results are available from Bresler and Pister (1957) and McHenry and Kani (1958). However, if the intrinsic shear strength of the material is high, failure is possible by cleavage in biaxial compression at values of stress rather lower than the uniaxial compression strength. Clearly, the analysis is in error here, most experimental results indicating a bonus of strength in biaxial compression, although Hilsdorf (1965) considers that many of these results are suspect and that under ideal testing conditions the intermediate principal stress may be shown to have negligible effect. This result could be obtained by arbitrarily stating that the failure is by shear, but there are no grounds for this in the present analysis.

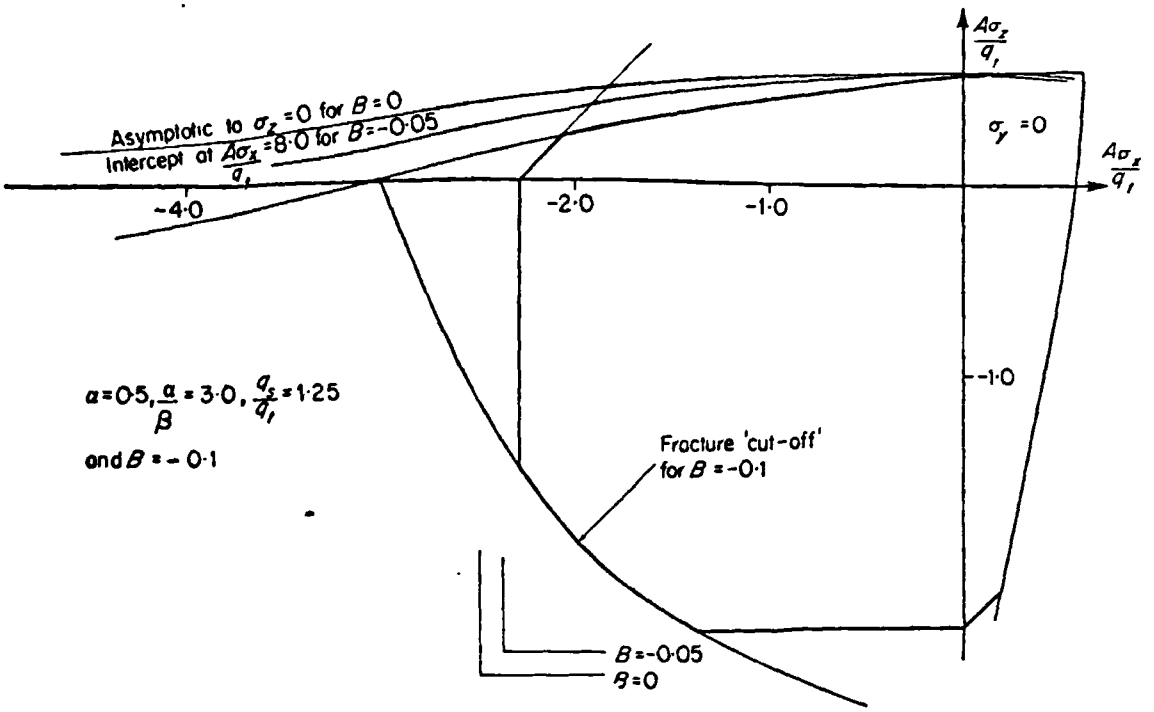


Figure 6. Biaxial strength envelope for a material with $\alpha = 0{\cdot}5$, $\alpha/\beta = 3{\cdot}0$, $q_s/q_t = 1{\cdot}25$ and $B = -0{\cdot}1$

Moreover, although the form of the transformation matrix used appears plausible for combined compression and tension, it may well be entirely unsatisfactory in biaxial compression.

7. CONCLUDING REMARKS

The main object of this paper has been to present an alternative method of studying the failure of concrete systems by means of an indirect description of the material based on the effects of structural heterogeneity. The work is still in a preliminary stage and it is possible that some details may need to be modified if the full range of behaviour of different concrete systems is to be adequately represented. The most likely modification may be to include some dependence on mean normal stress in the yield criterion adopted for the micro-elements. The effect of such a change has already been considered (Dougill, 1965) and may be included in the present treatment without difficulty.

The results obtained from the mathematical model for the micro-inhomogeneous material itself and 'mortars' are encouraging but require additional experimental support. It appears that the form of the failure surface under combined tensile and compressive stresses is very much influenced by heterogeneity and that different modes of failure may be obtained under similar stress conditions with materials of differing heterogeneity. It is interesting that the model reproduces the concavity, observed by Vile (1965), in this part of the biaxial stress envelope, and that the extent of this region is also affected by heterogeneity.

Mair's (1968) experimental results are particularly valuable in judging the model, if the comparison with cast iron can be considered valid. His results cover the whole possible range of biaxial stress combinations and show general agreement with the trends obtained from the model (see Figure 5), both under combined tension and compression and in the biaxial tension quadrant. The agreement is not so satisfactory in biaxial compression.

Although most emphasis has been put on biaxial states of stress, the results given in Figure 4 can be used to obtain the strength of the basic material and mortars under more general stress conditions. However, there appears to be a lack of empirical data to support or qualify results from the model for triaxial states of stress when one of the principal stresses is tensile.

An attempt has been made to apply the results to concrete, the aim being to illustrate the difficulties of the approach and to highlight the areas where more information and research are required. Here there are many additional difficulties. One of these, the description of the average stress condition in the matrix at incipient failure, has already been discussed but the other difficulty, that of assessing the change in effective heterogeneity caused by the addition of aggregate particles, may be equally important. To sum up: although more empirical support is required, the general approach using the mathematical model appears to have a genuine use in the study of the conditions at failure of mortars and possibly a whole range of other fine grained heterogeneous materials. However, more work is required before the approach can be applied satisfactorily to composites, in which the mode of interaction of the different phases changes considerably during progressive failure.

REFERENCES

Alexander, K. M., J. Wardlaw and D. J. Gilbert (1955). Aggregate-cement bond, cement paste strength and the strength of concrete. *Proc. Intern. Conf. Structure Concrete, London*, Paper B2.

Baker, A. L. L. (1959). An analysis of deformation and failure characteristics of concrete. *Mag. Concrete Res.*, **11**, No. 33, 119–128.

Brandtzaeg, A. (1927). Failure of a material composed of non-isotropic elements. *Kl. Norske videnskab. Selskabs Skrifter, No. 2.*

Bresler, B. and K. S. Pister (1957). Failure of plain concrete under combined stresses. *Trans. Am. Soc. Civ. Engrs.*, **122**, 1049–1060.

Cowan, H. J. (1952). Strength of reinforced concrete under the action of combined stresses, and the representation of the criterion of failure by a space model. *Nature*, **169**, p. 663.

Dantu, P. (1958). A study of stresses in heterogeneous materials; application to concrete. *Ann. Inst. Tech. Batiment Trav. Publ.*, **121**, 55ff.

Dougill, J. W. (1965). Some effects of thermal volume changes on the properties and behaviour of concrete. *Proc. Intern. Conf. Structure Concrete, London*, Paper I2.

Dougill, J. W. (1967). A mathematical model for the failure of cement paste and mortars. *Mag. Concrete Res.*, **19**, No. 60, 135–142.

Griffiths, A. A. (1920). The phenomena of rupture and flow in solids. *Phil. Trans. Roy. Soc., London*, **A221**, 163–198.

Hilsdorf, H. (1965). Determination of the biaxial strength of concrete. *Deutscher Ausschuss fur Stahlbeton.* Heft 173 Berlin.

Hughes, B. P. and G. P. Chapman (1966). The deformation of concrete and micro-concrete in compression and tension with particular reference to aggregate size. *Mag. Concrete Res.*, **17**, No. 54, 19–24.

Jones, R. (1952). A method of studying the formation of cracks in a material subjected to stress. *Brit. J. Appl. Phys.*, **3**, No. 7, 229–232.

Jones, R. (1965). Cracking and failure of concrete test specimens under uniaxial quasi-static loading. *Proc. Conf. Structure Concrete, London*, Paper B5.

Kaplan, M. F. (1961). Crack propagation and the fracture of concrete. *J. Am. Concrete Inst., Proc.*, **58**, 591–610.

Mair, W. M. (1968). Fracture criteria for cast iron under biaxial stresses. *J. Strain Analysis*, **3**, 254–263.

McHenry, D. and J. Kani (1958). Strength of concrete under combined tensile and compressive stress. *J. Am. Concrete Inst., Proc.*, **54**, 829–839.

Newman, K. (1964). The structure and engineering properties of concrete. In *Proceedings of an International Conference of the Theory of Arch Dams*, Pergamon Press, London, 1965, pp. 683–712.

Paul, B. (1961). A modification of the Coulomb–Mohr theory of fracture. *J. Appl. Mech.*, **28**, No. 2, 259–268.

Reinius, E. (1955). A theory of the deformation and failure of concrete. *Betong*, **40**, 15–43. Cement and Concrete Association Library Translation cj. 63.

Rös, M. and A. Eichinger (1928). Versuche zur klarung der trage der Bruchgerfahr II Nichtrutallische Stoffe, Zurich. *Eidgenossiche Materialprufung-Sanstalt and der Eidgenossischen*, Technischen Hochschule, p. 27.

Shah, S. P. and G. Winter (1966). Inelastic behaviour and fracture of concrete. *J. Am. Concrete Inst., Proc.*, **63**.

Terzaghi, K. (1945). Stress conditions for the failure of saturated concrete and rock. *Proc. A.S.T.M.*, **45**, 777–792.

Vile, G. W. D. (1965). Strength of concrete under short-term static biaxial stress. Paper F2 *Proc. Intern. Conf. Structure Concrete*, London, Paper F2.

Volkov, S. D. (1962). *Statistical Strength Theory.* (Translated from the Russian) Gordon and Breach, New York. Russian Monographs and Texts on Advanced Mathematics and Physics, Vol. XI.

KEY WORDS

Concrete systems, mathematical model, mortars, concrete, statistics, heterogeneity, strength, combined stresses, failure criteria, yield and fracture,

UDC 666.97.017:539.4

Some results for the average stresses induced in the principal components of concrete

J. W. Dougill, MSc(Eng), DIC, MICE

UNIVERSITY OF LONDON, KING'S COLLEGE

SYNOPSIS

Results are obtained for the average stresses in the separate phases of a range of conventional concretes. These results show that the larger particles of aggregate are more highly stressed than the smaller material in the concrete mix and also confirm that, for a concrete in uniaxial compression, the cement paste or mortar is in a state of average triaxial compression during the early stages of loading. It is suggested that the sign of the average stress in the separate phases may be used as an indicator of the mode of failure likely to occur in a concrete under any particular stress combination. Results for conventional concretes support this view and it is considered that the indicator will also be useful in studying the behaviour of high-strength and of lightweight-aggregate concretes.

Introduction

It has been suggested[1-3] that a criterion for cleavage failure of a quasi-brittle heterogeneous material should be based upon the distribution of micro-stress in the material under load, and that this may be described by the mean value of each stress component and some measure of the way in which the local values of micro-stress are distributed about the mean. This approach appears to be possible for cement pastes and mortars[4] but will be unsuitable for concretes which contain a high proportion of hard aggregate. Here, there is an appreciable volume within which failure is unlikely to occur and the criterion of failure must then be based upon the stresses in the cement paste matrix rather than in the material as a whole. Although both the average stress and the distribution of micro-stress are required in a full analysis of the condition at failure, this paper is concerned only with the mean stresses in the separate phases of the concrete structure. However, it is thought that these partial results are of interest, as it seems possible that the average stress in the material will affect the manner in which failure is propagated and may indicate the different circumstances in which failure is likely to be stable or unstable. It is this aspect of the problem which is the main concern of this paper.

In the analysis, concrete is considered to be a two-phase material in which both phases, the aggregate and the cement paste, are each regarded as being homogeneous and isotropic. The analysis applies to other materials of this form and a similar approach, in two dimensions, may have some application in studying fibre-reinforced composites and such structural problems as the stresses in the concrete within the heavily penetrated end cap of a reactor pressure vessel.

Notation

ξ_{ij}	typical micro-stress component
σ_{ij}	typical average stress component
ϵ_{ij}	typical average strain component (i and j may each take the values 1, 2 or 3)
$\sigma_1, \sigma_2, \sigma_3$	average principal stresses
g	volume concentration
E	Young's modulus
ν	Poisson's ratio
V	a representative volume
S	a representative area

All the above quantities may be referred to the cement paste by a single prime or to the aggregate by a double prime. Thus g' and g'' refer to the concentration of cement paste and of aggregate respectively. Unprimed quantities refer to the concrete as a whole.

Under the assumptions used in this paper, the components of micro-stress can be regarded as being the actual local stresses at each point within the composite material. However, Dantu's[3] analysis remains unaltered if the wider view of micro-stress, developed in references 2 and 3, is adopted.

Method of analysis

The particular problem, of determining the average stresses within the aggregate and cement paste that make up a concrete specimen, appears to have been taken up first by Dantu[5,6]. A brief account of the relevant theory is given in this section, as previous workers appear to have concentrated their attention on the experimental aspects of Dantu's work. The presentation may differ somewhat from Dantu's own, but the general procedure is the same.

Dantu defines the statistical stress components σ_{ij}, acting at a point P, by

$$\sigma_{ij} = \frac{1}{S}\int_S \xi_{ij} dS \quad \ldots\ldots\ldots\ldots\ldots (1)$$

In this expression, the micro-stress components are summed over a small plane surface, of area S, that includes the point P. Each statistical stress component thus represents the average value of the corresponding component of micro-stress acting on the surface S. In general, S can be chosen so that the statistical stresses are smoothly varying functions of position that approach the conventional values of stress in a continuum. If these conventional stresses do not vary throughout the material, the result from equation 1 becomes effectively independent of the choice of S, provided that S is sufficiently large compared with the grain size of the material. From this it follows that, in these circumstances of uniform macroscopic stress, Dantu's alternative definition for the statistical stresses,

$$\sigma_{ij} = \frac{1}{V}\int_V \xi_{ij} dV \quad \ldots\ldots\ldots\ldots\ldots (2)$$

gives a result identical with that obtained from equation 1. Here the statistical stress is the mean value of the micro-stress ξ_{ij} within a volume V that surrounds the point P and which is large compared with the grain size of the material.

Equation 2 can be written

$$\sigma_{ij} = \frac{V'}{V}\left(\frac{1}{V'}\int_{V'} \xi_{ij} dV\right) + \frac{V''}{V}\left(\frac{1}{V''}\int_{V''} \xi_{ij} dV\right)$$

where the separate integrations are taken throughout the volume of the cement paste, V', and the volume of the aggregate, V'', contained within the representative volume V. In a statistically homogeneous material, the ratios V'/V and V''/V are the respective concentrations (g' and g'') of the cement paste and the aggregate in the concrete. Also, the terms in parentheses represent the average values of the stress components (σ_{ij}' and σ_{ij}'') in each of the two phases. Thus we obtain equation 3, connecting the average stress in the composite with the average stress in the separate phases,

$$\sigma_{ij} = g'\sigma_{ij}' + g''\sigma_{ij}'' \quad \ldots\ldots\ldots\ldots\ldots (3)$$

A similar argument leads to the corresponding equation for the strains,

$$\varepsilon_{ij} = g'\varepsilon_{ij}' + g''\varepsilon_{ij}'' \quad \ldots\ldots\ldots\ldots\ldots (4)$$

where ε_{ij}' and ε_{ij}'' are the average strains in the cement paste and the aggregate and ε_{ij} is the strain in the concrete.

If the relationship between stress and strain is linear for the material in one phase, the average stresses and strains in that phase will also be related in a linear manner. Thus, if the values of the elastic constants for the composite and for the material in each phase are known, equation 4 can be rewritten in terms of stresses. The stress components in one of the phases can then be eliminated, by using equation 3, to give equations for the average stresses, in the other phase, in terms of the over-all average stresses σ_{ij}.

If this procedure is followed and the effects of creep and shrinkage are ignored, the following equations are obtained relating the average stresses in the cement paste (σ_{ij}') with those in the composite (σ_{ij}).

$$\sigma_{11}' = P'\sigma_{11} - Q'(\sigma_{11} + \sigma_{22} + \sigma_{33}) \quad \ldots\ldots (5a)$$

together with two similar equations for σ_{22}' and σ_{33}' and three equations of the form

$$\sigma_{12}' = P'\sigma_{12} \quad \ldots\ldots\ldots\ldots\ldots (5b)$$

for the average values, σ_{12}', σ_{23}' and σ_{31}', of the shear stress components.

In these expressions,

$$P' = \frac{1}{g'}\left(\frac{1+\nu}{E} - \frac{1+\nu''}{E''}\right)\Big/\left(\frac{1+\nu'}{E'} - \frac{1+\nu''}{E''}\right) \quad \ldots\ldots (5c)$$

and

$$Q' = \frac{1}{3}\left[P' - \frac{1}{g'}\left(\frac{1-2\nu}{E} - \frac{1-2\nu''}{E''}\right)\Big/\left(\frac{1-2\nu'}{E'} - \frac{1-2\nu''}{E''}\right)\right] \quad \ldots\ldots (5d)$$

Here, the symbols E and ν represent Young's modulus and Poisson's ratio. The particular values of these constants for the cement paste and the aggregate carry a single and a double prime respectively and the unprimed values refer to the concrete as a whole. Also, it should be noted that the corresponding group of equations, that relates the average stress in the aggregate to that in the concrete, may be obtained from equations 5 by merely replacing the quantities carrying a single prime by the corresponding double-primed quantity and vice versa. Alternatively, the average stresses in the aggregate can be found from those in the cement paste by means of equation 3 and using $g' + g'' = 1$.

Results

In order to obtain values of the average stresses in the separate phases, the elastic constants and concentration of the aggregate and cement paste in the concrete must be known as well as the over-all properties. Such complete data are rare, and in applying his analysis Dantu[5] was forced to make assumptions, concerning the relationship between the individual elastic constants, that were not generally valid and which had a considerable effect upon the results presented. The main difficulty arises because Q is highly dependent upon the values of Poisson's ratio. For equal values of the three Poisson's ratios, Q would be zero. Thus it is clear that Q is determined by the differences of quantities that are each difficult to measure and are often regarded as of only secondary importance in stress analysis.

Fortunately for this investigation, Anson and Newman[7] have reported the results of a comprehensive series of tests to determine the values of Poisson's ratio and Young's modulus for a range of concretes, mortars and cement pastes made with ordinary Portland cement and Thames Valley river gravel and sand. Also conveniently, they give values of Young's modulus and Poisson's ratio for the aggregate (as "about 10 × 10^6 lb/in²" and "about 0·22"), and so their results can be used without addition to calculate the coefficients P and Q corresponding to their range of concretes and mortars.

The properties of the cement paste used in Anson and Newman's investigation are given in Table 1, which also includes estimated values for a cement paste having a water/cement ratio of 0·6. The calculated values of the average stress coefficients P and Q are given in Table 2, together with the details of the mix proportions and concrete properties taken from Anson and Newman's paper. Their paper also contains results for the elastic constants found from dynamic measurements. These are ignored in the

TABLE 1: **Properties of cement pastes, from reference 7.**

Water/cement ratio by weight	Young's modulus (kN/mm²)	Poisson's ratio
0·3	23·2	0·249
0·4	17·0	0·250
0·5	12·0	0·249
0·6	8·1*	0·25†

*extrapolated value
†estimated value

TABLE 2: **Average stress coefficients, P and Q.**

Mix proportions by weight to one part of cement				Concrete properties		Average stress coefficients			
						Paste		Aggregate	
Water	Fine aggregate	Coarse aggregate	g'	E (kN/mm²)	υ	P'	Q'	P''	Q''
0·3	1·0		0·387	33·2	0·193	0·823	−0·143	1·280	0·226
0·3	1·5		0·486	39·2	0·185	0·672	−0·156	1·347	0·165
0·4	1·0		0·352	27·9	0·219	0·722	−0·051	1·511	0·094
0·4	1·5		0·449	31·8	0·196	0·649	−0·097	1·430	0·119
0·4	2·0		0·520	31·2	0·188	0·761	−0·134	1·221	0·124
0·4	2·5	0	0·576	34·2	0·178	0·709	−0·160	1·214	0·118
0·5	1·0		0·322	21·9	0·222	0·649	−0·035	1·739	0·073
0·5	1·5		0·417	26·0	0·210	0·573	−0·050	1·597	0·069
0·5	2·0		0·487	28·0	0·186	0·557	−0·090	1·467	0·095
0·5	2·5		0·544	28·3	0·171	0·602	−0·128	1·333	0·107
0·5	3·0		0·589	30·4	0·168	0·583	−0·135	1·291	0·094
		1·0	0·625	34·9	0·172	0·491	−0·118	1·306	0·071
		1·5	0·657	34·2	0·152	0·540	−0·173	1·240	0·090
		1·8	0·673	35·4	0·160	0·532	−0·157	1·227	0·076
0·5	2·5	2·0	0·682	36·2	0·156	0·518	−0·166	1·225	0·077
		2·5	0·704	38·5	0·145	0·470	−0·187	1·223	0·079
		3·0	0·725	39·6	0·153	0·481	−0·178	1·197	0·067
	1·0		0·298	22·1	0·227	0·392	−0·015	2·433	0·036
	1·5		0·389	21·4	0·209	0·461	−0·039	1·846	0·061
0·6	2·0	0	0·459	23·2	0·197	0·458	−0·054	1·639	0·063
	2·5		0·515	24·5	0·181	0·457	−0·076	1·511	0·071
	3·0		0·561	25·6	0·169	0·465	−0·095	1·419	0·075

Coefficients calculated using the paste properties from Table 1 and values of Young's modulus and Poisson's ratio for the aggregate of 68·9 kN/mm² and 0·22. The mix proportions and concrete properties are taken from reference 7.

present work, as it is felt that such results are not necessarily appropriate material for the present analysis.

Before coming to the subject of failure, there are a couple of points of immediate interest that arise from the results in Table 2. The first follows from the sign of the coefficient Q', and the other is concerned with the structural role of the coarse aggregate in concrete.

The coefficient Q' (relating to the stress in the cement paste) is negative for the entire range of materials investigated showing, for instance, that the cement paste, in a concrete or mortar specimen loaded in uniaxial compression, is in a state of average triaxial compression. This result has already been deduced by Anson[8], from strain measurements on idealized concretes and rubber models, and can also be obtained by analysis[9] when the aggregate concentration is low and the Poisson's ratio of the paste is greater than that of the concrete.

In his earlier paper, Anson[8] reports that the coarse aggregate used in making the concretes consisted of a 19 mm maximum size gravel of which 90% was retained on a 9·5 mm sieve whilst the sand used for both mortars and concretes was uniformly graded with 100% passing the 4·75 mm sieve. There is thus a clear division between the composition of the concretes and mortars, and the separate data from these can be used to examine the role of the larger sizes of aggregate in the concrete structure.

Table 2 gives the average stress coefficients for the aggregate in a range of six concretes whose composition varies only on account of differences in the quantities of coarse aggregate used in the concrete mix. These concretes can be regarded as composite materials of two phases comprising the coarse aggregate and a mortar of constant composition. The properties of this mortar are known, so that the average stresses in the coarse aggregate alone can be determined in the manner already described. Then, by using these results and knowing the relative proportion of coarse and fine aggregate, the average stresses in the fine aggregate can also be found from the results given in Table 2.

The results of these calculations are shown in Figure 1. In the calculations, it was assumed that the coarse aggregate and sand had the same values of specific gravity, Poisson's ratio and Young's modulus and, in drawing the Figure, the values obtained for the concrete with aggregate/cement ratio equal to one have been ignored. This was done because the value given for Young's modulus of this concrete is considerably 'out of step' with the other values and the calculated average stress coefficients were far removed from the trends obtained when the other results were used.

In looking at the Figure, it must be remembered that the same mortar is used throughout and that an increase in the coarse aggregate/cement ratio implies an increase in the total quantity of aggregate in the concrete. Thus, although the average stress in the coarse aggregate is relatively unaffected by an increase in the proportion of coarse aggregate, this increase in volume is sufficient to reduce significantly the average stresses in the fine aggregate and the cement paste. To some extent, these results support Baker's[10] view that the larger closely packed particles of aggregate form stiff thrust rings that carry an appreciable proportion of the total load and tend to span around the enclosed pockets of mortar. In this respect, the results shown in Figure 1 suggest that the sand itself fulfils the structural role of the coarse aggregate when there is no larger material present. Also, it appears that, as coarse aggregate is added to the concrete mix, the sand becomes increasingly associated with the role of the cement paste.

The concrete mixes examined here are deficient in 9·5 to 4·75 mm aggregate and may be thought to be over-sanded when compared with typical concretes. It is considered that Baker's thrust ring concept is also applicable to concretes made with continuously graded aggregates. However, it would be expected that the results of an investigation on such a material would not show such distinct trends as those of Figure 1, because of the necessarily arbitrary classification of coarse and fine aggregates within the continuous grading.

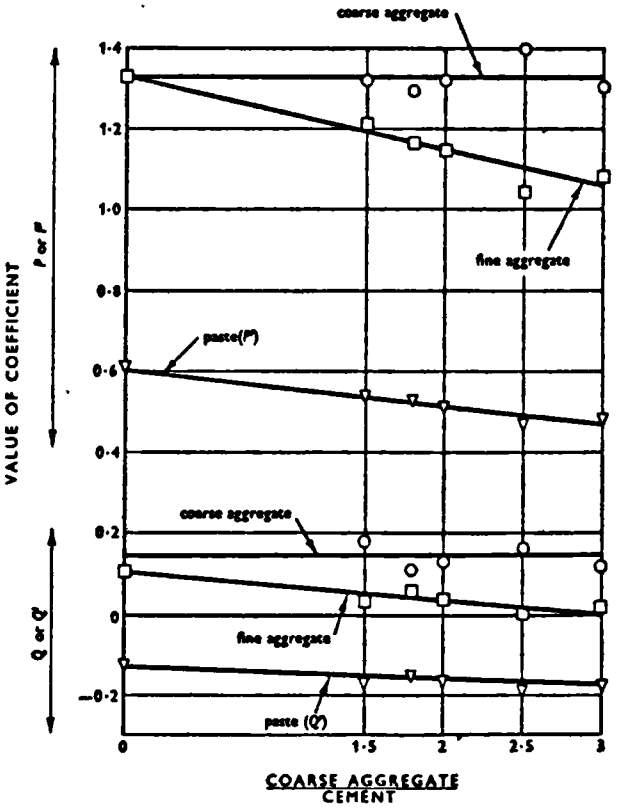


Figure 1: Average stress coefficients.

Failure

Although the present analysis is restricted to linear behaviour, it seems possible that the results can be used to provide some information on the mode of failure of concrete under different stress combinations.

In attempting this, it must be realized that the average stresses are no guide to local conditions and that it is quite possible for some regions, within the cement paste say, to be in tension when the average stress is compressive. Some cracking could occur in these regions at quite low loads, but it seems unlikely that these cracks could propagate easily in a stress field that is, on average, overwhelmingly compressive. Thus, if the average stress in the cement paste is compressive, it is reasonable to assume that the early cracking will be stable and, being localized, will also have little effect upon the over-all stress-strain behaviour. On the other hand, it is thought that any cracks initiated in a predominantly tensile stress field are likely to propagate rapidly under only small increases in stress and lead to over-all failure in an apparently brittle mode.

The mode of failure under conditions of average compressive stress is not so easily visualized. Slow growth of cracks could occur within the cement paste or at the interface with the aggregate. As these cracks extend, they will have a progressively greater effect upon the stress-strain behaviour of the cement paste and concrete and so cause some redistribution of the average stresses. In this way an unstable situation could develop, leading to sudden failure, but it seems probable that this can occur only after a comprehensive redistribution of the internal stresses which must be accompanied by loss in stiffness and significant departures from linearity of the concrete as a whole. On this basis, it seems that there are likely to be real differences in modes of failure under different stress combinations, depending upon whether cracking is initiated under conditions of average compressive or tensile stress. From this it appears that the sign of the average stress in the cement paste can be used as an indicator of the probable mode of failure of concrete under a particular stress combination. The use of this indicator is based upon the assumption that brittle failure occurs when the average stress in the cement paste is tensile during the propagation of cracking and that, if the average stress in the cement paste is entirely compressive, brittle failure is unlikely to occur.

The average stress component, σ_1', in the cement paste is tensile for $\sigma_1' \geqslant 0$ or, if equation 5a is used to express this in terms of the stresses $(\sigma_1, \sigma_2, \sigma_3)$ applied to the concrete as a whole, for

$$\sigma_1 - \frac{Q'}{P' - Q'}(\sigma_2 + \sigma_3) \geqslant 0 \quad \ldots\ldots\ldots (6)$$

Similar conditions, for σ_2' and σ_3' to be positive, can be found by interchanging the suffices in 6. The equalities included within these conditions represent three planes drawn in principal stress space $(\sigma_1, \sigma_2, \sigma_3)$, and the sign of each component of the average stress in the cement paste is constant within each of the eight open-ended pyramidal regions formed by the intersection of these planes.

Figure 2 shows the sign of the average stress components in the cement paste of a concrete specimen subject to biaxial stresses. The Figure has been drawn with the present results in mind, that is with Q' negative, so that the region within which the stresses in the cement paste are entirely compressive is larger than the compression quadrant of the Figure. As can be seen from Figure 3, the absolute value of the slope of the line $\sigma_1' = 0$ increases with the proportion of aggregate in the concrete mix but it is relatively unaffected by the water/cement ratio, only the two points for the mortars with water/cement ratio 0·3 being far removed from the general trend. From this Figure we see that, for concretes in combined compression and tension, the paste is, on average, entirely in compression if the applied tensile stress is numerically less than 0·2 to 0·3 of the applied compressive stress. Also, this range changes to 0·03 to 0·1 for the mortar to be entirely in compression.

These ranges are shown in Figure 4 superimposed upon recent results of Kupfer et al.[11] for the strength of concrete under biaxial stress. In their paper, the authors remark that the mode of failure of specimens tested in combined tension and compression and in biaxial compression was similar, provided that the applied tensile stress was numerically less than one-fifteenth (0·067) of the applied compressive stress. This ratio is within the range (0·03 to 0·1) within which the stresses in the mortar may change from being entirely compressive, and it is in this range also that the most obvious changes in slope of the experimental curves occur. Thus, if the results from Figure 3 can be taken to apply to Kupfer's range of concretes, it appears that it is the sign of the stress in the mortar matrix rather than that in the cement paste that should be used as the indicator of the mode of failure.

In spite of this limited agreement, it is clear that the change of sign of the average stress in the mortar does not mark an abrupt transition from a progressive type of failure to one that is very much more sudden. The stress-strain curves obtained by Kupfer et al. for combined tension and compression all show departures from Hooke's law, the non-linearity decreasing with an increase in the ratio of applied tension to compression. It thus seems important to recognize that the proposed indicator is an uncertain guide to the mode of failure in combined compression and tension. Here, there seems to be a transition region between the mode of failure in which comprehensive stress redistribution must occur between the separate phases and the other mode in which the strains are almost linear up to failure. These two modes of behaviour could be cate-

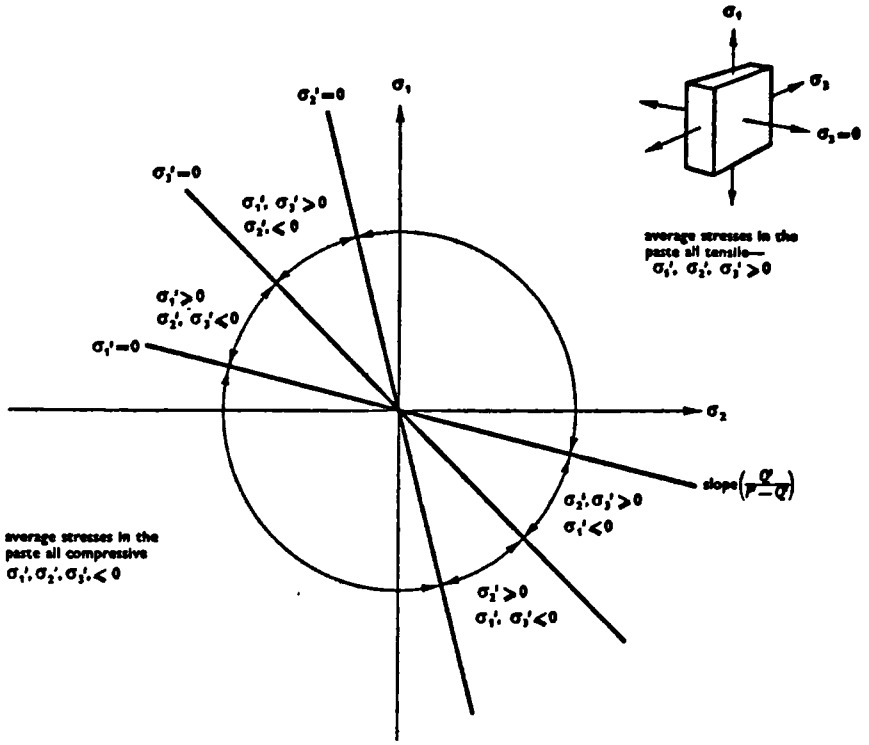


Figure 2: Isonomic regions for the average stresses in the cement paste for a biaxially stressed concrete.

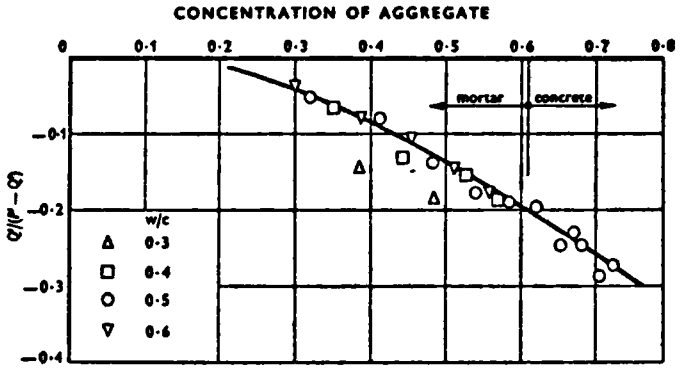


Figure 3: Range of values of $Q'/(P' - Q')$ derived from Anson and Newman's results[7].

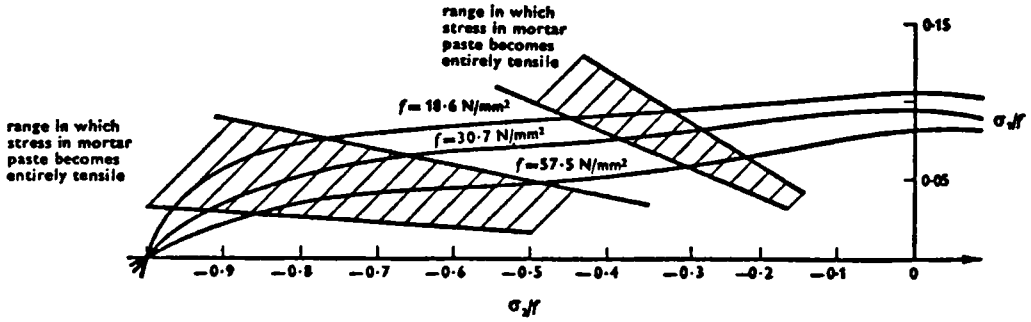


Figure 4; Behaviour in combined tension and compression, from Kupfer et al.[11] with additions.

gorized as compression and tension failures respectively. Vile[12] has described the probable mechanism of compression failure, in which major micro-cracking is promoted by shear bond failure at the aggregate/cement paste interface and development of slip planes within the cement paste itself. At the other extreme, it is considered (by Alexander[13] and Newman and Newman[14], for instance) that shear plays little part in tensile failure, which is principally due to the rapid propagation of micro-cracks, that have been initiated either in the cement paste or at the interface with the aggregates, in planes approximately normal to the maximum principal tensile stress. The transitional behaviour between these two extremes has been considered by Isenberg[15] and Johnson and Lowe[16], who find that this occurs when the ratio of the applied compressive stress to tensile stress is in the range 11 to 25. This occurs within the range of uncertainty of the proposed indicator. That is, within the range of stress when one of the average stresses in the mortar is tensile but the cement paste is entirely in compression.

The probable existence of two principal failure mechanisms for concretes of normal density has been recognized for some considerable time.[1,17,18] In this context, then, consideration of the internal stresses provides a plausible explanation for the occurrence of one mode of failure, rather than the other, under particular combinations of stress. With dense concretes, the results are possibly obvious on intuitive grounds alone, but the approach may have real diagnostic value when applied to less conventional concretes. These could include high-strength or lightweight-aggregate concretes in which the strength of the aggregate may set an upper limit to the concrete strength under some combinations of stress.

The signs of the average stress components in the aggregate of a concrete tested under biaxial stress are shown in Figure 5, which has been drawn with Q^* positive, following the results given in Table 2. The Figure shows that there is no combination of biaxial stress for which the average stresses in the aggregate are entirely compressive. Thus, if the matrix is capable of transmitting high stresses to the aggregate, brittle failure of the aggregate is possible under all combinations of biaxial stress. In general, small particles of natural aggregate must be stronger than large particles from the same source, because of the inevitable elimination of major flaws during the processes of size reduction. Therefore, if failure of the aggregate occurs, it will almost certainly do so preferentially in the large particles which are weaker and also carry higher

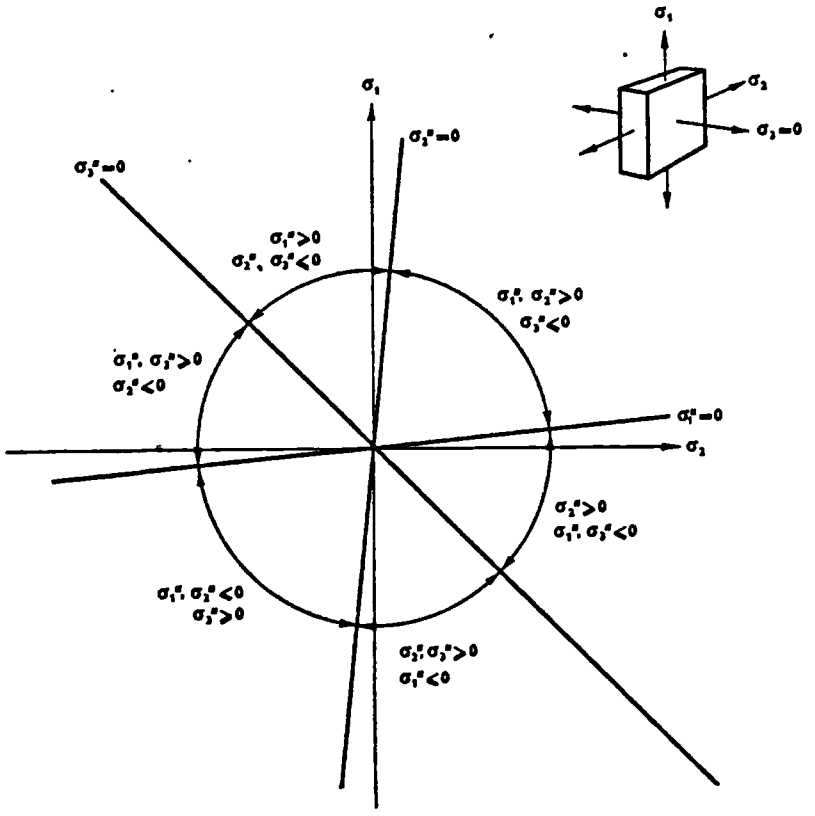


Figure 5: Isonomic regions for the average stresses in the aggregate in a biaxially stressed concrete.

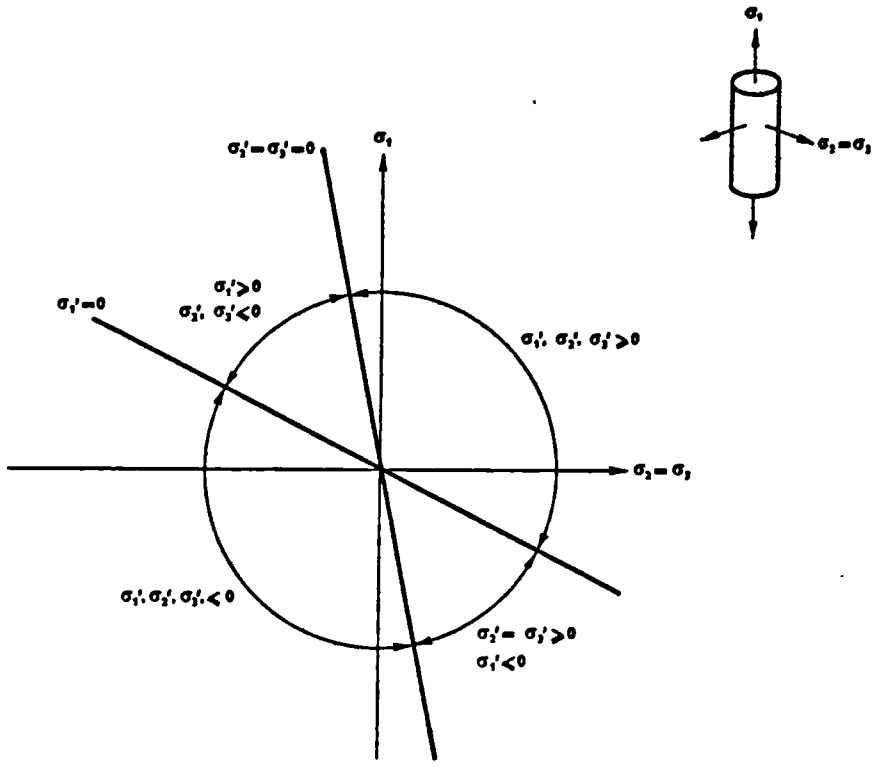


Figure 6a: Isonomic regions for the average stresses in the cement paste in a triaxially stressed concrete.

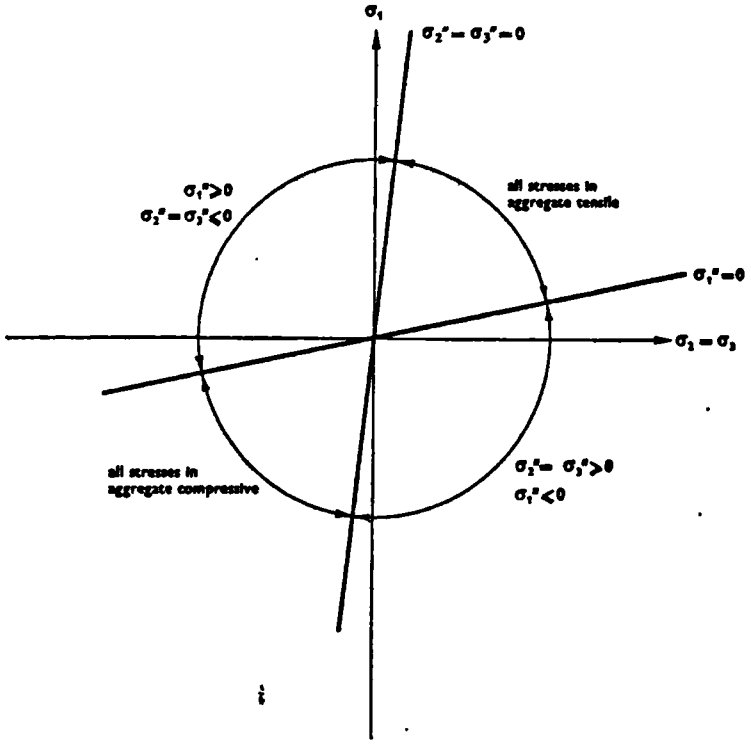


Figure 6b: Isonomic regions for the average stresses in the aggregate in a triaxially stressed concrete.

average stresses than the smaller material.

There is ample quantitative evidence to show that fracture of a significant proportion of the aggregates does occur in moderately high-strength concretes tested in tension[19]. Also, it is clear that aggregate failure must be avoided if concretes are to be obtained having a high strength in uniaxial compression[20]. However, these considerations do not apply to triaxial compression where concretes employing normal aggregates can sustain stresses an order of magnitude greater than their strength in uniaxial compression[21]. An explanation for this behaviour is evident from Figure 6, which shows that, in most of the possible triaxial stress combinations, obtained in tests using a hydraulic cell, the average stresses in the cement paste and the aggregate are entirely compressive.

Concluding remarks

There is always some doubt concerning the properties of the matrix within a concrete, as it is possible that these properties may differ from those found for a nominally identical material tested on its own. The success of solid models, used for estimating such properties as Young's modulus and specific creep of concrete, suggests that errors of this sort must be small when the quantity considered is an average value for a fair-sized volume of concrete. On this basis, the results for the average stress coefficients (Table 2) are reasonably acceptable, the accuracy depending mainly upon the quality of the experimental results and the values used for the elastic properties of the aggregate. These latter values were considered to be the main source of uncertainty in the results. Accordingly, the calculations were repeated with a range of different values of E'' and ν''. These calculations show that the coefficients P in Table 2 are not more than 18% in error and the signs of the coefficients Q are correct, provided that the values used for E'' and ν'' are within $\pm 10\%$ of the true values. Errors of this magnitude would not affect any of the conclusions obtained relating to the average state of stress in the separate phases or the role of the larger particles of aggregate in the concrete mix.

The work on failure is based upon the idea that it is difficult to propagate cracks in a stress field that is, on average, entirely compressive. This idea seems unexceptionable and has been partially confirmed by experiments on two-dimensional concretes comprising circular discs cast into a mortar matrix[22]. However, there is some risk in applying results derived from Anson and Newman's data to the other workers' concretes discussed in this paper. For this reason, the numerical results dealing with the extent of different ranges of behaviour etc. must be regarded as only approximate.

The qualitative results concerning the modes of failure depend essentially upon the sign of the coefficient Q'. It would be useful to be able to anticipate the sign of Q' for concretes different in character from those of Anson and Newman. If the Poisson's ratios of the aggregate and the cement paste are the same, Q' is negative if the Poisson's ratio of the concrete is less than that of the aggregate. This may lead to a satisfactory working rule for the sign of Q', but more information on the Poisson's ratio of various aggregates is required before the present ideas can be applied unreservedly to lightweight and unconventional concretes.

In the main, the present study is concerned with the results for average stresses and their implications concerning the mode of failure of concrete tested under ideal laboratory conditions. However, it is clear that the extent of the different isonomic regions will be affected by changes in the ambient conditions and it is intended to take up this question on another occasion. At this stage of the work, it is considered that the results are encouraging and that the proposed indicator may prove to be a reasonable guide to the occurrence of brittle modes of failure in concrete.

REFERENCES

1. TERZAGHI, K. Stress conditions for the failure of saturated concrete and rock. *Proceedings of the American Society for Testing and Materials.* Vol. 45. 1945. pp. 777–792.
2. VOLKOV, S. D. *Statistical strength theory.* Translated from the Russian. New York, Gordon and Breach, 1962. pp. 267. Russian monographs and texts on advanced mathematics and physics. Vol. XI.
3. DOUGILL, J. W. A mathematical model for the failure of cement paste and mortars. *Magazine of Concrete Research.* Vol. 19, No. 60. September 1967. pp. 135–142.
4. DOUGILL, J. W. An approximate assessment of the effects of heterogeneity on the strength and mode of failure of concrete systems. Paper presented to the International Conference on Structure, Solid Mechanics and Engineering Design, Southampton, 21–25 April 1969. (To be published.)
5. DANTU, P. Etude des contraintes dans les milieux hétérogènes: application au béton. (Study of the stresses in heterogeneous materials: application to concrete.) *Annales de l'Institut Technique du Bâtiment et des Travaux Publics.* Vol. 11, No. 121. January 1958. pp. 55–77. Série Essais et Mesures 40.
6. DANTU, P. Etude de la repartition des contraintes dans un milieu hétérogène a deux corps. (Study of the distribution of stresses in a heterogeneous mixture of two substances.) *Non-homogeneity in elasticity and plasticity: Proceedings of an IUTAM Symposium, September 1958.* London, Pergamon Press, 1959. pp. 443–451.
7. ANSON, M. and NEWMAN, K. The effect of mix proportions and methods of testing on Poisson's ratio for mortars and concretes. *Magazine of Concrete Research.* Vol. 18, No. 56. September 1966. pp. 115–130.
8. ANSON, M. An investigation into a hypothetical deformation and failure mechanism for concrete. *Magazine of Concrete Research.* Vol. 16, No. 47. June 1964. pp. 73–82.
9. DOUGILL, J. W. Some effects of thermal volume changes on the properties and behaviour of concrete. *The Structure of Concrete and its behaviour under load: Proceedings of an International Conference, London, 1965.* London, Cement and Concrete Association, 1968. pp. 499–513.

10. BAKER, A. L. L. An analysis of deformation and failure characteristics of concrete. *Magazine of Concrete Research.* Vol. 11, No. 33. November 1959. pp. 119–128.
11. KUPFER, H., HILSDORF, H. K. and RÜSCH, H. Behaviour of concrete under biaxial stresses. *Journal of the American Concrete Institute. Proceedings* Vol. 66, No. 8. August 1969. pp. 656–666.
12. VILE, G. W. D. The strength of concrete under short-term static biaxial stress. *The Structure of Concrete and its behaviour under load: Proceedings of an International Conference, London, September 1965.* London, Cement and Concrete Association, 1968. pp. 275–288.
13. ALEXANDER, K. M. A study of concrete strength and mode of fracture in terms of matrix, bond and aggregate strengths. *Proceedings of the 1st Tewksbury Symposium on Fracture, 1963.* Melbourne, Faculty of Engineering, University of Melbourne, 1965. pp. 141–168.
14. NEWMAN, K. and NEWMAN, J. B. Failure theories and design criteria for plain concrete. Paper presented to the International Conference on Structure, Solid Mechanics and Engineering Design, Southampton, 21–25 April 1969. (To be published.)
15. ISENBERG, J. Moisture affects strength of concrete under combined stress. *Civil Engineering and Public Works Review.* Vol. 60. October 1965. pp. 1475–1476.
16. JOHNSON, R. P. and LOWE, P. G. Behaviour of concrete under biaxial and triaxial stress. Paper presented to the International Conference on Structure, Solid Mechanics and Engineering Design, Southampton, 21–25 April 1969. (To be published.)
17. COWAN, H. J. The strength of plain, reinforced and prestressed concrete under the action of combined stresses, with particular reference to the combined bending and torsion of rectangular sections. *Magazine of Concrete Research.* Vol. 5, No. 14. December 1953. pp. 75–86.
18. NEWMAN, K. The structure and engineering properties of concrete. *Theory of Arch Dams: Proceedings of an International Symposium, Southampton, 1964.* London, Pergamon Press, 1965. pp. 683–712.
19. BACHE, H. H. and NEPPER-CHRISTENSEN, P. Observations on strength and fracture in lightweight and ordinary concrete. *The Structure of Concrete and its behaviour under load: Proceedings of an International Conference, London, September 1965.* London, Cement and Concrete Association, 1968. pp. 93–108.
20. MATHER, K. High strength, high density concrete. *Journal of the American Concrete Institute. Proceedings* Vol. 62, No. 8. August 1965. pp. 951–960.
21. BALMER, G. G. *Shearing strength of concrete under high triaxial stress—computation of Mohr's envelope as a curve.* Denver, U.S. Department of the Interior, Bureau of Reclamation. October 1949. pp. 26. Structural Research Laboratory. Report No. SP-23.
22. McCREATH, D. R., NEWMAN, J. B. and NEWMAN, K. The influence of aggregate particles on the local strain distribution and fracture mechanism of cement paste during drying, shrinkage and loading to failure. *Materials and Structures.* Vol. 2, No. 7. January–February 1969. pp. 73–84.

Contributions discussing the above paper should be in the hands of the Editor not later than 31 January 1971.

UDC 666.97.539.382

Further consideration of a mathematical model for progressive fracture of a heterogeneous material

J. W. Dougill, MSc(Eng), DIC, MICE

UNIVERSITY OF LONDON, KING'S COLLEGE

SYNOPSIS

Uniaxial stress-strain curves are derived for a mathematical model designed to represent a heterogeneous material that fails in tension by progressive fracture. These results show qualitative agreement with the behaviour of real materials including mortars and concretes. The results suggest that the behaviour that occurs, after the peak stress has been achieved in a deformation-controlled test, is dependent upon the energy required to fracture the material. If this is sufficiently high, stable fracture propagation occurs. However, if the energy required for fracture is low, failure occurs by instability under reducing stress. The conditions for the occurrence of this instability are obtained in terms of the properties of the model material and the implications of this behaviour, for materials testing and the derivation of failure criteria, are briefly discussed.

Introduction

In an earlier paper[1] a mathematical model was proposed which possesses some of the characteristics exhibited by mortars and cement pastes during fracture in tension. The work was based on an assumed statistical distribution of the micro-stress components and the principal results followed directly from consideration of equilibrium. By adopting this approach, the difficulty of describing the micro-structural geometry of the material was avoided. However, the approach carried its own penalty in that no direct kinematic argument could be developed. The object of the present paper is to examine this problem further in an attempt to obtain some results for the relationship between stress and strain for the model material when this is loaded in uniaxial tension.

Notation

σ = macroscopic direct stress component
ξ = component of micro-stress
q_t = intrinsic tensile strength of the model material
α = stress variation or heterogeneity parameter
m = stress redistribution or micro-cracking parameter
$1/r$ = non-dimensional applied stress ($1/r = \sigma/q_t$)
u = $(r - m)/\alpha$
$P(u)$ = normal probability function
$Z(u)$ = derivative of normal probability function
V = a representative volume
E = Young's modulus
W = work done on unit volume of the model material
U = strain-energy density
D = energy dissipated per unit volume
λ = a material property
n = number of potential fracture planes per unit length
γ = surface energy
F = a function of u or, more particularly, $F = 1 - P(u)$
ε = macroscopic strain component
ε = $E\varepsilon/q_t$

Equilibrium

Before considering strain, it will be helpful to summarize some details of the earlier work[1,2]. In this, it is assumed that, under a uniaxial stress, σ, the distribution of the direct components of micro-stress, ξ, acting on a plane at right-angles to the direction of σ, is as shown in Figure 1. This is a normal distribution, with mean $m\sigma$ and standard deviation $\alpha\sigma$, which is truncated at $\xi = q_t$ and has a discontinuity at $\xi = 0$. The cut-off follows from the assumption that no micro-element can sustain a stress greater than the intrinsic strength, q_t, of the material. In this way, the shaded region of Figure 1 represents the proportion of material fractured under the stress σ and this also

corresponds to the discontinuity, at $\xi = 0$, representing the proportion of material carrying a micro-stress having a value of precisely zero. The quantity α is a property of the model material that describes heterogeneity through its effect upon the stress distribution. For a homogeneous material, α would be zero and the stresses in all the micro-elements would be the same. In a heterogeneous material, however, the micro-stress will vary about the mean and this variation is described, to some extent, by using the appropriate value of α.

If the additional notation,

$$u = \frac{r - m}{\alpha} \text{ and } \frac{1}{r} = \frac{\sigma}{q_t} \quad \ldots\ldots\ldots\ldots (1)$$

is introduced, the condition that the applied macroscopic stress, σ, must be statically equivalent to the mean value of the micro-stress, ξ, leads to the equilibrium equation,

$$\frac{1}{\alpha} = \frac{m}{\alpha} P(u) - Z(u) \quad \ldots\ldots\ldots\ldots (2)$$

in which $P(u)$ is the normal probability integral and $Z(u)$ is its derivative.

The quantity m may be eliminated from equations 1 and 2 to obtain the relationship between the applied stress q_t/r and the proportion of material fractured, $1 - P(u)$, for any particular value of the heterogeneity parameter, α. Some results of this sort are shown in Figure 2.

If the heterogeneity parameter, α, can be considered to be unaffected by stress or damage, the curves in Figure 2 represent the behaviour, during progressive fracture, of materials of differing heterogeneity. For a monotonic increase in the proportion of material fractured, the applied stress increases to a maximum value before decreasing to become zero when the entire section is fractured. A material of this type fails in a load-controlled test when the applied stress reaches the peak value and observation of behaviour beyond this point is only possible if the applied load can be relaxed during the continuing process of failure.

This type of behaviour has been noted in tensile tests on concretes and mortars[3], but not cement pastes[4], and these observations are supported by similar results from other tests in which the principal tensile stress in the concrete is the major influence upon the mode of failure[4,5]. These results suggest that the model material may provide a satisfactory description of some features of the behaviour of mortars and concretes. It is also apparent that the model may have a use in describing other materials in which progressive breakdown occurs in tension.

Instead of taking α to be constant, a better description of a particular material may require that the heterogeneity, α, is a function of stress or damage. However, the effects of any specified change in heterogeneity can easily be derived from Figure 2, and it is clear that such changes are not likely to change qualitative trends obtained when α is assumed to be constant. Thus, in the present state of knowledge, it seems reasonable to take α as constant and accept that the resulting description of the material is only approximate.

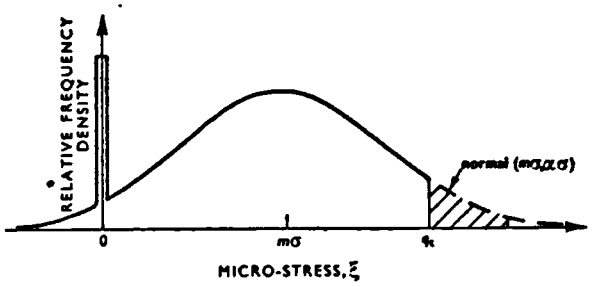


Figure 1: Assumed distribution of micro-stress.

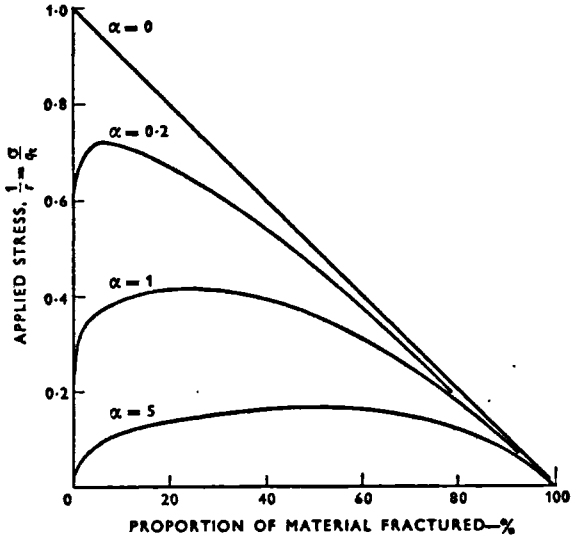


Figure 2: Relationship between the applied stress and the proportion of material fractured during progressive fracture.

Figure 2 can be looked at in another way. Suppose it were possible to perform an experiment on a real material in which the applied stress and the proportion of material fractured were both measured during loading. These results could be superimposed on Figure 2 in order to determine a value of α for the material and to determine the manner in which this property varies with stress. Clearly such an experiment would be difficult to perform and the interpretation of the term 'proportion of material fractured' may also be difficult in a real case. In spite of this, the experiment is conceptually sound and results of this type could lead to greater understanding of the failure process.

Energy considerations

Energy is supplied to a material during loading and this energy is equivalent to the work done, W, by the applied loads. Some of this energy may be stored in the form of strain energy, U, and the remainder, D, is dissipated. In the present problem, the loading comprises the single stress component σ, so that

$$dW = d(U + D) = \sigma d\varepsilon$$

the equations being written for unit volume of the loaded material. Thus the strain ε corresponding to the stress σ can be found, by integration, from the equation

$$\varepsilon = \int \frac{1}{\sigma} d(U + D) \quad \ldots\ldots\ldots\ldots\ldots (3)$$

In this way, the problem of determining strain in the model material is reduced to that of finding suitable expression for the stored and dissipated components of the energy supplied.

STRAIN ENERGY

Each element of the model material is taken to be linear elastic with Young's modulus E. In addition, the model is so arranged that the direct micro-stress component ξ is the only stress acting. On this basis, the average density of the strain energy, stored in a representative volume, V, is simply

$$U = \frac{1}{V} \int_V \frac{\xi^2}{2E} dV$$

If the volume V is large compared with the grain size of the material and the distribution of micro-stress is as shown in Figure 1, the expression for the strain-energy density may be written

$$U = \frac{1}{2E} \left(\frac{1}{\sqrt{2\pi}\alpha\sigma} \int_{-\infty}^{q_t} \xi^2 e^{-\frac{1}{2}\left(\frac{\xi - m\sigma}{\alpha\sigma}\right)^2} d\xi \right)$$

which gives, on again writing $r = q_t/\sigma$ and $(r - m)/\alpha = u$,

$$U = \frac{\sigma^2}{2E} [(m^2 + \alpha^2)P(u) - \alpha(2m + \alpha u)Z(u)] \ldots . (4)$$

DISSIPATED ENERGY

The structural behaviour of real materials depends very much upon the mechanism by which energy is dissipated and thus there is a marked contrast in behaviour between materials in which energy is dissipated primarily by plastic deformation and those in which fracture occurs and energy is required to form new surfaces within the material. The present model is intended to represent a material in which progressive fracture occurs and so it seems reasonable to suggest that the energy dissipated is used entirely in the formation of new surfaces. The work done in this is taken to be proportional to the amount of material fractured so that the energy dissipated per unit volume is given by

$$D = \lambda[1 - P(u)] \ldots\ldots\ldots\ldots\ldots (5)$$

Here, $1 - P(u)$ is the proportion of material fractured in any representative volume and λ is a constant. This constant may be considered to have the form

$$\lambda = n\gamma \ldots\ldots\ldots\ldots\ldots\ldots (6)$$

where γ is the surface energy of the model material and n is the number of separate fracture planes that can occur per unit length of the model material, measured in the direction of loading.

The work done in loading unit volume of material can now be found, by adding the expressions for the strain energy and the dissipated energy (equations 4 and 6). On substituting q_t/r for σ, the following expression is obtained

$$W = \lambda[1 - P(u)] + \frac{q_t^2}{2E}\left[\left(\frac{m^2}{r^2} + \frac{\alpha^2}{r^2}\right)P(u) - \frac{\alpha}{r}\left(1 + \frac{m}{r}\right)Z(u)\right] \ldots\ldots\ldots (7)$$

The quantity m in this equation can be found from the equilibrium equation in terms of u, as can the non-dimensionalized stress $1/r$. Thus, W can be regarded as a function of u or, alternatively, as a function of the damage, $1 - P(u)$, and the material properties.

Strain

The role of the different variables is seen more clearly if these are grouped by writing

$$\bar{\varepsilon} = E\varepsilon/q_t$$

and

$$\bar{W} = EW/q_t^2$$

so that $\bar{W}$ is a function of α, $\lambda E/q_t^2$ and F, a function of u. Equation 3 can now be rewritten in the form

$$\bar{\varepsilon} = \int r \frac{d\bar{W}}{dF} dF \ldots\ldots\ldots\ldots\ldots (8)$$

so that the strain parameter $\bar{\varepsilon}$ can be determined for different combinations of heterogeneity α and the dimensionless group $\lambda E/q_t^2$. These calculations are best undertaken numerically.

Some typical results, for a material with $\alpha = 1{\cdot}0$, are shown in Figure 3. The results for the two highest values of $\lambda E/q_t^2$ follow the pattern anticipated, for strain-controlled tests, in which the stress reaches a maximum value and is then reduced with continued deformation. Comparing these two results, more work is required to propagate fracture in the material having the highest value of $\lambda E/q_t^2$. Thus, the strain at any particular stress level is greater in this material than in that with the smaller energy dissipation.

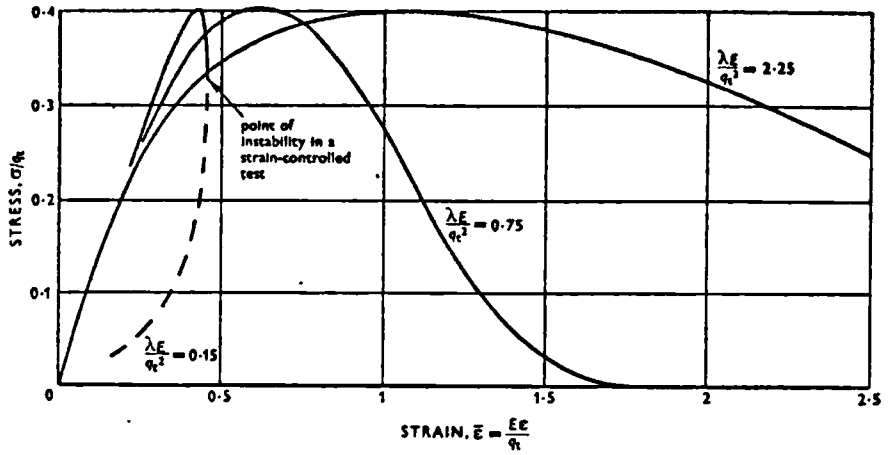


Figure 3: Stress-strain curves for a material with $\alpha = 1$, in tension, for various values of $\lambda E/q_t^2$.

The third curve in Figure 3, drawn for $\lambda E/q_t^2 = 0{\cdot}15$, suggests an interesting phenomenon. With this material, a stage is reached, under reducing stress, where no additional energy need be supplied in order to propagate failure throughout the material. At this point, the strain energy stored in the material is sufficient to fracture all the material that remains undamaged. If more strain energy is available than is necessary for the fracture process, much of the excess will be dissipated as kinetic energy and the process of failure may be violent. Thus, it appears that instability is possible even under conditions of monotonically increasing strain.

There are clearly difficulties in observing such instabilities in tests on real materials. However, this was possible in the work undertaken by Wawersik[6], in which this form of behaviour was obtained in uniaxial compression tests on a number of rock samples. When instability occurred in Wawersik's experiments, it did so at a stress not much below the peak stress achieved on loading. Accordingly, he classified the rocks he tested into two categories only: class I rocks, in which additional energy is required to propagate fracture, and class II rocks, in which fracture is self-sustaining. The particular results from the model shown in Figure 3 demonstrate class I behaviour and an additional failure mode in which instability occurs at a stress σ_{crit}, appreciably below the maximum stress σ_{max}. Other results show that the stress level at which instability occurs, $\sigma_{crit}/\sigma_{max}$, is affected by both heterogeneity, α, and the energy required for fracture, λ. It is, therefore, of interest to examine, in more detail, the manner in which these parameters affect behaviour under reducing stress.

Instability analysis

Once the peak stress has been reached, instability occurs if

$$\frac{d\varepsilon}{d\sigma} \geqslant 0$$

or, using equation 3, if

$$\frac{dW}{d\sigma} \geqslant 0$$

Now if we write $F = 1 - P(u)$, the proportion of material fractured, and note that $d\sigma/dF$ is negative once the peak stress has been achieved, the condition for the material to be unstable becomes

$$\frac{dW}{dF} \leqslant 0$$

In this criterion, $W = U + D$ and $D = F\lambda$, so that the material is unstable for

$$\lambda \leqslant -\frac{dU}{dF} \quad \ldots\ldots\ldots\ldots\ldots\ldots (9)$$

Here, the term $-du/dF$ can be regarded as the rate of release of strain energy, per unit volume of material, during the fracture process, so that λ is similar to G_c, the critical strain-energy release rate of fracture mechanics[7]. Clearly, this similarity is to be expected. However, there is a fundamental difference in dimensions between λ and G_c, and this occurs because the present analysis is concerned with variations in microstress that occur throughout a heterogeneous material rather than effects that are local to a single, abnormally large imperfection.

The term dU/dF can be considered to be a function of the applied stress and the heterogeneity α. Thus the equality in condition 9 can be used to calculate the values of λ that correspond to the occurrence of instability at a particular stress level, for a range of model materials of different heterogeneities. Two stress levels are of particular interest. One of these is the peak stress and the other occurs when the material is at an incipient state of complete disintegration and the applied stress has been reduced to zero. It can be shown that $\lambda E/q_t^2$ must be equal to $\frac{1}{2}$ if instability is to occur in this situation and, thus, instability is not possible under conditions of controlled deformation for $\lambda E/q_t^2 > \frac{1}{2}$.

The condition for instability to occur at the peak stress has also been examined. Here the critical value of λ is a function of α (referred to as λ_c). Thus unstable behaviour can occur somewhere in the descending portion of the stress-strain curve for

$$\lambda_c < \lambda < \frac{q_t^2}{2E} \quad \ldots\ldots\ldots\ldots\ldots\ldots (10)$$

It is considered that, for real materials, λ must be greater than zero, on physical grounds, and must also be greater than λ_c if the peak stress is to be attainable in a deformation-controlled test.

Values of λ_c are given in Figure 4, which shows the various combinations of material properties for which instability is possible. It is interesting that instability can occur at the peak stress only if the heterogeneity is greater than a value of around 1·3. This suggests that some departure from uniformity is necessary in the micro-stress distribution if brittle fracture is to be possible. Clearly, this irregularity in the stress field must play the same role as a flaw or the elliptical crack in Griffith's[8] classical approach to brittle fracture.

A particular form of model behaviour is specified by a point in Figure 4. Thus, the behaviour of the model requires that the parameters $\lambda E/q_t^2$ and α should be related and it would be reassuring if some such interdependence could be established, on physical grounds, as being relevant to real materials. It is thought that the connexion is established by equation 6, in which it is suggested that λ is dependent upon the number of potential fracture planes that occur per unit length in the direction of loading. In a real material, these fracture sites would occur at structural discontinuities or flaws. These flaws would affect the local micro-stress distribution and this effect must be described by the appropriate value of α.

Concluding discussion

Many of the limitations of the model examined in this paper have been discussed in detail in the earlier work[1]. The major limitation follows from the fact that the model is not a statistical vehicle and so some effects, due to variations of the various parameters throughout the body of the material, are ignored.

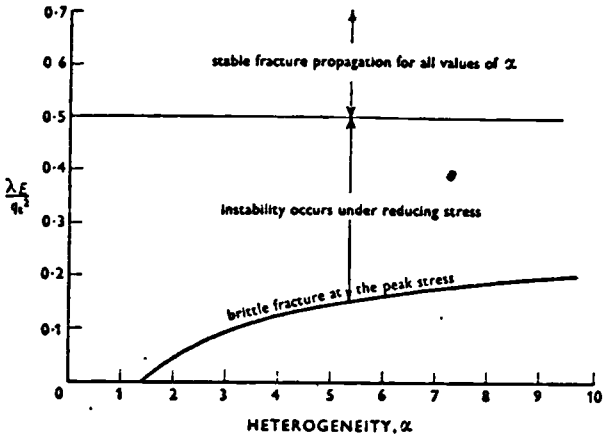


Figure 4: Modes of behaviour of a range of model materials.

The assumptions used in the analysis imply that the model has the character of a mathematical idealization which is used to define a range of ideal materials. However, there are real materials that show qualitative agreement with the behaviour of the model and, with this in mind, it is considered reasonable to put a physical interpretation upon the various parameters involved. Following this, the recognition that both α and λ are dependent upon the average flaw density may allow a limited approach to be made, in future work, to the question of size effects.

The stress-strain curves derived from the model show agreement with observed behaviour of mortars and concretes, and also suggest that failure, by instability, may occur for some materials under conditions of controlled deformation. This is an important result that has implications for both materials testing and analysis.

It is known that instabilities can occur in deformation-controlled tests on brittle materials. When this occurs, the material in the undamaged portion unloads into the fracture zone, to produce a violent failure. This behaviour is a result of heterogeneity in the specimen under test, in that failure occurs preferentially in one region, and the mechanism involved is similar to that shown by the model material. In experimental work, small specimens are often used in an attempt to avoid these effects. However, with heterogeneous materials, there is a minimum volume of specimen that can be used to provide a result, from a particular test[9], that is representative of the behaviour of the material in bulk. The results from the model suggest that instability is possible, with some materials, even if this minimum representative volume is used. If this occurs, the behaviour is not due to specimen size alone but is intrinsic to the material.

The effects of local gross heterogeneity and specimen size are questions of fracture mechanics. Here there is

a tendency to concentrate, in the analysis, upon the role of the most critical flaw in the initiation and propagation of failure in an otherwise perfect material. In practical terms, this means that the fracture mechanics approach is restricted to consideration of flaws that are considerably larger than the grain size of the material being examined. In the present work, the emphasis is different and an attempt has been made to describe the behaviour of a material that contains many imperfections of similar severity. Clearly, such a description is necessary if the local behaviour of a macroscopically heterogeneous material, like concrete or mortar, is to be understood. However, the two approaches are complementary and the effects of isolated major defects should not be ignored when large volumes of material are considered.

The complementary nature of the two approaches is evident when the possible forms of failure criteria for concrete are considered. Thus, although attempts have been made to apply criteria derived from the behaviour of individual flaws, the present work suggests that this approach is unlikely to be successful, for concretes, and that heterogeneity must be considered as a bulk, rather than a local, property. Criteria derived in this way would apply to the bulk material. However, the stress field in a structure or specimen may contain macroscopic regions of high stress concentration or gradient and these regions represent major flaws that should be investigated on a fracture mechanics basis. Clearly, it is to be expected that criteria for failure in the vicinity of a major local defect will differ from those of the bulk material.

REFERENCES

1. DOUGILL, J. W. A mathematical model for the failure of cement paste and mortars. *Magazine of Concrete Research.* Vol. 19, No. 60. September 1967. pp. 135–142.
2. DOUGILL, J. W. An approximate assessment of the effects of heterogeneity on the strength and mode of failure of concrete systems. Paper presented to the International Conference on Structure, Solid Mechanics and Engineering Design, Southampton, 21–25 April 1969.
3. HUGHES, B. P. and CHAPMAN, G. P. The deformation of concrete and micro-concrete in compression and tension with particular reference to aggregate size. *Magazine of Concrete Research.* Vol. 17, No. 54. March 1966. pp. 19–24.
4. HUGHES, B. P. and ASH, J. E. Short-term loading and deformation of concrete in uniaxial tension and pure torsion. *Magazine of Concrete Research.* Vol. 20, No. 64. September 1968. pp. 145–154.
5. DAVIES, J. D. A modified splitting test for concrete specimens. *Magazine of Concrete Research.* Vol. 20, No. 64. September 1968. pp. 183–186.
6. WAWERSIK, W. R. *Detailed analysis of rock failure in laboratory compression tests.* Thesis submitted to the University of Minnesota for the degree of PhD. July 1968. p. 165.
7. IRWIN, G. R. *Fracture dynamics. Fracturing of metals.* Cleveland, American Society for Metals, 1948. pp. 147–166.
8. GRIFFITH, A. A. The phenomena of rupture and flow in solids. *Philosophical Transactions of the Royal Society.* Series A. Vol. 221. 1920. pp. 163–198.
9. BROWN, C. B. Minimum volumes to ensure homogeneity in certain conglomerates. *Journal of the Franklin Institute.* Vol. 279, No. 3. March 1965. pp. 189–199.

Contributions discussing the above paper should be in the hands of the Editor not later than 30 September 1971.